ACTA CHIMICA

ACADEMIAE SCIENTIARUM HUNGARICAE

TOMUS 83 FASCICULUS 1

AKADÉMIAI KIADÓ, BUDAPEST

1974

ACTA CHIM. (BUDAPEST) ACASA 2 83 (1) 1–125 (1974)

ACTA CHIMICA

A MAGYAR TUDOMÁNYOS AKADÉMIA KÉMIAI TUDOMÁNYOK OSZTÁLYÁNAK IDEGEN NYELVŰ KÖZLEMÉNYEI

Az Acta Chimica német, angol, francia és orosz nyelven közöl értekezéseket a kémiai tudományok köréből.

Az Acta Chimica változó terjedelmű füzetekben jelenik meg, egy-egy kötet négy füzetből áll. Évente átlag négy kötet jelenik meg.

A közlésre szánt kéziratok a szerkesztőség címére (Budapest 112/91 Műegyetem) küldendők.

Ugyanerre a címre küldendő minden szerkesztőségi levelezés. A szerkesztőség kéziratokat nem ad vissza.

Megrendelhető a belföld számára az „Akadémiai Kiadó"-nál (1363 Budapest Pf 24. Bankszámla 215 11488), a külföld számára pedig a „Kultúra" Könyv- és Hírlap Külkereskedelmi Vállalatnál (1389 Budapest 62, P.O.B. 149 Bankszámla: 218 10990) vagy annak külföldi képviseleteinél és bizományosainál.

Die Acta Chimica veröffentlichen Abhandlungen aus dem Bereich der chemischen Wissenschaften in deutscher, englischer, französischer und russischer Sprache.

Die Acta Chimica erscheinen in Heften wechselnden Umfanges. Vier Hefte bilden einen Band. Jährlich erscheinen 4 Bände.

Die zur Veröffentlichung bestimmten Manuskripte sind an folgende Adresse zu senden

Acta Chimica
Budapest 112/91 Műegyetem

An die gleiche Anschrift ist auch jede für die Redaktion bestimmte Korrespondenz zu richten. Abonnementspreis pro Band: $ 32,00.

Bestellbar bei dem Buch- und Zeitungs-Außenhandels-Unternehmen »*Kultúra*« (1389 Budapest 62, P.O.B. 149 Bankkonto Nr. 218 10990) oder bei seinen Auslandsvertretungen und Kommissionären.

ACTA CHIMICA

ACADEMIAE SCIENTIARUM HUNGARICAE

TOMUS 83

AKADÉMIAI KIADÓ, BUDAPEST

1974

ACTA CHIMICA

TOMUS 83

FASCICULUS 1: 1974

FASCICULUS 2: 1974

FASCICULI 3—4: 1974

INDEX

Acta Chimica Academiae Scientiarum Hungaricae, Tomus 83 (1), pp. 1—13 (1974)

UNTERSUCHUNG DER ZUSAMMENSETZUNG VON EINHEIMISCHEN UND AUSLÄNDISCHEN ÄTHERISCHEN ÖLEN, III

KOMPONENTEN-ZUSAMMENSETZUNG DES DILLÖLES

K. BÉLAFI-RÉTHY*, E. KERÉNYI* und R. KOLTA**

(Ungarisches Erdöl- und Erdgas-Forschungsinstitut Veszprém und ** Betrieb für Kosmetik und Haushaltschemie, Budapest)*

Eingegangen am 28. August 1973

Es wurde durch Kombinierung wirksamer Trennmethoden und spektrometrischer Identifizierungsmethoden die qualitative und quantitative Zusammensetzung des ätherischen Öles der einheimischen Dillpflanze untersucht. Im Dillöl sind 14 Bestandteile (über einer Menge von je 0,01 Gew.-%) nachzuweisen. Davon betragen 3 Bestandteile (α-Phellandren, Limonen, Carvon) rund 90 Gew.-% bzw. zusammen mit 8 weiteren Bestandteilen — über 99,9 Gew.-%. Außer den 3 Hauptkomponenten ist das in ausländischen Dillöl-Proben bereits nachgewiesene α-Pinen, Dihydrocarvon und *p*-Cymol auch im einheimischen Dillöl vorzufinden. Viele Terpene und Terpenderivate, die in der Fachliteratur als Komponenten genannt werden, sind dagegen im gegebenen ätherischen Öl in nennenswerten Mengen nicht vorhanden. Andererseits gelang es den Verfassern, die Anwesenheit von α-Thujen, β-Myrcen, β-Phellandren, 1-Methyl-4-isopropenylbenzol und Carvotanaceton in dem untersuchten ätherischen Öl nachzuweisen. Schließlich wurden auch zwei in den Dillölen und allgemein in den ätherischen Ölen bisher unbekannte Bestandteile nachgewiesen.

Das durch Wasserdampfdestillation hergestellte ätherische Öl der Dillpflanze (Anethum graveolens) wird in beträchtlichen Mengen in der Konservenindustrie verwertet. Seine Bedeutung liegt außer der vielseitigen Untersuchung und der allgemeinen Verbreitung der Pflanze in unserem Lande [1] darin, daß die ungarische Dillölproduktion in der Weltproduktion, weiterhin der ungarische Dillölexport im Weltumsatz des Dillöles einen bedeutenden Anteil darstellt.

Fachliteratur-Angaben bezüglich der Zusammensetzung des ätherischen Öles

Trotz der Verbreitung des in Europa bekannten Anethum graveolens stehen über die Zusammensetzung des ätherischen Öles der Pflanze nur wenige zuverlässige Angaben zur Verfügung [2, 3]. Besonders wenig wurde bis jetzt das ätherische Öl der einheimischen Dillpflanze studiert, zumal sich die Untersuchungen lediglich auf die physikalischen Eigenschaften und Bestimmung der Hauptbestandteile des Dillöles erstreckt haben [3, 4]. Nach einigen Verfassern ist das ätherische Öl von Anethum graveolens hinsichtlich der Zusammensetzung dem Öl des in Indien geernteten Anethum sowa ähnlich

[5], mit dem Unterschied, daß das erstere einen höheren Gehalt an Carvon aufweist und kein Dillapiol enthält [6, 7]. Laut Fachliteratur-Angaben stimmen ferner die Hauptkomponenten des ätherischen Öles der Dillpflanze auch mit jenen des ätherischen Öles der Dillsamen überein, während bei den Nebenkomponenten Unterschiede festzustellen sind [5, 8].

Die Zusammensetzungs-Angaben für verschiedene Dillöle sind — unabhängig vom Ursprung der untersuchten Proben — in Tab. I angeführt. Jene Komponenten, deren Anwesenheit bis jetzt nur von einem einzigen Verfasser nachgewiesen oder von den Verfassern lediglich für wahrscheinlich gehalten wurde, sind in dieser Tabelle bezeichnet. Aus der Tabelle ist ersichtlich, daß in der Fachliteratur wenig gleichlautende Angaben bezüglich der Zusammensetzung der Dillöle zu finden sind. So konnte man auch die gesammelten Informationen für die Untersuchung des ätherischen Öles der einheimischen Dillpflanze vorerst nur als einen unsicheren Ausgangspunkt betrachten.

Tabelle I

Die in verschiedenen Dillölen bisher identifizierten oder wahrscheinlich vorhandenen Bestandteile

Bestandteil	Literatur	Bestandteil	Literatur
Limonen (Dipenten)	[9, 10]	Terpinen-4-ol (?)	[5]
α-Phellandren	[11, 12]	β-Terpineol (?)	[5]
γ-Terpinen	[5, 12]	Eugenol (?)	[18]
α-Pinen (?)	[10]	Thymol (?)	[18]
Camphen (?)	[10]	Carvon	[4, 12, 13]
p-Cymol (?)	[5]	Dihydrocarvon	[14, 17]
n-Oktanol (?)	[3]	Dillapiol	[6, 7, 15, 17]
2-Nonanol (?)	[5]	Myristicin (?)	[16]
Nonylaldehyd (?)	[5]	Isomyristicin (?)	[16]
Decylaldehyd (?)	[5]	α-Bergamott (?)	[5]

Das untersuchte ätherische Öl und die angewandte Untersuchungsmethode

Das den Untersuchungen unterworfene, durch Wasserdampfdestillation raffinierte ätherische Öl stammte aus der in Paks angebauten und 1969 geernteten Dillpflanze. Dichte ($d_{45}^{1} = 0{,}898$), Brechungsindex ($n_D^{20} = 1{,}4840$) und Drehungsvermögen ($\alpha_D = +\ 96{,}8°$) des Öles entsprachen den üblichen Charakteristiken des Dillpflazenöles [3].

Die Zusammensetzung des ätherischen Öles der Dillpflanze wurde von uns mit einer für ätherische Öle erarbeiteten, kombinierten Trennungs- und

Tabelle II

Zur Trennung und Analyse angewandte Methoden

Verfahren bzw. Methode	Ziel	Apparat bzw. Gerät	Versuchsbedingungen
1.	2.	3.	4.
Analytische Gaschromatographie	Quantitative Analyse, Kontrolle der Trennungsprodukte, Reinheitsprüfung der Bestandteile	Chrom III.; Kapillare: 50 m/0,25 mm; Flammenionisationsdetektor	Verteiler-Phase: Carbowax 1000; Temperatur: 130 °C; Trägergas: Argon, 3 ml/Min.; Abschwächung: 10%; Einwaage: 0,2 mm^3; Auswertung: mit der Dreieck-Methode
Halbmikro-Rektifikation	Vortrennung aufgrund des Siedepunktes	Säule mit Vakuum-Mantel, 500 mm/6 mm; Drehband: 5,5 mm breit aus Stahl	Drehzahl: ca. 2000 U/Min; Trennfähigkeit: 30 theor. Trennstufen; Betriebsinhalt: 0,1 cm^3; Druckverlust: 0,2 Torr; Einwaage: 20 cm^3; Destillationsdruck 200 Torr; Destillate: 1 cm^3-Fraktionen
Präparative Gaschromatographie	Herstellung reiner Bestandteile, Anreicherung der Bestandteile	Pye Unicam 105; Säule 7 m/5 mm	Verteiler-Phase: Carbowax 20 M auf Celite; Temperatur: abhängig vom Siedepunkt 120 bzw. 160 °C; Trägergas: Argon, 12 dm^3/Stde; Einwaage: zur groben Trennung — 1 cm^3, zur feinen Trennung — 50—100 mm^3
Infrarotspektrometrie	Identifizierung reiner Bestandteile, Strukturaufklärung	Carl Zeiss Jena, UR 20, mit Prismen aus KBr, NaCl u. LiF	Schichtdicke: für reine Substanz — 0,003 cm, für Lösung in Tetrachlormethan — 0,01 cm; Spektrumbereich: 4000—400 cm^{-1}
Massenspektrometrie	Identifizierung reiner Bestandteile, Strukturaufklärung	ZEME, MI 1305; Auflösungsvermögen: 300	Einwaage-System: eigene Konstruktion [22]; Beschleunigungsspannung: 50 V; Aufnahmegeschwindigkeit: 2 Masseneinheiten pro Minute; Spektrumbereich: 39—200 Masseneinheiten
Magnetische Kernresonanzspektrometrie	Identifizierung reiner Bestandteile, Strukturaufklärung	VARIAN T—60, Frequenz 60 MHz; Feldstärke 14 kG; Auflösungsvermögen: 0,4 Hz	Referenz-Substanz: Tetramethylsilan; Verschiebungsintervall: 0—8 ppm

Identifizierungsmethode [19] untersucht, die sich zur vollständigen Zusammensetzungsermittlung eines importierten »entmentholisierten« Minzöles und eines einheimischen Pfefferminzöles bereits gut bewährt hatte [20]. Die Anzahl der nennenswerten (in einer Menge von über 0,01 Gew.-% anwesenden)

Bestandteile und deren Mengenverhältnisse im ätherischen Öl wurden mittels Kapillar-Gaschromatographie bestimmt. Zur Identifizierung der Bestandteile ließ sich das ätherische Öl durch wirksame Halbmikro-Drehbandkolonnen-Destillation und dann mittels präparativer Gaschromatographie in einzelne Komponenten zerlegen, wobei die Trennvorgänge ebenfalls durch Kapillar-Gaschromatographie kontrolliert wurden. Die reinen oder beträchtlich angereicherten Bestandteile konnten danach aufgrund ihrer Massen-, Infrarot- und magnetischen Kernresonanz-Spektren, teils durch Studieren dieser Spektren, teils durch deren Vergleichen mit den Spektren bekannter, vermutlich anwesender Bestandteile identifiziert werden. Die charakteristischen Angaben der angewandten Trennvorgänge und analytischen Methoden sind in Tab. II zusammengefaßt.

Zwei Komponenten des ätherischen Öles der Dillpflanze ließen sich mit keinem bekannten Bestandteil der ätherischen Öle identifizieren. Zur Klärung ihrer Struktur wurden sie außer der Untersuchung ihrer Spektren chemischen Umwandlungen unterworfen, mit anschließender Identifizierung der dabei entstandenen, bereits bekannten Produkte [21]. Über die Strukturaufklärung der bis jetzt als Dillölkomponenten nicht bekannt gewesenen neuen Cumaranderivate berichten wir in einer folgenden Mitteilung.

Untersuchungsergebnisse

Das analytische Gaschromatogramm des untersuchten Dillöles ist in Abb. 1 gezeigt. Weniger flüchtige Komponenten (Sesquiterpene und ihre Derivate) konnten im ätherischen Öl wahrscheinlich wegen der Destillationsreinigung nicht gefunden werden. Die Trennung der ersten zwei Komponenten wurde durch nachträgliche Analyse bei niedrigerer Temperatur vollständiger gestaltet. Aufgrund der Aufnahme ist im ätherischen Öl der Dillpflanze die Anwesenheit von 14 Bestandteilen in einer Menge von über je 0,01 Gew.-% nachzuweisen.

Durch Verwendung der hergestellten reinen Komponenten wurden die Response-Faktoren ebenfalls untersucht. Dabei ließ sich feststellen, daß die Response-Faktoren zwischen 0,9 und 1,1 liegen. Da die quantitative Zusammensetzung der ätherischen Öle von der Vorgeschichte der Proben (Ursprung, Reifegrad, Herstellungs-, Reinigungs- und Behandlungsweise) beträchtlich abhängig ist, war eine genaue quantitative Analyse nicht von Bedeutung. So verzichteten wir auf die Berücksichtigung der Response-Faktoren. Die Angaben über die Mengenverhältnisse sind in Tab. V zu finden.

Über die Methoden zur spektrometrischen Untersuchung und zur Identifizierung der in reinem Zustand gewonnenen oder angereicherten Komponenten wird ein Überblick in Tab. III gegeben. Die charakteristischen gaschromato-

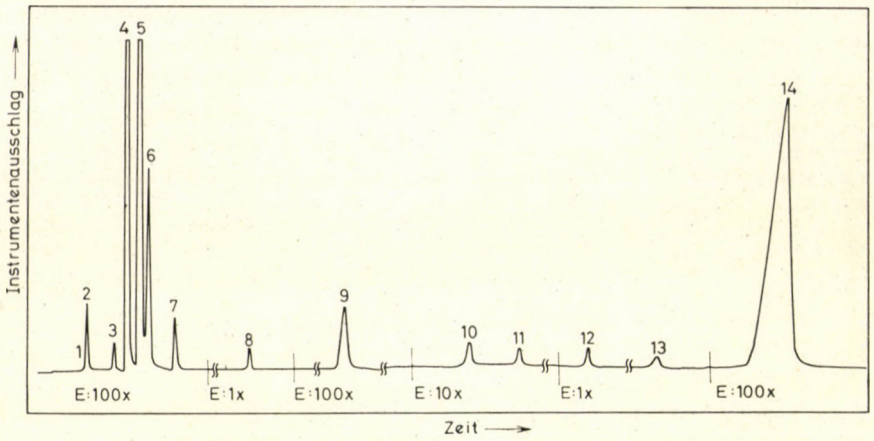

Abb. 1. Gaschromatogramm des untersuchten Dillpflanzenöles

Tabelle III

Untersuchung der aus dem ätherischen Öl gewonnenen reinen Komponenten oder Konzentrate

Komponenten-Nummer im Gaschromatogramm	Reinigung		Spektrumaufnahme			Identifizierung mittels			Spektrumangaben oder Spektren
	Reine Substanz	Angereicherte Substanz	Massenspektrum	Infrarotspektrum	Kernresonanzspektrum	bekannter Spektren [z. B. 23—26]	Spektrumzuordnung	chemischer Methoden	
1.		+		+		+	+		Tab. V
2.	+		+	+	+	+	+		Tab. IV
3.	+		+	+	+	+	+		Tab. IV
4.	+		+	+	+	+	+		Tab. IV
5.	+		+	+	+	+	+		Tab. IV
6.	+			+		+	+		Tab. IV
7.	+		+	+	+	+	+		Tab. IV
8.	+		+	+	+		+		Abb. 2—4, Tab. IV
9.	+		+	+	+		+	+	[21], Tab. IV, in separater Mitteilung
10.	+		+	+	+	+	+		Abb. 5—7, Tab. IV
11.		+	+	+	+		+		Tab. IV
12.	+				+		+		[21], Tab. IV, in separater Mitteilung
13.	+			+	+		+		Abb. 8—9, Tab. IV
14.	+		+	+	+	+	+		Tab. IV

graphischen und spektrometrischen Angaben der getrennten Bestandteile werden in Tab. IV zusammengefaßt. Die Qualität der Bestandteile wurde durch Untersuchung der Retentionsverhältnisse und der für die Struktur kennzeichnenden Spektrenteile verwahrscheinlicht, während ein Beweis für die

Tabelle IV

Gaschromatographische und spektrometrische

Nr. der Komponente	Relative Retention	Massenspektrum Massenzahl		Infrarotspektrum, cm^{-1}						
		Basis-Peak	Molek. Peak	$\nu=C\langle^{H}_{H}$ m	Olef. $\nu=C-H$ m	Arom. $\nu=C-H$ m	$\nu C=O$ st	Olef. $\nu C=C$ m	Arom. $\nu C=C$ m	$\delta-CH_3$ m
1.	81			—	3030	—	—	1650	—	1384
										1366
2.	82	93	136	—	3020	—	—	1660	—	1382
										1365
3.	91	91	136	3100	3016	—	—	1635	—	1382
								1596		
4.	94	119	136	—	3037	—	—	1660	—	1388
								1600		1370
5.	100	68	136	3090	3020	—	—	1645	—	1380
6.	102			3083	3032	—	—	1640		1387
								1597	—	1368
7.	111	119	134	—	—	3105	—	—	1592	1390
						3032			1528	1371
8.	155	117	132	3095	—	3095	—	1633	1572	1380
						3032		1682	1520	
9.	209	91	152	—	3020	—	—	1675	—	1380
10.	275	67	152	3090	—	—	1710	1642	—	1375
11.	291	67	152	3092	—	—	1710	1644	—	1380
12.	332									
13.	388			—	3030	—	1680	—	—	1370
14.	421	82	150	3090	3031	—	1676	—	—	1370

st = hohe Intensität, m = mittlere Intensität

Angaben der getrennten Komponenten

				Kernresonanzspektrum, ppm (δ)							
ν–C(=O)– st	γ=C(H)(H) st	Olef. γ=C–H m	Arom. γ=C–H st	HAr	HC=	H_2C=	HC(–O–)	HC(–)H_2C–	H_3CAr	H_3C–C(=)	H_3C–
—	—	783	—								
—	—	790	—	—	5,10	—	—	1,9— —2,6	—	1,62	0,80 1,29
—	900	825	—	—	5,0— —6,6	5,0— —6,6	—	2,1— —2,2	—	1,66 1,70	
—	—	800 734	—	—	5,42 5,73	—	—	2,06	—	1,70	0,90
—	890	800	—	—	5,43	4,68	—	2,00	—	1,66 1,76	—
—	882	822	—								
—	—	—	822 795	6,88	—	—	—	2,79	2,32	—	1,10
—	895	—	827	7,15 7 25	—	5,00 5,28	—	2,10	2,33	2,10	—
900— 1200	—	840 815	—	—	5,42	—	3,18 3,94 4,14	1,7— —2,2	—	1,65	1,05
—	895	—	—	—	—	4,75	—	1,8— —2,6	—	1,75	1,00
—	900	—	—	—	—	4,80	—	1,9— —2,7	—	1,72	1,00
				6,4— —7,0	—	—	3,98 4,60	2,2— —2,7	2,27	—	1,25
—	—	807	—	—	6,68	—	—	1,7— —2,7	—	1,75	0,95
—	900	806	—	—	6,36	4,78	—	2,1— —2,8	—	1,77	—

Tabelle V

Zusammensetzung des ätherischen Öles der Dillpflanze

Nr. der Komponente	Komponente	Menge, Gew.-%
1.	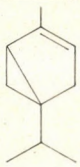 α-Thujen 	0,3
2.	α-Pinen	0,8
3.	 β-Myrcen 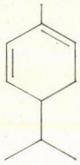	0,7
4.	α-Phellandren	29,0
5.	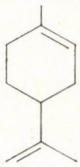 Limonen 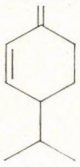	25,0
6.	β-Phellandren	4,2
7.	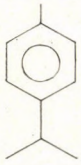 *p*-Cymol 	1,3
8.	1-Methyl-4-isopropenylbenzol	0,0X
9.	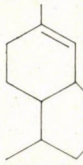 3,7-Dimethyl-4,5,6,7-tetrahydrocumaran 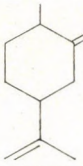	2,9
10.	Dihydrocarvon	0,3
11.	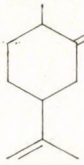 Isodihydrocarvon 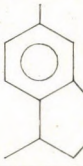	0,2
12.	3,6-Dimethylcumaran	0,0X
13.	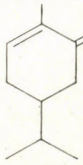 Carvotanaceton 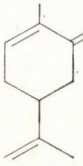	0,0X
14.	Carvon	35,2

Identifizierungsergebnisse durch den Vergleich mit bekannten Spektren von bekannten Bestandteilen oder durch spektrometrische Untersuchung des in ein bekanntes Derivat überführten Bestandteiles erhalten wurde.

Das Molekulargewicht ließ sich aus dem Massenspektrum ermitteln. Aufgrund des Infrarotspektrums orientierten wir uns über die Anwesenheit

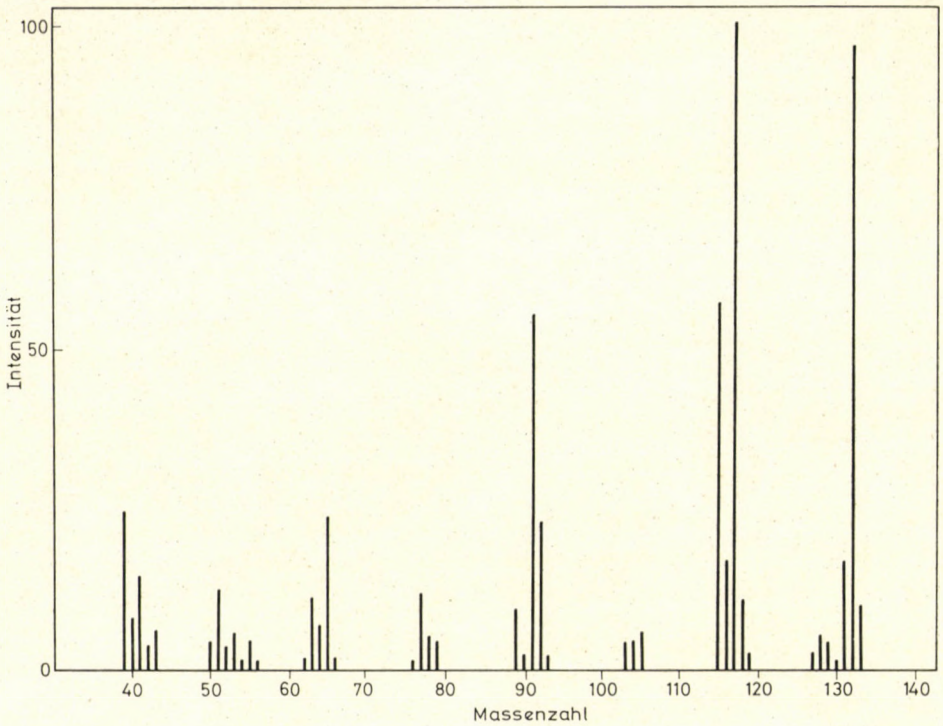

Abb. 2. Massenspektrum des 1-Methyl-4-isopropenylbenzols

oder Abwesenheit von charakteristischen Atomgruppen. Aufgrund dieser Angaben wurde auch entschieden, ob der betreffende Bestandteil eine aromatische, eine olefinische, eine cyklische Äther- oder Keton-Verbindung ist, weiterhin wurde dadurch der Grad und teilweise auch die Stellung der Ungesättigtheit des Kohlenwasserstoff-Teiles bestimmt. Aufgrund des Kernresonanzspektrums in Kenntnis der Peakverschiebung, der Multiplizität und der Mengenverhältnisse verschiedener Protone ließ sich die Bindungsweise der Atomgruppen feststellen und damit die vermutete Struktur bestätigen. Zur Identifizierung der Bestandteile wurde von uns nur die Molekül-Konfiguration ermittelt. Die Identifizierungsergebnisse wurden in Tab. V zusammengefaßt.

Qualitative und quantitative Zusammensetzung des ätherischen Öles

Die qualitative Zusammensetzung des ätherischen Öles der Dillpflanze und die Mengenverhältnisse zwischen den Komponenten sind in Tab. V angegeben. Die in der Fachliteratur nicht angegebenen Spektren der identifizierten reinen Komponenten wurden in Abb. 2—8 angeführt, wobei Abb. 2 ein Massenspektrum, Abb. 3, 5 und 7 Infrarotspektren, während Abb. 4, 6 und 8 magnetische Kernresonanzspektren zeigen. Die Abbildungen 2—4 beziehen sich auf

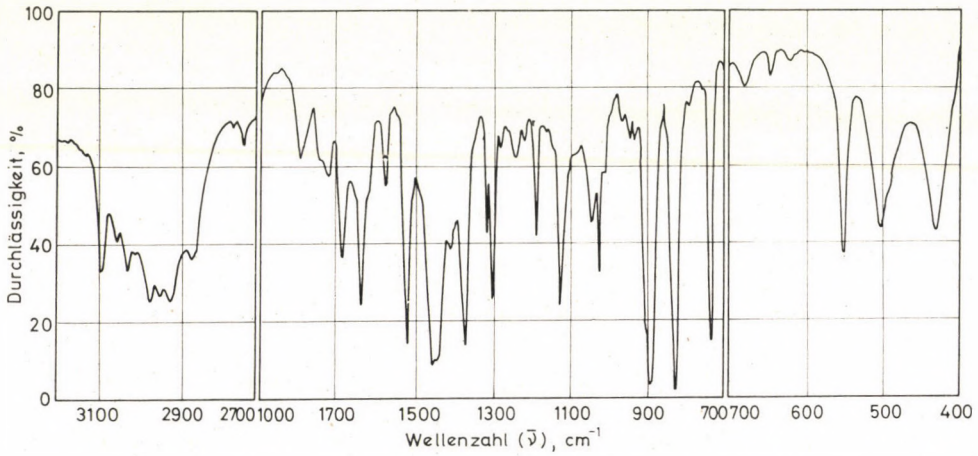

Abb. 3. Infrarotspektrum des 1-Methyl-4-isopropenylbenzols

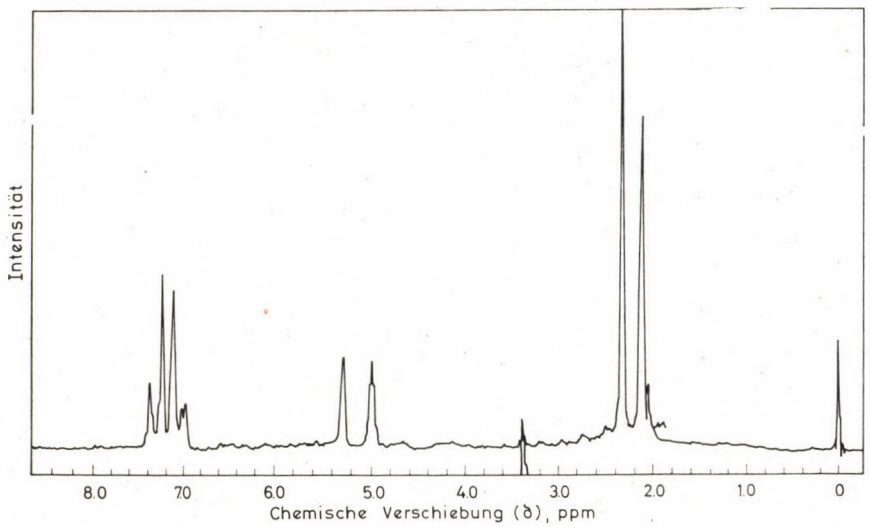

Abb. 4. Kernresonanzspektrum des 1-Methyl-4-isopropenylbenzols

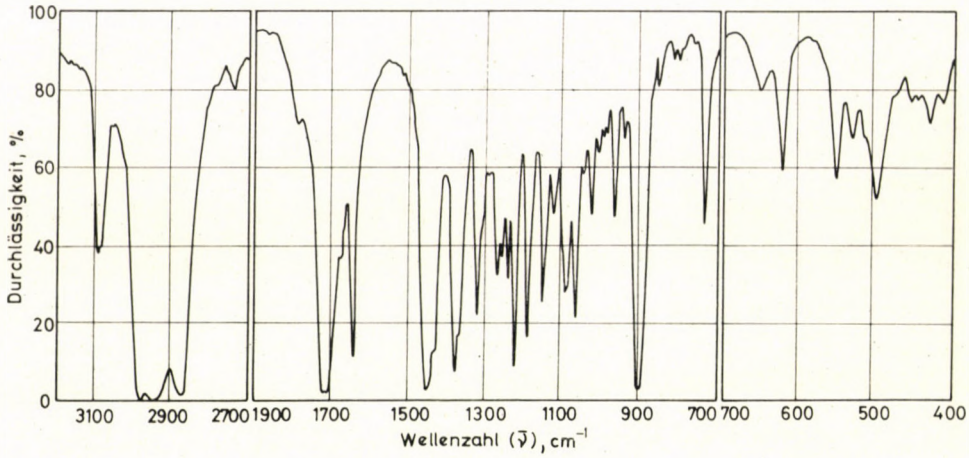

Abb. 5. Infrarotspektrum des Dihydrocarvons

das 1-Methyl-4-isopropenyl-benzol, die Abbildungen 5—6 auf das Dihydrocarvon und die Abbildungen 7 und 8 auf das Carvotanaceton. Die Spektren der bisher unbekannten Cumaranderivate und ihre Strukturermittlung werden in einer folgenden Mitteilung erörtert.

Aus der Tabelle ist festzustellen, daß die drei Hauptkomponenten des ätherischen Öles, entsprechend den Literaturangaben, das α-Phellandren, das Limonen und das Carvon sind. Ihre summarische Menge beträgt ungefähr 90% des Öles. Weitere acht Komponenten vertreten unter den Nebenkomponenten eine Menge von insgesamt ca. 10%. Zuletzt sind drei Bestandteile nur noch in

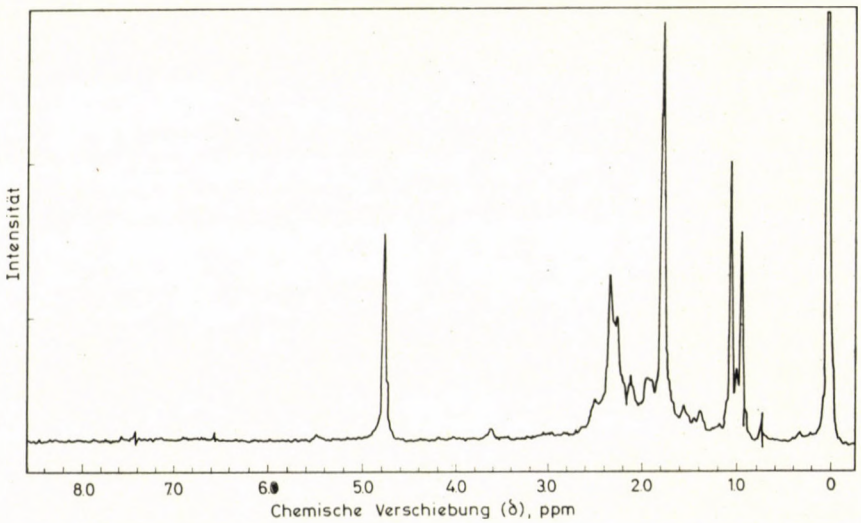

Abb. 6. Kernresonanzspektrum des Dihydrocarvons

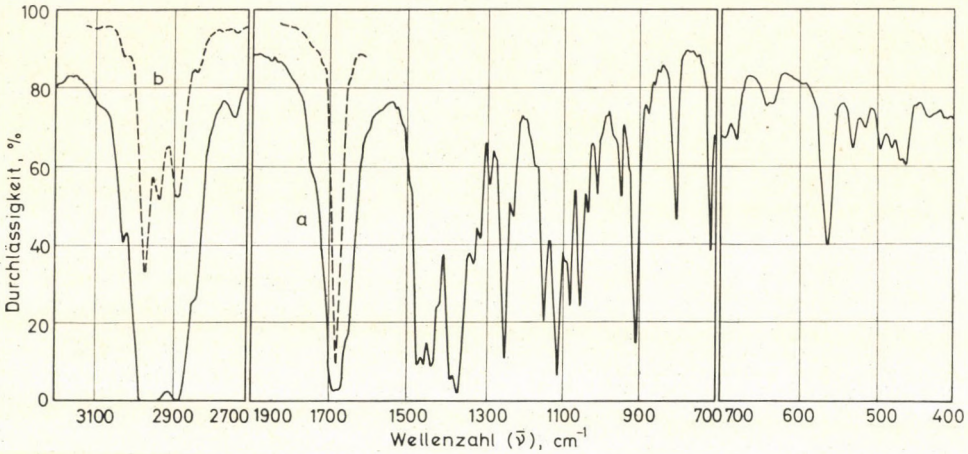

Abb. 7. Infrarotspektrum des Carvotanacetons ohne Lösungsmittel und in CCl_4-Lösung $a \sim 40$ g/l, $b \sim 16$ g/l

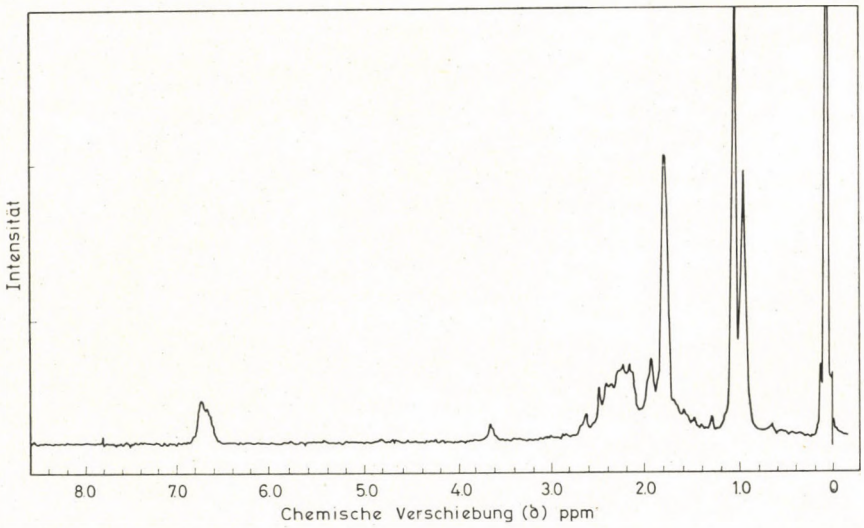

Abb. 8. Kernresonanzspektrum des Carvotanacetons

Spuren anwesend. Von den in der Fachliteratur als Dillölkomponenten beschriebenen Verbindungen waren zwar im ätherischen Öl der einheimischen Dillpflanze das α-Pinen, das Dihydrocarvon und das *p*-Cymol nachzuweisen, während zahlreiche vermutete Komponenten, so verschiedene Terpene, Terpenderivate — u. a. das Dillapiol —, ferner verschiedene nichtterpenische Verbindungen, beweisbar keine Bestandteile des ätherischen Öles der Dillpflanze sind. Von den in anderen ätherischen Ölen bekannten Bestandteilen wurde die Anwesenheit von α-Thujen, β-Myrcen, β-Phellandren, 1-Methyl-4-iso-

propenylbenzol und Carvotanaceton nachgewiesen. Für die gefundenen Cumaranderivate wurden in der Fachliteratur keine Angaben angetroffen. Diese Verbindungsgruppe war bisher zu den ätherischen Ölkomponenten nicht hinzugerechnet. Durch die strukturelle Verwandschaft beider Cumaranderivate miteinander, sowie mit dem 1-Methyl-4-isopropenylbenzol und dem *p*-Cymol, ferner durch die festgestellte Änderung ihrer Menge abhängig vom Reifegrad der Dillpflanze wird die pflanzenphysiologische Bedeutung dieser Komponenten unterstrichen.

LITERATUR

[1] Szujko-Lacza, J.: Acta Botanica, **17,** 189 (1971)
[2] Guenther, R.: The Essential Oils. Volume IV. Norstrand Co, New York, 1949
[3] Gildemeister, E., Hoffman, F.: Die ätherischen Öle. Band VI. Akademie Verlag, Berlin, 1961
[4] Tyihák, E.: Teil in der Abhandlung »Kulturflora von Ungarn. Band IV, Heft 10. Das Dillkraut.« Akademischer Verlag. Budapest, 1970
[5] Sethi, S., Nigam, M. C., Ra, R. R.: Indian Perfumer, **9,** (1) 17 (1965)
[6] Gulati, B. C., Duhan, S. P. S., Bhattacharya, A. K.: Perfum. Essent. Oil. Rec., **60,** 277 (1969)
[7] Gupta, G. L., Nigam, S. S., Sastry, S. D., Chakravarti, K. K.: Perfum. Essent. Oil. Rec., **60,** 329 (1969)
[8] Misra, K. P., Nigam, S. S.: Riechst., Aromen, Körperpflegen, **19,** 185 (1969)
[9] Wallach, O.: Liebigs Ann. Chem. **227,** 292 (1885)
[10] Branigan, C.: Amer. Perfumer, **48,** (2) 69 (1946)
[11] Schimmel et Co.: Ber. Schimmel (1898) 20
[12] Schimmel et Co.: Ber. Schimmel (1908) 38
[13] Gladstone, J. H.: J. Chem. Soc. (London), **25,** 1 (1872)
[14] Schmidt, H.: Ber. Schimmel (1954) 126
[15] Schimmel et Co.: Ber. Schimmel (1910) 36
[16] Schimmel et Co.: Ber. Schimmel (1927) 25
[17] Chakravarty, K. K., Bhattacharya, S. C.: Indian Pharmacist, **9,** 218 (1954)
[18] Malaviya, B. K., Dut, S.: Proc. Indian Akad. Sci. Sect., **A12,** 251 (1940)
[19] Bélafi-Réthy, K., Iglewski, St., Kerényi, E., Kolta, R.: Acta Chim. (Budapest) **76,** 1 (1973)
[20] Bélafi-Réthy, K., Iglewski, St., Kerényi, E., Kolta, R.: Acta Chim. (Budapest) **76,** 167 (1973)
[21] Bélafi-Réthy, K.: Dissertation, Universität für Chemische Industrie, Veszprém, 1973
[22] Iglewski, St., Fábián-Nagy, É., Szepesváry, P.: MÁFKI Kiadv., **318** (1968)
[23] Mitzner, B. M., Theimer, E. T., Freeman, S. K.: Appl. Spectroscopy, **19,** 169 (1965)
[24] Bellamoto, J., Hidalgo, A.: Infrared Analysis of Essential Oils. Heyden, Son Ltd., London, New-York, 1971
[25] Sato, T., Tsuchiya, T., Wasada, N.: J. Org. Chem. **33,** 1249 (1968)
[26] Grim, W., Kolbe, A.: Spectrochim. Acta, Part A, **24,** 1697 (1968)

Katalin Bélafi-Réthy
Ervin Kerényi
Rezső Kolta

8201 Veszprém 1. Wartha V. u. 1—3. Ungarn.

Acta Chimica Academiae Scientiarum Hungaricae, Tomus 83 (1), pp. 15—24 (1974)

ULTRAVIOLET SPECTROSCOPIC STUDY OF THE MOLECULAR STRUCTURE OF 4H-PYRIDO [1,2-a] PYRIMIDIN-4-ONE DERIVATIVES

G. HORVÁTH, Á. I. KISS,* Z. MÉSZÁROS and I. HERMECZ

*(CHINOIN Pharmaceutical and Chemical Works, Ltd., * Department of Physical Chemistry, Technical University, Budapest)*

Received March 19, 1973

The electronic spectra of 4H-pyrido[1,2-a]pyrimidin-4-one derivatives were recorded. On the basis of the substituent effect on the spectra the molecular structure and especially the conjugation in the unsaturated and partially saturated molecules were investigated. It has been established that nitrogen in position 1 is protonated in acidic media. The ionization constants of the protonation were calculated from the pH dependence of the spectra.

Several 4H-pyrido [1,2-a] pyrimidin-4-one derivatives were synthetized in the past years[1].These compounds exhibit significant biological activity [2], however, our knowledge on their spectra is rather vague. The ultraviolet spectra of 4H-pyrido [1,2-a] pyrimidin-4-one and some of its simple derivatives were published by ADAMS and PACHTER [3]. ANTAKI reported [4] the spectra of 3-monosubstituted and 3,6-, 3,8- and 3,9-disubstituted derivatives. Recently URBAN *et al.* [5] have published the spectra of polysubstituted 2-oxy-(alkoxy)-pyrido [1,2-a] pyrimidin-4-one derivatives in ethanol solution. The authors have concluded that the spectra considerably differ from each other, depending on the fact whether nitrogen in position 1 has a positive charge, or is neutral. The literature data indicate that the position of the substitution has a great influence on the spectra.

Systematic investigations have been carried out in order to reveal what informations can be gained on the molecular structures from the ultraviolet, infrared, nmr and mass spectra. The effect of both the solvent and ionization on the ultraviolet spectra were also studied. From the spectra measured at different pH the ionization constants were evaluated.

Investigation of the unsaturated derivatives

The spectrum of the basic compound (**I**) consists of two distinct bands at 336 nm and 239 nm

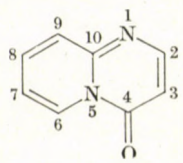

The high intensities of the bands indicate that these can be assigned to $\pi \rightarrow \pi^*$ transitions of charge transfer character.

The spectral data of some characteristic derivatives dissolved in ethanol are compiled in Table I. The spectra of 2-donor(methyl, chloro)-substituted derivatives are similar to that of the basic compound. Both bands are slightly red-shifted due to the effect of the donor substituent. The same holds for donor groups in position 3. It is evident from the spectra of the donor-substituted derivatives that the 7-, 8- and 9-donor groups exert also slight effect. The donor groups in positions 2 and 3 have nearly the same effect as in position 8, however, the 7- and 9-donor substituents exert a somewhat greater effect.

The greatest change (red shift) in the spectra is caused by donor groups in position 6. The greatest shift can be observed with the first band. A new band (*e. g.*, 2,6-di-donor derivative) appears at the place of the weak inflexion at around 320 nm, thus the spectrum consists of three $\pi \rightarrow \pi^*$ bands.

The red shift is caused by the conjugated system characteristic of structure A, which can be formed only in the presence of a donor group in

Table I

Spectroscopic data of 4H-pyrido[1,2-a]pyrimidin-4-one (I) derivatives in ethanol

	Compound	λ_{max}	logε	λ_{max}	logε	λ_{max}	logε	Ref.
I	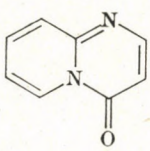	336	4.02	—	—	239	3.67	
II	2-methyl-	336	4.0	—	—	245	4.0	[3]
III	2-chloro-	343	4.00	(315)	—	256	3.89	
IV	2-methyl-7-bromo-	340	4.0	—	—	256	4.0	[3]
V	2,6-dimethyl-	358	3.89	323	3.75	250.5	3.95	
VI	2-chloro-6-methyl-	360	3.99	319	3.75	260.5	3.95	
				308	3.74	253	3.98	
VII	3-cyano-	365	4.2	315	3.7	250	3.9	[4]
VIII	3-acetyl-	360	4.3	310	3.7	255	4.0	[4]
IX	3-carbethoxy-	362	4.18	314	3.62	252	3.92	
				304	3.60			
X	3-carbethoxy-9-methyl-	370	4.24	311	3.68	259	3.91	
				300	3.69			
XI	3-carbethoxy-8-methyl-	364	4.28	312	3.64	252	3.88	
						245	3.90	
XII	3-carbethoxy-7-methyl-	371	4.23	310	3.61	260	4.06	
				302	3.61			
XIII	3-carbethoxy-6-methyl-	389	4.24	316	3.68	258	4.07	
				306	3.73			
XIII	in 0.1 *N* HCl	354	4.15	301	3.86	252	3.90	
XIV	3-carbethoxy-1,6-dimethyl-	354	4.07	310	3.99	250	3.92	
XIV	in 0.1 *N* HCl	353	4.05	310	3.99	251	3.91	

The wave length values in parantheses refer to an inflexion.

position 6. Position 6 is the point of the molecule wherein a donor group has the largest effect and which is found farthest from the acceptor (carbonyl) group in position 4.

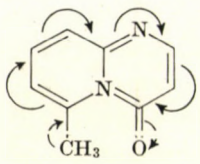

A

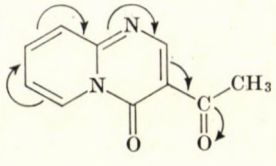

B

An acceptor (acetyl, carbethoxy, etc.) group in position 3 affects the spectrum to the same extent, as a donor group does in position 6. The spectra consist of three bands similar to that of 6—donor-derivatives. Position 3 is most favourable for an acceptor substitution, and structure B is formed.

This consideration is supported by the spectrum of compound **XIII** (Fig. 2), where the shift of the first band is approximately twice of that observed with the 6-methyl- and 3-carbethoxy-derivative, respectively. The spectra of the corresponding 7-, 8- and 9-methyl derivatives (**X**—**XII**) all have shorter wave length bands. The large shift in the spectra of **XIII** is due to the fact that a donor group and an acceptor group are in the most favourable position to form a conjugated system.

Based on the study of the substitution effect, it is probable that the first $\pi \rightarrow \pi^*$ band (above 350 nm) belongs to the excitation of the bicyclic conjugated system. This band is the most sensitive to changes in the conjugated system. The band near 320 nm can be assigned to the pyrimidinone ring, owing to its relatively constant position, and corresponds to a more localized excitation. The simple derivatives of mono- and diazines have characteristic bands in this region [6]. The band near 250 nm is a conjugation band of charge transfer character.

Pariser-Parr-Pople type calculations were carried out for **I** and some of its substituted derivatives on several models differing in the extent of the delocalization of the ring conjugated system and in the substituent effect of the methyl group, respectively [7]. The results of the calculations support the presence of a mobile π-electron system.

Solvent effect

The band assignment was proved by the study of the solvent effect. As an example the spectral data of **III** together with the dipole moment of the solvents are given in Table II. The red shifts of all the three bands increased with an increase in the dipole moment (μ) of the solvent, this refers to the $\pi \rightarrow \pi^*$ character of the bands.

Table II

The spectra of XIII in different solvents

Solvent	λ_{max}(nm)				$\mu(D)$
Chloroform	367	308	300	248	1.10
Water	381	312	302	255	1.82
Ethanol	389	316	306	258	1.73
Dimethylformamide	393	320	310	262	3.85

In ethanol a relatively large red shift was observable, this also occurred in the case of analogous compounds, *e. g.* 2-substituted-pyrimidines [6].

Effect of ionization

The pH-dependence of the spectra of some derivatives was investigated too. The spectra of **XIII** taken at different pH are shown in Fig. 1. The changes in the spectra refer definitely to the existence of an equilibrium. The spectra in alkaline and neutral media are identical with the spectrum in ethanol solution, which indicates the presence of the neutral form of the molecule. If the oxygen were ionized (enolic form), the molecule would have a different structure in neutral (C) and in alkaline medium (D), repectively, which would be in contradiction with the identity of the spectra.

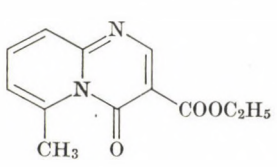

C

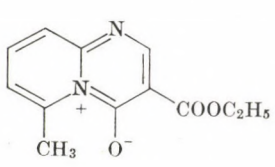

D

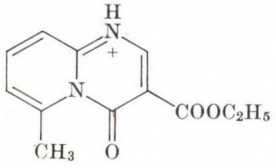

E

In acidic medium blue shift is observed (Table I). The spectrum of **XIV** in which the 1-nitrogen is methylated is identical in neutral and acidic media. The spectrum of **XIII** in acidic medium is the same as that of **XIV** which undoubtedly proves the protonation of nitrogen in position 1 (structure E). This spectral change is characteristic of the protonation of nitrogen in mono- and bicyclic azines.

The changes in the spectra as a function of the pH confirm that the proton is bound to nitrogen in position 1, in case of all the studied derivatives.

It is worth mentioning that both the studied bases and their salts with hydrochloric acid give identical spectra and their pH-dependence is the same, as well. It can be concluded from this fact that bases and salts possess the same structure in solution.

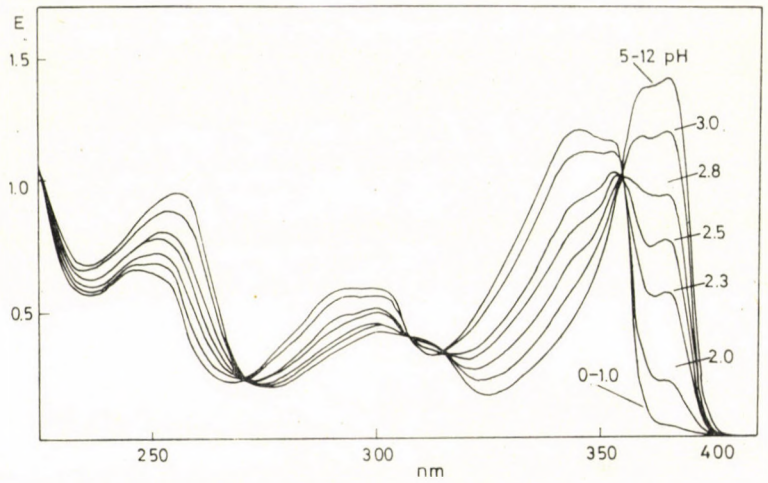

Fig. 1. The PH dependence of spectra of XIII

Equilibrium constant and basicity of the compounds

On the basis of the pH-dependence of the spectra, the equilibrium constant of the protonation of nitrogen in position 1 was calculated in order to obtain information on the basicity of the studied compounds. The values of the equilibrium constants (pK_a) are given in Table III. It is apparent that the

Table III

Ionization constants of I derivatives

	Compound	pK_a
I	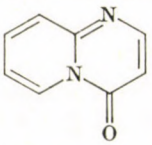	3.26
IX	3-carbethoxy-	1.80
X	3-carbethoxy-9-methyl-	1.70
XI	3-carbethoxy-8-methyl-	2.28
XII	3-carbethoxy-7-methyl-	2.20
XIII	3-carbethoxy-6-methyl-	2.40

basicity is reduced due to the acceptor effect of the 3-carbethoxy group. The 6-methyl group increases the basicity considerably, which refers this group being a strong donor.

Investigation of tetrahydro-derivatives

Ultraviolet spectroscopy was applied to reveal the structure of the 6,7,8,9-tetrahydro derivatives. The following two structures might form:

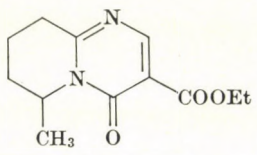

F

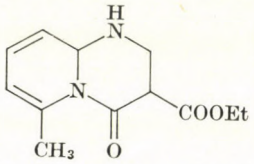

G

In order to solve the problem, the effect of substitution on the spectra of the tetrahydro derivatives as well as the pH-dependence of the spectra were investigated.

Effect of substitution

The spectroscopic data of the compounds investigated in ethanol are collected in Table IV. It is apparent from the table that the spectra consist of two well-separated bands which can be related to $\pi \rightarrow \pi^*$ transitions in the conjugated system. A comparison of the spectra of compounds **XV** and **XVIII,** shows that the carbethoxy group produces a large (25 nm) red shift of the first band. The same shift can be observed with the first band of 4H-pyrido [1,2-a] pyrimidin-4-one, due to the effect of the ester group. Such change is

Table IV

Spectra of 6,7,8,9-tetrahydro-4H-pyrido[1,2-a]pyrimidin-4-one derivatives

Compound		λ_{max}	logε	λ_{max}	logε
XV	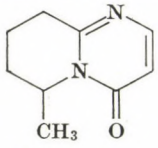	278	3.68	226	3.78
XVI	2,6-dimethyl-	276	3.60	228	3.72
XVII	3-carbethoxy-	301	3.96	230	3.80
XVIII	3-carbethoxy-6-methyl-	303	3.92	230	3.81

possible only if the substitution takes place in a π-electron system, it is impossible, however, with substitutions in a saturated ring. This proves the saturation of the pyridine ring. The spectral effect of substitution in the pyridine ring was also studied. The 6-methyl group does not cause changes in the spectrum, as it is seen from the comparison of the spectra of compounds **XVII** and **XVIII,** If the pyridine ring were unsaturated a significant change would be obtained similarly to that observed with the **I** derivatives.

Effect of ionization

The pH-dependence of compounds **XV, XVII** and **XVIII** showed identical behaviour. The spectral data of both the ionized and non-ionized forms are given in Table V. The spectra in alkaline solution and in water are identical in

Table V

Spectral data of the ionized and non-ionized forms of compounds XV, XVII, XVIII

Compound	pH	λ_{max}	pH	λ_{max}
XV	7—11	275	1—2	258
XVII	4—12	297	0	278
XVIII	4—11	300	0	280

all the three cases with the spectrum obtained in a neutral polar solvent. Due to the effect of acids, the first band gradually disappears and a new band develops at a wave length appr. 20 nm shorter than that of the original band. A definite isosbestic point can be seen between the two bands.

The changes in spectra as a function of pH are very similar to those observed with **XIII.** A definite blue shift can be observed in both cases. Thus it is probable that also in the case of compound **XVIII** the proton is bound to nitrogen in position 1.

The binding of proton to nitrogen in position 1 can follow the same mechanism in the cases of both unsaturated and tetrahydro derivatives, provided that the pyrimidine ring has the same structure in both cases, *i.e.*, the pyridine ring of compounds **XV—XVIII** is saturated.

The investigation on both the effects of substitution and ionization confirm the existence of structure F.

Bases **XV—XVIII** and their salts with hydrochloric acid show the same spectra in solution, and their pH dependence is also identical. Thus the bases and salts have the same structure in solution.

Equilibrium constants

On the basis of the pH-dependence of spectra, the equilibrium constant of the protonation of nitrogen in position 1 was calculated in order to obtain information on the basicity of these compounds. The values of the equilibrium constants (pK_a) are the following: **XVII** 1.76 and **XVIII** 1.07. The basicity of the compounds is less than that of the corresponding unsaturated compounds (**IX** and **XIII**). This may be interpreted in the following way. It can be expected by analogy (methylamines) that the basicity of nitrogen in position 5 is higher in the tetrahydro-derivatives. An electron migration from the carbonyl group, through the pyrimidine ring, towards nitrogen in position 5 can be presumed, and this reduces the basicity of nitrogen in position 1.

Hexahydro-derivatives

The results of the investigations with hexahydro-derivatives are explained on compound **XIX**:

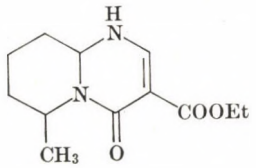

H

The spectrum of compound **XIX** consists of two bands (Fig. 2) (at 306 nm and 232 nm) in ethanol. The band at 306 nm can be related to the $\pi \rightarrow \pi^*$ transition of the alkylamine-ethylene-carbonyl conjugated system. The position of the band indicates a mobile π-electron system. The $\pi \rightarrow \pi^*$ character of the band is supported by the solvent effect too.

The red shift observed in polar solvents and concentrated acids excludes the existence of $n \rightarrow \pi^*$ bands. The two carbonyl groups are present in the form of carboxylic acid amide and ethyl ester, respectively, whose bands appear at about 250 nm.

The band at around 230 nm corresponds to the second $\pi \rightarrow \pi^*$ transition. This band is found in a position corresponding to α, β-unsaturated carbon compounds.

Ionization effect

The spectra of compound XIX were taken at different pH. The spectrum does not change between pH 1 and 13 and is identical with that in a neutral aqueous solution. This spectrum corresponds to the neutral structure of com-

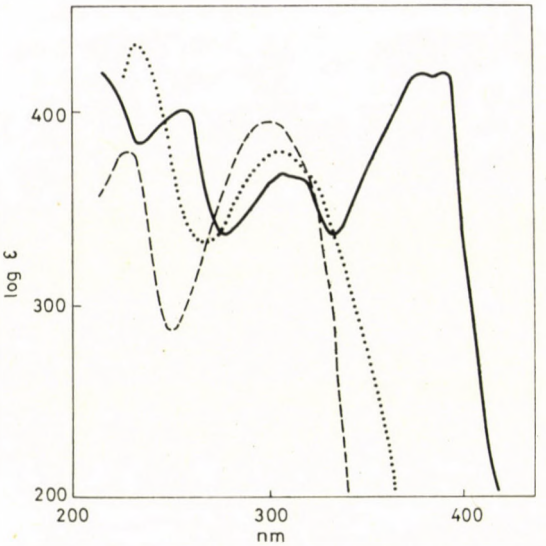

Fig. 2. Spectra of XIII ——, XVIII – – – –, and XIX · · · · in ethanol

Table VI

Effect of ionization on the spectrum of compound XIX

Solvent	λ_{max}(nm)	
1 *N* NaOH	(300)	265
pH = 1 to 13	308	236
2 *N* HCl	323	240

pound **XIX.** A red shift can be observed in a concentrated acid (2*N* HCl) due to the protonation of nitrogen in position 1, and the compound is transformed into cation form H. The observed change in the spectrum is in agreement with the experience [6].

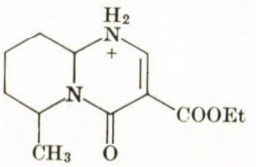

I

A great change is observed in the spectrum in alkaline solutions and this refers to a second equilibrium. An approximately 20 nm red shift of the second band indicates the existence of the enol (anion) form. The following equilibrium

is set up:

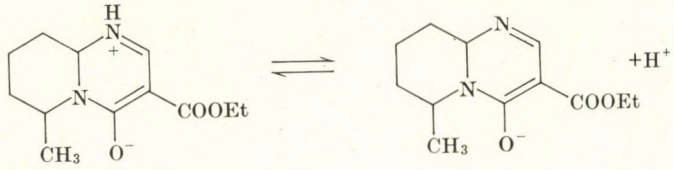

J K

The anion is formed by the loss of a proton.

REFERENCES

[1] MÉSZÁROS, Z., KNOLL, J., SZENTMIKLÓSI, P., DÁVID, Á., HORVÁTH, G., HERMECZ, I.: Arzneimittel-Forschung **22,** 815 (1972)
[2] KNOLL, J., MÉSZÁROS, Z., SZENTMIKLÓSI, P., FÜRST, S.: Arzneimittel-Forschung, **21,** 717 (1971)
[3] ADAMS, R., PACHTER, I. J.: J. Am. Chem. Soc. **74,** 5491 (1952)
[4] ANTAKI, H.: J. Am. Chem. Soc. **80,** 3066 (1958)
[5] URBAN, R., GROSJEAN, M. ARNOLD, W.: Helv. Chim. Acta **53,** 905 (1970)
[6] MASON, S. F.; J. Chem. Soc. 219 (1960)
[7] DUDAR, E., KISS, Á. I., HORVÁTH, G.: Acta Chim. (Budapest) **78,** 253 (1973)

Gábor HORVÁTH
Zoltán MÉSZÁROS
István HERMECZ
1045 Budapest, Tó u. 1—5.

Árpád István KISS
1111 Budapest, Budafoki út 8. Hungary.

Acta Chimica Academiae Scientiarum Hungaricae, Tomus 83 (1), pp. 25—35 (1974)

ENTROPY EFFICIENCY OF DISTILLATION WITH CONVENTIONAL AND 'STEPWISE HEAT TURNOVER'

Zs. Fonyó and P. Földes

(Department of Chemical Unit Operations, Technical University, Budapest)

Received May 8, 1973

The concept of net entropy efficiency of a separation process is introduced and defined: its variations are shown in conventional distillations and in distillations with stepwise heat turnover, for various operating characteristics. Results of these studies are in agreement with values in the literature, obtained from measurements in commercial plant. Approximate operating costs of distillations with stepwise heat turnover carried out with heating media at various levels of temperature can be calculated from the entropy production directly.

Introduction

The concept of entropy efficiency defined in the thermodynamic theory of stationary processes [1,2,3,4] can be utilized for a comparison of sources and consumers of entropy. Distillation may be uniformly understood as a stationary system of the first degree [5]. The analysis of distillation with stepwise heat turnover [6] has been extended to the computation of entropy production and this has made possible the study of the so-called net entropy efficiency.

Strength of thermodynamic coupling of various processes [4]

The common cross-effects are weakly coupled. Characteristic examples of cross-effects are thermodiffusion or the diffusional thermo effect where the value of the coupling factor is by several orders of magnitude less than unity. In commercial processes these effects are utilized only if no other method is available or when energetic factors can be left out of consideration.

In two-phase systems, larger coupling factors may be expected. Characteristically, the thermodynamic coupling of the so-called Lykow-effect (mechanical-chemical cross-effect) is of medium strength because the thermodiffusional factor increased by the partial enthalpies will produce a factor of rather high value. The entropy efficiencies for couplings of medium strength are within the range

$$0.1 > \eta_s > 0.01.$$

In such cases the entropy consumption is not yet comparable with the entropy production, thus these are of no importance in common chemical unit operations.

However, the mass transfer operations of chemical industry are strongly coupled, *viz.*: $\eta_s > 0.1$.

No quantitative analysis of the entropy efficiency of various mass transfer operations has been performed, though on its basis a characterization of the various operational units would be possible. In this paper an analysis will be given of the entropy efficiencies of distillations with special reference to those with stepwise heat turnover.

Coupling of transport processes in distillations

The entropy produced by the heat transport in the column is used up by the entropy-consuming process of the separation of the components. In this case coupling is an efficiency-like connection between the production and consumption of entropy:

$$\eta_s = p^2 = \frac{|\Phi_1|}{|\Phi_2|} . \tag{1}$$

In distillation, the net entropy change due to the transport of components is the useful consumption of entropy, *i.e.*

$$\Delta S_1 = R \, \Sigma_t \, A_t \, \Sigma_i \, x_{it} \ln x_{it} . \tag{2}$$

In the course of adiabatic distillation, the entropy produced in the steady state by a heat flow kept constant through external constraint is

$$\Delta S_2 = \frac{I_Q}{T_D} - \frac{I_Q}{T_B} = \left(\frac{T_B - T_D}{T_D \, T_B} \right) I_Q \tag{3}$$

or, if a constant molar overflow is supposed:

$$\Delta S_2 = \frac{(R+1) \, D + (q-1) \, F \; T_D \lambda - (R+1) \, D \lambda \, T_B}{T_D \, T_B} . \tag{4}$$

Besides entropy production by heat transport, other entropy producing processes also occur during rectification [7] (finite temperature differences in the heat exchangers, pressure drop in the column and heat exchangers, compression losses, loss of heat, etc.).

Insofar as the basis of reference is the total entropy production, one obtains the so-called 'standard thermodynamic efficiency'.* In this paper, however, we select, on practical considerations, the entropy production by heat transport in the column as a basis of reference, and the ratio thus obtained is referred to as the net entropy efficiency, η_s^n, of the separation process.

Analysis of the net entropy efficiency of distillation with stepwise heat turnover

In the course of stepwise heat turnover the total entropy production of heat transport decreases. Generally, for a cascade the entropy production is given as

$$\Delta S_2 = \int_{j=1}^{j=N} \frac{d\,Q_{j-j'}}{T_j T_{j'}} (T_j - T_{j'}) = \lambda \int_0^{V_{\max}} \frac{T_j - T_{j'}}{T_j T_{j'}}\, dV. \tag{5}$$

Clearly, in the case of a number of discrete heat turnover steps this entropy integral can be replaced by summation:

$$\Delta S_2 \sum_{j=1}^{N} \frac{\Delta Q_j}{T_j} = \sum_{j=1}^{N} \lambda_j \frac{\Delta V_j}{T_j}. \tag{6}$$

The scope of the analysis of stepwise heat turnover and of the variables involved have been discussed in some detail in a previous communication [6]. The entropy analysis has been carried out in the same range. The program has been written in PL-1 language for an IMB 360/40 computer. In the case of identical section numbers, the variant with the better entropy efficiency was regarded as the basis.

In Fig. 1 the variation of the net entropy efficiency for various values of α is presented as a function of the number of sections in stepwise heat turnover. The relative volatility does not significantly affect the shape of the η_s^n curves: also the shift is small.

Figure 2 shows changes caused by the variation of feed concentration. In conventional distillations with symmetric separation required, the entropy efficiency is maximal at medium feed mole fractions $x_F = 0.4 - 0.5$, and minimal at lower or higher feed mole fractions $x_F \cong 0.2$ and $x_F \cong 0.8$. In a thermodynamic sense, the application of stepwise heat turnover is most advantageous at low and at high feed concentrations. For example, if $x_F = 0.2$

* Since efficiency is computed not in energy but in entropy representation, 'standard' values will be obtained.

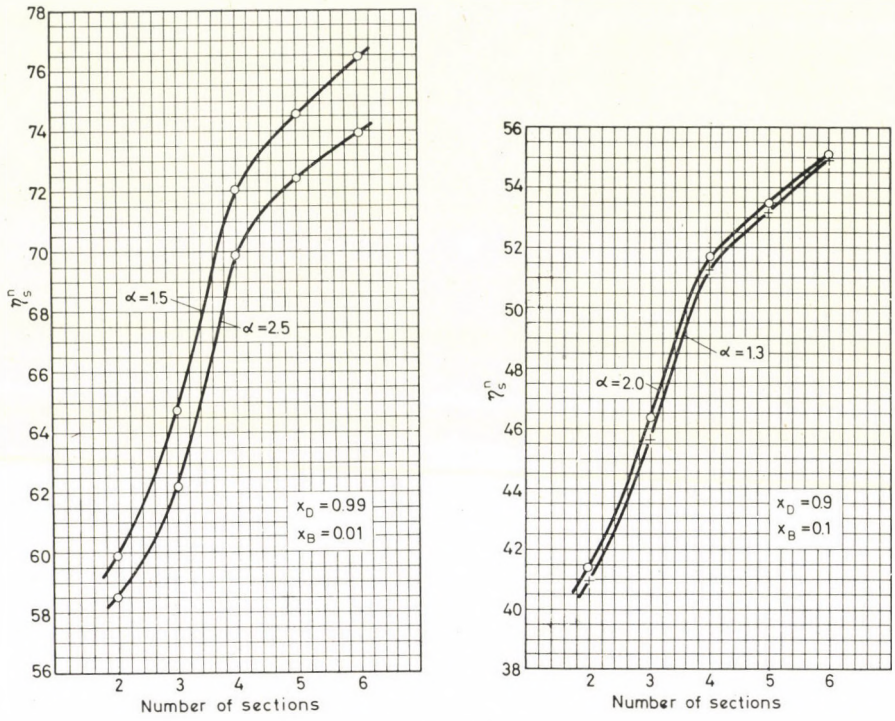

Fig. 1

or $x_F = 0.8$, two intermediate condensers, or two intermediate re-boilers improve the entropy efficiency by about 24%, (47% → 71%; 39% → 63%). This effect agrees well with the results of economic optimization, according to which interposed sectional heat turnover is economically better in 'long column sections' [6]. It can be seen that the interposing of sections 5 and 6 does not substantially alter the value of net entropy efficiency any more.

The 'flattening' of the net entropy efficiency curves at sections 5 and 6 can be observed also in Fig. 3 where the effect of the variation of product concentration is shown. At higher product concentrations the net entropy efficiency increases, *viz.* the entropy consumption of the separation process in the numerator of the efficiency term increases while entropy production by the other process (heat transport) does not change.

Figure 4 shows the effect of variations in the ratio $\Theta = \dfrac{R}{R_{\min}}$. When Θ is low, η_s is high; the entropy consumption needed for a prescribed separation can be reached with a smaller entropy production when Θ is high; the absolute magnitude of heat transport is directly proportional to Θ. Also this is in agreement with the picture presented by indices of process economics.

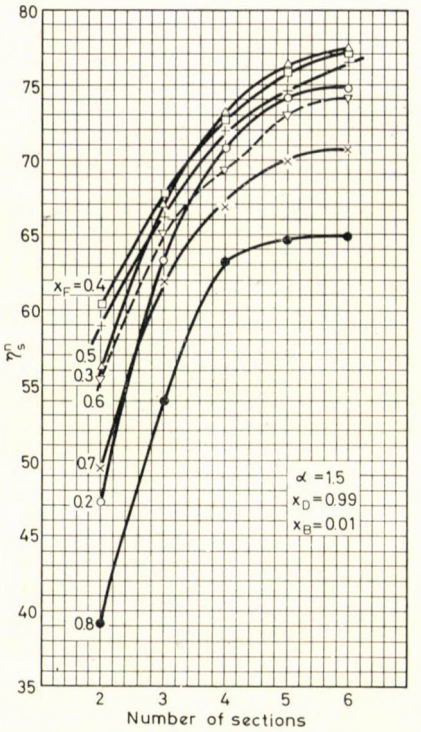
80
75
70
65
60
55
50
45
40
35
η_s^n
$x_F = 0.4$
0.5
0.3
0.6
0.7
0.2
0.8
$\alpha = 1.5$
$x_D = 0.99$
$x_B = 0.01$
2
3
4
5
6
Number of sections

Fig. 2

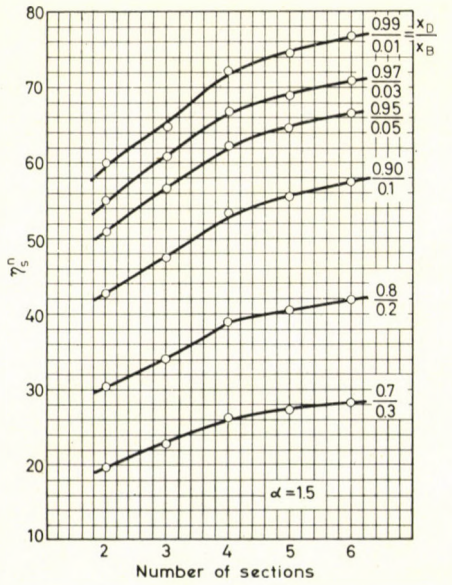
80
70
60
50
40
30
20
10
η_s^n
0.99/0.01 = x_D/x_B
0.97/0.03
0.95/0.05
0.90/0.1
0.8/0.2
0.7/0.3
$\alpha = 1.5$
2
3
4
5
6
Number of sections

Fig. 3

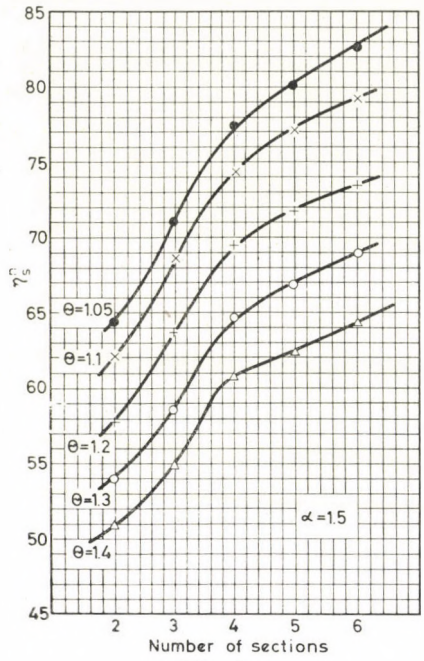
85
80
75
70
65
60
55
50
45
η_s^n
Θ=1.05
Θ=1.1
Θ=1.2
Θ=1.3
Θ=1.4
α=1.5
2
3
4
5
6
Number of sections

Fig. 4

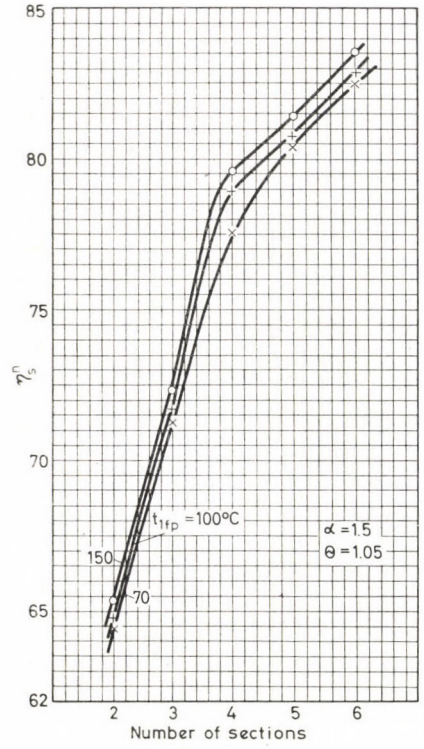
85
80
75
70
65
62
η_s^n
t_{1fp} =100°C
150
70
α =1.5
Θ =1.05
2
3
4
5
6
Number of sections

Fig. 5

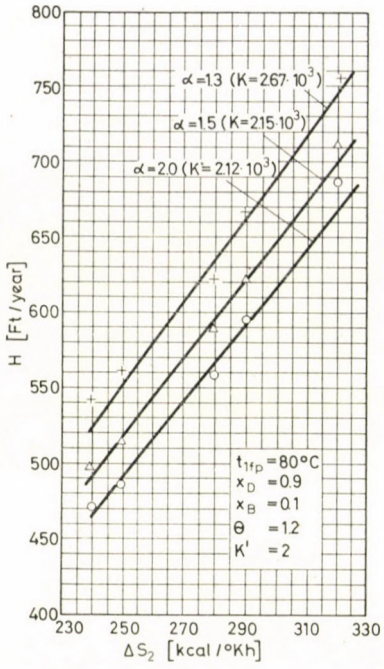

Fig. 6

When the relative volatilities and Θ values are identical, the increase of t_{1fp} values slightly improves the entropy efficiency, however, the change is small (Fig. 5).

These Figures give an adequate picture of how the stepwise heat turnover increases the entropy efficiency.

It should be noted that the net entropy efficiency of the separation process is not affected by the capacity of the distillation apparatus or by constructional or cost parameters.

Estimation of operational costs from entropy production

In the course of computer analysis [6], we have compared the operational cost of distillation apparatuses operated with heating media at various temperature levels, with the calculated entropy production (variant 1, Ref. [6]). In about 200 cases, at fixed operational, constructional and cost parameters (at K = const.) the correlation between operating costs and entropy production, having the form

$$H = K\Delta S_2 \tag{7}$$

Table I

Basis capacity 180 kmol/hr	Case 1			Case 2			Case 3			Case 4		
	$\alpha = 2.5$ $x_F = 0.5$ $x_B = 0.01$ $x_D = 0.99$			$\alpha = 1.5$ $x_F = 0.5$ $x_B = 0.01$ $x_D = 0.99$			$\alpha = 1.5$ $x_F = 0.8$ $x_B = 0.01$ $x_D = 0.99$			$\alpha = 1.5$ $x_F = 0.5$ $x_B = 0.3$ $x_D = 0.7$		
	Δs kcal/h K	η_s^n(%)	η_{therm}^{st}(%)	Δs kcal/h K	η_s^n(%)	η_{therm}^{st}(%)	Δs kcal/h K	η_s^n(%)	η_{therm}^{st}(%)	Δs kcal/h K	η_s^n(%)	η_{therm}^{st}(%)
Reversible rectification	227.90	1	—	227.90	1	—	158.96	1	—	29.43	1	—
Infinite adiabatic rectification	359.02	63.47	52.3	339.58	67.11	48.2	366.90	43.32	31.5	138.60	21.23	14.3
Finite adiabatic rectification	389.32	58.53	*48.9*	380.12	59.95	*44.4*	405.39	39.21	*29.3*	149.00	19.75	*13.6*
Stepwise heat turnover, 3 sections (c)	366.91	62.11	51.5	352.25	64.69	47.1	293.06	54.24	36	130.21	22.60	14.9
Stepwise heat turnover, 4 sections (c + r)	325.95	69.91	56.8	316.21	72.02	51.0	250.96	63.33	41	113.37	25.95	16.3
Stepwise heat turnover, 5 sections (c + 2r)	314.53	72.45	58.5	305.88	74.50	52.2	245.90	64.64	41.5	108.78	27.05	16.8
Stepwise heat turnover, 6 sections (2c + 2r)	308.23	73.93	59.6	297.81	76.52	53.2	244.72	64.95	53.2	105.00	28.2	17.0
Heat exchanger surface (m^2)	360.0			740			786			290		
$\Delta S_s = A \cdot K' \left(\frac{\Delta T}{T}\right)_m$ kcal/hK	51.7*			106.3*			111*			42*		
Heat isolation kcal/h K	3			5			5			5		
Hydraulic resistance kcal/h K	10			10			10			10		
Other losses kcal/h K	10			10			10			10		
Total loss kcal/h K	74 7			131.3			136			67		

* $K' = 200$ kcal/m^2 h °C; $\Delta T_m = 10$K; $T_m = 373$ K

agreed within 10% for the various stepwise heat turnover schemes. As an example we present the $H = H(\Phi_2)$ correlation with operational characteristics fixed for three different α-values (Fig. 6).

Thus, for changing prices of heat carrier media, the reduction of operating costs achieved by stepwise heat turnover can readily be estimated through an analysis of entropy production. The correlations mentioned are variants of the Gouy-Stodola relationship, $K = f(T_0) = \text{const}\ (T_0)$, applied to a concrete mathematical and cost model:

$$L_{\text{loss}} = T_0(S - S_0)\,. \tag{8}$$

Coupling strength and standard thermodynamic efficiency of distillation

In Table I the calculated entropy production of four variants is shown. The entropy production values refer to reversible, infinite adiabatic, and finite adiabatic (conventional) cases, for stepwise heat turnovers of 3, 4, 5 and 6 sections. In variants 1 and 2 the relative volatilities are $\alpha = 2.5$ and $\alpha = 1.5$ for the same feed and effluent concentrations. In variant 3 the entropy production is shown for a feed mole fraction of $x_F = 0.8$, in variant 4 for a required separation of $x_B = 0.3$ and $x_D = 0.7$, uniformly at a basis capacity of 180 kmol/hr. In the latter two cases the net entropy efficiency values η_s^n of the separation process are small, moreover, at product concentrations of $x_B = 0.3$ and $x_D = 0.7$ the application of stepwise heat turnover does not increase the efficiency to any substantial degree. It is of interest to note that the net entropy efficiency of adiabatic rectification with infinite dimensions is attained generally with 3 or 4 sections of the stepwise heat turnover system: this shows the significance of intermediate heat turnover.

Since in Table I the extreme cases of practical separation problems are collected, it can be seen that the range of net entropy efficiencies for conventional distillations is

$$20‰ < \eta_s^n < 60‰$$

i.e. the range of the thermodynamic coupling factor p in the entropy function

$$\Phi = L_{11} X_1^2 (1 - p^2) \tag{9}$$

is between $0.5 < p < 0.75$, where p can be derived from the theory of stationary processes as

$$p = \sqrt{\frac{(L_{12} + L_{21})^2}{4 L_{11} L_{22}}}\,. \tag{10}$$

With stepwise heat turnover value of η_s^n can be raised to 80%, accordingly p may increase to $p < \sim 0.9$.

In order to be able to determine the thermodynamic efficiency of distillation, other thermodynamic losses must be estimated; at the bottom of Table I these estimated figures are shown.

The entropy produced in the course of heat transfer, across a finite difference of temperature was calculated from the formula (flux multiplied by the driving force)

$$\Delta S_s = I_Q \Delta \left(\frac{1}{T}\right) = A K' \left(\frac{\Delta T}{T}\right)_m^2 . \tag{11}$$

The thermodynamic efficiency expressed in entropy representation provides a standard value; in the Table this is denoted by $\eta_{\text{therm}}^{\text{st}}$.

The range of the standard thermodynamic efficiency of conventional distillation falls between the limits of 10 and 50%, *i.e.*

$$10\% < \eta_{\text{therm}}^{\text{st}} < 50\% .$$

Under favourable circumstances these values can be improved by about 10% through the application of stepwise heat turnover.

The results of our analysis are in agreement with the low thermodynamic efficiencies of petroleum refining and petrochemical plants applying complex distillation apparatus: *cf.* Refs [9, 10, 11].

Conclusions

1. Conventional distillation is a strongly coupled stationary system of the first degree. The range of the thermodynamic coupling factor is $0.5 < p < 0.75$. The range of the standard thermodynamic efficiency of distillations is $10\% < \eta_{\text{therm}}^{\text{st}} < 50\%$.

2. The concept of net entropy efficiency of the separation process is introduced and defined; its variations according to different forms of a stepwise heat turnover are shown. For the various values of operational characteristics the change of the net entropy efficiency is given. The application of stepwise heat turnover improves, by about 10%, the standard thermodynamic efficiency of the process.

3. Using the correlation $H = K \Delta S_2$, where K is a function of the operational and constructional characteristics and price construction, the operating cost of a stepwise heat turnover system working with heating media of variable temperature levels can be calculated directly from the entropy production.

*

The authors wish to thank Mr. J. Szabó (DUNA Petroleum Co., Százhalombatta) for helping in the computations.

Symbols

A molar mass flow of the product, kmol/hr
A heat transfer area, m^2
B molar mass flow of the bottom product, kmol/hr
D molar mass flow of the head product, kmol/hr
F molar mass flow of the feed, kmol/hr
H operating cost, Ft/year
I_Q heat flow, kcal/hr
k constant
K coefficient defined by Eq. (7); a function of the parameters of operation, construction and costs
K' heat transfer coefficient, kcal/m^2 hr K
L general transport coefficient
L_{loss} operational loss, kcal/hr
p thermodynamic coupling factor
Q heat turnover at a given level, kcal/hr
q ratio of liquid in the feed
R reflux ratio
R gas constant, 1,9872 kcal/K kmol
$\overline{S}$ entropy production, kcal/K hr
T absolute temperature
V molar vapour flow, kmol/hr
X general driving force
x mole fraction in the liquid phase
y mole fraction in the vapour phase
η_s entropy efficiency
η_s^n net entropy efficiency of the separation process
η_{therm}^{st} standard thermodynamic efficiency
λ heat of evaporation
Φ density of entropy sources, kcal/K hr m^2
$\Theta = \frac{R_{act}}{R_{min}}$

Indices

i component
j plate
t product
act actual figure
min minimum figure
D head product
B bottom product
s value pertinent to heat-flow

REFERENCES

[1] Odum, H. T., Pinkerton, R. C.: American Sci., **43,** 331 (1955)
[2] Szolcsányi, P.: W. Z. der T. H. für Chemie 'Carl Schorlommer' (Leuna—Merseburg) **11,** 351 (1969)
[3] Szolcsányi, P.: Proc. 2nd Conf. on Appl. Phys. Chem., Veszprém 1971; Vol. 2, p. 601, Akadémiai Kiadó, Budapest
[4] Szolcsányi, P.: Analysis of the Energetics of Chemical Unit Operations (in Hungarian) Műszaki Könyvkiadó, Budapest 1972
[5] Fonyó, Zs.: Hung. Journ. of Industr. Chem. Veszprém, **1,** 293 (1973)
[6] Fonyó, Zs., Földes, P.: Acta Chim. (Budapest) **81,** No 1, 103 (1974)
[7] Fonyó, Zs., Nagy, S.: Paper presented at the Intern. CHISA '72 Congress, Praha, Sect. B, No 3.1.
[8] Haselden, G. G.: Trans. Inst. Chem. Engrs., **36,** 123 (1958)
[9] Haselden, G. G.: Der Ingenieur, **74,** No. 8, Ch. 9—16 (1962)
[10] Platonov, V. M., Bergo, B. G.: Rasdelenie mnogokomponentnych smesei. Khimia, Moscow 1965.
[11] King, J. C.: Separation Processes. McGraw-Hill, New York 1971

Zsolt Fonyó
Péter Földes
1521 Budapest, Műegyetem rkp. 3. Hungary.

Acta Chimica Academiae Scientiarum Hungaricae, Tomus 83 (1), pp. 37—52 (1974)

RECENT RESULTS ON METAL CATALYSIS

P. TÉTÉNYI, L. GUCZI and Z. PAÁL

(Institute of Isotopes of the Hungarian Academy of Sciences, Budapest)

Received July 2, 1973

Certain problems of adsorption, hydrogenolysis, isomerization and dehydrocyclization are discussed in the light of the interaction between the metal catalyst and the reacting substrate. On the basis of the authors' experiments, and of data taken from the literature, an interpretation is given for the role of hydrogen in certain catalytic reactions involving hydrocarbons, and it is discussed how hydrogen affects the nature and extent of the hydrocarbon–metal interaction. It is concluded that the various parameters characterizing the metal are insufficient to account for the catalytic effect, because this effect is due to the *catalytic system* as a whole, formed as a result of the interaction between the substrate and the metal.

On the basis an interpretation is given for the statement, made by one of the authors a few years ago that there is no characteristic difference between the catalytic effects of metals and metal oxides.

The phenomenon called catalysis was defined first by BERZELIUS in 1835 as follows:

"There exist certain special substances which affect chemical reactions in a peculiar way, different from chemical affinity, and induce a union wherein they take part, if at all, only to a minor extent. This effect is, presumably, the appearance of electricity, odd, catalytic force, which awakens the dormant chemical affinity. This process is catalysis."

Several definitions have since been given most of them disregarding the relations between the catalyst and the reaction, and emphasizing that the catalyst has no part in the chemical process:

"A catalyst is a substance which apparently plays no direct part in the reaction, but may initiate, accelerate, or control the process" (MITTASCH, 1933).

"Catalysis . . . is an influence on the rates of chemical processes by substances which do not undergo permanent changes during the reaction" (Contact Catalysis, Publ. House of the Hungarian Academy of Sci., Budapest, 1966).

A more general definition, which emphasizes clearly the main point of the phenomenon, was given by BALANDIN [1] in 1947: "Catalysis is the effect of a substance on the reaction, which changes selectively the kinetics of the reaction, while leaving unchanged the stoichiometric and thermodinamic conditions. The effect consists in replacing certain elementary steps of the reaction with other, cyclic steps, involving the active substance. This substance

is the catalyst which, as follows from the definition, in the limiting case does not change as a result of the reaction and does not influence the equilibrium."

This definition already implies unambiguously that the catalyst does take part in the reaction, but the emphasis is still on the feature that it is not changed during the process.

The results of recent investigations in the field of metal catalysis indicate that a further important step can be made in the interpretation of catalysis. Namely, increasingly numerous data show that the catalytic structure is the *result of interactions* between the catalyst and the other components of the system. The system is controlled, driven into a particular reaction path by this catalytic structure.

This phenomenon can be observed particularly well in the reactions of hydrocarbons catalyzed by metals. The course, rate, and the path of the reaction are all influenced, to a great extent, by the hydrogen content of the system.

The results of our experiments and those of other authors have shown that hydrogen is bonded, adsorbed on metals much more rapidly than are saturated hydrocarbons. For instance, tritium chemisorbed on nickel exchanges readily with hydrogen in the gas phase even at room temperature [2], as indicated by the radioactivity appearing in the gas phase. In contrast, the exchange between methane and tritium starts only above 200°C. Moreover, the rate of the hydrogen exchange in ethane is the same for deuterium and tritium [3]. The absence of an isotope effect proves that the rate-determining step of the exchange, *i.e.* the step with the lowest rate constant, is the adsorption of the saturated hydrocarbon, whereas the other steps, including the adsorption of hydrogen (deuterium, or tritium) are much faster. Thus, hydrogen occupies the surface of the metal catalyst, retards the reactions of hydrocarbons and decreases their reaction rates.

Such an effect can, indeed, be observed. When investigating the hydrogen–deuterium exchange for a number of substrates, we have found that the reaction is retarded by hydrogen, the reaction order with respect to hydrogen being negative. This result was found for the hydrogen–deuterium exchange of methane [2], ethane [3], and propane [14], on nickel and platinum [5] catalysts (*cf.* Table I). With increasing temperature, the negative reaction order gradually disappears, ceasing completely at about 250°C. This phenomenon can be explained by assuming that hydrogen is desorbed very easily at this temperature, and is thus displaced from the surface by the saturated hydrocarbon.

A similar phenomenon can be observed in the another typical reaction of hydrocarbons, namely the rupture of carbon–carbon bonds, or hydrogenolysis. Of the characteristic results, the data pertaining to the hydrogenolysis of ethane, propane [4] and butane [6] in the presence of nickel are shown in Table II.

Table I

*Variation of the order of exchange with temperature**

a) Ethane on nickel

T°C	$P_{C_2H_6}$	P_{H_2}	a	b	
174	7.89—15.2	8.38—31.54	1.1	—1.13	D_2
250	6.8 —34.0	34.0 —61.2	1.12	—0.15	D_2
250	22.4 —85.5	39.4 —69.5	1.1	—0.3	HT
310	25.0 —80.0	34.0 —136.0	0.68	0.52	HT
323	25.0 —86.5	41.0 —128.5	0.58	0.84	HT

b) Propane on nickel

T,°C	$P_{C_3H_8}$	P_{HT}	a	b
165	10—30	30—120	0.82	—0.6
200	10—35	45—120	0.8	—0.29
232	10—25	30—100	0.78	0.14
240	10—30	30—140	0.75	0.28

* $w = kp_{CH}^{a}p_{H_2}^{6}{}^{b}$

Table II

The change in the hydrogen exponent for the hydrogenolysis of ethane, propane, and n-butane

Temperature (°C)	Ethane*		Propanes*		*n*-Butane*	
	P_{H_2}	b	P_{H_2}	b	P_{H_2}	b
	(Torr)		(Torr)		(Torr)	
167					20—222	—1.6
174	8.4—31.5	—1.4				
182					34—200	—0.7
198			30—95	—0.6		
202					32—183	—0.03
210			27—100	—0.2		
227					34—192	0.0
240			30—110	0.0		
245					38—201	0.0
250	34—61.2	—0.7				
262	8.4—31.5	0.0				
270			40—120	0.0		
278	22—85	0.0				
310	25—130	0.0				
323	40—130	0.0				

* The pressure of hydrocarbons is approximately 10 Torr

Similar values were obtained for the hydrogenolysis of ethane, propane and butane in the presence of platinum [5].

It can be seen that hydrogen has a retarding effect both on hydrogen–deuterium exchange and the hydrogenolysis.

Hydrogen affects, however, not only the reaction rates, but also the direction of the reaction, as shown clearly by the effect of hydrogen on the selectivity of hydrogenolysis. The selectivity in the hydrogenolysis of a saturated hydrocarbon C_nH_{2n+2}, with respect to a component C_iH_{2i+2} (where $n > i > 1$), can be expressed, in complete generality, by the equation

$$S_i = \frac{nw_i^0}{\sum_{i=1}^{n-1} iw_i^0} \tag{1}$$

where w_i^0 is the initial rate of formation of the component with i carbon atoms. According to the definition, the selectivity with respect to any component is unity if only one C–C bond is broken, thus the selectivity of the hydrocracking reaction always means the transformation which involves the rupture of the first C–C bond.

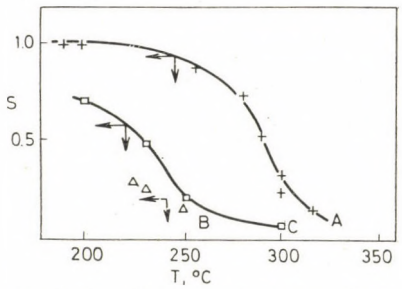

Fig. 1. Temperature dependence of the selectivity of propane hydrogenolysis on various nickel catalysts

In the decomposition of propane, for instance, the selectivity with respect to ethane is unity if the rates of the formation of ethane and the decomposition of propane are the same. If the rate of ethane formation is lower than this, because ethane molecules, in part, are decomposed into methane, the selectivity is less than 1.

Experimental results [4] have shown that the selectivity is temperature dependent.

It can be seen from Fig. 1 that the selectivity of the decomposition of propane *decreases* with increasing temperature.

The selectivity also depends on the activity of the catalyst, as can be seen from the data of Table III [4, 6]. The data also indicate that the selectivity increases with decreasing activity.

Table III

Dependence of the selectivity values on the catalytic activity

$-W^0_{C_3H_8}$	$S_{C_2H_6}$	$-W^0_{C_4H_{10}}$	$S_{C_3H_8}$
1.150×10^{-8}	0.330	2.34×10^{-9}	0.310
0.692×10^{-8}	0.360	1.42×10^{-9}	0.490
0.440×10^{-8}	0.454	8.31×10^{-10}	0.680
	0.493	3.61×10^{-10}	0.850
0.083×10^{-8}	0.500	1.63×10^{-10}	0.915
0.046×10^{-8}	1.000	6.36×10^{-11}	0.971
		4.22×10^{-11}	0.988

$-W^0_{C_3H_8}$ and $-W_{C_4H_{10}}$ are initial rates of propane and *n*-butane consumption in mol/m²
$S_{C_2H_6}$: selectivity of ethane production from propane;
$S_{C_3H_8}$: selectivity of propane production from *n*-butane.

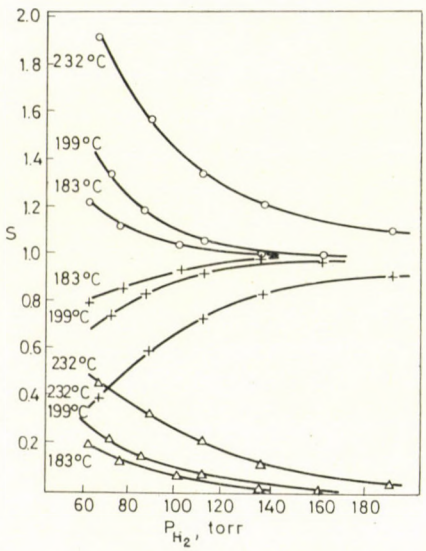

Fig. 2. Dependence of the selectivity of butane hydrogenolysis (catalyst: Pt) on the partia pressure of hydrogen; o—o $S_{methane}$, +—+ $S_{propane}$, Δ—Δ S_{ethane}

It has also been observed in the hydrogenolysis of *n*-butane on nickel that the probability of the selective rupture of one C–C bond increases with the hydrogen pressure. It can be seen in Fig. 2 that the propane yield increases, and the methane and ethane yields decrease with the hydrogen pressure, in-

dicating that the selective hydrogenolysis, which involves the fission of only one C–C bond, becomes more favoured with increasing hydrogen coverage.

Any effect that increase the free surface, such as decrease of the hydrogen pressure or hydrogen coverage and increase of the catalytic activity at elevated temperatures, decreases the selectivity.

These facts can be interpreted as follows. Saturated hydrocarbons are adsorbed on the surface of metals *via* the dissociation of C–H bonds. If the adsorption is weak, and only a single chemical bond is formed between the carbon atoms and the surface, a relatively fast desorption takes place, and if deuterium or tritium is present, a singly labelled product, containing heavy hydrogen, is formed. If, however, further hydrogen atoms are abstracted from the adsorbed species before desorption, a multiple carbon–metal bond is formed, and the surface species is bonded strongly. On the basis of hydrogen–deuterium exchange experiments with adsorbed methane, KEMBALL [7] assumed the formation of the structures.

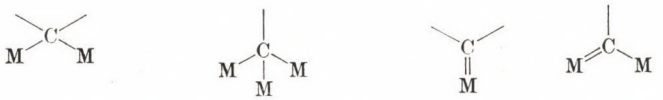

The rates of the multiple methane–deuterium exchange reactions (*i.e.* the formations of d_2- and d_3-methanes) and the rate of hydrogenolysis change in parallel on various catalysts. This fact led KEMBALL to the conclusion that hydrogenolysis is due to the presence of strongly adsorbed species bonded to the surface by multiple carbon–metal bonds [8]. Thus, the hydrogenolysis of propane can be conceived to proceed according to the scheme shown in Fig. 3. In this scheme the strongly adsorbed propane is converted into

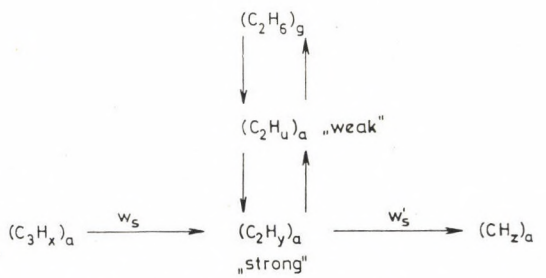

Fig. 3. Scheme of the hydrogenolysis of propane ($y < u$)

strongly adsorbed ethane. Because of the high hydrogen concentration on the surface, the formation of multiple metal–carbon bonds is less probable at low temperatures, and thus ethane is easily recombined with the hydrogens on the

surface of the metal, the reaction involving weakly adsorbed ethane molecules. In this case the selectivity is 1, and ethane and methane are formed in a ratio of 1 : 1.

At higher temperatures, on nickel above 220°C, and on platinum above 430°C, the selectivity decreases. The lower selectivity arises from the fact that more multiple carbon–metal bonds are formed owing to the lower hydrogen concentration, preventing thereby the recombination of ethane molecules, which are now converted, without desorption, into methane. Consequently, the selectivity drops below unity.

The same situation occurs if the selectivities are compared for the more active or less active surfaces.

The part played by hydrogen, thus, consists in occupying the free metal atoms, preventing the formation of multiple carbon–metal bonds, and decreasing thereby the probability of hydrogenolysis.

Is there any evidence, however, of the multiple carbon–metal bonds really playing such an important role in metal catalysis? Do such bonds exist at all?

It is known from a paper by EISCHENS and PLISKIN [9] that carbon monoxide is adsorbed to a metal surface in two main forms:

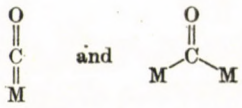

Low-energy electron diffraction (LEED) and flash desorption studies by MORGAN and SOMORJAI [10] have shown that the linear form, which is the dominant form of adsorption, does not exist on platinum over 200°C, whereas the bridge-form is stable up to 600°C. The linear form can be found both on the (111) and (100) faces, the bridge-form can be shown to exist only on the (100) faces, because the Pt–Pt distances allow the formation of an appropriate Pt–C–Pt angle ($\sim$ 131°) only in this case.

These facts explain why the rate of hydrogenolysis is lower than that of hydrogen exchange, and why the simple adsorption of hydrocarbon molecules does not lead, at the same time, to hydrogenolysis.

In this respect it is interesting to compare the effects of nickel and platinum. The latter is, as a catalyst, superior in hydrogen exchange, and weaker, but more selective, in the hydrogenolysis. Our most recent experiments also show that the adsorbing abilities of these catalysts are substantially different. The adsorption of ethane on nickel is partly irreversible already at —40°C, whereas on platinum it is completely reversible even at 80°C [11].

The differences between the catalytic activities and adsorption abilities of platinum and nickel can, in our view, be attributed to the following facts.

For platinum the two-point hydrocarbon adsorption, which involves the formation of the system,

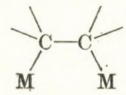

is more favourable from sterical aspects than for nickel. (The M–C–C angle is 106°40′ for platinum, and 103°40′ for nickel.) The different behaviour is also confirmed by the higher rates of the hydrogenation of ethylene [12] and dehydrogenation of cyclohexane [13]. Accordingly, the exchange is also more favourable on platinum. It has been shown in our previous papers [3, 4, 6] that two-point adsorption plays on extremely important role in the exchange reaction, which, consequently, also takes place more easily on platinum than on nickel.

The situation is different with the process of hydrogenolysis. On the (100) planes the Pt–C–Pt angle is 131°, whereas the Ni–C–Ni angle is 123°40′. Hence, it is much easier for a carbon atom to join two metal atoms on nickel than on platinum.

These considerations show that hydrogenolysis can be explained appropriately with the strong adsorption of the hydrocarbon, *i.e.* the two-point bonding of the carbon atoms, and this concept may also explain the effect of hydrogen on the selectivity of the reaction, and the differences observed between the catalytic behaviours of nickel and platinum.

The effect of hydrogen on the selectivity of the reactions catalyzed by metals is particularly prominent in the reactions of paraffins with higher molecular weight (*cf.* Fig. 4).

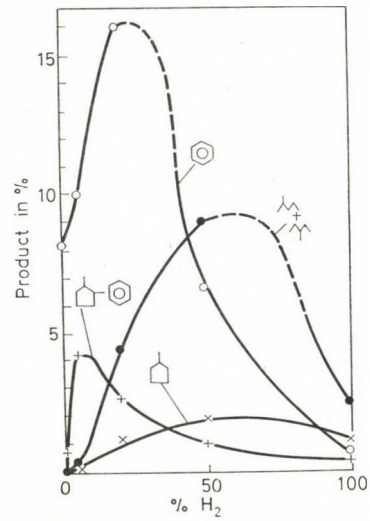

Fig. 4. The amounts of products formed from *n*-hexane in the presence of platinum catalyst, as the function of the hydrogen concentration in the carrier gas [14]

It can be observed that the ratio of the various products formed from *n*-hexane depends considerably on the amount of hydrogen present in the system. The isomerization of the carbon skeleton, and C_5-dehydrocyclization do not occur at all in the absence of hydrogen. The yields of the transformation of *n*-hexane to benzene and of the dehydrocyclization are increased, to a certain concentration limit, if hydrogen is present. The same phenomenon can be observed in the transformation of methylcyclopentane to benzene.

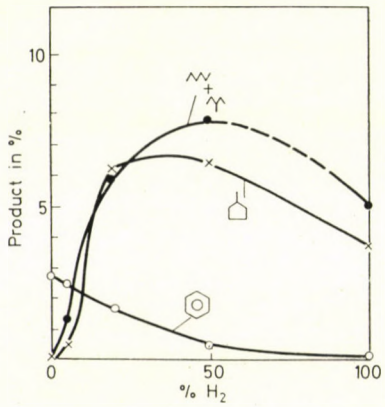

Fig. 5. The amounts of products formed from 2-methylpentane, in the presence of platinum catalyst, as a function of the hydrogen concentration in the carrier gas [14]

The relationship is similar, in many respects, between the products formed from 2-methylpentane, and the hydrogen pressure in the system (Fig. 5).

In this case, again, hydrogen has a positive effect on the rates of the chain-isomerization and C_5-dehydrocyclization, at the beginning, followed by a negative effect. The formation of benzene is now, however, retarded by hydrogen from the beginning of the reaction.

The above examples are peculiar in the sense that whereas only the *retarding effect* of hydrogen has so far been discussed, these examples show that hydrogen may also have a *positive effect* on the transformations of hydrocarbons, up to a certain concentration limit. The various reactions have optimum hydrogen concentrations [14] where the conversion exhibits a maximum (Fig. 6).

As can be seen, these optima for the different reactions appear at different hydrogen coverages; in one reaction a lower, in other reactions higher hydrogen coverages on the surface are optimal.

The fact that there is an optimum hydrogen coverage is extremely important in the practical realization of hydrocarbon reactions; it permits to

increase further the selectivity of metal catalysts, by the application of different partial pressures of hydrogen for the various processes.

It is indicated by the existence of optimum hydrogen coverages that the effect of hydrogen on the reactions is the result of several effects of opposite directions. Let us discuss some of these effects.

It has been shown that hydrogen, on one hand, has a *retarding effect* on the reactions, beyond a certain coverage. This effect can be attributed to the following facts.

(1) A part of the surface is occupied by hydrogen, hence the surface area, where reaction may take place, is reduced. Such an effect has been ob-

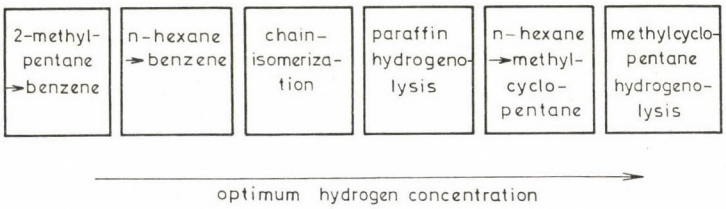

Fig. 6. Optimum hydrogen concentrations measured for various transformations of hydrocarbons

served in the dehydrogenation of various alcohols and hydrocarbons. The extent of this effect also depends on the nature of the metal. As regards the reactions of alcohols, the adsorption equilibrium constants of hydrogen are generally smaller, about 10—15%, of that of the alcohol [15]. The adsorption coefficient of benzene, however, is 15—20 times higher than that of hydrogen [16, 17].

(2) The adsorption of hydrocarbons according to the equation

$$R - H + 2M \rightarrow R - M + H - M$$

which involves the dissociation of the C–H bond, is suppressed by hydrogen. It is then obvious that the presence of hydrogen on the surface prevents the dissociation; chemisorption involving the dissociation of C–H bonds takes place more easily on a 'clean' surface. This fact has also been proved experimentally by EISCHENS and PLISKIN [9] for the adsorption of ethane on nickel.

(3) The formation of olefin products, or intermediates, from saturated hydrocarbons may also be suppressed for thermodynamic reasons by the presence of hydrogen.

(4) It can also be attributed to the effect of hydrogen that on hydrogen-occupied surfaces the processes which involve the formation of multiple carbon–metal bonds are, as has been pointed out, inhibited. LEED investigations by

MORGAN and SOMORJAI [18] show that every second atom on the surface of a platinum single crystal is blocked by hydrogen. Although this surface can adsorb carbon monoxide at the free sites, there is no way of forming strongly bonded, bridge-like structures, because the neighbouring platinum atoms are already blocked by hydrogens and thus the sites required to form strong multiple bonds are, at least in part, occupied.

These factors, however, which retard the reactions may, except factor (1), also promote the reactions of hydrocarbons, and this explains that the presence of hydrogen has a positive effect on the reaction rate up to a certain concentration limit, in agreement with the experimental data shown above. Let us discuss this question in more detail. The fact that the presence of hydrogen retards dissociative adsorption involves simultaneously that it promotes the desorption and recombination of molecules adsorbed in dissociated state, by hydrogenating the *C–M* bonds on the surface. The chemisorption of benzene (Table IV) provides a characteristic example [19].

Table IV

Chemisorbed amounts (10^{-3} STP ml/m²) of benzene
($t = 150$ °C, $P = 160$ Torr)

Catalyst	Quantity chemisorbed	Eluted with benzene	Eluted with hydrogen
Co	9.6	7.8	1.8
Ni	6.4	3.9	2.5
Pt	7.9	7.4	0.5

Using the method of radioactive labelling, we have found that only *a part* of the benzene molecules chemisorbed on the surface could be eluted with benzene, and hydrogen had to be used to remove the remaining part. It can be seen that the ratio of the fractions depends on the catalyst, the amount of irreversibly bonded benzene being higher in the case of certain metals (Ni, Co), and lower for others (Pt). Consequently, the presence of hydrogen ensures that in the reactions which involve benzene formation the catalyst resists the poisoning effect of the irreversibly bonded benzene molecules. Olefins, formed in catalytic reactions, exert, in general, a strong poisoning effect. If they are removed from the surface by hydrogenation, the original activity of the catalyst can be restored. Thus, also in this case, the effect of hydrogen on the reaction is favourable.

In the two cases discussed above the cleaning and regeneration of the surface is promoted by hydrogen. A different action of hydrogen is to prevent the formation of multiple carbon–metal bonds on the surface, whereby the

cracking of hydrocarbon molecules and the deposition of carbon is suppressed, and the surface is protected from coking.

These effects manifest in that the activities of metal catalysts are more constant, and the catalysts show less tendency towards being poisoned if hydrogen is present, as it is reflected in the diagrams of Fig. 7 [14].

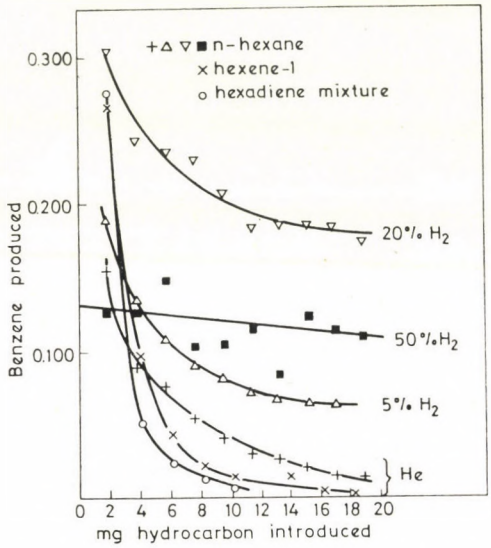

Fig. 7. Decrease on the aromatization activity of platinum catalyst in subsequent pulses

It can be seen that the activity for aromatization decreases much faster in the presence of helium than of hydrogen. Although at a hydrogen concentration of 50% the initial activity is much smaller than at lower hydrogen concentrations or in the absence of hydrogen, the activity remains neerly constant.

Each of these phenomena arises from the effect of hydrogen on the *reaction partners*. Hydrogen may, however, also affect the structure of the catalyst. It has been shown by BAIRD, PAÁL and THOMSON [20] that at high temperatures the grain size of platinum catalysts changes in the presence of hydrogen. The incorporation of hydrogen atoms into the metal lattice causes the lattice constant to increase, which also influences the catalytic activity.

The direct action of hydrogen on the surface state of metals can be illustrated by the following example. It is known that the metal atoms form a hexagonal layer on the (100) faces of gold, iridium and platinum [18, 21, 22]. Upon adsorbing an electron donor species (hydrogen, carbon monoxide or olefins) this layer disappears rapidly and a surface state which corresponds to

the original lattice is formed. In the presence of electron acceptors, such as O_2 or Cl_2, however, the hexagonal structure of the surface remains unchanged.

Consequently, in the reactions of hydrocarbons the catalytic effect is exerted *jointly* by hydrogen and the metal. The presence of hydrogen is of utmost importance in that the elementary steps of catalysis are cyclic with respect to the catalyst. The presence of hydrogen also influences the direction or path of the catalytic reaction, and the selectivity of the catalyst.

In the reactions of hydrocarbons hydrogen is only one of the reaction partners. Interactions occurring between the metal catalyst and the hydrocarbon molecule also change the original surface; and its structure, which is responsible for the catalytic effect, is formed jointly by the metal, the hydrocarbon molecule and hydrogen. Consequently, it appears more appropriate not to regard the catalyst and the various substances present in the system, as *the* catalyst and *the* reaction components. The catalytic structure, which promotes the reaction in the appropriate direction, is formed as a result of the interactions between the catalyst and the reaction partners.

Thus, when interpreting the catalytic properties of various elements, it is insufficient to rely only on the properties (geometry, electronic structure) of the given element; one must always endeavour to take into account the possibility of irreversible interactions between the substrate and the catalyst.

This approach has led to a successful interpretation, for instance, of the decomposition of formic acid on various metals. This interpretation was based on the properties of the oxalates of the metals in question [23]. The results referred here on the investigations on the reactions of hydrocarbons show that even in these, chemically less active systems the original properties of the metal undergo drastic changes, involving the formation of a catalytic structure on the surface.

The problems of catalytic effect have so far been discussed from the aspect of the interactions between the metal surface and the substrate. Metal oxide catalysts can be discussed in a similar way, as systems of metal ions which exert their effects in a medium formed by oxygen ions. It is very probable that under the conditions of catalytic reactions the surfaces of metals do really approach this state for a considerable part of metals.

On the basis of this presumption it becomes more understandable why the characteristic difference, which has formerly been assumed to exist between the catalytic effects of metals and their oxides, cannot be observed in the practice [24].

The catalytic reactions which were some ten years ago attributed only to the catalytic effect of oxides can, as has been discovered, also be promoted by metals. Thus, for instance, the dehydration of alcohols, the chain isomerization of hydrocarbons, and the alkylation reactions can equally be catalyzed by metals.

No characteristic differences can be observed, either, between the mechanisms of reactions catalyzed by these two types of catalyst. The hydro–dehydrogenation of six-membered hydrocarbon rings proceeds, for instance, in a stepwise manner, through the formation of cyclohexene and cyclohexadiene, both on metals and on metal oxides.

The sextet mechanism, which had been considered as valid for metal catalysts, must be inadequate for a series of metals (Fe, Mo, W, Au, Be, etc.), because the geometric factors contradict this hypothesis. Dehydrogenation

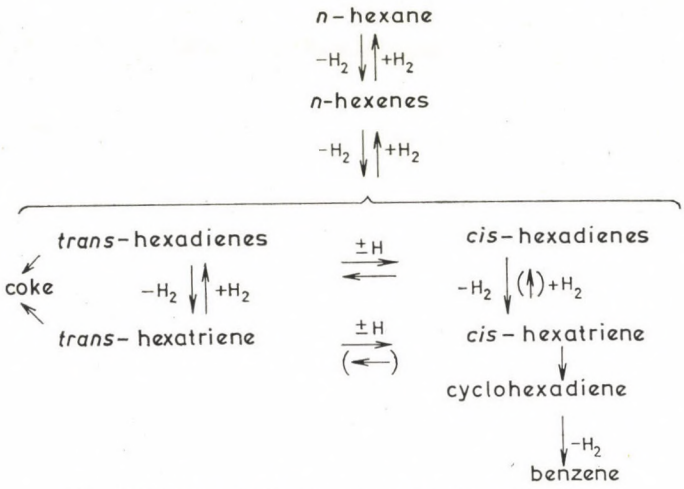

Fig. 8. Scheme of the dehydrocyclization of *n*-hexane

reactions, nevertheless, may proceed, indicating clearly that the mechanism must be similar to that on oxide catalysts.

The path of dehydrocyclization reactions is also stepwise both on metals and oxides (Fig. 8). This mechanism was proved successfully in our laboratory [14] for metal catalysts, and a similar result was found by KAZANSKY, *et al.* [25] for oxide catalyzed dehydrocyclization reactions.

Is there, then, any difference between metals and metal oxides in this respect, and if so, what is this difference?

In the presence of oxides the specific catalytic activity is, in general, lower but more steady, the catalysts showing less tendency towards being poisoned. In the presence of metals the reactions usually proceed at lower temperatures. However, the reactions which need higher temperatures for thermodynamic reasons cannot be promoted by metals because of the risk of catalyst poisoning.

The reversible adsorption of benzene and cyclohexane [19] offers a possibility to compare these types of catalyst (Table V). The data reveal the following facts.

Table V

Reversible adsorption of benzene and cyclohexane

		Fe	Fe_2O_3	Co	Co_3O_4	Ni	NiO	Pt	PtO
Benzene	Isotherm*	*L*	*L*	*F*	*F*	*F*	*F*	*F*	*L*
	V_m(STP ml/m²)	0.104	0.073	0.108	0.052	0.092	0.062	0.098	0.072
	$-\Delta H_a$ kcal	6.6	8.7	8.6	7.4	6.3	6.4	8.2	6.8
Cyclohexane	Isotherm	*L*	*L*	*F*	—	*L*	*L*	*L*	—
	V_m(STP ml/m²)	0.179	0.106	0.176	—	0.167	0.103	0.198	—
	$-\Delta H_a$ kcal	6.2	9.1	6.8	—	5.6	6.5	7.3	—

* *L* and *F*: Langmuir and Freundlich-type of adsorption isotherm respectively.

(1) There is no significant difference between the types of adsorption, both processes being described by the same isotherm equations and the values of adsorption enthalpy being also the same.

(2) The adsorption limits with respect to unit surface area are, however, different for the two types of adsorbent, being higher for metals than for oxides. The ratios of the corresponding pairs of V_m values are between 1 and 2, the actual ratio depending on the metal–metal oxide pair. The values are similar to the ratio of the surface concentrations of metal atoms in metals and oxides, respectively.

Consequently, the adsorption (now reversible, but not physical) takes place at the metal ions in the oxides, too, and oxygen atoms act merely as inert diluents. The lower specific catalytic activities of oxides (activity per unit surface area) can be attributed primarily to this fact.

This interpretation is in agreement with the conclusions of KOKES and DENT [26] drawn from the results of infrared spectrophotometric studies, according to which, the carbon atoms of the substrate (ethylene and ethanol) are bonded to the metal in ZnO catalysts, and only the hydrogen atoms are bonded to oxygens.

The weaker tendency of oxides, as compared to metals, towards being poisoned can also be related to the diluting effect of oxygen atoms, because a bridged, strong, multivalent, adsorbed surface species is of the

most unlikely to be formed in the case of oxides. This reasoning is proved by recent investigations [27], in agreement with the opinion of other authors [28]

who state that in oxides the main product of the hydrogen–deuterium exchange of hydrocarbons is the singly labelled, d_1-hydrocarbon.

The interpretation given here is, no doubt, mostly mechanistic, since it disregards the effects of the electronic structure, and its arguments are based primarily on geometrical considerations. This treatment does, however, not imply that electronic effects have no influence on the phenomena. It rather expresses the hope that, stemming from the intimate relationship between geometrical and electronic factors, this treatment can later be translated into the language of electronic behaviour, which enables one to reveal more advanced correlations.

REFERENCES

[1] BALANDIN, A. A.: Vestn Ak. Nauk. SSSR, **4,** 97 (1947)
[2] GUCZI, L., TÉTÉNYI, P.: Z. phys. Chem. Leipzig, **237,** 356 (1968)
[3] GUCZI, L., SÁRKÁNY, A., TÉTÉNYI, P.: Z. phys. Chem. (N. F.), **74,** 26 (1971)
[4] GUCZI, L., SÁRKÁNY, A., TÉTÉNYI, P.: Proc. 5th Intern. Congress on Catalysis, V. 2. 1111. North Holl. Publ.-Elsevier, Amsterdam 1973
[5] GUCZI, L., SÁRKÁNY, A., TÉTÉNYI, P.: J. C. S. Faraday Transactions I. (In press)
[6] SÁRKÁNY, A.: Studies on the catalytic hydrogenolysis of C_3 and C_4 hydrocarbons on Ni catalyst. Thesis, Budapest, 1972 (in Hungarian)
[7] KEMBALL, C.: Proc. Roy. Soc., **A207,** 539 (1951)
[8] KEMBALL, C.: Catalysis Rev., **5,** 33 (1971)
[9] EISCHENS, R. P., PLISKIN., W. A.: Adv. Catalysis, **10,** 1 (1958)
[10] MORGAN, A. E., SOMORJAI, G. A.: J. Chem. Phys., **51,** 3309 (1969)
[11] BABERNICS, L., GUCZI, L., TÉTÉNYI, P., SÁRKÁNY, A.: Paper № 73 on Conference "Mechanism of Catalytic Processes" Acad. Sci. USSR, Moscow, 1974
[12] BEECK, O.: Rev. Mod. Phys., **17,** 61 (1945)
[13] TÉTÉNYI, P., SCHÄCHTER, K.: Acta Chim. Acad. Sci. Hung., **56,** 15 (1968)
[14] PAÁL, Z., TÉTÉNYI, P.: Kém. Közl., **37,** 129 (1972)
[15] BALANDIN, A. A., TÉTÉNYI, P.: MTA Kém. Tud. Oszt. Közl., **11,** 299 (1959)
[16] TÉTÉNYI, P., KIRÁLY, J., BABERNICS, L.: Acta Chim. Acad. Sci. Hung., **29,** 35 (1961)
[17] TÉTÉNYI, P., BABERNICS, L., SCHÄCHTER, K.: Acta Chim. (Budapest) **61,** 367 (1969)
[18] MORGAN, A. E., SOMORJAI, G. A.: Surface Sci., **12,** 405 (1968)
[19] BABERNICS, L., TÉTÉNYI, P., KERTÉSZ, L.: Zeitschr. Phys. Chem. NF. **89,** 237 (1974)
[20] BAIRD, T., PAÁL, Z., THOMSON, S. J.: J. C. S. Faraday Transactions I., **69,** 50 (1973): **69,** 1237 (1973)
[21] FEDAK, A. G., GJOSTEIN, N. A.: Surface Sci., **8,** 77 (1967)
[22] PALMBERG, P. W., RHODIN, T. N.: Phys. Rev., **161,** 586 (1967)
[23] SACHTLER, W., FAHRENFORT, J.: Actes de 2ème Congr. Intern. de Catalyse. Vol. 1, p. 831, Technip. Paris (1961)
[24] TÉTÉNYI, P.: Kém. Közl., **36,** 59 (1971)
[25] KAZANSKY, B., ISAGULYANTS, G., ROZENGART, M., DUBINSKY, Y., KOVALENKO, L.: Proc. 5th Intern. Congress on Catalysis, V. 2. 1277. North Holl. Publ.-Elsevier, Amsterdam, 1973
[26] KOKES, R. J., DENT, A. L.: Adv. Catalysis, **22,** 1 (1972)
[27] KÁLMÁN, J.: Thesis on D. Techn. Budapest, 1974
[28] BURWELL, Jr. R. L., LITTLEWOOD, A. B., CAEDEW, M., PASS, G., STODDART, C. T. H.: J. Amer. Chem. Soc., **82,** 6272 (1960)

Pál TÉTÉNYI
László GUCZI
Zoltán PAÁL

H–1525 Budapest, POB 77. Hungary.

Acta Chimica Academiae Scientiarum Hungaricae, Tomus 83 (1), pp. 53—61 (1974)

PROPERTIES OF ALCOHOL–AMINE MIXTURES, IV

VISCOSITY AND AVERAGE DEGREE OF ASSOCIATION OF NORMAL BUTYLAMINE–1-BUTANOL MIXTURES

F. RATKOVICS, T. SALAMON and L. DOMONKOS

(Electrochemical Research Group of the Hungarian Academy of Sciences, Department of Physical Chemistry, University of Chemical Industries, Veszprém, Hungary)

Received October 22, 1973

A relation was found between the average degree of association and the viscosity of normal primary alcohols and some primary, secondary and tertiary amines. An approximate method was developed for the calculations of the average degree of association from viscosity data. It was shown that as regards order of magnitude the association equilibrium constants calculated from the average degree of association are in agreement with those determined by other methods. The method based on viscosity measurement was applied to the study of the average degree of association of the *n*-butylamine–1-butanol mixture. It was found that with regard to the formation of the mixed associated species the results exclude all assumptions which would attempt to explain the negative entropy of mixing and the exothermic heat of mixing the system by the formation of mixed species of the type A_iB_j, with higher average degree of association than the original species A_i and B_j.

The experimental results of studies on mixtures of primary alcohols and primary amines have led to the assumption that the strikingly high exothermic heat of mixing can be attributed to the formation of associated amine-alcohol species [1, 2]. The question arose as to the compositions of such associations.

The formation of mixed associated species can be used in various ways to explain not only the exothermic heat of mixing, but also the negative entropy of mixing. One possible assumption is that the entropy decrease and the exothermic heat of mixing are both due to binding between of the associated alcohol and amine species. In this case average degree of association must increase as a result of the mixing.

It is conceivable that only a limited number of amine molecules can be linked to the associated species of alcohol and even that cyclic species are formed, containing one molecule of amine and one molecule of alcohol, which combine with high energy only. The presence of these has been confirmed by the NMR spectroscopic measurements of HUYSKENS and HUYSKENS[3]. In this latter case the negative entropy of mixing would be explained by the extensive ordering, and the heat of mixing by the high energy accompanying the formation of cyclic species AB. To narrow down the number of possibilities in this question, it was necessary to find a method with which the average degree of association could be determined at least semiquantitatively with an independent experimental method in both the pure components and the mixture. The present paper deals with this subject.

Determination of the degree of association by viscosity measurements

In a study of the thermodynamic properties of mixtures of aliphatic alcohols and amines with paraffins, KEHIAIAN [4] found that, as compared with the OH . . .O and NH . . . N interactions, the interactions between the aliphatic carbon chains are negligible. On this basis we assumed that since the transport properties of liquids are also determined by the masses of molecules and the intermolecular forces between them, then the masses of the associated species formed in mixtures of alcohols and amines can be determined from viscosity data.

The viscosity of an arbitrary polymer of the associative component was assumed to be the same as the viscosity of the paraffin with the identical, or nearly identical molecular weight; *i.e.* it was assumed that in the case of viscous flow only the weak interactions are important, and thus the extent of friction is controlled by the lengths of the hydrocarbon chains.

Although the associated species formed in the systems studied are not necessarily chain-like in form, the viscosities of the normal paraffins were selected as the basis for comparison. When the numbers of carbon atoms are the same, there is no essential difference between the viscosities of the iso and the normal paraffins. Certain relevant viscosity data are listed in Table I [8].

Table I

Viscosities of hydrocarbons at 20 °C

Hydrocarbon	Viscosity (cp)
Ethane	gas
Propane	gas
Butane	0.164*
2-methylbutane	0.223
n-pentane	0.226
2-methylpentane	0.300
n-hexane	0.308
n-heptane	0.413
n-octane	0.546
n-nonane	0.713
n-decane	0.907
n-hendecane	1.186
n-tetradecane	2.18
n-hexadecane	3.34

* at the equilibrium vapour pressure.

The average molecular weight of the associated polymers was defined as:

$$\overline{M} = \sum_{i=1}^{k} x_i M_i . \tag{1}$$

For solutions of linear polymeric molecules the following relation holds between the viscosity and the average molecular weight [5]:

$$\eta = k \overline{M}^{\alpha} . \tag{2}$$

In this relation k and α are constants, and η is the dynamic viscosity. Accordingly, the log η *vs.* log $\overline{M}$ diagram plotted from the data for the straight-chain paraffins is to a good approximation a straight line; this can be used as

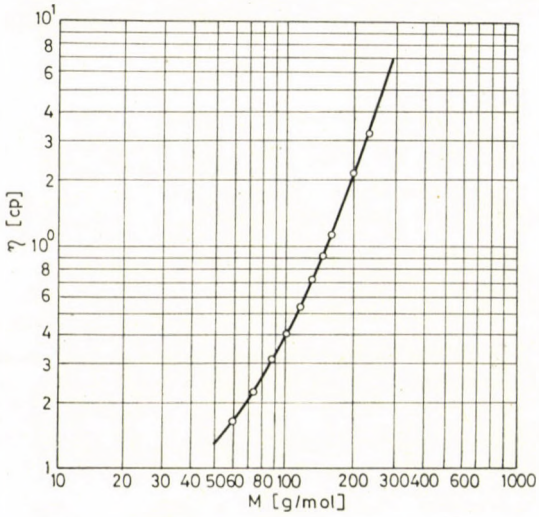

Fig. 1. Viscosities and molecular weights of normal hydrocarbons at 20 °C

a reference curve (Fig. 1) to read off the average molecular weight of the associative component.

When the average molecular weight is known, the association equilibrium constant can also be calculated, but this requires the assumption of some model of association. Calculations were carried out in this respect to asses the reliability of our method by comparison with literature data. A special note must be made that while the calculations referring to the average molecular weight are preceded in every case by the choice of a concrete model of association, in the determination of the average molecular weight from viscosities there is no need for this. Some model must be used for the calculation of the equilibrium constant of association from the viscosity data.

In the simplest case, using the MECKE-KEMPTER model [6], *i.e.* assuming an ideal, infinite chain-association, for one nominal mole of the pure associative component we can write:

$$n_1 + 2n_2 + \ldots + in_i + \ldots = 1 \tag{3}$$

where n_i is the number of moles of the chain-association containing i monomers. On dividing by Σn_i, one obtains for the mole fraction:

$$x_1 + 2x_2 + \ldots + ix_i + \ldots = \frac{1}{\Sigma n_i} . \tag{4}$$

On multiplication by the molecular weight of the monomer, M_1, we have for the average molecular weight:

$$\overline{M} = \frac{M_2}{\Sigma n_i} \tag{5}$$

or

$$\frac{\overline{M}}{M_1} = \frac{1}{\Sigma n_i} .$$

The average molecular weight can also be expressed by means of the equilibrium constant K and the mole fraction of the monomer x_1:

$$\overline{M} = M_1 x_1 + 2M_1 K x_1^2 + \ldots + iM_1 K^{i-1} x_1^i + \ldots \tag{6}$$

Dividing throughout by $M_1 x_1$:

$$\frac{\overline{M}}{M_1 x_1} = 1 + 2Kx_1 + 3K^2 x_1^2 + \ldots + iK^{i-1} x_1^{i-1} + \ldots = \sum_0^\infty i(Kx_1)^{i-1} . \tag{7}$$

Denoting the product Kx_1 by y, and taking into account that in the case of $y < 1$

$$\sum_{i=1}^{\infty} iy^i = y \sum_{i=1}^{\infty} iy^{i-1} = y \frac{1}{(1-y)^2} \tag{8}$$

we may write:

$$\frac{\overline{M}}{M_1} = \frac{x_1}{(1-Kx_1)^2} = \frac{\dfrac{1}{K+1}}{\left(1-\dfrac{K}{K+1}\right)^2} = K + 1 \tag{9}$$

i.e. using the single-constant MECKE-KEMPTER model for the pure substance:

$$\frac{\overline{M}}{M_1} = \frac{1}{\Sigma n_i} = K + 1 .$$

If cyclic dimers may form in addition to the ideal chain-associations, then a simultaneous association equilibrium is set up in the pure component. In this case the simplifying assumption can be made that the formation of the two hydrogen bridges in the cyclic dimers is accompanied by twice the free enthalpy change for the hydrogen bridges uniting the chain-associations. The equilibrium constant for the chain-association is then:

$$K = \frac{x_i}{x_{i-1}\, x_1} \qquad i = 1, 2, 3, \ldots \tag{10}$$

while the equilibrium constant of cyclic dimerization is:

$$K^* = K^2 = \frac{x^*}{x_1^2} \tag{11}$$

where x^* is the mole fraction of cyclic dimers. If the presence of the cyclic dimers is taken into consideration, the average molecular weight is:

$$\overline{M} = M_1 x_1 + M_2 x_2 + \ldots + M_i x_i + \ldots M_2 x^* . \tag{12}$$

On rearrangement, and introduction of $y = Kx_1$:

$$\frac{\overline{M}}{M_1} = x_1 [2 + 2y + 3y^2 + \ldots + iy^{i-1} + \ldots] + 2y^2$$

which, on the basis of relation (8), can be brought into the following simple form:

$$\frac{\overline{M}}{M_1} = \frac{x_1}{(1-y)^2} + 2y^2 . \tag{13}$$

Let us now seek the relation between the equilibrium constant and the mole fraction of monomers. We know that

$$x_1 + x_2 + x_3 + \ldots + x_i + \ldots + x^* = 1 \tag{14}$$

and thus, using relations (10) and (11):

$$x_1 + Kx_1^2 + K^2 x_1^3 + \ldots + K^{i-1} x_1^i + \ldots + K^2 x_1^2 = 1 . \tag{15}$$

That is:

$$\frac{x_1}{1-y} + y^2 = 1 \tag{16}$$

or

$$x_1 - (1 - y^2)(1 - y) \tag{17}$$

and

$$K = \frac{y}{(1 - y^2)(1 - y)} . \tag{18}$$

If this is substituted into Eq. (13), then according to the above two-constant model:

$$\frac{\overline{M}}{M_1} = \frac{1 - y^2}{1 - y} + 2y^2 . \tag{19}$$

It can be seen from relations (17) and (18) that if $y \to 1$ then $x_1 \to 0$ and $K \to \infty$, *i.e.* this case corresponds to maximum association.

A surprising result is obtained for the average molecular weight in the case of maximum association:

$$\lim_{y \to 1} \frac{\overline{M}}{M_1} = \lim_{y \to 1} \frac{1 - y^2}{1 - y} + 2y^2 = 4 . \tag{19a}$$

The model where the formation of cyclic dimers is also taken into account thus gives the maximum average molecular weight as 4.

The relations derived above are now going to be applied to the pure components. The relevant literature data [3, 4, 6, 7] indicate that if ideal chain-association is assumed for the pure amines, while for the pure alcohols

Table II

Viscosities and degrees of association of alcohols and amines at 20 °C

Component	η [cp]	$\overline{M}$ [g/mol]	$\overline{M}/M_1$	Model applied	K	x_1
methanol	0.584*	116	3.70	ideal chain-association	200	0.005
ethanol	1.200*	164	3.58	+ cyclic dimers	65.8	0.014
1-propanol	2.20*	205	3.48	+ cyclic dimers	42.8	0.021
1-butanol	2.95*	240	3.24	+ cyclic dimers	16.7	0.050
1-heptanol	5.42*	350	3.18	+ cyclic dimers	14.2	0.058
n-propylamine	0.411	95	1.64	ideal chain-association	0.64	0.790
di-*n*-propylamine	0.524	105	1.06	ideal chain-association	0.06	0.943
tri-*n*-propylamine	0.67	123	0.88	ideal chain-association	—	1.000
n-butylamine	0.545	110	1.51	ideal chain-association	0.51	0.663
di-*n*-butylamine	0.900	135	1.05	ideal chain-association	0.05	0.952
tri-*n*-butylamine	1.45	175	0.94	ideal chain-association	—	1.000

* The viscosities of the alcohols are literature data [8].

cyclic dimerization is also taken into account, calculations can be made with the help of the two-constant model. The results thus obtained are listed in Table II.

Comparison of the results reveals that the equilibrium constants calculated from the viscosity agree, as regards order of magnitude, with reported equilibrium constants [4,9] determined by different experimental methods (measurement of thermodynamic and dielectric properties, infrared spectroscopy, etc.). The results calculated from the viscosity, generally give a smaller equilibrium constant and accordingly a higher monomer mole fraction than those of the other methods. This can probably be attributed to the fact that the associations are not chain-like, and thus the reference curve based on the viscosities of the normal hydrocarbons results in a degree of association lower than the actual one, for the viscosity of the branched-chain compound is always less than that of the straight-chain molecule with the same molecular weight. This is also indicated by the fact that a degree of association lower than one was obtained for the tertiary amines. It follows from what has been said that the method needs refining, but even in its present form it is suitable for the estimation of the degree of association and for the demonstration of changes in the extent of association. It is utilized in the evaluation of the viscosity data for the *n*-butylamine–1-butanol mixture.

Viscosity of the 1-butanol–n-butylamine mixture

In the course of its application to the pure materials it was observed that this method gives a reliable qualitative description of the autoassociation of alcohols and amines. Accordingly, an attempt was made to apply it to the 1-butanol–*n*-butylamine mixture. The necessary viscosity data were determined with a Höppler rheoviscometer. The results obtained at 20°C are presented in Table III and Fig. 2.

Table III

Dynamic viscosity of the 1-butanol–n-butylamine mixture as a function of the composition at 20 °C

x_{amine}	η (cp)	$\overline{M}$	$\overline{M}/M_1$
0.0	2.95	240	3.24
0.1	2.51	225	3.04
0.3	1.85	195	2.63
0.5	1.25	164	2.21
0.7	0.95	145	1.96
0.9	0.68	123	1.66
1.0	0.55	110	1.51

The results were evaluated by the earlier procedure, *i.e.* a reference curve based on the viscosities of the normal hydrocarbons was used. When establishing the relation between the average molecular weight and degree of association, use was made of the fact that there is only a negligible difference between the molecular weights of the monomers of the components. Thus,

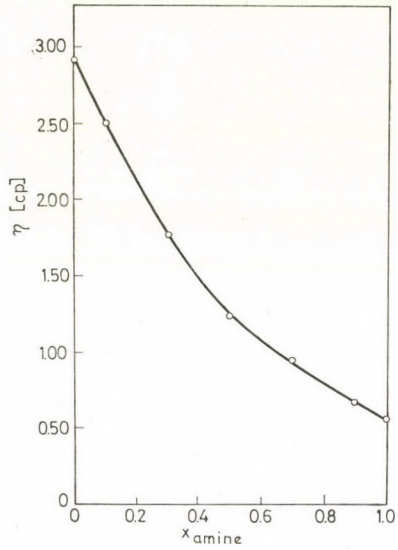

Fig. 2. Viscosity of the *n*-butylamine – 1-butanol mixture as a function of composition at 20 °C

the degree of association can be calculated without attributing any composition, structure or composition ratio to the associations. The results nevertheless permit one to exclude the possibility of simple coupling of the alcohol and amine associations from among the many possible mixed association species. This can be done for the reason that if on mixing the amine and alcohol associations simply combine:

$$A_i + B_j \rightleftharpoons A_i B_j$$

then the only explanation for the exothermic heat of mixing would be that extra hydrogen bonds are formed. It would also explain the negative entropy of mixing, for the coupling of the associates would result in a decrease of the number of particles. However, this is in contrast with the degree of association *vs.* composition relation determined from the viscosity measurements, for it was observed that the decrease of the number of particles was not accompanied by the increase of the average degree of association: instead, the average degree of association of the mixture gradually decreases on proceeding from

the alcohol towards the amine on the concentration scale (Fig. 3). No matter how qualitative we consider the degree of association calculated from the viscosity, it seems beyond doubt that it does not exhibit a maximum as a function of the composition; thus, as regards the conceivable possibilities for the formation of the mixed species, it is possible to exclude those which assume the increase of the average degree of association of mixing.

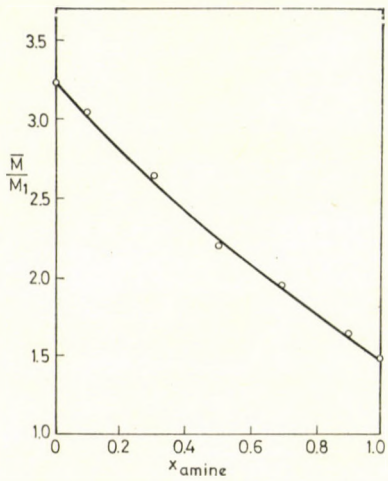

Fig. 3. Average degree of association of the *n*-butylamine – 1-butanol mixture at 20 °C

REFERENCES

[1] RATKOVICS, F., LISZI, J., LÁSZLÓ, A.: Magy. Kém. Foly., **79**, 273 (1973)
[2] RATKOVICS, F., LÁSZLÓ, A.: Magy. Kém. Foly., **79**, 276 (1973)
[3] HUYSKENS, P., HUYSKENS, T. Z.: Bull. Soc. Chim. Belg., **69**, 267 (1960)
[4] KEHIAIAN, H.: Bull. Acad. Polon. Sci. chim., **14**, 703 (1966)
[5] SIGWALT, P.: Chimie macromoléculaire. Soc. Edit. Techn. Paris 1967
[6] PRIGOGINE, I., DEFAY, R.: Chemische Thermodynamik. VEB Deutscher Verlag, Leipzig 1962
[7] VON THIEL, M., BECKER, E. D., PIMENTEL, G. C.: J. Chem. Phys., **27**, 95 (1957)
[8] D'ANS, LAX: Taschenbuch für Chemiker und Physiker. Springer Verlag, Berlin 1967
[9] SADRON, C., BENOIT, H.: J. Chim. Phys., **43**, 145 (1946)
[10] SADRON, C., BENOIT, H.: J. Chim. Phys., **44**, 18 (1947)

Ferenc RATKOVICS
Tamás SALAMON
László DOMONKOS
8201 Veszprém, POB 28. Hungary.

Acta Chimica Academiae Scientiarum Hungaricae, Tomus 83 (1), pp. 63—70 (1974)

PROPERTIES OF ALCOHOL–AMINE MIXTURES, V

HEATS OF MIXING OF DIBUTYLAMINE–NORMAL PRIMARY ALCOHOL MIXTURES

F. RATKOVICS and ZS. GUTI

(Electrochemical Research Group of the Hungarian Academy of Sciences, Department of Physical Chemistry, Chemical Industries of University, Veszprém)

Received October 23, 1973

The heats of mixing of di-*n*-butylamine and normal primary alcohols were measured at 20 ± 1 °C. It was found that the exothermic heat of mixing measured at the equimolar composition practically agrees with the results for the similar mixtures of *n*-butylamine. It turned out that the exothermic heat effect for the alcohol–amine interaction is to a good approximation independent of whether the alcohol molecules interact with a primary or a secondary amine. The data for mixtures with low amine contents revealed that the differences found between the properties of the alcohol–di-*n*-butylamine and alcohol–*n*-butylamine mixtures can be attributed to the different extents of autoassociation of the primary and secondary amines. This assumption was supported by the difference in the endothermic heats of mixing for the *n*-butylamine–*n*-hexadecane and di-*n*-butylamine–*n*-hexadecane mixtures.

An earlier paper [1] dealt with the considerable exothermic heat of mixing for *n*-butylamine–*n*–primary alcohol mixtures. The conclusion was reached that the mixing heat is practically independent of the length of the hydrocarbon chain in the molecules of the alcohol component (the only exception being methanol), and thus can be regarded to a good approximation as the reaction heat accompanying the binding of alcohol and amine molecules. It was also shown that neither the experimental results nor the literature data permit a clear-cut answer to the question of what mixed associations are formed. In this connection a study has been made of the heat effect arising on the mixing of di-*n*-butylamine and normal primary alcohols. The alcohol component was methanol, ethanol, 1-propanol, 1-butanol, or 1-heptanol. The measurements were made as previously [2], at 20 ± 1°C. The experimental results are listed in Tables I—V. The quotient of the heat of mixing and the product of the mole fractions is shown in Fig. 1.

It is immediately clear from both the Figure and the data in the Tables that all the qualitative conclusions made earlier for the *n*-butylamine–alcohol mixtures also hold for the *n*-butylamine–alcohol mixtures. The heat of mixing decreases slightly with the increase of the molecular weight of the alcohol component. With methanol an exceptionally high heat of mixing was found, but in the other cases the results are practically independent of the length of the hydrocarbon chain in the alcohol. It can be said that in these systems the heat of mixing may be attributed to the energy resulting from the interaction of the =NH and —OH groups.

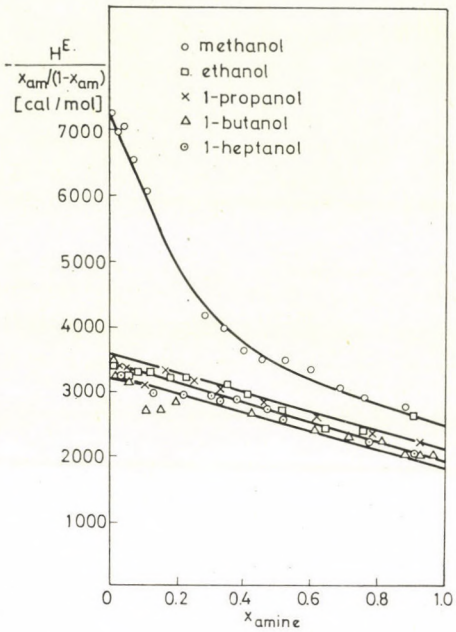

Fig. 1. Quotient of the heat of mixing and the product of the mole fractions in mixtures of di-*n*-butylamine and *n*-primary alcohols at 20 °C

Table I

Heat of mixing of di-n-butylamine and methanol at 20 °C

x_{am}	$-H^E$ (cal/mol)	$-\frac{H^E}{x_{am}(1-x_{am})}$ (cal/mol)
0.008	57.4	7240
0.023	153	6970
0.046	310	740
0.075	453	6520
0.108	582	6070
0.288	848	4130
0.346	907	4020
0.403	935	3660
0.462	913	3510
0.536	874	3490
0.605	795	3330
0.687	653	3040
0.773	509	2900
0.877	304	2790

Table II

Heat of mixing of di-n-butylamine and ethanol at 20 °C

x_{am}	$-H^E$(cal/mol)	$-\frac{H^E}{x_{am}(1-x_{am})}$ (cal/mol)
0.012	39.6	3370
0.025	82	3320
0.051	158	3260
0.080	243	3310
0.119	346	3310
0.178	471	3220
0.230	562	3240
0.351	717	3150
0.410	719	2970
0.515	678	2720
0.638	561	2430
0.747	452	2390
0.901	239	2690

Table III

Heat of mixing of di-n-butylamine and 1-propanol at 20 °C

x_{am}	$-H^E$ (cal/mol)	$-\frac{H^E}{x_{am}(1-x_{am})}$ (cal/mol)
0.019	62.5	3390
0.053	169	3380
0.103	289	3100
0.162	454	3350
0.251	628	3210
0.335	675	3040
0.463	692	2800
0.621	614	2610
0.794	380	2320
0.925	157	2230

A good basis for evaluation is obtained by comparising the results presented here with those found for the primary amine–alcohol mixtures [1].

Let us first consider the values of the heat of mixing for the equimolar mixtures. These are listed in Table VI.

It can be seen that there is practically no difference between the results for the primary and secondary amines. The only difference is observed in the

Table IV

Heat of mixing of di-n-butylamine and 1-butanol at 20 °C

x_{am}	$-H^E$ (cal/mol)	$-\frac{H^E}{x_{am}(1-x_{am})}$ (cal/mol)
0.012	40.5	3490
0.023	74.5	3320
0.035	108	3200
0.063	190	3230
0.104	251	2700
0.146	341	2730
0.197	445	2850
0.380	696	2910
0.436	659	2680
0.513	642	2570
0.616	579	2440
0.713	483	2350
0.805	359	2290
0.881	215	2050
0.919	151	2030
0.957	83.5	2040

Table V

Heat of mixing of di-n-butylamine and 1-heptanol at 20 °C

x_{am}	$-H^E$ (cal/mol)	$-\frac{H^E}{x_{am}(1-x_{am})}$ (cal/mol)
0.033	102	3220
0.127	324	2930
0.224	510	2940
0.310	621	2910
0.336	629	2820
0.379	668	2840
0.476	681	2730
0.621	602	2560
0.778	384	2220
0.914	160	2020

range of low amine concentrations. For a given alcohol the heat of mixing is higher for the secondary than for the primary amine. This can be seen well by comparison of the $H^E/x_{am}(1 - x_{am})$ values extrapolated to zero amine or zero alcohol concentration. This quantity is equal to the difference of the partial

Table VI

Excess enthalpy of primary and secondary butylamine–alcohol mixtures at 20 °C ($x_{am} = 0.5$)

Amine	Alcohol	$-H^E$ (cal/mol)	$-\frac{H^E}{x_{am}(1-x_{am})}$ (cal/mol)
n-butylamine	methanol	975	3900
n-butylamine	ethanol	745	2980
n-butylamine	1-propanol	727	2910
n-butylamine	1-butanol	720	2880
n-butylamine	1-heptanol	670	2680
di-*n*-butylamine	methanol	935	3740
di-*n*-butylamine	ethanol	718	2870
di-*n*-butylamine	1 propanol	705	2820
di-*n*-butylamine	1 butanol	690	2760
di-*n*-butylamine	1-heptanol	685	2740

Table VII

Heats of mixing of amine–alcohol mixtures at 20 °C

Components of the mixture	$-\frac{H^E}{x_{am}(1-x_{am})}$	
	$\lim_{x_{am} \to 0}$	$\lim_{x_{am} \to 1}$
n-butylamine – methanol	4000	2600
di-*n*-butylamine – methanol	7300	2600
n-butylamine – ethanol	2950	2400
di-*n*-butylamine – ethanol	3500	2200
n-butylamine – 1-propanol	2900	2350
di-*n*-butylamine – 1-propanol	3400	2100
n-butylamine – 1-butanol	2850	2200
di-*n*-butylamine – 1-butanol	3400	2050
n-butylamine – 1-heptanol	2700	2150
di-*n*-butylamine – 1-heptanol	3300	2000

molar and the molar enthalpies, or to the differential solution heat determined in infinitely dilute solution. These results are listed in Table VII.

It can be seen from the data that the heats of solution of the alcohols are practically independent of whether the solvent is a primary or a secondary amine. (The difference of 100—150 cal/mol can simply be explained by the higher molecular weight of the secondary amine.) However, the heats of solution of the primary and secondary amines differ considerably. For dissolution

in a given alcohol, the heat of solution of the secondary amine is always higher than that of the primary amine. For dissolution in methanol the difference is 3300 cal/mol, but for the other alcohols it is 450—550 cal/mol, independently of the molecular weight of the solvent alcohol. In our opinion, apart from the exceptional results for the mixtures containing methanol, the higher heat of solution of di-*n*-butylamine can be interpreted by taking into account that several endothermic and exothermic processes proceed simultaneously when amine–alcohol mixtures are formed. The $H^E/x_{am}(1 - x_{am})$ values extrapolated to zero alcohol concentration are characteristic of the alcohol, and arise from the difference of the exothermic heat effects (originating from the amine–alcohol interaction) and the endothermic heat effects (a result of the dissociation of the associated alcohol molecules). It also follows from this that with a high amine excess the alcohol–amine interaction is practically independent of whether the alcohol molecule interacts with a primary or a secondary amine.

The difference of the heats of solution of the amines can be explained in that even at low amine concentrations the energy observed as heat of mixing is the resultant of two enthalpy changes of opposite sign, but the energy necessary for the dissociation of the amines is different for the primary and the seconary amines. If it is assumed that in this concentration range the amine–alcohol interaction energy is to a first approximation independent of whether the alcohol interacts with a primary or a secondary amine, it follows that since a greater endothermic effect must be observed for the more strongly associated primary amine than for the secondary amine, the resultant of the heat effects will be a higher exothermic value for the secondary amines. This agrees with experience. The phenomenon that for all the alcohols (with the exception of methanol) the same difference in the heat of solution (450—550 cal/mol) is observed between the two types of amine permits the conclusion that energy of the amine–alcohol interaction is independent of the molecular weight of the alcohol.

In order to confirm the reality of the above qualitative picture, a study was also made of the heats of mixing in the *n*-butylamine–*n*-hexadecane and di–*n*–butylamine–*n*–hexadecane systems. From these series an answer is obtained to the question of whether it is justified to assume that more energy is required for the dissociation of the associated molecules of the primary amines than for the secondary amines.

In these mixtures the heat of mixing originates predominantly from the energy necessary to split the hydrogen bonds holding the associations together [3]. The experimental results are given in Tables VIII and IX.

The results are plotted in Fig. 2, in a similar manner as previously.

Fig. 2 shows that for *n*–butylamine and di–*n*–butylamine the heat of solution extrapolated to zero concentration is endothermic, 2700 and 920 cal/mol, respectively. These results prove that much more energy is required

Table VIII

Heat of mixing of n-butylamine and n-hexadecane at 20 °C

x_{am}	H^E (cal/mol)	$\frac{H^E}{x_{am}(1-x_{am})}$ (cal/mol)
0.021	56.1	2710
0.085	209	2680
0.163	398	2920
0.227	456	2610
0.337	583	2610
0.514	646	2590

Table IX

Heat of mixing of di-n-butylamine and n-hexadecane at 20 °C

x_{am}	H^E (cal/mol)	$\frac{H^E}{x_{am}(1-x_{am})}$ (cal/mol)
0.040	35.1	910
0.139	115	960
0.277	179	890
0.413	236	970
0.525	251	1000

to dissociate the primary amine associations than those of the secondary amines. This assumption with regard to the alcohol–amine mixtures therefore justified.

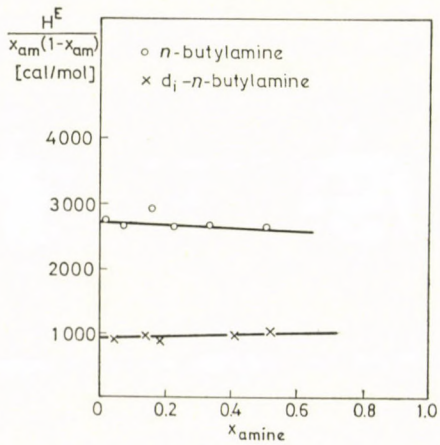

Fig. 2. Heats of mixing of amines and *n*-hexadecane at 20 °C

REFERENCES

[1] RATKOVICS, F., LÁSZLÓ, A.: Magyar Kém. Foly., **79**, 276 (1973)
[2] RATKOVICS, F., LÁSZLÓ, A., LISZI, J.: Magy. Kém. Foly., **79**, 273 (1973)
[3] WÓYCICKA, M. K., RECKO, W. M.: Bull. Acad. Polonaise des Sci. **20**, No 3. 783 (1972)

Ferenc RATKOVICS
Zsuzsanna GUTI
8201 Veszprém, POB 28. Hungary.

Acta Chimica Academiae Scientiarum Hungaricae, Tomus 83 (1), pp. 71—77 (1974)

PROPERTIES OF ALCOHOL–AMINE MIXTURES, VI

A METHOD FOR THE DETERMINATION OF THE AVERAGE DEGREE OF ASSOCIATION

F. RATKOVICS, T. SALAMON and L. DOMONKOS

(Department of Physical Chemistry, University of Veszprém, and Research Group for Electrochemistry of the Hungarian Academy of Sciences)

Received January 21, 1974

The viscosities of normal primary alcohols, normal hydrocarbons and tertiary aliphatic amines have been studied in the temperature range of 233 to 353 °K. The activation enthalpies of viscous flow have been determined, and for normal hydrocarbons and tertiary amines they have been found to be in a linear relationship with the molecular weight, practically independent of the homologous series concerned. Using this function as a calibration curve a molecular weight has been determined for the non-associated component with the same activation enthalpy as that of the alcohol, and this figure has been interpreted as the average molecular weight of alcohol species. It has been found that, in agreement with our previous results, the average degree of association in liquid phase alcohols is about 4, and is affected by temperature. This result can be interpreted by assuming the simultaneous formation of cyclic dimers and chain like associated species, since in this case the maximum degree of association may deviate only slightly from 4. It has also been found that the extent of association tends to decrease from methanol to *n*-heptanol.

In our previous paper [1] we have suggested a method for the determination of the average molecular weights of liquid phase association polymers of alcohols and amines. The method is based on the assumption that a polymer of the associative component has the same viscosity as the hydrocarbon with the same or nearly the same molecular weight.

The relationship between viscosity and the average molecular weight, defined as

$$\overline{M} = \sum_{i=1}^{k} x_i M_i \tag{1}$$

has been given by the equation

$$\eta = k \overline{M}^{\alpha} \tag{2}$$

where k and α are constants, and η is the dynamical viscosity. This paper is concerned with the determination of the average molecular weight for the polymers of normal aliphatic alcohols on the basis of the activation enthalpy of viscous flow (termed here as 'viscous enthalpy'). Viscous enthalpy can be defined as

$$\Delta H = - RT^2 \left(\frac{d \ln \eta}{dT} \right)_p \tag{3}$$

where η is the dynamical viscosity measured at a constant pressure, T is absolute temperature, and $R = 1.98$ cal · mole^{-1}K^{-1}.

Results

The dynamical viscosities of the various components were measured at atmospheric pressure, by a Höppler-type rheoviscosimeter, in the temperature range between —40 and 80 °C. The results, along with literature data, are given in Table I and in Figs 1 and 2.

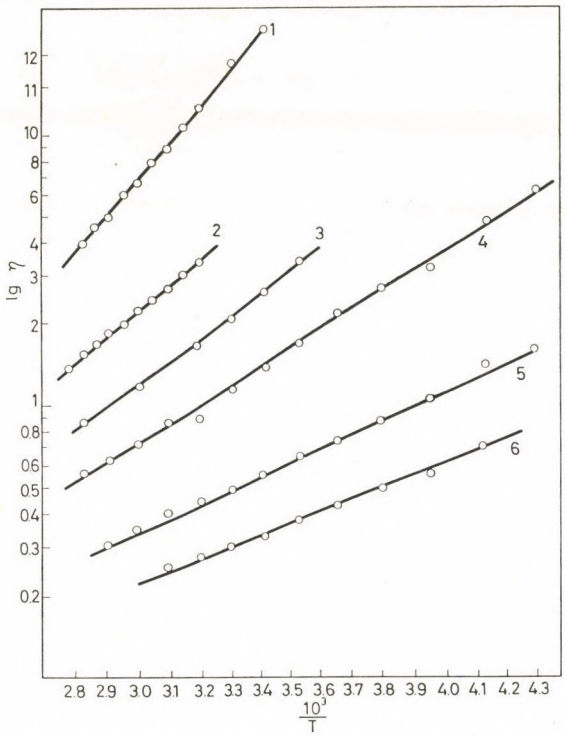

Fig. 1. log η *vs.* T^{-1} plots for *n*-hydrocarbons and tertiary amines.
1. Squalane; 2. eicosane; 3. tri-amylamine; 4. tri-butylamine; 5. tri-propylamine; 6. triethylamine

The diagrams show that when plotting the logarithm of the dynamical viscosity against the reciprocal of absolute temperature, straight lines are obtained for both the alcohols and the tertiary amines investigated. This behaviour is remarkable for alcohols, because the temperature range of the measurements exceeds 100 °K, and thus even if the average degree of association varies strongly as a function of temperature, it cannot be observed in the behaviour of viscous enthalpy. It is, however, also possible that there is a relationship between viscous enthalpy and the average degree of association of alcohols, but in practice the latter is nearly constant over the complete

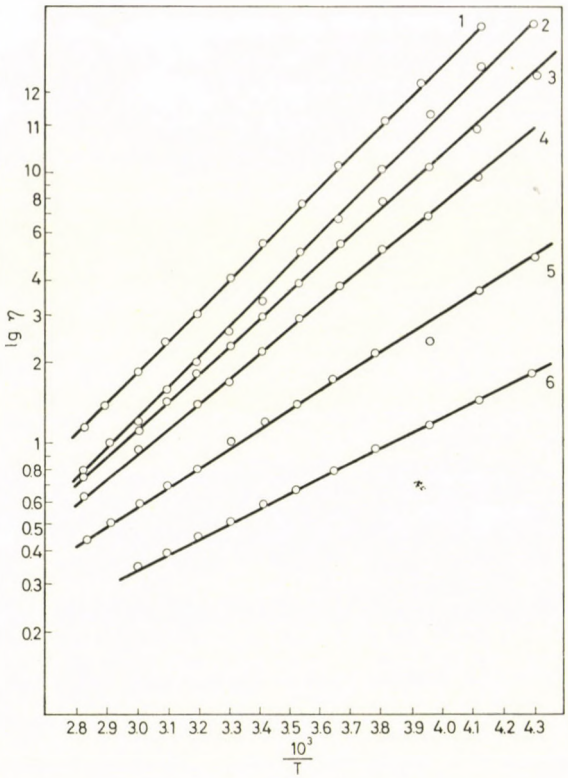

Fig. 2. log η *vs.* T^{-1} plots for normal primary alcohols

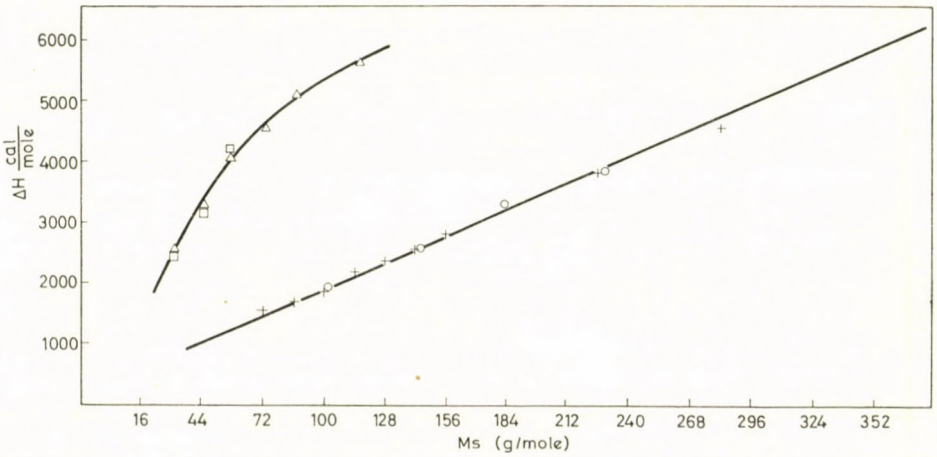

Fig. 3. Viscous enthalpy as a function of the molecular weight

Table I

Dynamical viscosities, in cp, as the functions of temperature

Temperature °K	233	243	253	263	273	283	293	303	313	323	333	343	353	Ref.
Methanol	1.75	1.39	1.16	0.970	0.817	0.686	0.584	0.510	0.450	0.396	0.350	—	—	[2]
Ethanol	4.79	3.65	2.38	2.23	1.78	1.46	1.19	1.0	0.825	0.701	0.591	0.503	0.43	[2]
1-Propanol	13.5	9.5	6.9	5.1	3.85	2.89	2.20	1.72	1.38	—	0.92	—	0.63	[2]
1-Butanol	22.4	14.1	10.3	7.41	5.18	3.86	2.94	2.28	1.79	1.41	1.14	0.76	0.74	
1-Pentanol	34.8	24.5	16.3	10.24	6.69	5.04	3.30	2.52	1.92	1.52	1.17	0.97	0.77	
1-Heptanol	—	34.21	21.89	16.30	10.56	7.62	5.42	3.97	2.99	2.25	1.82	1.37	1.11	
Triethylamine	—	0.708	0.569	0.509	0.440	0.385	0.330	0.303	0.275	0.251	—	—	—	
Tri-*n*-propylamine	1.61	1.431	1.087	0.894	0.725	0.642	0.555	0.495	0.445	0.399	0.353	0.312	—	
Tri-*n*-butylamine	6.25	4.98	3.33	2.73	2.22	1.70	1.39	1.17	0.903	0.863	0.863	0.731	0.572	
Tri-*n*-amylamine	—	—	4.72	—	—	3.43	2.62	2.06	1.67	—	1.17	—	0.87	[2]
n-Hexane	0.611	—	0.486	0.432	0.383	0.342	0.308	0.278	0.252	0.230	0.210	—	—	[3]
n-Heptane	0.865	—	0.682	0.600	0.525	0.464	0.413	0.370	0.334	0.302	0.274	—	0.230	[3]
n-Octane	1.22	—	0.955	0.828	0.714	0.621	0.546	0.485	0.433	0.389	0.351	—	0.291	[3]
n-Nonane	1.73	—	1.332	1.138	0.964	0.823	0.713	0.625	0.553	0.493	0.441	—	0.361	[3]
n-Decane	—	—	—	—	1.298	—	0.907	—	—	0.601	—	—	0.452	[3]
n-Undecane	—	—	—	2.167	—	—	1.186	—	—	0.761	—	—	—	[4]
n-Hexadecane	—	—	—	—	—	—	3.174	2.403	1.945	1.596	1.339	1.128	—	
n-Eicosane	—	—	—	—	—	—	—	—	3.421	2.688	2.238	1.871	1.559	
Hexamethyltetracosane	—	—	—	—	—	—	25.11	18.60	12.43	8.80	6.53	4.89	3.93	

temperature range of the liquid phase. This latter possibility is supported by the fact that alcohols contain free monomeric molecules only in very small amounts, *i.e.* are associated practically completely, even at temperatures close to their boiling points. It has been shown in our previous paper [1] that the maximum degree of association is 4 if a simultaneous cyclic dimerization and ideal infinite chain association is assumed. (The simplifications applied in the derivation may affect the final result to only a minor extent.) Therefore, even at temperatures considerably lower than the boiling point, the observed degree of association may not be much higher than near the boiling point. Consequently, similarly to *n*-paraffins and tertiary amines, the viscous enthalpy of alcohols is in practice also independent of temperature over the range of measurements.

Table II

Molecular weights and viscous enthalpies of the components

Component	Mol. weight g/mole	Viscous enthalpy cal/mole	Ref.
n-Pentane	72.15	1510	[5]
n-Hexane	86.18	1660	
n-Heptane	100.21	1895	
Triethylamine	101.19	1950	
n-Octane	114.23	2162	
n-Nonane	128.50	2344	
n-Decane	142.29	2573	
tri-*n*-Propylamine	143.27	2550	
n-Undecane	156.31	2810	
tri-*n*-Butylamine	185.36	3350	
n-Hexadecane	226.45	3860	
tri-*n*-Amylamine	227.44	3800	
n-Eicosane	282.56	4580	
Methanol	32.04	2568	
		2465± 40	[5]
Ethanol	46.07	3348	
		3225±130	[5]
1-Propanol	60.09	4170	
1-Butanol	74.12	4270±280	[5]
		4620	
1-Pentanol	88.15	5106	
1-Heptanol	116.20	5618	
Hexamethyltetracosane (squalane)	422.83	6430	

Table III

Degrees of polymerization for normal alcohols and tertiary amines

Component	Average degree of association, $\overline{M}/M$		
	From viscosities	From viscous energies	
		This work	Ref. [5]
Methanol	3.70	4.43	4.31
Ethanol	3.58	4.16	4.00
1-Propanol	3.48	4.04	4.06
1-Butanol	3.24	3.66	
1-Pentanol	—	3.40	
1-Heptanol	3.18	2.85	
tri-*n*-Propylamine	0.88	1	
tri-*n*-Butylamine	0.94	1	

The appropriate values of viscous enthalpy were calculated from the data given in Table I, on the basis of Eq. (3), with the method of least squares. The results, along with literature data, are listed in Table II. A plot of the viscous enthalpy against the molecular weights of the components is shown in Fig. 3. It can be seen clearly that in this type of plot the viscous enthalpies of paraffin hydrocarbons and aliphatic tertiary amines fall onto the same straight line, and vary linearly with the molecular weight. The viscous enthalpies of the alcohols investigated also increase with the molecular weight, but the relationship is non-linear, and the enthalpy values are substantially higher than those of hydrocarbons or triamines at about the same molecular weight. This phenomenon can be interpreted as follows.

The viscous enthalpy of hydrocarbons and tertiary amines depends, as can be seen in Fig. 3, primarily on the size of molecules, hence, according to the hole theory, on the number of atomic groups constituting the molecule. For these compounds the contributions to the molecular weight of CH_3 and CH_2 groups can be regarded practically the same as that of the nitrogen of tertiary amines. Consequently, the viscous enthalpy in either homologous series varies in the same way with the molecular weight. If this linear relationship for hydrocarbons and tertiary amines between the viscous enthalpy and the molecular weight is applied as a 'calibration curve', it can be used to determine an apparent molecular weight for normal aliphatic alcohols from the viscous enthalpy. According to the model of associated mixtures the molecular weight of the non-associated component, that has the same viscosity as the alcohol, is equal to the average molecular weight of the association polymers of the alcohol.

The degree of polymerization for normal alcohols calculated from the viscous enthalpy are listed in Table III, along with similar data calculated from the dynamical viscosities measured at 20°C, and given in our previous paper [1]. The results obtained from diverse sources are in a satisfactory agreement. It can be seen that one cannot decide unambiguously which is the more reliable method in the case of normal alcohols, but from the data on tertiary amines the comparison of viscous enthalpies appears to be more preferable. (The degree of polymerization of tertiary amines is 1, as they are unable to form hydrogen-bonded species.) For the first three members of the homologous series the calculated degree of association is greater than 4. This indicates primarily that the simplifying assumptions introduced in the derivation of the limiting degree of association are not completely valid. The discrepancy is probably the consequence of the fact that the change in standard free enthalpy of cyclic dimerzation is not exactly twice as high as that of chain formation. A lower value, which may be attributed to sterical reasons, could explain why the average degree of association may slightly exceed the value of 4, because under these conditions the equilibrium would be shifted towards chain association, increasing thereby the average degree of association.

We believe that the method presented here can be applied not only to the determination of the average degree of association but also to gain information, in certain cases, on the nature of association.

REFERENCES

[1] RATKOVICS, F., SALAMON, T., DOMONKOS, L.: Acta Chim. (Budapest), to be published
[2] RAZNJEVIC, K.: Hőtechnikai táblázatok. Műszaki Könyvkiadó, Budapest, Zágráb 1964
[3] D'ANS LAX: Taschenbuch für Chemiker und Physiker, Band I. Springer Verlag Berlin—Heidelberg—New York 1967
[4] HODGMAN: Handbook of Chemistry and Physics. Chemical Rubber Publishing Company, London 1959
[5] MOELWYN-HOGHES, E. A.: Physical Chemistry. Pergamon Press, New York 1957

Ferenc RATKOVICS
Tamás SALAMON
László DOMONKOS
8201 Veszprém, POB 28- Hungary.

Acta Chimica Academiae Scientiarum Hungaricae, Tomus 83 (1), pp. 79—89 (1974)

HERSTELLUNG UND UNTERSUCHUNG VON METALLHALTIGEN POLYMEREN MIT KOORDINATIVEN BINDUNGEN, I

REAKTION VON POLYESTERN MIT ZnO

I. VANCSÓ-SZMERCSÁNYI und P. HIRSCHBERG

(Forschungsinstitut der Kunststoffindustrie, Budapest)

Eingegangen am 18. Juni 1973

Es wurde die Weiterpolymerisation von Polyestern mit freien kettenendständigen COOH-Gruppen sowie von neutralen Polyestern durch koordinative Bindungen untersucht. Die Publikation berichtet vor allem über experimentelle Resultate, die für Polyester mit freien kettenendständigen COOH-Gruppen und Zink als Zentralatom erhalten wurden. Falls das Zinkatom in Oxidform in das System eingeführt wird, reagiert es infolge seiner Basenanhydrid-Natur im ersten Schritt in einer ionischen Reaktion mit den COOH-Gruppen. Das gebildete Metallcarboxylat ist dann zu weiteren koordinativen Reaktionen fähig, wobei der Mechanismus in entscheidendem Maße durch das Mengenverhältnis des zentralen Metallatoms und des Liganden bestimmt wird.

Nach den Ergebnissen der Untersuchungen ist das in Gegenwart von neutralen Polyestern aus Essigsäure und Zinkoxid *in situ* gebildete Salz hinsichtlich einer weiteren, mit Polyester verlaufenden Reaktion von koordinativem Charakter ebenfalls wirksam. Diese Reaktion ergibt einen äußerst thixotropen Polyester mit höherem Molekulargewicht. Hingegen findet die koordinative Reaktion zwischen Zinkacetat und Polyester unter den gegebenen Umständen nicht statt.

In unseren früheren Mitteilungen [1, 2] wurden Ergebnisse behandelt, die in unserem Laboratorium in Versuchen über die Reaktion von niedrigmolekularen Polyestern (Mol. gew. 1000—2000) mit Metalloxiden vom Baseanhydrid-Typ, vor allem mit MgO erhalten wurden. Dabei wurde festgestellt, daß eine Salzbildung zwischen den kettenendständigen COOH-Gruppen des Polyesters (Oligoester) und dem basischen Metalloxid stattfindet. Anschließend verläuft eine weitere Reaktion des gebildeten Salzes bzw. des daraus entstehenden Ions mit den Esterbindungen des Polyesters. Letztere Reaktion beruht auf dem Entstehen koordinativer Bindungen. Das Endprodukt ist eine sehr hochmolekulare Verbindung, in der die Polyestermoleküle des Ausgangsmaterials durch Metallatome gemäß nachstehenden Schemas miteinander verbunden sind:

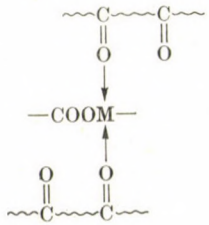

Diese Reaktionen, deren Mechanismus ziemlich kompliziert und nur im großen und ganzen geklärt ist, führten zu makromolekularen Komplexverbindungen.

Die verschiedenartig gebundenen Sauerstoffatome des als Ausgangsmaterial dienenden Polyesters können sich bei Komplexreaktionen als Elektronendonor verhalten. Die Polyestermoleküle können demgemäß als mehrzahnige gemischte Liganden betrachtet werden.

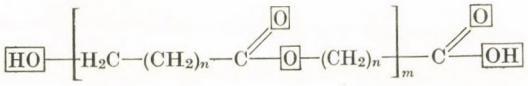

Bei näherer Betrachtung des ersten Schritts der angeführten Reihe von Reaktionen, namentlich der Salzbildung mit den COOH-Gruppen trifft man auf folgende Vorgänge.

Der saure Polyester wurde in einem organischen Lösungsmittel gelöst und darin ein kristallines Metalloxid mit Basenanhydrid-Charakter (Teilchengröße einige Mikrometer) suspendiert. Infolge der auf der Oberfläche der kristallinen Metalloxidteilchen mit den entständigen COOH-Gruppen der Polyestermoleküle verlaufenden Reaktion verschwinden nach einiger Zeit die Metalloxidkristalle aus dem System; das Metall wird in Form eines Salzes bzw. Carboxylat-Metallkomplexes molekular dispergiert (die im Verhältnis zu den COOH-Gruppen überschüssigen Metalloxid-Kristalle bilden dabei selbstverständlich auch im weiteren ein heterogenes System). Diese Reaktion ist diffusions kontrolliert. Ihre Geschwindigkeit ist vor allem von der »elektrischen Feldstärke« zwischen der Metallverbindung und dem Liganden abhängig. Je stärker der basische Charakter des Metalloxids ist, desto höher ist die Geschwindigkeit, mit der die Metalloxid-Kristalle aus dem System verschwinden.

Die weitere Koordinierung des entstandenen Salzes bzw. der Komplexverbindung sowie der daraus gegebenenfalls entstehenden Ionen durch die Esterbindungen des Oligoesters (Polyesters) hängt ebenfalls stark vom Charakter des zentralen Metallatoms ab.

Im vorliegenden Aufsatz werden vor allem Systeme behandelt, in denen das zentrale Metallatom Zink ist. Aus Literaturangaben [3, 4] ist bekannt, daß Zinkchelate stabiler als Magnesiumchelate sind. Auch im Verhalten gegenüber Wasser zeigt sich ein wesentlicher Unterschied. Nach unseren früheren Versuchen [5] sind z. B. aus bestimmten Dicarbonsäuren (Maleinsäure, Fumarsäure, Bernsteinsäure usw.) hergestellte Magnesiumkomplexe in Wasser gut löslich und können aus ihren wäßrigen Lösungen unter Bindung von beträchtlichen Mengen an Kristallwasser (4—5 Mol) kristallisiert werden. Dagegen werden aus Dicarbonsäuren mit Zinkionen hergestellte Komplexe aus Wasser in Form von Polymeren abgeschieden. Die herauspräparierte Verbindung

enthält äußererst wenig Wasser (1 Mol pro Metallatom) oder ist wasserfrei. Diese polymeren Carboxylatverbindungen sind praktisch weder in Wasser noch in organischen Lösungsmitteln löslich, sind jedoch durch Säuren und Alkalien zersetzbar.

Auf Versuchsergebnisse bezüglich der Zinkkomplexe mit Dikarbonsäuren soll an Hand des Beispiels Zinkmaleat im weiteren noch eingegangen werden.

Experimenteller Teil

In dieser Arbeit werden Prüfergebnisse der Reaktionen von Zinkverbindungen, vor allem Zinkoxid mit folgenden Liganden behandelt:

— Dicarbonsäuren;
— saurer Polyester (Kettenendgruppen: COOH bzw. alkoholische OH-Gruppe)
— neutraler Polyester (Endgruppe an beiden Enden der Kette: alkoholische OH-Gruppe).

Herstellung der Zinkkomplexe von Dicarbonsäuren in wäßrigem Medium

1 : 1-Komplex. Dieser Komplex wurde nach zwei Verfahren hergestellt:

a) Zinkoxid wurde in Wasser suspendiert und die äquivalente Menge an Dicarbonsäure bei 60 °C in Form ihrer wäßrigen Lösung oder Suspension stufenweise zugegeben.

b) Die wäßrige Lösung bzw. Suspension der Dicarbonsäure wurde mit Natriumhydroxid neutralisiert und die äquivalente Menge an Zinkchlorid, in Wasser gelöst, bei 60 °C unter ständigem Rühren zugefügt.

Die entstehenden Komplexe sind sowohl in Wasser als in organischen Lösungsmitteln äußerst wenig löslich oder unlöslich und sind unschmelzbar. Ihre Bruttoformel ist

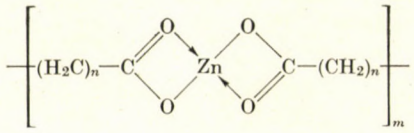

Herstellung des sauren Polyesters

1.2 Propylenglykol, Äthylenglykol, Maleinsäure und Phtalsäure wurden in äquivalentem Säure : Alkohol-Verhältnis, unter Stickstoff, bei einer Maximaltemperatur von 180 °C in der Schmelze kondensiert. Die Polykondensation wurde beim Erreichen eines Molekulargewichts von 700 bzw. 1000 unterbrochen. Die Komplexierversuche wurden mit der Lösung des erhaltenen Polyesters (Oligoesters) in monomerem Styrol (65 Gew.-teile Polyester, 35 Gew.-teile Styrol) durchgeführt.

Herstellung des neutralen Polyesters

Sebacinsäure und Äthylenglykol wurden äquimolar vermischt und in der Schmelze kondensiert, unter stufenweiser Steigerung der Temperatur bis maximal 190 °C. Nach Erreichen eines durchschnittlichen Molekulargewichts von 1300 wurden pro Mol sauren Polyesters 2 Mol Äthylenglykol zur Schmelze gegeben und die Kondensation wurde bis zum völligen Verschwinden der COOH-Gruppen fortgesetzt. Das überschüssige Äthylenglykol wurde im Vakuum abdestilliert. In den Komplexierversuchen wurde die 50%ige Lösung des erhaltenen neutralen Polyesters in Toluol verwendet.

Untersuchung der Zinkverbindungen von Dicarbonsäuren

Die aus Dicarbonsäuren hergestellten Metallcarboxylat-Verbindungen wurden nach verschiedenen Methoden geprüft. In Abb. 1 sind die Derivatogramme der nach den zwei verschiedenen Verfahren hergestellten Zinkmaleat-Polymeren dargestellt. Die Derivatogramme stimmen vollkommen überein, d. h. bei den auf zweierlei Art synthetisierten Komplexen handelt es sich um

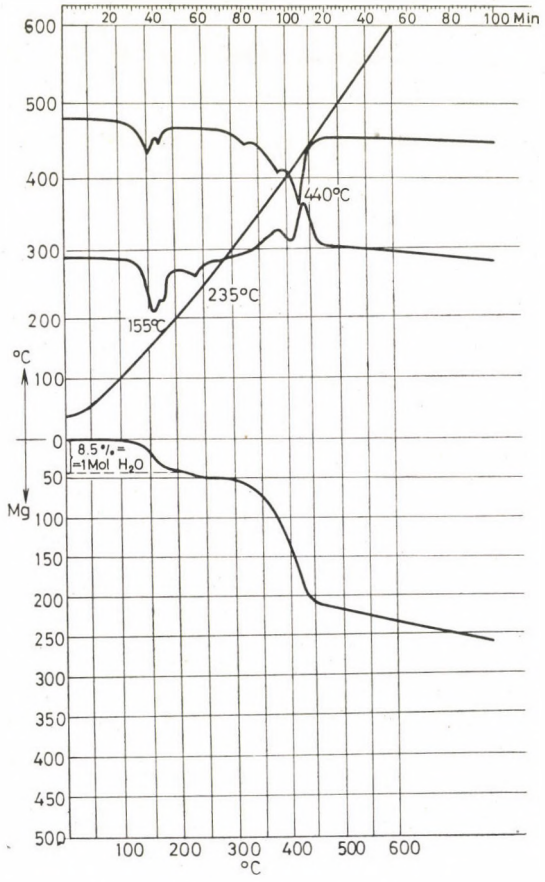

Abb. 1. Derivatogramm von Zinkmaleat

dieselbe Verbindung. Aus den DTA- und TG-Kurven geht hervor, daß bei einer Spitztemperatur von 155° C ein Gewichtsverlust von 8,5% auftritt. Dieser entspricht einem Mol Kristallwasser pro Zinkatom (die qualitative Untersuchung des abgespaltenen Wassers wurde auch nach einer anderen Methode durchgeführt).

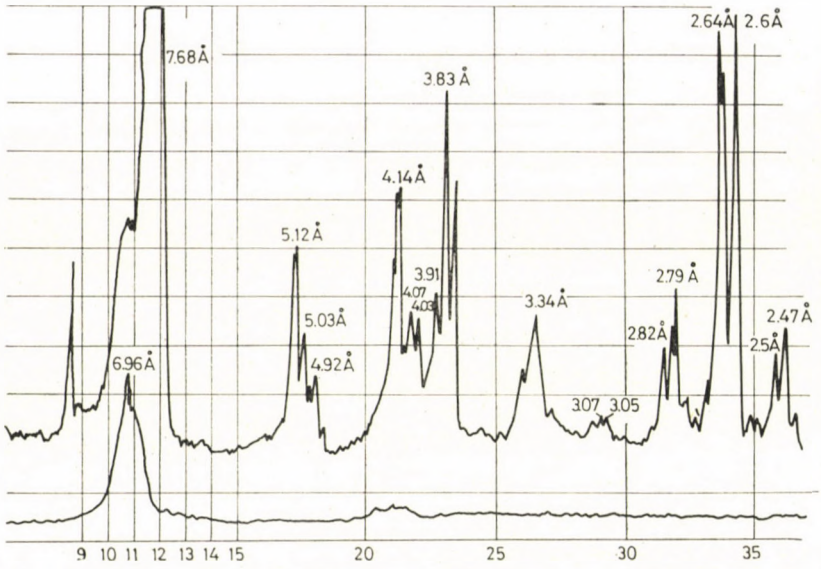

Abb. 2. Röntgendispersionsaufnahme von Zinkmaleat
Oberes Bild: Monohydrat; unteres Bild: dehydratierte Form

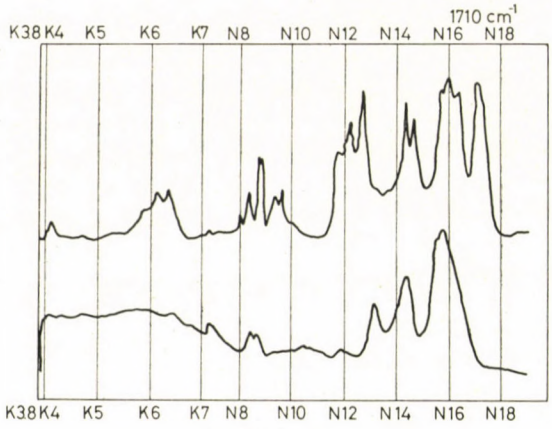

Abb. 3. IR-Spektren von Zinkmaleat (unten) und Maleinsäure (oben)

Abb. 2 zeigt Röntgendispersionsaufnahmen von Zinkmaleat-Monohydrat bzw. bei 150° C dehydratiertem Zinkmaleat. Wie ersichtlich, wird die Kristallstruktur durch das Dehydratieren wesentlich vereinfacht.

In Abb. 3 sind die Infrarot-Spektren des Zinkmaleats und der Maleinsäure dargestellt. Das Verschwinden der COOH-Bande bei 1710 cm^{-1} im

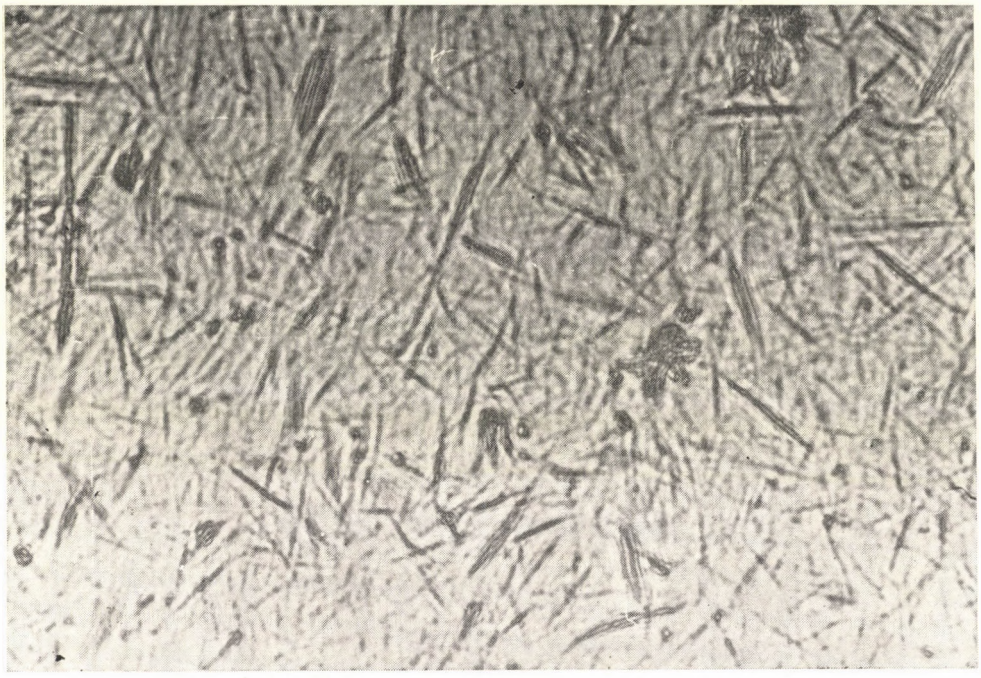

Abb. 4. Mikroskopisches Bild (882×) von Zinkmaleat-Monohydrat

Spektrum des Zinkmaleats weist eindeutig auf die Reaktion der Carboxylgruppen hin.

Abb. 4 ist eine mikroskopische Aufnahme des Zinkmaleat-Monohydrats, worin die faserige Struktur des Polymeren deutlich erkannt wird.

Untersuchung der aus saurem Polyester mit Zink als Zentralatom hergestellten komplexen Makromoleküle

Aus dem beschriebenen sauren Polyester wurden durch Reaktion mit Zinkoxid komplexe Polymere hergestellt, wobei die Menge des Zinkoxids unterschiedlich gewählt wurde.

1. *Äquivalent COOH zu 0,5 Äquivalenten ZnO*

Die Reaktion wurde nach dem Vermischen des Zinkoxids in die Lösung des Polyesters durch kontinuierliches Messen der Viskositätzunahme bei 25 °C verfolgt. (Das verwendete Gerät war Rheotest Type RV.) Eine der Proben enthielt 0,20%, die andere 1,20% Wasser. Die zeitliche Änderung der Viskosität ist in Abb. 5 dargestellt.

Aus der Abbildung geht folgendes hervor: Höhere Wassermengen steigern die Reaktionsgeschwindigkeit; die Erhöhung der Temperatur bewirkt das gleiche. Nach einer bestimmten Zeit hört jedoch die Viskositätszunahme auf. Bei geringerem Wassergehalt stellte sich dieser konstante Zustand bei einem höheren Viskositätswert ein. Die Erklärung dieser Erscheinung ist vermutlich folgende: da im gegebenen Fall die COOH-Gruppen in stöchiometri-

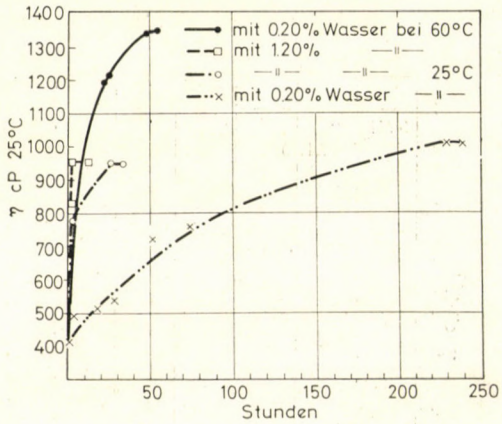

Abb. 5. Viskosität einer pro Äquivalent Carboxyl-Endgruppe 0,5 Äquivalente Zink oxid enthaltenden Polyesterlösung in Abhängigkeit von der Reaktionszeit

schem Überschuß bezogen auf Zinkoxid vorliegen, gelangen, in Gegenwart von Wasser, infolge der Dissoziation der Carboxylgruppen, Wasserstoffionen in das System. Es erfolgt ein teilweiser Austausch der gebildeten Salzkomplexe mit den Protonen, eine Reaktion, die zum Gleichgewicht führt.

Die Lage des Gleichgewichts ist von der Dissoziation der COOH-Gruppen, folglich vom Wassergehalt abhängig. Je weniger Wasser im System vorliegt, desto höher ist die Konzentration des Komplexes bei der sich das Gleich-

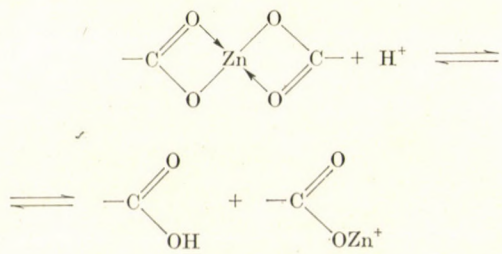

gewicht einstellt, d. h. desto höher ist die Viskosität beim Gleichgewicht. Im untersuchten Fall verläuft, allen Anzeichen nach, außer dem Verbinden der

endständigen COOH-Gruppen, keinerlei sekundäre koordinative Reaktion mit den Estergruppen.

Ergebnisse abweichenden Charakters wurden bei erhöhtem Zinkoxidverhältnis erhalten.

1 *Äquivalent COOH zu* 2,1 *Äquivalenten ZnO*

Hier wurde die Wirkung des Wassergehalts auf die Viskosität in einem breiteren Bereich untersucht. Die bei 45° C gewonnenen Ergebnisse sind in Abb. 6 dargestellt.

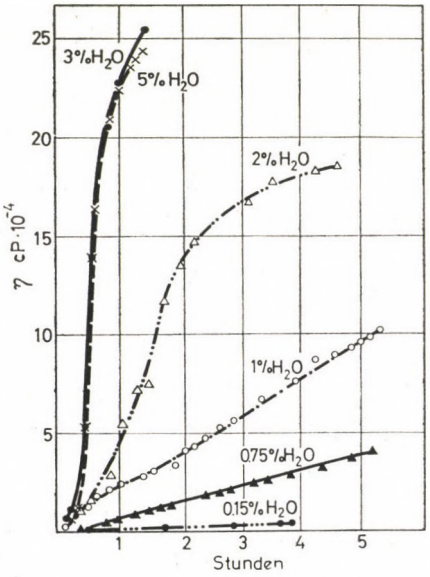

Abb. 6. Wirkung des Wassergehalts auf die Viskosität des Reaktionsgemisches aus Polyesterlösung und Zinkoxid

Wie ersichtlich, wirkt die Steigerung des Wassergehalts äußert günstig auf die Viskositätszunahme. Sogar durch 5% Wasser wird die Viskosität nicht herabgesetzt, im Gegensatz zu unseren Versuchen mit Magnesiumoxid, wo geringe Wassermengen zwar positiv wirkten, jedoch Wasser über 1% bereits die erreichbare maximale Viskosität verringerte. Die Erscheinung kann folgendermaßen erklärt werden: Wie bereits gesagt wurde, ist die Gegenwart einer geringen Wassermenge zur Salzbildung unerläßlich, da nur durch sie die Dissoziation der COOH-Gruppen erfolgen kann. Aus den Versuchen folgerten wird, daß im Fall von Zinkoxid eine größere Wassermenge als bei Magnesiumoxid nötig ist, um die Reaktion mit dem Polyester hervorzurufen. Andererseits ist aber Magnesium als Zentralatom viel mehr zur Bildung von Aquokomplexen geneigt als Zink. Es kann demgemäß angenommen werden, daß das koordinierte

Wasser in bestimmten Fällen die Magnesiumverbindung blockiert, so daß keine weiteren Komplexbindungen mit den im System vorliegenden sonstigen Liganden zustande kommen können. Höhere Mengen an Wasser (oberhalb 1%) hindern demnach die Bildung von Magnesium-Polyester Polymerenkomplexen, fördern dagegen die Bildung von Zink-Carboxylat-Komplexen. Da nun die Zink-Carboxylat-Komplexe wenig oder überhaupt nicht zur Bildung von

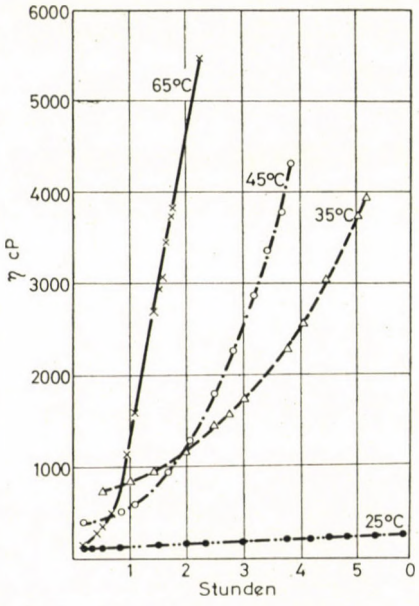

Abb. 7. Zeitliche Veränderung der Viskosität des Reaktionsgemisches aus Polyesterlösung und Zinkoxid bei verschiedenen Temperaturen

Aquokomplexen neigen, stört das anwesende Wasser die weitere Koordinierung in keiner Weise.

Die Wirkung der Temperatur in Gegenwart von 0,20% Wasser auf die Zunahme der Viskosität ist in Abb. 7 dargestellt. Wie ersichtlich, ist die Reaktion des Zinkoxids mit saurem Polyester stark temperaturabhängig.

Die Viskosität wurde auch bei verschiedenen Umdrehungszahlen gemessen. Dabei wurde bei hohen Viskositätswerten (20 000 cP) eine mäßige Thixotropie festgestellt.

Herstellung von polymeren Komplexverbindungen aus neutralem Polyester

Um den Komplexbildner unabhängig von den kettenendständigen Carboxylgruppen herzustellen, wurden folgende Versuche durchgeführt: in die Lösung des neutralen Polyesters (mit alkoholischen OH-Gruppen an beiden

Enden der Kette) wurden Essigsäure und eine damit äquivalente Menge Zinkoxid eingerührt. Das Verhältnis der Reagenzien betrug 4 Äquivalente Essigsäure bzw. Zinkoxid pro Molekül Polyester. Ein Polyester-Molekül enthielt durchschnittlich 11,2 Estergruppen. Wasser war im System nur in Spuren anwesend. Nach dem Mischen der Reagenzien wird das System stehen gelassen und von Zeit zu Zeit eine Probe entnommen, deren Viskosität mit einem

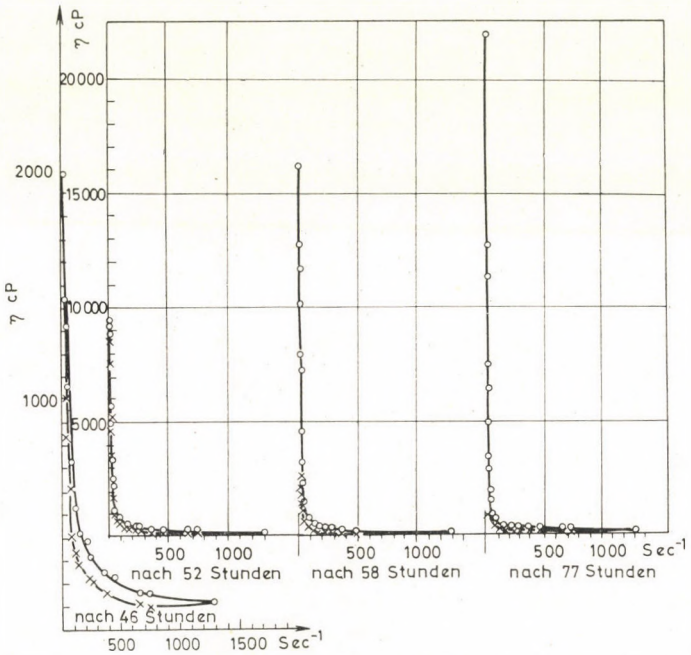

Abb. 8. Thixotrope Hysteresekurven bei einer neutralen Polyesterlösung in Gegenwart der aus Essigsäure und Zinkoxid im Reaktionsgemisch entstandenen Ionen

Rotationsviskosimeter bei 50°C und verschiedenen Umdrehungszahlen gemessen wurde. Die Ergebnisse waren überraschend: es wurde eine starke Thixotropie des Systems beobachtet. Aus den Kurven in Abb. 8 kann festgestellt werden, daß — nach 77 Stunden dauerndem Stehen — die Viskosität, in Abhängigkeit von der Umdrehungszahl, Werte zwischen >100 cP und 22 000 cP aufwies. Gegenüber diesem äußerst starken Effekt wurde, wenn die Salzbildung mit den endständigen COOH-Gruppen des Oligoesters (Polyesters) erfolgt, zwar eine bedeutende Zunahme der Viskosität beobachtet, jedoch trat Thioxtropie in einem unvergleichbar geringeren Ausmaß auf. Der Unterschied steht unbedingt mit dem Unterschied in der Molekularstruktur der zwei verschiedenartigen Komplexe in Zusammenhang.

Wird das Zinkacetat nicht *in situ* im System gebildet, sondern in Salzform zur Lösung des neutralen Polyesters zugefügt, so bleibt die ursprüngliche Viskosität der Lösung selbst nach längerem Erwärmen (48 Stunden) und intensivem Rühren unverändert.

Zusammenfassung der Ergebnisse

Es wurde die Weiterpolymerisation von Polyestern mit freien kettenendständigen COOH-Gruppen sowie von neutralen Polyestern durch koordinative Bindungen untersucht. Das zentrale Metallatom war dabei Zink. Der Polyester als mehrzahniger gemischter Ligand ist zu verschiedenen Reaktionen mit Zinkverbindungen fähig. Gelangt das Zinkatom in Oxidform in das System, so reagiert es infolge seiner Basenanhydrid-Natur zunächst derart mit den freien COOH-Gruppen, daß ionische Bindungen entstehen. Der auf diese Weise gebildete Carboxylatkomplex bildet dann weitere koordinative Bindungen. Der Reaktionsmechanismus wird unter anderem durch das Mengenverhältnis der Reaktionspartner bestimmt. Überschreitet die Menge der Zinkatome die äquivalente Menge im Vergleich zu den COOH-Gruppen nicht, so werden die Polyestermoleküle paarweise über die COOH-Gruppen durch das Metallatom verbunden. Oberhalb der äquivalenten Zinkoxidmenge tritt jedoch die entstehende, koordinativ vermutlich nicht gesättigte Carboxylatverbindung offensichtlich mit den Carbonylgruppen der Esterbindungen in Wechselwirkung. Derart werden nun die Polyestermoleküle nicht mehr paarweise, sondern zu Polymeren mit recht hohem Molekulargewicht verbunden. Ergebnisse von Modellversuchen mit Zinkoxyd bzw. Zinkchlorid und Dicarbonsäuren konnten mit den bei sauren Polyestern erhaltenen Ergebnissen in Korrelation gebracht werden.

Bei neutralem Polyester, an dessen beiden Enden alkoholische OH-Gruppen stehen, ergab sich aus den Viskositätsmessungen, daß eine aus Essigsäure und Zinkoxyd *in situ* gebildete Verbindung hinsichtlich einer weiteren koordinativen Reaktion wirksam ist. Diese Reaktion führt zu äußerst thixotropen Lösungen des entstehenden Polymeren.

LITERATUR

[1] Vancsó-Szmercsányi, I., Vöő, E.: Kunststoffe, **58**, 907 (1968)
[2] Vancsó-Szmercsányi, I.: Kunstsoffe, **60**, 1066 (1970)
[3] Jazimirsky, K. B.: Zh. Neorg. Chim., **5**, 264 (1960)
[4] Inczédi, J.: Die Analytik von Komplex-Gleichgewichten (ung.). Műszaki Könyvkiadó, Budapest, S. 307—308, 310—311, 313.
[5] Vancsó-Szmercsányi, I.: Wysokomol. Soed., **15**, 380 (1972)

Ibolya Vancsó-Szmercsányi
Péter Hirschberg
1950 Budapest, Hungária krt. 114. Ungarn.

Acta Chimica Academiae Scientiarum Hungaricae, Tomus 83 (1), pp. 91—94 (1974)

SOLANUM GLYCOSIDES, IX*
SOLANUM OLERACEUM

P. BITE and M. M. SHABANA

(Research Institute for Pharmaceutical Chemistry, Budapest, and Pharmacognosy Department, Faculty of Pharmacy, Cairo University)

Received August 6, 1973

The unripe fruits of *Solanum oleraceum* were found to contain solasonine and solamargine; a third unidentified steroid glycoside was also detected in trace amounts.

Introduction

During our search for new sources of steroid hormon precursors of new Solanum species, the National Agrobotanical Institute of Tápiószele, Hungary, sent us a Solanum plant which they identified as *Solanum oleraceum*. Upon reviewing the literature, it was found that no study had been made concerning this particular species. It has been of interest to carry out phytochemical study of this plant which might prove to contain valuable steroidal constituents.

Experimental

All m.p.'s were determined with a Boetius apparatus, and were uncorrected. The following solvent systems were used for chromatography:

a) chloroform–methanol–water (65 : 35 : 10) [1],
b) benzene–methanol (9 : 1) [2],
c) *n*-butanol–pyridine–water (6 : 4 : 3) [3],
d) *n*-butanol–ethanol–water (8 : 1 : 2) [2],
e) *n*-butanol–acetic acid–ether–water (9 : 6 : 3 : 1) [4],
f) ethyl acetate–isopropanol–water (65 : 23 : 12) [5].

The glycoalkaloids and aglycones were detected with antimony trichloride [6] (25% solution in chloroform), while the sugars were detected with aniline phthalate [6], triphenyltetrazolium chloride [6] or anisaldehyde-sulphuric acid [6]. For GLC a Gasofract 400 C-type (Dr. VIRUS K. G.) was used.

Isolation of the steroidal glycoalkaloids

The fresh immature fruits (4 kg) of *S. oleraceum* were minced in methanol, the mixture was stirred at room temperature three times, each for 1 hour. The combined extract was evaporated to give a syrup (350 g), which was shown on chromatoplates (solvent *a*) to consist of three antimony trichloride positive products; these, according to their decreasing order of R_f-values, were marked by *A*, *B*, and *C*.

The syrupy product was extracted with 1 l of absolute methanol three times at the boiling point. The combined extract gave on concentration in vacuum 145 g of a thick residue, which was treated with 5% acetic acid (1 l). The defatted acidic extract was heated to 60 °C, adjusted with ammonia to pH 9, then allowed to stand overnight. The dried precipitate

* Part VIII: Acta Chim. (Budapest) **73**, 361 (1972)

(97.5 g) was extracted by boiling with methanol 2×500 ml which removed 64.3 g of greenish basic glycoside mixture.

A column 5.5 cm in diameter was prepared from 1.5 kg of neutral Brockmann grade II alumina in a mixture of benzene–isopropanol–water (5 : 1 : 1). 40 g of the glycoside mixture (slurried with suitable weight of adsorbent in the same solvent) was introduced into the column and eluted with the same solvent mixture. Fractions of 15 ml were collected. The chromatographic results are summarized in Table I.

Table I

Fractionatio n of the glycoside mixture on an alumina column

Fraction no.	Weight of the evaporated residue (g)	Components according to TLC
1—110	0.6	—
111—250	20.2	*A*
251—285	4.2	*A* + (*B*)
286—580	3.8	*A* + *B*
581—720	8.1	*B*
721—800	0.5	*B* + (*C*)

Glycoside *A*

A was isolated by repeated crystallization of the residue obtained after evaporation of fractions 111—250 from aqueous methanol, as colourless needless, m.p. 295—300 °C, $(\alpha)_D^{23}$ —109° (pyridine); reported for solamargine [7]: m.p. 301 °C, $(\alpha)_D^{20}$ —114° in pyridine.

For analysis the samples were dried at 110 °C in vacuum for 48 hrs.

$C_{45}H_{73}O_{15}N \cdot {}^1/_2\ H_2O$ Calc. C 61.6; H 8.5; N 1.6;
Found C 62.4; H 8.6; N 1.7%.

Glycoside *B*

Fractions containing component *B* were combined and evaporated; recrystallization from methanol yielded the pure glycoside *B* as needles, m.p. 282—286 °C, $(\alpha)_D^{25}$ — 91° (pyridine) and $(\alpha)_D^{25}$ —70° (methanol); reported for solasonine [8]: m.p. 284.5 °C, $(\alpha)_D^{25}$ —68.7° in methanol.

For analysis, samples were dried at 110° over P_2O_5 in vacuum for 48 hrs.

$C_{45}H_{73}O_{16}N$ Calc. C 61.1; H 8.3; N 1.60;
Found C 60.8; H 8.4; N 1.52%.

Fraction *C*

This was found to be present in minute amounts. Isolation was difficult but further work is in progress.

Total hydrolysis [5] of glycosides A and B: 0.5 g of *A* and *B*, respectively was refluxed with 25 ml of 3 N HCl in 50% ethanol for 3.5 hrs.

Examination of the aglycone

This mixture was left standing in a refrigerator, the precipitate filtered off, washed with cold water and dissolved in 80% hot methanol. The free base was precipitated with ammonia which gave two spots on TLC (solvent *b*). After visualization with antimony trichloride the R_f of the main spot (0.34) was the same as that of authentic solasodine, and the R_f value of

the trace spot (0.70) agreed with that of solasodiene. Purification of the crude product on an alumina column followed by crystallization from aqueous methanol gave long plates of solasodine, m.p. 199—201 °C, $(\alpha)_D^{23}$ —99° (methanol). Reported: [9] m.p. 201 °C, $(\alpha)_D$ —100° (methanol).

$C_{27}H_{43}O_2N$ Calc. C 78.40; H 10.48; N 3.39;
Found C 77.10; H 10.20; N 3.15%.

Examination of sugar moiety

The acid hydrolysates from *A* and *B*, respectively were tested for sugars on Whatmann No. 1 filter paper and on silica gel or Kieselguhr chromatoplates. The results of the comparative run made with authentic sugars showed that the aqueous hydrolyzate from glycoside *A* contained glucose and rhamnose, and that from glycoside *B* contained glucose, galactose and rhamnose.

Quantitative estimation of sugars

60 mg of glycosides *A* and *B* were separately refluxed with 5% hydrogen chloride in absolute methanol for 5 hrs. The methylglycoside mixtures were then analyzed by GLC according to WULFF's method [10].

Detector: Flame ionization; *gas carrier:* hydrogen; *column:* 2.4 m, ID 4 mm; *stationary phase:* apiezon L; *solid support:* superthermolite fire-brick powder (0.25—0.3 mesh); *column temp.:* 200 °C; *detector temp.:* 220 °C; *gas flow rate:* 60 ml/min; *chart rate:* 0.5 cm/min.

Results of GLC indicate that in glycoside *A* the ratio of D-glucose to L-rhamnose is 1 : 2, while in glycoside *B*, D-glucose, D-galactose and L-rhamnose were found in equimolar quantities.

N-nitroso-glycoside A

100 mg of *A* was dissolved in 1 ml of acetic acid and mixed with a saturated aqueous solution of 50 mg sodium nitrite. After a few minutes a white precipitate was obtained [11].

After two crystallizations from hot aqueous ethanol, white needless of the nitroso derivative (32 mg) were obtained, m.p. 260 °C. Reported [12] m.p. for nitroso-solamargine 259—261 °C; mixture m.p. undepressed.

N-nitroso-glycoside B

The derivative was prepared as above. 38 mg of the pure N-nitroso *B* was obtained, m.p. 250 °C; reported [13] m.p. 251 °C; no depression of the mixture m.p. was observed.

Results

It was proved that the immature fruits of *S. oleraceum* contained two main solasodine glycosides, solamargine and solasonine. The identification of the isolated glycoalkaloids was made apart from direct comparison, on the basis of the preparation of their N-nitroso derivatives, their behaviour on chromatoplates, and acid hydrolysis, which afforded the same aglycone solasodine [14], (25 R)-22α-N-spirosol-5-en-3β-ol, m.p. 198—200°C, $(\alpha)_D^{23}$ — 99° (in methanol) from both. The sugars in the aqueous hydrolyzates from both isolated glycoalkaloids were also studied by PC, TLC and GC. Glycoside *A* was found to contain glucose and rhamnose in a ratio of 1 : 2 as in solamargine, while glycoside *B* was found to contain glucose, galactose and rhamnose in equimolar quantities as in solasonine.

*

Sincere thanks are due to Mr. Béla KOCH, the Vicedirector of National Agrobotanical Institute, Tápiószele, Hungary, for supply of plant material. The authors are grateful to the members of the analytical department for determinations.

Thanks are also due to Miss. É. SZEBENYI for her valuable technical assistance.

REFERENCES

[1] KAWASAKI, T., MIYAHARA, K.: Chem. Pharm. Bull. Japan, **11,** 1546 (1963)
[2] RASMUSSEN, M. B., BOLL, P. M.: Acta Chem. Scand., **12,** 802 (1958)
[3] BOGNAR, R., MAKLEIT, S.: Pharmazie, **20,** 40 (1965)
[4] BROWN, R. G., LINDBERG, B.: Acta Chem. Scand. **21,** 2379 (1967)
[5] SHABANA, M.: Ph. D. Dissertation, Hungarian Academy of Sciences, Budapest (1969)
[6] Dyeing Reagents for Thin-layer and Paper Chromatography Merck, S. A. G. (Darmstadt), p. 4
[7] BRIGGS, L. H., BROCKER, E. G., HARVEY, W. E., ODELL, A. L.: J. Chem. Soc., 3587 (1952)
[8] BELL, R. C., BRIGGS, L. H., CARROLL, J. J.: J. Chem. Soc. 12 (1942)
[9] TAYLOR, D. A. H.: J. Chem. Soc., 4216 (1958)
[10] WULFF, G.: J. Chromatog. **18,** 285 (1965)
[11] BITE, P., SHABANA, M., JÓKAY, L., PONGRÁCZ-STERK, L.: Acta Chim. (Budapest) **63** (3) 343 (1970)
[12] FAYEZ, M. B. E., SALEH, A. A.: Phytochemistry, **6,** 435 (1967)
[13] SCHREIBER, K., AURICH, O.: Z. Naturforschung, **18b,** 471 (1963)
[14] SCHREIBER, K.: Z. Chem., **3,** 433 (1963)

Pál BITE; 1325 Budapest, P. O. Box 82. Hungary
Marruan M. SHABANA; Faculty of Pharmacy, Cairo, University, Egypt.

Acta Chimica Academiae Scientiarum Hungaricae, Tomus 83 (1), pp. 95—105 (1974)

PYRIMIDINE DERIVATIVES, III*

SOME REACTIONS OBSERVED DURING THE SYNTHESIS OF CERTAIN 2-[2-(2,6-DI-R-PHENOXY)ETHYLAMINO]-5-METHYL-PYRIMIDIN-4(3*H*)-ONES**

J. REITER and L. TOLDY

(Research Institute for Pharmaceutical Chemistry, Budapest)

Received October 9, 1973

2-Alkylthio-5-methyl-pyrimidin-4(3*H*)-one and its 1- and 3-N-methyl derivatives, previously applied in the synthesis of 2-[2-(2,6-di-R-phenoxy)ethylamino]-5-methyl-pyrimidin-4(3*H*)-ones, were allowed to react with the appropriate 2-(2,6-di-R-phenoxy)-ethylamine at temperatures higher than 200 °C. The structures of products **8** and **14** obtained were determined by means of MS, IR, UV and NMR spectroscopy, and also proved by preparative methods. In the course of the structure-proving experiments compounds **7** and **19** being the isomers of **8** and **14**, respectively, as well as their demethyl- (**20**) and monosubstituted demethyl derivatives (**21**) were also prepared.

In the first two parts of this series [1,2] we reported that the reaction of 2-methylthio-5-methyl-pyrimidin-4(3*H*)-one (**1a**) [3] with 2-(2,6-dimethyl-phenoxy)ethylamine (**2a**) [4] at low temperature (160°C) gave 2-[2-(2,6-dimethylphenoxy)ethylamino]-5-methyl-pyrimidin-4(3*H*)-one (**3a**), as expected. When this reaction was carried out at higher temperature (200°C), or when **3a** was heated to this temperature, one molecule of 2,6-dimethylphenol(**6a**) was eliminated, resulting in two products; 2,3-dihydro-6-methylimidazo(1,2-*a*)-pyrimidin-7(1*H*)-one (**4**) and 2,3-dihydro-6-methylimidazo(1,2-*a*)pyrimidin-5(1*H*)-one (**5**).

Analogously, when **1a** was allowed to react with 2-(2,6-dichlorophenoxy)-ethylamine (**2b**) [5] at low temperature (135°C), **3b** was formed. Heating this product to 150°C, or carrying out the reaction at 160—180°C yielded compounds **4** and **5**, in addition to 2,6-dichlorophenol (**6b**).

When, however, **1a** was made to react with **2b** at 220°C, and the reaction mixture was separated on a chromatographic column, an additional compound *E* could also be isolated [6], which had the molecular formula $C_{12}H_{13}N_5O_2$, as determined from its mass spectrum.

Since the molecular formula of *E* differs from that of **4** or **5** by just one 5-methyl-4-oxo-pyrimidinyl group, it was reasonable to assume that *E* was the product of the reaction of **4** or **5** with an additional molecule of the starting material **1a**. Accordingly, *E* should be represented by one of the structures, **7** or **8**.

* Part II: Ref. [2].
** Preliminary papers on this topic: Refs [6] and [8].

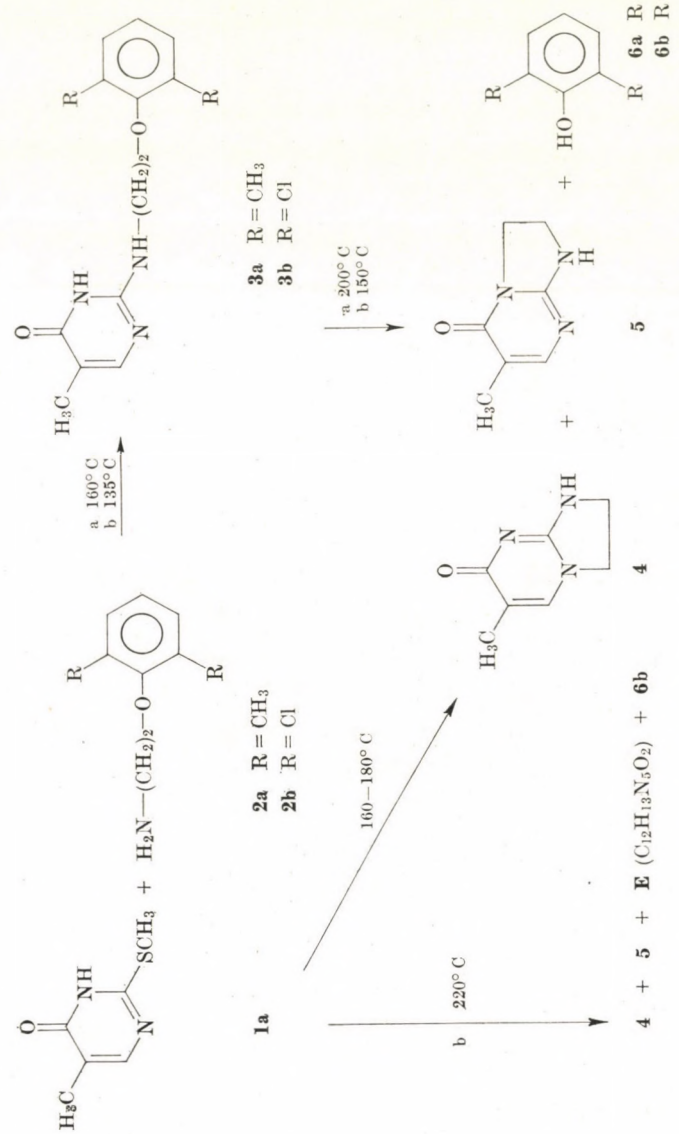
1a
2a R = CH3
2b R = Cl
a 160° C
b 135° C
3a R = CH3
3b R = Cl
a 200° C
b 150° C
160—180° C
b 220° C
4 + 5 + E (C12H13N5O2) + 6b
4
5
6a R = CH3
6b R = Cl

The IR spectrum of *E* has only one $\nu C{=}O$ band (1685 cm^{-1}), which can be brought in agreement with structure **8,** while structure **7** is excluded, since it contains two different carbonyl groups.

The UV spectrum of *E*, being analogous to that of **9,** is also in agreement with structure **8.**.

In the NMR spectrum of *E*, the methyl and methylene protons appear as singlets, their intensity ratios being 3 : 2 or 6 : 4, as predictable on the basis of structure **8.**

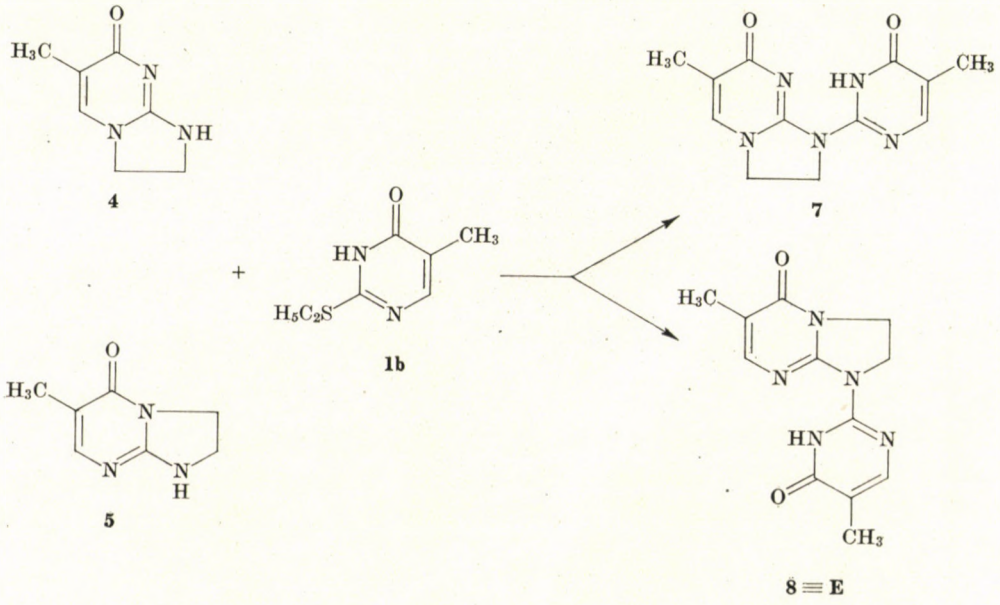

The spectroscopically established structure of *E* was also verified by preparative methods. For this purpose, **4** and **5,** respectively, was made to react with 2-ethylthio-5-methylpyrimidin-4(3*H*)-one (**1b**) [7], and the products were compared with *E*. The substance obtained from **5** was identical with *E*.

The reactions of 2-ethylthio-3,5-dimethylpyrimidin-4(3*H*)-one (**9**) and 1,5-dimethyl-2-ethylthiopyrimidin-4(1*H*)-one (**10**) with 2-(2,6-dichlorophenoxy)ethylamine (**2b**) [8] led to further interesting results. (Compounds **9** and **10** were prepared by the methylation of **1b** [2]).

When **9** was fused with **2b** at 170°C, 2-[2-(2,6-dichlorophenoxy)ethylamino]-3,5-dimethylpyrimidin-4(3*H*)-one (**11**) was formed, as expected. Effecting the reaction at 220°C, however, resulted in transformation of the intermediate **11,** and column chromatographic separation of the reaction mixture yielded 2,3-dihydro-6,8-dimethylimidazo(1,2-*a*)pyrimidin-7(8*H*)-one (**12**) [2], 3-methylthymine (**13**), 2,6-dichlorophenol (**6b**) and an additional product *F* having the molecular formula $C_{16}H_{22}N_6O_2$, on the basis of its mass spectrum.

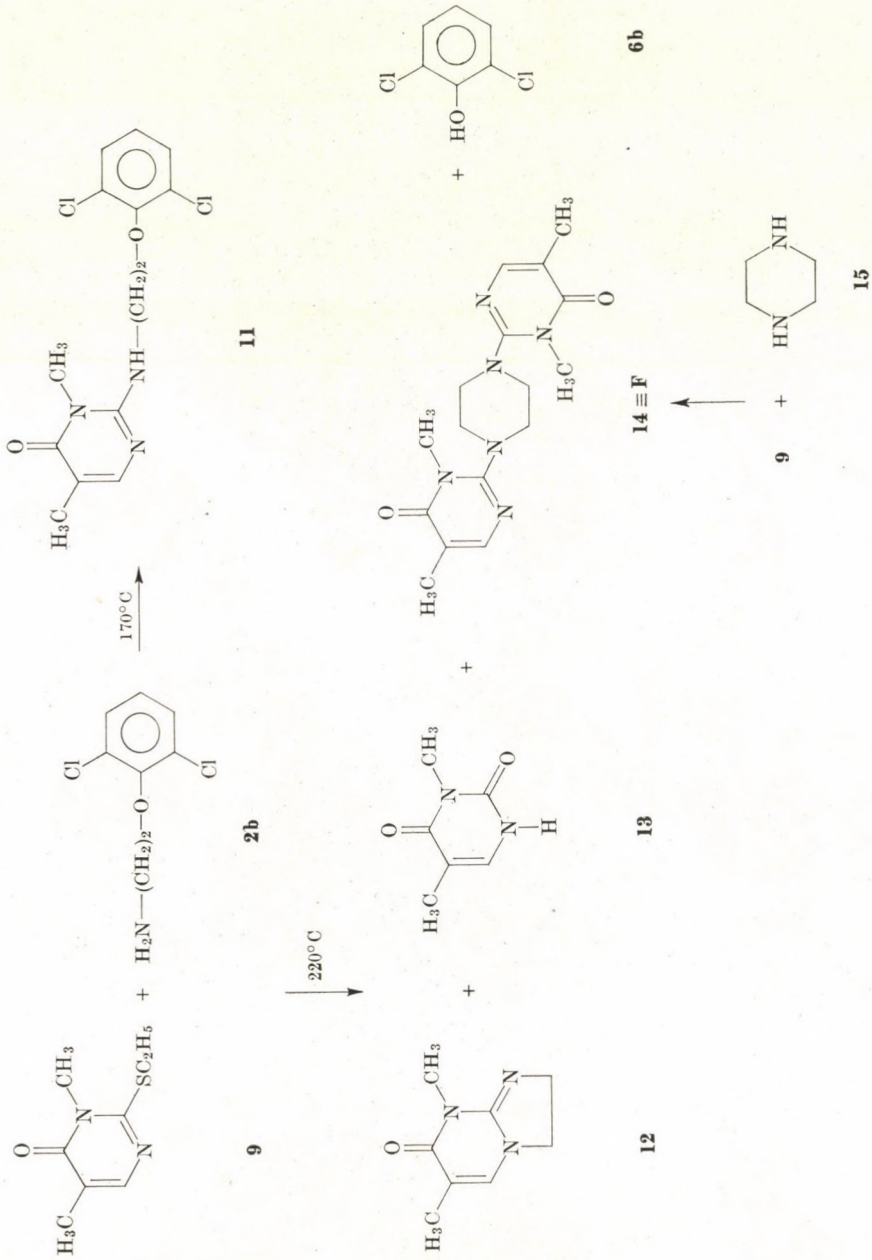

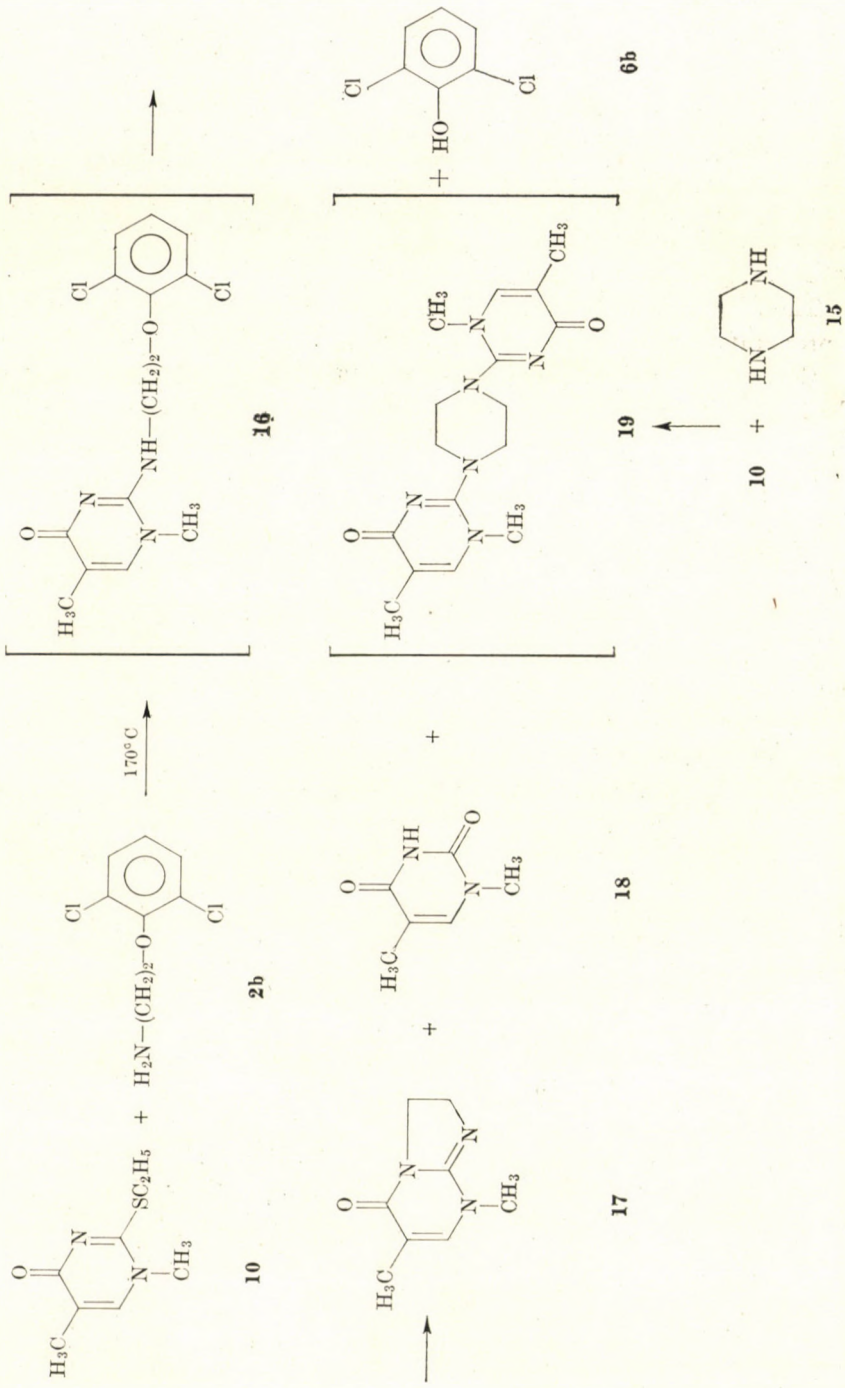

In the NMR spectrum of *F*, in addition to the singlets of the two methyl groups and pyrimidone proton, another singlet was found at $\delta = 3.3$ ppm, the intensity ratios being $CH_3 : CH_3 : H : X = 3 : 3 : 1 : 4$ or $6 : 6 : 2 : 8$. This result can well be explained by assuming the elimination of the terminal 2,6-dichlorophenols (**6b**) from two molecules of **11**, followed by an intermolecular N-alkylation yielding the piperazine derivative **14**..

The appearance of one single carbonyl band ($\nu C{=}O$ 1665 cm^{-1}) in the IR spectrum, as well as the analogous UV spectrum of *F* to that of **9** supports also the proposed structure **14.**

The structure of *F* as represented by formula **14** was later also proved in a preparative way by allowing **9** to react with piperazine.

Compound **16** presumably present as an intermediate in the reaction of the isomer **10** with **2b** at 170°C could not be isolated from the reaction mixture, but 2,3-dihydro-6,8-dimethylimidazo(1,2-*a*)pyrimidin-5(8*H*)-one (**17**), prepared already earlier [2], and 1-methylthymine (**18**) were directly obtained. The piperazine derivative **19** expected in the reaction mixture could not be isolated either, therefore this compound was synthesised by the reaction of **10** with **15.**

Analogously to the above procedures, the demethyl analogue (**20**) of compounds **14** and **19** was prepared in the reaction of **1b** with **15**; this compound was not formed in the reaction of either **1a** and **2a** or **1a** and **2b**, respectively, nor during the thermal decomposition of the reaction products **3a** or **3b.** The by-product of the reaction is the monosubstituted derivative **21,** isolated chromatographically from the reaction mixture.

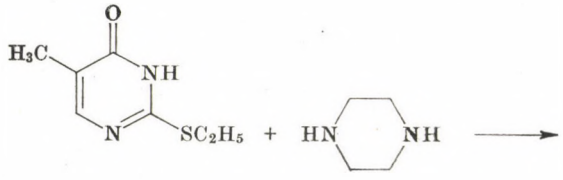

1b **15**

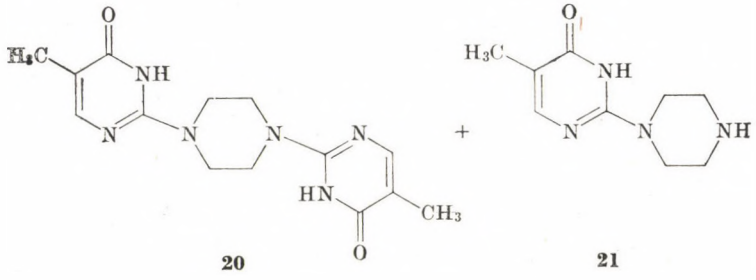

20 **21**

Compounds **20** and **21** were also prepared by an independent synthesis, that is, in the reaction of diguanylpiperazine (**23**) [9] with ethyl sodio-2-formylpropionate (**22**) obtained by the Claisen condensation of ethyl formate and ethyl propionate [7].

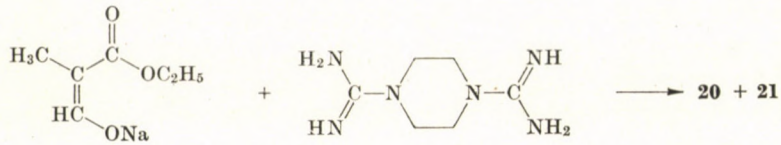

22 **23**

Experimental

M.p.'s were determined on a Kofler-Boetius melting point apparatus (Franz Küstner Nachf. KB, Dresden). In the MS measurements, a single-focussed instrument of type MX-1303 was used. The samples were introduced into the ion source by direct evaporation at 5—100 °C. The IR spectra were recorded with a Zeiss UR-10 and with a Perkin—Elmer 457 spectrophotometer, in KBr pellets. The UV spectra were obtained with a Unicam SP 700 instrument. In the NMR studies a Jeol C-60 (at 23 °C) and Varian A-60D instrument (at 36 °C) were used with tetramethylsilane and sodium 2,2-dimethyl-2-silapentanesulfonate internal standards.

The thin-layer chromatographic tests were made on plates coated with silica gel. The so-called chlorination technique [10] was used for the detection of the spots. The composition of the developing mixture No. 9 was the following: ethyl acetate (60 ml), pyridine (20 ml), water (11 ml), acetic acid (6 ml).

Reaction of 2-(2,6-dichlorophenoxy)-ethylamine with 2-methylthio-5-methylpyrimidin-4(3*H*)-one at 220 °C

A mixture of 2-(2,6-dichlorophenoxy)-ethylamine (**2b**) [5] (16.4 g; 0.0795 mole) and 2-methylthio-5-methylpyrimidin-4(3*H*)-one (**1a**) [3] (12.2 g; 0.078 mole) was refluxed on an oil bath at 220 °C for 6 hrs. After cooling, the half-crystallized honey-like product was rubbed with absolute ethanol (25 ml), cooled in salted ice, filtered off and washed with ice-cold absolute ethanol (15 ml). In this way 5.4 g (45.8%) of 2,3-dihydro-6-methylimidazo(1,2-*a*)pyrimidin-7(1*H*)-one was obtained. After recrystallization from absolute ethanol, m.p. 299—300 °C; the IR spectrum was identical with that of **4** obtained earlier [2].

When 16% HCl in absolute ethanol (35 ml) was added to the alcoholic mother liquor of the raw product, 2,3-dihydro-1-[5-methyl-4(3*H*)-oxo-pyrimidinyl-2]-6-methylimidazo(1,2-*a*) pyrimidin-5(1*H*)-one hydrochloride (**8** · HCl) (2.2 g; 9.5%) separated, m.p. 242—244 °C; $R_f = 0.65$ (in solvent system No. 9).

$C_{12}H_{14}ClN_5O_2$ (295.73). Calcd. C 48.74; H 4.77; N 23.68; Cl 11.99. Found C 48.81; H 4.92; N 23.56; Cl 12.13%.

Recrystallization of **8** · HCl from water yielded the semihydrochloride of **8** (1.6 g; 7.4%), m.p. 276—277 °C. IR: νC=O 1715 cm^{-1}.

$C_{12}H_{13}N_5O_2 \cdot \frac{1}{2}$ HCl (277.50). Calcd. C 51.93; H 4.90; N 25.24; Cl 6.39. Found C 51.76; H 5.04; N 25.31; Cl 6.52.

This semihydrochloride was recrystallized from conc. ammonium hydroxide solution (15 ml) to obtain the base, 2,3-dihydro-1-[5-methyl-4(3*H*)-oxo-pyrimidinyl-2]-6-methylimidazo-(1,2-*a*)pyrimidin-5(1*H*)-one (**8**=*E*) (1.0 g; 5.0%), m.p. 280—281 °C.

IR: νC=O 1685 cm^{-1}. UV (in ethanol): λ_{max} 245 nm ($\log \varepsilon = 4.18$) and 301 nm ($\log \varepsilon = 4.26$); λ_{min} 223 nm ($\log \varepsilon = 3.94$) and 266 nm ($\log \varepsilon = 3.92$); $\Delta \log \varepsilon$ [11] = + 0.08. NMR: $\delta CH_3 = 2.05$ s (6H), $\delta CH_2 = 3.30$ s (4H), $\delta ArH = 7.60$ s (2H).

$C_{12}H_{13}N_5O_2$ (259.26). Calcd. C 55.63; H 5.05; N 27.01. Found C 55.68; H 5.15; N 27.20%.

The ethanolic mother liquor of **8** · HCl was evaporated to dryness in vacuum and the residue subjected to chromatographic separation on a silica gel column in solvent mixture No.9.

2,6-Dichlorophenol (**6b**) (7.2 g; 55.4%) was obtained first, m.p. 66—67 °C; next 2,3-dihydro-6-methylimidazo(1,2-*a*)pyrimidin-5(1*H*)-one (**5**) (2.3 g; 19.5%) was eluted, m.p. 299—300 °C (from methanol). Its IR spectrum was identical with that of compound **5** obtained earlier [2].

2,3-Dihydro-1-[5-methyl-4(3*H*)-oxo-pyrimidinyl-2]-6-methylimidazo(1,2-*a*)pyrimidin-7(1*H*)-one (7)

A mixture of 2,3-dihydro-6-methylimidazo(1,2-*a*)pyrimidin-7(1*H*)-one (**4**) [2] (0.453 g; 0.003 mole) and 2-ethylthio-5-methylpyrimidin-4(3*H*)-one (**1b**) [7] (0.511 g; 0.003 mole) was refluxed on an oil bath at 210—215 °C for 3 hrs. The mixture melted first during the reaction, then solidified while ethanethiol was formed. The reaction mixture was dissolved, while still warm, in hot 80% ethanol (50 ml), filtered, and allowed to crystallize. 2,3-Dihydro-1-[5-methyl-4(3*H*)-oxo-pyrimidinyl-2]-6-methylimidazo(1,2-*a*)pyrimidin-7(1*H*)-one (**7**) (0.710 g; 91.5%) was obtained, m.p. 368—370 °C (from dimethyl sulfoxide); $R_f = 0.62$ (in solvent mixture No. 9). According to the mass spectrum, the molecular weight of the product was 259, the molecular formula being $C_{12}H_{13}N_5O_2$.

IR: νC=O 1660 cm^{-1} and 1680 cm^{-1}. UV (ethanol): λ_{max} 225 nm ($\log \varepsilon = 4.35$), 235 nm ($\log \varepsilon = 4.33$) shoulder, 277 nm ($\log \varepsilon = 4.18$) and 302 nm ($\log \varepsilon = 3.99$) shoulder; λ_{min} 263 nm ($\log \varepsilon = 4.16$).

2,3-Dihydro-1-[5-methyl-4(3*H*)-oxo-pyrimidinyl-2]-6-methylimidazo(1,2-*a*)pyrimidin-5(1*H*)-one (8)

A mixture of 2,3-dihydro-6-methylimidazo(1,2-*a*)pyrimidin-5(1*H*)-one (**5**) [2] (0.230 g; 1,52 mmole) and 2-ethylthio-5-methylpyrimidin-4(3*H*)-one (**1b**) [7] (0.272 g; 1.6 mmole) was refluxed on an oil bath at 230 °C for 2 hrs. During this time the reaction mixture melted with the formation of ethanethiol. The still hot reaction mixture was dissolved in hot absolute ethanol (50 ml), filtered and allowed to crystallize. 2,3-Dihydro-1-[5-methyl-4(3*H*)-oxo-pyrimidinyl-2]-6-methylimidazo(1,2-*a*)pyrimidin-5(1*H*)-one (**8**) (0.390 g; 80.6%) was obtained; m.p. 280—281 °C; the IR spectrum was identical with that of *E*.

2-[2-(2,6-Dichlorophenoxy)-ethylamino]-3,5-dimethylpyrimidin-4(3*H*)-one semi-(2,6-dichloro)phenolate ($11 \cdot \frac{1}{2} C_6H_4Cl_2O$)

A mixture of 2-(2,6-dichlorophenoxy)ethylamine (**2b**) [5] (10.3 g; 0.05 mole) and 2-ethylthio-3,5-dimethylpyrimidin-4(3*H*)-one (**9**) [2] (9.2 g; 0.05 mole) was refluxed at 170 °C on an oil bath for 13 hrs. During this time the reaction mixture melted with the formation of ethanethiol. Absolute ethanol (10 ml) was added to the still warm reaction mixture, then it was filtered and allowed to stand to crystallize. The product which separated was filtered off, washed with absolute ethanol to obtain 2-[2-(2,6-dichlorophenoxy)-ethylamino]-3,5-dimethylpyrimidin-4(3*H*)-one semi-(2,6-dichloro)phenolate ($11 \cdot \frac{1}{2} C_6H_4Cl_2O$) (8.90 g; 72,3%), m.p. 137—137.5 °C (from absolute ethanol); $R_f = 0.1$ (in solvent mixture No. 9).

IR: νC=O 1680 cm^{-1} (base) and 1708 cm^{-1} (salt). On the basis of the IR spectrum, the substance is a molecular adduct formed from the base and dichlorophenolate in 1 : 1 ratio. NMR: $\delta CCH_3 = 1.86$ s (3H), $\delta NCH_3 = 3.35$ s (3H), $\delta CH_2 = 3.90$ s (4H), $\delta ArH = 6.4—7.25$ m (3 + 1.5H) (phenoxy + $\frac{1}{2}$ phenolate), $\delta ArH = 7.5$ s (1H) (pyrimidinone).

$C_{14}H_{15}N_3Cl_2O_2 \cdot \frac{1}{2} C_6H_4Cl_2O$ (409.70). Cald. C 49.83; H 4.18; N 10.26; Cl 25.97. Found C 49.69; H 4.56; N 10.10; Cl 25.86%.

Reaction of 2-ethylthio-3,5-dimethylpyrimidin-4(3*H*)-one (9) with 2-(2,6-dichlorophenoxy)ethylamine (2b) at 220 °C

A mixture of 2-ethylthio-3,5-dimethylpyrimidin-4(3*H*)-one (**9**) [2] (5.53 g; 0.03 mole) and 2-(2,6-dichlorophenoxy)ethylamine (**2b**) [5] (6.4 g; 0.0311 mole) was refluxed on an oil bath at 220 °C for 8 hrs. During this time the reaction mixture melted with the formation of

ethanethiol. The residual dark brown honey-like reaction mixture was dissolved in solvent mixture No. 9 and subjected to chromatographic separation on a silica gel column. The following compounds were eluted subsequently from the column:

(1) 2,6-Dichlorophenol (**6b**) (4.2 g; 85.8%), m.p. 65—66 °C (from gasoline) (Ref. [12] m.p. 66—67 °C). $R_f = 0.95$ (in solvent mixture No. 9).

(2) 3,5-Dimethylpyrimidin-2,4(1*H*, 3*H*)-dione (3-methylthymine, **13**) (1.2 g; 28.6%), m.p. 210—211 °C (from ethanol) (Ref. [13] m.p. 202—203 °C). $R_f = 0.7$ (in solvent mixture No. 9). IR: νC=O 1670 and 1720 cm^{-1}.

(3) 1,4-Bis-[3,5-dimethyl-4(3*H*)-oxo-pyrimidinyl-2]-piperazine (**14** = *F*) (1.8 g; 36.4%), m.p. 316—316.5 °C (from dimethylformamide); $R_f = 0.6$ (in solvent mixture No. 9).
IR: νC=O 1665 cm^{-1}; UV (in dimethylformamide): $\lambda_{max} = 296$ nm ($\log \varepsilon = 4.27$). NMR: $\delta CCH_3 = 2.00$ s (6H), $\delta NCH_3 = 3.50$ s (6H), $\delta CCH_2 = 3.30$ s (8H), $\delta ArH = 7.55$ s (2H). $C_{16}H_{22}N_6O_2$ (330.38). Calcd. C 58.16; H 6.71; N 25.44. Found C 57.92; H 6.98; N 25.50%. MS: molecular weight: 330, molecular formula: $C_{16}H_{22}N_6O_2$; the fragmentation pattern is consistent with structure **14** given.

(4) 2,3-Dihydro-6,8-dimethylimidazo(1,2-*a*)pyrimidin-7(8*H*)-one hydrochloride (**12** · HCl) (0.8g; 14.2%), m.p. 280—284 °C, $R_f = 0.15$ (in solvent mixture No. 9).
When the hydrochloride was dissolved in a mixture of chloroform and aqueous NaOH and, after the separation of the phases, the chloroform solution was dried, the solvent removed, and the residual solid product recrystallized from ethyl acetate, base **12**, m.p. 130—131 °C, was obtained; its IR spectrum was identical with that of **12** prepared earlier [2].

1,4-Bis-[3,5-dimethyl-4(3*H*)-oxo-pyrimidinyl-2]-piperazine (14)

A mixture of freshly distilled anhydrous piparazine (**15**) (1.70 g; 8.75 mmole) and 2-ethylthio-3,5-dimethylpyrimidin-4(3*H*)-one (**9**) [2] (3.12 g; 17.5 mmole) was refluxed on an oil bath at 240 °C for 11 hrs. The warm reaction mixture was dissolved in absolute ethanol (10 ml), filtered and allowed to crystallize. The procedure yielded 1,4-bis-(3,5-dimethyl-4(3*H*)-oxo-pyrimidinyl-2]-piperazine (**14**) (0.62 g; 21.9%), m.p. 316—317 °C (from dimethylformamide). The IR spectrum of the product was identical with that of *F* obtained in the previous experiment.

Reaction of 1,5-dimethyl-2-ethylthiopyrimidin-4(1*H*)-one (10) with 2-(2,6-dichlorophenoxy)ethylamine (2b)

A mixture of 1,5-dimethyl-2-ethylthiopyrimidin-4(1*H*)-one (**10**) [2] (9.21 g; 0.05 mole) and 2-(2,6-dichlorophenoxy)ethylamine (**2b**) [5] (11.33 g; 0.055 mole) was refluxed on an oil bath at 170 °C for 6 hrs. During this period, the reaction mixture melted with the evolution of ethanethiol. The brown-red melt was dissolved in solvent mixture No. 9 and subjected to chromatographic separation on a silica gel column. The following compounds were eluted from the column in the order given:

(1) 2,6-Dichlorophenol (**6b**) (7.5 g; 92.1%), m.p. 65—67 °C (from gasoline) (Ref. [12], m.p. 66—67 °C); $R_f = 0.95$ (in solvent mixture No. 9).

(2) 1,5-Dimethylpyrimidin-2,4(1*H*, 3*H*)-dione (1-methylthymine, **18**) (1.7 g; 24.3%), m.p. 278—280 °C (from dimethylformamide) (Ref. [13], m.p. 280—282 °C); $R_f = 0.65$ (in solvent mixture N. 9).
IR: νC=O 1670 and 1730 cm^{-1}.

(3) 2,3-Dihydro-6,8-dimethylimidazo(1,2-*a*)pyrimidin-5(8*H*)one (**17**) (1.5 g; 18.4%), m.p. 134—135 °C (from water); $R_f = 0.05$ (in solvent mixture No. 9). The IR spectrum of the substance was identical with that of **17** obtained earlier [2].

1,4-Bis-[1,5-dimethyl-4(1*H*)-oxo-pyrimidinyl-2]-piperazine (19)

A mixture of anhydrous, freshly distilled piperazine (**15**) (1.15 g; 5.9 mmole) and 1,5-dimethyl-2-ethylthiopyrimidin-4(1*H*)-one (**10**) [2] (2.18 g; 11.8 mmole) was refluxed on an oil bath at 240—260 °C for 6 hrs. During this time, the reaction mixture fused with the evolution of ethanethiol. Absolute ethanol (100 ml) was then added to the still warm reaction mixture, it was brought to boiling, and filtered while hot. 1,4-Bis-[1,5-dimethyl-4(1*H*)-oxo-pyrimidinyl-2]-piperazine (**19**) (1.50 g; 81.1%) was obtained, m.p. 368—370 °C (from dimethyl sulfoxide).
IR: νC=O 1665 cm^{-1}.
$C_{16}H_{22}N_6O_2$ (330.38). Cald. C 58.16; H 6.71; N 25.44. Found C 58.02; H 7.07; N 25.35%.
MS: molecular weight: 330, molecular formula: $C_{16}H_{22}N_6O_2$; the fragmentation pattern is consistent with structure **19.**

Preparation of 1-[5-methyl-4(3*H*)-oxo-pyrimidinyl-2]-piperazine (21) and 1,4-bis-[5-methyl-4(3*H*)-oxo-pyrimidinyl-2]-piperazine (20) from piperazine

A mixture of piperazine hexahydrate (4.85 g; 0.025 mole) and 2-ethylthio-5-methyl-pyrimidin-4(3*H*)-one (**1b**) [7] (8.5 g; 0.05 mole) was refluxed in a distillation apparatus on an oil bath at 160—170 °C for 6 hrs. During the reaction the mixture melted, while water and ethanethiol distilled off. The product was rubbed with hot absolute ethanol; in this way 1,4-bis-[5-methyl-4(3*H*)-oxo-pyrimidinyl-2]-piperazine (**20**) (6.2 g; 82.3%) was obtained, m.p. > 380 °C (from dimethyl sulfoxide); $R_f = 0.1$ (in solvent mixture No. 9).

IR: νC=O 1670 cm^{-1}.

$C_{14}H_{18}N_6O_2$ (302.34). Cald. C 55.61; H 6.00; N 27.80. Found C 55.58; H 6.24; N 28.03%.

MS: molecular weight: 302, molecular formula: $C_{14}H_{18}N_6O_2$; the fragmentation pattern is consistent with structure **20.**

The alcoholic filtrate of **20** was evaporated to dryness and the residue subjected to chromatographic separation on a silica gel column in solvent mixture No. 9, to yield 1-[5-methyl-4(3*H*)-oxo-pyrimidinyl-2]-piperazine (**21**) (0.5 g; 10.6%), m.p. 207—208 °C (from ethanol). $R_f = 0.5$ (in solvent mixture No. 9).

IR: νC=O 1685 cm^{-1}; NMR: $\delta CCH_3 = 1.85$ s (3H), $\delta CH_2 = 3.75$ m (8H), δArH = = 7.65 s (1H), δNH = 8.15 s (1H).

$C_9H_{14}N_4O$ (194.23). Calcd. C 55.65; H 7.27; N 28.85. Found C 55.70; H 7.56; N 29.03%.

MS: molecular weight: 194, molecular formula: $C_9H_{14}N_4O$; the fragmentation pattern s consistent with structure **21.**

Preparation of 1-[5-methyl-4(3*H*)-oxo-pyrimidinyl-2]-piperazine (21) and 1,4-bis-[5-methyl-4(3*H*)-oxo-pyrimidinyl-2]-piperazine (20) from diguanylpiperazine

Metallic sodium (11.2 g; 0.488 g-atom) was dissolved in absolute ethanol (240 ml), then the solution was evaporated to dryness in vacuum on an oil bath at 220 °C. After cooling, the alcoholate was ground, absolute ether (200 ml) was added, and an ester mixture prepared from ethyl formate (32.0 g; 0.432 mole) and ethyl propionate (40.8 g; 0.400 mole) was slowly added by drops, under stirring and cooling in salted ice; the mixture was then allowed to stand overnight. On the next day, the reaction mixture was decomposed by the addition of water (100 ml), separated, and a solution of diguanylpiperazin sulfate (**23**) [9] (26.8 g; 0.1 mole) in water (50 ml) was added to the aqueous phase, and the solution was allowed to stand overnight. The solution was then refluxed on a water bath for 2 hrs., acidified with conc. HCl and evaporated to dryness in vacuum. The residue was subjected to chromatographic separation in solvent mixture No. 9 on a silica gel column. First, 1-[5-methyl-4(3*H*)-oxo-pyrimidinyl-2]-piperazine (**21**) (6.8 g; 35.1%) was obtained, m.p. 207—208 °C (from ethanol). The IR spectrum of the substance was identical with that of **21** prepared earlier.

Continuing the chromatographic separation, 1,4-bis-[5-methyl-4(3*H*)-oxo-pyrimidinyl-2]piperazine (**20**) (2.8 g; 9.3%) was eluted, m.p. > 380 °C (from dimethyl sulfoxide). The IR spectrum of the product was identical with that of **20** prepared earlier.

*

The autors' thanks are due to Dr. J. TAMÁS (Center for Studies on Chemical Structure of the Hungarian Academy of Sciences) for the MS spectra; to Dr. P. SOHÁR for recording the IR and NMR spectra; to Dr. L. LÁNG (Department for Nuclear Physics of the Technical University, Budapest) and Dr. J. LIPTÁK for the UV spectra and their valuable help in the interpretation.

REFERENCES

[1] REITER, J., TOLDY, L.: Pyrimidine derivatives, I., Acta Chim. (Budapest) (In press)
[2] REITER, J., TOLDY, L.: Pyrimidine derivatives, II., Acta Chim. (Budapest) (In press)
[3] WHEELER, H. L., MERRIAM, H. F.: Am. Chem. J. **29,** 487 (1903)
[4] BARRON, D. J., BAVIN, P. M. G., DURANT, G. J., NATOFF, I. L., SPICKETT, R. G. W., WALLANCE, D. K.: J. Med. Chem. **6,** 705 (1963)

[5] U. S. Pat. 3,099.599 (July 30, 1963); C. A. **60**, 2824 (1964)
[6] REITER, J., TOLDY, L.: Tetrahedron Letters **1970** (28), 2451
[7] WITTENBURG, E.: J. prakt. Chem. **4/33**, 165 (1966)
[8] REITER, J., TOLDY, L.: Tetrahedron Letters, 1970 (28), 2455
[9] PIOVANO, V.: Gazz. Chim. Ital. **58**, 245 (1928)
[10] ZAHN, H., REXROTH, E.: Z. anal. Chem. **148**, 181 (1955)
[11] ÁGAI, B., HORNYÁK, GY., LÁNG, L., LEMPERT, K., SOHÁR, P.: Periodica Polytechnica, **15**, 43 (1971)
[12] HUSTON, R. C., NEELY, A. H.: J. Am. Chem. Soc. **57**, 2176 (1935)
[13] JOHNSON, T. B., CLAPP, S. H.: J. Biol. Chem. **5**, 49 (1908)

József REITER
Lajos TOLDY } 1045 Budapest, Szabadságharcosok útja 47—49. Hungary.

Acta Chimica Academiae Scientiarum Hungaricae, Tomus 83 (1), pp. 107—114 (1974)

TRITYLATION AND TRANSTRITYLATION REACTIONS OF ETHANOLAMINE*

K. KÖRMENDY and MOHAMED M. EL-SAWY**

*(Institute of Organic Chemistry, Eötvös Loránd University, Budapest and ** Polytechnical Institute of Cairo, Shoubra, Department of Organic Chemistry, Cairo, A. R. Egypt)*

Received November 18, 1973

Direct tritylation of ethanolamine (**I**) affords N-tritylethanolamine (**II**) as the sole product. In boiling pyridine, however, the tritylation gives a mixture of N-tritylethanolamine (**II**), O-tritylethanolamine (**III**), N,O-ditritylethanolamine (**IV**) and triphenylcarbinol (**V**) under the conditions of BUCKUS *et al.* [1], who isolated only compound **II**. The **II** · HCl and **III** · HCl salts form alkyl trityl ethers with primary alcohols in intermolecular N → O and O → O' transtritylation reactions.

With tertiary alcohols, such as *t*-butyl alcohol, **II** · HCl or **III** · HCl does not enter either intermolecular or intramolecular transtritylation reaction, thus the alkyl trityl ether or N,O-dityrityl derivative (**IV**) is not formed. The proton-catalyzed transformation of **II** and **III** to **IV** can be achieved in the presence of tertiary bases (*e.g.* pyridine), which are suitable for trityl transfer.

The tritylation of amino alcohols is a reaction of interest; some derivatives proved to be important in the preparation of biologically active molecules. They also offer a good model to examine the two known types of tritylation, direct tritylation and transtritylation. The latter process might involve the following cases:

N → N'	O → O'
N → O	O → N
N → C	O → C, etc.

The tritylation of ethanolamine (**I**) is herein described, particularly in view of the paper published by BUCKUS *et al.* [1]. These authors reported that **I** was selectively N-tritylated with trityl chloride in boiling pyridine to give N-tritylethanolamine (**II**) as the sole product. The formation of O-tritylethanolamine (**III**) and other products were not noted by these authors.

We repeated the work of BUCKUS [1]; the product so obtained was a mixture of **II, III,** N,O-dityrityl-ethanolamine (**IV**), and triphenylcarbinol (**V**)*** formed in 85%, 4.83%, 6% and 4.17%, respectively.

* Some of the material of this paper had been the subject of a lecture, held at the Conference of Organic Chemistry of the Hungarian Chemical Society, Pécs, August 22—24, 1973.

*** The formation of **V** can presumably be due to either hydrolysis of TrCl or **IV** during manipulation.

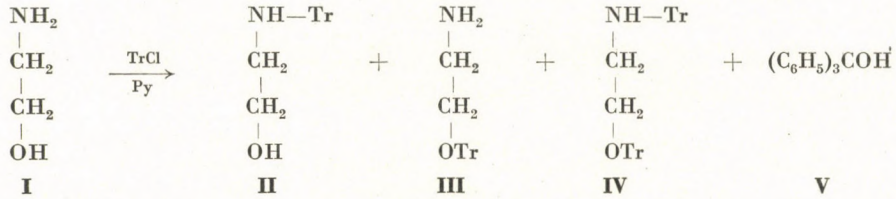

Thin-layer chromatography of the reaction mixture showed 4 spots: *i* R_f 0.64; *ii* R_f 0.08 and *iii* R_f 0.84, which corresponded to compounds **II, III** and **IV,** respectively. The fourth spot had R_f 0.77 of triphenylcarbinol (**V**). The structure of each compound was examined by IR spectroscopy and microanalysis.

The isolation of the compounds from the mixture according to the method of BUCKUS was found rather tedious in our experiments, therefore we tried to modify the procedure in an attempt to minimize the formation of by-products. Thus pure N-tritylethanolamine (**II**; yield: 99.6%) was obtained when the reaction was carried out in ethanolamine used in a large excess (1 mole trityl chloride in 60 moles ethanolamine, at room temperature). Under such conditions direct N-tritylation of **I** took place, no transtritylation being involved. Using 1 : 30 molar ratio of the reactants in chloroform solution, a mixture of **II, III, IV** and **V** was obtained again.

While the direct N-tritylation of amino alcohols is possible, selective O-tritylation can only be achieved through special syntheses:

(*a*) Reaction of carbobenzoxy chloride with **I** afforded N-carbobenzoxyethanolamine (**VI**). Tritylation of the latter, either at room temperature or in boiling pyridine gave O-trityl-N-carbobenzoxyethanolamine (**VII**). Hydrogenolysis of **VII** either in ethyl acetate or in dimethylformamide yielded **III.**

(*b*) Chemically homogeneous O-tritylethanolamine (**III**) can also be obtained by the hydrazinolysis of ω-trityloxyethylphthalimide (**VIII**).

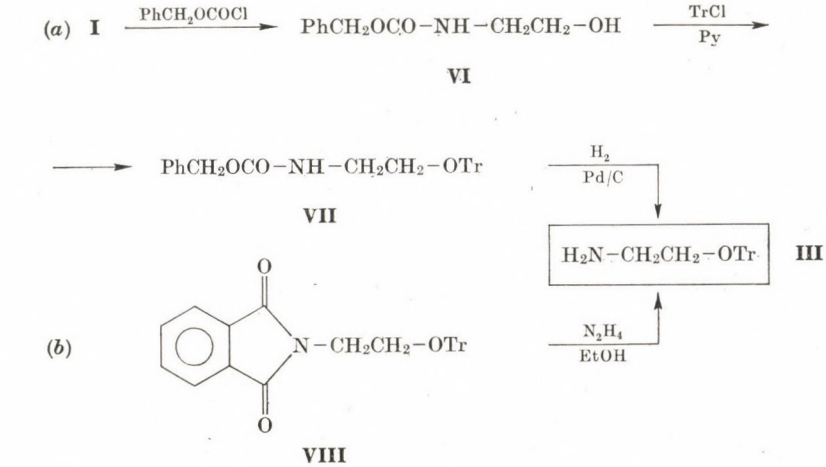

The purity of O- and N-tritylethanolamine, their structure and the stability of the isomers were checked by mass spectroscopy (Fig. 1). The molecular ion of both isomers has the mass number 303. In the course of the fragmentation, the C–C bond in β-position both to the oxygen and nitrogen, splits homolytically, though the mass numbers of the ions differ by one unit.

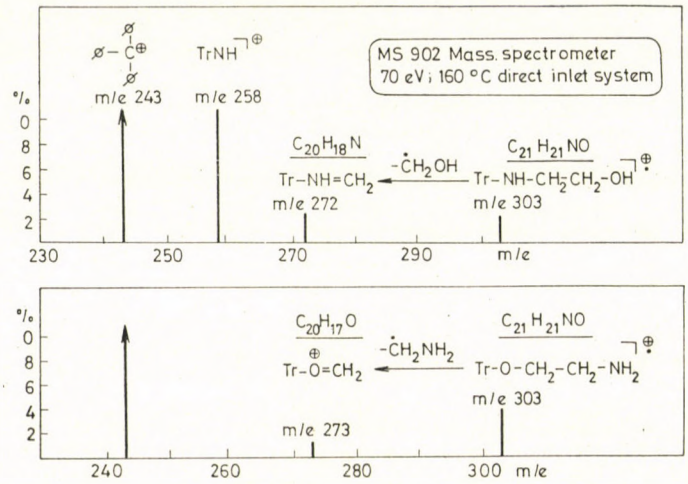

Fig. 1

N-trityl compounds have a characteristic fragment ($TrNH^+$) at the mass number 258. The latter is completely missing from the spectrum of the O-trityl compound, which means that this compound is quite pure, and that the isomers do not transform into each other as bases. Even prolonged heating of these compounds (**II** and **III**) (20 hrs at 100°C) produced no change.

Tritylamino alcohols called our attention to trityl migration, a problem similar to the acyl migration of acylamino alcohols which latter has been studied in great detail. The main problem is whether the different ways of formation and the different modes of cleavage of the N- and O-trityl compounds [2] correspond to a reversible *intramolecular* transtritylation ("trityl migration"), or tritylethanolamine is capable of undergoing only *intermolecular* transtritylation reaction. An N → O trityl migration can be expected in acidic medium, while O → N trityl migration might take place in basic medium with these compounds.

Trityl migration has only been described for aryl trityl ethers an for N-tritylarylamines. The proton-catalyzed reaction takes place as an intramolecular O → C or N → C migration, accompanied by intermolecular transtritylation [3,4] (*e.g.*, $C_6H_5OTr \rightarrow p\text{-Tr-}C_6H_4OH$, or $C_6H_5NHTr \rightarrow p\text{-Tr-}C_6H_4NH_2$).

The hydrochloride of N-tritylethanolamine (**II** · HCl) is a very reactive compound, and the heterolysis assisted by proton catalysis can easily take place. The cleavage of the trityl group in the isomeric salt (**III** · HCl) is more difficult, because the oxygen atom is not easily protonated even in the presence of equimolecular hydrochloric acid. However, BUCKUS reported that the O-trityl bond in the N,O-ditrityl compound (**IV**) can be cleaved easily when this compound (**IV**) is treated with a great excess of hydrogen chloride gas in dry benzene, to afford the hydrochloride of **II.**

It is probable that the proton-catalyzed transtritylation of **II** · HCl can easily take place if the salt is boiled in a solvent indifferent to tritylation, *e.g.* *t*-butanol, as the monotrityl compound can be transformed into the corresponding ditrityl derivative. After boiling for several hours, **II** · HCl showed no remarkable change. As the hydrochloride of **II** quickly transtritylates ethanol (**II** · HCl → **IX**), the absence of transtritylation in the former case can be explained by steric hindrance, or alternatively, as probably due to the electrostatic effect of the $Tr\text{-}\overset{+}{N}H_2$-group.

The boiling of **II** · HCl with *t*-butanol for 20 hours, under strictly anhydrous conditions afforded only triphenylcarbinol (**V**) in 83% yield, together with unchanged starting material. The formation of triphenylcarbinol might be explained as a result of dehydratation of *t*-butanol.

On account of the reasons mentioned above, the O-tritylethanolamine salt (**III** · HCl) reacts with primary alcohols more slowly, and its behaviour with *t*-butanol is also different because here we could observe a strange reaction; namely the formation of *β*-triphenylethyl trityl ether (**X**); the mechanism of this reaction will be studied later.

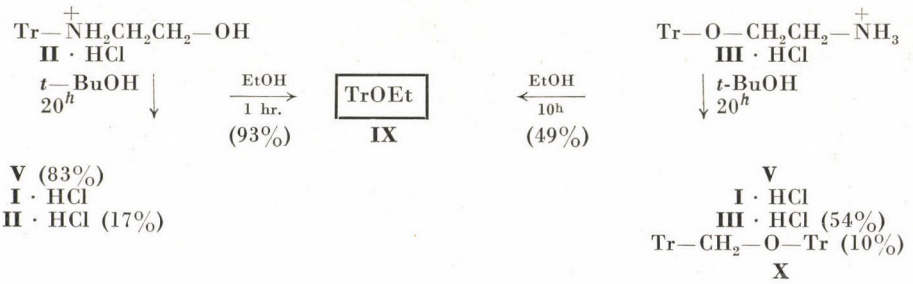

It is true that, in the cases of **II** · HCl and **III** · HCl derivatives, in *t*-butyl alcohol, the reaction only goes as far as the tritylation of water formed by dehydration of the tertiary alcohol, and neither trityl migration nor intermolecular transtritylation reaction (*i.e.* the formation of N,O-ditritylethanolamine) could be observed.

This might be ascribed to the fact that the monotritylethanolamines **II** and **III** are incapable of trityl migration under the applied experimental condi-

tions. So they cannot be transtritylated (N → O or O → N) intramolecularly, owing to steric reasons. But the salts **II** · HCl and **III** · HCl showed different behaviour in the presence of tertiary bases capable of transferring a trityl group. Thus boiling these salts in absolute pyridine converted them to N,O-ditritylethanol-amine (**IV**). Transtritylation can occur only in the presence of a suitable transferring material, *e.g.* pyridine, which assists the formation of a transition complex and in this way also the transient heterolysis of the N-trityl or O-trityl bonds.

$$\textbf{II} \cdot \text{HCl or } \textbf{III} \cdot \text{HCl} \xrightarrow[\text{pyridine}]{\text{Reflux in}} \text{TrNH}-\text{CH}_2\text{CH}_2-\text{OTr}$$

Experimental

All melting points were determined on a Boetius micro melting point apparatus. The infrared spectra were obtained with an UR-10 (Zeiss, Jena) spectrometer in KBr pellets, the mass spectra were recorded with an AEI MS 902 mass spectrometer. The elemental composition of the molecular ions was determined by exact mass measurements.

Conditions of thin-layer chromatography: silica gel; solvent systems: benzene–methanol 95 : 5 v/v (Solvent *a*), or benzene–ether 10 : 90 v/v (Solvent *b*); detection with methanol–conc. H_2SO_4 3 : 1; yellow spots appear after warming the plates.

Preparation of N-tritylethanolamine

N-Tritylethanolamine (II)

(a) Ethanolamine (7.33 g; 0.12 mole) and trityl chloride (0.55 g; 0.002 mole) were shaken (30 min) at room temperature till dissolution. Excess ethanolamine (6.35 g) was recovered at 68—70°/0.4 mm. The product (0.6 g; 96%), m.p. 71—88 °C* (from ethanol) gave one spot on TLC in Solvent *a*, R_f 0.64. The IR spectrum of **II** showed peaks at 3500—3150 cm^{-1}: νOH, and 3362 cm^{-1}: νNH. Recrystallization from 96% ethanol, aqueous acetone, benzene–ligroin or ethanol, gave feathery needles, m.p. 71—88 °C (dried over P_2O_5 in vacuum at room temperature). The molecular weight, determined by mass spectrometer, was 303. The material contained no accompanying contaminations.

$C_{21}H_{21}NO \cdot \frac{1}{2} H_2O$ (312.4). Calcd. C 80.7: H 7.1; N 4.5; O 7.7. Found C 81.1, 81.1; H 7.2, 7.4; N 3.9, 4.2; O 7.6, 7.7%.

Buckus *et al.* [1] reported m.p. 75—76 °C for compound **II.**

(b) Ethanolamine (2.4 g; 0.039 mole) and trityl chloride (5.6 g; 0.02 mole) were refluxed in abs. pyridine (15 ml). The reaction mixture was poured in water, the solid filtered off and air-dried, as described by Buckus *et al.* [1]. The crude product (6.0 g; m.p. 110—135 °C) gave 4 spots on TLC; R_f 0.08, R_f 0.64, R_f 0.77 and R_f 0.84.

The solid was boiled with abs. ethanol, and filtered to yield 0.36 g (6%) of a substance, m.p. 169—170 °C, R_f 0.84. Its IR spectrum showed a stretching vibrational band at 3320 cm^{-1}: νNH.

$C_{40}H_{35}NO$ (545.7). Calcd. C 88.1; H 6.4; N 2.6. Found C 88.2, 88.3; H 6.3, 6.5; N 2.5, 2.6%.

This compound is N,O-ditritylethanolamine (**IV**), reported by Buckus *et al.* [1] with m.p. 148—150 °C.

The above alcoholic filtrate was mixed with water, when feathery needles separated. Yield: 5.1 g (85%), m.p. 71—88 °C, R_f 0.64 (in Solvent *a*). The IR spectrum was similar to that of compound **II** prepared as described under *(a)*.

$C_{21}H_{21}NO \cdot \frac{1}{2} H_2O$ (312.4). Calcd. C 80.7; H 7.1; N 4.5; O 7.7. Found C 80.1, 80.6; H 7.5, 7.4; N 4.4, 4.6; O 8.1, 8.1%.

* The wide range of this melting point is not due, most likely, to a chemical change, because heating this material for 20 hrs. at 100 °C left the starting material unchanged, as demonstrated by TLC and mass spectroscopy.

The alcoholic mother liquor from the above filtrate was evaporated to leave a pale yellow gum. This was treated with dry ether (3 × 10 ml), and the ether extract was concentrated at the pump. The solid [(0.25 g; 4.1%), m.p. 163—164 °C (from ethanol), R_f 0.77 (in Solvent *a*)] showed in the IR spectrum a peak at 3478 cm^{-1}: νOH. This was triphenylcarbinol (**V**). The remaining gum crystallized well from abs. acetone (0.29 g; 4.83%), m.p. 180—181 °C, R_f 0.08. IR spectrum: $\nu\overset{+}{N}H_3$ at 3150—2200 cm^{-1} and νC—O—C at 1048 cm^{-1}.

$C_{22}H_{23}NO_4$ (365.4). Calcd. C 72.3; H 6.3; N 3.8. Found C 71.6; H 6.6; N 4.3%.

This compound is a hydrogen carbonate derivative of O-tritylethanolamine (**III**). The tendency of aminoethanol to absorb carbon dioxide on exposure to the air is known [6]. The base, (m.p. 91—91.5 °C, undepressed upon admixture with an authentic sample) was obtained by warming the above salt with aqueous potassium hydroxide solution: R_f 0.08 (in Solvent *a*).

(c) Ethanolamine (3.75 g; 0.06 mole) and trityl chloride (0.55 g; 0.002 mole) were dissolved in dry chloroform (10 ml) and allowed to stand at room temperature for 30 min. Similar results as described under *(b)* were obtained.

Preparation of O-tritylethanolamine

Method A

ω-Trityloxyethylphthalimide (VIII)

A solution of ω-hydroxyethylphthalimide (18.1 g; 0.1 mole) and trityl chloride (31.0 g; 0.11 mole) in abs. pyridine (200 ml) was heated at 50 °C for 1 hr., then kept at room temperature (24 hrs.). The product which separated upon the addition of water (1000 ml) was dried, and extracted with alcohol in a Soxhlet apparatus. The insoluble residue was recrystallized from acetone to yield 34.2 g (78.9%), m.p. 163—164 °C.

IR spectrum: νCO at 1770 cm^{-1}; ν_sCO at 1712 cm^{-1}; νAr at 1615, 1600 and 1495 cm^{-1}; νC—O—C at 1085 cm^{-1}; 1,2-disubstituted aromatic ring at 720, 728 cm^{-1}; monosubstituted aromatic ring at 768, 755, 710, 701 cm^{-1}.

O-Tritylethanolamine (III)

The above phthalimide derivative (**VIII**) (4.33 g; 0.01 mole) was dissolved in ethanol (25 ml) and refluxed with 72% hydrazine hydrate (5 ml) for 5 hrs. The phthalazine-1,4-dione was filtered off and the filtrate was mixed with 10% hydrochloric acid adjusting pH 7, whereupon the O-tritylethanolamine salt (**III** · HCl) separated; yield 2.9 g (85%), m.p. 197—199 °C (after washing with dry ether).

$C_{21}H_{22}ClNO$ (339.9). Calcd. C 74.2; H 6.5; N 4.1; Cl 10.4. Found 74.4; H 6.8; N 4.3; Cl 10.1%.

The base (**III**) was prepared from 1.0 g of the above salt (**III** · HCl), by mixing it with aqueous potassium hydroxide (30%, 20 ml). Yield: 0.7 g, m.p. 91—91.5 °C (from aqueous ethanol).

$C_{21}H_{21}NO$ (303.4). Calcd. C 83.2; H 6.6; N 4.6. Found C 83.0; H 6.5; N 4.7%.

Method B

N-Carbobenzoxyethanolamine (VI)

To freshly distilled ethanolamine (21 ml; 20.6 g; 0.336 mole), carbobenzoxy chloride (7.5 g; 0.044 mole) was added by drops, with cooling and stirring. The white crystalline product (from cold dry petroleum ether) was 8.3 g (97.6%, calcd. for the benzyl ester); m.p. 45—50 °C.

$C_{10}H_{13}NO_3$ (195.2). Calcd. N 7.2. Found N 7.3, 7.4%.

IR spectrum: νNH at 3327 cm^{-1}; νOH at 3500—3150 cm^{-1}; νC_{Ar}—H at 3064—3036 cm^{-1}. νCH_2 at 2942, 2888 cm^{-1}; νCO at 1696 cm^{-1}; δNH at 1532, 1540 cm^{-1}; νC_{Ar}—O—C at 1278 cm^{-1}; νC—O at 1040 cm^{-1}; mono-substitution at 748, 698 cm^{-1}.

N-Carbobenzoxy-O-tritylethanolamine (VII)

A well-dried sample of **VI** (0.5 g; 0.0025 mole) and trityl chloride (0.8 g; 0.0028 mole) were refluxed for 2 hrs in abs. pyridine (10 ml). The product separated after dilution with water; 0.95 g (87%); m.p. 75—76 °C (from abs. ethanol).

IR spectrum: νNH at 3352 cm^{-1}; mono-aromatic substitution at 768, 702 cm^{-1}.

$C_{29}H_{27}NO_3$ (437.5). Calcd. C 79.6; H 6.2; N 3.2; O 11.0. Found C 79.9, 80.8; H 6.3, 6.4; N 3.0, 3.1; O 10.9, 11.0%.

O-Tritylethanolamine (III)

The above compound (**VII**) (2.0 g; 0.0045 mole) was shaken with hydrogen in the presence of 10% palladium-on-carbon catalyst at room temperature and atmospheric pressure in abs. ethyl acetate (100 ml); about 100 ml hydrogen was absorbed. The solvent was evaporated at the pump; on the addition of dry ether (20 ml) a solid (0.5 g; 31.7%) separated. This was the *hydrogen carbonate derivative* of **III**. The base (**III**) was liberated by the addition of aqueous potassium hydroxide solution; m.p. 91—91.5 °C.

N-Benzoyl derivative of III

O-Tritylethanolamine (**III**) (0.10 g) was acylated with benzoyl chloride (0.10 ml) in abs. pyridine (3 ml). After a short time the solution was diluted with water whereupon a gum separated. This gum slowly crystallized from a mixture of chloroform and petroleum ether to give a colourless powder, m.p. 135—136 °C.

IR spectrum: νNH 3296 cm^{-1}; νCO (amide) 1635 cm^{-1}; δNH (amide) 1552 cm^{-1}; νC—O 1068 cm^{-1}; monosubstituted Ar ring at 763, 750, 710, 702 cm^{-1}.

$C_{28}H_{25}NO_2$ (407.5). Calcd. C 82.6; H 6.1; N 3.4. Found C 82.4, 82.7; H 6.3, 6.2; N 3.5, 3.5%

Ditritylation of ethanolamine, O-tritylation of II, and intermolecular transtritylation of II · HCl and III · HCl

N,O-Ditritylethanolamine (IV)

(a) Ethanolamine (2.4 g; 0.039 mole) and trityl chloride (33.6 g; 0.12 mole) were allowed to react in abs. pyridine (55 ml) under the conditions used by BUCKUS *et al.* The product was 17 g (80%), m.p. 168—169 °C (from ethanol), R_f 0.84 (in Solvent *a*).

IR spectrum: νNH at 3320 cm^{-1}.

$C_{40}H_{35}NO$ (545.7). Calcd. N 2.6. Found N 2.6, 2.7%.

(b) N-Tritylethanolamine (**II**) (2.5 g; 0.008 mole) and trityl chloride (3.4 g; 0.012 mole) were refluxed in abs. pyridine (20 ml) under the conditions given by BUCKUS *et al.* Yield: 4.0 g (91.7%); m.p. 168—169 °C (from ethanol or acetone), undepressed in admixture with a sample of the product made according to *(a)*. R_f 0.84 (in Solvent *a*).

(c) The hydrochloride (**II** · HCl or **III** · HCl: 1.0 g; 0.003 mole) and abs. pyridine (15 ml) were refluxed for 7 hrs., then kept at room temperature for 24 hrs. The solvent was evaporated in vacuum to leave a pale yellow syrup. This crystallized from abs. ethanol to yield 0.95 g (57.9%) of a substance, m.p. 168—169 °C R_f 0.84. It was identical with the products described under *(a)* and *(b)*.

Detritylation of IV. N-Tritylethanolamine hydrochloride (II · HCl)

The above ditrityl compound (**IV**) (1.4 g; 0.0025 mole) was dissolved in dry benzene (30 ml) and cooled in ice-water, then treated with dry hydrogen chloride gas. The product was 0.80 g (94.1%), m.p. 180—181 °C (BUCKUS *et al.* [1] reported m.p. 167—168 °C). R_f 0.80 (in Solvent *b*).

IR spectrum: $\nu\overset{+}{N}H_2$ at 3102—2500 cm^{-1}; νOH at 3360 cm^{-1}.

$C_{21}H_{21}ClNO$ (339.9). Calcd. N 4.1; Cl 10.5. Found N 4.1; Cl 10.6%.

Reactions of the isomeric monotritylethanolamine salts with primary alcohols

Reaction of ethanol with II · HCl (a) and III · HCl (b)

(a) N-Tritylethanolamine hydrochloride (**II** · HCl) (1.0 g; 0.003 mole) and abs. ethanol (30 ml) were refluxed for 40 min. Removal of the solvent and the addition of water gave 0.76 g (88%) of colourless cubes, m.p. 82—83 °C (from 96% ethanol), R_f 0.36 (in Solvent *a*). Mixed

m.p. with an authentic sample [5] was 82—83 °C. When this experiment was repeated with 1-hr. reflux, the yield was 0.80 g (93%) of trityl ethyl ether.

(b) The isomeric salt (**III** · HCl) (1.0 g) was refluxed for 10 hrs. with abs. ethanol (30 ml); work-up according to *(a)* gave 0.42 g (49%) of trityl ethyl ether [5], m.p. and mixed m.p. 82—83 °C.

Reaction of t-butanol with II · HCl (a) and III · HCl (b)

(a) *t*-Butanol (100 ml) and N-tritylethanolamine hydrochloride (**II** · HCl) (1.0 g; 0.003 mole) were heated at the boiling temperature under strictly anhydrous conditions for 20 hrs. The solvent was removed at the pump to leave a solid (0.85 g), m.p. 135—180 °C. This was taken up in dry ether (40 ml). The insoluble material, after recrystallization from ethanol, was 0.14 g (14%), m.p. 174—176 °C (unchanged **II** · HCl). The ether filtrate was evaporated at the pump to leave a solid, 0.65 g (83%), m.p. 163—164 °C (from ethanol), which proved to be triphenylcarbinol, its IR spectrum showing a peak at 3478 cm^{-1}; νOH. The mother liquor contained no ditrityl derivative.

(b) 1.0 g (0.003 mole) O-tritylethanolamine hydrochloride (**III** · HCl) was refluxed in abs. *t*-butanol (100 ml) for 20 hrs. The solid left behind after evaporation of the solvent, was suspended in abs. ether (40 ml) and filtered to yield 0.64 g, consisting of a mixture of unchanged **III** · HCl, **X** and **I** · HCl. This mixture was shaken with 10 ml 25% aqueous KOH solution and after 3 hrs. the solid was filtered off and washed with hot ethanol. On the filter paper there remained 0.10 g of a gleaming, crystal-like powder, which was recrystallized from a mixture of dioxan and ethanol; m.p. 185—186 °C. The analytical data showed the product to be β-triphenylethyl trityl ether (**X**).

Molecular weight (from mass spectrum): 516. Most important bands of the IR spectrum: νOH: —; νAr 1605, 1498, 1453 cm^{-1}; νCH: 772, 759, 704 cm^{-1}; νC—O 1038 (979?) cm^{-1}.

The compound could not be acylated with acetic anhydride in pyridine.

$C_{39}H_{32}O$ (516.6). Calcd. C 90.5; H 6.2. Found C 90.9, 90.4; H 6.4, 6.1%.

*

We wish to thank Dr. F. RUFF for the infrared spectra, P. BRUCK for the mass spectra, Dr. H. MEDZIHRADSZKY and the members of the microanalytical laboratory, and Gy. KORONCZAY technical assistant for the thin-layer chromatography.

REFERENCES

[1] BUCKUS, P. F., SABONIENE, R. U., LAMESIENE, D.: Zh. Org. Khim. **6** (10), 1984 (1970); C. A. **74**, 12723d (1971)

[2] BUCKUS, P. F.: Usp. Khim. **39** (1), 112 (1970); C. A. **72**, 100171m (1970)

[3] BUCKUS, P. F., SABONIENE, R. U.: Zh. Org. Khim. **5**, 533 (1969); SHORIGIN, P. P.: Ber. **59**, 2510 (1926); SHORIGIN, P. P., SKOBLINSKAJA, S. A.: Dokl. Akad. Nauk **14**, 505 (1937); ALPHEN, J. VAN: Rec. trav. chim. **46**, 287 (1927); IDDLES, H., FRENCH, K., MELLON, E.: J. Am. Chem. Soc. **61**, 3192 (1939); MACKENZIE, C., CHUCANI, G.: J. Org. Chem. **20**, 336 (1955); IDDLES, H., MINCKLER, H.: J. Am. Chem. Soc. **62**, 2757 (1940); IDDLES, H., MILLER, W., POWERS, W., *ibid.* **62**, 71 (1940); FUNAKUBO, E., HIROTANI, T.: Ber. **69**, 2123 (1936); FUNAKUBO, E., *ibid.* **70**, 1981 (1937); BURTON, H., CHEESEMAN, G.: J. Chem. Soc. **1953**, 832; BUCKUS, P. F., RAGUOTENIE, N. V., BUCKENIE, A. J.: Zh. Org. Khim. **4**, 4413 (1968); *idem.*, *ibid.* **4**, 2120 (1968); PARSONS, G., PORTER, C.: J. Am. Chem. Soc. **54**, 363 (1932)

[4] CHUCHANI, G., RODRIGUEZ-UZCANGA, V.: Tetrahedron **22**, 2665 (1966); BUCKUS, P. F., RAGUOTENIE, N. V., BUCKENIE, A. J.: Zh. Org. Khim. **4**, 181 (1968); ALPHEN, J. VAN: Rec. trav. chim. **46**, 501 (1927); BOYD, D., HARDY, D.: J. Chem. Soc. **1928**, 630; HARDY, D., *ibid.*, **1929**, 1000

[5] FRIEDEL, C., CRAFTS, J. M.: Ann. de Chim. et de Phys. **6**, 1, 503

[6] GUYER, A., PÜRNER, G.: Helv. Chim. Acta **21**, 1341 (1938); GRÜN, Ad., LIMPÄCHER, R.: Ber. **59**, 1349 (1926); SHNEERSON, A. L., LEIBUSH, A. G.: Zh. prikl. Khim. **19**, 871 (1946); *cf.* C. A. **41**, 4340f (1947) and the references cited therein

Károly KÖRMENDY; 1088 Budapest VIII., Múzeum krt. 4/b. Hungary
Mohamed M. EL-SAWY; 20A, Road 510, Maadi, Cairo, A. R. Egypt.

Acta Chimica Academiae Scientiarum Hungaricae, Tomus 83 (1), pp. 115—117 (1974)

NOTE ON THE ACYLATION OF 1-(3,4-DIMETHOXYPHENYL)-5-ETHYL-7,8-DIMETHOXY-4-METHYL-5*H*-2,3-BENZODIAZEPINE

(SHORT COMMUNICATION)

M. LEMPERT-SRÉTER

(Department of Organic Chemistry, Eötvös Loránd University, Budapest)

Received February 22, 1974

Acylations of the title compound (**2**) take place at N-3 under migration of the endocyclic double bond between N-3 and C-4 into the semicyclic position.

In connection with another research project we became interested in the acylations of the title compound (**2**). The latter has been prepared essentially according to a Hungarian patent [1] by reacting 1-(3,4-dimethoxyphenyl)-4-ethyl-6,7-dimethoxy-3-methyl-2-benzopyrylium chloride (**1**) with hydrazine hydrate.* Both the IR and NMR spectra (which do not exhibit NH bands and signals, respectively) are in agreement with the assumed tautomeric structure of the starting compound.

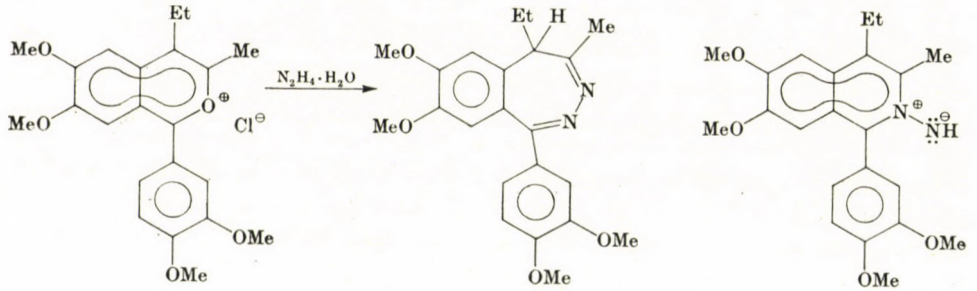

1 **2** **3**

When **2** was allowed to react with *p*-nitrobenzoyl chloride in pyridine and with acetic anhydride, smooth acylations took place. The positions of the carbonyl bands in the IR spectra of the resulting acyl derivatives clearly demonstrated that they were N-substituted products. The proton, lost in exchange for the acyl groups, came in both cases from the 4-methyl group of **2**, since the signal of this group disappeared from the NMR spectra as a result of the acylation and became replaced by the AB doublet of a newly formed

* Originally the 1-(3,4-dimethoxyphenyl)-4-ethyl-6,7-dimethoxy-3-methylisoquinolinioamide structure **3** has been assigned to the product in Ref. [1], but in an addendum to the patent this structure assignment has been revised [2].

terminal methylene group. The structures of the acyl derivatives are therefore represented by the general formula **4.**

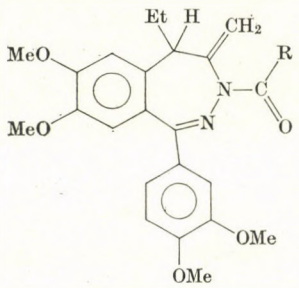

4

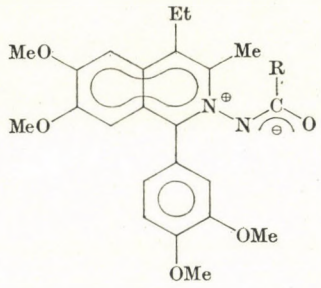

5

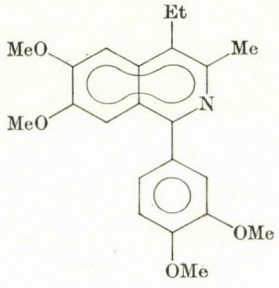

6

An analogous *N*-acylation under migration of the endocyclic C=N double bond into the semicyclic position has been observed in the reaction of 1-methyl-3,4-dihydroisoquinoline with aryl isocyanates [3].

Synthesis of the isomeric isoquinolinioamidates **5** by acylation of the isoquinolinioamide **3** could not be carried out since *N*-amination of the isoquinoline **6** to yield **3** could not be performed [4] even with the powerful amination reagent *O*-(2,4,6-trimethylphenylsulfonyl)-hydroxylamine [5].

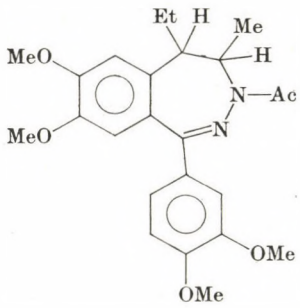

7

Experimental

NMR and IR spectra were obtained at 60 MHz in $CDCl_3$ solution with TMS as internal reference and in KBr pellets, respectively, with the aid of a Perkin—Elmer spectrometer, Type R-12 and a Carl Zeiss spectrometer, Type UR-10, respectively.

NMR spectrum of 1-(3,4-dimethoxyphenyl)-5-ethyl-7,8-dimethoxy-4-methyl-5H-2,3-benzodiazepine (2)

δ 1.1 ppm, t, $J = 7.3$ Hz, 3H, $CH_2—\mathbf{CH_3}$; δ 2.0 ppm, s, 3H, 4-**Me**; δ 2.15 ppm, m, 2H, $CH—\mathbf{CH_2}—CH_3$; δ 2.8 ppm, t, $J = 7.3$ Hz. 1H, $>\mathbf{CH}—CH_2$; δ 3.75, 3.91, 3.93, 3.97 ppm, s, 3H, each, $(CH_3O)_4$; δ 6.7—7.7 ppm, m, 5H, Ar**H.**

3-Acetyl-1-(3,4-dimethoxyphenyl)-5-ethyl-7,8-dimethoxy-4-methylene-4,5-dihydro-3H-2,3--benzodiazepine (4, R=Me)

A mixture of **2** (0.38 g; 1 mmole), pyridine (3 cm^3) and acetic anhydride (0.6 cm^3) was allowed to stand overnight in a refrigerator and for a day at room temperature. The solution was poured into ice-water, the product was extracted with ether and the ether solution was washed with water and evaporated to dryness. The residue was recrystallized from ethanol to yield 0.28 g (67%) of **4** (R = Me), m.p. 151—153 °C.

$C_{24}H_{29}N_2O_5$ (425.5). Calcd. C 67.74; H 6.87; N 6.59. Found C 68.10; H 6.92; N 6.79%.
IR: νCO 1680 cm^{-1}.

NMR: δ 0.95 ppm, t, J = 7.5 Hz, 3H, $CH_2-\mathbf{CH_3}$; δ 1.8 ppm, m, 2H, $CH-\mathbf{CH_2}-CH_3$; δ 2.5 ppm, s, 3H, Ac; δ 3.55 ppm, t, J = 7.5 Hz, 1H, $>\mathbf{CH}-CH_2$; δ 3.70, 3.90, 3.95, 3.98 ppm, s, 3H, each, $(CH_3O)_4$; δ 5.1 and 5.25, s, 1H, each, $=CH_2$; δ 6.7—7.45 ppm, m, 5H(Ar**H**).

3-Acetyl-1-(3,4-dimethoxyphenyl)-5-ethyl-7,8-dimethoxy-4-methyl-4,5-dihydro-3H-2,3-benzodiazepine (7)

The above product was reduced in ethyl acetate solution at room temperature and atmospheric pressure in the presence of a Pd/C catalyst to yield 62% of compound **7**, m.p. 174—175 °C (EtOH).

$C_{24}H_{31}N_2O_5$ (427.5). Calcd. C 67.42; H 7.31; N 6.56. Found C 67.73; H 7.32; N 6.49%.
IR: νCO 1640 cm^{-1}.

NMR: δ 0.85 ppm, d, J = 6 Hz, 3H, 4-**Me**; δ 1.05 ppm, t, J = 7 Hz, 3H, $CH_2-\mathbf{CH_3}$; $\delta \sim$ 1.9 ppm, m, 4H, $CH-\mathbf{CH_2}-CH_3$, 4**H** + 5**H**; δ 2.4 ppm, s, 3H, Ac; δ 3.70, 3.85, 3.90, 3.95 ppm, s, 3H, each, $(CH_3O)_4$; δ 6.7—7.4 ppm, m, 5H (Ar**H**).

1-(3,4-Dimethoxyphenyl)-5-ethyl-7,8-dimethoxy-4-methylene-3-(*p*-nitrobenzoyl)-4,5-dihydro--3H-2,3-benzodiazepine (4, R = $p-O_2NC_6H_4$)

p-Nitrobenzoyl chloride (0.4 g, 100% excess) was added to a solution of **2** (0.4 g) in pyridine (3 cm^3). Heat was evolved and the crystalline product started to precipitate within a few minutes. The mixture was allowed to stand for a couple of hours and poured into water. The lemon yellow crystalline crude product was recrystallized from ethyl acetate–ethanol to yield 0.2 g (38%) of **4** (R = $p-O_2NC_6H_4$), m.p. 222—223 °C.

$C_{29}H_{29}N_3O_7$ (531.6). Calcd. C 65.53; H 5.50; N 7.91. Found C 65.35; H 5.75; N 7.90%.
IR: νCO 1670 cm^{-1}.

NMR: δ 1.08 ppm, t, J = 7.5 Hz, 3H, $CH_2-\mathbf{CH_3}$; δ 1.9 ppm, m, 2H, $CH-\mathbf{CH_2}-CH_3$; δ 3.6 ppm, t, J = 8 Hz, 1H, $>\mathbf{CH}-CH_2$; δ 3.7, 3.75, 3.9, 4.0 ppm, s, 3H, each, $(CH_3O)_4$; δ 5.15 and 5.4, s, 1H, each, $=CH_2$; δ 6.6—7.4 ppm, m, 5H, Ar**H**, benzodiazepine: δ 7.65 and 8.23 ppm, AA'BB' quadruplet, J = 8.5 Hz, 4**H**, *p*-nitrobenzoyl.

*

The author's thanks are due to Dr. H. MEDZIHRADSZKY—SCHWEIGER for the microanalyses, to Dr. F. RUFF for the IR and to Dr. P. KOLONITS (Technical University, Budapest) for the NMR spectra.

REFERENCES

[1] KŐRÖSI, J., LÁNG, T., KOMLÓS, E., PETŐCZ, L.: Hung. Pat. No. 155 572 (December 9, 1966); Chem. Abstr. **70**, 115 026 (1969)
[2] KŐRÖSI, J., LÁNG, T., KOMLÓS, E., PETŐCZ, L.: Addendum to Hung. Pat. No. 155 572 (December 9, 1966)
[3] RICHTER, R.: Chem. Ber. **105**, 82 (1972)
[4] ÁGAI, B., private communication
[5] TAMURA, Y., MINAMIKAWA, J., KITA, Y., KIM, J. H., IKEDA, M.: Tetrahedron **29**, 1063 (1973)

Magda LEMPERT-SRÉTER; 1088 Budapest, Múzeum krt. 4/b. Hungary.

INDEX

Printed in Hungary

A kiadásért felel az Akadémiai Kiadó igazgatója — Műszaki szerkesztő: Zacsik Annamária

A kézirat nyomdába érkezett: 1974. VII. 4. — Terjedelem: 10,5 (A/5) ív, 71 ábra

74.634 Akadémiai Nyomda, Budapest — Felelős vezető: Bernát György

ACTA CHIMICA
ТОМ 83 — ВЫП. 1

РЕЗЮМЕ

Исследование отечественных и иностранных летучих масел, III

К. РЕТИ-БЕЛАФИ, Э. КЕРЕНИ и Р. КОЛЬТА

Был исследован качественный и количественный состав летучего масла отечественного растения укропа с помощью совокупности методов эффективного разделения и спектрометрической идентификации. В летучем масле было обнаружено 14 компонентов (в количестве, превышающем 0,01 вес.%), из которых 3 компонента (α-фелландрен, лимонен и карвон) вместе составляют 90 вес.%, а с дальнейшими 8 компонентами уже — 99,9 вес.%. Помимо трех основных компонентов в образцах летучего масла заграничного укропа были обнаружены α-пинен, дигидрокарвон и п-цимол, которые присутствуют и в летучем масле отечественного укропа. Терпены и их производные, которые согласно специальной литературе являются компонентами масел, не были найдены в исследованном летучем масле в количествах, заслуживающих упоминания. Однако, было доказано, что присутствуют α-туен, β-мирцен, β-фелландрен, 1-метил-4-изопропенил-бензол и карвотанацетон. Наконец, удалось обнаружить два новых компонента, до сих пор не известных в литературе для укропного масла и для летучих масел вообще.

Исследование молекулярной структуры производных 4H- пиридо (1,2-a) пиримидин-4-она с помощью УФ спектроскопии

Г. ХОРВАТ, А. И. КИШ, З. МЕСАРОШ и И. ХЕРМЕЦ

Были сняты электронные спектры производных 4H-пиридо [1,2-a] пиримидин-4-она. На основе эффекта заместителей были изучены молекулярное строение и, в особенности, сопряжение в ненасыщенных и частично насыщенных молекулах. На основе эффекта ионизации было установлено, что атом азота в положении 1 протонируется в кислых средах. Исходя из изменения спектров с pH, были рассчитаны константы ионизации протонирования.

Эффект энтропии обычной дестилляции и дестилляции со «ступенчатым переносом» тепла

Ж. ФОНЁ и П. ФЁЛЬДЕШ

Было введено и определено понятие кпд нетто эффекта энтропии процесса разделения, и приводится его изменение в случае обычной дестилляции и дестилляции со ступенчатым переносом тепла (ДСПТ) при различных параметрах процесса. Результаты анализа находятся в согласии с литературными величинами термодинамических кпд, полученными на основе промышленных измерений. Было указано, что стоимость работы ДСПТ, осуществленной с помощью теплоносителей с изменяющимся уровнем температур, может быть приблизительно рассчитана непосредственно из продукции энтропии.

Новые достижения в области катализа на металлах

П. ТЕТЕНИ, Л. ГУЦИ и З. ПААЛ

Принимая в учет взаимодействие между металлическим катализатором и реагирующим субстратом, авторами рассматриваются некоторые вопросы адсорбции, гидрогенолиза, изомеризации и дегидроциклизации. На основе собственных и литературных данных была

обсуждена, в первую очередь, роль водорода в некоторых каталитических реакциях углеводородов, принимая во нимание его эффект на характер и меру взаимодействия углеводорода с металлом. Было сделано заключение, что для интерпретации каталитического влияния недостаточно знание различных характерных параметров металла, т. к. каталитическое влияние оказывает каталитическая система, образующаяся в результате взаимодействия между реагирующим субстратом и металлом.

На этой остнове дискутируется заключение, сделанное одним из авторов несколько лет тому назад, согласно которому между каталитическими свойствами металлов и их окислов нет принципиальной разницы.

Свойства смесей аминов со спиртами, IV

Ф. РАТКОВИЧ, Т. ШАЛАМОН и Л. ДОМОНКОШ

Исследуя первичные спирты, а также некоторые первичные, вторичные и третичные амины, была найдена зависимость между средней степенью ассоциации перечисленных компонентов и их вязкостью. Был разработан метод приближенного расчета средней степени ассоциации, исходя из данных вязкости. Было показано, что порядок констант ассоциации, рассчитанных из средней степени ассоциации, находится в согласии с равновесными константами, определенными другими способами. Для исследования средней степени ассоциации смеси н-бутиламин — 1-бутанол был использован метод, основанный на измерении вязкости. Было установлено, что результаты, полученные при образовании смешанных ассоциатов, исключают всякое такое предположение, которое на основе отрицательной энтропии смешения системы и экзотермической теплоты смешения ассоциатов A_i и B_j объясняет образование смешанных ассоциатов A_i B_j со средней степенью ассоциации, превышающей исходную.

Свойства смесей аминов со спиртами, V

Ф. РАТКОВИЧ, и Ж. ГУТИ

Была измерена теплота смешения ди-н-бутиламина с нормальными первичными спиртами при температуре 20 $\pm$ 1°С. Было установлено, что при эквимолярном составе измеряемая экзотермическая теплота смешения практически совпадает с результатами, полученными в подобных смесях с н-бутиламином. Было доказано, что экзотермический тепловой эффект взаимодействия спирта с амином не зависит, в хорошем приближении, от того, что с молекулой спирта взаимодействует превичный или вторичный амин. Из данных, полученных в смесях с небольшим содержанием амина, вытекает, что те различия, которые наблюдаются между свойствами смесей спирт- ди-н-бутиламин и спирт — н-бутиламин, могут быть приписаны различной степени самоассоциации первичных и вторичных аминов. Это подтверждается расхождением целого порядка между величинами эндотермической теплоты смешения смесей н-бутиламин — н-гексадекан и ди-н-бутиламин — н-гексадекан.

Свойства смесей, содержащих амины и спирты, VI

Ф. РАТКОВИЧ, Т. ШАЛАМОН и Л. ДОМОНКОШ

Вязкость нормальных первичных спиртов, нормальных углеводородов и третичных ароматических аминов была исследована в интервале 233—353 °К. Была определена энтальпия активации вязкого потока. В случае нормальных углеводородов и третичных аминов она является линейной функцией молекулярного веса и практически не зависит от данной гомологической серии. Используя эту кривую в качестве калибровочной кривой, был рассчитан молекулярный вес неассоциированного компонента, имеющего ту же самую энтальпию активации. Этот молекулярный вес полагался средним молекулярным весом ас-

социированных частиц спирта. Было найдено, что — в согласий с нашими более ранними результатами в этой области — средняя степень ассоциации равна приблизительно 4 в жидких спиртах и лишь слегка зависит от температуры. Этот результат может быть объяснен совместным появлением циклических полимеров и ассоциации цепей, т. к. в этом случае максимальная величина степени ассоциации лишь слегка отличается от 4. Было определено, что в ряду метанол — 1-гептанол наблюдается уменьшение ассоциации.

Получение металлосодержащих, координационно-связанных полимеров из конденсационных олигомеров

И. СМЕРЧАНИ-ВАНЧО и П. ХИРШБЕРГ

Была исследована полимеризация по координационным связям нейтральных олигоэфиров, содержащих свободные концевые группы COOH. Центральным атомом металла в данном случае являлся атом цинка.

Если атом цинка включен в систему в форме окиси, то, соответственно его природе щелочного ангидрида, он реагирует с группами COOH, уже на первой стадии, по ионному механизму. Однако, в зависимости от количества цинка, по всей вероятности, следует считаться и с другими механизмами реакций.

Согласно результатам исследований, ион, образующийся в самой системе из уксусной кислоты и окиси цинка, является активным с точки зрения дальнейшей реакции координационного характера, однако, данные условия не способствуют достаточной диссоциации ацетата цинка и дальнейшей координационной реакции.

SOLANUM Гликозиды, IX

П. БИТЕ и М. М. ШАБАНА

Было найдено, что незрелые фрукты Solanum oleraceum содержат соласонин и соламаргин. Были обнаружены также следы третьего неидентифицированного стероидного гликозида.

Некоторые прочие реакции, наблюдаемые при синтезе отдельных 2-[2-(2,6-ди-R-фенокси)-этиламино]-5-метил-пиримидин-4(3H)-онов

Й. РЕЙТЕР и Л. ТОЛЬДИ

2-Алкилтио-5-метилпиримидин-4(3H)-он, а также его 1- и 3-N-метил-замещенные производные, используемые в синтезе 2-[2-(2,6-ди-R-фенокси)-этильамино]-5-метил-пиримидин-4(3H)-онов, реагируя при температуре выше 200°C с соответствующими 2-(2,6-ди-R-фенокси)-этиламинами, дают *8* и *14*. Строение этих соединений было определено с помощью МС, ИК, УФ и ЯМР исследований, а также подтверждено препаративным путем. В ходе этих исследований были получены *7*, изомер соединения *8*, *19*, изомер соединения *14*, а также его деметилированные *(20)* и монозамещенные деметилированные производные *(21)*.

Реакции тритилирования и транстритилирования этаноламина

К. КЁРМЕНДИ и М. М. ЭЛЬ-САВИ

Тритилирование аминоспиртов представляет интерес, т. к. некоторые из них оказались важными в приготовлении биологически активных молекул. Они также могут служить исходным пунктом при проверке двух известных типов тритилирования, а именно,

непосредственное тритилирование и транстритилирование. Последний процесс может включать следующие превращения:

N — N'		O — O'
N — O	или	O — N
N — C		O — C и т. д.

Тритилирование этаноламина (I), в частности, описывается здесь в связи с работой Бакуса и сотр. [1]. Этими авторами утверждается, что (I) был селективно N-тритилирован с помощью хлористого тритила в кипящем пиридине, давая в качестве единственного продукта N-тритилэтаноламин (II). Однако, образование O-тритилэтаноламина (III) и других продуктов не отмечалось этими авторами.

Работа Бакуса была повторена и была получена смесь следующих продуктов: II (85%), III (4,83%), N,O-дитритилэтаноламин (6%) и трифенилкарбинол (4,17%).

The Acta Chimica publish papers on chemistry in English, German, French and Russian.

The Acta Chimica appear in volumes consisting of four parts of varying size, 4 volumes being published a year.

Manuscripts should be addressed to

Acta Chimica
Budapest 112/91 Műegyetem

Correspondence with the editors should be sent to the same address.

The rate of subscription is $ 32.00 a volume.

Orders may be placed with "*Kultúra*" Foreign Trade Company for Books and Newspapers (1389 Budapest 62, P. O. B. 149. Account No. 218 10990) or with representatives abroad.

Les Acta Chimica paraissent en français, allemand, anglais et russe et publient des mémoires du domaine des sciences chimiques.

Les Acta Chimica sont publiés sous forme de fascicules. Quatre fascicules seront réunis en un volume (4 volumes par an)

On est prié d'envoyer les manuscrits destinés à la rédaction à l'adresse suivante:

Acta Chimica
Budapest 112/91 Műegyetem

Toute correspondance doit être envoyée à cette même adresse.

Le prix de l'abonnement est de $ 32.00 par volume.

On peut s'abonner à l'Entreprise pour le Commerce Extérieur de Livres et Journaux «*Kultúra*» (1389 Budapest 62, P. O. B. 149. Compte-courant No. 218 10990) ou à l'étranger chez tous les représentants ou dépositaires.

«*Acta Chimica*» издают трактаты из области химической науки на русском, французском, английском и немецком языках.

«*Acta Chimica*» выходят отдельными выпусками разного объема. 4 выпуска составляют один том. 4 тома публикуются в год.

Предназначенные для публикации рукописи следует направлять по адресу:

Acta Chimica
Budapest 112/91 Műegyetem

По этому же адресу направлять всякую корреспонденцию для редакции.

Подписная цена — $ 32.00 за том.

Заказы принимает предприятие по внешней торговле книг и газет «*Kultúra*» (1389 Budapest 62, P. O. B. 149. Текущий счет № 218 10990) или его заграничные представительства и уполномоченные.

Reviews of the Hungarian Academy of Sciences are obtainable at the following addresses:

ALBANIA

Drejtorija Qëndrone e Përhapjes
dhe Propagandimit të Librit
Kruga Konferenca e Pazes
Tirana

AUSTRALIA

A. Keesing
Box 4886, GPO
Sydney

AUSTRIA

GLOBUS
Höchstädtplatz 3
A-1200 Wien XX

BELGIUM

Office International de Librairie
30, Avenue Marnix
Bruxelles 5
Du Monde Entier
5, Place St.-Jean
Bruxelles

BULGARIA

HEMUS
11 pl Slaveikov
Sofia

CANADA

Pannonia Books
2, Spadina Road
Toronto 4, Ont.

CHINA

Waiwen Shudian
Peking
P. O. B. 88

CZECHOSLOVAKIA

Artia
Ve Směčkách 30
Praha 2
Poštovní Novinová služba
Dovoz tisku
Vinohradská 46
Praha 2
Mad'arská Kultura
Václavské nám. 2
Praha 1
SLOVART A. G.
Gorkého
Bratislava

DENMARK

Ejnar Munksgaard
Nörregade 6
Copenhagen

FINLAND

Akateeminen Kirjakauppa
Keskuskatu 2
Helsinki

FRANCE

Office International de Documentation
et Librairie
48, rue Gay-Lussac
Paris 5

GERMAN DEMOCRATIC REPUBLIC

Deutscher Buch-Export und Import
Leninstraße 16
Leipzig 701
Zeitungsvertriebsamt
Fruchtstraße 3—4
1004 Berlin

GERMAN FEDERAL REPUBLIC

Kunst und Wissen
Erich Bieber
Postfach 46
7 Stuttgart S.

GREAT BRITAIN

Blackwell's Periodicals
Oxenford House
Magdalen Street
Oxford
Collet's Subscription Import
Department
Dennington Estate
Wellingsborough, Northants.
Robert Maxwell and Co Ltd.
4—5 Fitzroy Square
London W. 1

HOLLAND

Swetz and Zeitlinger
Keizersgracht 471—487
Amsterdam C.
Martinus Nijhof
Lange Voorhout 9
The Hague

INDIA

Hind Book House
66 Babar Road
New Delhi 1

ITALY

Santo Vanasia
Via M. Macchi 71
Milano
Libreria Commissionaria Sansoni
Via La Marmora 45
Firenze
Techna
Via Cesi 16.
40125 Bologna

JAPAN

Kinokuniya Book-Store Co. Ltd.
826 Tsunohazu 1-chome
Shinjuku-ku
Tokyo
Maruzen and Co. Ltd.
P. O. Box 605
Tokyo-Central

KOREA

Chulpanmul
Phenjan

NORWAY

Tanum-Cammermeyer
Karls Johansgt 41—43
Oslo 1

POLAND

RUCH
ul. Wronia 23
Warszawa

ROUMANIA

Cartimex
Str. Aristide Briand 14—18
Bucureşti

SOVIET UNION

Mezhdunarodnaya Kniga
Moscow G—200

SWEDEN

Almquist and Wiksell
Gamla Brogatan 26
S—101 20 Stockholm

USA

F. W. Faxon Co. Inc.
15 Southwest Park
Westwood Mass. 02090
Stechert Hafner Inc.
31. East 10th Street
New York, N. Y. 10003

VIETNAM

Xunhasaba
19, Tran Quoc Toan
Hanoi

YUGOSLAVIA

Forum
Vojvode Mišića broj
Novi Sad
Jugoslavenska Knjiga
Terazije 27
Beograd

ACTA CHIMICA

ACADEMIAE SCIENTIARUM HUNGARICAE

TOMUS 83 FASCICULUS 2

AKADÉMIAI KIADÓ, BUDAPEST

1974

ACTA CHIM. (BUDAPEST) ACASA 2 83 (2) 119–222 (1974)

ACTA CHIMICA

A MAGYAR TUDOMÁNYOS AKADÉMIA KÉMIAI TUDOMÁNYOK OSZTÁLYÁNAK IDEGEN NYELVŰ KÖZLEMÉNYEI

Az Acta Chimica német, angol, francia és orosz nyelven közöl értekezéseket a kémiai tudományok köréből.

Az Acta Chimica változó terjedelmű füzetekben jelenik meg, egy-egy kötet négy füzetből áll. Évente átlag négy kötet jelenik meg.

A közlésre szánt kéziratok a szerkesztőség címére (Budapest 112/91 Műegyetem) küldendők.

Ugyanerre a címre küldendő minden szerkesztőségi levelezés. A szerkesztőség kéziratokat nem ad vissza.

Megrendelhető a belföld számára az „Akadémiai Kiadó"-nál (1363 Budapest Pf 24. Bankszámla 215 11488), a külföld számára pedig a „Kultúra" Könyv- és Hírlap Külkereskedelmi Vállalatnál (1389 Budapest 62, P. O. B. 149. Bankszámla: 218 10990) vagy annak külföldi képviseleteinél és bizományosainál.

Die Acta Chimica veröffentlichen Abhandlungen aus dem Bereich der chemischen Wissenschaften in deutscher, englischer, französischer und russischer Sprache.

Die Acta Chimica erscheinen in Heften wechselnden Umfanges. Vier Hefte bilden einen Band. Jährlich erscheinen 4 Bände.

Die zur Veröffentlichung bestimmten Manuskripte sind an folgende Adresse zu senden:

Acta Chimica
Budapest 112/91 Műegyetem

An die gleiche Anschrift ist auch jede für die Redaktion bestimmte Korrespondenz zu richten. Abonnementspreis pro Band: $ 32.00.

Bestellbar bei dem Buch- und Zeitungs-Außenhandels-Unternehmen »*Kultúra*« (1389 Budapest 62, P. O. B. 149 Bankkonto Nr. 218 10990) oder bei seinen Auslandsvertretungen und Kommissionären.

Acta Chimica Academiae Scientiarum Hungaricae, Tomus 83 (2), pp. 119—126 (1974)

DIELECTRIC PROPERTIES AND POLYMERIZATION OF ALLYL ALCOHOL, I

DIELECTRIC PROPERTIES OF MONOMERIC ALLYL ALCOHOL

J. Liszi and Zs. Hartyáni

(Electrochemical Research Group of the Hungarian Academy of Sciences, Department of Physical Chemistry, of Chemical Industries, Veszprém)

Received October 22, 1973

The complex relative permittivity of monomeric allyl alcohol has been determined as a function of temperature and frequency. The Cole-Davidson equation was used to describe the results. The activation enthalpy of the dielectric relaxation was calculated and compared with the viscous energy. Comparison of the results for allyl alcohol and 1-propanol show that the double bond does not appreciably change the properties studied.

1. Introduction

The present paper deals with the study of some dielectric properties of allyl alcohol. The complex relative permittivity of monomeric allyl alcohol has been determined as a function of temperature and frequency. The Cole—Davidson equation is used for the description of the results. The activation energy of dielectric relaxation is calculated and compared with the viscous energy. After polymerizing the alcohol to a molecular weight of about 400, the same studies have been carried out with the resulting liquid-phase oligomer as with the monomeric alcohol. The polymerization leads to large changes in the dielectric properties examined. The first part of this series deals with monomeric liquid allyl alcohol.

2. Experimental

The normal boiling point of the allyl alcohol used was 97°C, its density at 20°C 0.855 g cm^{-3} and its refractive index $n_D^{20} = 1.4132$. The specifications of the instruments used for the determination of the complex relative permittivity are given in Table I.

Cylindrical, direct-contact cells made from a combination of stainless steel and teflon were used for the measurements. The double-walled cells were thermostated in a mixture of methanol and ethanol. The liquid in the cell was protected from atmospheric moisture by a teflon cap. The experimental results are presented in Tables II and III, and Figs 1 and 2.

For the calculation of the viscous energy, the viscosity of allyl alcohol was measured as a function of temperature. The instrument used was a Rheo-

Table I

Specifications of the instruments used for the determination of the complex relative permittivity

Specification	Frequency range
SIEMENS Scheinwiderstandsmess-brücke, Rel. 3R. 277	$\leqslant$ 1 MHz
RADELKIS, Universal Dielectrometer, Type OH-301	= 3 MHz
WAYNE KERR V. H. F. Admittance bridge, Type B 901	50—250 MHz

Table II

Low-frequency relative permittivity of allyl alcohol (ε_0) as a function of temperature (t °C)

t(°C)	ε_0
30	18.3
20	19.7
10	21.2
0	22.6
−10	24.1
−20	25.6
−30	27.0
−40	28.5
−50	29.9
−60	31.4

Viscosimeter (Rheo-Viscosimeter nach Höppler, GDR, Patent No. 210). For technical reasons the viscosity measurements could not be performed in the same wide temperature range as the dielectric measurements. The results are listed in Table IV.

3. Discussion

For the description of the complex relative permittivity of substances characterized by an asymmetrical COLE-COLE diagram [1], COLE and DAVIDSON [2] proposed the following equation:

$$\frac{\varepsilon^* - n^2}{\varepsilon_0 - n^2} = \frac{1}{(1 + j\omega\tau)^\alpha} \tag{1}$$

Table III

Real (ε') and imaginary (ε'') parts of the relative permittivity of allyl alcohol as functions of temperature and frequency

t (°C)	50 MHz		75 MHz		100 MHz		150 MHz		200 MHz	
	ε'	ε''	ε'	ε''	ε'	ε''	ε'	ε''	ε'	ε''
−60	10.3	9.6	7.2	8.5	6.3	7.4	5.8	4.3	4.3	5.3
−55	13.7	11.7	9.2	10.1	8.3	9.0	6.0	7.3	4.6	6.3
−50	16.5	11.6	11.4	11.0	9.1	10.7	6.7	8.6	5.1	7.5
−45	18.8	11.2	13.9	12.6	11.2	11.5	7.9	10.3	5.8	8.8
−40	20.4	9.7	16.4	12.0	13.5	13.0	9.5	12.1	6.6	10.3
−35	21.6	8.3	18.3	10.6	15.6	13.4	11.5	13.5	7.8	12.0
−30	22.0	6.9	19.9	9.1	17.5	12.7	14.0	14.2	9.5	13.7
−25	22.2	5.7	20.7	7.8	19.2	11.4	16.5	14.1	11.7	15.4
−20	22.1	4.6	21.3	6.4	20.5	9.8	18.6	13.4	14.3	16.4
−15	21.8	3.6	21.0	5.2	21.5	8.2	20.3	11.9	17.1	16.3
−10	21.3	2.9	20.5	4.2	21.8	6.8	21.4	10.1	19.7	15.5
−5	20.7	2.3	19.9	3.4	21.2	5.6	22.0	8.4	21.6	14.0
0	20.0	1.9	19.4	2.8	20.5	4.6	21.9	6.9	22.7	12.1
5	19.4	1.6	18.9	2.4	19.8	3.7	21.6	5.6	23.0	10.2
10	18.8	1.3	18.3	2.1	19.3	3.1	21.0	4.6	22.9	8.5
15	18.1	1.1	17.8	1.9	18.4	2.7	20.2	3.8	22.6	6.9
20	17.4	0.9	17.3	1.8	17.8	2.3	19.5	3.2	22.0	5.7
25	17.1	0.8	16.6	1.6	17.0	2.0	18.8	2.7	21.2	4.7
30	16.2	0.6	16.0	1.5	16.4	1.8	18.0	2.3	20.1	4.3

where ε^* — complex relative permittivity;
ε_0 — static relative permittivity;
n — 'internal' refractive index [3];
ω — angular frequency;
τ — macroscopic relaxation time;
j — the imaginary unity; and
α — an empirical constant: $0 < \alpha \leqslant 1$.

If $\alpha = 1$, the COLE—DAVIDSON equation (1) simplifies to the DEBYE equation [4].

Rationalization of Eq. (1) gives the following relations:

$$\frac{\varepsilon' - n^2}{\varepsilon_0 - n^2} = \cos^{\alpha}(\omega\tau)\cos(\alpha\omega\tau) \tag{2}$$

$$\frac{\varepsilon''}{\varepsilon_0 - n^2} = \cos^{\alpha}(\omega\tau)\sin(\alpha\omega\tau). \tag{3}$$

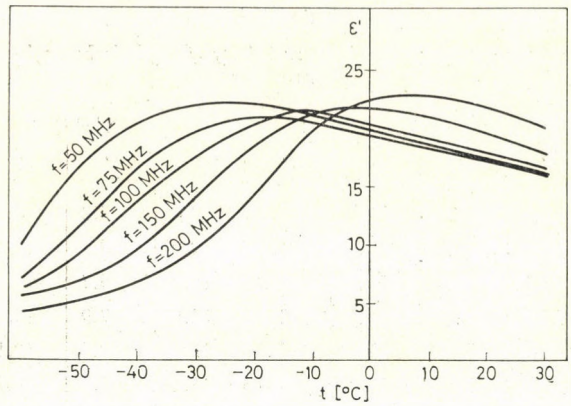

Fig. 1. Real part of the relative permittivity of allyl alcohol as a function of temperature and frequency

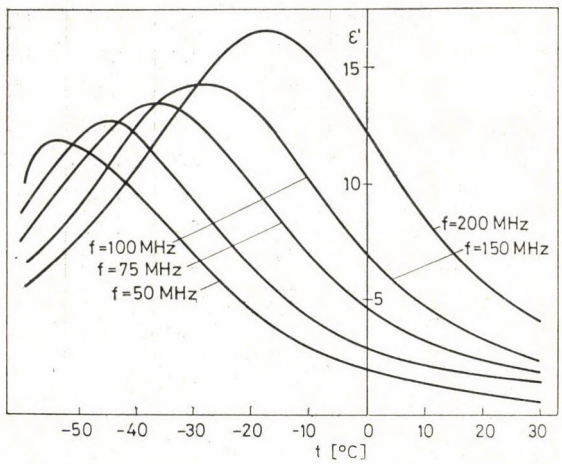

Fig. 2. Imaginary part of the relative permittivity of allyl alcohol as a function of temperature and frequency

Table IV

Viscosity of allyl alcohol as a function of temperature

t (°C)	η (cP)
15	1.401
20	1.191
25	0.965
30	0.852
40	0.632

In latter equations ε' is the real part and ε'' the imaginary part of the complex relative permittivity. In the $\varepsilon''/(\varepsilon_0 - n^2)$ *vs.* $(\varepsilon' - n^2)/(\varepsilon_0 - n^2)$ diagram "deformed semicircles" are obtained, the extent of the 'deformation' depending on the value of α; if $\alpha = 1$, the diagram gives the DEBYE semicircle [4]. From the data of Table III the value of the constant α in the COLE—DAVIDSON equation is 0.8 ± 0.1. The corresponding diagram is shown in Figure 3. With the use of the known value of α and equations (2) and (3), the macroscopic relaxation time of allyl alcohol was calculated as a function of temperature. The results are listed in Table V.

Table V

Macroscopic relaxation time of allyl alcohol as a function of temperature

t (°C)	$\tau \times 10^{10}$
0	2.5
−20	7.5
−40	12.4
−60	14.3

Dielectric relaxation is a process requiring activation energy. The temperature-dependence of the relaxation time can be described to a good approximation by the Arrhenius equation:

$$\tau = A \exp\left\{\frac{\Delta H^*(\tau)}{RT}\right\} \tag{4}$$

where A is a constant;

$\Delta H^*(\tau)$ — the activation enthalpy;
R — the gas constant; and
T — the absolute temperature.

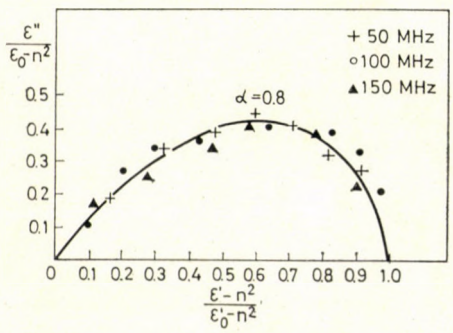

Fig. 3. Reduced COLE—DAVIDSON diagram of allyl alcohol

Figure 4 depicts an Arrhenius representation of the data in Table V. It can be seen that the macroscopic relaxation time of allyl alcohol can be readily described by Eq. (4). On the above basis, the activation enthalpy of the dielectric relaxation of allyl alcohol is 5.05 kcal mol^{-1}. This is naturally to be regarded as the average value for the temperature range in equation.

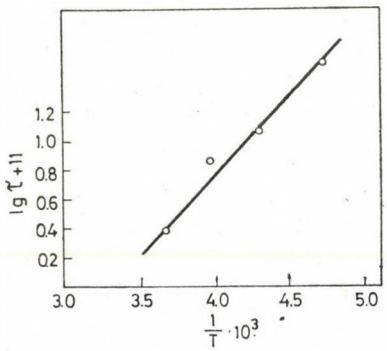

Fig. 4. log τ as a function of $1/T$

The activation enthalpy of the dielectric relaxation of the corresponding saturated alcohol, 1-propanol, is 5.54 kcal mol^{-1} [5] and according to that work can be regarded as essentially constant in the temperature range 180—300 °K. The only significant deviation from the given value is observed near the freezing point (120 °K) (in that region $\Delta H^*(\tau) = 6.3$ kcal mol^{-1}). This shows that the double bond in allyl alcohol gives rise to change in the activation enthalpy of only about 10%, while at the same time it appears to confirm the calculation method used to determine $\Delta H^*(\tau)$ from the experimental data in a relatively broad temperature range.

Dielectric relaxation is frequently correlated with the viscosity of the liquid. According to the early theory of DEBYE [6]

$$\tau = \frac{4\pi r^3}{kT}\eta \tag{5}$$

where r — radius of the molecule regarded as a rigid sphere;
k — the Boltzmann constant; and
η — viscosity of the liquid.

If the molecule cannot be regarded as spherical, then it can be modelled with an ellipsoid with semi-axes a, b and c, the relaxation time referred to the given axis [7] is

$$\tau_i = \frac{4\pi\eta}{kT} abc\, s_i \tag{6}$$

where s_i a 'form factor' dependent on the ratio of the semi-axes, has been tabulated [8]. Often, the variation of the viscosity with temperature can similarly be described with an Arrhenius-type equation:

$$\eta = A\,(\eta) \exp \left\{\Delta H^*(\eta)/RT\right\} \tag{7}$$

where A is a constant; and

$\Delta H^*(\eta)$ — the activation enthalpy of viscous flow.

$\Delta H^*(\eta)$ and $\Delta H^*(\tau)$ are not identical, but usually the difference is within one

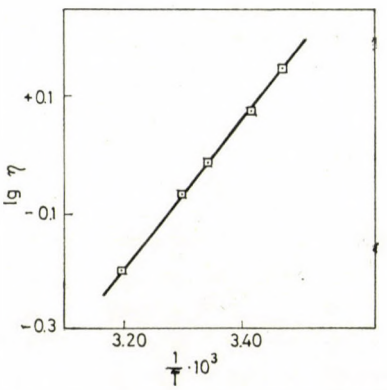

Fig. 5. log η as a function of $1/T$

order of magnitude [9]. (It can be mentioned that relatively few $\Delta H^*(\eta)$ and $\Delta H^*(\tau)$ data can be found for pure liquids, most of the literature data referring to solutions.)

From Eq. (7) and the data of Table IV, for allyl alcohol $\Delta H^*(\eta) = 5.75$ kcal mol^{-1}. The Arrhenius plot of the data in Table IV is shown in Figure 5. For the system studied, therefore, $\Delta H^*(\tau)/\Delta H^*(\eta) \simeq 0.88$. In the evaluation of the latter value it must also be taken into account that $\Delta H^*(\eta)$ was determined from data relating to a comparatively narrow temperature range. For 1-propanol $\Delta H^*(\eta) = 4.3$ kcal mol^{-1} and thus $\Delta H^*(\tau)/\Delta H^*(\eta) \simeq 1.28$.

Comparison of the activation enthalpies of 1-propanol and allyl alcohol shows that the double bond does not appreciably change the properties studied. The dielectric relaxation of the two alcohols in the liquid phase presumably occurs by similar mechanisms.

Part II of this series will examine the effect of polymerization on dielectric relaxation.

REFERENCES

1. Cole, K. S., Cole, R. H.: J. Chem. Phys., **9**, 341 (1949)
2. Davidson, D. W., Cole, R. H.: J. Chem. Phys., **18**, 1417 (1951)
3. Onsager, L. J.: J. Amer. Chem. Soc., **58**, 1486 (1936)
4. Hill, N. E., Vaughan, W. E., Price A. H., Davies, M.: Dielectric Properties and Molecular Behaviour. p. 48. Van Nostrand — Reinhold Co., London, 1969
5. Hill, N. E., Vaughan, W. E., Price A. H., Davies, M.: Dielectric Properties and Molecular Behaviour. p. 329, Van Nostrand — Reinhold Co., London, 1969
6. Debye, P.: Polar Molecules. Chem. Catalog Co., New York, 1929
7. Fischer, E.: Phys. Z., **60**, 645 (1939)
8. Budó, A., Fischer, E., Miyamoto, S.: Phys. Z., **40**, 337 (1939)
9. Hill, N. E., Vaughan, W. E., Price A. H., Davies, M.: Dielectric Properties and Molecular Behaviour. Chapter 5, Van Nostrand — Reinhold Co., London, 1969.

János Liszi
Zsuzsanna Hartyáni } 8021 Veszprém, Vegyipari Egyetem, Hungary.

Acta Chimica Academiae Scientiarum Hungaricae, Tomus 83 (2), pp. 127—133 (1974)

DIELECTRIC PROPERTIES AND POLYMERIZATION OF ALLYL ALCOHOL, II

EFFECT OF POLYMERIZATION ON THE DIELECTRIC PROPERTIES OF THE LIQUID PHASE

J. LISZI and ZS. HARTYÁNI

(Electrochemical Research Group of the Hungarian Academy of Sciences, Department of Physical Chemistry, Chemical Industries of University, Veszprém)

Received October 23, 1973

Liquid polyallyl alcohol with a molecular weight of approximately 400 was prepared. The complex relative permittivity of the polymerization product was determined as a function of temperature and frequency, as was the temperature-dependence of its viscosity. The dielectric data and the viscosity values show that the polymerization causes an extremely strong change in the properties of allyl alcohol. The results indicate that a new relaxation range appears as a consequence of polymerization.

1. Introduction

The first part of this series dealt with the dielectric properties of monomeric liquid allyl alcohol. The present paper describes the preparation of the liquid-phase polymer. The complex relative permittivity of the resulting material is determined as a function of temperature and frequency. The results are evaluated by comparison with the viscous energy.

2. The polymerization of allyl alcohol

On the action of molecular oxygen, ultraviolet light or peroxides, together with thermal treatment, allyl alcohol and β-alkyl-substituted allyl alcohols slowly polymerize to give a viscous product oligomer with a low degree of polymerization [1]. For example, in the presence of 2.8 *w/w*% dibenzoyl peroxide at 80°C, 4.2% polyallyl alcohol is formed in an evacuated ampoule in 240 hrs [2]. In order to attain a better conversion, fresh dibenzoyl peroxide must be added during the polymerization, to replace the initiator rapidly consumed as a consequence of chain termination steps. The literature indicates [3] that polyallyl alcohol is formed in 87% yield at 100°C if 1.3 *w/w*% hydrogen peroxide is added to the system initially, and again at intervals during the polymerization. When purified from the unreacted monomer the polymer has a honey-like consistency; its refractive index $n_D^{20} = 1.5143$, while according to the literature [2, 4] its average degree of polymerization is about 5.

The polymerization of allyl alcohol was carried out into two ways: photocatalytically and in the presence of an initiator, together with thermal treatment. Allyl alcohol was dehydrated with $CaCl_2$ and placed in a quartz vessel,

and bulk-polymerization was effected under an AK 02 UV lamp at 25°C, in the absence of solvent and chemical initiator. In the other method the polymerization was carried out at the normal boiling point of allyl alcohol in a two-necked flask fitted with a reflux condenser and an initiator-dispenser. 1 *w/w*% of stabilized 33% hydrogen peroxide was used as initiator in the

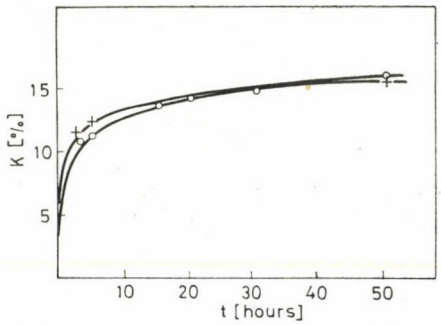

Fig. 1. Yield of the polymerization product as a function of time

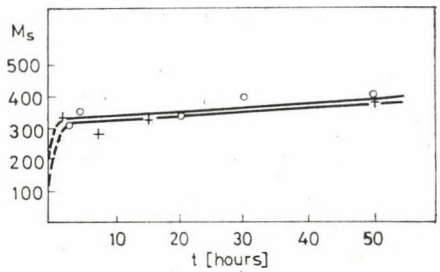

Fig. 2. Molecular weight of the product as a function of the polymerization time

thermocatalytic process. Since the free radicals were fairly rapidly consumed because of rapid chain-termination, the initiator consumed was replaced after each sampling.

The unreacted monomer and the polymer were separated by distillation at 25°C and 35 Torr. The products obtained were viscous, translucid materials with a honey-like consistency, they were soluble in methanol and common organic solvents, but on the action of acetone they separated from the monomer in the form of a precipitate. The yield of the polymer in weight per cent is shown in Fig. 1 as a function of time.

The molecular weights of the polymerization products were determined with a Knauer vapour pressure osmometer. The measurements were made at 45°C, with freshly distilled methanol as solvent. The calibration curve was obtained using a series of dinonyl phthalate solutions of known concentration. Figure 2 shows the molecular weights of the polymerization products as a function of the polymerization time. The data relating to the products ob-

tained by means of the two different polymerization methods are listed in Table I.

In the Table t is the polymerization time in hours, M is the molecular weight of the product, P is the degree of polymerization and Y is the per cent yield. The data show that the two methods give practically the same degree of polymerization after polymerization for 50 hrs. The products proved to be stable.

Table I

Properties of polymerization products

Photocatalytic polymerization				Thermocatalytic polymerization			
	M	P	Y (%)	t	M	P	Y (%)
2.5	223	4.55	11.7	3	301	5.18	11.1
5	275	4.90	12.5	5	338	5.80	11.5
15	324	5.80	14.0	15	340	5.85	13.9
20	332	5.72	14.7	20	342	5.90	14.3
25	354	6.10	15.1	30	390	6.71	14.8
50	388	6.68	15.7	50	400	6.90	16.0

3. Results

The complex relative permittivity of the product of the 50 hour polymerization was determined by the following methods:

at a frequency less than 1 MHz: SIEMENS Scheinwiderstandsmessbrücke, Rel. 3R. 277;

at a frequency of 3 MHz: RADELKIS Universal Dielectrometer, Type OH-301.

The experimental results are presented in Tables II and III, and Figures 3 and 4.

Table II

Real part of the complex relative permittivity of the polymerization product as a function of temperature and frequency

t (°C)	ε'			
	100 kHz	500 kHz	1 MHz	3 MHz
−30	7.1	5.4	4.9	4.1
−20	9.6	7.1	6.2	4.8
−10	12.0	9.1	8.5	6.0
0	14.0	11.2	10.2	7.6
10	15.0	12.9	12.5	9.5
20	15.4	13.9	13.3	11.2
30	15.5	14.3	13.8	12.4
40	15.6	14.5	14.1	12.8
50	15.5	14.6	14.3	13.1

Table III

Imaginary part of the complex relative permittivity of the polymerization product as a function of temperature and frequency

t (°C)	$10\,\varepsilon''$			
	100 kHz	500 kHz	1 MHz	3 MHz
−30	17.6	10.2	9.8	5.3
−20	25.0	16.5	16.3	9.1
−10	28.7	21.9	21.6	13.2
0	26.0	25.0	24.8	17.7
10	21.2	23.1	23.6	20.6
20	16.5	19.6	20.3	21.4
30	17.6	17.0	17.2	18.8
40	21.1	15.5	15.2	15.9
50	26.6	15.1	14.0	13.9

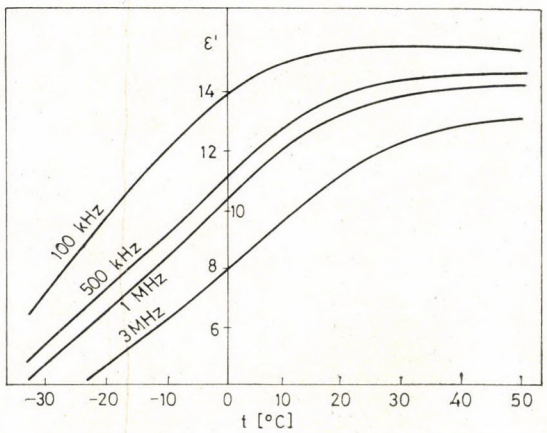

Fig. 3. Real part of the complex relative permittivity as a function of temperature and frequency

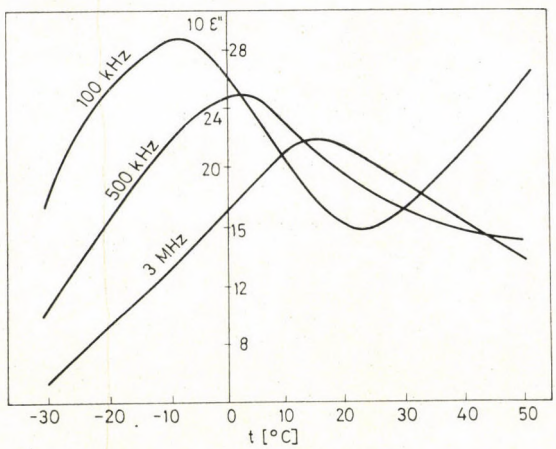

Fig. 4. Imaginary part of the complex relative permittivity as a function of temperature and frequency

The viscosity of the polymer was determined as a function of temperature for the calculation of the viscous energy; a "Rheo-Viscosimeter nach Höppler, GDR, Patent No. 210" was used. The results are given in Table IV.

Table IV

Viscosity of the polymerization product as a function of temperature

t (°C)	η (cp)
20	17815
25	9768
30	7126
40	2969

4. Discussion

The dielectric properties was evaluated as in the case of monomeric allyl alcohol. The COLE—DAVIDSON equation [5] was used for the description of the complex relative permittivity:

$$\frac{\varepsilon^* - n^2}{\varepsilon_0 - n^2} = \frac{1}{(1 + j\omega\tau)^\alpha} \tag{1}$$

where ε^* — complex relative permittivity;
ε_0 — static relative permittivity;
n — 'internal' refractive index;
j — the imaginary unit;
ω — the angular frequency;
τ — the macroscopic relaxation time; and
α — an empirical constant: $0 < \alpha \leq 1$.

By rationalization of Eq. (1):

$$\frac{\varepsilon' - n^2}{\varepsilon_0 - n^2} = \cos^\alpha(\omega\tau)\cos(\alpha\omega\tau) \tag{2}$$

$$\frac{\varepsilon''}{\varepsilon_0 - n^2} = \cos^\alpha(\omega\tau)\sin(\alpha\omega\tau). \tag{3}$$

The COLE—DAVIDSON diagram, $(\varepsilon' - n^2)/(\varepsilon_0 - n^2)$ *vs.* $\varepsilon''/(\varepsilon_0 - n^2)$, for the polymerization product is depicted in Fig. 5. From Eqs. (2) and (3), and the data of Tables 2 and 3, $\alpha = 0.2 \pm 0.1$. For monomeric allyl alcohol this value was 0.8 ± 0.1. It can be seen that polymerization leads to an extremely strong "deformation" of the reduced COLE—DAVIDSON diagram. In the

Table V

Macroscopic relaxation time of the polymerization product as a function of temperature

t (°C)	$\tau \times 10^4$ (s)
0	8.4
10	8.1
20	7.3
30	6.4

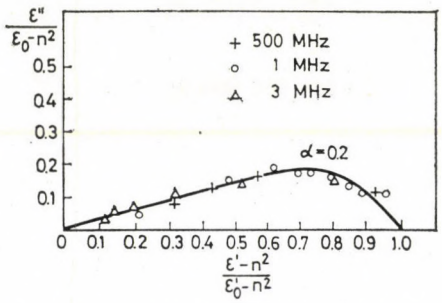

Fig. 5. Reduced COLE—DAVIDSON diagram of the polymerization product

knowledge of α, the macroscopic relaxation time of the polymerization product was determined as a function of temperature. The results are listed in Table V.

The data in the Table indicate that the relaxation time of the polymerization product is about six orders of magnitude larger than that for monomeric allyl alcohol.

The activation enthalpy of dielectric relaxation was calculated with the Arrhenius equation:

$$\tau = A \exp\left\{\frac{\Delta H^*(\tau)}{RT}\right\} \tag{4}$$

where A is a constant;

$\Delta H^*(\tau)$ — the activation enthalpy;
R — the gas constant; and
T — the absolute temperature.

The activation enthalpy of the dielectric relaxation of the polymerization product was found to be 2.1 kcal mol^{-1}. This is substantially smaller than the value of 5.05 kcal mol^{-1} obtained for monomeric allyl alcohol. At the same time the viscous energy increased considerably during polymerization. The activation enthalpy of viscous flow was similarly calculated with an Arrhenius-type equation:

$$\eta = A(\eta) \exp\left(\Delta H^*(\eta)/RT\right) \tag{5}$$

where $A(\eta)$ is a constant and $\Delta H^*(\eta)$ is the activation enthalpy of viscous flow. From Eq. (5) and the data of Table IV, $\Delta H^*(\eta) = 16.2$ kcal mol^{-1}. The quotient of the two activation enthalpies, $\Delta H^*(\tau)/\Delta H^*(\eta) \simeq 0.13$. This is almost one order of magnitude less than the value for monomeric allyl alcohol. For comparison, for glycerine [6] $\Delta H^*(\tau) = 32$ kcal mol^{-1} and $\Delta H^*(\eta) = 21.4$ kcal mol^{-1} at about 210 and 234 °K. The extremely large difference of the $\Delta H^*(\tau)$ and $\Delta H^*(\eta)$ values for polyallyl alcohol indicates that the mechanism of relaxation is different here than for the monomer. As regards the dielectric relaxation of alcohols, three ranges can be distinguished [7]. The first range is connected with the motion of the alcohol associations; the second may be due to the rotation of the monomer molecules, or the —OR group (where R is an alkyl group); and the third range may result from the rotation of the —OH group around the C—O bond. In the case of polymeric molecules it is also necessary to reckon with the rotation of the individual parts 'segments' of the polymer [8]. With monomeric allyl alcohol it is presumably the first relaxation range which is determined, for the other two ranges should appear at essentially higher frequencies [9, 10]. Our results for polyallyl alcohol do not permit a decision as to which relaxation range appears in the frequency and temperature intervals examined; it can be concluded that the first relaxation range (for the lowest frequencies) is not involved. This conclusion is confirmed by the curve belonging to a frequency of 100 kHz (Fig. 4). The rising section at temperatures higher than 20°C points to a new relaxation, associated with lower frequencies. Further studies are necessary to clarify the phenomenon: it appears desirable to study the dielectric dispersion of the polymerization product at frequencies lower than 100 kHz, and the effect of dilution with an inert solvent.

REFERENCES

[1] Reinhard, R. H.: Monsato Chemical Co. Erf. A. P. 2897, 174 (1959)
[2] Adelson, D. E., Gray, H. F.: Shell Develop. Erf. A. P. 2555, 775 (1951)
[3] Ullmanns: Encyklopädie der technischen Chemie, Vol. III, p. 315. 3rd revised edition, Urban und Schwarzbert, Munich, Berlin
[4] Oster, G., Mizutani, U. Y.: J. Polymer Sci., **22,** 173 (1956)
[5] Davidson, D. W., Cole, R. H.: J. Chem. Phys., **18,** 1417 (1951)
[6] Hill, N. E., Vaughan, W. E., Price, A. H., Davies, M.: Dielectric Properties and Molecular Behaviour. p 331, Van Nostrand — Reinhold Co, London, 1969
[7] Liszi, J.: Acta Chim. (Budapest) **72,** 207 (1973)
[8] Ferry, J. D.: Viscoelastic Properties of Polymers. John Wiley, New York, 1961
[9] Grag, S. K., Smyth, C. P.: J. Phys. Chem., **69,** 1294 (1965)
[10] Brot, C., Magat, M.: Chem. Phys., **39,** 841 (1963)

János Liszi
Zsuzsanna Hartyáni
8201 Veszprém, Vegyipari Egyetem, Hungary.

Acta Chimica Academiae Scientiarum Hungaricae, Tomus 83 (2), pp. 135—149 (1974)

EFFECT OF A SMALL AMOUNT OF NOBLE-METAL ADDITIVE ON THE BEHAVIOUR OF ACTIVE AND INACTIVE SUPPORTS IN CATALYTIC HYDROGENATION

G. VÉRTES, G. HORÁNYI and GY. KISS

(Central Research Institute for Chemistry of the Hungarian Academy of Sciences, Budapest)

Received 31 October, 1973

The effects of a small amount of platinum or palladium on the behaviours of various catalyst supports in aqueous-phase catalytic hydrogenation were investigated.

The rate of the hydrogenation reaction was examined in the case of two model compounds, *p*-nitro-phenol and maleic acid, using aluminium oxide, tungsten trioxide, active carbon, tantalum and tungsten carbide supports, and support-free palladium or noble-metal-free hydrogen tungsten bronze

In contrast with literature findings, it was concluded that tungsten oxide cannot be regarded as an active support.

It was found that in the absence of noble metal hydrogen tungsten bronze is not able to activate molecular hydrogen.

Tungsten carbide containing 0.1% noble metal is well applicable as a catalyst in the hydrogenation of unsaturated compounds.

In a previous communication [1] it has been described that tungsten carbide can be well utilized as a catalyst in the hydrogenation of compounds containing a nitro or a quinoidal group, *i.e.* ionically reducible compounds.

Literature data led to the assumption that the reaction is catalyzed by tungsten bronze formed on the surface of the tungsten carbide. Hydrogen tungsten bronze was prepared from tungsten oxide in the presence of a small amount of noble metal, and its catalytic activity was investigated. Our experiments showed that the tungsten blue thus obtained may serve as a catalyst in hydrogenation reactions. This result seemed to support the fact that also in the case of tungsten carbide tungsten bronze was catalytically active. In the hydrogenation of unsaturated compounds on tungsten blue, however, the noble metal present in the system cannot be ignored, for this may well take part directly in the reaction. Similarly, an explanation is required for the fact that the specific activity, referred to unit weight, of the catalyst containing hydrogen tungsten bronze in its entire mass practically agrees with that of tungsten carbide, for which it is assumed that the tungsten bronze is contained only on part of the surface. In the present paper we wish to deal with a more detailed analysis of this question, and also to show possibilities which may the comparatively low rates of hydrogenation achieved on tungsten carbide.

Experimental

The experiments were performed in two types of hydrogenation apparatus. On was a 100 cm^3, thermostatable vessel, fitted with a magnetic stirrer, which was connected by a glass tube to a gas burette. The majority of the experiments were carried out in a simple, thermostat-

able hydrogenation bulb (70 cm^3), connected by thick-walled rubber tubing to a gas burette. We found that the diffusion of hydrogen through the walls of the rubber tubing was less than 1 cm^3 per hour, and thus loss in hydrogen in this way during the measurements could be neglected.

In the deposition of the noble metal, the procedure generally followed was to saturate 1 g support in 2 *N* H_2SO_4 solution in the hydrogenation bulb with hydrogen and then H_2PtCl_6 of $PdCl_2$ solution was added in appropriate amount and concentration.

Measurements were performed at 80°C. The temperature of the water circulating in the thermostating jacket was thermostated within ± 0.1°C.

2 *N* H_2SO_4 used as a stock solution was prepared from sulfuric acid of p.a. grada (Apolda). The tungsten carbide support was a Murex product, tungsten oxide, aluminium oxide and active carbon were Merck products, and tantalum was a BDH product. Aqueous solutions of $PdCl_2$ or H_2PtCl_6 (Reanal, analytical purity) were used for the activation of the catalysts, generally in a concentration of 1 mg metal/1 cm^3 solution. The substances to be hydrogenated were of p.a. or puriss. grada. Prior to use the hydrogen was carefully freed from oxygen.

The specific surface of the supports exhibiting metallic conductivity, was determined by the BET method.* The following values were obtained from Kr isotherms taken at −196°C: active carbon: 1100 m^2/g; tungsten carbide: 1.0 m^2/g; tantalum: 0.2 m^2/g.

Tungsten carbide as a catalyst support

From earlier studies on the catalytic properties of tungsten carbide [1]—[4] it has been concluded that the rate-determining step in the hydrogenation reaction was the activation of hydrogen. If our aim is to accelerate the hydrogenation reaction, then the rate of this step should be increased in some way. The adsorption of hydrogen on noble metals is known to proceed at a comparatively high rate. We assume, therefore, that in the presence of a small amount of noble metal the rate of hydrogenation is significant.

This is supported by the results of MUND *et al.* [5], who added silver to tungsten carbide (in an amount of ca. 20%) and thus obtained higher hydrogenation rates. BINDER *et al.* [6]—[7] in their investigations on fuel elements mixed platinum powder into tungsten carbide or tungsten dioxide and (under certain conditions) obtained electrodes more active than platinum.

In a preliminary experiment we too mixed platinum powder (1%) with tungsten carbide powder. As can be seen from Fig. 1, a rate increase of 150% was then observed in the reduction of the Fe(III) ion at 70°C. However, HOBBS and TSEUNG [8] showed that much more effective than simply to mix the powders is to reduce the noble metal from solution directly onto the surface of the support. Accordingly, in the experiments described below we followed this procedure for the deposition of the noble metal.

For a given tungsten carbide powder, on which a rate of 12 cm^3/hour was reached without noble metal, addition of 0.1% palladium resulted in an initial hydrogen-uptake rate of 320 cm^3/hour (Fig. 2). This rate is already in the range of those achieved with platinum powder. However, the increase of

* The authors wish to express their thanks to J. KIRÁLY for the careful performance of the measurements.

the catalytic activity in this way also brings about a change in the selectivity of the catalyst. Although three moles of hydrogen were still consumed in the hydrogenation of aromatic nitro compounds, *i.e.* the aromatic ring was not hydrogenated, compounds containing double bonds could be reduced by the platinized or palladized tungsten carbide. For example (see Table II), the hydrogenation of maleic acid proceeded at a rate of 300 cm^3/hour on tungsten carbide containing 0.1% palladium. In contrast with other supports to be

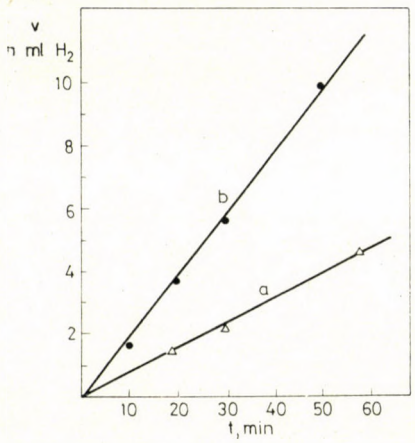

Fig. 1. Effect of platinum powder on catalytic activity of tungsten carbide. (a) tungsten carbide; b) tungsten carbide +1% platinum powder

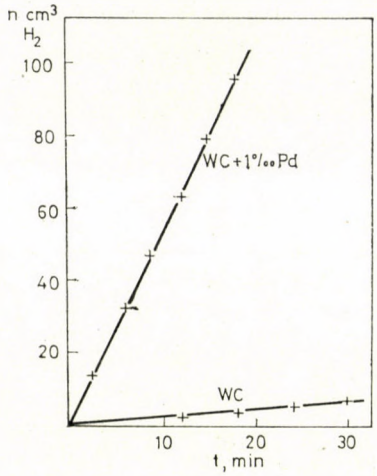

Fig. 2. Hydrogen-uptake of *p*-nitrophenol in 2 *N* H_2SO_4 solution at 80°C, in presence of tungsten carbide or tungsten carbide containing 0.1% palladium

discussed later, the use of a tungsten carbide support in the hydrogenation of double-bond-containing compounds was not accompanied by the rapid decrease in activity of the catalyst.

The conditions of deposition of the noble metal can affect the properties of the catalyst. In our experience this is primarily to be observed in the deposition of platinum. In the case of palladium chloride, which can be easily reduced with hydrogen the activity of the catalyst depends only slightly on the conditions of deposition. Our experiments showed that a more active catalyst can be obtained if the solution containing the noble metal is mixed with hydrogen-saturated tungsten carbide, than if the noble metal solution is added to the powder in contact with the air and reduced subsequently. As shown in Fig. 3, a hydrogen-uptake rate of about 30 cm^3/hour could be achieved in the reduction of *p*-nitrophenol in the presence of 0.01% platinum in the former case, while in the latter case the rate of about 12 cm^3/hour attained with pure

tungsten carbide could be increased only to 20 cm^3/hour. However, the best result, 300 cm^3/hour, was obtained by adding the chloroplatinic acid solution to the system when the nitro compound was already present and its hydrogenation was under way. As mentioned above, this phenomenon is hardly observable with palladium, the differences between the catalysts prepared in various ways barely exceeding the differences of 10% often found even between samples prepared in the same way.

In the case of a palladium additive the catalytic activity of tungsten carbide was studied as a function of the quantity of the additive. The results

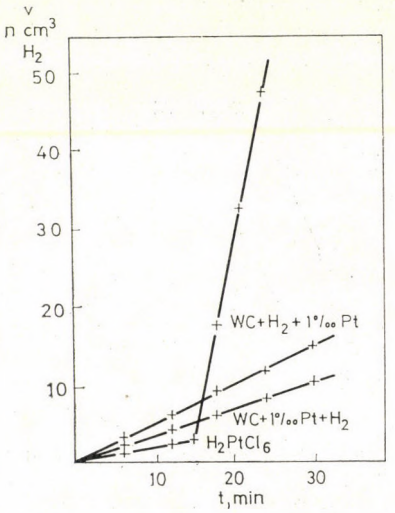

Fig. 3. Hydrogenation curve for *p*-nitrophenol in 2 *N* H_2SO_4 solution at 80°C in the presence of tungsten carbide treated in different ways

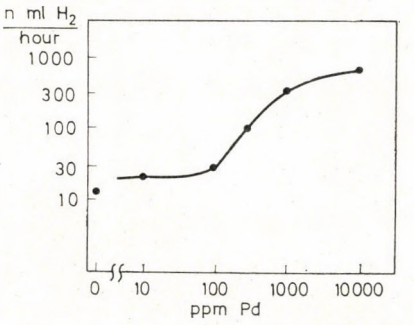

Fig. 4. Effect of the amount of palladium on the catalytic activity of tungsten carbide in the hydrogenation of *p*-nitrophenol in 2 *N* H_2SO_4 solution at 80°C on 1 g tungsten carbide

are depicted in Fig. 4. It can be seen that up to about 100 ppm the increase in the rate of hydrogenation is not too significant. After this an almost linear range follows, but at a palladium content of 1% it already approaches a limiting value, which is presumably connected with the transport of hydrogen (the diffusion or absorption limiting rate under the given conditions).

Metallic conductors as catalyst supports

A study was made on the catalytic properties of small amounts of noble metal deposited on supports of various types, in the case of the liquid-phase hydrogenation of compounds reduced by both ionic and radical mechanisms.

With metallic conductors as catalyst supports under the generally applied condition, two basic differences can arise compared with insulators. For

noble-metal deposition as described above in the case of metallically conducting supports, the entire surface is at approximately the same electrode potential, while for the insulators this is not so. The other difference may appear in the course of the hydrogenation, when, although the activation of hydrogen takes place only on the noble-metal surface, electron-uptake by the ionically reacting compounds can occur on the entire surface, since in this case too the whole surface may be found to be at roughly the same potential.

Our investigations were started with the commonly-used support, the active carbon. The hydrogenation of the nitro group on active carbon containing 0.1% palladium proceeds with a very high rate, of about 800 cm^3/hour. From the amount of hydrogen absorbed it could be established that only the nitro group was reduced, and not the aromatic ring, or if the latters was reduced, then the reduction proceeded at a rate of at least two orders lower than the reduction of the nitro group. The hydrogenation of unsaturated compounds also takes place at a relatively high rate initially on this catalyst. It can be seen from Fig. 5b, that as the reaction progresses the rate of the process decreases to about one fourth of the initial rate. Experience shows that the activity of catalysts containing such a small quantity of noble metal is not constant; it is affected considerably by trace contaminants. It appears probable that, similarly to the phenomenon observed with tungsten oxide, here too it is a matter of the poisoning of the small amount of noble metal, and the gradual decrease of its surface. This is supported by the experiment in which *p*-nitrophenol was added to the system after the reduction of maleic acid (Fig. 5c); the rate attained on the clean surface could not be approached then, nor even the initial rate of reduction of maleic acid.

Similar experiments were also carried out in the presence of catalytically completely inactive tantalum powder. Although the specific surface of this support was almost four orders less than that of active carbon, there was no significant difference between the rates of reduction of the nitro group on the two types of support in the presence of 0.1% palladium. The hydrogenation of maleic acid similarly proceeds on a tantalum-supported catalyst, and here too a considerable rate decrease was observed during the reaction. The poisoning of the surface is indicated by the fact that in this case too the rate of hydrogenation of the nitro compound added after hydrogenation of maleic acid did not attain the value found on the clean surface.

Insulator as a catalyst support

Al_2O_3 was used in our investigations; under other conditions it is frequently used as a support. The conditions for noble-metal deposition were exactly the same as described above. The catalyst thus obtained can be employed for the hydrogenation of both nitro compounds and unsaturated bonds.

It may be seen from Table II that, similarly to the previous observations, the rate of hydrogenation of nitro compounds exceeds that measured for maleic acid, but after the hydrogenation of an unsaturated compound it is no longer possible to attain the rate referring to the clean surface in this case either.

As regards the rate of hydrogenation, this section also includes tungsten oxide, which was dealt with in detail in the preceding publication. This draws attention to the fact that under the present conditions tungsten blue, which can otherwise be well used as an electrode, shows similar properties to insulators; thus, it is apparently not the electric properties of the prepared catalyst which determine the rate of the reaction.

In a comparatively narrow concentration interval, a study was made of the effect of the quantity of platinum on the rate of hydrogenation on tungsten oxide. The experimental data and the rates calculated from these and referring to 1 mg platinum are given in Table 1.

The rate values obtained in the presence of 1 mg palladium activator for the different supports are listed in Table II.

Table I

Effect of the amount of platinum deposited on 1 *g tungsten oxide on the rate of hydrogenation of p-nitrophenol in* 2 *N* H_2SO_4 *at* 80 °C

Pt mg	Rate n cm³ H_2/hour	Rate n cm³ H_2/hour/mg Pt
0.3	8	27
1	30	30
4	130	32
10	180	18

Table II

Initial hydrogenation rates, in n cm³/hour, measured in 2 *N* H_2SO_4 *solution at* 80 °C, *on* 1 *g support, in the presence of* 1 *mg palladium*

Support	NO_2[a]	C=C[b]	NO_2[c]
Active carbon	800	180	100
Ta	300	60	60
Al_2O_3	60	20	20
WO_3	50	20	20
WC	320	300	
Without support	20	10	

[a] rate of hydrogenation of *p*-nitrophenol
[b] rate of hydrogenation of maleic acid
[c] rate of hydrogenation achieved in the presence of *p*-nitrophenol, after complete hydrogenation of maleic acid.

Some supplementary hydrogenation experiments

Hydrogenation on 1 mg palladium, without a support

With the aim to facilitate the evaluation of the previous experiments, it appeared necessary in the interest of both the interpretation of the deposition conditions and the comparison of catalysts obtained under given experimental conditions, to carry out experiments without supports, where only the noble metal was present.

In the preparation of the catalyst, 20 cm^3 2 *N* H_2SO_4 solution was saturated with hydrogen at 80°C in a hydrogenation bulb, and then a $PdCl_2$ solution (1 cm^3) containing 1 mg Pd/cm^3 was added. The catalyst formed initially floated in the solution as a fine powder, but after one or two minutes it became saturated with hydrogen and coagulated, and the bulk of it settled to the bottom of the bulb.

Our experiments showed (*cf.* Table II) that, even though at not too high a rate, the catalyst prepared under such conditions catalyzed the hydrogenation of both nitro compounds and compounds containing an unsaturated bond. On comparison of the reaction rates with those measured in the case of Al_2O_3 or WO_3 supports, the differences were not considerable, and thus, as regards the rate, this catalyst can be classified together with those catalysts deposited on the insulators.

Experiments with tungsten blue not containing noble metal

GLEMSER *et al.* [9] elaborated methods for the preparation of hydrogen tungsten bronze without the use of noble metals. For our purposes, the most favourable of these appeared to be the one in which tungsten oxide was reduced with zinc dust in an acid solution. In this case, at the end of the reduction the residual reductant dissolves in the excess acid and can play no part at all later during the hydrogenation reaction. In addition to the hydrogen tungsten bronze thus formed, the system contains only dissolved zinc sulfate, which is presumed not to interfere in the hydrogenation reaction. A further possibility is that zinc is incorporated into the tungsten oxide during the reduction, with the possible formation of a bronze, but GLEMSER *et al.* found no evidence for that in their X-ray measurements.

In our experiment, 1 g tungsten oxide was suspended in 2 *N* H_2SO_4 in a hydrogenation bulb, and 1 g zinc dust was added at 80°C. After one or two minutes the system became blue, indicating the reduction of the tungsten oxide. The completion of the dissolution of all the zinc was indicated by the cessation of gas evolution. *p*-Nitrophenol was then added to the system. Similarly to platinized tungsten oxide, the colour of the suspension initially became greyish-blue, and then greenish, but in this case hydrogen uptake was not

observed. The oxidation of the hydrogen tungsten bronze not containing a noble metal is fairly convincingly indicated by the colour change, although complete oxidation could not be achieved even in four hours. This could be established from the facts that the suspension remained green, while on addition of potassium dichromate it instantaneously turned yellow. However, hydrogen was not adsorbed in the presence of $K_2Cr_2O_7$ either.

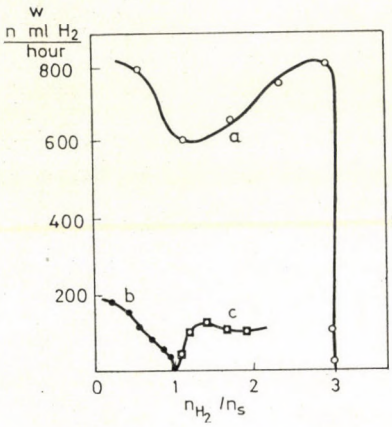

Fig. 5. Dependence of hydrogenation rate on the amount of hydrogen absorbed, on 1 g active carbon containing 0.1% palladium, in 2 *N* H_2SO_4 solution at 80°C. (n_{H_2}/n_S = moles of hydrogen adsorbed/moles of substance taken.) a) *p*-nitrophenol; b) maleic acid; c) *p*-nitrophenol after complete hydrogenation of maleic acid

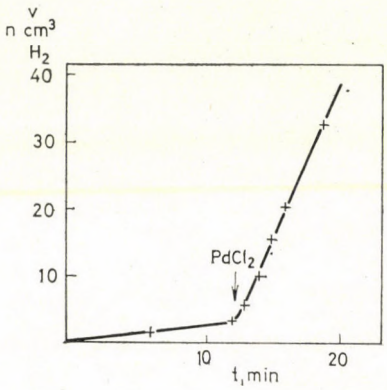

Fig. 6. Effect of addition of palladium chloride on rate of hydrogenation

Some examples of practical application

In our earlier investigation [1—4] it was found that tungsten carbide is excellently applicable to the selective reduction of quinones and aromatic nitro compounds. The rate of the reaction is fairly low, however, and thus the possibilities for practical applications are rather limited. A method was earlier presented which was suitable to enhance the catalytic activity. In the following we shall illustrate the applicability of the catalyst thus prepared.

1 g 4-amino-3-nitrobenzophenone (4.03 mmole) was hydrogenated at 60°C in a mixture of 6 cm^3 2 *N* HCl and 14 cm^3 2-propanol. It can be seen in Fig. 6 that in the presence of 1 g tungsten carbide the initial rate of the reaction is fairly low. After the addition of a $PdCl_2$ solution containing 1 mg palladium (after 12 minutes), the reaction rate increases considerably. After the absorption of about 280 *n* cm^3 hydrogen (12.5 mmole) the rate of the reaction decreased by more than one order, and thus the hydrogenation can be regarded

as completed. On cooling of the solution filtered from the catalyst, 0.70 g pale-brown material separates; after evaporation of the mother liquid and crystallization from 2-propanol, an additional 0.23 g of 3,4-di-aminobenzophenone monohydrochloride can be obtained (yield: 91%; m.p. 220°C).

It can be seen from the above example that on a tungsten carbide catalyst containing 0.1% palladium the nitro group can be hydrogenated without an attack on the oxo group and the aromatic nucleus; in this sense, therefore, the selectivity is further upheld.

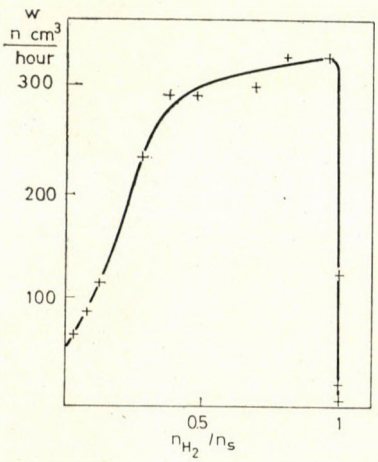

Fig. 7. Hydrogenation of lg 2,6-dinitro-4-acetato-hydroquinone (4.7 mmole) in 30 cm³ 2 *N* HCl at 80°C in the presence of 1 g tungsten carbide. After 15 minutes a palladium chloride solution containing 2 mg palladium was transferred into the bulb

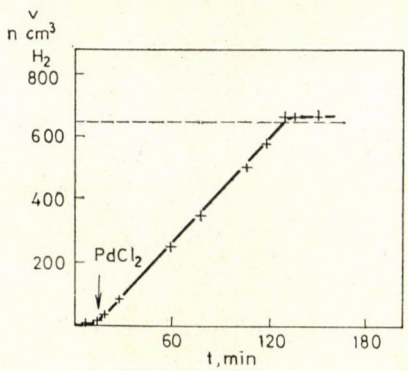

Fig. 8. Hydrogenation of 1 g 2,5-dimethoxy-1,4-benzoquinone in 30 cm³ 75% acetic acid at 80°C in the presence of 1 g tungsten carbide containing 0.1% platinum

Fig. 7 shows the hydrogenation of 2,6-dinitro-4-acetato-1,4-hydroquinone at 80°C in 2 *N* HCl. The Figure again clearly illustrates the significant rate increase accompanying the addition of palladium. After the absorption of 10% of the amount of hydrogen calculated as required for complete hydrogenation, no volume change was observed, and thus the aromatic nucleus remained unchanged here too. Crystallization after filtration of the catalyst and evaporation of the solution leads to pale-brown, light- and air-sensitive crystals of 2,6-diamino-4-acetatohydroquinone monochlorohydrate in a yield of 80% (the product sublimes at 190°C).

Fig. 8 shows the rate of hydrogenation of 2,5-dimethoxy-1,4-benzoquinone in 75% acetic acid at 80°C in the presence of a tungsten carbide catalyst containing 0.1% platinum, as a function of the number of moles of hydrogen adsorbed per mole of material. On the completion of the hydrogenation,

the rate decreases suddenly here too. With evaporation of the solution and recrystallization, 2,5-dimethoxyhydroquinone (which rapidly turns brown in the air) is obtained in a yield of about 85% (m.p. 161°C).

The above examples were presented to show that tungsten carbide containing a small amount of noble metal preserves its selective catalytic properties, as regards the aromatic nucleus and the oxo group, catalyzing only the hydrogenation of the nitro group and quinones. This fact is also proved by the identification of the product, over and above the amount of hydrogen absorbed.

Discussion

Hydrogenation on inactive support

The experimental results in Table II show that in all the cases studied, when noble metal too was present in the system it was possible to hydrogenate both compounds containing the nitro group and compounds containing double bonds. The hydrogenation of unsaturated compounds is assumed to proceed only if the double bond is first chemisorbed on the surface. Activated adsorption of such type has not been observed so far on the supports examined.

The presence of a small number of catalytically active sites is indicated by the ageing observed in the hydrogenation of maleic acid, and by the fact that in the hydrogenation of nitro compounds on such a poisoned surface it is not even possible to attain the reaction rate found on the pure surface. Since both the chemisorption of the double bond and the surface decrease at times connected with this can primarily be conceived on the surface of the noble metal, it may be assumed that, at least in the hydrogenation of maleic acid, the reaction rate observed is due completely to the reaction on the surface of the platinum or palladium.

If the hydrogenation rates observed in the case of palladium without a support are compared with the data obtained with a small amount of palladium deposited on an aluminium oxide or tungsten oxide support, it can be seen that the difference is not too significant, and can easily be explained in that the surface of the palladium without support is somewhat smaller as a result of coagulation, and thus in the case of the same surface the same rate may arise, which again supports the above finding.

For the catalysts examined, with the exception of tungsten carbide, it was found that the rates of hydrogenation of nitro compounds are about three to four times larger than that of maleic acid. Since a similar difference was also obtained in the experiments with palladium powder without a support, it may be assumed to a first approximation that in the hydrogenation of nitro compounds the reaction similarly takes place on the surface of the noble metal.

A significant difference of nearly one order of magnitude was observed in the hydrogenation of the two types of compound, depending on whether the

support was electrically an insulator or a conductor. Different, ionically reacting compounds are found to undergo reduction at almost the same rate in the case of a given support, and thus the rate-determining step of the process is to be sought on the side of the hydrogen. Adsorbed hydrogen can be conceived only on the surface of the noble metal, however, and thus the other surface parts of the catalyst do not play a role in the formation of the hydrogen ion. It is in vain, therefore, for a potential identical to that measurable on the noble metal to develop on the surface of the electrically conducting support, and it is in vain for the compound to be reduced to be able to ionize on the whole of the catalyst surface, for it is not the rate-determining step of the reaction which is 'accelerated' in this way. Accordingly,the cause of the above-mentioned difference must be sought not in the electric properties of the catalyst containing the small amount of noble metal, but in the conductivity of the original support.

We have experienced that the reduction of the noble metal in the homogeneous phase is a slow process. The metal deposition can be conceived in that the metal particles separating in the solution saturated with hydrogen are themselves saturated with hydrogen relatively quickly, and in the vicinity of 0 mV the electrochemical reduction of the noble metal is already a fast process. Thus, the slowly commencing deposition of metal accelerates on metal surfaces present or forming in the solution. If the potential of around 0 mV develops only on the forming noble metal in the solution, the further metal deposition too will take place on these sites. In contrast, if the noble metal separates out on some metallically conducting substance, then the rapid electrochemical reduction may continue on the entire surface of this particle, and so the noble metal may form in a substantially greater dispersity. Hence, the rate difference observed for the different supports may be ascribed to the difference in the surface of the noble metal.

The difference between the catalysts containing platinum and palladium can be explained in a similar way. The homogeneous reduction of platinum in an acid solution is found to be an essentially slow process, which means that the nucleus formation is slow. On a metallically conducting support, in the presence of a redox system (which establishes the potential at a value more negative than $+1.2$ V, the standard potential of Pt/Pt^{2+}), the metal deposition may proceed on the entire surface and the catalytic activity of the finely divided platinum thus formed nearly agrees with that observed for palladium.

The above conception relating to metal deposition is not directly applicable to the electrically well-conducting hydrogen tungsten bronze, and in the case of tungsten carbide too it is striking that the rate of hydrogenation of maleic acid agrees with those observed for nitro compounds. These two supports are dealt with in the following section.

Results relating to tungsten oxide

Tungsten oxide is dealt with separately primarily because, according to HOBBS and TSEUNG [10], it cannot be regarded as an inactive support. They investigated the oxidation of hydrogen on tungsten oxide electrodes containing various amounts of platinum. They found that the oxidation of hydrogen can proceed partly by the 'normal' mechanism:

$$H_2 + Pt \rightarrow Pt2(H)_{ads} \quad (1)$$

$$Pt2(H)_{ads} \rightarrow Pt + 2H^+ + 2e \quad (2)$$

and partly by a 'bronze route':

$$Ptx(H)_{ads} + WO_3 \rightarrow H_xWO_3 + Pt \quad (3)$$

$$H_xWO_3 \rightarrow xH^+ + WO_3 + xe\,. \quad (4)$$

Referring to BENSON *et al.* [11, 12], they conceive process (3) in that the hydrogen atoms forming on the platinum enter the tungsten oxide lattice, where they rapidly attain a uniform distribution.

A rate increase compared to platinum, however, or in other words an active role of the support, can be expected only if the rates of reactions (3) and (4) under the given conditions are at least comparable with those of the parallel process (2), and if the rate-determining step on the platinum is not the dissociative adsorption of hydrogen, but the ionization. Reliable experimental data regarding this latter condition are not available, and under such conditions the adsorption can generally be regarded as rate-determining, in spite of the fact that neither possibility can be excluded.

Nevertheless, it is difficult to conceive that in the given case either the solid-phase reaction (3), followed by solid-phase diffusion, or the electrochemical reaction (4), would result in a higher rate than that of hydrogen ionization with large exchange current. Reaction (4) is in effect a reversible process, since hydrogen tungsten bronze can also be prepared by reduction with tin(II) chloride, for instance [9]. Since the standard potential of Sn^{2+}/Sn^{4+} is +150 mV, it is obvious that the standard potential of the redox system H_xWO_3/WO_3 is much more positive than 0 mV. This is also proved by the fact that in the presence of noble metal it can also be prepared with hydrogen at a pressure lower than 1 atm [11]. If it is not assumed that the exchange current of the equilibrium corresponding to equation (4) is several orders higher than the exchange current of hydrogen on platinum, then at a potential more positive than 0 mV it is inconceivable that the rate of reaction (4) exceeds the rate of reaction (2).

The slowness of the diffusion of hydrogen in the solid phase, and also that of the establishment of the redox equilibrium H_xWO_3/WO_3, are shown

by the fact that on tungsten oxide containing noble metal the hydrogenation rate practically agrees with those found for catalysts deposited on insulators. The first noble-metal particles separating from the solution are capable of recharging the entire surface of metallically conducting supports to about 0 mV, even before metal deposition can continue on these few nuclei. This means that the charging of the surface, *i.e.* the penetration of the hydrogen atom into the oxide lattice and the development of redox equilibrium (4), is slower than the rate of noble-metal nucleus formation, which has been seen above to be lower than the rate of ionization of hydrogen.

On this basis, we feel that the importance of the parallel route consisting of reactions (3) and (4) is negligible in practice in comparison with reaction (2).

The catalytic activity of tungsten oxide in the presence of a small amount of noble metal has recently been confirmed by HOBBS and TSEUNG [10] in that the specific rate referred to the noble metal decreases hyperbolically after a maximum at a platinum content of about 0.4%. The decrease of the specific rate in this sense on the increase of the quantity of noble metal is well known in the literature on catalytic processes, and has been observed in cases when it is not possible to speak of the active role of the support. In many instances the experimental curves could be well explained, for example by the geometrical theory of KOBOZJEV. In our own experiments it would be somewhat artificial to speak of a maximum in connection with the hydrogenation of *p*-nitrophenol (Table II); here it is rather a matter of a constant specific activity.

It may be stated on the basis of our examinations that tungsten oxide cannot be regarded as an active support in catalytic hydrogenation in the presence of a small amount of noble metal (and presumably in the ionization of hydrogen, which comprises the rate-determining partial process of this). Among the inactive supports it may be classified with the catalysts deposited on insulators, since under the conditions of deposition not even its electric conductivity is sufficient for the metal deposition to take place on the entire surface.

Results relating to tungsten carbide

In our earlier paper we assumed on the basis of the works of HOBBS [8] and SANDSTEDE [13] that the tungsten oxide formed on the oxidation of hydrogen tungsten bronze is identical with the assumed oxide which, when developing on the surface of tungsten carbide, gives rise to the catalytic activity of the latter. It proved in our experiments that the oxide forming on the partial or total oxidation of hydrogen tungsten bronze prepared without noble metal is not able to activate molecular hydrogen; thus, the catalytic activity of tungsten carbide in such a sense cannot be attributed to tungsten oxides or tungsten bronzes forming on its surface.

As can be seen from Table II, tungsten carbide can be classified among the electrically well-conducting supports. However, in spite of the fact that the support too is catalytically active, its catalytic activity is not outstandingly high. This further supports our finding that the noble metal does not activate the support; the noble metal is catalytically active and the activity of the support, if it has any, is simply added to that of the former.

Examination of the data in Table II reveals that nitro compounds are hydrogenated at a significantly higher rate than unsaturated compounds on every support, with the exception of tungsten carbide. For the unsaturated compounds the highest rate was attained in fact with tungsten carbide. Thus, the peculiar case arose that while tungsten carbide can be favourably employed as a catalyst primarily for the hydrogenation of nitro compounds, as a support it has advantages over other supports in the hydrogenation of unsaturated compounds. A further advantage of this support is that, as already mentioned, the reaction rate decrease generally observed as a consequence of the small noble-metal content occurs to the lowest extent in this case, and thus a possibility arises for the practical utilization of the catalyst.

The explanation of the considerable rates achieved for unsaturated compounds could be given if the adsorption conditions on the surface of the tungsten carbide were known. It is conceivable that unsaturated compounds are adsorbed on tungsten carbide, but that the strength is such that hydrogenation cannot take place in the absence of noble metal. Some extent of adsorption of organic materials is indicated by those experiments in which the electrochemical oxidation of formaldehyde and methanol was achieved on a tungsten carbide electrode. It may be assumed that, as observed by BAGOTZKY *et al.* [14] in the case of platinized pyrographite, the noble metal deposited on tungsten carbide changes the energetic conditions of the surface to such an extent that the compound adsorbed on the tungsten carbide will undergo hydrogenation too.

A study of the adsorption properties of tungsten carbide does not seem unconditionally necessary for an interpretation of the phenomenon. A more detailed examination of this question will be treated in the following publication.

REFERENCES

[1] VÉRTES, G., HORÁNYI, G.: (In press)
[2] HORÁNYI, G., FÉZLER, G., VÉRTES, G.: Magy. Kém. Foly. **78,** 575 (1972)
[3] HORÁNYI, G., VÉRTES, G., FÉZLER, G.: Z. phys. Chem. N. F. **83,** 322 (1973)
[4] VÉRTES, G., HORÁNYI, G., SZAKÁCS S.: J. Chem. Soc. Perkin II., **1973** 1400
[5] MUND, K., RICHTER, G., STURM, F. V.: Coll. Czech. Chem. Comm. **36,** 439 (1971)
[6] BINDER, H., KÖHLING, A., SANDSTEDE, G.: Energy Conversion **11,** 17 (1971)
[7] BINDER, H., KÖHLING, A., SANDSTEDE, G.: From Electrocatalysis to Fuel Cells. Ed.: Sandstede, G., Battelle Seattle Research Center. 1972. p. 59.
[8] HOBBS, B. S., TSEUNG, A. C. C.: J. Electrochem. Soc. **119,** 580 (1951)

[9] GLEMSER, O., NAUMANN, C.: Z. anorg. allg. Chem. **265.** 288 (1951)
[10] HOBBS, B. S., TSEUNG, A. C. C.: J. Electrochem. Soc. **120,** 766 (1973)
[11] BENSON, J. E., KOHN, H. W., BOUDART, M.: J. Catalysis **5,** 307 (1966)
[12] BOUDART, M., VANNIE, M. A., BENSON, J. E.: Z. phys. Chem. N. F. **64,** 171 (1969)
[13] BENDA, K. V., BINDER, H., KÖHLING, A., SANDSTEDE, G.: From Electrocatalysis to Fuel Cells. Ed.: Sandstede, G., Battelle Seattle Research Center. 1972. p. 87.
[14] BAGOTZKY, V. S., KANEVSKY, L. S., PALANKER, V. SH.: Electrochim. Acta **18,** 473 (1973)

György VÉRTES
György HORÁNYI
Györgyi KISS
1025 Budapest, Pusztaszeri út 59—67. Hungary.

Acta Chimica Academiae Scientiarum Hungaricae, Tomus 83 (2), pp. 151—158 (1974)

INVESTIGATION OF THE IONIZATION OF METALS AND OF THE NEUTRALIZATION OF METAL IONS WITH ROTATING RING-DISC ELECTRODE, X

L. KISS and J. FARKAS

(Department of Physical Chemistry and Radiology, L. Eötvös University, Budapest)

Received November 25, 1973

The $\frac{I}{I_h}$ *vs.* $f^{-1/2}$ relationship (where I is the disc current of the rotating ring-disc electrode, I_h the limiting current of the intermediate measurable at the ring electrode, and f the speed of the electrode) has been rived for anodic metal dissolution proceeding *via* the reactions $M \rightleftarrows M^{z_1^+} + z_1 e$; $M^{z_1^+} \rightleftarrows M^{z_2^+} + (z_2 - z_1)e$; $M \rightleftarrows M^{z_2^+} + z_2 e$. The reaction routes are given in the case of which the relationship obtained is suitable for establishing the mechanism of the process.

As has been shown in our earlier communications, short-lived interme diates formed in the anodic dissolution of metals can be detected with the aid of the rotating ring-disc electrode [1]. Attention has been drawn to the possibilities provided by this electrode system in the study of the mechanisms of electrode process [1, 2].

On the basis of results obtained with the rotating ring-disc electrode DAMJANOVIC, GENSHAW and BOCKRIS [3] have discussed the processes

$$A \rightarrow C \qquad \text{(I)}$$

$$A \rightarrow B \qquad \text{(II)}$$

$$B \rightarrow C \qquad \text{(III)}$$

giving those criteria which permit finding the reaction route through which product C is formed from starting material A. Upon plotting the value of $\frac{I}{I_h}$ as a function of $\frac{1}{f^{-1/2}}$ (where I is the current passing through the disc, I_h the limiting current measured for intermediate B at the ring electrode, and f the speed of rotation of the electrode), straight lines are obtained at a constant disc electrode potential, from the course and mutual position of which conclusions can be drawn on the reaction route. The considerations of the authors mentioned concern those cases in which reactions (I)—(III) proceed only in one direction, owing to the large overvoltage of the electrode processes.

A similar relationship has been found by BAGOTSKII, TARASEVITCH and FILINOVSKII [4] for the reduction of oxygen according to the following scheme:

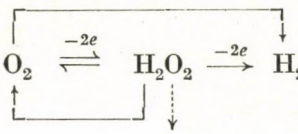

(IV)

The relationship deduced permits also to determine the rate constants of the individual steps.

In some cases the criteria relevant to reactions (I)—(III) have been applied without a sound justification to the analysis of data obtained in the anodic dissolution of metals. [5, 6]

Therefore, our present work was undertaken with the aim to investigate the conditions under which conclusions can be drawn from the shape of the $\frac{I}{I_h}$ *vs.* $f^{-1/2}$ ploton the mechanism of the stepwise anodic dissolution of metals. For the sake of simplicity, let us assume that the ionization of metal M proceeds in two steps, *i.e.* the following processes may take place:

$$M \underset{k_{k_1}}{\overset{k_{a_1}}{\rightleftharpoons}} M^{z_1^+} + z_1 e \qquad \text{(V)}$$

$$M^{z_1^+} \underset{k_{k_2}}{\overset{k_{a_2}}{\rightleftharpoons}} M^{z_2^+} + (z_2 - z_1)\, e \qquad \text{(VI)}$$

$$M \underset{k_{k_3}}{\overset{k_{a_3}}{\rightleftharpoons}} M^{z_2^+} + z_2 e \qquad \text{(VII)}$$

where $M^{z_1^+}$ and $M^{z_2^+}$ are metal ions with charge z_1 and z_2, respectively, and k_{a_i} and k_{k_i} $(i = 1, 2, 3)$ are rate constants depending on the electrode potential.

As can be seen from the schemes written for reactions (V)—(VII), it is assumed in this case that the processes can proceed in the directions of both the upper and the lower arrows. This assumption is justified in the anodic dissolution of metals and in the neutralization of metal ions, because these processes often proceed at a low overvoltage. This is a substantial difference as compared to processes (I)—(VI).

In order to derive the expression for $\frac{I}{I_h}$ as a function of $f^{-1/2}$, first the polarization curve describing processes (V)—(VII) must be determined, and the limiting current intermediate $M^{z_1^+}$, to be measured at the ring electrode, must be known.

For the steady state, when the slow diffusion of the components participating in the reaction affects also the rate of the process, the equation of the polarization curve can be written as follows:

$$j = k_{a_1} + k_{a_3} + k_{a_2} c_{10} - k_{k_1} c_{10} - k_{k_2} c_{20} - k_{k_3} c_{20} \qquad (1)$$

where j is the current density passing through the disc electrode, c_{10} and c_{20} is the concentration at the surface of the disc electrode of the ions $M^{z_1^+}$ and $M^{z_2^+}$, respectively.

Assuming that no $M^{z_1^+}$ ions are present in the bulk of the solution, the limiting current (I_h) of the oxidation of the $M^{z_1^+}$ ions to $M^{z_2^+}$ ions at the ring electrode is:

$$I_h = r_1^2 \pi (z_2 - z_1) X_1 N c_{10} \tag{2}$$

where r_1 is the radius of the disc electrode, $X_1 = 0.62\ FD^{2/3}\omega^{1/2}\nu^{-1/6}$, F being Faraday's number and D_1 the diffusion coefficient of the $M^{z_1^+}$ ion, $\omega = \frac{2\pi}{60} f$, f being the speed of rotation of the electrode, $\min^{-1}$, ν is the kinematic viscosity of the solution, and N is the geometric factor of the electrode.

The unknown concentrations c_{10} and c_{20} needed for solving the task, can be determined from the following relationships derived from the mass balance, under the assumption that the concentration of the $M^{z_2^+}$ ions in the bulk of the solution is also practically zero:

$$\frac{k_{a1}}{z_1} - \frac{k_{k1}}{z_1} c_{10} - \frac{k_{a2}}{(z_2 - z_1)} c_{10} + \frac{k_{k2}}{(z_2 - z_1)} c_{20} = X_1 c_{10} \tag{3}$$

$$\frac{k_{a3}}{z_2} + \frac{k_{a2}}{(z_2 - z_1)} c_{10} - \frac{k_{k3}}{z_2} c_{20} - \frac{k_{k2}}{(z_2 - z_1)} c_{20} = X_2 c_{20} \tag{4}$$

where the meaning of X_2 is completely analogous to that of X_1.

From relationships (1)—(4), the following expression can be obtained for $\frac{I}{I_h}$ ($I = j\pi r_1^2$):

$$\frac{I}{I_h} = \frac{1}{(z_2 - z_1)N}\left[z_1 \left(1 + \frac{z_2}{z_1(z_2 - z_1)} \cdot \frac{k_{a2}}{X_2 + \frac{k_{k2}}{z_2 - z_1} + \frac{k_{k3}}{z_2}} \right) + \right.$$

$$\left. + \frac{X_1 + \frac{k_{k1}}{z_1} + \frac{k_{a2}}{z_2 - z_1} \cdot \frac{X_2 + \frac{k_{k3}}{z_2}}{X_2 + \frac{k_{k2}}{z_2 - z_1} + \frac{k_{k3}}{z_2}}}{\frac{k_{a1}}{k_{a3}}\left(X_2 + \frac{k_{k2}}{z_2 - z_1} + \frac{k_{k3}}{z_2} \right) + \frac{z_1}{z_2(z_2 - z_1)} k_{k2}} \right]. \tag{5}$$

As can be seen, in the general case, when the process occurs through reactions (V)—(VII), $\frac{I}{I_h}$ as a function of $f^{-1/2}$ does not give a straight line, and neither can it be linearized.

The conceivable reaction routes for anodic metal dissolution and the pertinent relationships for $\frac{I}{I_h}$ are listed in Table I. For simpler treatment, the diffusion coefficients of the ions $M^{z_1^+}$ and $M^{z_2^+}$ have been taken as identical in the table, so that $X_1 = X_2 = X$. The following symbols have been used:

$$\frac{k_{a_3}}{k_{a_1}} = A\,; \quad \frac{k_{k_1}}{z_1 X} = B; \quad \frac{k_{k_2}}{(z_1 - z_2)\,X} = C\,; \quad \frac{k_{k_3}}{z_2 X} = D\,;$$

$$\frac{k_{a_2}}{(z_2 - z_1)\,X} = E\,; \quad \gamma = \frac{1}{(z_2 - z_1)\,N}\,.$$

As can be seen from the table, when all three processes [(V)—(VII)] take place, the plot of $\frac{I}{I_h}$ *vs.* $f^{-1/2}$ gives a straight line only in two cases (*ad* and *ag*). In both cases, the slope and the intercept of the straight lines, determined at various electrode potentials, increase when the electrode potential becomes more positive. Case *ad* corresponds to the process described by Eq. (IV) [4], provided that the intermediate does not decompose spontaneously, while case *ag* has been discussed by DAMJANOVIC, GENSHAW and BOCKRIS [3] as a general case.

In the table, the stepwise mechanism is realized in the processes of the *b* series. As shown by the relationships and as can be seen from Fig. 1, the $\frac{I}{I_h}$ *vs.* $f^{-1/2}$ plot does not give straight lines in cases *b* and *ba* but the curves deflect in the direction of the abscissa. However, at a sufficiently high speed of the rotating electrode and at a sufficiently high anodic polarization, an approximately straight line is obtained, and the straight lines belonging to different potentials of the disc electrode reach the ordinate at the same point (see solid curves in Fig. 1). It should be mentioned that when the process occurs via reactions *b* and *ba*, and when, according to current practice in the literature the section of the curve between points $f_1^{-1/2}$ and $f_2^{-1/2}$ is extrapolated as a straight line to the ordinate axis, the diagram corresponding to the *ad* and *ag* mechanisms is obtained (see Fig. 1). This may lead to erroneous conclusions concerning the mechanism.

In cases *bb* and *bc*, the plot of $\frac{I}{I_h}$ *vs.* $f^{-1/2}$ gives straight lines. The slope of the straight lines belonging to different potentials increases with increasing potential of the disc electrode, and the straight lines reach the ordinate axis at the same point.

In cases *bd* and *be* the plot of $\frac{I}{I_h}$ *vs.* $f^{-1/2}$ gives a straight line parallel to the abscissa; the position of this line is independent of the electrode potential.

Table I

Processes proceeding during anodic dissolution	Relationship obtained for the value of $\frac{I}{I_h}$
a) $M \rightleftarrows M^{z_1^+} + z_1 e$ $M^{z_1^+} \rightleftarrows M^{z_2^+} + (z_2 - z_1)e$ $M \rightleftarrows M^{z_2^+} + z_2 e$	$\frac{I}{I_h} = \gamma \left[z_1 + \frac{z_2 E}{1 + C + D} + \frac{1 + B + \frac{E(1+D)}{(1+C+D)}}{\frac{1}{A}(1 + C + D) + \frac{z_1}{z_2} C} \right]$
aa) $M \rightarrow M^{z_1^+} + z_1 e$ $M^{z_1^+} \rightleftarrows M^{z_2^+} \rightleftarrows (z_2 - z_1)e$ $M \rightleftarrows M^{z_2^+} + z_2 e$	$\frac{I}{I_h} = \gamma \left[z_1 + \frac{z_2 E}{1 + C + D} + \frac{1 + \frac{E(1+D)}{1+C+D}}{\frac{1}{A}(1 + C + D) + \frac{z_1}{z_2} C} \right]$
ab) $M \rightleftarrows M^{z_1^+} + z_1 e$ $M^{z_1^+} \rightarrow M^{z_2^+} + (z_2 - z_1)e$ $M \rightleftarrows M^{z_2^+} + z_2 e$	$\frac{I}{I_h} = \gamma \left[z_1 + \frac{z_2 E + A(1 + B + E)}{1 + D} \right]$
ac) $M \rightleftarrows M^{z_1^+} + z_1 e$ $M^{z_1^+} \rightleftarrows M^{z_2^+} + (z_2 - z_1)e$ $M \rightarrow M^{z_2^+} + z_2 e$	$\frac{I}{I_h} = \gamma \left[z_1 + \frac{z_2 E}{1 + C} + \frac{1 + B + \frac{E}{1+C}}{\frac{1}{A}(1 + C) + \frac{z_1}{z_2} C} \right]$
ad) $M \rightleftarrows M^{z_1^+} + z_1 e$ $M^{z_1^+} \rightarrow M^{z_2^+} + (z_2 - z_1)e$ $M \rightarrow M^{z_2^+} + z_2 e$	$\frac{I}{I_h} = \gamma \left[z_1 + A + z_2 E + A(B + E) \right]$
ae) $M \rightarrow M^{z_1^+} + z_1 e$ $M^{z_1^+} \rightleftarrows M^{z_2^+} + (z_2 - z_1)e$ $M \rightarrow M^{z_2^+} + z_2 e$	$\frac{I}{I_h} = \gamma \left[z_1 + \frac{z_2 E}{1 + C} + \frac{1 + C\frac{E}{1+C}}{\frac{1}{A}(1 + C) + \frac{z_1}{z_2} C} \right]$
af) $M \rightarrow M^{z_1^+} + z_1 e$ $M^{z_1^+} \rightarrow M^{z_2^+} + (z_2 - z_1)e$ $M \rightleftarrows M^{z_2^+} + z_2 e$	$\frac{I}{I_h} = \gamma \left[z_1 + \frac{z_2 E + A(1 + E)}{1 + D} \right]$
ag) $M \rightarrow M^{z_1^+} + z_1 e$ $M^{z_1^+} \rightarrow M^{z_2^+} + (z_2 - z_1)e$ $M \rightarrow M^{z_2^+} + z_2 e$	$\frac{I}{I_h} = \gamma \left[(z_1 + A) + E(z_2 + A) \right]$

Table I continued

Processes proceeding during anodic dissolution	Relationship obtained for the value of $\frac{I}{I_h}$
b) $M \rightleftarrows M^{z_1^+} + z_1 e$ $M^{z_1^+} \rightleftarrows M^{z_2^+} + (z_2 - z_1)e$	$\frac{I}{I_h} = \gamma \left(z_1 + \frac{z_2 E}{1 + C} \right)$
ba) $M \rightarrow M^{z_1^+} + z_1 e$ $M^{z_1^+} \rightleftarrows M^{z_2^+} + (z_2 - z_1)e$	$\frac{I}{I_h} = \gamma \left(z_1 + \frac{z_2 E}{1 + C} \right)$
bb) $M \rightleftarrows M^{z_1^+} + z_1 e$ $M^{z_1^+} \rightarrow M^{z_2^+} + (z_2 - z_1)e$	$\frac{I}{I_h} = \gamma (z_1 + z_2 E)$
bc) $M \rightarrow M^{z_1^+} + z_1 e$ $M^{z_1^+} \rightarrow M^{z_2^+} + (z_2 - z_1)e$	$\frac{I}{I_h} = \gamma (z_1 + z_2 E)$
bd) $M \rightleftarrows M^{z_1^+} + z_1 e$	$\frac{I}{I_h} = \gamma z_1$
be) $M \rightarrow M^{z_1^+} + z_1 e$	$\frac{I}{I_h} = \gamma z_1$
c) $M \rightleftarrows M^{z_1^+} + z_1 e$ $M \rightleftarrows M^{z_2^+} + z_2 e$	$\frac{I}{I_h} = \gamma \left[z_1 + \frac{A(1 + B)}{1 + D} \right]$
ca) $M \rightleftarrows M^{z_1^+} + z_1 e$ $M \rightarrow M^{z_2^+} + z_2 e$	$\frac{I}{I_h} = \gamma \left[(z_1 + A) + AB \right]$
cb) $M \rightarrow M^{z_1^+} + z_1 e$ $M \rightleftarrows M^{z_2^+} + z_2 e$	$\frac{I}{I_h} = \gamma \left[z_1 + \frac{A}{1 + D} \right]$
cc) $M \rightarrow M^{z_1^+} + z_1 e$ $M \rightarrow M^{z_2^+} + z_2 e$	$\frac{I}{I_h} = \gamma (z_1 + A)$
cd) $M \rightarrow M^{z_2^+} + z_2 e$ or $M \rightleftarrows M^{z_2^+} + z_2 e$	

Table I continued

	Processes proceeding during anodic dissolution	Relationship obtained for the values of $\frac{I}{I_h}$
dj	$M_1^{z_1^+} \rightleftarrows M$ $M \rightleftarrows M$	$\frac{I}{I_h} = \gamma \left[z_1 + \frac{z_2 E}{1+C+D} + \frac{1+\frac{E(1+D)}{1+C+D}}{\frac{z_1}{z_2} C} \right]$
da)	$M_1^{z_1^+} \leftarrow M_2^{z_2^+} + (z_2 - z_1)\, e$ $M \rightleftarrows M_2^{z_2^+} + z_2 e$	$\frac{I}{I_h} = \gamma \left(z_1 + \frac{z_2}{z_1 C} \right)$
db)	$M_1^{z_1^+} \rightleftarrows M_2^{z_2^+} + (z_2 - z_1) e$ $M \rightarrow M_2^{z_2^+} + z_2 e$	$\frac{I}{I_h} = \gamma \left[z_1 + \frac{z_2 E}{1+C} + \frac{1+\frac{E}{1+C}}{\frac{z_1}{z_2} C} \right]$
dc)	$M_1^{z_1^+} \leftarrow M_2^{z_2^+} + (z_2 - z_1)\, e$ $M \rightarrow M_2^{z_2^+} + z_2 e$	$\frac{I}{I_h} = \gamma \left(z_1 + \frac{z_1}{z_2 C} \right)$

In the case of the processes listed in the table under reaction series *c*, the anodic process occurs according to a so-called parallel mechanism. As can be seen, in case *ca* a straight line similar to those for *ad* or *ag* is obtained for the plot of $\frac{I}{I_h}$ *vs.* $f^{-1/2}$. In case *cc*, the plot of this relationship gives a straight line parallel to the abscissa; the position of this line depends on the potential of the disc electrode.

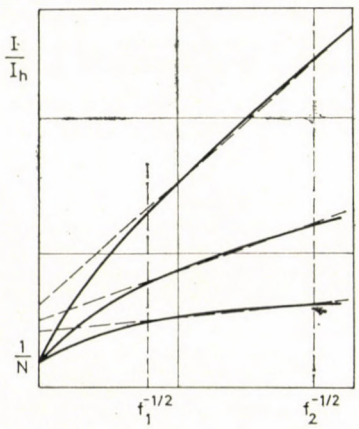

Fig. 1. Schematic diagram of the $\frac{I}{I_h}$ *vs.* $f^{-1/2}$ curves corresponding to cases *b* and *ba*

Reaction series *d* of the table represents a reaction type, which is probably seldom realized in practice. In this case, the stable ion of higher charge number is formed in one step, and the ion of lower charge number is produced by the reduction of this ion, *i.e.* process (V) does not take place. As can be seen, the plot of $\frac{I}{I_h}$ *vs.* $f^{-1/2}$ gives in none of the cases a straight line. However, when under conditions *da* and *dc* the value of $\frac{I}{I_h}$ is plotted as a function of $f^{+1/2}$, a straight line is obtained.

It should be mentioned that in their discussion DAMJANOVIC, GENSHAW and BOCKRIS [3] regarded case *ag* as general, reaction routes marked with *bc*, *be* and *cc* in our table being special cases.

Thus it can be established $\frac{I}{I_h}$ *vs.* $f^{-1/2}$ relationship cannot always be used for the investigation of the anodic dissolution of metals and unequivocal conclusions on the reaction route can be drawn only in certain cases. In those cases where the extrapolated curves belonging to different disc electrode potentials do not intersect the ordinate in the same point conclusions must be drawn with extreme care (see Fig. 1).

REFERENCES

[1] KISS, L.: Magy. Kém. Foly. **72,** 191 (1966), KISS L., KŐRÖSI, A., FARKAS, J.: Ann. Univ. Sci. Bp. Sect. Chim., **9,** 3 (1967); KISS, L., FARKAS, J.: Acta Chim. Acad. Sci. Hung., **64.** 241 (1970)
[2] KISS, L., FARKAS, J.: Acta Chim. Acad. Sci. Hung., **66,** 395 (1970); **69,** 167 (1971); KISS, L., FARKAS, J., FÓTHI, A.: Acta Chim. (Budapest), **74,** 123 (1972)
[3] DAMJANOVIC, A., GENSHAW, M., BOCKRIS, J. O'M.: J. Chem. Phys., **45,** 4057 (1966)
[4] BAGOTSKII, V. S., TARASEVITCH, M. P., FILINOVSKII, V. YU.: Elektrokhimia, **5,** 1218 (1969); PLESKOV, YU. V., FILINOVSKII, V. YU.: The Rotating Disc Electrode (In Russian). Izd. Nauka, Moscow, 1972. p. 269.
[5] KOZIN, L. F., SOKOLSKII, D. V.: Trudy Inst. Org. Kataliza i Elektrokhimii. Vol. 2, p. 3, Izd. Nauka Kazak. SSR, Alma-Ata, 1971
[6] ECKERT, J., FORKER, W.: Z. phys. Chem., **253,** 153 (1973)

László KISS
József FARKAS
} 1088 Budapest, Puskin u. 11—13. Hungary.

Acta Chimica Academiae Scientiarum Hungaricae, Tomus 83 (2), pp. 159—163 (1974)

STEREOCHEMICAL STUDIES, XIX*

CYCLIC AMINOALCOHOLS AND RELATED COMPOUNDS, XI* INVESTIGATION OF *CIS*- AND *TRANS*-2-HYDROXYMETHYLCYCLOHEXYLAMINE BY NMR SPECTROSCOPY**

Zs. MÉHESFALVY-VAJNA, G. BERNÁTH*** and P. SOHÁR

*(Research Institute for Pharmaceutical Chemistry, Budapest and Institute of Organic Chemistry, A. József University, Szeged***)*

Received December 14, 1973

The NMR spectra of N-acyl derivatives of *cis*- and *trans*-2-hydroxymethylcyclohexylamines were studied to obtain information concerning the structure of the transition state of the N → O acyl migration reaction. The most advantageous conformation of the bicyclic transition state of the *trans*- and *cis*-isomers has been established. In the *trans*-isomers the original *diequatorial* conformation remains intact on protonation, while the cyclohexane ring of the *cis*-isomers is present probably in the twist form in which the acylamide and the hydroxymethyl groups are forced into *quasi-equatorial* position.

We studied earlier the N → O acyl migration in N-benzoyl derivatives of *cis*- and *trans*-2-hydroxymethylcyclohexylamine and *cis*- and *trans*-2-aminomethylcyclohexanol [1—3], as well as in the corresponding cyclopentane [4, 5] and cycloheptane [6] derivatives. In cyclohexane and cycloheptane derivatives, the *trans*-isomers undergo N → O acyl migration faster than the *cis*-isomers, whereas for the cycloheptane derivatives the reaction rate is reversed. The reaction rate depends upon the stability of the bicyclic transition state, which, in the case of the *cis*- and *trans*-cyclohexane derivatives, resembles monoazamonooxa *cis*- and *trans*-decaline, respectively.

Cis- and *trans*-2-aminomethylcyclohexanol and *cis*- and *trans*-2-hydroxymethylcyclohexylamine were converted to tetrahydrooxazines [7] related to the bicyclic transition state of the N → O acyl migration reaction of N-benzoyl derivatives of these aminoalcohols. IR and NMR analyses of the tetramethylenetetrahydro-1,3-oxazine-2-ones derived from these aminoalcohols and those of the related pentamethylene analogues derived from the corresponding cycloheptane derivatives were also discussed [8, 9].

The preferred conformations of the above perhydroheterocycles proved to be analogous to those suggested by us for the most probable transition state of the acyl migration reactions. Namely, the *cis*-derivatives may exist in the transition states of acyl migrations as well as in the above perhydroheterocycles in two conformations, differing in the *equatorial* or *axial* orientation of the

* Part XVIII (X): BERNÁTH, G., GÖNDÖS, GY., GERA, L., TÖRÖK, M., KOVÁCS, K., SOHÁR, P.: Acta Phys. et Chem. Szeged, 19, 147 (1973).

** Presented in part at the XVII. Colloquium Spectroscopicum Internationale, Firenze, Sept. 17, 1973. See: Proceedings, Acta Vol. III. p. 123.

methylene group and of the oxygen atom (or NH group), respectively. Of these conformations those with the methylene group in *equatorial* and the hetero atom in *axial* position are the more stable.

In order to get a deeper insight into the formation of the bicyclic transition state of the N → O acyl migration reaction, we investigated the NMR spectra of the N-acyl derivatives of the above cyclic 1,3-aminoalcohols. Especially the NMR spectra of the N-*o*-, *m*- and *p*-methylbenzoyl derivatives of *cis*- and *trans*-2-hydroxymethylcyclohexylamine measured in deuterochloroform and trifluoroacetic acid (TFA) solutions proved to be highly informative. In this paper these investigations are reported.

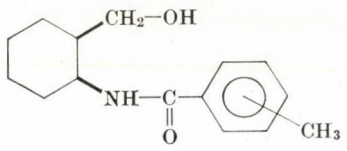

I a–c

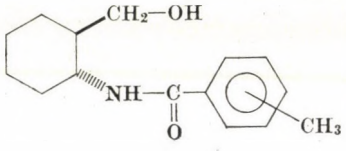

II a–c

a: $o-CH_3$
b: $m-CH_3$
c: $p-CH_3$

The structures of the signals corresponding to the hydroxymethyl protons in N-*o*-, N-*m*- and N-*p*-methylbenzoyl-*cis*- and *trans*-2-hydroxymethylcyclohexylamine (**Ia—c**, **IIa—c**) differ significantly in the case of the *cis*- and *trans*-isomers in $CDCl_3$ solution. The *cis*-isomers give a doublet, whereas the corresponding signal of the *trans*-isomers appears as an AB part of one ABX multiplet (Table). This may be explained by the assumption that in the case of *cis*-isomers the ABX spin system of the methylene protons and their adjacent ring hydrogen approach the A_2X pattern. The A and B protons are practically isochronic ($\delta A \sim \delta B$).

This difference is due to the anisotropic effect of the acylamido group, causing an opposite shift of the two methylene protons in the *trans*-isomers as compared with the *cis*-isomers.

The chemical shift of the ring proton adjacent to the acylamino group differs significantly in the corresponding *cis*- and *trans*-isomers. From this it could be concluded that this ring proton is *axial* in the *trans*-, and *equatorial* in the *cis*-isomers.

The changes of the spectrum parameters in TFA are due to protonation on the nitrogen atom, causing a dramatic decrease in the electron density of the adjacent ring carbon atom. The signal of the methine proton adjacent to the nitrogen is paramagnetically shifted in the *trans*-isomers by 0.7 ppm. The

Table
PMR Data of compounds **Ia—c** and **IIa—c**

Compound		δCH_2 ppm			$\Delta\delta$	δCH ppm*		$\Delta\delta$
		$CDCl_3$		TFA		$CDCl_3$	TFA	
ortho (**a**)	*cis* (**I**)	3.35**		3.9	0.55	4.4	4.6	0.2
meta (**b**)	*cis* (**I**)	3.45**		4.0	0.55	4.4	4.6	0.2
para (**c**)	*cis* (**I**)	3.47**		3.9	0.45	4.4	4.6	0.2
ortho (**a**)	*trans* (**II**)	3.65	3.25	3.9	0.45	3.8	4.5	0.7
meta (**b**)	*trans* (**II**)	3.67	3.33	3.9	0.45	3.8	4.5	0.7
para (**c**)	*trans* (**II**)	3.70	3.25	4.0	0.50	3.8	4.5	0.7

* Signal of the CH(NHAc) group.
** $\delta A \sim \delta B$ ($ABX \rightarrow \sim A_2X$)
$\Delta\delta$ = chemical shift difference between $CDCl_3$ and TFA solvents.

supposition that this shift is caused by protonation is supported by the fact that the methylene protons of the hydroxymethyl group are similarly shifted in both isomers. Thus it may be taken for granted that in the *trans* isomers the original *diequatorial* conformation remains intact on protonation. Obviously, this conformation is the most advantageous for the formation of the bicyclic transition state of the acyl migration.

In the *cis*-isomers, on protonation the signal of the methine proton adjacent to the nitrogen is shifted only by 0.2 ppm.

This can be explained by a change in the conformation occurring during protonation. Accordingly, the ring proton originally *equatorial* in the basic state, becomes *quasi-axial* and more shielded in the protonated transition state. The result of this shielding and of the somewhat stronger deshielding caused by the protonation is a small downfield shift.

The *quasi-axial* orientation of the methine proton in the protonated *cis*-isomers suggests a twist conformation for the cyclohexane ring due to which the acylamide and the hydroxylmethyl group are forced into *quasi-equatorial* position. Nevertheless, this arrangement is favourable for the N → O acyl migration enabling the formation of the energetically preferred chair conformation of the second ring of the hypothetical intermedier.

Of the four most probable conformers **IIIa—d, IIIb** and **IIId** probably do not play an important role in the conformer distribution of the transition state because of the *axial* orientation of the phenyl group. Moreover, even the two diastereomers **IIIa** and **IIIc** are energetically different; accordingly, **IIIa** can be taken as the preferred conformation. In this steric arrangement only

one hydrogen and one hydroxyl group is involved in a 1,3-*diaxial* interaction, whereas in **IIIc** the hydroxyl group and a C–C bond are situated *diaxially*.

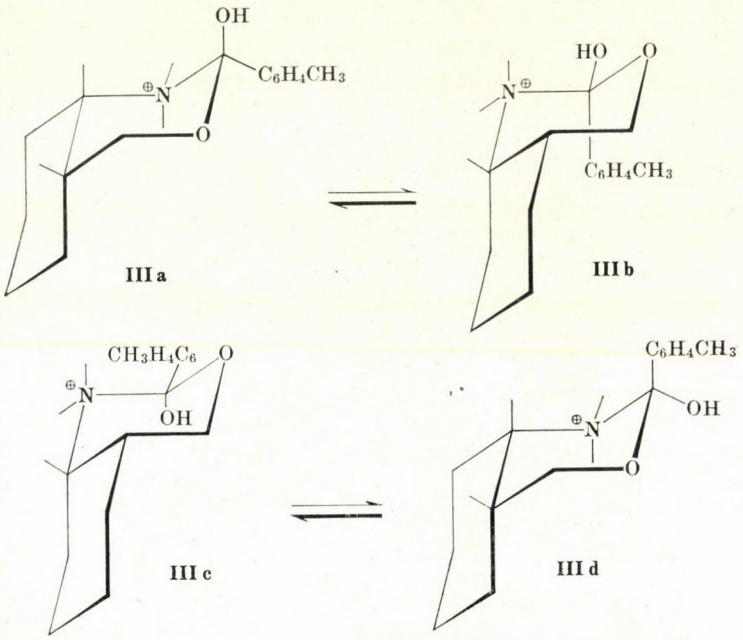

The formation of transition state **IIIa** of the acyl migration reaction is in accordance with the conformation deduced from the NMR spectra of the unprotonated N-acyl derivatives. Namely, as shown above, in *cis*-N-acyl derivatives the hydroxymethyl group is *equatorial*, while the acylamino group is *axial*. After protonation, as the cyclohexane ring takes up the twist form, an even more favourable condition for the formation of the bicyclic transition state is obtained.

Summing up, it can be stated that these investigations support the conformation deduced earlier for the bicyclic transition state of the N → O acyl migration reaction of *cis*-derivatives, which is also analogous with that found in the case of the related perhydrooxazines and perhydrooxazinones. It can be concluded that on protonation the unfavourable steric interactions appearing in the formation of the bicyclic transition state are further diminished by the more advantageous twist chair form of the cyclohexane ring.

REFERENCES

[1] Bernáth, G., Kovács, K., Láng, K. L.: Tetrahedron Letters **1968,** 2713
[2] Bernáth, G., Kovács, K., Láng, K. L.: Acta Chim. (Budapest) **65,** 347 (1970)
[3] Bernáth, G., Láng, K. L., Kovács, K.: Acta Phys. et Chem. Szeged **18,** 227 (1972)

[4] BERNÁTH, G., LÁNG, K. L., GÖNDÖS, GY., MÁRAI, P., KOVÁCS, K.: Tetrahedron Letters **1968,** 4441
[5] BERNÁTH, G., LÁNG, K. L., GÖNDÖS, GY., MÁRAI, P., KOVÁCS, K.: Acta Chim. (Budapest) **74,** 479 (1972)
[6] BERNÁTH, G., GÖNDÖS, GY., LÁNG, K. L.: Unpublished results
[7] BERNÁTH, G., LÁNG, K. L., KOVÁCS, K., RADICS, L.: Acta Chim. (Budapest) **73,** 81 (1972)
[8] SOHÁR, P., BERNÁTH, G.: Org. Magnetic Resonance **5,** 159 (1973)
[9] BERNÁTH, G., GÖNDÖS, GY., KOVÁCS, K., SOHÁR, P.: Tetrahedron **29,** 981 (1973)

Zsuzsa MÉHESFALVY-VAJNA
Pál SOHÁR
} 1325 Budapest, Ujpest 1, POB 82

Gábor BERNÁTH; 6720 Szeged, Dóm tér 8, Hungary.

Acta Chimica Academiae Scientiarum Hungaricae, Tomus 83 (2), pp. 165—170 (1974)

INVESTIGATION OF THE ANODIC DISSOLUTION OF COPPER IN ANHYDROUS ACETIC ACID SOLUTIONS, II

EFFECT OF CHLORIDE IONS

L. KISS and M. L. VARSÁNYI

(Department of Physical Chemistry and Radiology, L. Eötvös University, Budapest)

Received December 23, 1973

The anodic dissolution of copper has been studied in acetic acid solutions containing LiCl. It has been established that copper is oxidized practically only to Cu(I), and the transfer and diffusion overvoltages are comparable. Cu(I) ions form chloride complexes of the type $CuCl_2^-$. Calculation of the transfer coefficient gave a value of 0.65 ± 0.05.

In our previous communication [1], the anodic dissolution of copper has been studied in acetic acid and in acetic acid–water mixtures containing perchlorate ions. It has been established that the rate-determining step of metal dissolution in anhydrous acetic acid solutions is the diffusion of Cu^+ ions. However, in aqueous acetic acid the rate of further oxidation of Cu^+ ions at the electrode plays also a considerable role in addition to the diffusion of Cu^+ ions.

In this communication we report on investigations of the anodic dissolution of copper in acetic acid solutions containing chloride.

Results and discussion

The experimental equipment and the preparation of the electrode were the same as described earlier [1]. LiCl of analytical grade used in the measurements was dried at 160°C, and the residual water content was determined by preparing a stock solution in methanol. The solvent was dried in the usual way [2]. The acetic acid calomel electrode described in our earlier communications was used as reference electrode [2]. The experiments were carried out at room temperature under oxygen-free nitrogen.

In preliminary experiments, the apparent charge number of copper (Ne) in a 0.5 mol/dm^3 solution of LiCl in acetic acid has been determined. The value of $Ne \sim 1$ is indicative of the fact that in the anodic dissolution copper is oxidized only to Cu(I), similarly to the experimental results obtained in perchloric acid solution.

Fig. 1 shows the galvanostatic curves (φ—lg j), determined for the copper rotating disc electrode at three different speeds of rotation of the electrode. As compared to curves recorded in perchlorate media the polarization

curves are shifted considerably in the negative direction and moreover, the $\varphi - \lg j$ function is not a straight line. Though polarization curves are shifted with increasing speed of rotation of the electrode towards more negative potentials, on plotting the $j - f^{1/2}$ function no straight line is obtained. The analysis of these data in combination with the finding that the apparent valency of copper in LiCl solution is ~ 1, permits the conclusion that copper is oxidized

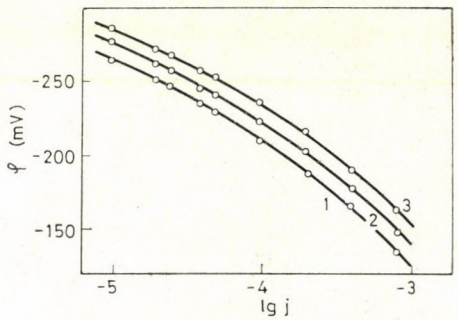

Fig. 1. Relationship between the potential of the rotating disc electrode and the logarithm of the anodic current density in 0.5 mol/dm³ LiCl solution in acetic acid. Speed of rotation of the electrode: 1. $f = 160$ min^{-1}; 2. $f = 610$ min^{-1}; 3. $f = 3070$ min^{-1}

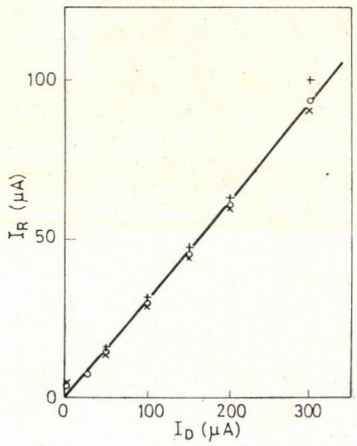

Fig. 2. Limiting oxidation current measurable at the ring electrode as a function of the anodic current measured at the disc electrode in 0.5 mol/dm³ LiCl solution in acetic acid. Speed of rotation of the electrode: + $f = 160$ min^{-1}; × $f = 610$ min^{-1}; ○ $f = 3070$ min^{-1}

in this solution practically to Cu(I), and the transfer and diffusion overvoltages are comparable. The conclusion that only Cu(I) ions are formed in the solution is supported also by measurements with the rotating ring-disc electrode. According to data shown in Fig. 2, the limiting current of the Cu(I) ions, formed by the anodic dissolution of the copper disc, which can be measured at the ring, is independent of the speed of rotation of the electrode and is proportional to the current passing through the disc [3, 5].

The general relationship describing the polarization curve for a two-step process, when the concentration of the ions participating in the reaction is zero in the bulk of the solution [3] is

$$j = k_{a_1} \frac{X_1 + \dfrac{2k_{a_2}}{1 + \dfrac{k_{k_2}}{X_2}}}{X_1 + k_{k_1} + \dfrac{k_{a_2}}{1 + \dfrac{k_{k_2}}{X_2}}} \qquad (1)$$

where k_{a_1}, k_{k_1} k_{a_2} and k_{k_2} are the rate constants of the corresponding processes, depending on the electrode potential. In the case of the rotating disc electrode X_1 and X_2 mean the following expression:

$$X_i = 0.62\, FD_i^{2/3} \nu^{-1/6} \omega^{1/2} \qquad i = 1, 2 \tag{2}$$

where F is Faraday's number, D_i is the diffusion coefficient of Cu^+ and Cu^{2+} ions, respectively, ω is the angular velocity of the rotating electrode, $\omega = \frac{2\pi}{60} f$, if f is the speed of rotation in min^{-1}, and ν is the kinematic viscosity of the solution.

According to the above, in the present case the rate constants of Cu(I) formation and reduction (k_{a_1} and k_{k_1}) are comparable with respect to their order of magnitude with the 'rate constant' of the diffusion of the complex containing the Cu(I) ions (X_1) and, as compared to these quantities, the rate constant of the oxidation of Cu(I) to Cu(II) (k_{a_2}) is negligible. Thus, the following condition is fulfilled:

$$k_{a_1} \gtrless k_{k_1} \simeq X_1 \gg k_{a_2}\,. \tag{3}$$

With this condition, relationship (1) can be written in the following form:

$$\frac{1}{j} = \frac{1}{k_{a_1}} + \frac{k_{k_1}}{k_{a_1} X_1} \tag{4}$$

or under consideration of the dependence of k_{a_1} and k_{k_1} on the electrode potential (3):

$$\frac{1}{j} = \frac{1}{k'_{a_1}} \exp\left(-\frac{\alpha_1 F\varphi}{RT}\right) + \frac{k'_{k_1}}{k'_{a_1}} \frac{1}{X_1} \exp\left(-\frac{F\varphi}{RT}\right) \tag{5}$$

where k'_{a_1}, and k'_{k_1}, are rate constants independent of the electrode potential.

Thus, when condition [3] is fulfilled, j^{-1} is a linear function of $f^{-1/2}$. The plot of j^{-1} *vs.* $f^{-1/2}$ is shown in Fig. 3 for a constant potential. The plot is actually a straight line, which supports the correctness of assumption [3].

If the diffusion term is eliminated from relationship [5], the determination of the value of α_1 becomes possible. JOHN and VIELSTICH [4] used this method in the case of the redox system Fe^{3+}/Fe^{2+} for the determination of the transfer coefficient.

For the case of $\frac{1}{X_1} = 0$ relationship [5] can be written in the following form:

$$j_0 = k'_{a_1} \exp \frac{\alpha_1 F\varphi}{RT}\,. \tag{6}$$

If the $\varphi - \lg j_0$ relationship is plotted on the basis of the j_0^{-1} values belonging to $\frac{1}{X_1} = 0$, the value of α_1 can be calculated from the slope of the straight line. The $\varphi - \lg j_0$ plot is shown in Fig. 4. The value of α_1 calculated on the basis of these data is 0.65 ± 0.05.

It can be established on the basis of these data that in the anodic dissolution of copper in acetic acid solution containing LiCl, only Cu(I) ions are

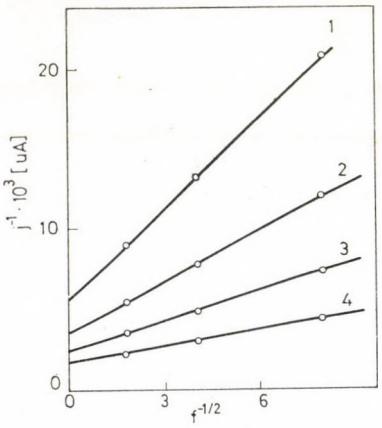

Fig. 3. The relationship $j^{-1} - f^{-1/2}$ in 0.5 mol/dm³ LiCl solution in acetic acid at constant potential. 1. $\varphi = -230$ mV; 2. $\varphi = -215$ mV; 3. $\varphi = -200$ mV; 4. $\varphi = -185$ mV

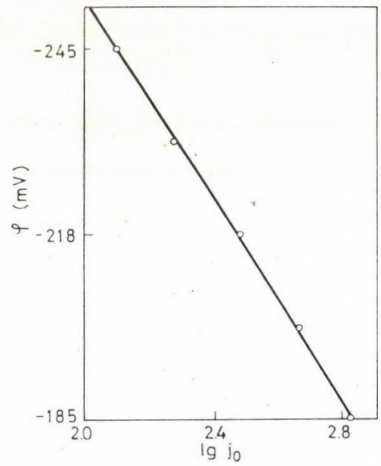

Fig. 4. The relationship $\varphi - \lg j_0$ in 0.5 mol/dm³ LiCl solution in acetic acid j_0 is the current density belonging to $f^{-1/2} = 0$

formed but, in contrast to results obtained in acetic acid solution containing perchlorate ions, in LiCl the diffusion and transfer overvoltages are comparable.

It is known from our earlier investigations [5] as well as from other sources [6, 7] that in aqueous chloride solutions copper(I) complexes are formed, and the potential of the copper electrode is determined by the concentration of these complexes. In the general cases, the potential of the metal electrode in the presence of a complexing agent is [8]

$$\varphi = \varphi^{0'} + \frac{RT}{zF} \ln \frac{c_{M^{z+}}}{c_x^n} \tag{7}$$

where $\varphi^{0'}$ is the formal potential of the electrode, c_x is the initial concentration of the ligand, $c_{M^{z+}}$ is the metal ion concentration of the solution, n is the coordination number, and the conditions are fulfilled that $c_x \gg c_{M^{z+}}$, and predominantly only complexes of ligand number n are formed.

From Eq. [7], the coordination number of the ion or neutral molecule bound in the complex can be determined. Using this equation, it was our object to determine the number of chloride ion bound in the complex in acetic acid medium. With this aim, it was first investigated, whether the Nernst relationship is valid. At a relatively high foreign ion concentration (0.2 mol dm^{-3} $LiClO_4$) and at a constant chloride ion concentration (0.3 mol dm^{-3} LiCl),

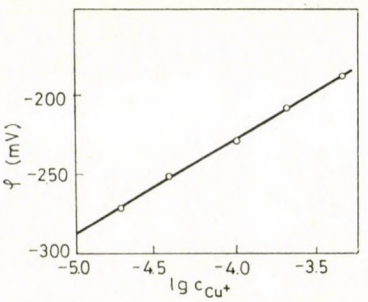

Fig. 5. The relationship φ — lg c_{Cu^+} in 0.3 mol/dm^3 LiCl + 0.2 mol/dm^3 $LiClO_4$ solution in acetic acid

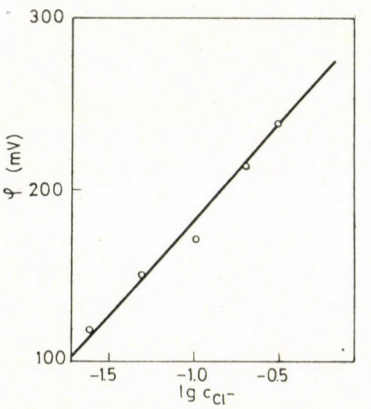

Fig. 6. The relationship φ — lg c_{Cl^-} in x mol/dm^3 LiCl + (0.5 — x) mol/dm^3 $LiClO_4$ solution in acetic acid at constant Cu^+ ion concentration. $c_{Cu^+} = 2 \times 10^{-4}$ mol/dm^3

the relationship φ *vs.* lg c_{Cu^+} has been determined, changing the CuCl concentration in the region from 10^{-5} to 6×10^{-4} mol dm^{-3}. The results of these measurements are shown in Fig. 5. As can be seen, Nernst's relationship is fulfilled, the slope of the straight line being 59 mV per decade.

For the determination of the coordination number, a concentration of 2×10^{-4} mol dm^{-3} was selected for Cu(I), while the chloride ion concentration was changed between 0.025 and 0.3 mol dm^{-3}, and relationship φ — lg c_{Cl^-} was determined at constant ionic strength. As can be seen from Fig. 6, the slope of the straight line is 114 mV per decade, *i.e.* $n = 2$. Accordingly, Cu(I) ion forms chloride complexes of the type $CuCl_2^-$.

REFERENCES

[1] KISS, L., VARSÁNYI, M. L.: Magy. Kém. Foly. **80,** 29 (1974); Acta Chim. (Budapest) **81** 61 (1974)
[2] KISS, L., DO NGOC, L., VARSÁNYI, M. L.: Annales Univ. Sci. Budapest, Sect. Chim., **12,** 145 (1971)
[3] KISS, L., FARKAS, J., FÓTHI, Á.: Magy. Kém. Foly., **78,** 202 (1972); Acta Chim. (Budapest), **74,** 123 (1972)

[4] JAHN, D., VIELSTICH, J.: J. Electrochem. Soc., **109,** 849 (1962)
[5] KISS, L., FARKAS, J., KŐRÖSI, A.: Magy. Kém. Foly., **77,** 35 (1971); Acta Chim. Acad. Sci. Hung., **68,** 359 (1971)
[6] STEPHENSON, L., BARTLETT, J. H.: J. Electrochem. Soc., **101,** 571 (1954)
[7] BACARELLA, A. L., GRIESS, J. C.: J. Electrochem. Soc., **120,** 459 (1973)
[8] KRAVTSOV, V. I.: Elektrodnye protsessy v rastvorakh kompleksov metallov. Izd. LGU 1969 p. 25

László KISS
Magda L. VARSÁNYI
1088 Budapest, Puskin u. 11—13. Hungary.

Acta Chimica Academiae Scientiarum Hungaricae, Tomus 83 (2), pp. 171—183 (1974)

RADIOLYSIS OF ALKENES, II*

LIGHT HYDROCARBON PRODUCTS FROM SOME NORMAL AND CYCLIC ALKENES

GY. CSERÉP and G. FÖLDIÁK

(Institute of Isotopes of the Hungarian Academy of Sciences)

Received December 27, 1973

Various normal and cyclic alkenes with different molecular sizes were irradiated in liquid phase with a ^{60}Co γ-radiation source. On the basis of the yields of C_1–C_5 fragments it has been concluded that in spite of the very high primary energy, the primary decomposition of the molecules occurs at bonds which are loosened. Owing to the delocalization of π electrons in the alkenes, σ-bonds in β-position have the smallest energy of dissociation, however, other effects such as chain ends or unpaired electrons of free radicals, as well as the strain energy of the molecula may also influence the product composition.

Introduction

Dehydrogenation of alkenes under irradiation was treated in our previous papers [1, 2] and π-bonds were established to play a predominant role in determining hydrogen yields. In addition to hydrogen yields usually smaller by an order of alkanes, preferred splitting of individual C–H bonds is observed: in general, hydrogen atoms in allylic positions split off with higher probabilities than others. A strong antibat correlation is observed between the probability of hydrogen removal and the bond dissociation energy

This paper deals with the radiolysis of unbranched aliphatic and cyclic C_5–C_{10} alkenes, that is with the influence of π-bonds on the position of decomposition.

1. Literature survey

In comparison with the literature on radiation-induced polymerization, few papers deal with the fragmentation of alkenes. This may be attributed to the great number of fragments as well as to experimental difficulties due to the very low yields — and, last but not least, to the fact that polymerization is a much more important process in practice.

Of open chain alkenes, the radiolysis of propene was studied by WAGNER [3] but only the yields of products higher than C_3 were evaluated. *n*-butenes were investigated by KAUFMAN [4] both in the gas and liquid phases; although more attention was paid to products of higher molecular weight, the G-values

* Ref. [2] is regarded as Part I of the series.

of fragmentation products were found to be much higher with the irradiation carried out in the gas phase. Though no conclusions have been drawn by the author on the mechanism of fragment formation, the importance of ion-molecule combination in the formation of higher molecular weight products has been pointed out. Radiolysis of *cis*-2-butene was investigated by HATANO *et al.* [5] in the liquid phase. Their results differ considerably from those of KAUFMAN (Table I); according to their experiments in the presence of additives, the prod-

Table I

Fragmentation products of the radiolysis of liquid cis-2-butene [4, 5]

Product	G(molecule/100 eV)	
	Ref. [5]	Ref. [4]
Methane	0.21	0.13
Ethane	0.03	0.09
Ethylene	0.08	0.26
Acetylene	0.11	0.26
Propane	—	0.22
Propene	0.13	0.26

ucts were formed partly by radical and partly by molecular mechanisms. No interpretation has been given for the fact of why the carbon skeleton splits at particular positions. The dimeric products formed during radiolysis of 1-pentene were determined by WAGNER [6] in the presence of various additives but no data on the fragments were reported. The radiation chemistry of *n*-hexenes was investigated by CHANG *et al.* [7], BRASH and GOLUB [8] and that of 1-octene by KOURIM [9]. These investigations included the determination of $G(H)_2$ as well as yields of dimers and telomers. Of higher *n*-alkenes, COLLINSON and coworkers studied the radiolysis of 1-hexadecene [10]. They have drawn conclusions on the mechanism of H_2 formation and polymerization and, in addition, reported data on the overall yields of some light hydrocarbon fragments.

Of cyclic monoalkenes, cyclohexene was studied in detail by FREEMAN [11], with considerable attention to products of higher yields and of higher molecular weight. Individual yields of methane and ethylene and the overall yield of the C_4 fraction were determined. Ethylene was found to have the highest yield.

FREEMAN assumes two kinds of decomposition, namely:

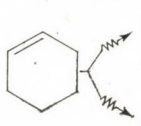

$$2\,C_2H_4 + C_2H_2 \qquad (1a)$$

$$C_2H_4 + C_4H_6 \qquad (1b)$$

We have not found any information about the radiolysis of cyclic monoalkenes of higher molecular weight.

2. Experimental

Experiments were carried out according to a technique described earlier [2]. Hydrocarbons to be irradiated were supplied by FLUKA; their purity was, as a rule, 98—99%. Cyclodecene was synthesized in this Institute. All hydrocarbons were purified prior to irradiation. Irradiations took place at room temperature, using a 80 000 Ci nominal activity ^{60}Co γ-radiation source, with a dose rate of 3—5 $m^2 s^{-3}$ (1.0—1.5 Mrad h^{-1}); the total doses were as high as 4—8 10^4 $m^2 s^{-2}$ (4—8 Mrad). Fragmentation products were analyzed by gas chromatography.

3. Results and discussion

Different normal terminal and internal alkenes as well as cycloalkenes of different ring sizes without side chains were irradiated. The yields obtained are listed in Tables II—IV. The values given are averages of at least three parallel experiments. In all cases, more fragments were observed than those shown in the Tables; however, the products whose yields were too low to permit an accurate determination were omitted.

3.1. *Open chain alkenes*

3.1.1. n-Hexene isomers

Table II contains data for light hydrocarbons produced from different *n*-hexenes.

The yield of methane increases significantly with the shift of the π-bond towards the middle of the chain. A similar variation of the hydrogen yield was observed in our previous work [2]. Assuming that methane is primarily produced from methyl groups of the molecule, the increase of methane yield from internal hexenes may be attributed to the relative position of the methyl groups and the π-bond, on the other hand, to the fact that the number of methyl groups is twice as high in internal hexenes than in terminal 1-hexene. The highest methane yield was observed in the case of 3-hexene having both of its methyl groups in β-position with respect to the π-bond. More methane was formed from 2-hexene than expected; this may be due to the formation of a transition state prior to decomposition which is similar to the one formed from 3-hexene. The fact that this complex is more similar to 3-hexene than to 1-hexene may be explained in terms of the secondary allylic C–H bond having a lower bond energy and, hence, a smaller stability. Our assumption is supported by studies of *n*-hexene isomers in the mass spectrometer where migration of the π-bond also manifests itself [12]. In addition to the higher methane yield of 2-hexene, the formation of propene from 3-hexene also suggests an isomerization prior to decomposition.

Table II

*Yields of light hydrocarbons from n-hexene isomers**

Product	C=C–C~C–C–C	C–C=C–C~C–C	C~C–C=C–C~C
	G (molecule/100 eV)		
C	0.030	0.132	0.233
C–C	0.028	0.107	0.160
C=C	0.133	0.122	0.073
C≡C	0.091	0.049	0.045
C–C–C	0.043	0.003	0.008
C=C–C	0.113	0.063	0.035
	0.015	0.003	0.004
C=C=C	0.031	0.003	0.004
C≡C–C	0.006	0.027	0.004
C–C–C–C	0.035	0.008	0.002
C=C–C–C	0.044	0.022	0.074
C–C=C–C	0.005	0.006	0.002
C=C–C=C	0.003	0.003	0.004
C–C–C–C–C	0.001	0.001	0.002
C=C–C–C–C	0.003	0.003	0.002
C–C=C–C–C	0.004	0.001	0.040

* H-atoms were omitted from the formulae for the sake of clarity
~ denotes the position of allyl-interaction

The variation of the yield of ethane with the position of the π-bond is similar to that of methane, while no such phenomenon can be observed for the ethylene and acetylene yields. As expected, much less ethane was produced from 1-hexene than from 2-hexene, since ethane (and also much of the ethylene) is formed from 2-hexene via rupture of allylic C–C bonds whose bond dissociation energy is lower by about 54 kJ mol^{-1} than those of other C–C bonds, owing to interactions with the π-bond:

$$CH_3CH{=}CHCH_2{-}CH_2CH_3 \rightsquigarrow CH_3CH{=}CHCH_2^{\cdot} + C_2H_5^{\cdot} \qquad (2)$$

$$2\ C_2H_5^{\cdot} \rightarrow C_2H_6 + C_2H_4\,. \qquad (3)$$

The large amount of ethane produced from 3-hexene may be explained, in addition to combination of methyl radicals, by the rupture of C–C bonds in α-position to the π-bond (as supported by the formation of acetylene in the case of both 2- and 3-hexene) as well as by the isomerization mentioned before.

Further studies will be necessary to clear finally the problem of ethane formation from 3-hexene.

The double bond in 1-hexene favours the formation of C_3 products instead of ethyl group elimination but still the G-value of ethylene is remarkably high. One may assume that this is due to loosening effect of the end of the saturated chain which favours the splitting of the molecule into fragments with two carbon atoms each (*e.g.* ethylene). The unpaired electron of alkyl radicals exerts an effect similar to that of the π-bond, *viz.* favours the splitting of σ-bonds in β-position. This may explain the presence of some ethylene among the radiolysis products of every hydrocarbon:

$$C{=}C{-}C{-}C{-}C{-}C \xrightarrow{\sim} C{=}C{-}C{-}\dot{C}H_2 + \dot{C}H_2{-}C \qquad (4)$$

$$C{=}C{-}C{-}\dot{C}H_2 \longrightarrow C{=}C\dot{H} + C{=}C \qquad (5)$$

$$2\,C{-}\dot{C}H_2 \longrightarrow C{-}C + C{=}C \qquad (6)$$

$$C{=}C\dot{H} \longrightarrow C{\equiv}C + \dot{H} \qquad (7)$$

The assumption of reaction (4) is justified by the fact that the second weakest bond of the molecule is between the fourth and fifth carbon atoms of the 1-hexene chain:

$$C = \overset{391}{C}{-}\overset{299}{C}{-}\overset{342}{C}{-}\overset{354}{C}{-}C$$

Numbers above the bonds denote dissociation energies (in kJ mol^{-1}) calculated from literature data [13]. Although the formation of both ethylene and acetylene can be explained by reactions (4)—(7), in agreement with the experimental data, reaction (8) cannot be excluded either:

$$C{=}C{-}C{-}C{-}C{-}C \xrightarrow{\sim} 3\,C{=}C. \qquad (8)$$

This reaction involves the decomposition of a 1-hexene radical ion, *e.g.* according to reactions (9)—(11):

$$C{=}C{-}C{-}C{-}C{-}C \xrightarrow{\sim} \overset{+}{C}H{-}\dot{C}H{-}C{-}C{-}C{-}C + e^- \qquad (9)$$

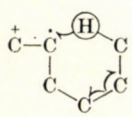

$$\xrightarrow{} \overset{+}{C}H{-}C{-}C{-}\dot{C}H_2 + \dot{C}H{=}C \qquad (10)$$

$$\overset{+}{C}H{-}C{-}C{-}\dot{C}H_2 \xrightarrow{+e^-} 2\,C{=}C \qquad (11)$$

Of *n*-hexene isomers, 1-hexene produces the most C_3 products. The nature of these C_3 fragments suggests that they have been formed *via* fission of the loosened C–C bond between the third and fourth carbon atoms. The G-

value of propene is three times higher than that of propane, which may be due to several reasons. One may be an internal rearrangement in the transition state involving H-atom transfer simultaneously with the rupture of the C–C bond in β-position in part of the decomposing ions or excited molecules reaction (12):

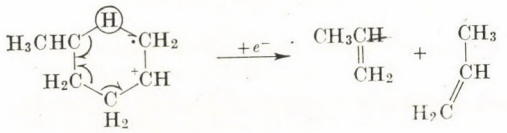

(12)

A similar rearrangement has been described in mass spectrometry and, according to WAGNER [6], it may take place in the liquid phase too.

Another explanation may involve further reactions of propyl radicals leading to lower propane and higher propene yields:

$$2\ C_3H_7^{\cdot} \rightarrow C_3H_6 + C_3H_8 \tag{13}$$

$$C_3H_7^{\cdot} \rightarrow C_2H_4 + CH_3^{\cdot}. \tag{14}$$

Fragments of primary decomposition possess considerable energy and the decomposition of propyl radicals according to Eq. (14) requires an energy as low as 108 kJ mol^{-1}. *i.e.* $\approx$ 1 eV/particle. Since the disproportionation of allyl radicals is unfavourable energetically this has no appreciable influence on the propene yield.

As a rule, low yields of C_4 products were observed although both 2-hexene and 3-hexene contain σ-bonds in β-position with respect to the π-bond, whose rupture could result in the formation of C_4 products. The very low yield of butenes from 2-hexene indicates secondary reactions of the 1-methylallyl radicals or ions formed via removal of an ethyl group from hexene. The methylallyl intermediates are resonance stabilized, therefore, they have longer lifetimes than *e.g.* the alkyl and alkenyl radicals to interact with reactive radicals and other intermediates present in the system. The formation of C_4 products from 3-hexene would involve (assuming a directing effect of the π-bond) a simultaneous elimination of two methyl groups; the very low yield of butadiene indicates that the probability of such a simultaneous decomposition is very low. It is remarkable that, of C_4 products, 1-butene is produced with the highest yield from all hexenes irradiated. This phenomenon may be interpreted by rearrangement or by the splitting of the σ-bond in α-position to the π-bond; α-splitting leads to the formation of acetylene, *n*-butane and 1-butene from 1-hexene [reactions (15)—(17)], and ethane, ethylene and 1-butene from 3-hexene [reactions (18)—(20)]:

$$CH_2{=}CH(CH_2)_3CH_3 \xrightarrow{\sim} CH_2{=}\dot{C}H + \dot{C}H_2(CH_2)_2CH_3 \quad (15)$$

$$CH_2{=}\dot{C}H \longrightarrow H^{\cdot} + CH{\equiv}CH \quad (16)$$

$$2\,CH_3(CH_2)_2\dot{C}H_2 \longrightarrow CH_2{=}CHCH_2CH_3 + CH_3CH_2CH_2CH_3 \quad (17)$$

$$CH_3CH_2CH{=}CHCH_2CH_3 \xrightarrow{\sim} \begin{cases} CH_2{=}CH_2 + CH_2{=}CHCH_2CH_3 & (18a) \\ CH_3\dot{C}H_2 + \dot{C}H{=}CHCH_2CH_3 & (18b) \end{cases}$$

$$2\,CH_3\dot{C}H_2 \longrightarrow CH_2{=}CH_2 + CH_3CH_3 \quad (19)$$

$$CH_3CH_2CH{=}\dot{C}H + RH \longrightarrow CH_3CH_2CH{=}CH_2 + R^{\cdot} \quad (20)$$

The yield of C_5 products is even lower than those of the C_4 fragments. The only C_5 compound worth mentioning is 2-pentene from 3-hexene, indicating the splitting of a σ-bond in β-position with respect to a π-bond.

3.1.2. *n*-Octene isomers

The data on the decomposition of n-octene isomers (Table III) permit to draw similar conclusions as in the case of hexenes, although, owing to the longer carbon chain, the fraction of fragments not connected with the directing effect of the π-bond increases in comparison with the amount of fragments where this directing effect manifests itself; hence, it is still more difficult to distinguish between various effects.

The methane yields show an identical variation to those observed with hexenes: the G-values increase in the following order: 1-octene $<$ 2-octene $<$ $<$ 4-octene $<$ 3-octene. The smallest value corresponding to 1-octene is due to the presence of only a single methyl group in this hydrocarbon. The highest $G(CH_4)$ value is observed with 3-octene; the loosening effect of the π-bond in β-position with respect to one of the methyl groups causes an enhancement as high as 20%.

The yield of ethane + ethylene is the highest from 4-octene. This may be explained by the symmetrical loosening effect of the π-bond in the middle of the chain on both terminal ethyl groups:

$$C{-}C{-}C{-}C{=}C{-}C{-}C{-}C{-}C \xrightarrow{\sim} C{-}\dot{C} + \dot{C}{-}C{=}C{-}C{-}C{-}C \quad (21)$$

$$2\,C{-}\dot{C} \longrightarrow C{=}C + C{-}C \quad (22)$$

This phenomenon is analogous to that observed for the methane yield of 3-hexene.

The conclusions that can be drawn from the G-values of ethane are analogous to those obtained on the basis of methane formation. The G-value of ethane from 2-octene is twice as high as that from 1-octene in spite of the fact that both isomers contain only one ethyl group. This may be interpreted in terms of a cumulative loosening effect of the π-bond and chain end on the σ-bonds in β-position with respect to both.

Table III

*Yields of light hydrocarbons from n-octene isomers**

Product	C=C–C–C–C–C–C–C–C	C–C=C–C–C–C–C–C–C	C–C–C=C–C–C–C–C	C–C–C–C=C–C–C–C
	G (molecule/100 eV)			
C	0.015	0.058	0.077	0.055
C–C	0.016	0.031	0.047	0.115
C=C	0.081	0.066	0.056	0.111
C≡C	0.031	0.010	0.008	0.010
C–C–C	0.013	0.020	0.055	0.067
C=C–C	0.051	0.056	0.052	0.028
C–C–C–C	0.009	0.048	0.035	0.005
C=C–C–C	0.018	0.036	0.041	0.013
C–C–C–C–C	0.029	0.030	0.003	0.002
C=C–C–C–C	0.029	0.022	0.013	0.045
C–C=C–C–C	0.002	0.017	0.420	0.066

* H-atoms were omitted from the formulae for the sake of clarity
–≀– denotes the position of allyl-interaction

The G-values of ethylene decrease in the following order: 4-octene > > 1-octene > 2-octene > 3-octene; the length of the saturated parts of the molecules becomes shorter in the same order, except the 4-octene. This can be interpreted by breaking up the longer alkyl or alkenyl radicals by units of two carbon atoms. Identical G-values of ethylene and ethane were observed in the case of 4-octene. This may be attributed to the disproportionation of ethyl radicals with one another [reaction (22)] or with other alkyl radicals.

The acetylene yields from octenes are analogous to those of hexenes; acetylene is produced in higher yield from terminal than from internal alkenes.

There are only small differences between the yields of C_3 fragments produced from octene isomers under irradiation. $G(C_3)$ is highest from 3-octene; this is in good agreement with the loosening effect of the π-bond; at the same time the low (propene + propane) yield from 1-octene is unexpected. This may perhaps be interpreted in analogy to hexenes, *i.e.* by the ability of allyl radicals to form not only propene but also higher hydrocarbons. C_3 formation from 2- and 4-octene is only possible via fission of the σ-bond in α-position with respect to the π-bond, eventually after rearrangement of the energy-rich activated complex.

Of all octenes, 2-octene produces the most C_4 products, although their amount is not as high as one would expect from the known loosening effect of the π-bond:

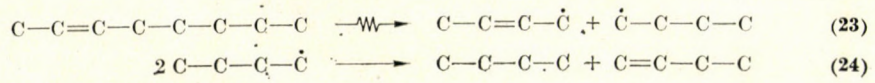

(23)

(24)

In order to explain this apparent discrepancy, it has to be assumed that part of the methylallyl radicals is transformed into higher molecular weight products. On the basis of yields from 3- and 4-octene, it may be assumed that simultaneous rupture of two allylic C–C bonds has a very low probability, since only traces of 1,3-butadiene are formed.

Owing to the directing effect of the π-bond, the radiolysis of 3-octene produces the largest amount of C_5 fragments. At the same time, the relatively high yield of C_5 products from 4-octene can be explained in a way analogous to the explanation offered for C_3 products from 2- and 4-octene.

3.2. *Cycloalkenes*

The hydrogen yields observed during the radiolysis of alkenes show that cyclic compounds are characteristically different from open chain ones [1, 2]. Similarly, the yields of light (C_1–C_5) hydrocarbon fragments produced via fragmentation of the molecule also indicate that there is a difference between the cyclic and the corresponding open chain hydrocarbons (Table IV).

Table IV

Yields of light hydrocarbons from cycloalkenes

Product	Cyclo-pentene	Cyclo-hexene	Cyclo-heptene	Cyclo-octene	Cyclo-decene	Cyclo-dodecene
	G (molecule/100 eV)					
Methane	0.008	0.005	0.007	0.004	0.002	0.002
Ethane	0.001	0.001	0.001	0.001	0.002	0.001
Ethylene	0.15	0.14	0.07	0.054	0.035	0.02
Acetylene	0.06	0.021	0.01	0.006	0.009	0.005
Propane	0.01	0.001	—	—	0.004	0.001
Propene	0.05	0.005	0.01	0.006	0.017	0.002
Cyclopropane		—	0.007	0.002	—	0.001
Propadiene	0.10	—	0.002	0.001	0.001	0.001
n-butane	—	0.001	—	—	0.002	0.001
Butenes	—	0.006	0.003	0.005	0.011	0.002
1,3-butadiene	—	0.06	0.015	0.009	0.014	0.005
C_5 fraction	—	—	0.017	0.007	0.006	—

The stabilization of fragments formed during ring fission of cyclopentene leads mainly to ethylene and propadiene (C_3H_4):

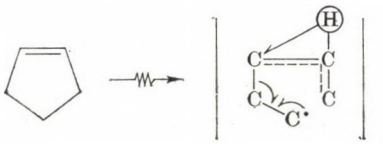

$$\longrightarrow C{=}C + C{=}C{=}C \qquad (25)$$

Presumably, the first bond to be split is one of the allylic C–C bonds; the formation of the two end-products involves rearrangement of electrons and one H-atom. The first of the two subsequent bond ruptures is favoured by allyl-interaction, and the second one by the pairing tendency of the unpaired electron of the activated complex not participating in the allyl-interaction. Another process also taking place with a probability of about 0.5 in comparison with that of reaction (25) is:

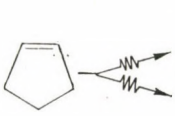

$$C{\equiv}C + C\overset{C}{\diagup\!\diagdown}C \qquad (26a)$$

$$C{\equiv}C + C{=}C{-}C \qquad (26b)$$

The yield of the higher one of the two complementary fragments is lower, but the difference is not too great in the case of this parent cycloalkene.

On comparing the products of radiation-chemical and thermal decomposition, it has been found that any analogy between the products depends mainly on the conditions of pyrolysis. The products obtained upon pyrolysis of short contact time and high temperature [14] are almost the same as those observed in the case of radiolysis (although there is less C_3H_4 among the products of pyrolysis), whereas pyrolysis at lower temperatures (479—520°C) carried out in a static system gives ethylene and propene as the main products [15]. The latter phenomenon may be explained by further conversion of C_3H_4 into propene, since — in correspondence with the activation energies of individual processes — at lower temperatures chain initiation is less extensive than chain propagation, whereas this ratio is reversed at higher temperatures.

The fragment composition from cyclohexene was investigated in more detail (Table IV) than by FREEMAN. We have shown that the C_4 fraction consists mainly of 1,3-butadiene. Thus, the reaction mechanism assumed in section (1b) has been verified. The ethylene yield is 2.3 times higher than that of butadiene; apart from reaction (1a), this may be explained by the fact that while ethylene is stable, butadiene may react easily; *e.g.* the addition of H-atoms [16,17] and methyl radicals [18] is, respectively, about one and two orders of magnitude faster for butadienes than for monoalkenes. In addition — owing to the rather high energies applied radiolysis involves decomposition of both ionic and excited states. As has been established in mass-spectrometric studies of cyclohexene [19], the main direction of cyclohexene ion decomposition leads to the formation of a stable ethylene molecule and a butadiene ion-radical

(27)

The butadiene ion-radical produced during the radiolysis of cyclohexene is a very reactive activated complex — both as a radical and an ion — stabilized by resonance [23], thus it may react in processes requiring hardly any energy of activation.

The data indicate that while in pyrolysis the difference between the yields of complementary products — *i.e.* butadiene and ethylene — is not higher than 5—20% [20,21], in our radiolysis experiments, the yield of 1,3-butadiene is hardly exceeds 1/3 of the yield of ethylene. Presumably, this difference may be attributed to reactions of ion-radicals which are produced during radiolysis but not during pyrolysis.

The preferred splitting of C–C bonds in β-position with respect to the double bond can still be observed in the radiolysis of cycloheptene. This is

supported by the G-values of butadiene, propene and cyclopropane. Because of this type of splitting, butadiene is also formed from cyclooctene, cyclodecene and cyclododecene but the small yields and numerous other fragments make the directing effect rather ambiguous.

On the basis of our experiments with unbranched cycloalkene homologues between 5 and 12 carbon atoms, it can be established that the yield of light hydrocarbon fragments produced *via* C–C bond rupture decreases with increasing carbon atom number, *i.e.* the fragmentation of larger rings is less likely then that of smaller cycles. We assume that this may have energetic reasons; one of the factors of importance may be that the strain energy of the ratio of the components of strain energy (the compression of van der Waals radii, the distorsion of bond angles and bond opposition forces) varies with increasing ring dimensions [22]. Another factor may be the increasing importance of energy dissipation without decomposition. This may be attributed to the fact that in larger molecules the amount of surplus energy per bond is smaller, therefore, the probability that a sufficiently high amount of energy may be concentrated on a given bond, to cause dissociation before deactivation without reaction, becomes lower and lower.

Conclusions

Owing to the high energies absorbed by the system during irradiation, any of the σ-bonds of the molecules activated (excited and/or ionized) by radiation energy may split. In spite of this, a certain selectivity is characteristic of the decomposition, especially in the case of lower molecular weight parent compounds, *i.e.* the rupture of some bonds may occur with a higher probability that of others. This may be correlated with energetic factors. Double bonds (π-bonds) have a loosening effect on other bonds in β-position with respect to them; this effect may be observed in the case of both open chain and cyclic alkenes. A similar but smaller loosening effect is caused by the unpaired electrons of free radicals and chain ends on the σ-bond in β-position to them. The effect of strain energy in cyclic alkenes, whose extent is a function of the ring dimensions, manifests itself mainly in the case of smaller rings, resulting in their enhanced decomposition into smaller fragments.

REFERENCES

[1] CSERÉP, GY., FÖLDIÁK, G.: Int. J. Rad. Phys., **5,** 235 (1973)
[2] CSERÉP, GY., FÖLDIÁK, G.: Acta Chim. (Budapest), **77,** 407 (1973)
[3] WAGNER, C. D.: Tetrahedron, **14,** 164 (1961)
[4] KAUFMAN, P. C.: J. Phys. Chem., **67,** 1971 (1963)
[5] HATANO, Y., SHIDA, S., SATO, S.: Bull. Chem. Soc. Japan, **37,** 1854 (1964)
[6] WAGNER, C. D.: Trans. Faraday Soc., **57,** 163 (1968)
[7] CHANG, P. C., YANG, N. G., WAGNER, C. D.: J. Amer. Chem. Soc., **81,** 2060 (1959)

[8] BRASH, J. L., GOLUB, M. A.: Canad. J. Chem., **45,** 101 (1967)
[9] KOURIM, P.: Int. J. Rad. Phys. Chem., **1,** 345 (1968)
[10] COLLINSON, E., DAINTON, F. S., WAGNER, C. D.: Trans. Faraday Soc., **57,** 1732 (1961)
[11] FREEMAN, G. R.: Canad. J. Chem., **38,** 1043 (1960)
[12] LOUDON, A. H. and MACCOL, A.: The Mass Spectrometry of the Double Bond, in The Chemistry of Alkenes, Ed.—J. Zabicky. Interscience, London, 1970
[13] KERR, J. A.: Chem. Rev., **66,** 465 (1966)
[14] RICE, F. O., MURPHY, M. T.: Amer. Chem. Soc., **64,** 869 (1942)
[15] KNECKT, D. A.: Diss. Abst., *B* **29,** 1627 (1968)
[16] DABY, E. E., NIKI, H., WEINSTROCK, B.: J. Phys. Chem., **75,** 1601 (1971)
[17] CVETANOVIC, R. J., DOYLE, L. C.: J. Chem. Phys., **50,** 4705 (1969)
[18] COLLIN, G. J., PERRIN, M., GAUCHER, C. M.: Canad. J. Chem., **50,** 2391 (1972)
[19] BUDZIKIEWITCZ, H., BRAUMAN, J. I., DJERASSI, C.: Tetrahedron, **21,** 1855 (1965)
[20] SMITH, S. R., GORDON, A. S.: J. Phys. Chem., **65,** 1124 (1961)
[21] UCHIYAMA, M., TOMIOKA, T., AMANO, A.: J. Phys. Chem., **68,** 1878 (1964)
[22] BROWN, H. C., HAM, G.: J. Amer. Chem. Soc., **78,** 2735 (1956)
[23] MCLAFFERTY, F. W.: Interpretation of Mass Spectra. W. A. Benjamin, New York, 1967

György CSERÉP
Gábor FÖLDIÁK } H-1525, Budapest 114, P.O.B. 77, Hungary.

Acta Chimica Academiae Scientiarum Hungaricae, Tomus 83 (2), pp. 185—194 (1974)

RADIOLYSIS OF ALKENES, III

LIGHT HYDROCARBON PRODUCTS FROM SOME BRANCHED ALIPHATIC AND CYCLIC ALKENES

GY. CSERÉP and G. FÖLDIÁK

(Institute of Isotopes of the Hungarian Academy of Sciences, Budapest)

Received December 27, 1973

Various branched-chain aliphatic and side-substituted cyclic alkenes were irradiated in liquid phase with a ^{60}Co γ-radiation source. The yields of light hydrocarbons produced show that branching, *i.e.* the presence of tertiary carbon atoms also has a significant influence upon the decomposition of these hydrocarbons. The loosening effect of tertiary carbon atoms competes in some cases with that caused by the π-bond in β-position, in other cases the two effects are cumulative. Chain ends as well as secondary processes may also influence the product composition.

Introduction

It was found in earlier experiments that π-bonds may considerably influence the composition of radiolysis products since they exert a directing effect on the rupture of both C–H and C–C bonds, making the decomposition selective [1, 2, 3].

In order to further elucidate the correlation between molecular structure and radiation-chemical decomposition, branched-chain aliphatic and cyclic alkenes were also included into our experimental program. This has the advantage that the methyl group leads to a 'pseudo-labelling' of one or another carbon atom of the parent molecule, thus permitting to determine the position of molecular decomposition with greater certainty on the basis of the products. In addition, one may obtain data on the radiolysis of bonds linked to tertiary carbon atoms. In the present paper, results on this subject are reported.

1. Experimental

Experiments were carried out by the method described earlier [2]. Hydrocarbons for irradiation were supplied by FLUKA; their purity was, as a rule, 98—99%, and they were further purified prior to irradiation.

Irradiations took place at room temperature, using 80 000 Ci nominal activity ^{60}Co γ-radiation source, with a dose rate of 5 $m^2 s^{-3}$ (1.5 Mrad h^{-1}) in the dose range of $4—8 \times 10^4$ $m^2 s^{-2}$ (4—8 Mrad). The products were analyzed by gas chromatography.

2. Results and discussion

2.1. *Open-chain branched alkenes*

The data from the evaluation of gas chromatograms are listed in Table I.

Table I

*Yield of light hydrocarbons in the radiolysis of methylhexene isomers**

Product	C=C–C–C–C–C | C 2M1H	C=C–C–C–C–C –C– C 3M1H	C=C–C–C–C–C | C 4M1H	C=C–C–C–C–C | C 5M1H	C–C–C=C–C–C | C 2M3H
	G (molecule/100 eV)				
C	0.06	0.12	0.07	0.15	0.27
C–C	0.025	0.025	0.065	0.005	0.057
C=C	0.079	0.140	0.158	0.087	0.032
C≡C	0.012	0.110	0.060	0.056	0.015
C–C–C	0.035	0.120	0.003	0.022	0.073
C=C–C	0.101	0.110	0.238	0.202	0.060
C–C–C–C	0.029	0.010	0.075	0.002	0.001
C=C–C–C	0.022	0.020	0.102	0.095	0.056
C–C=C–C		0.042	0.146		
C=C–C=C		0.035			
△–C		0.025			
C–C–C | C	0.000	0.000	0.001	0.112	0.001
C–C=C | C	0.060	0.000	0.000	0.125	0.000

* The H-atoms were omitted from most of the formulae for the sake of clarity
–C– denotes the position of allyl interaction
△–C = methylcyclopropane

It can be seen that one of the main effects of methyl groups is that the methane yields become higher as compared with *n*-hexenes [3]. This result verifies our earlier statement that methane is derived from methyl groups split off from the molecule.

Although all methylhexenes in Table I contain only one branching, the values of $G(CH_4)$ are nevertheless different: they increase in the following order: 2M1H < 4M1H < 3M1H < 5M1H < 2M3H. This order may be attributed to two factors: the loosening effect of π-bonds exerted on the σ-bond in β-position and that of the tertiary carbon atom on the σ-bond in α-position. The directing effect of the π-bond, due to its tendency to delocalization, on the σ-bond in β-(allylic) position manifests itself mainly in the case of 3M1H and 2M3H: in 3M1H one, whereas in 2M3H three methyl groups are loosened, thus, the corresponding methane yields $[G(CH_4)]$ are in the ratio of 1 : 3.

Loosening by the tertiary carbon atom increases first of all the methane yield from 5M1H, since both methyl groups of this molecule are linked to a tertiary carbon atom. This is the reason why its methane yield is twice as high as that of 4M1H.

The weakening effect of tertiary carbon atoms is also supported by the G(ethane) values. The order is reverse in this case: the G(ethane) value of 4M1H is higher by more than one order of magnitude than that of 5M1H, and is about three times as high as those of 2M1H and 3M1H. The small ethane yield of 5M1H may be due to the fact that, at the dose rates applied, ethane is formed mainly via ethyl group elimination rather than combination of methyl radicals.

The yield of ethylene from methyl-1-hexenes has a maximum as a function of the position of the methyl substituent with respect to the π-bond. It is not clear why the ethylene yields from 3M1H and 4M1H are as high as measured, but it can be assumed that C_4 fragments produced via β-splitting in the middle of the molecule, breaking into two fragments, may partly decompose into hydrocarbon fragments with two carbon atoms. The G-values of acetylene are obviously strongly dependent on the position of the π-bond and the branching with respect to each other. The smallest acetylene yield was measured with 2M1H, and the highest with 3M1H. The G(acetylene) values from 4M1H and 5M1H are identical, and again, that from 2M3H is very small. Thus, it may be concluded that acetylene is derived almost completely from the bridgehead carbon atoms of the original double bond and its formation is promoted by the tertiary carbon atom in the case of 3M1H. The low G-value of acetylene from 2M3H supports our earlier concept on the higher acetylene yield from terminal alkenes as compared with internal ones [3].

As a consequence of 'labelling' with a methyl group, it may be expected that the elimination of the group containing the double bond from 2M1H (C=C—) will result in the formation of mainly C_3 products (propene, propyne
|
C

and propadiene) instead of acetylene. Actual data are in good agreement with our assumption: G(propyne) = 0.027, G(propadiene) = 0.024. Propyne and propadiene were formed only in negligible amounts from other methylhexenes, therefore, these data were not included into Table I.

The propane and propene yields from methyl-1-hexene isomers show the loosening effect of the π-bond in β-position. Owing to allyl-interaction, one of the main products of decomposition of these molecules always contains three carbon atoms:

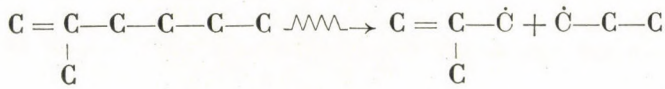

(1)

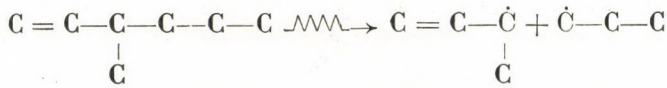

(2)

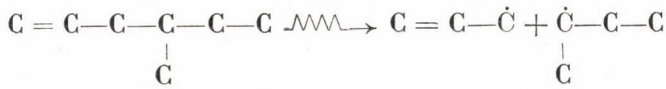

(3)

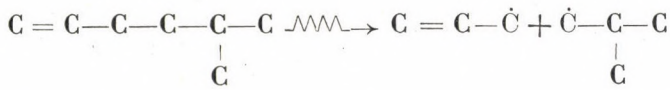

(4)

The reaction mechanism outlined shows that the intermediate containing three carbon atoms is saturated in the case of 2M1H and 3M1H, whereas it is unsaturated with 4M1H and 5M1H. In correspondence with this, of methyl-1-hexene isomers 2M1H and 3M1H produce more propane, whereas 4M1H and 5M1H produce more propene. The considerable amount of propene observed with 2M1H and 3M1H isomers originates from the disproportionation of propyl radicals; this gives practically all propene from 3M1H and about 1/3 of it from 2M1H:

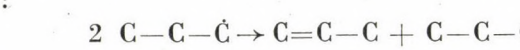

(5)

Propane from 5M1H and 2M3H originates not from the splitting of the σ-bond loosened by the allylic interaction but from the fission of the bond loosened by the tertiary carbon atom:

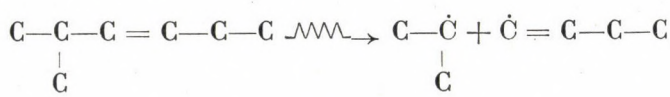

(6)

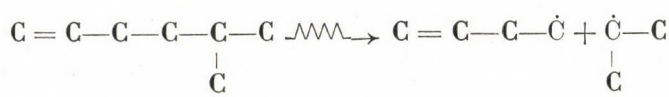

(7)

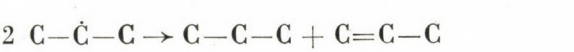

(8)

This assumption is supported by the facts that the G-value of propane produced from 2M3H is nearly identical with that of propene, and that only traces of propane are formed from 4M1H where neither splitting of the σ-bond in β-position with respect to the π-bond, nor fission of the σ-bond in the vicinity of the tertiary carbon atom produce propyl radicals.

The C_4 products may be divided into groups since the *sec*-butyl- and methylallyl-radicals produced in primary processes may transform into various products, *e.g.* via disproportionation or ring closure reactions.

The G-value of *n*-butane is usually very small: 4M1H is the only hydrocarbon producing somewhat more *n*-butane. This is due to the fact that the loosening effect of both the π-bond and the tertiary carbon atom promotes the formation of *sec*-butyl radicals. The comparison of the G-values of *n*-butanes produced from various methylhexene isomers also indicates that there is no, or hardly any, combination between two ethyl radicals in the systems investigated, under the conditions of the experiments, *i.e.* upon irradiation in the liquid phase. The highest yield of *n*-butenes was observed with 4M1H, suggesting the importance of sec-butyl radicals formed under the combined directing effect of the π-bond and the tertiary carbon atom, like in the case of *n*-butane. In agreement with the reactivities of primary and secondary C–H bonds, more 2-butene was found than 1-butene. Though only the sum of *cis*- and *trans*-2-butene was included into the Table their separate determination revealed that the amount of the trans-isomer was 2.5 times higher than that of the cis-isomer from both 3M1H and 4M1H. Since the free enthalpies of formation of the two isomers show the trans-isomer to be more stable, its formation in higher proportion is due to thermodynamic reasons.

C_4 products were formed in much lower proportion from 3M1H than from 4M1H, although the main decomposition of the molecule [Eq. (3)] should have produced one fragment with four carbon atoms. This methylallyl radical, however, has several possibilities for stabilization, as is actually shown by the product spectrum:

$$C{=}C{-}\dot{C}{-}C \xrightarrow{RH} C{=}C{-}C{-}C + R^{\cdot} \qquad (9)$$

$$\dot{C}{-}C{=}C{-}C \xrightarrow{RH} C{-}C{=}C{-}C + R^{\cdot} \qquad (10)$$

$$2\ C{=}C{-}\dot{C}{-}C \begin{cases} \nearrow\ C{=}C{-}C{=}C + C{=}C{-}C{-}C & (11a) \\ \searrow\ C{=}C{-}C{=}C + C{-}C{-}C \ (\text{ring}) & (11b) \end{cases}$$

The sum of the G-values of all these products, however, is hardly equal to one half of that of the complementary products, *i.e.* propane and propene. The difference between the yields of complementary C_3 and C_4 products from

3M1H, *i.e.* the C_4 deficit, can be interpreted in terms of acetylene and ethylene production via further decomposition of the C_4 hydrocarbon as well as by reactions of the methylallyl radical with other reactive intermediates (*e.g.* combination).

Branched-chain C_4 fragments are formed only from 2M1H and 5M1H, demonstrating clearly the directing effect of the π-bond. These branched-chain fragments form only in those cases where allyl interaction promotes the formation of isobutyl and 2-methylallyl radicals. As shown in Table I, 2M1H produces only isobutene, whereas 5M1H gives both isobutane and isobutene in nearly identical amounts. This indicates that — in the case of 5M1H — these products may have been formed in the disproportionation of isobutyl radicals formed in reaction (4):

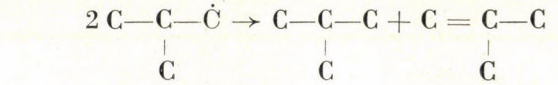

(12)

The structure of the 2M1H molecule explains why no isobutane is produced together with isobutene. Isobutene formation may have occurred in this case *via* hydrogen abstraction by the 2-methylallyl radical, produced primarily in reaction (1) from another molecule, or via intermolecular hydrogen migration in a unimolecular process. The latter possibility may also explain why the propene yield from 2M1H is higher than that of propane:

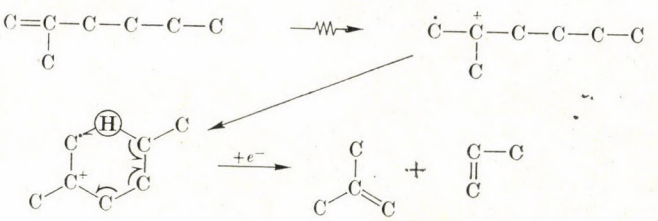

(13)

(14)

2.2. *Cycloalkenes with side chains*

The branched-chain cycloalkenes with six-membered rings listed in Table II can be divided into three groups according to their π-bonds:
the first group contains methylcyclohexenes with one π-bond in the ring (1MC, 3MC, 4MC);
4-vinylcyclohexene (4VC) represents the second group with two π-bonds, one in the ring and one in the side chain;
methylenecyclohexane with a semicyclic π-bond is the only member of the third group.

Table II

Yield of light hydrocarbons in the radiolysis of branched-chain cycloalkenes

Product	1-methyl-cyclohexene	3-methyl-cyclohexene	4-methyl-cyclohexene	4-vinyl-cyclohexene	methylene-cyclohexane
	G (molecule/100 eV)				
Methane	0.016	0.059	0.038	0.002	0.033
Ethane	0.003	0.002	0.002	—	0.001
Ethylene	0.17	0.16	0.03	0.044	0.05
Acetylene	0.02	0.03	0.03	0.023	0.005
Propane	0.005	0.001	0.002	—	0.005
Propene	0.02	0.02	0.15	0.001	0.001
Cyclopropane	—	—	—	—	0.003
Propadiene	—	—	—	—	0.007
Butanes	0.004	0.001	0.002	0.001	—
1-butene	0.003	0.006	0.005	0.001	0.002
2-butene	0.005	0.008	0.002	0.001	0.001
1,3-butadiene	0.002	0.007	0.06	0.163	0.001
Isoprene	0.05	0.002	—	—	0.001
1,3-pentadiene		0.077	—	—	—
C_5-fraction	0.004	0.007	0.005	0.002	0.007

denotes the position of allyl interaction

The methane yields from methylcyclohexene isomers containing one methyl group per molecule are nevertheless different: the lowest methane yield was found from the methyl group in α-position with respect to the π-bond (1MC) and the highest value was observed with a methyl group in β-position (3MC). In the first case, hyperconjugation while in the second case, allyl-interaction can be recognized.

Methylcyclohexenes together with 4-vinylcyclohexene — in spite of the two π-bonds of the latter — decompose in a way similar to cyclohexene, discussed earlier [3], according to a reverse Diels-Alder reaction. The main products of decomposition of methylcyclohexene isomers are different, in correspondence with the position of the methyl 'label'; these are ethylene and 2-methyl-1,3-butadienes (isoprene) from 1MC, ethylene and 1,3-pentadienes from 3MC, and propene and 1,3-butadiene from 4MC:

Of the complementary products of these main decomposition processes, the yield of the one with the higher molecular weight is lower in the case of methylcyclohexenes, too, similarly to the radiolysis of cyclohexene [3, 4]. Our data give, however, evidence, that this difference may not be attributed to the decomposition of the molecule into three parts as suggested by FREEMAN for

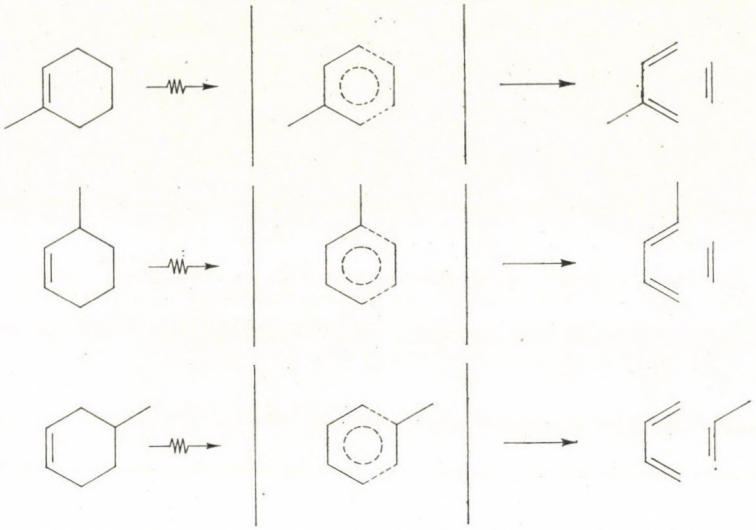

(15)

(16)

(17)

cyclohexene [4], but rather to further reactions of the higher molecular weight fragment, *i.e.* 1,3-pentadiene and 2-methyl-1,3-butadiene. If the difference were due to simultaneous fragmentation into three parts, then *e.g.* the G-value of propene produced from 4MC in reaction (17) would have to be lower than that of ethylene in the radiolysis of cyclohexene [3, 4], since the decomposition of the other part of the molecule would give ethylene and acetylene and not propylene. Since ethylene yields from cyclohexene [3] as well as from 1MC and 3MC are comparable with that of propylene from 4MC, and further, since the G-values of ethylene and acetylene from 4MC are as low as 0.03, and the yield of propylene from 1MC and 3MC is a similarly low value (0.02), it can be stated that the difference between the yields of complementary products may be attributed to the fission of the molecule into three parts only to a very low extent, not more than $G = 0.02-0.03$. The greater part of the discrepancy must be attributed to reactions of the resonance stabilized radical-ion and/or biradical containing the original double bond as well as stable conjugated products with neutral molecules and active intermediates in the system, in a similar way, as it was suggested in the case of cyclohexene [3].

In the radiolysis of 4VC — as expected — only one main product is formed when the carbon skeleton suffers decomposition, and this is butadiene. The most important decomposition process involves the rearrangement of unpaired electrons formed upon the splitting of allylic C–C bonds together with the π-electrons of the double bonds, resulting in the formation of new double bonds at the expense of the σ-bonds cleaved:

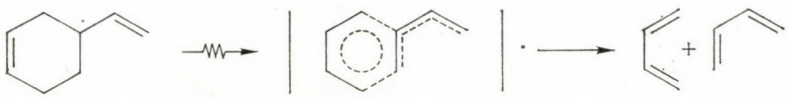

(18)

The amount of acetylene and ethylene is to be mentioned among the fragmentation products, too, ethylene being, however, twice as much as acetylene. The difference may be due to the elimination of a vinyl group, which is promoted by the loosening effect of the tertiary carbon atom. This may lead to ethylene in reaction (19):

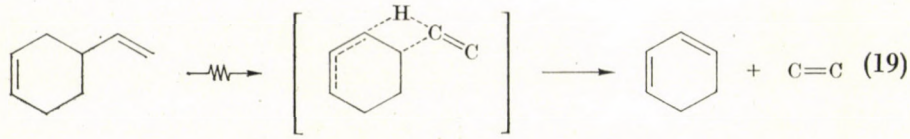

(19)

or may be eliminated as a vinyl radical interacting with other molecules in hydrogen abstraction reactions resulting also in ethylene. Since both the simultaneous fragmentation of the ring into three parts (20):


(20)

and the decomposition of butadiene (21):

$$1,3\text{—}C_4H_6^* \rightarrow C_2H_2 + C_2H_4 \qquad (21)$$

give ethylene and acetylene in equal amounts, the surplus ethylene must have formed in other processes [*e.g.* in reaction (19)].

The radiolysis of methylenecyclohexane containing a semicyclic double bond is very different from those of cyclohexene and substituted cyclohexene. This manifests itself first of all in the very low C_1–C_5 yields. This behaviour is similar to that observed in the photolysis of methylenecyclopentane [5], where only traces of products were observed apart from a small amount of hydrogen. Of the fragmentation products of methylenecyclohexane, we have found that ethylene and propadiene were produced in the highest yields; their formation is represented in Scheme (22):

On energetic grounds, first the rupture of one of the allylic C–C bond should occur, thereafter the unpaired electron of the biradical formed, which does not take part in allyl interaction will direct the decomposition. We assume that the large difference between the yields of ethylene and propadiene is mainly due to the high reactivity of propadiene.

Summary

The radiolysis of branched-chain alkenes — similarly to that of unbranched ones [3] — is selective in spite of the random 'background' molecular splitting because of the high energies absorbed by the system: the G-values of products originating from the rupture of bonds with lower bond energies are generally higher. The π-bond of alkenes considerably decreases the dissociation energy of σ-bonds in β-position with respect to it. The effect of chain ends is smaller but has the same character. Tertiary carbon atoms of branched-chain alkenes exhibit a similar effect.

The radiolysis of the branched open chain and side-substituted cyclic alkenes investigated do not differ considerably from each other. The product spectrum of open-chain species is more complicated, which may be attributed — in addition to the effect of the chain end — to the formation of biradicals from cyclic alkenes when bond splitting occurs. These biradicals may be stabilized in unimolecular rearrangements and thus give a smaller number of products than do the transition species from aliphatic alkenes.

REFERENCES

[1] CSERÉP, GY., FÖLDIÁK, G.: Int. Rad. Phys. Chem., **5,** 235 (1973)
[2] CSERÉP, GY., FÖLDIÁK, G.: Acta Chim. (Budapest) **77,** 407 (1973)
[3] CSERÉP, GY., FÖLDIÁK, G.: Acta Chim. (Budapest) **83** (*1*), 179 (1974)
[4] FREEMAN, G. R.: Canad. J. Chem., **38,** 1043 (1960)
[5] BRINTON, R. K.: J. Phys. Chem., **72,** 321 (1968)

GYÖRGY CSERÉP
GÁBOR FÖLDIÁK
H—1525 Budapest, 114, P. O. B. 77, Hungary.

Acta Chimica Academiae Scientiarum Hungaricae, Tomus 83 (2), pp. 195—199 (1974)

THE DETERMINATION OF SOME SURFACTANTS BY THE DROPPING MERCURY ELECTRODE CAPACITY MEASUREMENTS

(SHORT COMMUNICATION)

S. K. SHARMA

(Department of Chemistry, Birla Institute of Technology and Science, Pilani, Rajasthan, India)

Received January 3, 1974

BREYER and HACOBIAN [1] observed that when a mixture of two surfactants was present in an indifferent electrolyte, only one tensammetric wave was obtained corresponding to the substance whose peak potential occurred at the more cathodic potential. GUPTA and SHARMA [2] studied the influence of tensammetric waves on one another by a.c. polarography and found that in most of the cases, the influence of more cathodic tensammetric peak on less cathodic peak is due to the greater adsorbability of surfactant corresponding to more cathodic peak and consequently forming an adsorbed film on the electrode surface. In some cases, the influence is due to some chemical interaction between two surfactants to form a complex [3, 4] which is more surface active than the individual surfactants.

The communications deals with the determination of some surfactants in dilute solutions with a view to ascertain the applicability of complexation method by dropping mercury electrode (dme) capacity measurements (tensammetry). The determination of these surfactants is of significance since conventional polarography gives no indications to the presence of these surfactants whereas tensammetry provides flat peak or no peak at all in very diluted solutions.

o-Cresol, aniline, benzylamine, diethylamine, *n*-hexylamine, *n*-heptylamine, piperidine and triethanolamine were of either BDH or Merck's quality. Pyridine and *n*-amyl alcohol were of Baker's analytical grade reagents. These were distilled before used from an all-glass fractionating column and the middle one thirds of the distillates were collected. Mercury used for the dme was purified as described previously [2]. Potassium chloride used was of AnalaR quality of BDH.

The technique of dme capacity measurements (tensammetric technique) was the same as that described earlier [5]. This is done by superimposing to the dme, a 50 c/sec $\pm$ 20 m V sinusoidal a.c. potential on the d.c. potential and observing the alternating component of the current. As the capacitive impedance of the dme is much higher than the impedance of the rest of the system, the magnitude of the alternating current gives a measure of the dme capacity.

0.1 *M* KCl (BDH., AR) solution was used as supporting electrolyte. Dropping mercury electrode capacity measurements are taken with the electrolyte and the effect of the surfactants has been expressed in the terms of a.c. (microampers). Negative d.c. potentials were applied to the dme with respect to the saturated calomel electrode. The experiments were carried out at 30 $\pm$ 0.5°. The constants of the dme were: m = 4.564 mg/sec. and t = 1.8 sec/drop in 0.1 *M* KCl (open circuit).

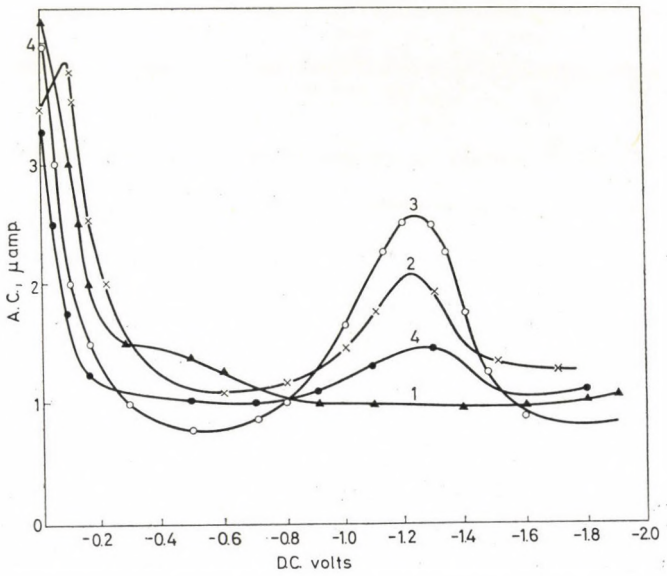

Fig. 1. Interaction of *o*-cresol with triethanolamine by tensammetry. pH = 7.0. Curve 1 — 0.1 *M* KCl; Curve 2 — 1.0% *o*-cresol; Curve 3 — 1.0% *o*-cresol + 0.3% triethanolamine; Curve 4 — 0.3% triethanolamine

The shift of peak potential of the mixture by varying the concentration of one of the surfactants and keeping the other constant, has been utilised in determining the molar ratio of the compounds in the complex [3]. Since the magnitude of the peak of the mixture of surfactants (complex) is greater than those of individual surfactants, it was thought desirable to determine individual surfactants by complexation using tensammetry. As the capacity minimum is not sharp and is sometimes flat over a considerable range of potentials, the estimation of low concentration of surfactant becomes difficult by tensammetry and therefore enhanced magnitude of desorption peak of the mixture of surfactants at potentials differing from the zero value of electrocapillarity has been utilised for determining various surfactants in low concentrations.

Fig. 1 shows the typical tensammetric waves depicting the interaction of *o*-cresol with triethanolamine at pH 7.0 in which curves 2 and 4 are individ-

ual tensammetric waves of 1.0% *o*-cresol and 0.3% triethanol-amine, respectively, whereas curve 3 is the tensammetric wave of the mixture of 1.0% *o*-cresol and 0.3% triethanol-amine. The enhanced desorption peak of the mixture of both the surfactants is further supported by its adsorption. The enhanced peak of the mixture of *o*-cresol and triethanolamine indicates greater surface activity of the complex than the individual surfactants. The desorption peaks of the individual surfactants are not sharp, they cover a wide

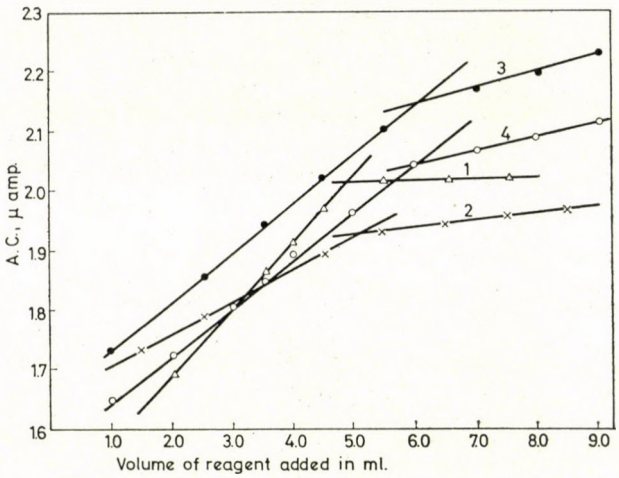

Fig. 2. Titration of *o*-cresol with piperidine and triethanolamine by tensammetry. pH = 7.0. Curve 1 — 50 ml of 1.5×10^{-3} *M* triethanolamine *vs.* 1.0×10^{-1} *M* *o*-cresol; Curve 2 — 50 ml of 2.0×10^{-2} *M* piperidine *vs.* 1.3×10^{-1} *M* *o*-cresol; Curve 3 — 50 ml of 1.0×10^{-2} *M* *o*-cresol *vs.* 5.7×10^{-2} *M* piperidine; Curve 4 — 50 ml of 1.0×10^{-2} *M* *o*-cresol *vs.* 5.7×10^{-2} *M* triethanolamine

range of potentials; with hydrogen-bonded complexation, however, the peaks are sharper and greater.

The enhanced magnitude of the peak of the complex is utilised in determining the surfactants in lower concentrations. Fig. 2 shows the typical results obtained by titrating *o*-cresol with triethanolamine and piperidine and vice-versa at different concentrations of surfactants by tensammetry. The intersections of straight lines gave a 3 : 1 stoichiometry for the hydrogen-bonded *o*-cresol-amine complexes. In order to determine various surfactants, a series of tensammetric direct and reverse titrations of surfactants with other surfactants were carried out. Results on the 3 : 1 complexes (*o*-cresol : amine [6]), as well as pyridine: *n*-amyl alcohol [3], 1 : 1 complex (*o*-cresol : pyridine [3]) and 2 : 1 complex (*o*-cresol : *n*-amyl alcohol [2]) are given in Table I.

The determinations of the surfactants by complexation should be carried out in alkaline solutions where surfactants have pronounced effect.

Table I

Determination of some surfactants by tensammetry in aqueous solutions
Surfactant solution = 50.0 ml
pH = 7.0

Surfactant	Titrant	Concentration (mole/litre)		Titre values (ml)		Error %
		C_S	C_T	calculated	Observed	
Pyridine	*n*-Amyl alcohol	1.2×10^{-3}	2.0×10^{-2}	2.0	1.98	−1.0
n-Amyl alcohol	Pyridine	1.0×10^{-2}	7.5×10^{-1}	4.0	4.02	+0.63
o-Cresol	Pyridine	1.0×10^{-3}	2.0×10^{-2}	5.0	4.96	−0.8
Pyridine	*o*-Cresol	1.0×10^{-3}	2.0×10^{-2}	5.0	4.94	−1.2
Aniline	*o*-Cresol	1.2×10^{-3}–3.0×10^{-4}	2.0×10^{-1}–2.0×10^{-2}	1.8	1.78	−1.1
Benzylamine	*o*-Cresol	1.0×10^{-2}–1.0×10^{-3}	7.5×10^{-1}–1.0×10^{-2}	4.0	4.05	+1.25
Diethylamine	*o*-Cresol	1.2×10^{-3}–2.5×10^{-4}	7.2×10^{-2}–1.0×10^{-3}	5.0	5.03	+0.6
n-Hexylamine	*o*-Cresol	1.0×10^{-3}–2.0×10^{-4}	1.0×10^{-1}–1.0×10^{-2}	3.0	3.03	+1.0
n-Heptylamine	*o*-Cresol	1.5×10^{-3}–2.5×10^{-4}	1.0×10^{-1}–2.0×10^{-2}	4.5	4.5	0
Piperidine	*o*-Cresol	2.0×10^{-3}–5.0×10^{-4}	1.0×10^{-1}–2.5×10^{-2}	6.0	5.95	−0.8
Triethanolamine	*o*-Cresol	2.0×10^{-3}–4.0×10^{-4}	1.0×10^{-1}–2.0×10^{-2}	6.0	5.93	−1.1
Phenol	Piperidine	1.0×10^{-1}	6.6×10^{-1}	5.0	4.96	−0.8
Phenol	Triethanolamine	2.0×10^{-2}	1.3×10^{-1}	5.0	4.96	−0.8
Triethanolamine	Phenol	1.0×10^{-2}–5.0×10^{-3}	7.5×10^{-1}	4.0	3.95	−1.25
Piperidine	Phenol	1.5×10^{-3}	1.0×10^{-1}	4.5	4.52	+0.5

Surfactant	Titrant	Concentration (mole/litre)		Titre values (ml)		(Error) (%)
		C_S	C_T	Calculated	Observed	
o-Cresol	Aniline	1.0×10^{-3}–2.5×10^{-4}	3.0×10^{-2}–2.0×10^{-3}	1.11	1.1	−0.9
o-Cresol	Diethylamine	1.0×10^{-3}–1.2×10^{-4}	6.6×10^{-3}–5.0×10^{-2}	5.0	4.98	−0.4
o-Cresol	*n*-Hexylamine	5.0×10^{-3}–1.2×10^{-4}	5.0×10^{-2}–6.0×10^{-3}	3.33	3.35	+0.6
o-Cresol	*n*-Heptylamine	2.5×10^{-3}–2.0×10^{-4}	4.0×10^{-2}–1.0×10^{-3}	2.08	2.05	−1.44
o-Cresol	Piperidine	1.0×10^{-2}–1.0×10^{-3}	5.7×10^{-2}–6.0×10^{-3}	5.84	5.86	−0.3
o-Cresol	Triethanolamine	1.0×10^{-2}–2.0×10^{-3}	5.7×10^{-2}–6.0×10^{-3}	5.84	5.83	−0.17

C_S — concentration of surfactant
C_T — concentration of titrant

Even $1.5 \times 10^{-4} M$ surfactant can be measured by complexation using tensammetry. The surfactants having higher surface activity can be determined even in lower concentrations since the magnitudes of the peaks of individual surfactant is higher. The accuracy of the method is $\pm$ 1.0%.

*

The author thanks authorities Birla Institute of Technology and Science, Pilani (Rajasthan) India for providing the facilities.

REFERENCES

[1] BREYER, B., HACOBIAN, S.: Aust. J. Sci. Res. **5,** (1952) 500
[2] GUPTA, S. L., SHARMA, S. K.: Electrochemica Acta **10,** (1965) 151
[3] GUPTA, S. L., SHARMA, S. K., SONI, R. N.: Electrochimica Acta **10,** (1965) 549
[4] GUPTA, S. L., SONI, R. N.: Electrochimica Acta, **14,** (1969) 1313
[5] SHARMA, S. K.: Kolloid-Z-u-Z Polymere **233,** (1969) 962
[6] SHARMA, S. K.: La Nuova Chimica (Italy) (under publication) 1974

S. K. SHARMA; Department of Chemistry, Birla Institute of Technology and Science, Pilani (Rajasthan) India.

Acta Chimica Academiae Scientiarum Hungaricae, Tomus 83 (2), pp. 201—204 (1974)

CARBOHYDRATE METHYL ETHERS, VII*

SYNTHESIS OF QUINOVOSE METHYL ETHERS. REACTION OF PARTIALLY SUBSTITUTED PHENYL-4,6-O-BENZYLIDENE-β-D-GLUCOPYRANOSIDES WITH N-BROMOSUCCINIMIDE

L. KISS, A. LIPTÁK and P. NÁNÁSI

(Biochemical Institute, L. Kossuth University, Debrecen)

Received December 20, 1973

The synthesis of 6-deoxy-2,3-di-O-methyl-D-glucose (2,3-di-O-methyl-D-quinovose) (**5**) and 6-deoxy-2,3,4-tri-O-methyl-D-glucose (2,3,4-tri-O-methyl-D-quinovose) (**11**) is reported. The starting material was phenyl-4,6-O-benzylidene-2,3-di-O-methyl-β-D-glucopyranoside, which was converted into the 6-bromo-6-deoxy derivative with N-bromosuccinimide (NBS), using HANESSIAN's method [1]. The bromine was eliminated by $LiAlH_4$ and, after the acid hydrolysis of the phenylquinovoside derivative, **5** was isolated. Phenyl-β-D-quinovoside, being well known [2], was methylated according to KUHN *et al.* [3] and thus **10** was prepared. Compound **4** was converted by methylation into this product, too. This gives the proof of the structures of two compounds, **5** and **11**.

2,3-Di-O-methyl- and 2,3,4-tri-O-methyl-D-quinovose have been isolated as the sugar components of heterosides from several natural sources [4], [5]. The structures of these compounds were elucidated by instrumental methods (NMR, IR, and mass spectrometry), but their syntheses have not yet been accomplished. This synthetic work has now been achieved in our laboratory. These compounds are also useful in investigating the activity of emulsin and in the structural investigation of naturally occurring heterosides.

The reaction routes are summarized in Table I.

Phenyl-4,6-O-benzylidene-β-D-glucopyranoside (**1**) was methylated to 2 according to KUHN *et al.* [3]. Treatment of **2** with NBS in boiling carbon tetrachloride gave **3**, which was debrominated and debenzoylated in abs. ether with $LiAlH_4$ to yield **4**. Hydrolysis of **4** with 0.5*N* sulfuric acid gave **5** as a syrupy, chromatographically pure compound. When **1** was treated with benzoyl chloride in dry pyridine, **6** was obtained. Treatment of **6** with NBS gave **7** which was deacylated according to ZEMPLÉN [6] to give **8**. Methylation of the latter according to KUHN [3] gave **9**, the bromine of which was eliminated with $LiAlH_4$ in abs. ether to obtain **10**. Hydrolysis of this product with 0.5*N* sulfuric acid gave 6-deoxy-2,3,4-tri-O-methyl-D-glucose (**11**) as a crystalline compound.

This compound (**11**) has also been synthesized by a different route. Compound **7** was treated with zinc powder in about 75% acetic acid to give **12**. ZEMPLÉN deacylation [6] of **12** gave **13**, first described by HELFERICH [2]. Methylation of **13** yielded **10**, proving the structure of **10** and **11**, respectively.

* Part VI: NÁNÁSI, P. and LIPTÁK, A.: Magy. Kém. Foly., **80**, 217 (1974).

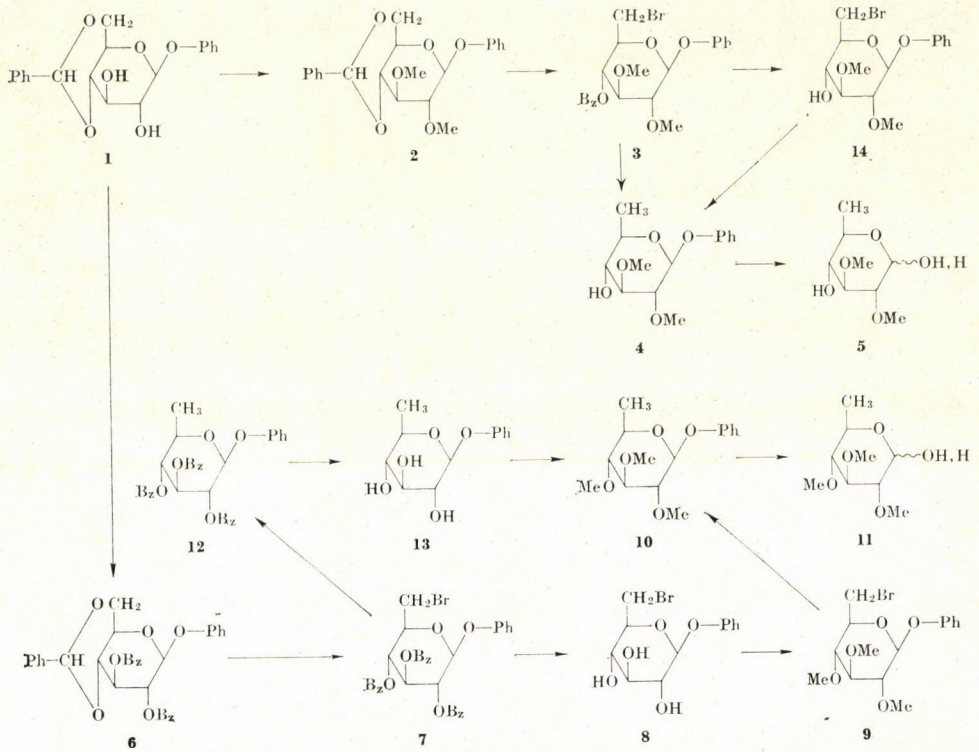

Since **4** can also be converted into **10** by methylation, it also affords evidence for the structures of **4** and **5**.

Experimental

M.p.'s were determined on a Boetius hot-stage apparatus and are uncorrected. TLC was performed on Kieselgel G Merck. Benzene–metanol 9 : 1 was used as the solvent mixture for the glucosides, and ethylmethyl ketone saturated with water for the free quinovose methyl ethers. Detection was made with sulfuric acid–water (1 : 1) and aniline hydrogen phthalate, respectively.

Phenyl-4,6-O-benzylidene-β-D-glucopyranoside (1)

This was synthesized according to McCloskey and Coleman [7].

Phenyl-4,6-O-benzylidene-2,3-di-O-methyl-β-D-glucopyranoside (2)

10 g of **1** was methylated and the mixture worked up in the manner as described by Kuhn [3], to obtain 7.26 g (60%) of **2**, m.p. 179°C; $[\alpha]_D^{25} - 55.8°$ ($c = 2$, chloroform) $C_{21}H_{24}O_6$ (372). Calcd. C 67.72; H 6.5 Found C 67.65; H 6.56.

Phenyl-4,6-O-benzoyl-bromo-6-deoxy-2,3-di-O-methyl-β-D-glucopyranoside (3)

5.57 g (0.015 mole) of **2** was dissolved in warm carbon tetrachloride (130 ml) and barium carbonate (11.84 g; 0.06 mole) and NBS (4 407 g; 0.0247 mole) were added. The reaction mixture was refluxed for 2 hours, then the $BaCO_3$ was removed by filtration and washed with

boiling carbon tetrachloride (10 ml). The filtrate was washed successively with water, saturated $NaHCO_3$ solution, and water, and dried over anhydrous Na_2SO_4. Thd dried solution was evaporated in vacuum to leave a syrup, which was recrystallized from alcohol to yield 5.4 g (80%) of **3**, mp. 122—123°C; $[\alpha]_D^{20}$ —60.7° ($c = 2$, chloroform).

$C_{21}H_{23}O_6Br$ (451). Calcd. C 55.87; H 5.1. Found C 55.6; H 5.3%.

Phenyl-6-deoxy-2,3-di-O-methyl-β-D-glucopyranoside (4)

0.9 g (0.002 mole) of **3** was dissolved in abs. ether (20 ml) and added to a solution of $LiAlH_4$ (1.52 g; 0.04 mole) in abs. ether (25 ml) during 5 min. The reaction mixture was stirred overnight at room temperature, and then refluxed for 2 hours. Ethyl acetate (3 ml) was then added to destroy any excess of $LiAlH_4$. The precipitate was filtered off and washed with acetone (3 × 20 ml). The filtrate was evaporated and the residue extracted with boiling chloroform (3 × 20 ml) .The solution was washed with water, dried and evaporated in vacuum. The crystalline residue was recrystallized from cyclohexane to yield 320 mg (60%) of **4**, mp. 124—126°C; $[\alpha]_D^{25}$ —69.8° ($c = 2$, chloroform).

$C_{14}H_{20}O_5$ (268.3). Calcd. C 62.67; H 7.51. Found C 63.12; H 7.3%.

Phenyl-6-bromo-6-deoxy-2,3-di-O-methyl-β-D-glucopyranoside (14)

450 mg of **3** was saponified according to ZEMPLÉN [6] affording 295 mg of **14**. It was recrystallized from cyclohexane to yield 283 mg (81%) of pure **14**, mp. 98—99°C; $[\alpha]_D^{25}$ —67.7° ($c = 2$, chloroform).

$C_{14}H_{19}O_5Br$ (347.2). Calcd. C 48.43; H 5.51, Found C 49.06; H 5.65%.

Debromination of 14

173.6 mg (5×10^{-4} mole) of **14** was dissolved in abs. ether (5 ml) and added to a solution of $LiAlH_4$ (190 mg) in abs. ether (10 ml) during 5 min. After the usual work-up as above, 82 mg (61%) of **4** was obtained, mp. 124°C; $[\alpha]_D^{25}$ —67.8° ($c = 2$, chloroform). The compound was chromatographically identical with **4**.

$C_{14}H_{20}O_5$ (268.3). Calcd. C 62.67; H 7.51. Found C 63.00; H 7.25%.

6-Deoxy-2,3-di-O-methyl-D-glucose (5)

344 mg of **4** was dissolved in 0.5 *N* sulfuric acid (35 ml) and kept at 90—95°C for 14 hours. The warm solution was neutralized with barium carbonate, filtered, the precipitate was washed with water (2 × 5 ml) and ethyl acetate (2 × 10 ml). The combined filtrate and washings were evaporated. The residue was extracted with ethyl acetate (2 × 10 ml), filtered and evaporated to yield a syrup (230 mg; 93.4%), which was chromatographically pure. $[\alpha]_D^{25}$ + +61.3° ($c = 2$, water), after mutarotation.

$C_8H_{16}O_5$ (192.2). Calcd. C 71.73; H 8.39. Found C 72.59; H 8.03%.

Phenyl-4,6-O-benzylidene-2,3-di-O-benzoyl-β-D-glucopyranoside (6)

17.2 g of **1** was benzoylated and working up in the usual manner to give **6** 13.7 g; (50%), mp. 212—213°C; $[\alpha]_D^{20}$ —51.5° ($c = 2$, chloroform).

$C_{33}H_{28}O_8$ (551.47). Calcd. C 71.73; H 5.11. Found C 72.59; H 5.35%.

Phenyl-2,3,4-tri-O-benzoyl-6-bromo-6-deoxy-β-D-glucopyranoside (7)

6.6 g (0.012 mole) of **6** was dissolved in a mixture of abs. carbon tetrachloride (300 ml) and abs. benzene (120 ml); then barium carbonate (4.8 g; 0.024 mole) and NBS (2.11 g; 0.024 mole) were added to the solution which was refluxed and stirred for 1.5 hours. The warm reaction mixture was filtered, washed successively with water, $NaHCO_3$ solution and water, dried and the solvent evaporated in vacuum. The residue was crystallized from methanol (52 ml). Recrystallization from methanol (68 ml) yielded 5 g (66.3%) of **7**, mp. 152—154°C; $[\alpha]_D^{25}$ —10.5° ($c = 2$, chloroform).

$C_{33}H_{27}O_8Br$ (631.47). Calcd. C 62.66; H 4.30. Found C 63.29; H 4.92%.

Phenyl-6-bromo-6-deoxy-β-D-glucopyranoside (8)

2.53 g (0.004 mole) of **7** was saponified according to ZEMPLÉN [6] to obtain 800 mg (62%) of **8**, mp. 145—146°C; $[\alpha]_D^{25}$ —76.8 ($c = 2$, chloroform).

$C_{12}H_{15}O_5Br$ (319.15). Calcd. C 45.15; H 4.74. Found C 45.18 H 4.78%.

Phenyl-6-bromo-6-deoxy-2,3,4-tri-O-methyl-β-D-glucopyranoside (9)

290 mg of **8** was methylated according to KUHN [3] to give 237 mg (72.2%) of **9** after recrystallization from cyclohexane; mp. 108°C; $[\alpha]_D^{25}$ —50.6° ($c = 2$, chloroform).

$C_{15}H_{21}O_5Br$ (361.24). Calcd. C 49.86; H 5.82. Found C 50.34; H 6.16%.

Phenyl-6-deoxy-2,3,4-tri-O-methyl-β-D-glucopyranoside (10)

108 mg (3×10^{-4} mole) of **9** was debrominated with $LiAlH_4$ (29 mg; 6×10^{-4} mole) in abs. ether (13 ml). The usual work-up gave 54.8 mg (65%) of **10**, 72—73°C; $[\alpha]_D^{25}$ —49.7° ($c = 2$, chloroform).

$C_{15}H_{22}O_5$ (282.34). Calcd. C 63.81; H 7.85. Found C 63.5; H 7.35%.

6-Deoxy-2,3,4-tri-O-methyl-D-glucose (11)

200 mg of **10** was dissolved in 0.5 *N* sulfuric acid (25 ml) and kept at 90—95°C for 18 hrs. After the usual work-up, the solvent was evaporated and the residue extracted with chloroform and evaporated again. The crystalline residue was recrystallized from cyclohexane (10 ml) to yield 140 mg (93.3%) of the product, mp. 64—67°C; $[\alpha]_D^{25}$ +48.2° ($c = 2$, water) (lit. $[\alpha]_D^{25}$ +49.2° ($c = 1.2$, water).

$C_9H_{18}O_5$ (206.24). Calcd. C 52.41; H 8.79. Found C 52.83; H 8.84%.

REFERENCES

[1] HANESSIAN, S.: Carbohydrate Res. **2**, 86 (1966)
[2] HELFERICH, B., ROHR, H., GÜNTHER, E.: Z. physiol. Chem. **221**, 90 (1933)
[3] KUHN, R., TRISCHMANN, H., LÖW, I.: Angew. Chem. **67**, 32 (1955)
[4] ALLGEIER, K., WEISS, EH., REICHSTEIN, T.: Helv. Chim. Acta **50**, 456 (1967)
[5] RIPPERGER, H., SCHREIBER, K.: Ber. **101**, 2450 (1968)
[6] ZEMPLÉN, G.: Ber. **59**, 1254 1926
[7] MCCLOSKEY, C. M., COLEMAN, G. H.: J. Org. Chem. **10**, 184 (1945)

László KISS
András LIPTÁK
Pál NÁNÁSI
H 4010 Debrecen POB 20, Hungary.

Acta Chimica Academiae Scientiarum Hungaricae, Tomus 83 (2), pp. 205—207 (1974)

CYCLOADDITION REACTIONS OF CEPHALOSPORIN COMPOUNDS, II
A STUDY ON 1-OXIDIZED 3-CEPHEMS AND PYRAZOLINO-CEPHAMS

(PRELIMINARY COMMUNICATION)

E. T. GUNDA, J. Cs. JÁSZBERÉNYI and E. R. FARKAS
(Institute of Organic Chemistry, L. Kossuth University, Debrecen)

Received April 17, 1974

The interaction of 3-methyl-cephem derivatives with diazomethane has already been described in our previous report [1]. In order to obtain more detailed information about the steric course of this reaction, we investigated the effect caused by the higher oxidation state of the sulfur atom.

The pyrazolino-cepham derivative **II** was oxidized by 1.1 eq. of *m*-chloroperbenzoic acid. The reaction products were separated by column chromatography on silicagel. The first compound eluted proved to be a small amount (~5%) of **V**, [m.p. 208—9 °C (d.); IR(KBr) 1788, 1527, 1268, 1060 cm^{-1}; NMR (d_6-DMSO, TMS)δ = 0.91(s, 3H), 3.58, 3.90 (ABq, 2H, J = 15 Hz), 4.69(s, 2H), 5.38(d, 1H), 5.05, 5.08(ABq, 2H, J = 18.5 Hz), 5.61(s, 2H), 6.01 (dd, 1H), 6.98—8.22(aromatic), 8.83(d, 1H); MS m/e 529 (M-28)]. The next compounds were the corresponding (*S*)- and (*R*)-sulfoxides, **III** and **IV**. **III** m.p. 186—7.5 °C (d.); IR (KBr) 1776, 1530, 1240, 1060 cm^{-1}; NMR (d_6-DMSO, TMS)δ = 0.81(s, 3H), 2.93, 3.87(ABq, 2H, J = 16 Hz), 4.65(s, 2H), 5.27 (d, 1H), 4.86, 5.54(ABq, 2H, J = 18.5 Hz), 5.55(s, 2H), 5.98(dd, 1H), 6.92—8.31(aromatic + NH); MS m/e 513 (M-28)] and **IV** [m.p. 146—7 °C (d.); IR (KBr) 1783, 1530, 1270, 1040 cm^{-1}; NMR (d_6-DMSO, TMS)δ = 1.17 (s, 3H), 3.02(s, 2H), 4.62(s, 2H), 4.53, 4.92(ABq, 2H, J = 18 Hz), 4.75(d, 1H), 5.51(s, 2H), 5.61(dd, 2H), 6.94—8.32(aromatic), 9.22(d, 1H); MS m/e 513 (M-28)].

Subsequent oxidation of **III** and **IV** with *m*-chloroperbenzoic acid or *p*-nitroperbenzoic acid yielded **V**. The preparation of this compound (**V**) was also possible by the addition of diazomethane to **VI**. Direct oxidation of **II** with 2.5 eq. of *m*-chloroperbenzoic acid is an alternative route to **V**.

Another possibility might have been the formation of **IX** or a mixture of **V** and **IX**. In the case of α,β-unsaturated sulfones the C-atom of the diazo

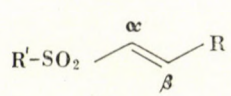

a

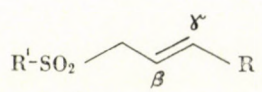

b

compound becomes attached to the β-position [2, 3] (*a*, R=H, alkyl). If in *a* R represents an electron-attracting substituent, *e.g.* phenyl, the directive effect of this group competes with that of the sulfone group, thus the formation of both the α- and β-adducts can be observed [3].

Obviously, in case of the allylsulfones (case *b*) the effect of group R is predominant, and the new C—C bond forms between the diazo C-atom and the β-C-atom of the unsaturated partner. Indeed, this is supported by the structure of the compounds obtained in the reaction of diazomethane and 5-phenyl-2*H*-thiopyrane-1.1-dioxide [4] and 2*H*-thiopyrane-1.1-dioxide [5], as well as by the directive effect of acrylic acid derivatives [6].

Diazomethane converts compound **VIII** into **IV**. After having prepared the (*S*)-sulfoxide **VII** by known methods, we could transform it to **III** neither in CH_2Cl_2/ether solution [1], because of solubility difficulties, nor in THF or DMSO/ether mixture. The stereospecific oxidation of **I** to **VIII** was carried out using N,N-dichlorourethane (DCU) [7, 8]. V-cephalosporin *p*-nitrobenzyl ester dissolved in a minimum amount of dry CH_2Cl_2 was allowed to react with an equimol. amount of DCU at room temperature for 3 min. Extraction work-up gave the (*R*)-oxide in a high yield. This compound is identical with the minor component of the paracidic oxidation of the parent compound.

The described facts show that any combination of the cycloaddition and oxidation steps gives rise to the formation of the same compound, **V** [9].

Further, we aimed at explaining the direction of the dipolarophilic attack. In the cycloaddition the β-side of the 3-cephem molecule is preferred, although the lactam moiety makes the interaction of diazomethane and the 3-double-bond on the β-side difficult; the ring strain of the α-face adduct would be stronger than that of the β-face adduct. This is supported by the fact that the chemical shift of one of the methylene protons of the pyrazoline ring is highly influenced by the S—βO bond in **III**, whereas in the (*R*)-oxide **IV** the effect of the diamagnetic anisotropy of the S||||αO bond cannot be noticed. On the other hand, the well-known "reagent approach control" caused by the 7-NH group [10] does not work so efficiently as in the peracidic oxidation process of **I**, since the rate of formation of **IV** and **III** [*i.e.* the (*R*)- and (*S*)-sulfoxides] is approximately 2 : 3 instead of the usual 5 : 95 ratio.

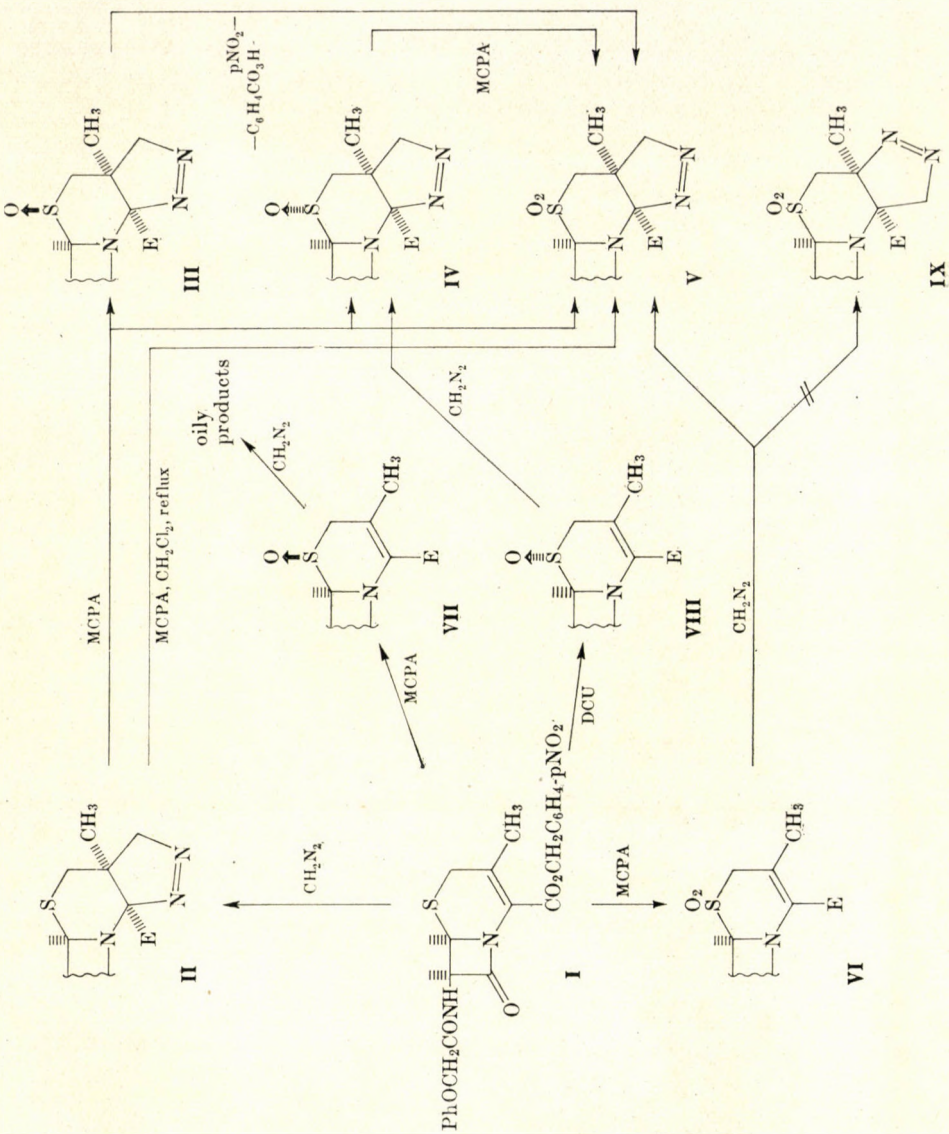
PhOCH2CONH
CO2CH2C6H4-pNO2
I
II
III
IV
V
VI
VII
VIII
IX
MCPA
MCPA, CH2Cl2, reflux
CH2N2
DCU
oily products
pNO2—C6H4CO3H

FOOTNOTES AND REFERENCES

[1] FARKAS, E. R., GUNDA, E. T., JÁSZBERÉNYI, J. Cs.: Tetrahedron Letters **1973,** 5127
[2] HELDER, R., DOORNBOS, T., STRATING, J., ZWANENBURG, B.: Tetrahedron **29,** 1375 (1973); PARHAM, W. E., BLAKE, F. D., THEISSEN, D. R.: J. Org. Chem. **27,** 2415 (1962)
[3] VAN AUKEN, T. V., RINEHART, K. L., Jr.: J. Am. Chem. Soc. **84,** 3736 (1962)
[4] BRADAMANTE, S., MAIORANA, S., MANGIA, A., PAGANI, G.: Tetrahedron Letters **1969,** 2921
[5] See Ref. [14] in our Ref. [4]
[6] ANDREWS, S. D., DAY, A. C., MCDONALD, A. N.: J. Chem. Soc. (C) **1969,** 787 and refs. cited therein
[7] BOUGAULT, J., CHABRIER, P.: Compt. rend. **213,** 310 (1941)
[8] OCHIAI, N., AKI, O., MORIMOTO, A., OKADA, T.: Tetrahedron Letters **1972,** 3241
[9] According to mass spectral data, azoxy derivatives do not form in the reaction
[10] COOPER, R. D. G., DEMARCO, P. V., CHENG, S. C., JONES, N. D.: J. Am. Chem. Soc **91,** 1408 (1969)

E. T. GUNDA
J. Cs. JÁSZBERÉNYI
E. R. FARKAS

L. Kossuth University, 4010 Debrecen, P.O.B. 33. Hungary
Present address: Technical University of Denmark, Dept. Org. Chem., DK–2800 Lyngby, Denmark.

Acta Chimica Academiae Scientiarum Hungaricae, Tomus 83 (2), pp. 209—215 (1974)

SYNTHESIS OF PYRANS, PYRONES AND PYRIDONES BY MICHAEL CONDENSATION WITH CINNAMALACETOPHENONE

A. SAMMOUR, A. RAOUF, M. ELKASABY, M. ABDALLA and M. A. HASSAN

(Chemistry Department, Faculty of Science, Ain Shams University, Abbassia, Cairo, Egypt)

Received August 9, 1973; in revised form February 4, 1974

The Michael reaction of cinnamalacetophenones with deoxybenzoin, malonamides, ethyl phenylacetate, diethyl malonate, ethyl cyanoacetate and malononitrile has been investigated. Some new pyrans, pyrones and pyridones have been obtained directly or by the action of acids or alkalies on the intermediate Michael adducts.

The Michael reaction of I with deoxybenzoin gave 1,2-diphenyl-5-aryl-3-styryl-1,5-pentanediones (**II**). Cyclization of II takes place on the action of a mixture of acetic acid and *p*-toluene-sulfonic acid to give 2,3-diphenyl-4-styryl-6-aryl-(4*H*)-pyrans (**III**).

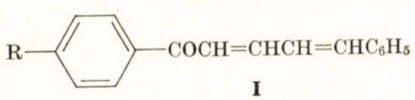

I

a, R = H
b, R = Cl

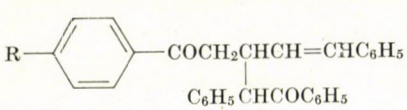

II

a, R = H
b, R = Cl

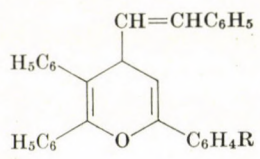

III

a, R = H
b, R = 4-Cl

Cinnamalacetophenone **I** were allowed to react with malonamide or malonanilide [1] to obtain 2-[α-phenacylcinnamyl] malonamides (**IVa** and **b**) and 2-[α-phenacylcinnamyl]malonanilides (**IVc** and d). Treatment of **IV** with alcoholic alkali gave two products: 3,4-dihydro-2-imino-4-styryl-6-aryl-2*H*-pyran-3-carboxamides (**V**) and 1,2,3,4-tetrahydro-2-oxo-4-styryl-6-aryl-nicotinic acids (**VI**).

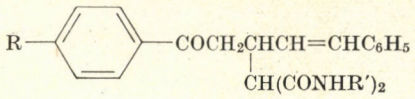

IV

a, R = R′ = H
b, R = Cl, R′ = H
c, R = H, R′ = C_6H_5
d, R = Cl, R′ = C_6H_5

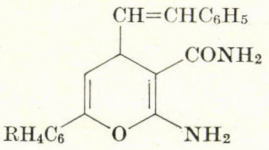

V

a, R = H
b, R = 4-Cl

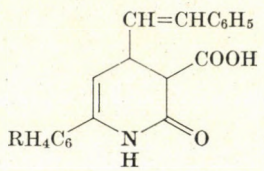

VI

a, R = H
b, R = 4-Cl

Treatment of **IVa** and **c** with a mixture of acetic acid and hydrochloric acid gave 3,4-dihydro-4-styryl-6-phenyl-2*H*-pyran-2-one-3-carboxylic acid (**VII**).

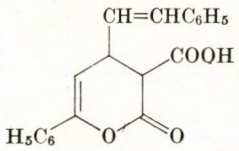

VII

It has been reported [2] that ethyl phenylacetate adds to benzalacetophenone in the presence of sodium ethoxide to give the normal Michael adduct. In the present investigation, the base-catalyzed reaction of ethyl phenylacetate with **I** leads to the formation of 3,4-dihydro-3-phenyl-4-styryl-6-phenyl (or *p*-chlorophenyl)-2*H*-pyran-2-ones (**VIII**). On the basis of steric considerations, the reaction proceeds *via* the stable conformation of the intermediate.

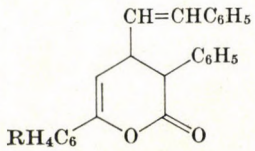

VIII

a, R = H
b, R = 4-Cl

The same compound (**VIII**) was obtained *via* the reaction of **I** with benzyl cyanide and treatment of the intermediate adduct **IX** with alcoholic potassium hydroxide.

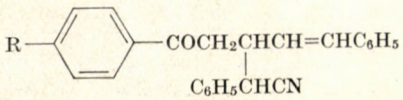

IX

a, R = H
b, R = Cl

The base-catalyzed cycloaddition of diethyl malonate to **I** giving 3,4-dihydro-4-styryl-6-aryl-2*H*-pyran-2-ones (**X**) proceeds *via* the more stable conformation of the intermediate adduct.

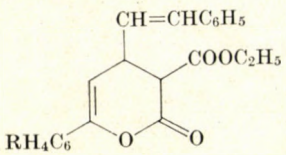

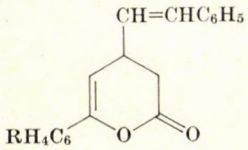

X

a, R = H
b, R = 4-Cl

The same compound (**X**) was obtained by the reaction of **I** with ethyl cyanoacetate in the presence of sodium methoxide.

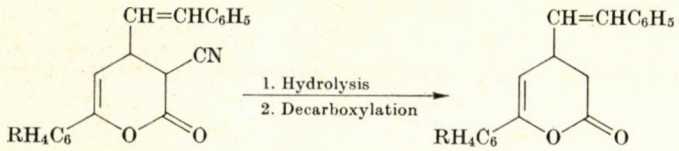

X

The base-catalyzed cycloaddition of malononitrile to **Ia** in the presence of sodium methoxide gave 3,4-dihydro-2-imino-4-styryl-6-phenyl-2*H*-pyran-3-carbonitrile (**XI**).

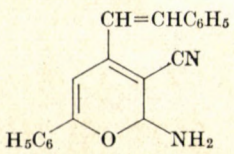

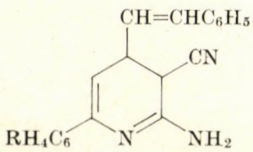

XI **XII**

On the other hand, the reaction of malononitrile and **I** in the presence of ammonium acetate at 170°C effected the formation of a mixture of two products: 2-amino-3,4-dihydro-4-styryl-6-aryl-nicotinonitriles (**XII**) and 2-amino-4-styryl-6-aryl-nicotinonitriles (**XIII**). The 1,2- or 1,4-dihydro derivatives of **XII** cannot be excluded.

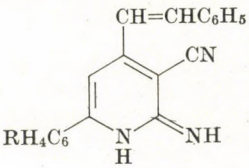

imino

XIII

The IR spectral data of the products are shown in Table I.

Table I

IR spectra (KBr), cm^{-1}

Compd.	ν C=O, open chain	ν C=O amide I	ν C=O, carboxyl	ν C=O, cyclic	ν C=C	ν C≡N	ν C=N	ν NH and OH
II	1680 1650	—	—	—	1608	—	—	—
III	—	—	—	—	1585	—	—	—
IV	1690	1665	—	—	1605	—	—	3200 and 3400
V	—	1660	1705	—	1605	—	—	3350 and 3145
VI	—	1670	—	—	1605, 1590	—	1625	3200
VII	—	—	1705	1670 (α-pyrone)	1605, 1585	—	—	3320 (chelated)
VIII	—	—	—	1665 (α-pyrone)	1600	—	—	—
IX	1688	—	—	—	1606	2248	—	—
X	—	—	—	1670 (α-pyrone)	1606, 1590	—	—	—
XI	—	—	—	—	1608, 1587	2220	1630 ketimine	1400
XII	—	—	—	—	1608	2220	1635 ketimine	3400
XIII	—	—	—	—	1608	2220	1635 ketimine	3400

Table II

Michael adducts with cinnamalacetophenones

Compound	M. p., °C	Solvent of crystn.	Yield, %	Formula (Mol. wt.)	Analysis, % Calcd./Found		
					C	H	N
IIa	248	X	86	$C_{31}H_{26}O_2$	86.5	6.1	—
				(430.5)	86.2	6.2	
IIb	255	B	78	$C_{31}H_{25}ClO$	80.0	5.4	—
				(465.0)	80.2	5.4	—
IVa	219	E	92	$C_{20}H_{20}N_2O_3$	71.4	6.0	8.3
				(336.4)	71.3	6.0	8.1
IVb	186	E	62	$C_{20}H_{19}ClN_2O_3$	64.7	5.1	7.5
				(370.9)	64.5	5.0	7.2
IVc	211	E	96	$C_{32}H_{28}N_2O_3$	78.7	5.8	5.7
				(488.6)	78.3	5.7	5.5
IVd	193	E	85	$C_{32}H_{27}ClN_2O_3$	73.4	5.2	5.4
				(523.1)	73.2	5.1	5.3
VIIIa	156	$P^{100-120}$	68	$C_{25}H_{20}O_2$	85.2	5.7	—
				(352.4)	84.9	5.8	—
VIIIb	145	$P^{100-120}$	42	$C_{25}H_{19}ClO_2$	77.6	4.9	—
				(386.9)	77.6	4.9	—
IXa	141	E	88	$C_{25}H_{21}NO$	85.4	6.0	4.0
				(351.4)	85.5	6.1	4.1
IXb	136	E	68	$C_{25}H_{20}ClNO$	77.7	5.2	3.6
				(385.9)	77.5	5.3	3.9
Xa	161	$B-P^{40-60}$	82	$C_{19}H_{16}O_2$	82.6	5.8	—
				(276.3)	82.8	5.6	—
Xb	123	$B-P^{40-60}$	68	$C_{19}H_{15}ClO_2$	73.3	4.8	—
				(310.8)	73.5	4.6	—
XIa	168	E	38	$C_{20}H_{16}N_2O$	80.0	5.4	9.3
				(300.3)	79.7	5.6	9.5
XIb	135	E	30	$C_{20}H_{15}ClN_2O$	71.7	4.5	8.4
				(334.8)	71.3	4.6	8.2
XIIa	155	E	18	$C_{20}H_{17}N_3$	80.5	6.3	5.2
				(299.4)	80.7	6.2	5.0
XIIb	165	E	15	$C_{20}H_{16}ClN_3$	71.9	4.8	12.3
				(333.9)	71.8	4.7	12.4
XIIIa	248	B	23	$C_{20}H_{15}N_3$	80.8	5.1	14.1
				(297.3)	81.0	5.2	13.9
XIIIb	240	B	19	$C_{20}H_{14}ClN_3$	72.3	4.2	12.1
				(331.8)	72.1	4.3	12.4

X = xylene; E = benzene;
E = ethanol; P = light petrol.

Experimental

The IR spectra were determined with a Unicam SP 1200 Spectrometer using the KBr pellet technique. All m.p.'s are uncorrected.

Michael reactions with cinnamalacetophenones (I)

(A) A solution of **I** (0.01 mole) and deoxybenzoin, malonamide, malonanilide, ethyl phenylacetate, benzyl cyanide, diethyl malonate, ethyl cyanoacetate or malononitrile (0.015 mole) in dry methanol (50 ml) was treated with sodium methoxide (prepared from 0.75 g of sodium and 5 ml of absolute methanol). The reaction mixture was refluxed for 4 hrs, then cooled and the solid product was crystallized from a suitable solvent (*cf.* Table II).

(B) A mixture of **I** (0.01 mole), malononitrile (0.015 mole) and ammonium acetate (0.1 mole) was heated for 8 hrs at 140—160 °C. After cooling, the reaction product was triturated with hot ethanol and the solid that separated was fractionally extracted with ethanol to give **XII**; the residue ethanol extraction was crystallized to give **XIII**.

Table III

2,3-Dyphenyl-4-styryl-6-phenyl or chlorophenyl-4H-pyrans **III** *and 3,4-dihydro-4-styryl-6-phenyl-2H-pyran-2-one-3-carboxylic acid* **VII**

Compound	M. p., °C	Yield, %	Formula Mol. wt.	Analysis, % Calcd. / Found	
				C	H
IIIa	231	48	$C_{31}H_{24}O$	90.3	5.9
			(412.5)	90.5	5.6
IIIb	220	30	$C_{31}H_{23}ClO$	83.0	5.1
			(447.0)	83.3	5.0
VII	178	38	$C_{20}H_{16}O_4$	75.0	5.0
			(320)	74.5	5.2

Table IV

Action of alkali on **IV**

Compound	M. p., °C	Solvent of crystn.	Yield, %	Formula Mol. wt.	Analysis, % Calcd. / Found		
					C	H	N
Va	234	Ac	28	$C_{20}H_{18}N_2O_2$	75.5	5.7	8.8
				(318.4)	75.2	5.8	8.6
Vb	268	Ac	38	$C_{20}H_{17}ClN_2O_2$	67.9	4.8	7.9
				(352.9)	67.6	4.9	8.2
VIa	228	E—B	38	$C_{20}H_{17}NO_3$	75.2	5.4	4.4
				(319.3)	75.1	5.4	4.6
VIb	245	E—B	42	$C_{20}H_{16}ClNO_3$	67.8	4.5	4.0
				(353.8)	67.6	4.3	4.2

Ac = acetic acid; E = ethanol; B = benzene.

Ring closure of II and IV

A solution of **IIa** and **b** or **IVa** and **c** 0.01 mole was prepared in a mixture glacial acetic and hydrochloric acid or acetic acid and *p*-toluenesulfonic acid 50 : 10 ml and the solution was heated under reflux for 72 hr; water was then added to the hot solution till turbidity appeared. The solid product which separated was filtered off and recrystallized from acetic acid to give **IIIa** and **b** or **VII**, as pale yellow crystals; *cf.* Table III.

Action of alkali on IV or IX

IV or **IX** 0.5 g was heated with 20% alcoholic potassium hydroxide 50 ml for 4 hrs. After the addition of 40 ml water to the reaction mixture, the solid which separated was filtered off and crystallized from the proper solvent to give, **V, VI,** and **VIII**, respectively; *cf.* Table IV.

REFERENCES

[1] Sammour, A., Selim, M. I. B., Abd Elhaim, M. S.: Egypt. J. Chem. **15,** 23 (1972)
[2] Connor, R., Andrews, D. B.: J. Am. Chem. Soc. **56,** 2713 (1934)
[3] Bellamy, L. J.: "The Infrared Spectra of Complex Molecules", Methuen and Co. Ltd., London 1967

A. Sammour
A. Raouf
M. Elkasaby
M. Abdalla
M. A. Hassan

Chemistry Department, Faculty of Science, Ain Shams University Abbassia, Cairo, Egypt.

Acta Chimica Academiae Scientiarum Hungaricae, Tomus 83 (2), pp. 217—222 (1974)

SYNTHÈSES DE POLYACYLSEMICARBAZIDES

E. COMANIȚĂ, M. TUTOVEANU, M. VÂȚĂ et A. SAVIN
(Institut Polytechnique, Jassy, Roumanie)

Reçu le 25 octobre 1973

Les hydrazides des acides *m*- et *p*-phénylènedioxydiacétiques se prêtent aux additions nucléophiles aux groupes C=N des diisocyanates. On obtient ainsi des polymères de type acyl-semicarbazidique. On a utilisé comme esters diisocyaniques hexaméthylènediisocyanate, dibenzyldiisocyanate, et toluylènediisocyanate. On a confirmé la structure de polyacylsemicarbazides par les spectres IR qui présentent des bandes caractéristiques. Indications sur le degré de polymérisation ont été obtenus déterminant la viscosité intrinsèque des polymères. On a trouvé des valeurs comprises entre 15,5—49 ml/g. Les données de l'analyse thermogravimétrique attestent que les polymères sont stables jusqu'à leur point de fusion.

L'utilisation des isocyanates comme produit de départ dans la synthèse de certains polymères homo- et hétérocaténaires a fait l'objet de nombreuses études. On a décrit les réactions de l'homopolymérisation des isocyanates [1—5], ainsi que la polycondensation des diisocyanates [6, 7], auxquelles s'ajoutent les réactions de polyaddition de certains composés polyfonctionnels à atomes d'hydrogène mobiles sur la liaison C=N. Cette dernière méthode a servi à préparer certains produits macromoléculaires de type polyurétanique et polyuréique de propriétés intéressantes pour leurs applications techniques [8, 9].

Parmi les groupes fonctionnels susceptibles de s'additionner à la liaison polaire C=N des isocyanates se trouvent les hydrazides des acides carboxyliques. Les hydrazides, bien que moins basiques que les amines, se prêtent aux additions nucléophiles au groupe C=N et cette réaction a été largement étudiée sur de petites molécules [10—15]. Finalement cette intéressante réaction a été appliquée aux composés bifonctionnels (dihydrazides et diisocyanates). On a préparé ainsi des polymères de type polyacylsemicarbazidique à radicaux aliphatiques et arylaliphatiques sur la chaîne macromoléculaire [16—20].

Discussion

Le présent travail se propose d'étendre la gamme de polymères acylsemicarbazidiques, de connaître leurs propriétés et en plus, d'étudier les possibilités d'applications. Les polymères synthétisés se différencient de ceux obtenus déjà dans notre laboratoire par l'hydrazide utilisée dans la réaction de

polyaddition. Il s'agit d'une hydrazide récemment synthétisée [21], celle de l'acide *p*-phénylène-dioxydiacétique et de son isomère *meta*-substitué que nous avons préparée selon [22]. La structure allongée ainsi que la réactivité du groupe NH_2 terminal de ces dihydrazides nous a suggéré l'idée de les faire réagir avec des diisocyanates pour aboutir aux polymères linéaires à radical aryl alternant avec des unités aliphatiques. Les hétéroatomes O et N présents dans la chaîne macromoléculaire permettent à ces liaisons une rotation libre, ce qui contribue à la flexibilité de la chaîne. En même temps, les groupes —CO—NH— favorisent la formation des liaisons d'hydrogène intermoléculaires ce qui pourrait améliorer les propriétés thermiques de ces polymères.

La série de polymères synthétisés présente des modifications de structure distinctes dues au radical introduit par l'ester isocyanique. On a utilisé les isocyanates suivants : hexaméthylènediisocyanate (HMDI), toluylènediisocyanate (TDI), et dibenzyldiisocyanate (DBDI) qui par addition des hydrazides *m*- et *p*-phénylènedioxydiacétiques ont conduit aux polyacylsemicarbazides (PASC) suivants.

$$NH_2-NH-CO-CH_2-O-C_6H_4-O-CH_2-CO-NH-NH_2 +$$
$$+ O=C=N-R-N=C=O \rightarrow$$
$$[NH-CO-NH-NH-CO-CH_2-O-C_6H_4-O-CH_2-CO-NH-NH-$$
$$- CO-NH-R-]_n \qquad R: -CH_2-(CH_2)_4-CH_2-$$

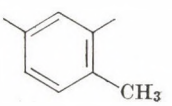

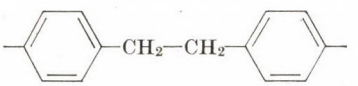

Pour la synthèse on utilise des quantités équivalentes des produits de départ dans DMF comme solvant. Les hydrazides phénylènedioxydiacétiques y sont partiellement solubles. A mesure que la réaction s'avance, le milieu devient homogène et on constate finalement la séparation du polymère. Par addition de l'eau, le PASC de la structure indiquée plus haut se précipite sous forme des fibres. Après séchage et pulvérisation on obtient une poudre blanche, insoluble dans la majorité des solvants organiques. Les points de fusion sont compris entre 190—300 °C. Les valeurs les plus élevées ont été observés chez les produits préparés avec DBDI. La purification par lavages à l'eau chaude ou par dissolution dans DMSO et la précipitation par l'eau n'ont pas donné en tous les cas de résultats. Les analyses centésimales pour l'azote indiquent parfois un taux en N moins élevé que celui calculé ce qui peut être expliqué en partie par la rétention de solvant par le polymère. Néanmoins les spectres IR confirment la structure donnée de PASC, comme nous le verrons plus loin.

Afin d'obtenir le degré de polymérisation on a déterminé les valeurs de la viscosité intrinsèque à la température de 25°C. Les concentrations des solutions a été 0,1—0,5 g/100 ml DMSO dans lesquelles on fait dissoudre par agitation de longue durée les polymères finement moulus. On a trouvé les valeurs de la viscosité intrinsèque comprises entre 15 et 45 ml/g.

Le tableau suivant contient les constantes physiques caractérisant les PASC synthétisées.

Tableau I

Les PASC obtenus des dihydrazides p- et m-phénylènedioxydiacétique

Nr.	Substances de départ		Point de fusion	Viscosité intrinsèque ml/g
	Hydrazide	Diisocyanate		
I	*p*-phénylènedioxydiacétique	HMDI	220	37,00
II	*p*-phénylènedioxydiacétique	TDI	241	15,50
III	*p*-phénylènedioxydiacétique	DBDI	300	49,00
IV	*m*-phénylènedioxydiacétique	HMDI	210	45,00
V	*m*-phénylènedioxydiacétique	TDI	190	23,50
VI	*m*-phénylènedioxydiacétique	DBDI	280	18,50

On constate que l'indice de viscosité est plus élevé dans les polymères obtenus des hydrazides *p*- et *m*-phénylènedioxydiacétiques et HMDI ainsi que de l'hydrazide *p*-substituée et de DBDI.

Dans le but de confirmer la structure de PASC on a fait appel aux spectres d'absorption en IR. L'identification des bandes a été effectuée par comparaison avec une substance modèle à petite molécule 1,1-[*p*-phénylènedioxydiacétyl]-bis-(4-phénylsemicarbazide) (**VII**). Dans le spectre de ce composé apparaît distinctement une série de vibrations caratéristiques aux éléments structuraux présents dans la molécule. On retrouve les mêmes bandes d'absorptions dans les spectres des polymères où on peut remarquer en général la tendance des pics à se confondre en plus larges bandes, c'est ce qu'on peut observer dans la figure 1.

Afin de pouvoir mieux suivre la structure des polymères, on a groupé dans le tableau ci-dessous les bandes considérées les plus représentatives:
La bande amide **I** apparaît constante dans tous les produits avec deux maximums d'absorption dus aux vibrations νC=O des groupes CO—NH et NH—CO—NH. Les bandes amide **II** et **III** présentent des nombres d'onde moins élevés, respectivement dans les intervalles 1475—1600 et 1200—1300 cm^{-1}, sont difficilement localisables à cause de la présence d'autres absorptions dans le même domaine. Dans le cas du polymère préparé avec HMDI (**I**) on observe une intensité accrue de la bande correspondante a νC—H aliphatique de 2960 cm^{-1}. De même, les absorptions caractéristiques de N–H apparaissant

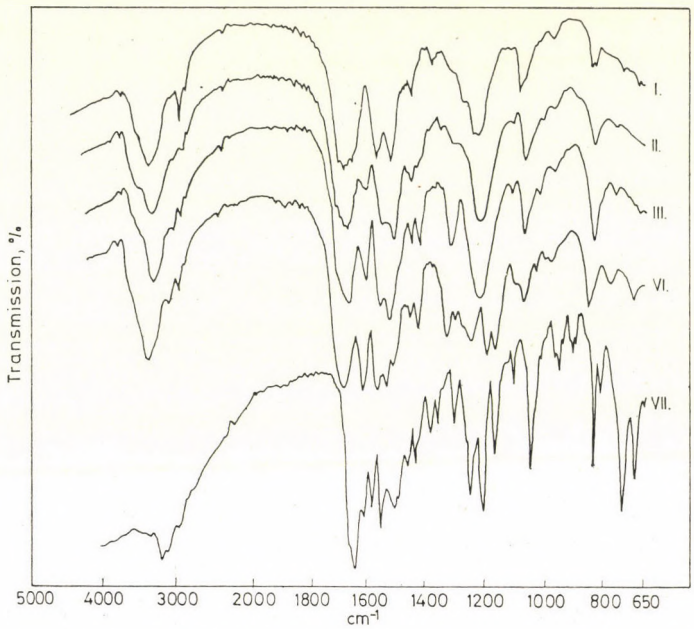

Fig. 1. Spectres IR des polymères I, II, III, VI et de la substance modèle VII

Tableau II

Bandes caractéristiques présentes dans les spectres IR des polymères

Absorptions	Polymères				Substance modèle
	I	II	III	IV	
νC=O (amide I)	1660; 1680	1660; 1675	1660	1680	1640; 1660
νC=C	1630	1610	1605	1620	1605
νC—O—C	1088	1078	1078	1080	1055
νN—H	3360	3310	3300	3350	3200; 3340
νC—H arom.		3050	3050	3100	3100
νC—H aliph.	2960	2870; 2930	2860; 2950	2900; 2980	3030
benzène *p*-subst.	845	840	840	—	840

dans l'intervalle 3200—3360 cm^{-1} sont spécifiques à la structure des PASC. Dans leur proche voisinage, entre 3050 et 3100 cm^{-1} se trouvent les absorptions des liaisons C–H aromatiques. D'autres caractéristiques des vibrations se trouvent dans le tableau précédant.

Il nous a semblé intéressant d'envisager le comportement des polymères dans l'analyse thermique. On a étudié la stabilité des PASC **II, III** et **VI** enregistrant des courbes thermogravimétriques par le Dérivatographe de type PAULIK F., PAULIK I., ERDEY L., MOM Budapest dans l'intervalle de tempéra-

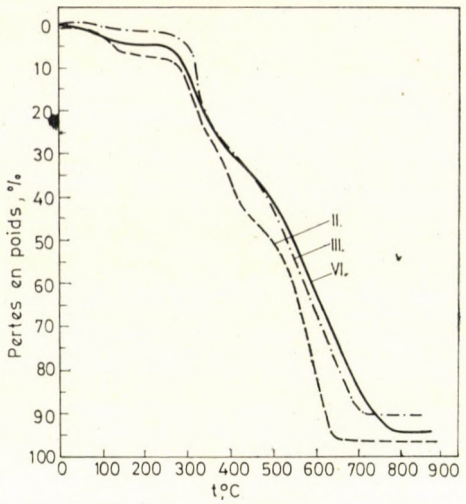

Fig. 2. Courbes thermogravimétriques des polymères II, III et VI

ture de 20—900°C. Les enregistrements ont été effectués en présence de l'air à une vitesse de chauffage de 9,8°C minute. En examinant les données de l'analyse thermogravimétrique (voir la figure 2), on constate que les PASC préparées des hydrazides *m*- et *p*-phénylènedioxydiacétiques se comportent d'une manière semblable.

Jusqu'au point de fusion la perte de poids est faible et due à l'élimination du solvant retenu par le polymère. Elle s'accentue jusqu' au dessus de la température de fusion. Selon certains auteurs [23] dans ces conditions la décomposition caractéristique des acylsemicarbazides a lieu avec dégagement d'eau, d'aniline, etc., et il se forme ainsien partie de cycles triazoliques. Les pertes atteignent 50% dans l'intervalle de 460—500°C.

Partie expérimentales

On décrit dans ce qui suit la synthèse de deux polymères isomères obtenus en partant des hydrazides des acides *p*- et *m*-phénylènedioxydiacétiques et MHDI. Utilisant de TDI et de DBDI les conditions de travail sont identiques.

Poly-(1,1'p-phénylènedioxydiacétyl-4,4'-hexaméthylène)-semicarbazide (I)

Une suspension de 2 g hydrazide *p*-phénylènedioxydiacétique dans 75 ml DMF anhydre est chauffée au bain-marie pour être partiellement dissoute. On ajoute 1,46 g MHDI, et continue le chauffage pendant deux heures. On obtient le polymère par précipitation dans l'eau.

Poly-(1,1-m-phénylènedioxydiacétyl-4,4'hexaméthylène)-semicarbazide (IV)

A la suspension de 2 g hydrazide *m*-phénylènedioxydiacétique dans 60 ml DMF on ajoute 1,46 g HMDI. Après chauffage de deux heures au bain-marie et agitation intermittente on obtient une solution visqueuse, de laquelle le polymère se sépare sous forme de gel. On peut le filtrer ou le précipiter par eau.

BIBLIOGRAPHIE

[1] NATTA, G., DI PIETRO, J., CAMBINI, M.: Makromol. Chem., **56,** 200 (1962)
[2] SCHNEIDER, N. S., FURUSAKI, S.: J. Polymer Sci., A **3,** 933 (1965)
[3] SHASHOUA, V. E.: J. Amer. Chem. Soc., **81,** 3156 (1959)
[4] NATTA, G., DI PIETRO j., PREGALIA, G.: Ital. Pat. 678, 634 (1964) C. A. **64,** 8343 (1966)
[5] SOBUE, H., TABATA, Y., HIRAOKA, M., OSHIMA, K.: J. Polymer Sci., C **943,** (1963)
[6] NEUMANN, W., FISCHER, P.: Angew. Chem., **74,** 801 (1962)
[7] CAMPBELL, T. W., MONAGLE, J. J., FOLDI, V. S.: J. Amer. Chem. Soc., **84,** 3673 (1962)
[8] BAYER, O.: Angew. Chem., **59,** 275 (1947)
[9] BAYER, O., RINKE, I.: Ger. Pat. 728, 981, nov. 12, (1942)
[10] BUU HOI, N. P., XUONG, N. D., NAM, N. H.: Comptes rendus (Paris) **238,** 295 (1954)
[11] BUU HOI, N. P., XUONG, N. D., LESCOT, E.: Bull. Soc. chim. France, **24,** 441 (1957)
[12] BUU HOI, N. P. et collab.: Bull. Soc. Chim. France, **23,** 365 (1956)
[13] MATEI, I., COMANIȚĂ, E.: Bul. Inst. Polit. Iași, tom XII (XVI), fasc. 1—2, 189 (1966)
[14] MATEI, I., COMANIȚĂ, E.: Bul. Inst. Polit. Iași, tom XII (XVI), fasc. 3—4, 175 (1966)
[15] TUTOVEANU, M., COMANIȚĂ, E., ANDREI, A.: Bul. Inst. Polit. Iași, tom XVII (XXI), fasc. 3—4, 89 (1971)
[16] CAMPBELL, T. W., FOLDI, V. S., FARAGO, I.: J. Appl. Polymer Sci., **2,** 155 (1959)
[17] CAMPBELL, T. W., TOMIC, E. A.: J. Polymer Sci., **62,** 379 (1962)
[18] TOMIC, E. A., CAMPBELL, T. W., FOLDI, V. S.: J. Polymer Sci., **62,** 387 (1955)
[19] BUDEANU, C.: An. Stiinț. Univ. "Alex. I. Cuza" Iași, sect. I C, 13 (1) 93 (1967)
[20] STILMAN, M. I., FEDOTOVA, O., KOLESNICOV, G.: Vîșokomolek. soed., (A) X, 2, 283 (1968)
[21] LANGE, J., URBANSKI, T.: Diss. Pharm. Pharmacol., 20 (6) 589 (1968)
[22] TUTOVEANU, M., COMANIȚĂ, E.: Compt. rend. acad. bulgare sci., tome 26, 3, 375 (1973)
[23] DYMEK, W., DZIEWONKA, M.: Diss. Pharm. Pharmacol., 13, 313 (1961)

Eugenia COMANIȚĂ
Maria TUTOVEANU
M. VÂȚĂ
Alex. SAVIN

Institut Polytechnique, Jassy, Roumanie.

INDEX

Printed in Hungary

A kiadásért felel az Akadémiai Kiadó igazgatója — Műszaki szerkesztő: Zacsik Annamária

A kézirat nyomdába érkezett: 1974. VII. 18. Terjedelem: 9,8 (A/5) ív, 63 ábra

74.691 Akadémiai Nyomda — Felelős vezető: Bernát György

ACTA CHIMICA

ТОМ 83—ВЫП. 2

РЕЗЮМЕ

Диэлектрические свойства и полимеризация аллилового спирта, I

Диэлектрические свойства мономерного аллилового спирта

Я. ЛИСИ и Ж. ХАРТЯНИ

Была определена комплексная относительная перметивность в зависимости от температуры и частоты. Для описания результатов было использовано уравнение Коль—Давидсона. Была рассчитана энтальпия активации диэлектрической релаксации, которая затем сравнивалась с энергией вязкости. Путем сравнения данных аллилового спирта и 1-пропанола было показано, что двойная связь не оказывает значительного влияния на изученные свойства.

Диэелектрические свойства и полимеризация аллилового спирта, II

Влияние полимеризации на диэлектрические свойства жидкой фазы

Я. ЛИСИ и Ж. ХАРТЯНИ

Был получен жидкофазный полиаллиловый спирт с молекулярным весом, равным приблизительно 400. Была определена комплексная относительная перметивность продукта полимеризации в зависимости от температуры и частоты, а также зависимость вязкости от температуры. Диэлектрические данные и величины вязкости указывают на то, что полимеризация в значительной степени изменяет свойства аллилового спирта. Согласно результатам, эффект полимеризации сказывается в появлении новой области релаксаций.

Влияние добавок благородных металлов на поведение активных и неактивных носителей при каталитическом гидрировании в водной фазе

Дь. ВЕРТЕШ, Дь. ХОРАНИ и Дь. КИШ

Было исследовано влияние платины и палладия на поведение различных носителей катализаторов при каталитическом гидрировании в водной фазе.

Была измерена скорость реакции гидрирования двух модельных соединений — п-интрофенола и малеиновой кислоты — используя в качестве носителей окись алюминия, трехокись вольфрама, активный углерод, карбиды тантала и вольфрама, а в качестве катализаторов палладий и водород-вольфрамовую бронзу без благородного металла.

В противоположность литературным данным, согласно нашим исследованиям и окись вольфрама нельзя считать активным носителем.

Было установлено, что без благородных металлов водород-вольфрамовая бронза не способна к молекулярной активации водорода.

Карбид вольфрама, содержащий одну тысячную долю благородного металла, может быть с успехом использован в качестве катализатора при гидрировании ненасыщенных соединений.

Изучение ионизации металлов и восстановления ионов металлов с помощью вращающегося дискового электрода с кольцом, X

Л. КИШ и Й. ФАРКАШ

Была выведена зависимость $\frac{I}{I_h} - f^{-1/2}$ (где I — сила тока на вращающемся дисковом электроде, I_h — предельный ток промежуточного продукта на кольцевом электроде, f — число оборотов электрода) для того случая, когда при анодном растворении металла происходят следующие процессы:

$$M \rightleftarrows M^{z_1^+} + z_1 e\,;\; M^{z_1^+} \rightleftarrows M^{z_2^+} + (z_2 - z_1)\, e\,;\; M \rightleftarrows M^{z_2^+} + z_2 e\,.$$

Было определено, в каких случаях полученную зависимость можно использовать для выяснения механизма процесса.

Стереохимические исследования, XIX

Циклические аминоспирты и их производные, XI

Исследование *цис*- и *транс*-2-гидроксиметилциклогексиламинов с помощью ЯМР спектроскопии

Ж. ВАЙНА-МЕХЕШФАЛЬВИ, Г. БЕРНАТ и П. ШОХАР

На основе исследования ЯМР спектров N-ацил-производных *цис*- и *транс*-2-гидроксиметилциклогексиламинов были получены сведения относительно структуры переходного состояния реакции ацильной миграции N → O. Были определены наиболее возможные конформации бициклического переходного состояния *транс*- и *цис*-изомеров. Исходные диэкваториальные конформации в транс-изомерах остаются незатронутыми при протонировании, в то время как циклогексановое кольцо *цис*- изомера присутствует, вероятно, в скрученной форме, в которой ациламидная и гидроксиметильная группы вынуждены занимать квази-экваториальное расположение.

Изучение анодного растворения меди в уксуснокислых растворах, II

Влияние ионов хлорида

Л. КИШ и Л. М. ВАРШАНИ

Было изучено анодное растворение меди в растворах LiCl в безводной уксусной кислоте. Установлено, что медь окисляется только до одновалентного состояния, а перенапряжения перехода и диффузии соизмеримы. В результате анодного растворения образуются комплексы $CuCl_2^-$. Был рассчитан коэффициент переноса анодного процесса $\alpha = 0{,}65 \pm 0{,}05$.

Радиолиз алкенов, II

Легкие углеводородные продукты радиолиза некоторых нормальных и циклических алкенов

Дь. ЧЕРЕП и Г. ФЕЛЬДИАК

Нормальные и циклические алкены, с различными размерами молекул, подвергались γ-облучению Co^{60} в жидкой фазе. На основе выхода фрагментов C_3—C_5 было сделано заключение о том, что первичное разложение молекулы — несмотря на высокую первичную энергию — протекает чаще по тем связям молекулы, которые ослаблены вследствие какого-либо влияния. Так, у алкенов энергия диссоциации σ-связи, находящейся в β-положении к π-связи, является наименьшей, вследствие стремления к делокализации валентных электронов π-связи; однако, на состав продуктов реакции оказывает влияние также конец цепи или неспаренный электрон свободного радикала, а также энергия напряжения.

Радиолиз алкенов, III

Легкие углеводородные продукты радиолиза некоторых разветвленных алифатических алкенов и циклических алкенов с заместителями

Дь. ЧЕРЕП и Г. ФЕЛЬДИАК

Были облучены γ-излучением 60 Co разветвленные алифатические алкены и циклические алкены с боковыми заместителями. На основе выхода образующихся легких углеводородов было заключено, что в случае изученных углеводородов важное значение в вероятности разрыва связей имеют третичные углероды и присоединяющиеся к ним связи. Это ослабляющее влияние третичных углеродных атомов в отдельных случаях является конкурирующим с влиянием связи, находящейся в β-положении к π-связи, а в других случаях складывается с последним. Состав продуктов зависит также от природы конца цепи и от вторичных реакций.

Метиловые эфиры углеводов, VII

Синтез метиловых эфиров квиновозы Взаимодействие 4,6-O-бензилиден-β-*D*-глюкопиранозидов с N-бромсукцинимидом

Л. КИШ, А. ЛИПТАК и П. НАНАШИ

Был осуществлен синтез G-дезокси-2,3-ди-O-метил-D-глюкозы (2,3-ди-O-метил-D-квиновозы) (5) и 6-дезокси-2,3-4-три-O-метил-D-глюкозы (2,3,4-три-O-метил-D-квиновозы) (11). Исходным продуктом был 4,6-O-бензилиден-2,3-ди-O-метил-0-D-глюкопиранозид, который, согласно методу Ханессиана [1], взаимодействуя с N-бромсукцинимидом, превращается в 6-бром-6-дезокси-производное. Бром был удален с помощью $LiAlH_4$, и полученный фенил квиновозид под действием кислого гидролиза был превращен в соединение 5. Хорошо известный фенил-β-D-глюкопиранозид [2] был метилирован согласно Куну [3], давая при этом соединение 10. Метилирование соединения 4 приводило к тому же самому продукту. Оба соединения являются доказательством структуры соединений 5 и 10.

Синтез пиранов, пиронов и пиридонов с помощью конденсации Михаэля с циннамальацетофеноном

А. САМУР, А. РАОУФ, М. ЭЛЬКАСАБАЙ и М. А. ХАССАН

Была исследована реакция Михаэля циннамальацетофенона с дезоксибензоином, малонамидом, этил фенилацетатом, диэтил малонатом, этил цианоацетатом и малононитрилом. Некоторые новые пираны, пироны и пиридоны были получены непосредственно или действием кислот или щелочей на промежуточные аддукты Михаэля.

Синтез полиацилсемикарбазидов

Э. КОМАНИТА, М. ТУТОВЕАНУ, М. ВАТА и А. САВИН

Гидразиды м- и п-фенилендиоксидиуксусных кислот обнаруживают способность к нуклеофильному присоединению к группе C = N диизоцианатов, давая при этом полимеры ацилсемикарбазидного типа. HMDI, DBDI, и TDI были использованы в качестве диизоцианатных эфиров. Структура PASC определялась на основе его ИК спектра с характерными полосами. Определение характеристической вязкости, значения которой находятся в интервале 15,5÷49 мл/г, позволяет судить о степени полимеризации. Данные термодифференциального анализа указывают на то, что полимер стабилен вплоть до его точки плавления.

ABSORPTION SPECTRA IN THE ULTRAVIOLET AND VISIBLE REGION

Series edited by L. LÁNG

According to international book reviews, this series is highly useful in both structure research and chemical analysis. This applies especially to problems of analytical character or structure determination encountered in the pharmaceutical, dye and other industries, i.e. in organic chemical industry in general. A great advantage of this collection is that the spectra published may, in many cases, directly be used for solving the particular problems in question.

The series dealing with *ultraviolet and visible spectra* was started by the Publishing House of the Hungarian Academy of Sciences in 1959, and by now the project has got as far as Vol. 18. The editors invite the users of the collection to contribute to the success of this work by submitting for publication spectra of new compounds.

Each volume contains about 400 pages spectra graphs and tables of about 190 compounds + indexes.

Cumulative index: I–V, VI–X, X–XV

AKADÉMIAI KIADÓ
Budapest

ACADEMIC PRESS
New York

The whole series is a co-edition, – distributed on the American Continent by ACADEMIC PRESS, New York, in all other countries by KULTURA, H-1389 Budapest, P. O. B. 149

JOURNAL OF RADIOANALYTICAL CHEMISTRY

International journal dealing with all aspects of nuclear analytical methods

Journal of Radioanalytical Chemistry has an international Editorial Board, whose members are distinguished specialists from all parts of the world – from Moscow to San Diego, from Prague to Tokyo.

The main subjects covered are:

Activation analysis
Radiometric analysis
Radioreagent analysis
Radiometric titration
Isotope dilution analysis
Beta, gamma, X-ray and neutron absorption and backscattering
Analytical separations involving radionuclides
Instrumentation and automation for radioanalytical chemistry

Journal of Radioanalytical Chemistry provides the reader with important and up-to-date information on research being carried out all over the world. Data and Bibliography Sections and a section entitled Laboratory of the Issue help to serve this purpose.

Journal of Radioanalytical Chemistry appears generally in three or four volumes per year of some 480 to 500 pages each, published in several issues in English, French or German. Size: 17 × 25 cm. Subscription rate per volume: US $32.00

Journal of Radioanalytical Chemistry is published jointly by

AKADÉMIAI KIADÓ
Budapest

ELSEVIER SEQUOIA S. A.
Lausanne

JOURNAL OF THERMAL ANALYSIS

An international forum for communications on thermal investigations

Journal of THERMAL ANALYSIS has an international Editorial Board, the members of which are distinguished specialists from all over the world.

AIMS AND SCOPE

The main subjects covered are: thermogravimetry, derivative thermogravimetry, differential thermal analysis, dilatometry, differential scanning calorimetry, thermometry, evolved gas detection, evolved gas analysis, multiple techniques and miscellaneous thermal methods (including the thermal method with various instrumental techniques), instrumentation for the thermal method. Papers dealing with these subjects are published in the following sections: Original Research Papers, Short Communications, Special Reviews, Bibliography Section, Modern Instruments. The Special Reviews section is reserved for papers that have been published in greater detail in some journal for a special branch of scientific field or industry.

Papers submitted to the journal may deal with any field of chemistry, metallurgy or mineralogy, e.g. they may deal with inorganic, organic or polymeric materials and they may cover biochemical, mineralogical or metallurgical applications.

Journal of THERMAL ANALYSIS is published bimonthly comprising about 720 pages per year. Size: 17×25 cm. Subscription rate per volume: US $32.00

Journal of THERMAL ANALYSIS is published jointly by

AKADÉMIAI KIADÓ
Budapest

HEYDEN & SON LIMITED
London

ACTA ALIMENTARIA

ACADEMIAE SCIENTIARUM HUNGARICAE

publishes original papers in the field of food science and technology (physico-chemistry, chemistry, analysis, biology, microbiology, enzymology, engineering, automation and economics related to fundamental principles of the production, preparation, preservation, packaging and examination of foods) in English.

Contributions to ACTA ALIMENTARIA are regularly abstracted or indexed in all reference journals.

ACTA ALIMENTARIA is as a rule a quarterly. Four issues make up a volume of some 400 to 500 pages yearly.
Subscription rate per volume: US $32.00

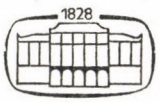

AKADÉMIAI KIADÓ
Publishing House of the
Hungarian Academy of Sciences
BUDAPEST

AKADÉMIAI KIADÓ, H-1363 Budapest P.O.B. 24

☐ Please enter my/our subscription for ACTA ALIMENTARIA for one volume

☐ Please enter a standing order for ACTA ALIMENTARIA, beginning with

DATE . . . . . .

☐ Please send a specimen-copy free of charge

NAME . . . . . .

ADDRESS . . . . . .

The Acta Chimica publish papers on chemistry, in English, German, French and Russian.

The Acta Chimica appear in volumes consisting of four parts of varying size, 4 volumes being published a year.

Manuscripts should be addressed to

Acta Chimica
Budapest 112/91 Műegyetem

Correspondence with the editors should be sent to the same address.

The rate of subscription is $ 32.00 a volume.

Orders may be placed with "*Kultúra*" Foreign Trade Company for Books and Newspapers (1389 Budapest 62, P. O. B. 149. Account No. 218 10990) or with representatives abroad.

Les Acta Chimica paraissent en français, allemand, anglais et russe et publient des mémoires du domaine des sciences chimiques.

Les Acta Chimica sont publiés sous forme de fascicules. Quatre fascicules seront réunis en un volume (4 volumes par an).

On est prié d'envoyer les manuscrits destinés à la rédaction à l'adresse suivante:

Acta Chimica
Budapest 112/91 Műegyetem

Toute correspondance doit être envoyée à cette même adresse.

Le prix de l'abonnement est de $ 32.00 par volume.

On peut s'abonner à l'Entreprise pour le Commerce Extérieur de Livres et Journaux «*Kultúra*» (1389 Budapest 62, P. O. B. 149. Compte-courant No. 218 10990) ou à l'étranger chez tous les représentants ou dépositaires.

«*Acta Chimica*» издают трактаты из области химической науки на русском, французском, английском и немецком языках.

«*Acta Chimica*» выходят отдельными выпусками разного объема. 4 выпуска составляют один том. 4 тома публикуются в год.

Предназначенные для публикации рукописи следует направлять по адресу:

Acta Chimica
Budapest 112/91 Műegyetem

По этому же адресу направлять всякую корреспонденцию для редакции.

Подписная цена — $ 32.00 за том.

Заказы принимает предприятие по внешней торговле книг и газет «*Kultúra*» (1389 Budapest 62, P. O. B. 149. Текущий счет № 218 10990) или его заграничные представительства и уполноченные.

Reviews of the Hungarian Academy of Sciences are obtainable at the following addresses:

ALBANIA
Drejtorija Qändrone e Pärhapjes
dhe Propagandimit tä Librit
Kruga Konferenca e Päzes
Tirana

AUSTRALIA
A. Keesing
Box 4886, GPO
Sydney

AUSTRIA
GLOBUS
Höchstädtplatz 3
A-1200 Wien XX

BELGIUM
Office International de Librairie
30, Avenue Marnix
Bruxelles 5
Du Monde Entier
162. rue du Midi
1000 Bruxelles

BULGARIA
HEMUS
11 pl Slaveikov
Sofia

CANADA
Pannonia Books
2, Spadina Road
Toronto, 4. Ont.

CHINA
Waiwen Shudian
Peking
P. O. B. 88

CZECHOSLOVAKIA
Artia
Ve Smečkách 30
Praha 2
Poštovní Novinivá Služba
Dovaz tisku
Vinohradská 46
Praha 2
Mad'arské Kultura
Václavské nám. 2
Praha 1
SLOVART A. G.
Gorkého
Bratislava

DENMARK
Ejnar Munksgaard
Nörregade 6
Copenhagen

FINLAND
Akateeminen Kirjakauppa
Keskuskatu 2
Helsinki

FRANCE
Office International de Documentation
et Librairie
48, rue Gay-Lussac
Paris 5

GERMAN DEMOCRATIC REPUBLIC
Deutscher Buch-Export und Import
Leninstraße 16
Leipzig 701
Zeitungsvertriebsamt
Fruchtstraße 3—4
1004 Berlin

GERMAN FEDERAL REPUBLIC
Kunst und Wissen
Erich Bieber
Postfach 46
7 Stuttgart S.

GREAT BRITAIN
Blackwell's Periodicals
Oxenford House
Magdalen Street
Oxford
Collet's Subscription Import
Department
Dennington Estate
Wellingsborough, Northants.
Robert Maxwell and Co. Ltd.
4—5 Fitzroy Square
London W. 1.

HOLLAND
Swetz and Zeitlinger
Keizersgracht 471—487
Amsterdam C.
Martinus Nijhof
Lange Voorhout 9
The Hague

NDIA
Hind Book House
66 Babar Road
New Delhi 1

ITALY
Santo Vanasia
Via M. Macchi 71
Milano
Libreria Commissionaria Sansoni
Via La Marmora 45
Firenze
Techna
Via Cesi 16.
40135 Bologna

JAPAN
Kinokuniya Book-Store Co. Ltd.
826 Tsunohazu 1-chome
Shinjuku-ku
Tokyo
Maruzen and Co. Ltd.
P. O. Box 605
Tokyo-Central

KOREA
Chulpanmul
Phenjan

NORWAY
Tanum-Cammermeyer
Karl Johansgt 41—43
Oslo 1

POLAND
Ruch
ul. Wronia 23
Warszawa

ROUMANIA
Cartimex
Str. Aristide Briand 14—18
Bucureşti

SOVIET UNION
Mezhdunarodnaya Kniga
Moscow G—200

SWEDEN
Almquist and Wiksell
Gamla Brogatan 26
S—101 20 Stockholm

USA
F. W. Faxon Co. Inc.
15 Southwest Park
Westwood Mass. 02090
Stechert Hafner Inc.
31. East 10th Street
New York, N. Y. 10003

VIETNAM
Xunhasaba
19, Tran Quoc Toan
Hanoi

YUGOSLAVIA
Forum
Vojvode Mišića broj
Novi Sad
Jugoslavenska Knjiga
Terazije 27
Beograd

ACTA CHIMICA

ACADEMIAE SCIENTIARUM HUNGARICAE

TOMUS 83 FASCICULI 3—4

AKADÉMIAI KIADÓ, BUDAPEST

1974

ACTA CHIM. (BUDAPEST) ACASA 2 83 (3—4) 223—435 (1974)

ACTA CHIMICA

A MAGYAR TUDOMÁNYOS AKADÉMIA KÉMIAI TUDOMÁNYOK OSZTÁLYÁNAK IDEGEN NYELVŰ KÖZLEMÉNYEI

Az Acta Chimica német, angol, francia és orosz nyelven közöl értekezéseket a kémiai tudományok köréből.

Az Acta Chimica változó terjedelmű füzetekben jelenik meg, egy-egy kötet négy füzetből áll. Évente átlag négy kötet jelenik meg.

A közlésre szánt kéziratok a szerkesztőség címére (Budapest 112/91 Műegyetem) küldendők.

Ugyanerre a címre küldendő minden szerkesztőségi levelezés. A szerkesztőség kéziratokat nem ad vissza.

Megrendelhető a belföld számára az „Akadémiai Kiadó"-nál (1363 Budapest Pf 24. Bankszámla 215 11488), a külföld számára pedig a „Kultúra" Könyv- és Hírlap Külkereskedelmi Vállalatnál (1389 Budapest 62, P. O. B. 149. Bankszámla: 218 10990) vagy annak külföldi képviseleteinél és bizományosainál.

Die Acta Chimica veröffentlichen Abhandlungen aus dem Bereich der chemischen Wissenschaften in deutscher, englischer, französischer und russischer Sprache.

Die Acta Chimica erscheinen in Heften wechselnden Umfanges. Vier Hefte bilden einen Band. Jährlich erscheinen 4 Bände.

Die zur Veröffentlichung bestimmten Manuskripte sind an folgende Adresse zu senden:

Acta Chimica
Budapest 112/91 Műegyetem

An die gleiche Anschrift ist auch jede für die Redaktion bestimmte Korrespondenz zu richten. Abonnementspreis pro Band: $ 32.00.

Bestellbar bei dem Buch- und Zeitungs-Außenhandels-Unternehmen »*Kultúra*« (1389 Budapest 62, P. O. B. 149 Bankkonto Nr. 218 10990) oder bei seinen Auslandsvertretungen und Kommissionären.

Acta Chimica Academiae Scientiarum Hungaricae, Tomus 83 (3—4), pp. 223—228 (1974)

DETERMINATION OF PHOSPHORUS IN SILICATE ROCKS BY ACTIVATION ANALYSIS

S. O. KHALIL

(Department of Geology, Faculty of Science, Alexandria University, Egypt)

Received November 25, 1973

A neutron activation method for the determination of phosphorus as silver thallium(I) phosphate (Ag_2TlPO_4) from ammonium phosphomolybdate precipitate is applied to silicate rocks.

Ammonium phosphate is added as carrier to the irradiated rock powder and the phosphorus recovered as ammonium phosphomolybdate, which is precipitated several times in the presence of appropriate holdback carriers to ensure its radiochemical purity and then finally dissolved and reprecipitated as silver thallium(I) phosphate (Ag_2TlPO_4) for weighing and counting.

Introduction

On irradiation with thermal neutrons ^{31}P undergoes the ^{31}P (n, γ) ^{32}P reaction, the thermal neutron cross-section of which is 0.19 barns. ^{32}P decays by β-emission only, the particles having a maximum energy of 1.707 Mev, with a half-life of 14.3 days.

Ammonium phosphomolybdate was chosen by VINCENT and CURREN [1] as a weighing form. This compound, for a variety of reasons is not very suitable for a final weighing or counting form for phosphorus: it has an uncertain composition, it is hygroscopic, and the precipitate self-absorps the β-particles of ^{32}P, except in very thin layers.

HENDERSON [2] used an initial zirconium phosphate precipitation as a weighing form. The choice of a final weighing form is difficult as many phosphorus compounds have an uncertain stoichiometry (*e.g.* ammonium phosphomolybdate), or are difficult to plate out (*e.g.* magnesium phosphate).

SPACU and DIMA [3], prepared a new compound of phosphorus: silver thallium (I) phosphate (Ag_2TlPO_4). This compound has a definite composition and can be dried and weighed as such after being brought to any temperatures between 20°C and 720°C [4]. Some further experiments were performed by the author in order to ascertain whether self-absorption of ^{32}P β-particles would be a serious drawback to the use of Ag_2TlPO_4 as a weighing form for phosphorus in radioactivation analysis, for which purpose it seems otherwise to be well suited. SPACU and DIMA [3] prepared the new phosphate compound from disodium hydrogen phosphate solution, while in this present work the

main problem is to prepare silver thallium (I) phosphate (Ag_2TlPO_4) from ammonium phosphomolybdate precipitate.

Anhydrous potassium dihydrogen phosphate was chosen as an irradiation standard, since it is obtainable in very pure form and is commonly used. The "Analar" salt was found to contain no elements which would interfere in the procedure.

Method

Preparation of samples and standards and irradiation

Weigh 100 mg rock powder (sample) into short polyethylene tubing and seal the open ends. Similarly, weigh accurately and seal 100 mg "Analar" disodium hydrogen phosphate (standard) and a similar weight of "Analar" potassium sulphate (monitor for the $^{32}S \rightarrow {}^{32}P$ reaction). Pack sample, standard and monitor in a standard Harwell aluminium irradiation can, and irradiate in the thermal column of BEPO for 3 1/2 days in a thermal flux of 2×10^{10} neutrons/cm^2/sec.

Reagents:

(a) Ammonium molybdate; dissolve 100 g "Analar" ammonium molybdate in 700 ml distilled water and pour into 300 ml concentrated nitric acid. A clear solution should result. The reagent should be freshly prepared in every 2 or 3 days and kept in a polyethylene bottle.
(b) Ammonium nitrate solution: 50 per cent w/v.
(c) Ammonia solution, "Analar"; S.G. 0.88—0.90.
(d) Nitric acid, "Analar": Concentrated.
(e) Ethyl alcohol, absolute.
(f) Phosphate carrier solution: dissolve 0.7027 g "Analar" diammonium phosphate in distilled water and make up to 500 ml. Five ml of this solution is equivalent to 100.0 mg of ammonium phosphomolybdate (1.65 per cent P).
(g) Holdback carrier solution: prepare a solution containing about 1 mg per ml of each of the following metals, in the form of chloride or nitrate: Al, Ba, Ca, Cr, Ni, Co, Cu, Fe, Mg, Mn, K, Na and Zn.
(h) 0.1 *N* $AgNO_3$: dissolve 8.4960 g of "Analar" $AgNO_3$ in 500 ml distilled water after drying at 110°C for 2 hours (keep in a dark bottle).
(i) 4% thallium(I) acetate (TlOAc) in water: dissolve 4 g of thallium(I) acetate in distilled water.
(j) 3% thallium(I) acetate in alcohol: dissolve 3 g of thallium(I) acetate in 95% ethyl alcohol.
(k) 10% acetic acid v/v.
(l) Sodium acetate salt.
(m) Ethyl alcohol.

Treatment of irradiated samples

A. Precipitation of phosphorus as ammonium phosphomolybdate:

Allow the irradiated samples to cool for a few days until the radioactivity has decayed to a safe working level. Taking the usual precautions, and working behind a lead shield, transfer the rock powders to teflon vessels, and add to each 5 ml of the ammonium phosphate carrier using a pipette filler. Add 10 ml conc. HNO_3 and then 10 ml 40% HF. Evaporate carefully to dryness on a sand bath, cool, add 5 ml HNO_3 and repeat the evaporation. In the same way evaporate repeatedly with conc. HNO_3. Cool, add to the residue 5 ml HNO_3 and 10 ml water, warm until the dissolution is as complete as possible.

Pour the hot solution into a centrifuge tube containing 5 ml of 50% ammonium nitrate solution, 5 ml of ammonium molybdate reagent and 2 ml of the holdback carrier solution. Allow the tube to stand for 30—45 minutes in a beaker containing hot water, until all phosshorus has been precipitated as ammonium phosphomolybdate, centrifuge and discard the dawhings. From this stage onwards, activity in the samples is reduced to tracer level.

Redissolve the precipitate in the centrifuge tube in a few drops of strong ammonia solution, add 5 ml ammonium nitrate solution and 2 ml of the holdback carrier solution; then 5 ml conc. HNO_3 and 5 ml of the ammonium molybdate reagent to precipitate the phosphorus. In the absence of foreign ions the precipitation is now generally complete within a few minutes. Centrifuge and wash the precipitate as before, redissolve and reprecipitate twice more in the presence of holdback carrier solution, and wash thoroughly with hot water.

B. Separation of molybdenum as thallium(I) molybdate:

Decant the excess water and dissolve the ammonium phosphomolybdate precipitate in the centrifuge tube in a few drops of conc. ammonia solution. Transfer the solution to a conical flask, wash the centrifuge tube carefully with water and pour the washings into the conical flask. Neutralize the solution with 10% acetic acid using phenolphtalein as an indicator.

Add 60 ml 95% ethyl alcohol and warm to 70—80°C (on a water bath). Thallium(I) molybdate is precipitated from the hot solution by adding 25—30 ml 3% thallium(I) acetate in alcohol. The mixture is digested at 60—70°C on a water bath for about one hour until the precipitate completely coagulates. Cool, centrifuge, and decant the supernatant liquid into a clean conical flask for the precipitation of phosphorus as silver thallium(I) phosphate (Ag_2TlPO_4). This solution should be free from molybdenum, and this is easy to check: add a few drops of 3% thallium(I) acetate (TlOAc) reagent to the solution; if a white precipitate is formed, this means that some molybdenum is still in the solution; and the separation procedure should be repeated. If no precipitate is formed the solution is free from molybdenum.

C. Precipitation of phosphorus as silver thallium(I) phosphate:

If the decanted solution from step B is alkaline, neutralize it by adding a few drops of 10% acetic acid. It is important to adjust the pH value of the solution, which should not exceed 9, since it has been found experimentally that thallium(I) phosphate precipitates at pH values higher than 9, while a pH range of 7.5—8.5 seems to offer the best conditions for the precipitation of silver thallium(I) phosphate.

Now, the solution is ready for the precipitation of Ag_2TlPO_4 if SPACU and DIMA's method is to be applied. Add 1 g of sodium acetate as a buffer, warm to dissolve, cool, add a few ml of 10% acetic acid, and then 15 ml of 4% TlOAc in water, followed by 15—20 ml of 0.1 *N* $AgNO_3$ solution, added dropwise from a burette with continuous shaking and keeping the solution away from sunlight. A white precipitate of Ag_2TlPO_4 will be formed. The solution with the Ag_2TlPO_4 precipitate is left on a water-bath for about 30 minutes.

Centrifuge and wash the precipitate several times with an ethyl alcohol–water mixture, and finally with absolute ethyl alcohol. Decant the excess alcohol and transfer the slurry of the precipitate in alcohol with a pipette to a pre-weighed aluminium counting tray. Dry the precipitate under an infrared lamp. Cool and weigh to determine the chemical yield.

Treatment of standards

Open the polyethylene tube containing the irradiated potassium dihydrogen phosphate standard and transfer it quantitatively into a 500 ml volumetric flask. Using a pipette filler, transfer exactly 10 ml of the active solution to a 100 ml volumetric flask, and further dilute to volume. Transfer 5 ml portions of the diluted standard solution to centrifuge tubes, add 5 ml of the ammonium phosphate carrier solution and then precipitate the ammonium phosphomolybdate, separate the molybdenum as thallium(I) molybdate (Tl_2MoO_4). Then precipitate the silver thallium(I) phosphate (Ag_2TlPO_4) and plate out in the same manner as for the samples (two precipitations of the ammonium phosphomolybdate are enough).

Treat the irradiated potassium sulphate monitor similarly, this time adding the phosphate carrier to the solution of the whole sample.

Counting

Count the silver thallium(I) phosphate precipitates from samples and standards for β-activity, using and end-window Geiger–Müller counter. Record the time to accumulate at least 10^4 counts. The total recovery time of the Geiger–Müller tube used may be of the order 300—400 microseconds and depends on the applied voltage. It is therefore usual to impose an

external "paralysis time", greater than the recovery time, by electronic means (in this case, 300 microseconds).

Under these conditions, the observed counting rate C_0 is related to the count rate corrected for paralysis (C) by the equation:

$$C = \frac{C_0}{(1-C_0 T)}$$

where T is the artificially imposed paralysis time in the same units as C. C_0 may therefore be corrected for the lost counts which could have been recorded during the time the counter was paralysed. In the present work, $T = 300$ microseconds.

The natural background was measured immediately before and after a batch of samples was counted, and this value was deduced from the counting rate corrected for paralysis.

Self-absorption

Self-absorption and back-scattering effects of Ag_2TlPO_4 in specimens of different thickness on the counting trays, were studied. This was done by plating out varying weights of an active Ag_2TlPO_4 precipitate on to similar aluminium counting trays, and determining their specific activities, (Table I). A straight line relationship between weight of precipitate and counting rate is obtained, (Fig. 1), which indicates that Ag_2TlPO_4 as a weighing form of phosphorus would be satisfactory, self-absorption and back-scattering effects being negligible.

Table I

Effects of self-absorption and back-scattering of P^{32} in a precipitate of silver thallium phosphate

No. of samples	Time in sec for 10^4 counts	Time in sec for 10^4 counts	Time in sec for 10^4 counts	Mean time in sec	Observed counting rate C°/sec	Count rate corrected for paralysis in sec	Count rate corrected for paralysis in sec	Weights of Ag_2TlPO_4 in mg
1	16.756	16.776	16.735	16.756	596.8	727.0	726.8	21.6
2	67.141	67.806	67.667	67.538	148.1	154.9	154.8	5.2
3	38.913	38.496	38.384	38.597	259.1	280.9	280 8	8.9
4	16.675	16.793	16.821	16.763	596.6	726.6	726.4	21.7
5	13.918	13.900	13.749	13.855	721.8	921.2	921.1	26.8
6	13.191	13.249	13.284	13.241	755.2	976.5	976.3	28.4
7	53.916	54.847	53.919	54.227	184.4	195.2	195.0	6.5
8	66.732	66.273	66.336	66.447	150.5	157.6	157.4	5.2
9	23.461	23.657	24.175	23.764	420.8	481.6	481.4	14.9
10	9.881	9.871	9.810	9.854	1014.8	1459.0	1458.8	42.0

Discussion

The results of triplicate activation analysis for phosphorus in the international rock standards granite G-1 and diabase W-1 are given in Table II, together with values determined by either methods reported in the literature.

Agreement between the radiochemical results for W-1 and those obtained by other methods is fairly satisfactory, while results for G-1 are higher than the neutron activation results obtained by the present work. VINCENT

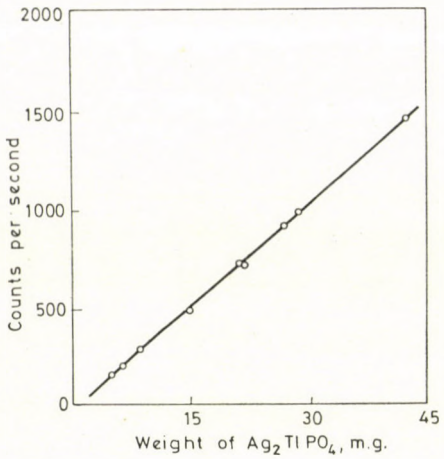

Fig. 1

Table II

Determination of phosphorus in G-1 and W-1

Granite G-1 % P_2O_5	Diabase W-1 % P_2O_5	Method and reference
0.04 (0.04, 0.04, 0.03)	0.11 (0.11, 0.11, 0.12)	Neutron activiation, this work
0.088 (range not quoted)	0.119 (range not quoted)	Neutron activation, [2]
0.076, 0.077, 0.080, 0.080	0.15, 0.14, 0.15, 0.15, 0.14	Neutron activation, [1]
0.10 (range 0.03—0.41)	0.13 (range 0.06—0.24)	Average of 34 analyses, chiefly gravimetric, [5]
0.09 (range not quoted)	0.15 (range not quoted)	Average of 5 spectrophotometric analyses as molybdi-vanado-phosphoric acid, [6]
0.08 (range 0.07—0.08)	0.13 (range 0.12—0.14)	Average of 4 spectrophotometric analyses as molybdenum blue, [7]
0.012 (range not quoted)	0.088 (range not quoted)	Spark source, mass spectrometer, [8]

and CURREN [1] and HENDERSON [2] obtained a higher P_2O_5 (0.08) and (0.088) respectively for G-1 which is about double the value obtained by the present method. Those authors chose ammonium phosphomolybdate and zirconium phosphate as the weighing form of phosphorus, in contrast to the silver thallium (I) phosphate used in the present work.

High results would be expected from the neutron activation method if radiochemical purification of the phosphorus has not been achieved. The formation of the phosphomolybdate complex appears to be hindered by the presence in the solution of large amounts of other elements contributed by the rock sample, while incomplete elimination of silicon during the initial decomposition leads to erroneous results due to the formation of some silicomolybdate.

In the present work, silver thallium (I) phosphate is chosen as the weighing form for phosphorus. In this case, the purification of phosphorus is completely achieved and, in addition, the new compound has a definite composition.

*

The author wishes to thank Dr. J. Esson (Manchester University) for his advices in radiochemical problems. The work was initially encouraged by Prof. E. A. Vincent, who has taken a keen interest in the development of the method. The irradiations were carried out in the Harwell pile BEPO by arrangement with the Isotope Division of the Atomic Energy Research Establishment.

REFERENCES

[1] Vincent, E. A., Curren, W. O.: unpublished results
[2] Henderson, P.: Anal. Chim. Acta **39,** 512 (1967)
[3] Spacu, G., Dima, L.: Z. anal. Chem. **120,** 317 (1940)
[4] Duval, C.: Inorganic Thermogravimetric Analysis. Second and revised edition. Elsevier Publ. Co., Amsterdam—London–New York 1963
[5] Fairbairn, H. W. *et al.:* U. S. Geolog. Surv. Bull. 980 (1951)
[6] Shapiro, L., Brannock, W. W.: U. S. Geol. Surv. Bull. 1036 C (1956)
[7] Riley, J. P.: Anal. Chem. **19,** 413 (1958)
[8] Brown, R., Wolstenholme, W. A.: Nature, London **201,** 598 (1964)
[9] Daly, R. A.: Igneous Rocks and their Origin. New York (1933)

S. O. Khalil; Department of Geology, Faculty of Sciences,
Alexandria University, Alexandria, Egypt.

Acta Chimica Academiae Scientiarum Hungaricae, Tomus 83 (3—4), pp. 229—235 (1974)

SEPARATION OF SMALL QUANTITIES OF PALLADIUM FROM PLATINUM AND IRIDIUM BY HYDROLYTIC PRECIPITATION ON WEAKLY ACIDIC CATION-EXCHANGE RESINS

L. L. KOCHEVA and B. TABAKOVA

(Department of Chemistry, University of Sofia, Bulgaria)

Received March 7, 1974

A method has been suggested for the separation of small quantities of palladium (0.15—1.50 mg) from platinum and iridium. The method is based on the sorption of palladium on the weakly acidic cation-exchange resin Amberlite IRC-84 in sodium form, due to hydrolytic precipitation taking place at room temperature. Under these conditions platinum and iridium remain completely in solution. The palladium sorbed is eluted with 20 ml 2 *M* hydrochloric acid. The method has been applied for the analysis of binary mixtures of palladium and platinum or palladium and iridium.

The sorption mechanism of palladium is also discussed.

It is well known, that in solutions which contain the chloride complexes of platinum metals the substitution reactions of the co-ordinated chlorine atoms with molecules or ions of the solvent proceed with different rates [1]. Among the platinum metals, the complexes of palladium (II) hydrolyze most readily, forming insoluble compounds. The complexes of platinum (IV) hydrolyze more slowly and the products obtained are soluble. The complex chlorides of iridium (IV) and rhodium (III) form likewise slightly soluble compounds on hydrolysis, but these reactions proceed very slowly at room temperature.

BLASIUS and REXIN [2] have shown that palladium is sorbed on weakly acidic cation exchange resins in the sodium form and may in this way be separated from platinum and iridium. The sorption of palladium under these conditions has been explained in terms of hydrolytic precipitation. No numerical data are given in the above cited paper.

The separation by precipitation on ion exchange resins offers certain advantages to the classic precipitation method. The precipitation takes place slowly and when a chromatographic band is formed on the ion exchange column, one could create conditions for a repeated formation and subsequent dissolution of the precipitate which is actually a purification procedure. Furthermore, very small quantities can be precipitated and sorbed on the ion-exchange resin which in the classic way of precipitation would be associated with difficulties.

In the present work we report on our investigations on the behaviour of palladium (II), platinum (IV), rhodium (III) and iridium (IV) chloride complexes towards weakly acidic cation-exchange resins in the sodium form. The sorption mechanism of palladium was elucidated and the influence of various

factors on this process was studied. A method was elaborated for the separation of small quantities of palladium from platinum and iridium which practically enables a complete separation of 0.150—1.50 mg of palladium from platinum and iridium. The method is easy and quick to carry out and the separated elements are obtained in the form of pure hydrochloric acid solutions which facilitates their subsequent determinations.

Experimental

Reagents

Standard solutions of palladium(II), platinum(IV) and rhodium(III) were prepared from $PdCl_2$, p.a., $H_2PtCl_6 \cdot 6H_2O$, p.a. and $RhCl_3 \cdot 3H_2O$, p.a., respectively, by dissolution in 1 *M* hydrochloric acid. The solutions were standardized gravimetrically; palladium with dimethylglyoxime [3], platinum with ammonium chloride [3], and rhodium with 2-mercaptobenzothiazole [4].

A standard iridium solution was prepared from metallic iridium by dissolution in 6*M* hydrochloric acid using alternating current [5].

Weakly acidic cation-exchange resin Amberlite IRC-84 (pK = 5.3) in sodium form.

Strongly acidic cation-exchange resin Dowex 50×8, 50—100 mesh in sodium form.

All reagents were analytically pure.

Ion-exchange columns

In the experiments columns of resin, 15, 20, 25 cm long and 0.8 cm in diameter were used. Before use the resin is converted to the sodium form with 0.5 *M* sodium hydroxide and washed with distilled water until a pH value of 7 is obtained. After preparation of the sodium form, prolonged washing is necessary since NaOH adheres very strongly to the resin.

Determination of the elements

Concentration of the platinum metal solutions was determined photometrically: platinum with stannous chloride, palladium with potassium iodide, rhodium with stannous chloride [6] and iridium by evaporation in presence of high-boiling oxidizing acids [7].

Preliminary work

Experiments to investigate the sorption behaviour of the platinum metals towards cation-exchange resins were carried out in the following manner. The sample was evaporated to dryness in the presence of 20 mg of sodium chloride. The residue was dissolved in 20 ml of hydrochloric acid of a definite concentration and passed through the column at a rate of 0.5 ml/min. The column was washed with 20 ml of hydrochloric acid of the same concentration. The whole volume of the filtrate and the washing liquid was examined for the respective elements.

In order to find the optimal elution conditions, after a definite quantity of palladium had been sorbed, the column was washed with 20 ml 0.1 *M* hydrochloric acid. The eluent solution was passed with the same rate and fractions of 5 ml each were taken in which palladium was determined.

Recommended procedure for separating palladium and platinum from iridium

The solution is placed in a 50 ml beaker and a solution containing 20 mg sodium chloride is added. Then it is evaporated cautiously to dryness under an infrared heater. The dry residue is dissolved in 20 ml 0.1 *M* hydrochloric acid and passed through a 20-cm column with a rate of 0.5 ml/min. The column is washed with 20 ml 0.1 *M* hydrochloric acid. The filtrate is collected in a 50 ml graduated flask and is filled to the mark. In aliquot portion of this solution platinum or iridium is determined. Palladium is eluted with 20 ml 2 *M* hydrochloric acid and in the eluate palladium is determined.

Results and discussion

The experiments for studying the ion-exchange behaviour of the chloride complexes of platinum metals showed that on the weakly acidic cation-exchange resin Amberlite IRC-84 (in the sodium form) palladium is sorbed almost completely, rhodium only partially while platinum and iridium remain completely in the solution. When sorbed, palladium forms a wide, diffuse brown ring which moves slowly when the column is washed. Single grains of the weakly acidic cation-exchange resin, saturated with the palladium solution, when observed under the microscope are brown in colour, with a smooth surface and no precipitate on it. Under the same conditions, however, on the strongly acidic ion-exchange resin Dowex 50, only rhodium is sorbed partially.

When hydrochloric acid solutions of the platinum metals are passed through cation-exchange resins in the sodium form, pH of the solutions becomes higher:

$$\mathrm{RCOONa} + \underset{\mathrm{Cl^-}}{\mathrm{H_3O^+}} = \mathrm{RCOOH} + \underset{\mathrm{Cl^-}}{\mathrm{Na}} + \mathrm{H_2O}$$

$$\mathrm{RSO_3Na} + \underset{\mathrm{Cl^-}}{\mathrm{H_3O^+}} = \mathrm{RSO_3H} + \underset{\mathrm{Cl^-}}{\mathrm{Na^+}} + \mathrm{H_2O}$$

Some of the anion complexes can be transformed as a result of substitution into electroneutral or positively charged complexes. The sorption of palladium on weakly acidic cation-exchange resins could be explained in terms of an exchange reaction between $PdCl^+$ and Na^+ counter-ions of the resin. However, if this retaining mechanism were true, this would involve the sorption of palladium on strongly acidic cation-exchange resins, as well, which we did not observe. The appearance of the chromatographic band and that of the grains, as well as the infra-red spectra of the cation-exchange resin Amberlite IRC-84 in the H-form, in the Na-form and saturated with palladium (which differ only in the peaks, characteristic of the carboxyl–the H-form, and the carboxylate–the Na-form, groups) give ground for the assumption that palladium is sorbed as a result of a precipitation preferentially inside the grains of the cation-exchange resin. The precipitation takes place according to the following reactions.

$$\mathrm{PdCl_4^{2-}} + 4\mathrm{H_2O} = \mathrm{Pd(OH)_2} + 4\mathrm{Cl^-} + 2\mathrm{H_3O^+}$$

$$\mathrm{RCOONa} + \mathrm{H_3O^+} = \mathrm{RCOOH} + \mathrm{Na^+} + \mathrm{H_2O}$$

During this process the other solution acquires a pH of 7. The solution inside the grains of the resin has a pH of 9 (pK = 5.3; capacity 3.5 mg equiv./ml) prior to passing the sample for investigation. When the resin is half transformed into the H-form, the pH inside the grains is 5.3. It is difficult to cal-

culate the pH necessary for the beginning of the precipitation, as well as the value needed for the practically complete precipitation of palladium at the concentrations employed by us (10^{-4} mol/l), as there are no reliable data on the composition and solubility of the products of hydrolysis obtained. According to approximate calculations there are conditions for the precipitation of palladium both inside the grains of the weakly acidic cation-exchange resin and in the solution which is among them. The complete retaining of palladium on the ion-exchange column, however, depends not only on its quantitative conversion into a weakly soluble compound but also on retaining the precipitate thus obtained on the resin. The precipitate formed in the outside solution is quickly washed down the column with dilute hydrochloric acid or it is dissolved and — on coming in contact with new portions of the ion exchange resin — it is again sorbed or precipitated according to the equilibria given above. The precipitate inside the grains of the resin dissolves more slowly due to the buffering action of the functional groups. Washing of the sorption column with 20 ml 0.1 *M* hydrochloric acid causes a shifting of the chromatographic band by 2—3 cm. The dissolution and precipitation of palladium hydroxide, occurring repeatedly on the ion-exchange column, offers a possibility of obtaining a precipitate free of admixtures. In the experiments on strongly acidic cation-exchange resins, a precipitate can be formed only in the solution between the grains and when the column is washed, it quickly passes into the filtrate. Inside the grains of the strongly acidic cation-exchange resin the hydrogen-ion concentration is substantially higher and no precipitation occurs.

To establish the conditions of complete sorption of palladium on weakly acidic cation-exchange resins, it was necessary to investigate the effect of the various parameters of the experiment which would influence the quantitative precipitation and retaining of palladium, such as acidity of the solution, palladium concentration, depth of the sorption layer, etc.

Table I shows the effect of hydrochloric acid concentration.

Table I

Effect of the acid concentration

Pd content in the sample, mg	HCl, *M*	Pd in the filtrate, mg	Pd in the filtrate, %
1.000	0.50	passes	passes
1.000	0.10	0.025	2.5
1.000	0.05	0.005	0.5
1.000	0.01	traces	traces

Experiments were carried out on a column of a height of 15 cm, at a rate of 0.5 ml/min. With the decrease of the acid concentration in the solution investigated and in the washing liquid, the sorption of palladium is improved.

Further experiments were carried out on columns of different height — 15, 20 and 25 cm — at one and the same hydrochloric acid concentration. The increase in column height improves the sorption of palladium because palladium passing into the washing liquid has a greater possibility of being precipitated and sorbed repeatedly.

A decrease in the rate of passing the solution through the column down to 0.2 ml/min has no effect on the quantitative sorption.

Table II illustrates the effect of palladium concentration. As the palladium concentration in the solution is decreased, the percentage of palladium passing into the filtrate increases, as it should be expected. However, the losses are insignificant and within the limits of the experimental error, stated by the respective methods of determination.

Table II

Effect of the palladium concentration

Pd, *M*	HCl, *M*	Pd in the filtrate, %
7.1×10^{-5}	0.1	2.6
2.3×10^{-4}	0.1	2.2
5.7×10^{-4}	0.1	1.3

The investigations on the eluation of palladium, sorbed on a column of a height of 20 cm, 0.8 cm in diameter with solutions of 1 and 2 *M* hydrochloric acid indicated 2 *M* hydrochloric acid being a better eluent (Figs 1 and 2).

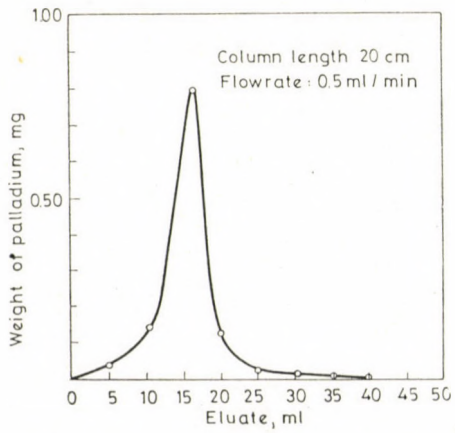

Fig. 1. Elution of palladium with 1 *M* hydrochloric acid

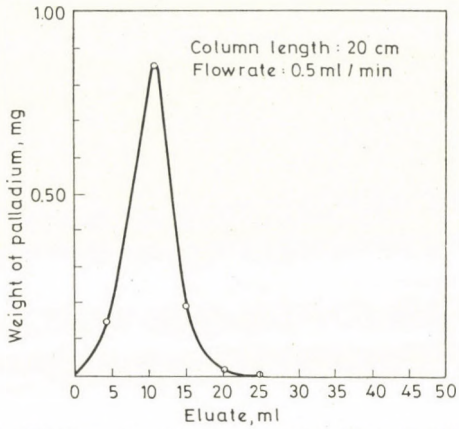

Fig. 2. Elution of palladium with 2 *M* hydrochloric acid

The optimal conditions for the separation of palladium from platinum and iridium (described in the experimental part) could be established.

The separation of palladium from rhodium proved to be more difficult. A series of experiments were carried out for complexing rhodium(III) to be not sorbed on the weakly acidic cation-exchange resin, however, this did not succeed so far.

Table III

Separation of palladium from platinum

Pd, mg		Pt, mg	
taken	found	taken	found
1.22	1.22	1.51	1.47
1.22	1.24	1.51	1.52
1.22	1.22	1.51	1.48
1.22	1.21	1.51	1.49
	average 1.222		
	→		
	S = 0.013		
0.488	0.477	1.51	1.49
0.488	0.487	1.51	1.55
0.488	0.488	1.51	1.50
	average 0.4840		
	→		
	S = 0.0061		
0.152	0.148	1.51	1.56
0.152	0.153	1.51	1.50
0.152	0.147	1.51	1.52
	average 0.1493		average 1.508
	→		→
	S = 0.0027		S = 0.029

Table IV

Separation of palladium from iridium

Pd, mg		Ir, mg	
taken	found	taken	found
1.22	1.19	1.35	1.37
1.22	1.21	1.35	1.34
1.22	1.22	1.35	1.36
1.22	1.19	1.35	1.33
	average 1.202		average 1.350
	S = 0.015		S = 0.018

S denotes standard deviation

The accuracy and reproducibility of the method developed for the separation of palladium from platinum and iridium were studied by analysing mixtures of standard solutions. The results obtained are very good (Tables III and IV).

REFERENCES

[1] PROKOF'EVA, I. V., FEDORENKO, N. V.: J. neorgan khimii **13,** 1348 (196)
[2] BLASIUS, E., REXIN, D.: Z. anal. Chem. 1961, **179,** 105
[3] CHARLOT, G.: Les methodes de la chimie analytique, Analyse quantitative minerale, Masson et Cie, Paris 1961
[4] BEAMISH, F. E.: The Analytical Chemistry of the Noble Metals. (Russ transl.) Mir, Moscow 1969
[5] YUFA, T., CHENTYSOVA, M. A.: Sb: Analiz blagorodn'ikh metallow, Akad. Nauk USSR, Moscow 1959 p. 176
[6] SANDELL, E. B.: Colorimetric Determination of Traces of Metals, 3rd Ed. Interscience, New York 1959
[7] PSHENITS'IN, N. K., GINSBURG, S. I., SAL'SKAYA, L. G.: Sb: Analiz blagorodn'ikh metallow, Akad. Nauk USSR, Moscow 1959 p. 48

L. L. KOCHEVA
B. TABAKOVA
Department of Chemistry, University of Sofia, Bulgaria.

Acta Chimica Academiae Scientiarum Hungaricae, Tomus 83 (3—4), pp. 237—245 (1974)

INVESTIGATION OF SUPERCOOLED WATER BY LIGHT SCATTERING

GY. BEKE, GY. INZELT and L. JANCSÓ

(Department of Physical Chemistry and Radiology, L. Eötvös University, Budapest)

Received December 30, 1972

The light scattering of water has been investigated between −8 and +8°C. The dependence of the scattered light intensity on the temperature does not differ significantly in the ranges above and below the freezing point. The range on the aggregation degree *vs.* concentration plane has been determined where light scattering experiments exclude the presence of ice embryos in supercooled water.

Introduction

Among the numerous publications devoted to the structure of water there are several studies dealing with the supercooled water itself while other papers report on investigations contributing to the studies of water structure in general by means of comparing some experimentally determined parameters of water above and below its freezing point ([1—9] as reviewed in [10]). The interest of many authors was aroused by the phenomenon of supercooling itself [11—17]. The results of these studies were discussed in several cases in the light of the theory of the crystallization process. According to the theory [18—20], the process starts with the formation of small clusters, the so-called crystal embryos, consisting of several molecules only but already having the same structure as the solid phase to be formed. The clusters can grow spontaneously and their presence in the liquid may result in actual crystallization only if their sizes attain a certain value. This critical size depends, among other parameters, upon the temperature. Thus, in agreement with the theory, crystal embryos can be present in supercooled water even in a very great amount without the real chance of crystallization unless their size attains the critical value at the given temperature. It would not be unexpected therefore if some properties of the supercooled liquid were detectably influenced by the presence of crystal embryos owing to their great amount, regardless of their small size. And indeed, the experimental data are in accordance with these considerations. Though no evidence of any molecular clusters appears in the temperature dependence of density [11, 13], surface activity, heat capacity and vapour pressure [11], there are several other parameters pointing to the presence of crystal embryos. Namely, by analyzing the temperature de-

pendence of the viscosity [11—13], electric conductivity [11], dielectric constant and ultrasonic absorption [15], thermal expansion, refractive index [12] and X-ray diffraction [17], it can be concluded that some new effect appears in the temperature range below the freezing point which might be due to the crystal embryos formed.

The investigation of water as a model is of interest not only because of the importance of this liquid but also because of the fact that in this case the available data are not controversial with respect to the hypothesis of crystal embryos. Neither the vapour pressure [4], heat conductivity [5], refractive index [6], dielectric constant nor the relaxation time [7], does indicate any change in the structure of water in the supercooled state. Likewise, the structure of water was found to be uniform by analyzing the distribution of oxygen isotopes [21] and the coefficient of self-diffusion [22] in the temperature ranges (—2, +85) and (—20, +30°C), respectively. Therefore it is the more interesting that a paper has recently been published which reports experiments pointing to the presence of ice embryos in supercooled water. KULES and SCHILLER have investigated the radiochemical decomposition of water [10]. They have concluded that within the experimental accuracy the yields of the decomposition products as a function of temperature can be approximated linearly both above and below the freezing point. However, these two lines do not coincide. This can be interpreted by taking into consideration the crystal embryos in supercooled water. These findings have prompted us to obtain some experimental evidence by the method of light scattering against or for the ice embryo hypothesis. It should be emphasized that for discussing the results of light scattering experiments one need not be restricted to the idea that the anomalous temperature dependence of some parameters in the range of supercooling should point to the existence of crystal embryos. The phenomenon of light scattering is known to be due to the lack of ideally uniform distribution of liquid particles in space and, generally speaking, the intensity of the scattered light at a given instant is a measure of the statistically expected nonuniformity. It is evident, therefore, that such a drastical change in the uniform distribution of particles as cluster formation must be accompanied by an increase in the intensity of scattered light. On the other hand, an unexpectedly high value of the intensity under given conditions cannot be explained in any way other than the increased lack of ideal uniformity.

The quantitative treatment of light scattering was given very long ago (see *e.g.* [25] and [27]). In the following we shall attempt to adapt it to ice clusters in supercooled water. It should be noted finally that many authors assume the presence of ice-like clusters in water even in temperature ranges far above the freezing point (as reviewed *e.g.* in [23]) while others regard this assumption as inconsistent with the fact that water can be easily supercooled [8].

Method

The intensity of light scattered by a pure liquid I can be given as the sum of intensities due to the fluctuation of density I_d and orientation I_{or}. For a system of two components the intensity, due to the fluctuation of the concentration I_c, contributes as well. Thus, if below the freezing point a new 'component' consisting of ice clusters appears in water, it can be detected experimentally from the $I_c(t)$ function superimposed on the $I_d(t)$ and $I_{or}(t)$ functions, presuming that two conditions are fulfilled. The first is that the $I_d(t) + I_{or}(t)$ function determined experimentally in the temperature interval $(0, t_1)$ should be valid in the interval $(t_2, 0)$ too, where $t_2 < 0 < t_1$. This condition is *a priori* fulfilled since, according to our approach, I_d and I_{or} characterize the unchanged 'solvent' and any change in the structure of the liquid is treated as an increase in the amount of the new 'component' of the structure, differing from that of water and reflected by I_c. The other obvious condition is that the ratio $I_c/(I_d + I_{or})$ should be great enough to be detected. In order to check this condition, one should analyze I_c written in the form [24—27]:

$$I_c = C \left(\frac{\partial n}{\partial c}\right)^2_{\varrho,T} n^2 v \overline{(\Delta c)^2_v} \tag{1}$$

where n is the refractive index, ϱ the density, c the concentration, T the absolute temperature, v a small part of the scattering volume, $\overline{(\Delta c)^2_v}$ the fluctuation of concentration in v and C is a constant depending on the experimental conditions only. Eq. (1) shows that at a given value of the fluctuation of concentration I_c is determined mainly by the refractive index increment. If one whises to determine the molecular weight of a macromolecule by light scattering, the solvent chosen should have a refractive index strongly different from that of the macromolecular material so that the effect observed were detectable. However, this is not possible therefore, when studying the water–ice embryo system, one will encounter an inherent restriction in the conclusions to be drawn. As has been shown by DEBYE, the molecular weight of the solute M can be expressed in terms of light scattering data in the following way (see *e.g.* [24—27]):

$$\frac{Kc}{R_c(\Theta, c)} = \frac{1}{MP(\Theta)} + 2Bc + \ldots, \tag{2}$$

Here B is the second virial coefficient, $P(\Theta)$ the scattering function and

$$K = \frac{2\pi^2 n_0^2 \left(\frac{dn}{dc}\right)^2}{\lambda^4 N_A} \tag{3}$$

where n_0 is the refractive index of the solvent, λ the wavelength of the applied monochromatic light in vacuum and N_A the Avogadro number. In Eq. (2) the intensity of light is replaced by the reduced intensity R_c which is independent of the experimental conditions, namely the intensity of incident light I_0, the scattering volume V, the distance between the scattering point the detector r and the angle between the incident and scattered light beams Θ, and is expressed as

$$R_c(\Theta, c) = \frac{r^2 I(\Theta, c)}{I_0 V(1+\cos^2 \Theta)} \quad . \tag{4}$$

It must not be left out of consideration that R_c could be connected with M owing to the correlation between fluctuations in the concentration and the concentration dependence of the free energy. The linear approximation of the latter at $c = 0$ leads to Eq. (2). Thus, the more dilute the solution, the nearer is Eq. (2) to reality. When studying macromolecules, one measures the scattered light intensity for a series of solutions in the dilute concentration range and extrapolates to $c = 0$. With another extrapolation to $\Theta = 0$ (since $P(0) = 1$) one can evaluate the molecular weight of the solute. As consistent $I_c(\Theta, c)$ data in principle could not be obtained in the whole ice embryo concentration range, it is impossible to evaluate the molecular weight of the embryos. However, their presence in supercooled water can be detected if the value of I_c exceeds the experimental error. The size of the detectable crystal embryos can be estimated.

Experimental

The light scattering photometer has been described earlier [28, 29]. Water was twice distilled and passed through a Millipore filter (0.22 μ). Benzene was used as a standard with $R_b = 48.4 \times 10^{-6}$ cm^{-1} [25]. The cell to be cooled was cylindrical with three walls to avoid the condenzation of vapour on the outer surfaces. Measurements were carried out in the temperature interval between -8 and $+8$°C.

Results and discussion

Figure 1 represents the scattered light intensities with the 99.7% confidence intervals. The intensity data from different experiments cannot be averaged at a given temperature since supercooling is not a reversible process and the quantity and size of the possible crystal embryos at a given pressure are not expected to be determined unambiguously by the temperature. Thus, the data presented in Fig. 1 should be regarded as representative samples of the experimental results. It can be concluded that no significant effect appears pointing to the presence of any structural changes in the supercooled region. To make further conclusions we must return to Eq. (2).

For a given refractive index increment, the higher the molecular weight of the dissolved particles, the stronger is the light scattering effect expected. From the known refractive index increment and the second virial coefficient, the molecular weights of particles and the concentrations, necessary for detection with the given experimental accuracy, can be evaluated. The second virial coefficient can be determined experimentally. For this purpose, *e.g.* light

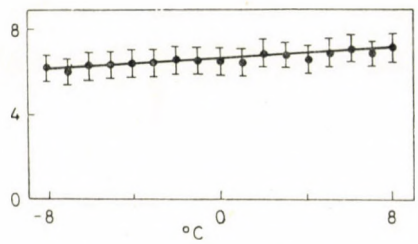

Fig. 1. Temperature dependence of the intensity of scattered light on an arbitrary scale

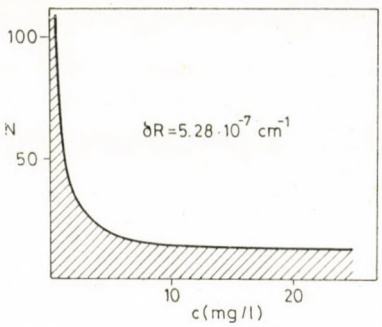

Fig. 2. The $N(c)$ function

scattering should be measured in the whole concentration and scattering angle range. However, one cannot prepare ice embryo "solutions" of systematically different concentrations. If the concentrations in two cases happen to be different and known, the identity of the size of crystal embryos (or size distributions) still cannot be taken for granted. These circumstances preclude the experimental determination of the refractive index increment as well. Thus, having no experimental data, one needs to be satisfied with their estimated values. Taking the approximations for B and dn/dc as given in the Appendix, the detectable concentration of crystal embryos consisting of N water molecules can be related to N by

$$c = \frac{\delta R N}{K' Q N^2 - 1} . \tag{5}$$

The symbols Q and K' are defined in the Appendix. In Eq. (5) the reduced intensity is replaced by the width of the reduced intensity interval δR significant at a certain confidence level. The $N(c)$ function evaluated from Eq. (5) for the given experimental conditions at a 99.7% confidence level is demonstrated in Fig. 2.

The following conclusions seem to be consistent with the experimental data. The crystal embryos in supercooled water, if present at all, must be characterized by pairs of values of concentration and degree of association

falling into the shaded range in Fig. 2. In principle this range can be decreased by a greater experimental accuracy. One should emphasize, however, that these results have been obtained assuming that the clusters have the same structure and the same refractive index as ice. Clusters of water molecules with a structure organized to a lesser extent than that of ice, and with a refractive index between those of water and ice, could be present in greater amounts than is shown in Fig. 2 without significantly influencing the light scattering data. It should be emphasized, however, that it is not a loose structure but clusters of real ice structure that are assumed to be present in supercooled water [18—20].

Appendix

1. Regarding the water–ice embryo system as an ideal mixture, the chemical potential can be expressed as a power series of the concentration and from this the k-th virial coefficient can be obtained in the form [24, 26]:

$$B_k = \frac{V_w^{k-1}}{kM^k} \tag{6}$$

where V_w and M are the molar volume of water and the molecular weight of the ice embryos, respectively. With the approximation that the density of supercooled water equals unity and by expressing M with the number of water molecules in the embryo N and the molecular weight of water M_w, using (6), one obtains

$$2\,B_2 = \frac{1}{M_w N^2}\,. \tag{7}$$

2. In order to evaluate the refractive index increment, let us regard the refractive index of supercooled water as a function of the mole fraction x of ice embryos and express x by c using, the equation $xM = V_w c$ valid for dilute solutions. If we utilize again that the density of supercooled water equals unity, we have

$$\frac{\mathrm{d}n}{\mathrm{d}c} = \frac{\mathrm{d}n}{\mathrm{d}x}\,\frac{1}{N} \tag{8}$$

and so our task is simplified to determine the derivative $\mathrm{d}n/\mathrm{d}x$.

Consider the molar polarization function of a water–ice embryo system

$$P(n, M, \varrho) = \frac{n^2 - 1}{n^2 + 2}\,\frac{M}{\varrho} \tag{9}$$

where the arguments n, M and ϱ depend on x. Suppose that $P(x)$, $M(x)$ and $\varrho(x)$ are linear. Let the following notation be introduced:

$$\frac{n^2(x)-1}{n^2(x)+2} = P'(x)\,, \qquad \frac{6\,n(x)}{(n^2(x)+2)^2} = S(x) \tag{10}$$

and $P'(1) = P'_i$, $P'(0) = P'_w$, $\varrho(1) = \varrho_i$ and $S(0) = S_w$. By taking the derivative of $P(x)$ one obtains

$$\frac{\mathrm{d}n}{\mathrm{d}x} = \frac{\dfrac{P'_i N\varrho(x)}{\varrho_i} - \dfrac{P'_w o(x)}{\varrho_w} - P'(x)(N-1) + (\varrho_i - 1)\left[P'_w + \left(\dfrac{P'_i N}{\varrho_i} - P'_w\right)x\right]}{S(x)\,[1+(N-1)\,x]}\,. \tag{11}$$

Suppose now that x is small enough to fulfil the following conditions

$$\frac{1+x}{x} \gg N, \qquad |\,\varrho(x)-1\,| \ll \varrho(x)\,, \qquad |\,P'(x)-P'_w\,| \ll P'(x) \tag{12}$$

and

$$|\,S(x)-S_w\,| \ll S(x)\,.$$

Then Eq. (11) becomes

$$\frac{\mathrm{d}n}{\mathrm{d}x} = \frac{\dfrac{P'_i}{\varrho_i}(N\,[1-x(\varrho_i-1)]) + P'_w\,[(\varrho_i-1)(1+x)-N]}{S_w}\,. \tag{13}$$

If

$$|\,x(\varrho_i-1)\,| \ll 1\,, \qquad |\,(1+x)\,(\varrho_i-1)\,| \ll N\,, \tag{14}$$

it is readily seen that

$$\frac{\mathrm{d}n}{\mathrm{d}x} = \frac{\left(\dfrac{P'_i}{\varrho_i} - P'_w\right)N}{S_w}\,. \tag{15}$$

3. Let I_w be the intensity of light scattered by pure water and I the nearest value to I_w distinguishable from it significantly at a certain confidence level. Let $\delta I = |\,I_w - I\,|$ and δR the respective reduced intensity. Let point

(c', M') of the c, M plane correspond to a solution of concentration c', of a material of molecular weight M' in water. Writing now δR instead of R in Eq. (2), one has a curve $F(c, M; \delta R, K, B) = 0$, which separates from one another the aqueous solutions that can and cannot be distinguish from pure water by light scattering at a given confidence level. The form of the curve is affected by the type of material through parameters K and B. For the special case of the water–ice embryo system, using Eq. (7), (8) and (15) we have Eq. (5).

Here M is replaced by the more descriptive degree of aggregation and

$$K' = \frac{K}{\left(\frac{dn}{dc}\right)^2} \tag{17}$$

$$Q = \frac{\left(\frac{P_i'}{\varrho_i} - P_w'\right)^2 M_w}{S_w^2} . \tag{18}$$

We have assumed that the scattering function in Eq. (2) is equal to unity. The error of this assumption depends on the shape and size of the clusters [27]. However, the error is appreciable only for clusters of "macromolecular size" regardless of the shape.

*

We express our gratitude to Dr. Róbert SCHILLER for drawing our attention to this problem.

REFERENCES

[1] MASON, B. J.: Advan. Phys. **7**, 221 (1958)
[2] CHANAL, R. S., MILLER, R. D.: Brit. J. Appl. Phys. **16**, 231 (1965)
[3] YANNAS, I.: Science **160**, 298 (1968)
[4] EISENBERG, D., KAUZMANN, W.: The Structure and Properties of Water. Clarendon, Oxford 1969
[5] POWELL, R. W.: Advan. Phys. **7**, 276 (1958)
[6] DASS, N., GILRA, N. K.: J. Phys. Soc. Jap. **21**, 2039 (1966)
[7] SAXTON, J. A.: Proc. Roy. Soc. Ser. A **213**, 473 (1952)
[8] KOEFOED, J.: Discuss. Faraday Soc. **24**, 216 (1957)
[9] KAVANAU, J. L.: Water and Solute–Water Interaction. Holden Day, San Francisco 1964
[10] KULES, J., SCHILLER, R.: J. Phys. Chem. **75**, 2997 (1971)
[11] GREENWOOD, N. N., MARTIN, R. L.: Proc. Roy. Soc. Ser. A **215**, 46 (1952)
[12] NECHAI, F. I.: Uch. Zap. Beloruss. Gos. Univ. Ser. Fiz. **41**, 231 (1958)
[13] BARLOW, A. J., LAMB, J., MATHESON, A. J.: Proc. Roy. Soc. Ser. A **292**, 322 (1966)
[14] DODD, C., ROBERTS, G. N.: Proc. Roy. Soc. London, Sect. B **63**, 814 (1950)
[15] HUNTER, A. N.: Proc. Roy. Soc. London, Sect. B **64**, 1086 (1960)
[16] PANTHASARATHY, S., BANDAL, V. N.: Indian J. Phys. **34**, 272 (1960)
[17] LEVASHEVICH, M. A., PODOSICHNIKOV, N. N., VARIVOSA, I. CH.: Trudy Dnepropetrovsk. Khim. Technol. Inst. **4**, 84 (1955)
[18] TURNBULL, D., FISCHER, J. I.: J. Chem. Phys. **17**, 71 (1949)
[19] HOLOMON, J. H., TURNBULL, D.: Progr. Metal. Phys. **4**, 333 (1953)
[20] FRENKEL, YA. I.: Izv. Akad. Nauk SSSR, 336 (1945)

[21] O'Neil, J. R., Adami, L. H.: J. Phys. Chem. **75,** 1553 (1969)
[22] Pruppacher, H. R.: J. Chem. Phys. **56,** 101 (1972)
[23] Erdey-Gruz, T.: Transport Processes in Aqueous Solutions (in Hungarian). Akadémiai Kiadó, Budapest 1971
[24] Beke, G., Gilányi, T.: Kémiai Közlemények **35,** 207 (1971)
[25] Fabelinskii, I. L.: Molekularnoe rasseianie sveta. Nauka, Moskva, 1965
[26] Tanford, C.: Physical Chemistry of Macromolecules. Wiley, London 1961
[27] Stacey, K. A.: Light Scattering in Physical Chemistry. Academic Press, London, 1956
[28] Czuppon, A.: Magy. Kém. Lapja **19,** 204 (1964).
[29] Beke, G., Gilányi, T.: Magy. Kém. Foly. **75,** 440 (1969)

Gyula Beke
György Inzelt
László Jancsó
H—1088 Budapest, Puskin u. 11—13. Hungary.

Acta Chimica Academiae Scientiarum Hungaricae, Tomus 83 (3—4), pp. 247—257 (1974)

POLARIZATION OF THE INDIUM ANTIMONIDE ELECTRODE

T. M. SALEM and A. A. ISMAIL

(Chemistry Department, Faculty of Science, Alexandria University, Egypt)

Received March 26, 1973, in revised form December 8, 1973

Indium antimonide as an intermetallic compound with a small energy gap has chosen for this study. The single crystal electrode has been examined with and without illumination in the presence of a redox system. It has been observed that the anodic dissolution is increased by illumination as holes are injected into the valence band. For all oxydizing agents the current depends on the light intensity. It is suggested that excess carriers may be generated optically by using a beam of light and that illumination is useful in the application of carrier injection into an electrode of *n*-type semiconductor.

Introduction

Most semiconductor substances with a small energy gap have a tendency to possess high values of electron mobility. Small gaps imply small effective masses which favour high mobilities. This behaviour helps to apply electrochemical measurements to silicon, germanium [1] and gallium phosphide electrodes [2].

Actually, indium antimonide has an energy gap equal to 0.18 eV at room temperature. Accordingly, the intrinsic single crystal of InSb has an average carrier mobility of 77,000 electrons and 1250 holes at room temperature. This would influence the electronic structure of this intermetallic compound, with these electrons taking part directly as reactants and/or products in the reaction itself.

It is the purpose of this study to examine the electron transfer occurring at the surface of indium antimonide electrodes with and without illumination and in the presence of a redox electrolyte system.

Experimental

Measurements were carried out using the single crystal indium antimonide electrode (prepared Dr. PARKER, Texas Instruments Inc.) having structures with 111 (A) and $\overline{111}$ (B) faces. Ohmic metal/semiconductor contact potentials were assumed to be zero, *n*-type single crystals of indium antimonide with a resistivity of $10^3\ \Omega$/cm were used. The circuit and the Amel potentiostat used were as described before [3]. The single crystal was pretreated in an etchant solution of HF : HNO_3 in the ratio of 1 : 3 before its use as an electrode [4].

Nitrogen was bubbled through the cell to free the solution from oxygen. All potential measurements were made against a saturated calomel or a mercury–mercuric sulfate reference electrode. Solutions were prepared from conductivity water and AR materials. Measurements were performed with and without illumination. All results are relative to the hydrogen scale.

Results and discussion

Redox measurements in the dark

The potential of indium antimonide of single crystal was measured in a variety of solutions. Figure 1 shows the anodic and cathodic current *vs.* potential curves characteristic for the single crystal electrode structure *A*, in sulfuric acid with and without added oxidizing agent (ferric sulfate). Without

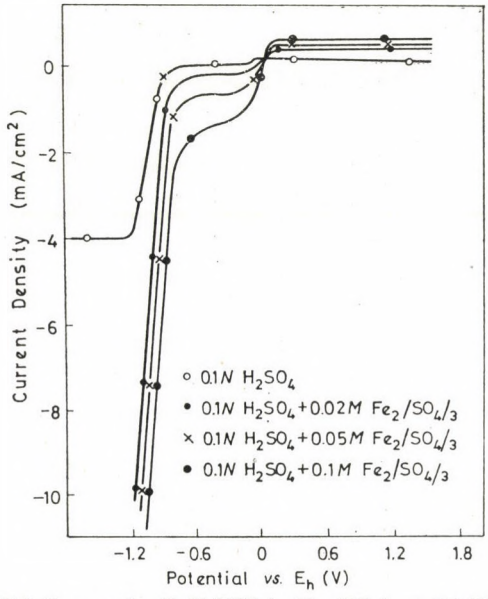

Fig. 1. E/1 Curves for InSb(III) in $Fe_2(SO_4)_3 + 0.1N\ H_2SO_4$

addition of ferric sulfate, current flows when the electrode is cathodic until the potential reaches the value required for hydrogen ion discharge. Both the anode and cathode are increasingly polarized with increasing concentration of $Fe_2(SO_4)_3$ *i.e.* the limiting current i_A increases with increasing concentration of the oxidizing agent.

Similar curves are obtained with InSb(III) in acid solutions after addition of cerium sulfate, potassium ferricyanide and potassium permanganate.

The current *vs.* potential curves (Fig. 2) for potassium dichromate in the presence of sulfuric acid show a decrease in the limiting anode current with increasing concentration of the added substance. The anodic plateaus merge into one line at zero current. On the other hand, there is an increase in the limiting cathode current. Figure 3 shows the current–potential characteristics for the InSb(III) electrode in hydrochloric acid with and without the redox agent oxalate. The redox system appears to be unique in that the electron transfer mechanism involves the conduction band electrons. In the case of

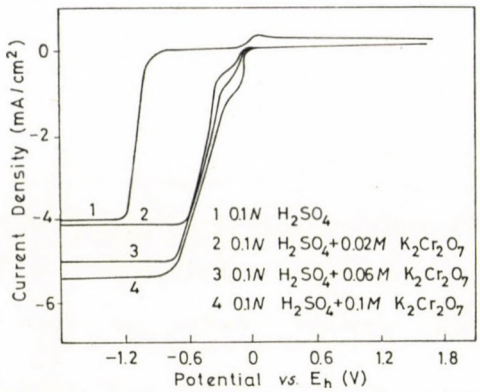

Fig. 2. E/1 Curves for InSb(III) in 0.1*N* H_2SO_4 + $K_2Cr_2O_7$

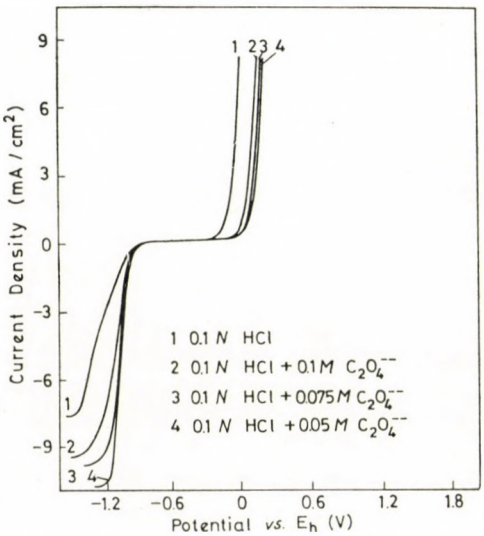

Fig. 3. E/1 Curves for InSb(III) in $C_2O_4^{2-}$ + 0.1*N* HCl

hydrogen peroxide both the cathodic and anodic limiting currents decrease.

Figure 4 is a representative diagram for the InSb (*B*) electrode in sulfuric acid with and without the oxidant ferric sulfate.

From the curves, it can be seen that the saturation current for anodic dissolution increases owing to hole depletion at the surface of the electrodes [5]. Since holes are the minority charge carriers, the saturation current of the limiting current represents the point at which holes are used up in the anode reaction as fast as they are made available at the electrode surface either by diffusion from the bulk or by generation in the surface region. The cathodic current i_C than decreases the parallel reduction process in these acid solutions when used alone. The anodic oxidation of ions in these redox solutions occurs

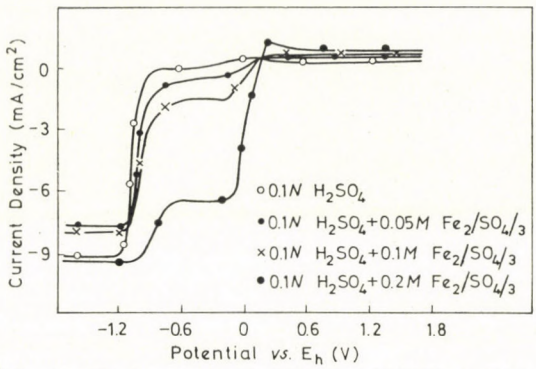

Fig. 4. E/1 Curves for InSb(III) in $H_2SO_4 + Fe(SO)_3$

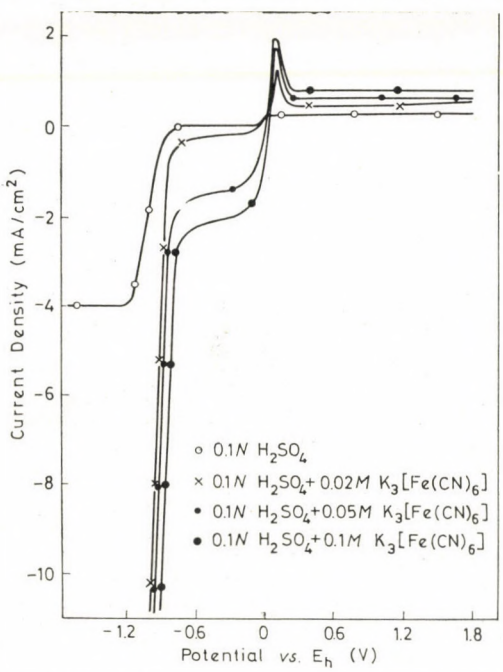

Fig. 5. E/1 Curves for InSb(III) in $K_3[Fe(CN)_6] + 0.1N\ H_2SO_4$

without either the anodic or cathodic process only in a potential range of about 1200 mV in sulfuric acid and hydrochloric acid between —1.0 and 0.2V *vs.* the hydrogen electrode. The anodic saturation current increases from 0.25 mA to 6.4 mA depending on the oxidizing system used. It should be noted that the increase of the anodic limiting current or the decrease in the cathodic current i_C is much greater for the single crystal (*B*) electrode than for the (111) electrode face. The amount of either increase or decrease depends on the oxidizing system used and it is proportional to its concentration (Table I) (Figs 5—8).

Table I

Oxidizing or reducing agent	i_A(μA/cm^2)	i_c(μA/cm^2)
S.C.E.; Structure (A)		
A — 0.1N H_2SO_4	250	— 2
(1) $H_2SO_4 + 0.02M\ Fe_2(SO_4)_3$	320	— 250
$H_2SO_4 + 0.05M\ Fe_2(SO_4)_3$	450	— 750
$H_2SO_4 + 0.1\ M\ Fe_2(SO_4)_3$	550	— 1500
(2) $H_2SO_4 + 0.01M\ Ce(SO_4)_2$	350	— 150
$H_2SO_4 + 0.02M\ Ce(SO_4)_2$	450	— 350
$H_2SO_4 + 0.1\ M\ Ce(SO_4)_2$	650	— 750
(3) $H_2SO_4 + 0.02M\ K_3Fe(CN)_6$	450	— 250
$H_2SO_4 + 0.05M\ K_3Fe(CN)_6$	600	— 1500
$H_2SO_4 + 0.1\ M\ K_3Fe(CN)_6$	750	— 2200
(4) $H_2SO_4 + 0.004M\ KMnO_4$	300	— 250
$H_2SO_4 + 0.01\ M\ KMnO_4$	350	— 500
$H_2SO_4 + 0.02\ M\ KMnO_4$	400	— 900
(5) $H_2SO_4 + 0.02M\ K_2Cr_2O_7$	150	— 500
$H_2SO_4 + 0.06M\ K_2Cr_2O_7$	150	— 750
$H_2SO_4 + 0.1\ M\ K_2Cr_2O_7$	150	— 1200
(6) $H_2SO_4 + 1\%\ H_2O_2$	50	— 3600
$H_2SO_4 + 2\%\ H_2O_2$	100	— 3300
$H_2SO_4 + 4\%\ H_2O_2$	150	— 3100
B — 0.1N HCl		— 30
(7) $0.1N\ HCl + 0.05\ M\ C_2O_4^{--}$		— 10000
$0.1N\ HCl + 0.075M\ C_2O_4^{--}$		— 9500
$0.1N\ HCl + 0.1\ M\ C_2O_4^{--}$		— 7700
Structure (B)		
A — 0.1N H_2SO_4	250	— 2
(1) $0.1N\ H_2SO_4 + 0.05M\ Fe_2(SO_4)_3$	400	— 700
$0.1N\ H_2SO_4 + 0.1\ M\ Fe_2(SO_4)_3$	600	— 1700
$0.1N\ H_2SO_4 + 0.2\ M\ Fe_2(SO_4)_3$	700	— 6500
(2) $0.1N\ H_2SO_4 + 0.01M\ Ce(SO_4)_2$	700	— 100
$0.1N\ H_2SO_4 + 0.02M\ Ce(SO_4)_2$	1200	— 200
$0.1N\ H_2SO_4 + 0.1\ M\ Ce(SO_4)_2$	1700	— 400

Table I (Continued)

Oxidizing or reducing agent	i_A(μA/cm^2)	i_c(μA/cm^2)
(3) 0.1*N* H_2SO_4 + 0.02*M* $K_3Fe(CN)_6$	1200	— 700
0.1*N* H_2SO_4 + 0.1 *M* $K_3Fe(CN)_6$	1200	— 2600
0.1*N* H_2SO_4 + 0.1 *M* $K_3Fe(CN)_6$	1200	— 8100
(4) 0.1*N* H_2SO_4 + 0.1 *M* $K_2Cr_2O_7$	500	— 3500
0.1*N* H_2SO_4 + 0.15*M* $K_2Cr_2O_7$	500	— 4500
0.1*N* H_2SO_4 + 0.2 *M* $K_2Cr_2O_7$	500	— 5500
(5) 0.1*N* H_2SO_4 + 2% H_2O_2	6400	— 150
0.1*N* H_2SO_4 + 4% H_2O_2	5600	— 100
0.1*N* H_2SO_4 + 5% H_2O_2	5000	— 50
(6) 0.1*N* H_2SO_4 + 0.01*M* $KMnO_4$	400	— 350
0.1*N* H_2SO_4 + 0.02*M* $KMnO_4$	500	— 400
B — 0.1N HCl	—	— 30
(7) 0.1*N* HCl + 0.03*M* $C_2O_4^{--}$	—	— 1000
0.1*N* HCl + 0.05*M* $C_2O_4^{--}$	—	— 800
0.1*N* HCl + 0.075 *M* $C_2O_4^{--}$	—	— 600
0.1*N* HCl + 0.1 *M* $C_2O_4^{--}$	—	— 400

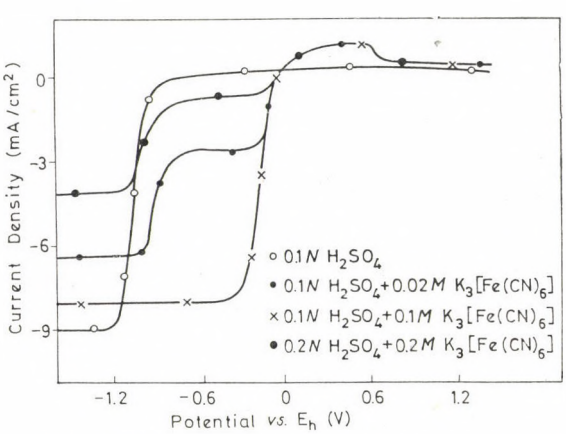

Fig. 6. E/1 Curves for InSb(III) in H_2SO_4 + $K_3[Fe(CN)_6]$

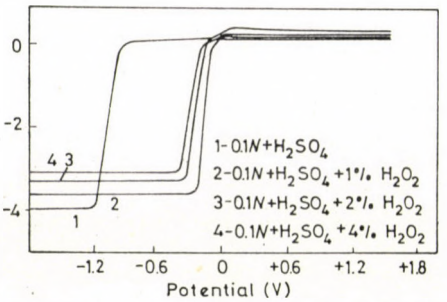

Fig. 7. E/1 Curves for InSb(III) in $0.1N$ $H_2SO_4 + H_2O_2$

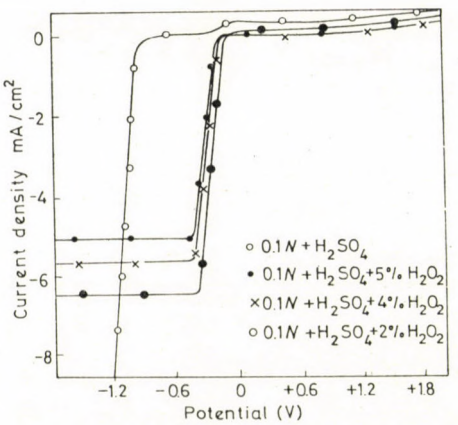

Fig. 8. E/1 Curves for InSb(III) in $H_2O_2 + 0.1N$ H_2SO_4

However, the variation of dissolution rate of the electrode surface depends mainly on the type of its surface orientation [4, 7]. This means that the unit cell with group V atoms at the origin have a tendency to be dissolved faster than those consisting of group III atoms. This conclusion was arrived at by FAUST and SAGAR [5], GATOS [7] and others [7] from X-ray evidence.

The mechanism in these redox systems could be explained by assuming that large numbers of electrons and holes are produced at the surface of the electrode during chemical anodization processes. The only cathode reaction at potentials less than 1 V *vs.* the hydrogen electrode can be explained by the processes

$$Fe^{3+} \rightarrow Fe^{2+} + p^+$$
$$Cr^{6+} \rightarrow Cr^{3+} + 3p^+$$
$$Ce^{4+} \rightarrow Ce^{2+} + 3p^+$$

These ions are reduced with the injection of hole into the indium antimonide surface. Thus the limiting saturation current i_C is reached when these ions are

reduced as fast as they arrive at the surface by mass transport. If Sb_2O_3 is cathodically reduced in the presence of these redox systems, the reaction at the cathode sites of the (111)single crystal surface is

$$Sb_2O_3 + H_2O + 3np^+ \rightarrow 2\,Sb^{3+} + 6\,e^- + 2\,H^+ + (3 - n)e\,.$$

In highly oxidizing redox systems, it is expected that the Fermi level on the surface is near the valence band and the concentration of holes at the surface is much higher than that of free electrons. Hence the exchange of holes should be predominating.

Hole reactions are produced on applying redox systems with very positive potentials where reactions take place by way of the valence band mechanism.

This is pronounced in the reduction of $K_3[Fe(CN)_6]$ where the cathodic (i_C) and anodic (i_A) limiting currents increase with the concentration of the oxidizing agent in these solution. It is observed that after the addition of the oxidizing agent to the solutions, there is again a shift of the rest potential in the positive direction to $\sim$0.1 V.

During the oxidation of oxalate or hydrogen peroxide, the cathodic limiting current decreases. The redox systems appear to be unique in that the electron transfer mechanism involves the conduction band electrons.

Redox measurements in light

Indium antimonide is characterized by a relatively low concentration of holes. This is noted when comparing the increase of i_A or i_C during anodic o r cathodic process in the presence of a redox system. However, the anodic current can be increased by providing additional holes at the surface as a result of illuminating the semiconductor.

In the luminescence measurements, an a.c. voltage was applied to obtain a modulated light emission. A mercury lamp was used with 5461 Å. Indium antimonide of structure A was chosen for these measurements. Typical E–I curves are obtained with the indium antimonide single crystal (III) electrodes under illumination in sulfuric acid and ferric sulfate (Fig. 9) and in hydrochloric acid and ferric chloride (Fig. 10). For comparison the curves measured in the dark under the same experimental conditions are also given. Figures 11, 12 and 13 show the indium antimonide single crystal electrodes under illumination in different redox systems.

For all oxidizing agents the current depends upon the illumination, *i.e.*, the conduction electrons are consumed at the surface. Upon illumination, the photogenerated holes move to the surface and react with the components of the solution and the corresponding anodic current is obtained. The limiting current density is greater than that obtained in the dark. The anodic current

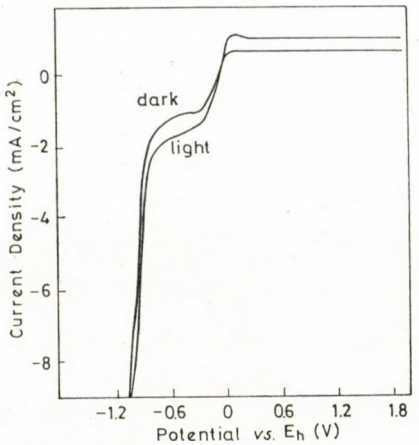

Fig. 9. E/1 Curves for InSb(III) in $0.1M$ $Fe_2(SO_4)_3 + 0.1N$ H_2SO_4

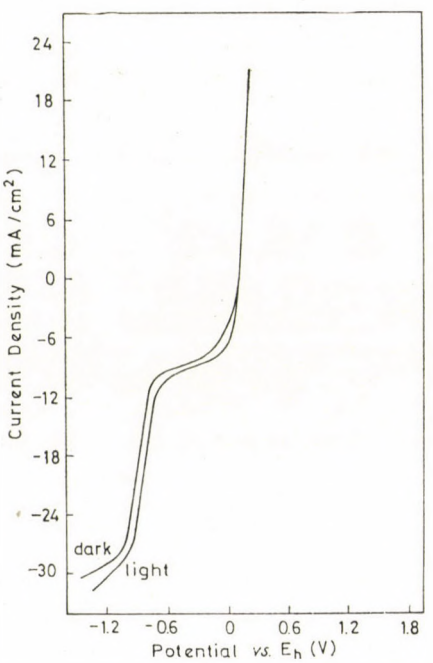

Fig. 10. E/1 Curves for InSb(III) in $0.25M$ $FeCl_3 + 0.1N$ HCl

density observed is the difference between the enhanced anodic dissolution current density and the reduction saturation current. The anodic dissolution is increased as holes are injected into the valence band by illumination. This affects not only the average hole participation factor but also the increase of the anodic limiting current density. This increase is altered to different degrees

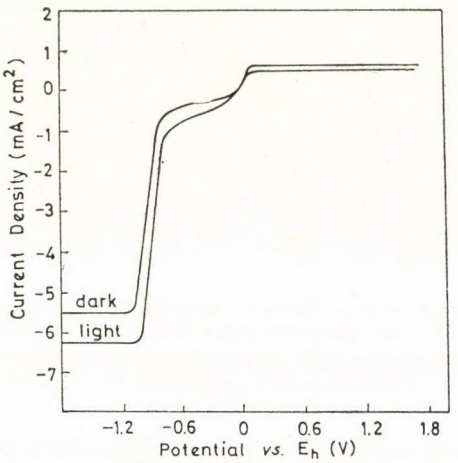

Fig. 11. E/1 Curves for InSb(III) in 0.02M Ce^{4+} + 0.1*N* H_2SO_4

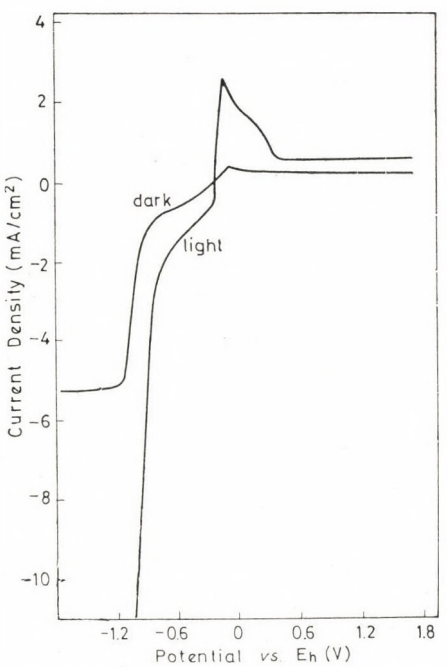

Fig. 12. E/1 Curves for InSb(III) in 0.02*M* $KMnO_4$ + 0.1*N* H_2SO_4

with various oxidizing agents used. In the potential range where the cathodic current is decreasing (−1.0 — +0.2 V), the reduction rate is lower than in the saturation region. This result is different from that obtained in the dark. On all curves a distinct increase in i_A is obtained, *i.e.*, a lower dark current and a higher photocurrent are observed (Table II).

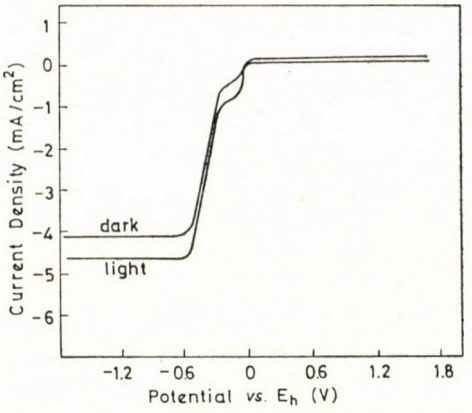

Fig. 13. E/1 Curves for InSb(III) in 0.02*M* $K_2Cr_2O_7$ + 0.1*N* H_2SO_4

Table II

Oxidizing or reducing agent	i_A(μA/cm²) Light	i_A (μA/cm²) Dark	i_c (μA/cm²) Light	i_c (μA/cm²) Dark
0.1*N* H_2SO_4 + 0.1 *M* $Fe_2(SO_4)_3$	+800	+500	−2000	−1500
0.1*N* H_2SO_4 + 0.02*M* $Ce(SO_4)_2$	+550	+450	− 900	− 500
0.1*N* H_2SO_4 + 0.02*M* $KMnO_4$	+500	+250	−1850	−1000
0.1*N* H_2SO_4 + 0.02*M* $K_2Cr_2O_7$	+150	+ 50	−1000	− 700
0.1*N* HCl + $FeCl_3$	—	—	− 700	− 500

On the basis of this study, one can suggest that excess carriers may be generated optically by using a beam of light to give a sharp boundary in the *n*-type indium antimonide material or, in other words, illumination is useful in the application of carrier injection into an *n*-type semiconductor electrode.

REFERENCES

[1] Brattain, W. H., Garrett, G. G.: Bell Syst. Techn. J. **34,** 129 (1955)
[2] Memming, R., Schwandt, G.: Electrochim. Acta **13,** 1299 (1968)
[3] Salem, T. M., Ismail, A. A.: J. Chem. Soc. 2415, 2419 (1970)
[4] Ismail, A. A., Salem, T. M.: J. Electroanal. Chem. Interfac. Electrochem. **42,** 105 (1973)
[5] Dewald, J. F., Hannoy, N. B., Ed.: Semiconductors, Reinhold Publishing Co., 1959 p. 727.
[6] Faust, J. W., Sagar, A.: J. Appl. Phys. **31,** 331 (1960)
[7] Gatos, H. C.: The Surface Chemistry of Metals and Semiconductors, p. 149, 1960
[8] Warekois, E. P., Metzger, P.[1]*U.*: J. Appl. Phys. **30,** 960 (1959)

T. M. Salem, A. A. Ismail — Chemistry Department, Faculty of Science, Alexandria University, Alexandria, Egypt.

Acta Chimica Academiae Scientiarum Hungaricae, Tomus 83 (3—4), pp. 259—263 (1974)

FORMATION AND STABILITIES OF PALLADIUM(II), PLATINUM(IV), GOLD(III) AND BISMUTH(III) CHELATES OF L-ASPARAGINE AND L-GLUTAMINE

R. C. TEWARI and M. N. SRIVASTAVA*

(Chemical Laboratories, University of Allahabad, Allahabad, India)

Received May 14, 1973; in revised form March 30, 1974

The metal chelates of Pd(II), Pt(IV), Au(III) and Bi(III) formed with L-asparagine and L-glutamine have been studied potentiometrically and their stepwise stability constants are repeated.

In earlier communications we reported the stability constants of some bivalent metal ion chelates of L-glutamine [1] and V(IV), Mo(VI) and W(VI) chelates of L-asparagine and L-glutamine [2]. Their formation was studied potentiometrically by IRVING and ROSSOTTI's method [3]. This paper describes the results of a similar study of Pd(II), Pt(IV), Au(III) and Bi(III) chelates formed with L-asparagine and L-glutamine.

Materials used: Palladium(II) chloride (Chempure), platinum(IV) chloride (Sisco), gold(III) chloride (Sisco), bismuth nitrate (B.D.H. AnalaR). Solutions of palladium, platinum and gold were standardized gravimetrically [4]; palladium as dimethylglyoxime complex, and platinum and gold as metals. Bismuth was determined by EDTA titration [5]. Other reagents, apparatus and procedure have been described earlier [1].

Results and discussion

The protonation constants are log K_1H 8.70, log K_2H 2.16 for L-asparagine and log K_1H 8.90, log K_2H 2.21 for L-glutamine.

The pH titrations (Figs 1 and 2) reveal that in Bi(III)-asparagine or glutamine systems a precipitate appears above pH 5.0, but in other cases the solutions remain clear throughout. Further in Pd(II)-asparagine system the titration curve first shows an inflexion at $m = 2$ (pH ~ 5) and then a buffer region from $m = 2$ to $m = 4$ (pH 5.5—8.0) whereas in Pd(II)-glutamine system the first inflexion observed at $m = 2$ occurs in pH 4—7 region and beyond that it shows a buffer region in pH 7—8.5 range. It thus indicates that in the higher pH region some hydroxochelates may also be formed. Similarly with Au(III) systems the first inflexion occurs at $m = 3$ (pH ~ 5) and then there is another buffer region from $m = 3$ to $m = 4$ (pH range 5—8) indicating the addition of an extra OH^- ligand to the gold chelate.

* *Postal address:* Dr. M. N. SRIVASTAVA, 266 (Near Distillery), Mumfordganj, Allahabad 211002 (India).

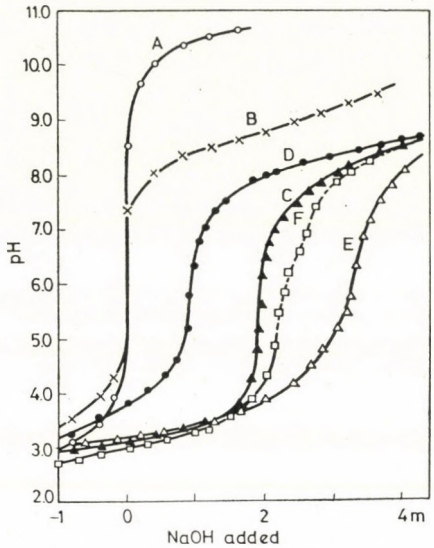

Fig. 1. pH Titration curves for Pd(II), Pt(IV), Au(III) and Bi(III) chelates of L-asparagine A ○ „0,1 *M* $NaClO_4$ + 0.004*M* $HClO_4$. All metal conc. 0.001*M*. B x A + 0.004*M* L-asparagine. C ▲ Pd(II); D ● Pt(IV), E △ Au(III); F □ Bi(III) (- - - - - indicates precipitation)

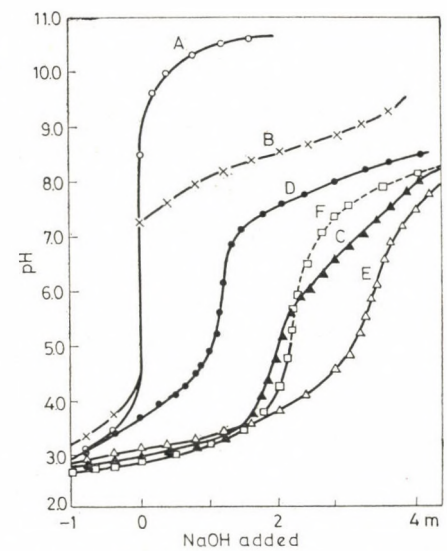

Fig. 2. pH Titration curves for Pd(II), Pt(IV), Au(III) and Bi(III) chelates of L-glutamine. A ○ 0.1*M* $NaClO_4$ + 0.004*M* $HClO_4$. All metal conc. 0.001*M*. B x A + 0.004*M* L-glutamine. C ▲ Pd(II); D ● Pt(IV); E △ Au(III); F □ Bi(III) (- - - - - indicates precipitation)

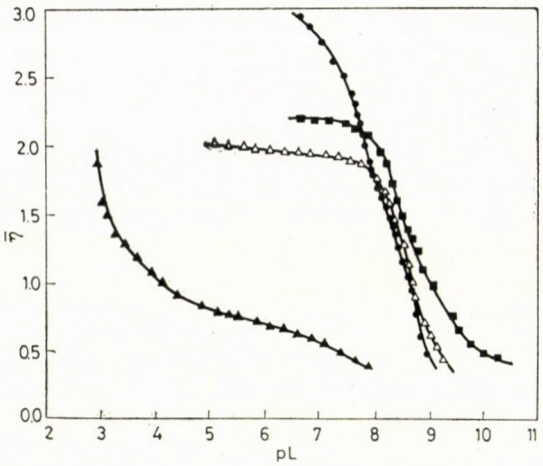

Fig. 3. Formation curves for L-asparaginate chelates. △ Pd(II); ▲ Pt(IV); ● Au(III); ■ Bi(III)

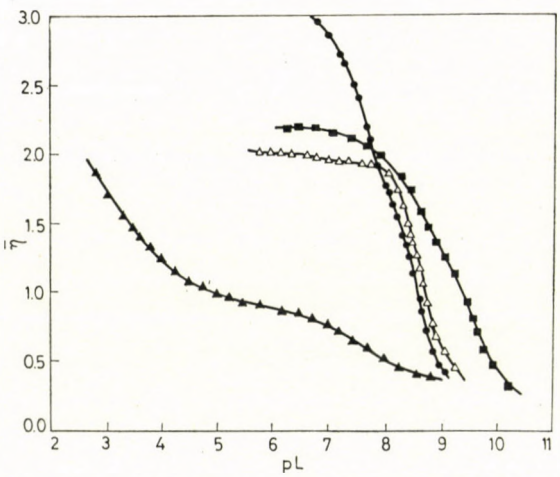

Fig. 4. Formation curves for L-glutaminate chelates. △ Pd(II); ▲ Pt(IV); ● Au(III); ■ Bi(III)

Figures 3 and 4 contain the formation curves ($\bar{n}$ *vs.* pL) of the metal chelates formed with L-asparagine and L-glutamine, respectively. The pH ranges employed for $\bar{n}$ calculations are given in Tables I and II. It is observed that for Pd(II) and Pt(IV) chelates $N = 2$, whereas for Au(III) chelates $N = 3$. In Bi(III) systems, before the precipitation point, $\bar{n}$ approaches a maximum value of approximately 2. However in Pd(II) and Bi(III) systems, it is quite probable that at lower pH values (1.9—2.5) the complexes formed may be protonated ones, since in that region the ligand species are also protonated as H_2L^+, and the relative displacements in the complex and ligand titration curves are not more than one equivalent of alkali.

Table I

Stability constants of palladium(II), platinum(IV) and bismuth(III) chelates, formed with L-*asparagine and* L-*glutamine*

(Temp. 25°C, μ 0.1 M $NaClO_4$)

Metal ion	pH range for $\bar{n}$ calculations	Method	L-Asparagine			L-Glutamine		
			log K_1	log K_2	log β_2	log K_1	log K_2	log β_2
Pd(II)	2.2—5.0	Half $\bar{n}$ values	9.30	8.35	—	9.20	8.25	—
		Correction term method	9.22	8.45	17.67	9.08	8.32	17.40
		Successive approximation method	9.15	8.50	17.65	9.10	8.35	17.45
Pt(IV)	2.8—8.6	Half $\bar{n}$ values	8.05	3.50	11.55	7.30	3.10	10.40
		By interpolation at various $\bar{n}$ values	7.98	3.52	11.50	7.31	3.15	10.46
Bi(III)	1.9—4.0	Half $\bar{n}$ values	9.85	8.80	—	9.85	8.40	—
		Correction term method	9.78	8.89	—	9.83	8.30	—
		Successive approximation method	9.76	8.88	—	9.81	8.44	—

Table II

Stability constants of Au(III) chelates formed with L-*asparagine and* L-*glutamine*

(Temp. 25 °C, μ 0.1 M $NaClO_4$)

pH range for $\bar{n}$ calculations	Method	L-Asparagine				L-Glutamine			
		log K_1	log K_2	log K_3	log β_3	log K_1	log K_2	log K_3	log β_3
2.5—5.0	Half $\bar{n}$ values	9.00	8.25	7.50	—	9.00	8.25	7.45	—
	Successive approximation method	8.88	8.14	7.60	24.62	8.88	8.13	7.58	24.59

Further in Bi(III) systems, since $\bar{n}$ approaches a maximum value of 2.2 before precipitation starts, it was considered desirable to determine its stoichiometry working at different metal–ligand ratios. Potentiometric titrations reveal that when Bi(III) : ligand ratio is 1 : 1 the first inflexion occurs at $\sim$1.8 m, which is further displaced towards 2 m in 1 : 2 Bi(III) : ligand system, and occurs at 2 m when Bi(III) : ligand ratio is 1 : 2.5 or more as in 1 : 3, and 1 : 4 systems. It thus indicates that for the first inflexion to occur (pH range 4—7) at most two equivalents of alkali are consumed in all cases. Thus the reactions may be explained in the following way.

In 1 : 1 system, with insufficient amount of ligand, the addition of the ligand and one OH occurs almost simultaneously to result in a hydroxochelate

$[BiL(OH)]^+$ which may further polymerize, whereas at higher ligand ratios as 1 : 2, 1 : 2.5 etc., primarily first a $[Bi\ L_2]^+$ chelate is formed in two overlapping steps, which of course at higher pH values can further take up OH^- ions to form a hydroxochelate. Moreover, since Bi(III) is much prone to hydrolysis, its effects can not be ruled out. It appears that above pH 4 even $[Bi\ L_2]^+$ may undergo hydrolysis, and consequent solation and polymerization reactions.

REFERENCES

[1] TEWARI, R. C., SRIVASTAVA, M. N.: J. Inorg. Nucl. Chem. **35,** 2441 (1973)
[2] TEWARI, R. C., SRIVASTAVA, M. N.: Talanta **20,** 133 (1973)
[3] IRVING, H., ROSSOTTI, H. S.: J. Chem. Soc. **3397** (1953)
[4] HILLEBRAND, W. F., LUNDELL, G. E. F., BRIGHT, H. A., HOFFMAN, J. A.: Applied Inorganic Analysis, John Wiley, New York 1953, p. 379, 364 and 366
[5] WELCHER, F. J.: The Analytical Uses of Ethylenediamine Tetraacetic Acid, D. Van Nostrand, New York 1957, p. 209

R. C. TEWARI, M. N. SRIVASTAVA } Chemical Laboratories, University of Allahabad, Allahabad, India.

Acta Chimica Academiae Scientiarum Hungaricae, Tomus 83 (3—4), pp. 265—270 (1974)

POSSIBILITIES OF USE OF TUNGSTEN OXIDE IN LIQUID-PHASE CATALYTIC HYDROGENATION

G. VÉRTES and G. HORÁNYI

(Central Chemical Research Institute of the Hungarian Academy of Sciences, Budapest H-1525/17)

Received October 3, 1973; in revised form March 18, 1974

The possibilities of utilizing tungsten oxide catalysts activated with noble metal additives were analyzed.

It was found that tungsten oxide containing a small amount of platinum or palladium can be well applied in the hydrogenation of various organic compounds.

It is known from the literature that certain research workers correlate the catalytic effect of tungsten carbide with the oxide layer developing on its surface. For example, VOORHIES [1] conceives an oxidation process on the tungsten carbide surface:

$$WC + 5\,H_2O \rightarrow WO_3 + CO_2 + 10\,H^+ + 10\,e^- \qquad (1)$$

followed by the formation of a "surface hydrogen tungsten bronze" in a subsequent reduction:

$$WO_3 + xH^+ + xe^- \rightarrow H_xWO_3 \qquad (2)$$

where the value of x may be between 0.1 and 0.5.

With the above processes, however, it is still not possible to explain the mechanism of ionization of molecular hydrogen on tungsten carbide, since here it is merely a matter of an electrochemical process between tungsten oxide and the hydrogen ion. No reference was found in the literature, suggesting the conversion of tungsten oxide to hydrogen tungsten bronze on the action of gaseous hydrogen. Our own experiments also showed that tungsten oxide does not take up hydrogen in acidic solution.

SANDSTEDE *et al.* [2] similarly observed that tungsten carbide is activated at a positive potential, but only in the case of some oxidizable substance, such as hydrogen, being present in the solution. In such a case, two types of tungsten oxide are formed, one inactive and one active. This latter is presumably able to activate hydrogen. Accordingly, the following equations can be given formally:

$$WO_3^* + \frac{x}{2}H_2 \rightarrow H_x\,WO_3 \qquad (3)$$

$$H_xWO_3 \rightleftharpoons WO_3^* + xH^+ + xe^- \qquad (4)$$

where WO_3^* denotes the at present unidentified active tungsten oxide. It must be emphasized that equation (2) differs from (4) in that the latter is a reversible process, while on the electrochemical oxidation of hydrogen tungsten bronze a compound is formed which can be reconverted with molecular hydrogen to hydrogen tungsten bronze.

Preparation of hydrogen tungsten bronze

Hydrogen tungsten bronze can be prepared "pure" independently of the tungsten carbide. If tungsten oxide is brought into contact with gaseous hydrogen in the presence of a relatively small amount of platinum, then the hydrogen undergoing dissociative adsorption on the platinum is capable of

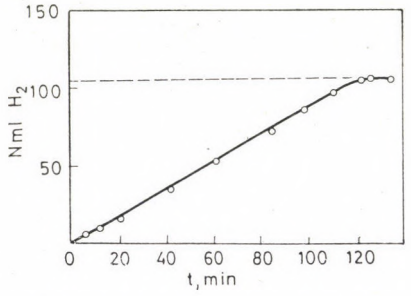

Fig. 1. Reduction of tungsten oxide on addition of 1 ml H_2PtCl_6 solution containing 1 mg Pt/ml (1 g WO_3, 2*N* H_2SO_4, 80°C)

penetrating into the oxide lattice through the metal oxide interface [3—6]. This means that the platinum-containing tungsten oxide is able to take up such an amount of hydrogen from the gas that x in the formula H_xWO_3 be $0.1 < x < 0.5$. When the earlier considerations are taken into account, it can be seen that the compound prepared in this way can in all probability be utilized to effect in the anodic oxidation of hydrogen, as has been confirmed in the recent investigations by HOBBS and TSEUNG [7].

Hydrogen tungsten bronze was prepared in the following way. One g tungsten oxide in 20 ml 2 *N* H_2SO_4 solution at 80°C was saturated with hydrogen in a hydrogenation vessel. Subsequently, 1 ml H_2PtCl_6 solution containing 1 mg Pt/ml was added to the system, and shaken vigorously. The hydrogen uptake curve is shown in Fig. 1. In the course of the reduction the initially yellow slurry becomes greenish, and later, on the completion of the uptake of hydrogen, a deep-blue (tungsten blue).

From Fig. 1 it is possible to estimate the quantity of hydrogen absorbed, and thus the composition of the hydrogen tungsten bronze. If the initial volume increase, resulting from the temperature and vapour pressure equali-

zation, is corrected then the hydrogen consumption involved is about 7—8 ml, *i.e.*, ca. 300 μmole. Compared to this, it is possible to neglect the amount of hydrogen necessary for the reduction of the 1 mg platinum, roughly 5 μmole, and for any adsorption on the monomolecular Pt layer. Calculation shows the value of x in the formula H_xWO_3 to be about 0.15 in our experiment, which is in good agreement with the value of 0.13 found by HOBBS and TSEUNG [6] for a platinum content of 0.1%.

In so far as the role of the platinum here was simply to activate the hydrogen, then this can be performed with other noble metals too. The above experiment was carried out with a $PdCl_2$ solution of similar concentration in place of the H_2PtCl_6 solution. The same phenomena could be observed in the course of the experiment as in the case of platinum.

Hydrogenation in presence of platinized tungsten oxide

If the processes of equations (3) and (4) can really be achieved, *i.e.*, if the oxide formed on the electrochemical reduction of hydrogen tungsten bronze can be reconverted on the action of gaseous hydrogen, then the hydrogen tungsten bronze can be used as a catalyst for the hydrogenation of compounds reduced according to the electrochemical mechanism.

Our experiments were performed with tungsten blue formed on the reduction of tungsten oxide containing a small amount (0.1%) of platinum or palladium. The investigations revealed that its blue colour is lost on the action of Fe^{3+}, nitrobenzene, *p*-nitrophenol and *p*-nitrocinnamic acid, and the oxidation of the bound or adsorbed hydrogen is indicated by a greenish or yellowish-green colour. A similar phenomenon can also be observed on the action of air. If the compound stands in air for a prolonged period, or is shaken in the hot solution in the presence of air, its entire hydrogen content can be oxidized. After the removal or consumption of the oxidant, both the completely oxidized tungsten blue and that containing noble metal only partially oxidized by the organic compounds can be reduced by gaseous hydrogen, and thus the process is reversible.

A study was also made of the possibility of hydrogenation of various organic compounds in the presence of platinized or palladized tungsten oxide. A typical hydrogenation curve is presented in Fig. 2. The Figure shows that, similarly as in the presence of tungsten carbide [8—10], the rate of hydrogenation is practically constant throughout the entire course of the reaction, a rate decrease being observed only on the completion of the reaction. The quantity of hydrogen taken up indicates that only the nitro group is reduced. Compared to tungsten carbide, however, there is a difference in the hydrogenation of compounds containing double bonds. The hydrogen-uptake curve for *p*-nitrocinnamic acid is shown in Fig. 3. It can be seen that although the

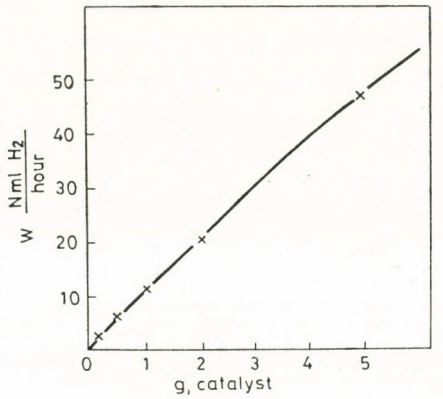

Fig. 2. Typical hydrogen uptake curve
(1 g WO_3 + 1 mg Pd, 2*N* H_2SO_4, 80°C, 0.2 g *p*-nitrophenol)

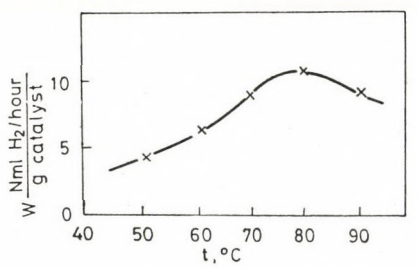

Fig. 3. Hydrogenation of *p*-nitrocinnamic acid on tungsten blue
(1 g WO_3 + 1 mg Pd, 2*N* H_2SO_4, 80 °C)
n_{H_2}/n_S = No. of moles of hydrogen taken up/No. of moles or org. compd. taken

aromatic ring cannot be hydrogenated, besides the three moles of hydrogen required for the nitro group a fourth mole of hydrogen is consumed by the double bond. A further examination was made of the hydrogenation of maleic acid on tungsten oxide containing 0.1% palladium. The experiments showed that although the initial rate of hydrogenation is perhaps not significantly less than the value found for the nitro compounds, the rate at first decreases very rapidly, and later too very perceptibly. The poisoning or aging of the catalyst is indicated by the fact that if some nitro compound is added to the system after the maleic acid, although a rate increase can be observed, the rate found with the nitro compounds can no longer be approached.

The temperature dependence of the rate of hydrogenation of *p*-nitrophenol on tungsten blue prepared by reduction of palladized tungsten oxide is presented in Figure 4. The rate decrease observed at higher temperature can be explained by the decrease of the partial pressure of the hydrogen, as treated in detail in the case of tungsten carbide [10].

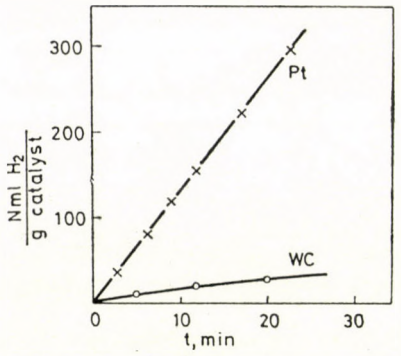

Fig. 4. Temperature-dependence of rate of hydrogenation (1 g WO_3 + 1 mg Pd, 2*N* H_2SO_4, *p*-nitrophenol, 80°C)

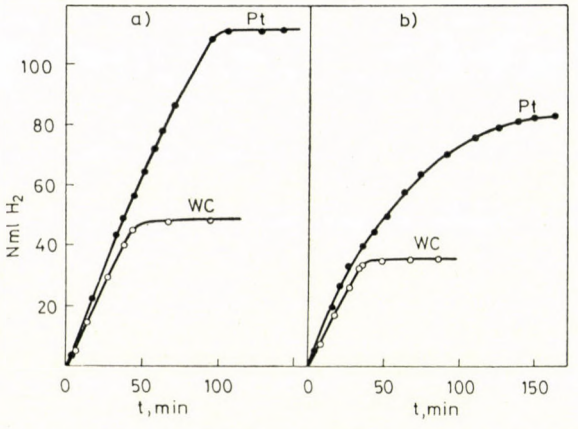

Fig. 5. Hydrogen uptake on WO_3 containing 1% Pd (1 g WO_3 + 10 mg Pd, 2*N* H_2SO_4, 80°C). (a) reduction of tungsten oxide; (b) reduction of *p*-nitrophenol

Some informatory experiments were also carried out using tungsten oxide with a higher noble metal content. The catalytic activity of the tungsten blue appears to be nearly proportional to the amount of noble metal taken up. Proof of this is given in Fig. 5. One ml palladium chloride solution with a concentration of 10 mg Pd/ml was added to 1 g tungsten oxide in 20 ml 2 *N* H_2SO_4 solution at 80°C. The first part of the Figure gives the rate of uptake of hydrogen as a function of the amount of hydrogen taken up. (From the amount of hydrogen absorbed, the value of x is obtained as ca. 0.3). After a considerable decrease in the rate of hydrogen uptake, *p*-nitrophenol was added to the system (indicated by an arrow). The rate maximum observed in the preparation of tungsten blue was then again attained.

Discussion

It was established in the experiments that tungsten oxide containing a small amount of noble metal can well be used for the hydrogenation of various organic compounds. The data presented to date permit the following conclusions as regards the mechanism of the hydrogenation.

The experiment illustrated in Fig. 5 clearly indicates that a transport process cannot play a rate-controlling role in the hydrogen uptake rate of ca. 50 ml/hour observed for tungsten oxide containing 0.1% of noble metal, for a rate larger by one order of magnitude can also be achieved under completely identical conditions.

The hydrogenation of unsaturated compounds too can be achieved on tungsten blue containing noble metal. This observation shows that, in contrast with tungsten carbide, the adsorption of the unsaturated compounds takes place to at least a certain extent on the surface. A difference from platinum, however, is that the aromatic ring is not hydrogenated, and thus its adsorption is presumably different from the simple double-bond adsorption. The appreciable rate decrease observed on the hydrogenation of maleic acid indicates that the catalytically active sites are relatively quickly poisoned. This can be conceived, for instance, in that these active sites on which the unsaturated compound may be adsorbed consist of noble metal bound on the surface of the tungsten oxide. The reaction initially proceeds fairly rapidly on the still clean noble metal surface, but later, as a result of the adsorption various molecular fragments and possibly polymers are formed on the surface, and these soon cover the comparatively small active surface available.

Further investigations are required to extend the utilizability of catalysts containing a small amount of noble metal, to clarify in greater detail their mechanisms of action, and to confirm our assumptions. These will be reported in a subsequent paper.

REFERENCES

[1] VOORHIES, J. D.: J. Electrochem. Soc. **119,** 219 (1972)
[2] VON BENDA, K., BINDER, H., KÖHLING, A., SANDSTEDE, G.: From Electrocatalysis to Fuel Cells. (Ed).: Sandstede, G., Battelle Seattle Research Center, 1972, p. 87.
[3] BENSON, J. E., KOHN, H. W., BOUDART, M.: J. Catalysis **5,** 307 (1966)
[4] BOUDART, M., VANNICE, M. A., BENSON, J. E.: Z. phys. Chem. N. F. **64,** 171 (1969)
[5] HOBBS, B. S., TSEUNG, A. C. C.: Nature **222,** 556 (1969)
[6] HOBBS, B. S., TSEUNG, A. C. C.: J. Electrochem. Soc. **119,** 580 (1972)
[7] HOBBS, B. S., TSEUNG, A. C. C.: J. Electrochem. Soc. **120,** 766 (1973)
[8] HORÁNYI, G., FÉZLER, G., VÉRTES, G.: Magy. Kém. Foly. **78,** 575 (1972)
[9] HORÁNYI, G., VÉRTES, G., FÉZLER, G.: Z. phys. Chem. N. F. **83,** 322 (1973)
[10] VÉRTES, G., HORÁNYI, G., SZAKÁCS, S.: J. Chem. Soc., Perkin II. **1973,** 1400

György VÉRTES
György HORÁNYI
Központi Kémiai Kutató Intézet,
1025 Budapest, Pusztaszeri út 57—69, Hungary.

Acta Chimica Academiae Scientiarum Hungaricae, Tomus 83 (3—4), pp. 271—279 (1974)

SPECTROPHOTOMETRIC STUDIES ON PURPURIN AND QUINALIZARIN IN BUFFER SOLUTIONS CONTAINING ORGANIC SOLVENTS

I. M. ISSA, R. M. ISSA*, K. A. IDRISS and A. M. HAMMAM

(Chemistry Department, Faculty of Science, University of Assiut, Assiut, Egypt (A.R.E.))

Received October 8, 1973; in revised form April 10, 1974

The electronic absorption spectra of purpurin and quinalizarin were studied in both water and water–organic solvent mixtures at different pH's. The solvents used include methanol, ethanol, ethylene glycol, glycerol and acetone. The effect of solvent polarity on the band position is discussed. The pK values have been determined for different equilibria and are discussed in relation to the nature and amount of the organic solvent. The pK_1 and pK_2 values for both compounds decrease with increasing proportion of ethylene glycol or glycerol but increase with increasing amount of methanol, ethanol or acetone.

Introduction

Purpurin (1,2,3-trihydroxyanthraquinone) and quinalizarin (1,2,5,8-tetrahydroxyanthraquinone) are known as histological reagents and chelating agents in analytical chemistry. The spectra of these compounds in buffer solutions and in some organic solvents were previously studied [1—4]. The present work deals with the effect of pH on the electronic absorption spectra in the presence of organic solvents. The pK values have been determined and will be discussed with reference to the nature of the medium used.

Experimental

The solid materials (AR or CP grade) were obtained from commercial sources (E. Merck or B.D.H.). 10^{-3} M solutions of the anthraquinone derivatives were prepared by dissolving the appropriate amount of the solid in 0.1M NaOH. More dilute solutions were prepared by accurate dilution. The pH was adjusted by the modified universal buffer series of BRITTON [5] which also served as supporting electrolyte. The organic solvents were purified by recommended procedures [6].

The absorption spectra were recorded on a UNICAM SP 500 Spectrophotometer at the wavelength range of 320—700 nm, using matched 1 cm silica cells. The pH measurements were carried out with a Radiometer pH-meter (Model 28bM) accurate to within ± 0.05 pH units. All pH and spectral measurements were carried out at room temperature ($\sim$25 °C).

Results and discussion

The spectral behaviour of purpurin and quinalizarin in aqueous buffer solutions was studied by ISSA and ZEWAIL [3], who found that only two equi-

* Present Adress: Chemistry Department, Faculty of Science, Tanta, Egypt.

libria existed for these compounds. The spectral behaviour was discussed with reference to the different species that may exist in solution. It seemed of interest to determine the first and second dissociation constants of the two compounds in water and to compare them with the values obtained in media containing organic solvents.

I. Purpurin

The spectra of purpurin solutions of constant concentration, recorded as a function of the pH and in the presence of various amounts of different organic solvents consist of three bands. The position of the bands is mainly affected by the pH and to some extent by the nature and amount of the solvent added. The first band with a maximum at about 400 nm is presumably due to the neutral molecule.

This band increases in intensity upon increasing the pH to 8. At higher pH's, the band decreases and shifts to the red. The absorption at this wavelength is mostly higher than at other bands. As the ionization of purpurin proceeds, the asymmetry or splitting of the bands becomes quite apparent. The different organic solvents cause various changes in the absorbance of the divalent anions, and the corresponding λ_{max} is affected by the nature and amount of the solvent added.

The second ionization step of purpurin starts at the pH range of 10—11 in all the mixtures investigated. Under such conditions the spectra show strongly overlapping and asymmetrical bands presumably as a result of the existence of various species. In solutions containing ~4—40% (by weight) of the different solvents, the absorbance *vs.* pH curves obtained at selected wavelenghts are similar in character and show two apparent staps. The absorbance increases with the pH up to 8—10 and then decreases rapidly at higher pH's, owing to the formation of divalent anions. The absorbance *vs.* pH plots obtained at 550 nm exhibit a continuous increase with the pH and show two inflections indicating two equilibria:

$$H_3A \rightleftharpoons H_2A^- + H^+$$
$$H_2A^- \rightleftharpoons HA^{--} + H^+$$

The separation of the two stages is sharper at high concentrations of glycerol or ethylene glycol but appears to be poor in solutions containing methanol or ethanol.

The pK_1 and pK_2 values of the two equilibria were evaluated by the following methods:

a) Modified COLLETER method [7, 8], whereby the dissociation constant (K) can be determined from the relation:

$$K = \frac{[H^+]_2 - M[H^+]_3}{M - 1}$$

$$M = \left(\frac{A_3 - A_1}{A_2 - A_1}\right) \cdot \frac{[H^+]_1 - [H^+]_2}{[H^+]_1 - [H^+]_3}$$

where

A_1, A_2 and A_3 are absorbance values at $[H^+]_1$, $[H^+]_2$ and $[H^+]_3$.

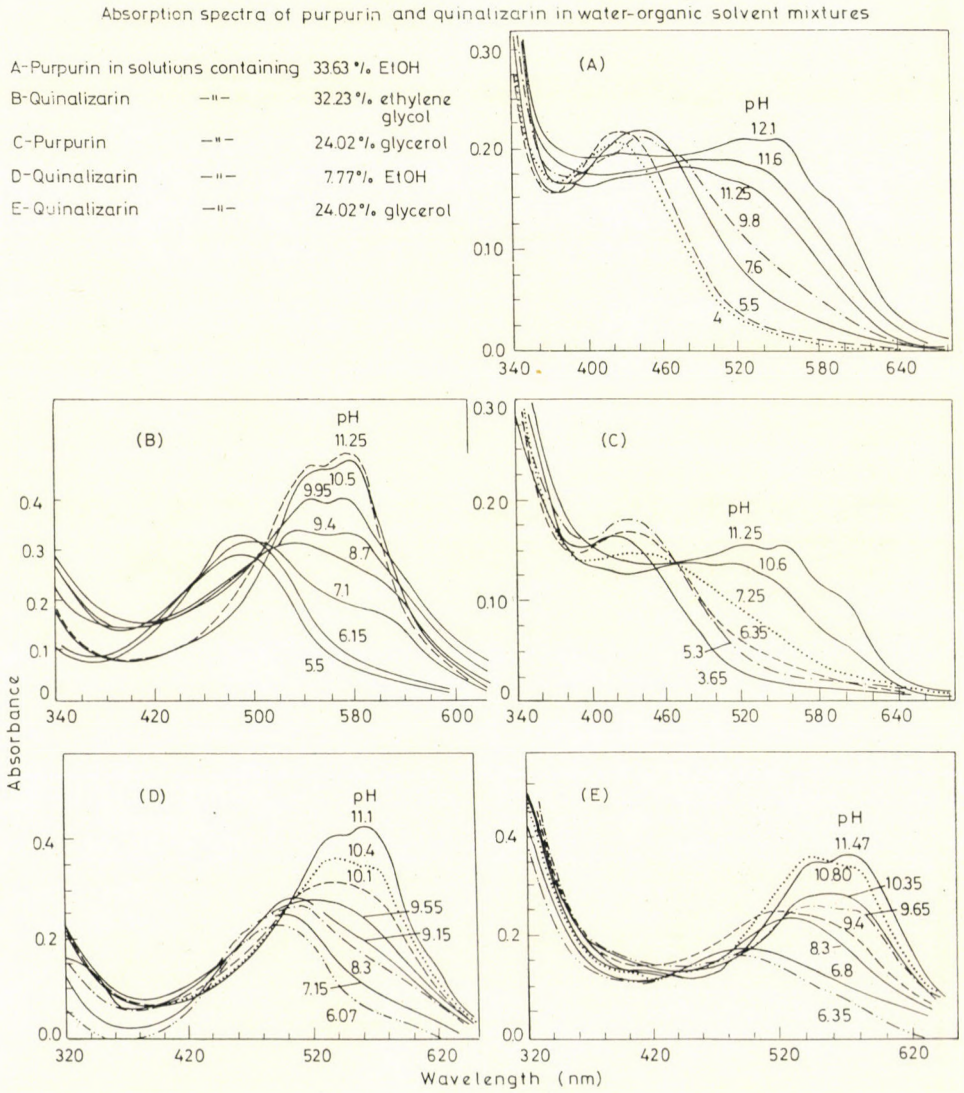

Fig. 1

b) Limiting absorbance method [9] according to which:

$$\mathrm{pH} = (pK + \log\gamma) + \log\frac{A}{A_1 - A}$$

where A_1 is the limiting absorbance, A is the absorbance at at given pH and γ is the activity coefficient of the ionic form.

Thus the pK can be determined from the plot of $\log A/(A_1 - A)$ against the pH.

The mean values of pK_1 and pK_2 in the presence of various amounts of organic solvents are listed in Table I.

Table I

Mean values of pK_1 and pK_2 for purpurin (10^{-4} M) and quinalizarin (4×10^{-5} M) in water–organic solvent mixtures

Organic solvent mixed	% (w/w) of organic solvent	Dielectric constant of the medium	Purpurin		Quinalizarin	
			pK_1	pK_2	pK_1	pK_2
Methanol	4.1	79.8	6.33	11.3	8.3	9.32
	8.2	78.12	6.85	10.84	7.32	9.45
	16.6	74.96	7.25	10.92	8.06	10.1
	25.1	71.47	7.28	11.08	8.4	10.3
	34.7	67.71	7.17	11.42	8.45	10.4
Ethanol	3.9	77.5	6.32	11.1	6.71	9.65
	7.8	76.6	6.34	10.23	6.42	9.59
	15.9	74.7	6.57	10.25	6.64	9.82
	24.6	72.7	6.6	10.7	6.65	10.16
	33.6	68.7	6.89	10.82	6.8	10.58
Acetone	4.1	80.13	5.95	10.3	7.68	9.28
	7.1	79.28	6.2	10.45	7.88	9.45
	16.6	77.49	6.65	10.65	8.28	10.1
	25.5	75.41	8.0	11.15	9.05	10.86
Ethylene glycol	5.6	80.22	6.7	10.7	8.65	9.96
	11.0	79.47	6.52	10.5	7.12	9.75
	21.7	77.92	5.65	10.15	6.95	9.54
	32.2	76.12	5.55	9.4	6.82	9.13
	42.5	73.91	5.15	9.1	6.85	8.66
Glycerol	6.3	81.06	6.85	11.06	8.29	9.52
	12.3	80.02	6.72	11.0	8.1	9.32
	24.6	78.8	6.6	10.65	7.45	9.3
	35.2	77.23	6.25	10.45	7.31	8.99
	45.8	75.51	6.2	10.08	7.14	8.8
Aqueous medium	—	75.5	6.9	11.35	8.89	10.22

It is apparent that both pK_1 and pK_2 decrease on increasing the amount of ethylene glycol or glycerol but increase as the proportion of methyl or ethyl alcohol is increased. This behaviour indicates that the former solvents act as acceptors rather than donors and hence cause protonation of the lone pairs of the OH-groups and facilitate proton dissociation from the hydroxyl groups. The change in behaviour is due to the differences in structure and polarity of the solvent molecules mixed with purpurin solutions. The decreasing ionization in the presence of high proportions of methanol, ethanol or acetone may be attributed to the blocking of the π-electrons of the carbonyl group by solvent molecules which renders excitation of the π electrons more difficult, thus higher pK values are obtained. The displacement of the absorption bands to shorter wavelengths caused by increasing ethanol, methanol or acetone concentration at constant pH can be attributed to the decreasing concentration of the ionized forms as a result of association with the solvent molecules. On the other hand, the bands are shifted to longer wavelengths on mixing increasing amounts of ethylene glycol and glycerol at any specific pH.

II. Quinalizarin

Within the pH range of 6—8.5, the spectra of quinalizarin exhibit one nearly symmetrical band with maximum absorption at wavelengths varying from 470 to 490 nm. The next band with λ_{max} at 520 nm appears at pH 8.5—9 and is due to the monoanion of the compound. At pH $\leq$ 9.5, the spectrum reveals two peaks at 540 and 570 nm resulting from absorption by the mono- and dianion.

In Table I are given the data obtained on mixing a solution of quinalizarin, at different pH's, with various amounts of each of methanol, ethanol, ethylene glycol, glycerol or acetone. The plots of absorbance *vs.* pH at specific wavelengths for some of the solutions are shown in Fig. 2-B.

The curves reveal a more or less pronounced *S*-shape with a break on the rising section at a certain pH range which depends on the composition of the solution.

The pK_a values corresponding to the first and second dissociation steps of quinalizarin were determined by applying the methods mentioned above.

The effect of different solvents on the pK are similar to that observed in the case of purpurin and can be explained on the same basis.

Discussion

As the amount of organic solvent in the medium increases, the pH range for spectral measurements increases owing to the higher solubility of the uncharged molecules. This is apparent from the spectra and the absorbance *vs.* pH plots shown in Figs 1 and 2.

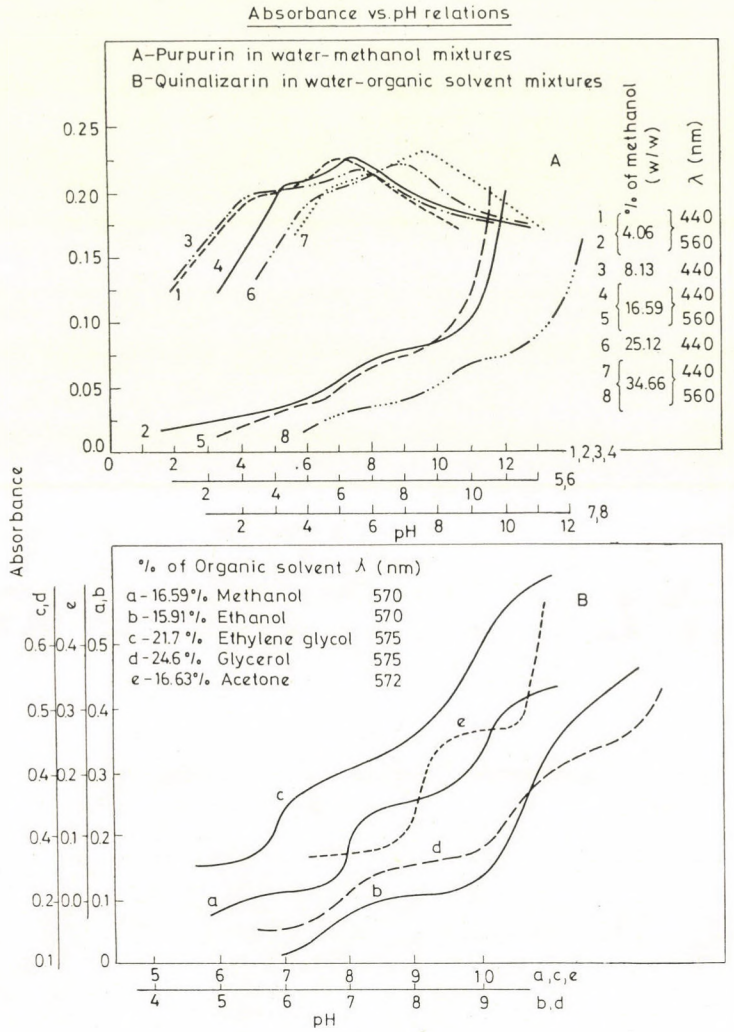

Fig. 2

The bands undergo a red shift on increasing the concentration of glycerol and ethylene glycol. This behaviour depends on solvation effects [10] rather than the dielectric constant of the medium as shown by the non-linearity of the ν or λ_{max} *vs.* $1/D$ plots.

The pK values in aqueous solutions are higher than those obtained in mixed solvents (see Table I), which thus favour ionization. The rate with which the ionic forms are produced is influenced by both the nature and amount of the organic solvent added. The removal of the proton is facilitated by the increasing amounts of ethylene glycol or glycerol, whereas the increase of the proportion of alcohol or acetone decreases ionization.

The change of pK with solvent concentration is due to factors such as changes in the dielectric constant of the medium, solvolysis of ions and basicity of the solvent mixture. The variation of pK with dielectric constant (D) in solvent mixtures is given by the relation [11]

$$pK_a = pK_0 + \frac{0.43\,Ne^2}{RT}\,\frac{Z_1 Z_2}{r_1 + r_2}\,\frac{1}{D}$$

where: pK_a — acid dissociation constant in the solvent mixture;
pK_0 — acid dissociation constant in pure water;
Z_1, Z_2 — charges carried of the ions involved in the equilibrium;
r_1, r_2 — radii of the ions involved in the equilibrium.

The plots of pK_a against $1/D$ are, however, not strictly linear except in a few cases. This indicates that changes in the pK_a with the solvent concentration, though mainly governed by the dielectric constant, are strongly influenced by solvent basicities too. The decrease in solvent basicity is quite apparent with alcohols and acetone and this in turn leads to a decreased ionization of the OH groups in the compounds investigated. Glycerol and ethylene glycol, though less basic than water [11], can still solvate the organic molecules and its ions more strongly than water, thus increasing the solvolysis constant. This leads to a lower acid dissociation constant in accordance with the relation:

$$K_a = \frac{K_D}{1 + K_s}$$

where: K_D — dissociation constant of the solvated ion pairs;
K_s — solvolysis constant.

Accordingly, it seems that the contribution of any single factor to the total effect on the pK_a values in water–organic solvent mixtures will depend on the properties of the solvent and solute used.

Correlation of the pK values

The pK_1 values determined for purpurin and quinalizarin indicate that the latter compound is a stronger acid in all the solvent systems investigated. This behaviour can be explained in terms of the structure. The first dissociation step in both compounds will involve the release of a proton from the β-OH group since the latter is not liable to participate in hydrogen bonding.

In the case of purpurin, the presence of the other two OH groups on the same ring carrying the β-OH group lowers the contribution of this group in charge donation to the anthraquinone nucleus. Charge migration from the β-OH

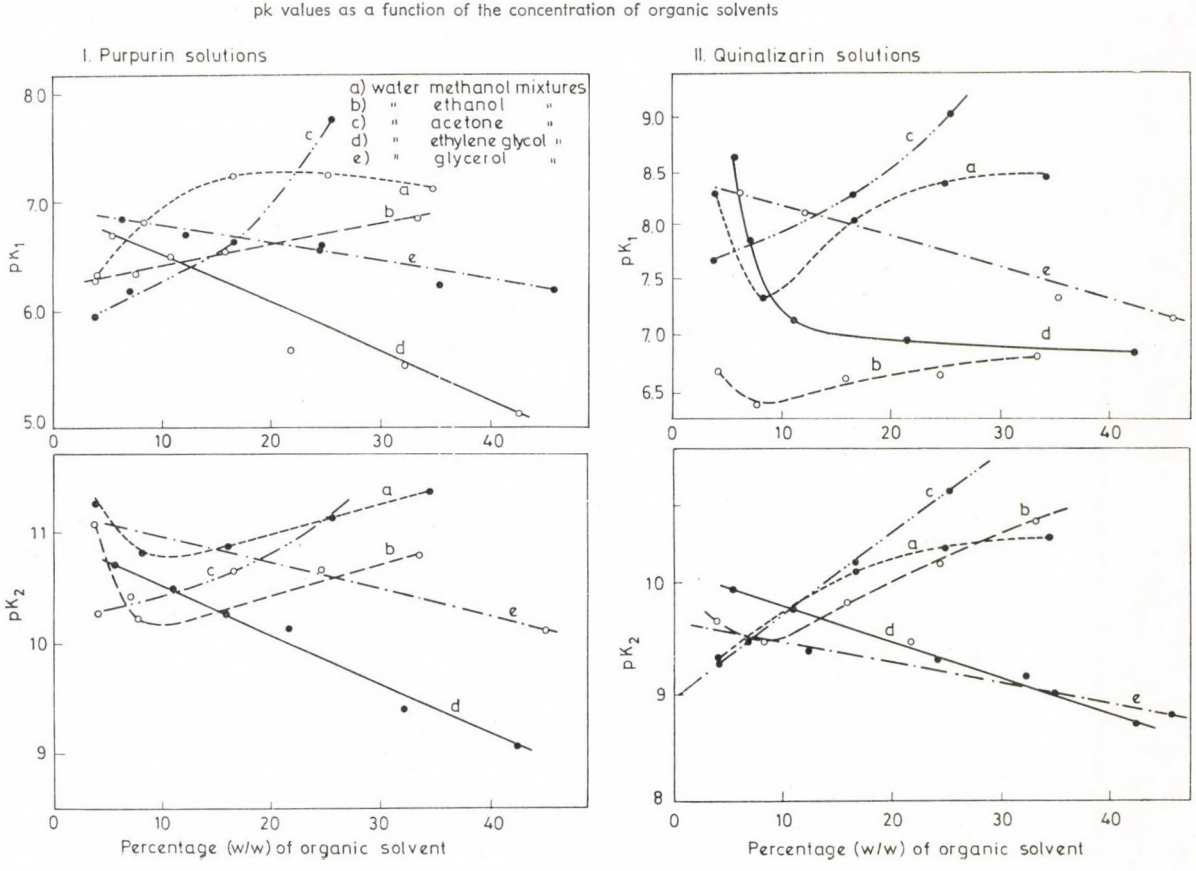
pk values as a function of the concentration of organic solvents
I. Purpurin solutions
II. Quinalizarin solutions
a) water methanol mixtures
b) " ethanol "
c) " acetone "
d) " ethylene glycol "
e) " glycerol "
pK1
pK2
Percentage (w/w) of organic solvent
Percentage (w/w) of organic solvent

Fig. 3

group through mesomeric interaction with the 9-C=O group will be counteracted by the OH group in position 4. This occurs by a tautomeric shift of the type:

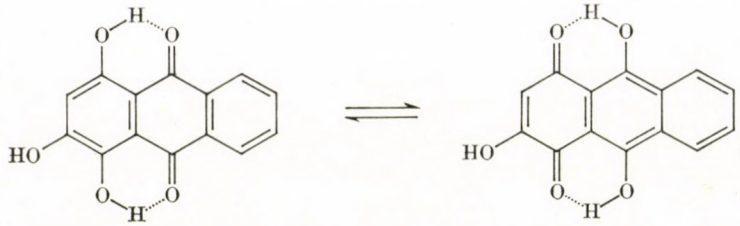

The higher charge density on the oxygen atom of the OH group in purpurin affords stronger bonding of the protons. The opposing effect of the tautomeric shift is of minor influence in the case of quinalizarin since the α-OH groups occupy the 1, 5 positions.

The second proton in the case of purpurin is dissociated from an OH group involved in a stronger H-bonding than that of quinalizarin and hence the pK_2 is higher for the former compound.

REFERENCES

[1] Pavlovskaya, M. P., Kishinev, Tr.: Sel. Khoz. Inst. **43,** 97 (1966)
[2] El-Ezaby, M. S., Salem, T. M., Zewail, A., Issa, R. M.: J. Chem. Soc. **1333** (1969)
[3] Issa, R. M., Zewail, A. H.: J. Chem. A. R. E. **14,** 461 (1971)
[4] Issa, R. M., Idriss, K. A., Hammam, A. M.: J. Chem. A. R. E. **17** (1972)
[5] Britton, H. T. S.: Hydrogen Yons. 4th Edition, Chapman & Hall 1952
[6] Vogel, A. I.: Practical Organic Chemistry. Longmans, London 1956.
[7] Colleter, I. C.: Annal. Chim. **5,** 415 (1960)
[8] Issa, R. M., Abdel-Halim, F. M., Hassanein, A. A.: Electrochim. Acta **14,** 561 (1969)
[9] Issa, R. M.: J. Chem. A. R. E. **14,** 113 (1971)
[10] Gáti, L., Szalay, L.: Acta Univ. Szegediensis, Acta Phys. et Chem. **5,** 87 (1959)
[11] Charlot, G., Tremillon, B.: Chemical Reactions in Solvents and Melts, Pergamon Press 1969. pp. 55, 306.

I. M. Issa
R. M. Issa
K. A. Idriss
A. M. Hammam

Chemistry Department, Faculty of Science,
University of Assiut,
Assiut, Egypt (A.R.E.)

Acta Chimica Academiae Scientiarum Hungaricae, Tomus 83 (3—4), pp. 281—289 (1974)

ON THE α-DIOXIMINE COMPLEXES OF TRANSITION METALS, XLVII

CYANO-HALOGENO-BIS-DIMETHYLGLYOXIMATO-COBALT(III) COMPLEX ACIDS AND THE AQUATION OF THE $[Co(DH)_2(CN)X]^-$ IONS

Z. FINTA and Cs. VÁRHELYI

(Faculty of Chemistry, Babes-Bólyai University, Cluj, Romania)

Received December 14, 1973; in revised form June 10, 1974

Three new monobasic complex acids: $H[Co(DH)_2(CN)X]$ (DH_2 = dimethylglyoxime, X = Cl, Br and I) were obtained by means of ligand exchange reactions from the corresponding dihalogeno acids: $H[Co(DH)_2X_2]$ and KCN. A number of 18 salts of these mixed acids were isolated and characterized. pH measurements were performed in order to test the strength of these acids. Their IR spectra were recorded and discussed. In aqueous solutions of these complex anions the halide ions are substituted by water. Kinetics of this aquation process in acidic medium was followed and kinetic parameters are derived. The mechanism of the aquation was discussed.

Complex compounds of cobalt(III) with cyano ligands were described and studied only in a few cases. The well known $K_3[Co(CN)_6]$ is formed easily by oxidation of cobalt(II)-salts in the presence of KCN [1]. The free acid: $H_3[Co(CN)_6]$ and some aquocyano acids, as $H_2[Co(CN)_5(H_2O)]$ [2], $H[Co(CN)_4(H_2O)_2]$ [3] and the halogeno pentacyano-acids $H_2[Co(CN)_5X]$ (X = Cl, Br, I) [4] were also isolated and kinetically studied [4—7]. Substitution reactions of the $[Co(CN)_4(SO_3)(OH)]^{4-}$ anion with CN^- and NH_3 were investigated by TEWARI *et al.* [8].

The first cyano-complex of the cobalt(III)-dioximine class, the $K[Co(DH)_2(CN)_2] \cdot 3/2\ H_2O$, was described by MAKI [9, 10]. In a previous paper [12] the chemical properties of some analogous derivatives of the acids $H[Co(Diox.\ H)_2(CN)_2]$ (Diox. H_2 stands for 1,2-cyclohexanedionedioxime and 1,2-cyclopentanedionedioxime) are reported.

The interest for this class of co-ordination compounds has been increased after the discovery of the analogy in the structure of the B_{12}-vitamine-type substances and the cyano-dioximine complexes of the trevalent cobalt, which have similar molecular skeleton [13—15]. Complex compounds of this type are used actually for the study '*in vitro*' of the kinetics and mechanism of different enzymatic reactions, catalyzed by B_{12}-vitamin derivatives [16, 17].

The strong nucleophilic cyano group easily enters in the inner co-ordination sphere of different mixed dioximine chelates of cobalt(III), as $[Co(Diox.\ H)_2(H_2O)X]$ and $[Co(Diox.\ H)_2X_2]^-$ with X = Cl, Br, I, etc. We observed that a large excess of CN^- replaces also other neutral ligands, as NH_3 and primary amines (aniline derivatives) or pyridine bases. In hot aqueous

KCN solutions even the Co-dioxime rings are split and $[Co(CN)_6]^{3-}$ is formed (*e.g.* in the case of $[Co(DH)_2(NH_3)_2]^+$ and $[Co(DH)_2(aniline)_2]^+$).

The substitution reaction of the dihalogeno-acids of the type $H[Co(DH)_2X_2]$ with stoichiometric amount of KCN at room temperature leads to the formation of mixed cyano–halogeno complexes:

$$[Co(DH)_2X_2]^- + CN^- = [Co(DH)_2(CN)X]^- + X^- . \qquad (1)$$

By using an excess of KCN, the second halide ion is also exchanged and the dicyano-ion, $[Co(DH)_2(CN)_2]^-$, is formed.

The free acids $H[Co(DH)_2(CN)X]$ can be separated from the aqueous solutions of their salts with an excess of diluted sulfuric acid.

Table I

Cyano–halogeno complex acids of the type $H[Co(DH)_2(CN)X]$

Formula	Mol. wt. calcd.	Yield (%)	Aspect	Analysis	
				Calcd.	Found
$H[Co(DH)_2(CN)Cl] \cdot 1\ H_2O$	369.6	60	Irregular yellow plates	Co 15.94 N 18.95	15.84 18.70
$H[Co(DH)_2(CN)Br] \cdot 2\ H_2O$	432.1	70	Irregular brown-yellow plates	Co 13.64 N 16.20	13.42 16.35
$H[Co(DH)_2(CN)I] \cdot 2\ H_2O$	479.1	80	Sparkling brown-yellow hexagonal plates	Co 12.30 N 14.62	12.20 14.53

$DH = C_4H_7N_2O_2$

Like other $[Co(DH)_2XY]^-$-type anions, the cyano–halogeno complexes readily form slightly soluble precipitates with monovalent ions as Cs^+, Tl^+, Cu^+, Ag^+ and Hg_2^{2+}, and with diacido-tetramine type complexes of cobalt(III) and chromium(III), as $[Me(NH_3)_4X_2]^+$, $[Me(en)_2X_2]^+$, $[Me(pn)_2X_2]^+$ ('en' and 'pn' are ethylenediamine and 1,2-propylenediamine, respectively). In aqueous suspensions, at higher temperatures, Ag^+- and Hg_2^{2+}-ions decompose them by the separation of the corresponding metal halides. One cannot perform double decomposition reactions with hexamine- and mono-acido-pentamine type complexes, as $[Me(NH_3)_6]^{3+}$, $[Me(en)_3]^{3+}$, $[Me(NH_3)_5(H_2O)]^{3+}$, $[Me(NH_3)_5X]^{2+}$, $[Me(en)_2X(amine)]^{2+}$, etc.

Like other $[Co(Diox.\ H)_2XY]^-$ anions, the cyano–halogeno complexes readily form $[Co(Diox.\ H)_2(amine)_2][Co(DH)_2(CN)X]$ type binary salts. (Diox. H_2 stands for a molecule of cyclopentane-, cyclohexane- or cycloheptane-dione-dioxime, dimethylglyoxime or diaminoglyoxime, respectively, 'amine' is ammonia, aromatic amines or pyridine bases.)

Table II

Cobalt(III)- and chromium(III)-amine derivatives of the $[Co(DH)_2(CN)X]^-$ ions

No.	Formula	Mol. wt. calcd.	Yield (%)	Aspect	Analysis	
					Calcd.	Found
1.	*trans*-$[Co(en)_2Cl_2]$ · $[Co(DH)_2(CN)Cl]$	600.5	40	Brown, long thin needles	Co 19.63 N 20.98	19.35 20.61
2.	*trans*-$[Co(en)_2Cl_2]$ · $[Co(DH)_2(CN)Br]$	644.9	45	green-yellow long plates	Co 18.28	18.60
3.	*trans*-$[Co(en)_2Cl_2]$ · $[Co(DH)_2(CN)I]$	691.9	55	long brown prisms	Co 17.04	17.23
4.	*trans*-$[Co(pn)_2Cl_2]$ · $[Co(DH)_2(CN)I]$	720.2	50	sparkling, brown rhomb. plates	Co 16.37 N 17.50	16.19 17.26
5.	*trans*-$[Cr(en)_2(NCS)_2]$ · $[Co(DH)_2(CN)Cl]$	638.8	60	brown-yellow microcryst.	1/3 Co_3O_4 + 1/2 Cr_2O_3 24.46 N 24.10	24.23 23.85
6.	*trans*-$[Cr(en)_2(NCS)_2]$ · $[Co(DH)_2(CN)Br]$	683.3	65	brown-yellow irregular plates	1/3 Co_3O_4 + 1/2 Cr_2O_3 22.87 N 22.54	22.60 22.70
7.	*trans*-$[Cr(en)_2(NCS)_2]$ · $[Co(DH)_2(CN)I]$	730.2	70	brown, long needles	1/3 Co_3O_4 + 1/2 Cr_2O_3 21.40 N 21.09	21.60 20.74
8.	$[Co(DH)_2(\beta\text{-naphtylamine})_2]$ · $[Co(DH)_2(CN)Cl]$	926.1	80	brilliant, brown irregular plates	Co 12.73 N 16.63	12.55 16.47
9.	$[Co(DH)_2(\beta\text{-naphtylamine})_2]$ · $]Co(DH)_2(CN)Br]$	970.1	85	brown, irregular sparkling dendrites	Co 12.14	12.06
10.	$[Co(DH)_2(\beta\text{-naphtylamine})_2]$ · $[Co(DH)_2(CN)I]$	1017.6	90	brown dendrites	Co 11.58 N 15.13	11.65 15.37
11.	$[Co(DH)_2(p\text{-phenetidine})_2]$ · $[Co(DH)_2(CN)Br]$	958.5	60	brown prisms	Co 12.30 N 16.06	12.08 16.29
12.	$[Co(DH)_2(m\text{-xylidine})_2]$ · $[Co(DH)_2(CN)Br]$	926.4	65	brown needles	Co 12.73	12.90
13.	$[Co(DH)_2(pyridine)_2]$ · $[Co(DH)_2(CN)Cl]$	798	60	short, brown prisms	Co 14.77 N 18.28	14.59 18.44
14.	$[Co(DH)_2(pyridine)_2]$ · $[Co(DH)_2(CN)Br]$	842.4	60	brilliant rhomb. plates	Co 13.99	13.69
15.	$[Co(DH)_2(pyridine)_2]$ · $[Co(DH)_2(CN)I]$	889.4	70	brown microcryst.	Co 13.25	13.21
16.	$[Co(pyridine)_4Cl_2]$ · $[Co(DH)_2(CN)Cl]$	796.9	80	yellow-green plates	Co 14.86	14.77
17.	$[Co(pyridine)_4Cl_2]$ · $[Co(DH)_2(CN)Br]$	841.3	80	brilliant, yellow dendrites	Co 13.69	13.79
18.	$[Co(pyridine)_4Cl_2]$ · $[Co(DH)_2(CN)I]$	888.3		brilliant, brown dendrites	Co 13.27 N 14.18	13.17 14.33

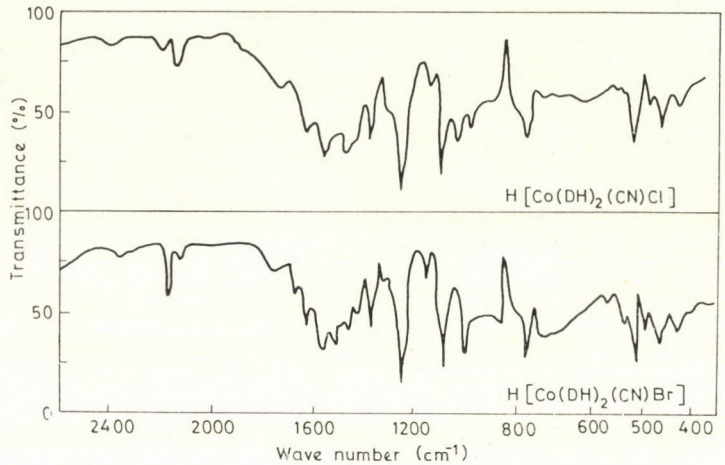

Fig. 1. IR spectra of the $H[Co(DH)_2(CN)Cl]$ and $H[Co(DH)_2(CN)Br]$ acids

The IR spectrum of the $H[Co(DH)_2(CN)Cl] \cdot H_2O$ and $H[Co(DH)_2(CN)Br] \cdot 2\,H_2O$ complex acids (see Fig. 1) shows the presence of strong intramolecular O—H ——— O hydrogen bridges (νO—H: 2350—2400 cm^{-1} (weak), δO—H: 1740—1760 and 1720 cm^{-1} (weak)), similar to those observed in the case of other bis-dimethylglyoxime cobalt(III)-complexes, as $H[Co(DH)_2X_2]$ or $[Co(DH)_2(amine)_2]X$. These hydrogen bridges stabilize the coplanar $Co(DH)_2$ ring system, *i.e.*, the '*trans*' configuration of the complexes of this type and therefore ligand exchange reactions occur with retention of their configuration.

The νC=N vibrations of the co-ordinated oxime groups have been found at 1575 and 1565 cm^{-1} (medium). This band is situated at 1620—1640 cm^{-1} in the spectrum of the non-co-ordinated dimethylglyoxime.

The two strong bands at 1085—1090 and 1241 cm^{-1}, respectively, belong to the νN–O valence vibrations, namely the former to the ionized, the latter to the non-ionized N—OH group of dimethylglyoxime.

The νC=N valence vibrations of the co-ordinated cyano group appear at 2155—2158 cm^{-1} (strong). This absorption band can be observed in the case of the free CN^- ion at 2080 cm^{-1} (in KCN). The shift of the cyano stretching vibrations to higher wave numbers can be explained on the basis of the resonance theory. Thus, for the free CN^- ion, the following resonance structures are available:

$$:\overline{C}\equiv N: \longleftrightarrow :C=\ddot{N}:^-$$ are availables:

a) b)

The corresponding structures for the coordinated CN^- are:

$$Me—C\equiv N: \longleftrightarrow Me^+=C=\ddot{N}:^-$$

c) d)

The formula (b) can be more probable for the free CN^-, while the structure (d) can be assumed for the complex-bonded cyano group [18—20].

Other absorption bands of the CN group appear in the 100—500 cm^{-1} wave-number range. The νCo—C stretching vibrations have been found at 490 cm^{-1} (medium) and 465 cm^{-1} (medium). The δCo—C=N and δC—Co—C deformation vibrations appear probably at 250—370 cm^{-1} and at about 100 cm^{-1}, respectively [21, 22].

The νCo-N (oxime) frequency has been identified at the same values as in the case of other Co(III)-amine- and Co(III)-dioximine-complexes [22], *i.e.*, at 512—515 cm^{-1} (medium).

The frequency of the corresponding absorption bands shows the Co—CN bond to be realized through the carbon atom. The position of the νC=N, νN—O, νCo–C and νCo—N bands demonstrates the strong covalent character of all Co–ligand bonds.

In aqueous solutions of the $[Co(DH)_2(CN)X]^-$ ions an aquation reaction occurs leading to the liberation of the halide ions and formation of the aquononelectrolite $[Co(DH)_2(CN)(H_2O)]$:

$$[Co(DH)_2(CN)X]^- + H_2O = [Co(DH)_2(CN)(H_2O)] + X^- \qquad (2)$$

Kinetics of this reaction was studied at different temperatures, in the pH range between 1.0 and 5.0 and at 0.1*M* ionic strength by following the change in time of the concentration of the free halide ions.

As seen from Fig. 2, the plot of log $[(c_0 - c)/c_0]$ values *versus* time give straight lines, but at higher temperatures a negative deviation appears, be-

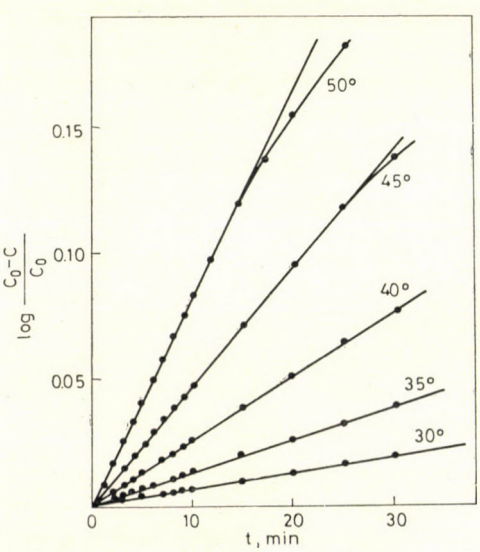

Fig. 2. Kinetic curves of the aquation of the $[Co(DH)_2(CN)Cl]^-$ ions at pH = 1.0 and μ = 0.1*M*

Table III

First order rate constants of the aquation of the $[Co(DH)_2(CN)X]^-$ ions at $\mu = 0.1$ M

X	pH	$k \times 10^5$, s^{-1}								
		30 °C	35 °C	40 °C	45 °C	50 °C	55 °C	60 °C	65 °C	70 °C
Cl	1.0	2.57	5.03	9.88	18.3	32.3	—	—	—	—
	2.0	2.61	4.98	10.1	18.0	32.8	—	—	—	—
	3.0	2.54	5.01	9.97	18.7	32.0	—	—	—	—
	5.0	2.59	5.09	9.74	18.3	32.7	—	—	—	—
Br	1.0	—	0.253	0.483	0.958	1.76	3.17	5.99	—	—
	2.0	—	0.261	0.472	0.972	1.80	3.10	5.87	—	—
	5.0	—	0.247	0.470	0.942	1.71	3.22	6.10	—	—
I	1.0	—	—	—	—	0.558	1.12	1.96	3.60	6.33
	2.0	—	—	—	—	0.542	1.17	2.07	3.69	6.18
	5.0	—	—	—	—	0.562	1.03	1.90	3.60	6.45

ginning after 30—40% reaction. This indicates the reversible character of the studied reactions. From the linear portion of these kinetic curves first order rate constants were derived, which are presented in Table III.

On the basis of the linear relationship between the $\log (k/T)$ and $1/T$ values, kinetic parameters of the studied reactions were calculated by means of the least square method. These values are given in Table IV.

Table IV

Kinetic parameters of the aquation of $[Co(DH)_2(CN)X]^-$ type complexes

X	$\Delta H^{\ddagger}$, kcal/mole	$\Delta^{\ddagger}$, e.u.	k_{298}
Cl	23.8 ± 0.2	-0.2	1.24
Br	25.1 ± 0.3	-2.1	1.51
I	25.7 ± 0.3	-3.1	2.06

Discussion

The kinetic data presented in Table IV indicate that the rate of aquation of the studied complexes is practically independent on the acidity of the solution even at pH = 1.0. This enables us to conclude that under our experimental conditions no protonation of the investigated anions occurs. This conclusion also agrees with the results of the pH-measurements presented in Table V, which shows a strong acidic character of the corresponding protonated species.

Table V

pH values of the half neutralized $H[Co(DH)_2(CN)X]$ acids

Complex acid	pH
$H[Co(DH)_2(CN)Cl]$	2.99
$H[Co(DH)_2(CN)Br]$	3.01
$H[Co(DH)_2(CN)I]$	3.01

Concentration of the complexes: $2 \cdot 10^{-3}$ *M*, t °C = 25°, μ = 0.1 *M*; neutralization with KOH up to 50%

No definitive conclusion can be drawn on the mechanism of the studied reactions. The reaction rate decreases, while the activation enthalpy increases in the order, Cl, Br, I, parallel with the increasing nucleophilic constants E_n of these ligands [24]. This indicates an increasing covalent character of the Co—X bond in the same order. This behaviour of the studied complexes differs from that observed in the case of other Co(III) complexes (*e.g.* $[Co(en)_2XA]^{2+}$ [25]) and indicates the 'soft' acid character of Co(III) in these dimethylglyoxime compounds. The strong dependence of the rate of aquation upon the nature of the substituted halide ions is a clear evidence for a dissociative mechanism. The negative activation entropy values, however, do not refer to an S_N1 mechanism. A 'pure' S_N2 pathway is improbable, since in this case the dependence of the rate of aquation on the nature of X cannot be interpreted. Thus, we conclude that the studied aquation reactions do not follow pure S_N1 mechanism. The rate determining step is the breaking of the Co—X bond, but the formation of the $Co—OH_2$ bond also plays a considerable role in the transition state.

The contribution of the $Co—OH_2$ bond in the formation of the activated complex may be expected on the basis of the π-acceptor ability of the '*trans*'--situated CN group. The Co → CNπ bonding leads to a considerable decrease of the electron density of the central atom, due to the charge transfer from this atom to the co-ordinated CN group. This effect makes possible a nucleophilic attack of a water molecule.

The trigonal bipyramidal rearrangement of the activated complex [25] is excluded in the case of the reactions studied here, because of the two short hydrogen bridges between the co-ordinated dimethylglyoxime molecules, which stabilize the tetragonal configuration of these complexes, even in the transition state.

Experimental

Synthesis of the $H[Co(DH)_2(CN)X]$ acids. To 0.1 mol $H[Co(DH)_2X_2]$ in 150—200 ml water 0.08—0.09 mole KCN in 20—25 ml aqueous solution was added. The dihalogeno-acids dissolve after 5—10 min by a continuous stirring, and dark brown solutions are formed. The mixture was cooled, filtered from the unreacted substances and the free acids were precipitated with an excess of 30—40% sulphuric acid.

Purification. The crude products are dissolved in 30—50 ml alcohol and added dropwise to a large excess of ice-cooled 30—40% sulphuric acid. The crystalline precipitates are filtered after 1/4—1/2 hr, washed with a small amount of ice-cooled water and with a 10 : 1 mixture of ether and alcohol, and dried in air.

Synthesis of $[Me(amine)_4Y_2]$ $[Co(DH)_2(CN)X]$ and $[Co(DH)_2(amine)_2]$ $[Co(DH)_2(CN)X]$ binary salts. 5 mmoles of the corresponding diacidotetramine salt: $[Co(en)_2Cl_2]Cl$, $[Cr(en)_2(NCS)_2]ClO_4$ or $[Co(DH)_2(amine)_2]OOC-CH_3$ in 80—100 ml water, or in 50% alcohol, respectively, are treated with 5 mmoles of $H[Co(DH)_2(CN)X]$ in 30—40 ml dilute alcohol (1 : 1). The crystalline precipitate is filtered after standing for 15—30 min, washed with a small amount of water and dried in air.

Analysis. Cobalt was determined complexometrically, by using murexide as an indicator. The organic ligands were mineralized by heating with concentrated sulphuric acid and several crystals of KNO_3. After diluting with water to a volume of 60—80 ml, the solution was neutralized with sodium acetate and ammonia. In the case of chromium derivatives the sum of the oxides ($Co_3O_4 + Cr_2O_3$) was determined after an hour of heating at 900°C. Nitrogen was determined by the micro-Dumas method.

Spectral investigations. The IR spectra of $H[Co(DH)_2(CN)X]$ were recorded in KBr pellets, on a UR 20 (Carl Zeiss, Jena) spectrophotometer, between 400 and 4000 cm^{-1}.

pH measurements. The titration of $H[Co(DH)_2(CN)X]$ acids with KOH could not been performed due to aquation which takes place with a considerable rate. The pH values of $2 \cdot 10^{-3}$ *M* $H[Co(DH)_2(CN)X]$ and $1 \cdot 10^{-3}$ *M* KOH mixtures were followed in time and results were extrapolated to $t = 0$. pH-measurements were carried out at 25° C and $\mu = 0.1M$ on an LPU-01 (USSR) pH-meter, using a glass electrode as an indicator and saturated calomel as a reference electrode.

Kinetic measurements. The concentration of the liberated halide ions was determined by SELBIN and BAILAR's method [26], by measuring the EMF of the following concentration cell: Ag/AgX, studied soln (0.1*M* $NaNO_3$) 10^{-3} *M* KX soln, AgX/Ag.

Both the sample solution and the standard one contained the same amounts of $HClO_4$ or acetic acid–sodium acetate buffer solution and $NaNO_3$, in order to ensure the acidity desired and an ionic strength of 0.1*M*. Samples were dissolved in the preheated solution and the system was thermostated at the working temperature, with an accuracy of ±0.01°.

Electrodes were prepared accordingly to the method of SELBIN and BAILAR, but a lower current density was used in order to improve their quality.

REFERENCES

[1] BILTZ, W., ESCHWEILER, W., BODENSIEK, A.: Z. anorg. allg. Chem. **170,** 161 (1928)
[2] RAY, P., DUTT, N. K.: Z. anorg. allg. Chem. **234,** 65 (1937)
[3] RAY, P., GUPTACHAUDKURI, T.: Z. anorg. allg. Chem. **220,** 154 (1934)
[4] ADAMSON, A. W.: J. Amer. Chem. Soc. **78,** 4260 (1956)
[5] BANERJEA, D., DAS GUPTA, T. P.: J. Inorg. Nucl. Chem. **29,** 1021 (1967)
[6] GRASSI, R., HAIM, A., WILMARTH, W. K.: J. Inorg. Chem. **6,** 237 (1967)
[7] BARCA, R., ELLIS, J., MAAK-SANG TSAO, WILMARTH, W. K.: J. Inorg. Chem. **6,** 243 (1967)
[8] TEWARI, P., GAVER, R. W., WILCOX, H. K., WILMARTH, W. K.: J. Inorg. Chem. **6,** 611 (1967)
[9] MAKI, N.: Nature **188,** 224 (1960)
[10] MAKI, N.: Bull. Chem. Soc. Japan **38,** 2013 (1965)
[11] VÁRHELYI, CS., GANESCU, I., SZOTYORI, L.: Z. anorg. allg. Chem. **386,** 232 (1971)
[12] BERNHAUER, K., MÜLLER, O., WAGNER, F.: Angew. Chem. **75,** 1145 (1963)
[13] LENHERT, P. G., CROWFOOT-HODGIN, D.: Nature **192,** 937 (1961)
[14] SCHRAUZER, G. N., KOHNLE, J.: Chem. Ber. **97,** 3056 (1964)
[15] SCHRAUZER, G. N., DEUTSCH, E.: J. Amer. Chem. Soc. **91,** 3341 (1969)
[16] MCBRIDGE, B. C., WOOD, J. M., SIBERT, J. W., SCHRAUZER, G. N.: J. Amer. Chem. Soc., **90,** 5276 (1968)
[17] SIBERT, J. W., SCHRAUZER, G. N.: J. Amer. Chem. Soc. **92,** 1022, 1421 (1970)
[18] HERRINGTON, E. F., KYNASTON, W.: J. Chem. Soc. **1955,** 3555
[19] GRIFFITH, W. P., WILKINSON, G.: J. Chem. Soc. **1959,** 2757
[20] EL-SAYED, M. F., SHELINE, R. K.: J. Inorg. Nucl. Chem. **6,** 187 (1958)
[21] NAKAGAWA, I., SHIMANOUCHI, T.: Spectrochim. Acta **18,** 101 (1962)

[22] JONES, L. H.: J. Chem. Phys. **36,** 1209 (1962)
[23] BLOCK, H.: Trans. Faraday Soc. **55,** 867 (1959)
[24] BASOLO, F., PEARSON, R. G.: Mechanism of Inorganic Reactions, J. Wiley, New York, 1958, p. 93
[25] CHAN, S. C., CHENG, C. Y., LEH, F.: J. Chem. Soc. (London) **1958,** 4536
[26] SELBIN, J., BAILAR, J. C.: J. Amer. Chem. Soc. **79,** 4285 (1957)

Z. FINTA
Cs. VÁRHELYI
Faculty of Chemistry, Babes-Bólyai University, Cluj, Romania.

Acta Chimica Academiae Scientiarum Hungaricae, Tomus 83 (3—4), pp. 291—298 (1974)

THE GREEN'S FUNCTION ANALYSIS OF ISOTOPICALLY SUBSTITUTED OZONE MOLECULAR VIBRATIONS

K. L. NARAYANA and B. P. SABALE

(Theoretical Physics, Shivaji University, Kolhapur)

Received December 18, 1973

The generalized and symmetrized mean square amplitude quantities, force constants, Coriolis coupling coefficients and potential energy distributions are obtained for isotopically substituted ozone molecules by the method of Green's function analysis and partitioning techniques, using the expressions given by DEWAMES *et al.* [12].

Introduction

Molecular vibrations of ozone has been the subject of study by a number of investigators [1—11] (WILSON and BADGER, CLEVELAND and PIERCE etc.). These authors have obtained the molecular constants with assumption of force field models except PIERCE [3] who however, has obtained force constants by the analysis of rotation-vibration data presumed to be the accurate set.

The object of the present work is to evaluate the set of unique force field constants by Green's function analysis and partitioning techniques of DEWAMES *et al.* [12—14] for the four isotopically substituted ozone molecules $O_3^{18-18-18}$, $O_3^{18-16-18}$, $O_3^{16-18-16}$ and $O_3^{16-16-16}$. The advantage of this method is obtaining molecular constants, without invoking any force field assumption. Mention may be made also of the force constants evaluated for ozone molecule by MULLER *et al.* [7—9] adopting constraints based on Green's function analysis and L-matrix approximation methods, and also involving a linear empirical relation $L_{12}/L_{21} = 0.325\ T + 0.63$. A comparison of the data obtained by them for force constants with those given by PIERCE [3] and CLEVELAND and KLEIN [2] indicates that the choice of the mixing parameter involved may not be an accurate value. Further they do not report the force field estimates for the other isotopic substitutions for ozone.

Method

The method of Green's function analysis and partitioning techniques suggested by DEWAMES and WOLFRAM [12] essentially involves solving the secular equation given below for a single isotopic substitution.

$$|\varepsilon\,\omega^2\,G(\omega^2) + 1| = 0$$

where $\varepsilon = (m^i - m)/m$, and m is the original mass, and m^i is the isotopic mass. $G(\omega^2)$ is the Green's function matrix for the unperturbed molecule, with the elements given by

$$Gij = \sum_l X_{il} X_{jl}/(\omega^2 - \omega_l^2)$$

where X_{ll} is the lth component of the normal co-ordinate for the mode the frequency of which is ω_l.

The normal co-ordinates for the unperturbed molecule have been constructed as a linear combination of symmetry co-ordinates with the coefficients of mixing involving a single parameter c.

This mixing parameter may easily be calculated in general for XY_2 type molecules under C_{2v} symmetry by means of the formulas (23), (24) and (25) of reference [7] for either type of isotopic substitution. $YXY \leftrightarrow (YX^iY$ or $Y^iXY^i)$. A knowledge of the mixing parameter allows us then to obtain generalized and symmetrized mean square amplitudes, force constants, Coriolis coupling coefficients and potential energy distribution.

Results

The method described above is applied for the isotopic substitutions $O_3^{18-18-18}$, $O_3^{18-16-18}$, $O_3^{16-18-16}$ and $O_3^{16-16-16}$. The numerical data of various molecular constants have been obtained by means of Computer Fortran program ming on CDC-3600 computer. This data is tabulated in Tables IA and II to IV. Table I gives the molecular parameters and frequencies adopted in this work [10].

Discussion

Since the expressions of product and sum rules of frequencies involve the square of mixing parameters, one obtains both positive and negative mixing parameters for evaluation of molecular constants. In Table IA we have listed

Table I

Molecular parameters of ozone molecules

Molecular parameter	(Ref. [10]) Observed frequencies in cm^{-1}							
	$O_3^{18-16-18}$		$O_3^{18-18-18}$		$O_3^{16-18-16}$		$O_3^{16-16-16}$	
	a_1	b_1	a_1	b_1	a_1	b_1	a_1	b_1
O—O distance = 1.278 Å	1056		1038		1085.84		1100	
O⟨O⟩O angle	671.67		660		672		695	
116.8°		1008		995		998		1030

a_1 and b_1 represent the species of C_{2v} symmetry group

Table I A

Urey-Bradley force-constants (mdyn/Å, 0.01 N/m)

		$O_3^{16-16-16}$	$O_3^{16-18-16}$	$O_3^{18-18-18}$	$O_3^{18-16-18}$
K	*a*	−1.334629	−1.34924	−1.354825	−1.483642
	b	5.532375	5.75232	5.596863	5.751824
H	*a*	1.3165	1.31826	1.42804	1.170007
	b	0.67118	0.71828	0.968282	0.95569
F	*a*	4.67739	4.68701	5.05728	5.08610
	b	2.1690	2.1646	2.3224	2.2543

a — positive mixing parameter
b — negative mixing parameter

Table II

Symmetry force constants (Units of mdyn/Å, 0.01 N/m)

		$O_3^{16-16-16}$	$O_3^{16-18-16}$	$O_3^{18-18-18}$	$O_3^{18-16-18}$	Results obtained by	
						PIERCE (Ref. [3])	CLEVELAND (Ref. [2])
F_{11}	*a*	5.4305621	5.4298663	5.9598223	5.8726888	7.22	5.659
	b	8.6695299	8.6831139	8.955889	9.0124112		
F_{12}	*a*	2.6614371	2.6669196	2.8775987	2.8939954	1.063802	0.3826259
	b	1.2342127	1.2316724	1.3214514	1.2827198		
F_{22}	*a*	2.9474056	2.9524184	2.9061663	2.9434186	2.0840	2.540
	b	1.4727469	1.472988	1.7780523	1.741728		
F_{33}		4.095695	4.1150328	4.2998366	4.10970522	4.180	4.181

a— values for positive mixing parameter
b — values for negative mixing parameter

the Urey—Bradley force field constants, evaluated as per an approach suggested by SHIMANOUCHI [15] and described in the book by NAKAMOTO [16]. The stretching, bending and repulsive force constants respectively denoted by K, H and F have a clearer physical meaning and are useful for transferability to other complex molecules in which the isotopic substitutions of ozone might occur. It is interesting to note from Table I A that (1) these constants show isotopic substitutional effects, (2) the stretching and bending force constants are extremely low with a positive mixing parameter, (3) the repulsive force constant F is constantly positive in all cases irrespective of the sign of the

mixing parameter. It is to be argued since K values are very low, compared, for example, to those reported [17] for H_2O, D_2O, T_2O etc., the positive mixing parameter is not physically reasonable to adopt for these molecules.

A comparison of calculated symmetry force constants for the two mixing parameters with those of previous investigators shows that the positive mixing parameter gives rise to a value for F_{11} comparable with that obtained by CLEVELAND and KLEIN [2] but differes considerably from the value given by PIERCE [3]. This has been observed similarly in the case of all four isotopic substitutions, while (for F_{11}) this is an exactly reverse situation with a negative mixing parameter value. F_{12} value of CLEVELAND *et al.* is too low, while that given by PIERCE and our results for all isotopic ozones (obtained using a negative mixing parameter) are in good agreement. F_{22} value surprisingly agrees (in our work with a positive mixing parameter) with both the values given by CLEVELAND and PIERCE. Since PIERCE's values are obtained on the basis of rotational–vibrational spectroscopic data, we are to conclude that a negative mixing parameter is reasonable for isotopic ozones, however, with the exception of not a good agreement, for F_{22} value. Determination of F_{33} value does not involve the mixing parameter at all and the slight variance in the different reported values is due to the adopted frequencies for anti-symmetric stretching vibration of ozone and the isotopic masses.

In the matrix method of F. G. WILSON L-matrix stands for the transformation of normal co-ordinates to internal displacement symmetry co-ordinates, and it is determined by an eigenvector solution of the secular equation $| GF - \lambda E | = 0$ where E is the unit matrix and λ-s are related to vibrational frequencies. The L-matrix elements thus determined are used in CYVIN's method [20] to determine the mean square amplitude through the well-known relations, given in reference No. [18—20] for XY_2 structures. The L-matrix comes out to be the product of the so-called B-matrix, and the mixing parameter A-matrix in the DEWAMES method [12]. Hence it is possible to [21—24] evaluate symmetrized mean square amplitudes using the mixing parameter matrix for the different isotopic substitutions of ozone. The data obtained by us are listed in Table III for the two mixing parameters, at two different temperatures 0 K and 273 K. Last row of the table lists the values reported by NAGARAJAN [11]. From Table III we note that Σ_{12} value is considerably lower, for a positive mixing parameter of $O_3^{16-16-16}$, than as obtained by NAGARAJAN. It is also positive for negative mixing parameter, unlike for other isotopic molecules which have a negative value for Σ_{12} irrespective of the sign of mixing parameter. Σ_{12} values are in reasonable agreement in all cases with that reported by NAGARAJAN, especially with positive mixing parameter. The isotopic effect on the mean square amplitudes is of significant magnitude.

In Table IV generalized mean square amplitudes are listed with last two columns pertaining to non-bonded atom pairs. The temperature effect on

Table III

Symmetrized mean square amplitudes (Units of (Å)²)

		Σ_{11}		Σ_{12}	
		$T = 0$ K	$T = 273$ K	$T = 0$ K	$T = 273$ K
$O_3^{16-16-16}$	*a*	0.0023552	0.0025275	−0.002463	−0.0026310
	b	0.0015177	0.0015388	0.0000702	+0.0001112
$O_3^{16-18-16}$	*a*	0.0023075	0.0024894	−0.0025979	−0.0027830
	b	0.0014853	0.0015077	−0.0001343	−0.0001878
$O_3^{18-18-18}$	*a*	0.0021829	0.0023688	−0.0027432	−0.0029544
	b	0.0014613	0.0014922	−0.0004939	−0.0005740
$O_3^{18-16-18}$	*a*	0.0022671	0.0024551	−0.0026126	−0.00281348
	b	0.0014865	0.0015150	−0.0001983	−0.0002634
Ref. [11] by NAGARAJAN		0.0017013	0.0017524	−0.0006984	−0.0004128

	Σ_{22}		Σ_{33}	
	$T = 0$ K	$T = 273$ K	$T = 0$ K	$T = 273$ K
$O_3^{16-16-16}$	0.0054706 0.0071457	0.0056667 0.0076440	0.0024950	0.0025364
$O_3^{16\ 18-16}$	0.0052811 0.0069255	0.0053774 0.0072299	0.0023491	0.0023881
$O_3^{18-18-18}$	0.0052919 0.0068078	0.0053645 0.0069288	0.0022931	0.0023310
$O_3^{18-16-18}$	0.0055577 0.0071222	0.0055602 0.0073421	0.00243289	0.0024732
Ref. [11] by NAGARAJAN	0.0052636	0.0053986	0.0024761	0.00251017

a— values for positive mixing parameter
b— values for negative mixing parameter

generalised mean square amplitudes and symmetrised mean square amplitudes is substantially different from the variation we note in the data of NAGARAJAN.

In Tables V and VI are given the potential energy distribution and the Coriolis coupling coefficients, respectively, for the four isotopically substituted ozone molecules. We note from Table V that the negative mixing parameter gives PED_{11} element predominant over PED_{12} while the reverse is the case with positive mixing parameter for $O_3^{16-16-16}$. This is not the similar case, when we consider PED_{21} and PED_{22} elements. Since force constants and mean square amplitudes indicate that the positive mixing parameter is reason-

Table IV

Generalized mean square amplitude

		$\langle \Delta z^2 \rangle$		$\langle \Delta x^2 \rangle$	
		$T = 0$ K	$T = 273$ K	$T = 0$ K	$T = 273$ K
$O_3^{16-16-16}$	*a*	0.0024251	0.00253201	0.0014820	0.0015329
	b	0.0020064	0.0020376	0.0019008	0.0020272
$O_3^{16-18-16}$	*a*	0.0023283	0.0024387	0.0014183	0.0014440
	b	0.0019172	0.0019479	0.0018294	0.0019071
$O_3^{18-18-18}$	*a*	0.2238005	0.2349932	0.0014462	0.0014462
	b	0.0018771	0.0019116	0.0018077	0.0018390
$O_3^{18-16-18}$	*a*	0.0023502	0.0024641	0.0015112	0.0015131
	b	0.00119597	0.0019441	0.0019020	0.0019590

able, we may be able to conclude from PED elements for $O_3{}^{16-16-16}$ the predominant symmetry co-ordinate to be the same as that indicated by PED_{11} element. PED_{33} is consistently unity since it refers to a pure symmetry co-ordinate.

The Coriolis coupling coefficients ξ_1 and ξ_2 are very high in magnitude for a positive mixing parameter. Interesting is a comparison of the values obtained for $O_3{}^{18-18-18}$ with those reported by NARAYANA [17] for F_2O molecule. The later author has given the values 0.8736 and -0.4898, respectively, for ξ_1

Table V

Potential energy distribution matrix elements

		PED_{11}	PED_{12}	PED_{21}	PED_{22}	PED_{33}
$O_3^{16-16-16}$	*a*	0.0065748	1.844531	0.8916515	0.9274773	1.00
	b	1.151788	0.0856748	0.04842785	1.202387	1.00
$O_3^{16-18-16}$	*a*	0.175638	1.837683	0.822599	1.0004544	1.00
	b	1.126206	0.1114658	0.0316437	1.219420	1.00
$O_3^{18-18-18}$	*a*	0.0286249	1.942292	0.7668863	1.175327	1.00
	b	1.139071	0.2076402	0.0252655	1.334454	1.00
$O_3^{18-16-18}$	*a*	0.0104517	1.989440	0.857871	1.111048	1.00
	b	1.176472	0.161017	0.0435358	1.307408	1.00

a— values for positive mixing parameter.
b — values for negative mixing parameter.

quantities (Units of (Å)²)

$\langle \Delta z \Delta x \rangle$		$\langle \Delta z^2 \rangle$		$\langle \Delta x^2 \rangle$	
$T = 0$ K	$T = 273$ K	$T = 0$ K	$T = 273$ K	$T = 0$ K	$T = 273$ K
−0.0004931	−0.0005462	0.0076129	0.0081164	0.0001419	0.0001442
0.0004088	0.0004176	0.0037085	0.003885		
−0.000579	0.0006389	0.0076499	0.0081689	0.0001540	0.0001565
0.0002786	0.0002919	0.0038882	0.0040432		
−0.0006227	−0.0006915	0.0076278	0.0081495	0.0001304	0.0001325
0.0001499	0.0001724	0.0042280	0.0043190		
−0.000539	−0.0006036	0.0076561	0.0081824	0.0001192	0.0001212
0.0002979	0.0003145	0.0039999	0.0041612		

a — values for positive mixing parameter
b — values for negative mixing parameter

and ξ_2. The sign of ξ_2 agrees when we take a negative mixing parameter but then the value of ξ_1 is only 0.2115 which is too low compared to 0.8736. The significant difference in the values of molecular constants relative to those in the literature is in turn due to the values of *L*-matrix elements. Thus essentially a different kind of mixing of symmetry co-ordinates is involved in the Green's function analysis [21—24] of molecular vibrations, unlike the mixing

Table VI

Coriolis coupling coefficients

Isotopic molecule		ξ_1	ξ_2	ξ_1^2	ξ_2^2
$O_3^{16-16-16}$	*a*	0.8406009	0.5416708	0.7066100	0.2934074
	b	0.3027236	−0.9530509	0.0916415	0.9083043
$O_3^{16-18-16}$	*a*	0.8449681	0.5664222	0.7139709	0.3208338
	b	0.2502426	−0.9700280	0.0626213	0.940954
$O_3^{18-18-18}$	*a*	0.785764	0.6204468	0.6174439	0.384954
	b	0.2115006	−0.9773536	0.0447325	0.9553918
$O_3^{18-16-18}$	*a*	0.8112024	0.5847797	0.6580486	0.3419664
	b	0.2768084	−0.9608994	0.0766228	0.9233268

a — values for positive mixing parameter
b — values for negative mixing parameter

of symmetry co-ordinates which is indicated by the conventional force field model calculations [25, 26].

*

One of the authors (B. P. S.) is thankful to the U.G.C. for financial support for this work and both authors wish to express their sincere thanks to the staff of CDC-3600 computer at T.I.F.R., Bombay-5.

REFERENCES

[1] WILSON, M. K., BADGER, R. M.: J. Chem. Phys. **16,** 741 (1948)
[2] CLEVELAND, F. F., KLEIN, M. J.: J. Chem. Phys. **20,** 337 (1952)
[3] PIERCE, L.: J. Chem. Phys. **24,** 139 (1956)
[4] UKA, T., MORINO, Y.: J. Mol. Spectros. **8,** 9 (1962)
[5] SUTHERLAND, G. B. B. M., PENNY, W. G.: Proc. Roy. Soc. (Lond.) **156,** 678 (1936)
[6] KIMURA, K.: J. Chem. Phys. **40,** 1213 (1957)
[7] MULLER, A., MOHAN, N., HEIBORN, U.: Z. für Naturforschung **270,** 129 (1972)
[8] MOHAN, N., MULLER, A.: Chemical Phys. Letters **14,** 205 (1972)
[9] MULLER, A., PEACOCK, C. J.: Mol. Phys. **14,** 393 (1968)
[10] BREWER, L., LING-FAIWANG, J.: J. Chem. Phys. **56,** 2 (1972)
[11] NAGARAJAN, G.: Acta Phys. Austriaca **17,** 241 (1963)
[12] DEWAMES, R. E., WOLFRAM, T.: J. Chem. Phys. **40,** 3 (1964)
[13] BASS, C. D., LYNDS, L., WOLFRAM, T., DEWAMES, R. E.: J. Chem. Phys. **40,** 12, 3611 (1964)
[14] WOLFRAM, T., BASS, C. D., DEWAMES, R. E.: Bull. Chem. Soc. of Japan **39,** 210 (1966)
[15] SHIMANOUCHI, T.: J. Chem. Phys. **25,** 660 (1956)
[16] NAKAMOTO, K.: Infrared Spectra of Inorganic and Co-ordination Compounds, John Wiley & Sons, 2nd ed. 1970, p. 55
[17] VANKTESWARALU, K.: Indian J. Pure and Appl. Phys. **1,** 377 (1963)
[18] NARAYANA, K. L.: Shivaji University Journal **2,** 115 (1969)
[19] MORINO, Y.: J. Chem. Phys. **18,** 395 (1956)
[20] CYVIN, S. J.: J. Mol. Spect. **11,** 195 (1963)
[21] NARAYANA, K. L., SABALE, B. P.: Curr. Sci. **41,** 412 (1972)
[22] NARAYANA, K. L., SABALE, B. P.: Curr. Sci. **42,** 535 (1973)
[23] NARAYANA, K. L.: Curr. Sci. **42,** 20, 712 (1973)
[24] SABALE, B. P.: Ph. D. Thesis (1973) submitted to Shivaji university, Kolhapur-416004, India.
[25] PILLAI, M. G. K., PILLAI, P. P.: Shivaji University Journal **2,** 41 (1969)
[26] NARAYANA, K. L., SABALE, B. P.: Indian Science Congress (1973) Nagpur Session, India.

K. L. NARAYANA, B. P. SABALE } Theoretical Physics, Shivaji University, Kolhapur 416004, India.

Acta Chimica Academiae Scientiarum Hungaricae, Tomus 83 (3—4), pp. 299—301 (1974)

INFRARED STUDIES ON ANILS AND THEIR COMPLEXES, I

R. K. UPADHYAY, M. L. SINGHAL, A. K. SAXENA and R. PRASAD*

*(N.R.E.C. College, Khurja and *J.A.S.I. College, Khurja, India)*

Received February 8, 1974

Infrared spectra of sixteen anils (condensation products of 3-phenanthrylglyoxal and primary aromatic amines) have been interpreted to assign the various modes of vibrations and to establish the structures of the compounds. The influence of the nature and position of the substituent on the azomethine group stretching frequency has also been studied.

In the Ni(II), Co(II) and Zn(II)complexes of the anil derived from *p*-dimethylaminoaniline and 3-phenanthrylglyoxal, infrared spectral studies show the oxygen and nitrogen atoms of the carbonyl and azomethine groups, respectively, to be sites of interaction in complex formation. The orders of metal–nitrogen and metal–oxygen bond stabilities have also been established.

Introduction

A large number of anils [1—4] derived from glyoxals, and primary aromatic amines have been characterized by elemental analysis and by preparing their derivatives. In the infrared spectra the appearance of a strong band at 1640—1690 cm^{-1} indicated [5] the presence of azomethine group ($>C=N$), but no efforts have been made so far to study extensively the infrared spectra of the anils. In the present work it has been attempted to characterize almost all the important bands in the spectra of anils [6] prepared from 3-phenanthrylglyoxal and aromatic primary amines. The influence of the nature and position of the substituent on the azomethine group stretching frequency has also been found to be a very important and interesting aspect of this study.

Anils with co-ordinating ability at the oxygen and nitrogen atoms of the carbonyl ($>C=O$) and azomethine groups, respectively, are well known to form chelates [7—10] with transition metal ions. Infrared spectral study of anil chelates has been done so far only to a limited extent; very important aspects, such as structural changes during complexation and the order of stability remained unexplained. Here such aspects are also discussed for chelates of the anil derived from *p*-dimethylaminoaniline and 3-phenanthrylglyoxal.

Results and discussion

Infrared spectra of all the products were recorded on a Perkin—Elmer Infracord Spectrophotometer, in KBr pellets. The characteristics frequencies and their assignments [5, 11, 12] are given in Table I.

The effects of the nature and position of substituents have been studied on the azomethine group of the anils. The nature of the substituent has been found to play a dominant role in determining the stretching frequency. To study this effect, *meta*-anils have been chosen, as this position contributes less to the intermolecular disturbance than the *ortho*- and *para*-positions. Further, the effect of the nature of the substituent is much more pronounced in *meta* position, than the influence due to the position itself. In *meta*-anils, the azomethine group stretching frequencies follow the order $N=R=CH_3 < COOH < OH < NO_2$, which is the same as the order of the electron withdrawing character of the substituents. This obviously shows that a substituent with weaker electron withdrawing character will provide greater stability to the carbon–nitrogen bond. From the survey of data given in Table I, it can easily be deduced that the azomethine group stretching frequency also depends on the position of the substituent. This effect has been studied in the ternary set of benzoic acid isomers and binary sets of nitroanilines, aminophenols, toluidines and α-, β-naphthylenes. The order in the azomethine group frequencies for isomeric anils is the following: *ortho* $\leq$ *meta* $<$ *para* and $\beta < \alpha$. Consequently, *ortho* and β substitutions contribute maximum to the stability of the C=N bond.

The spectral data for the anil derived from *p*-dimethylaminoaniline and its complexes indicate that most frequencies are perturbed on complex formation. Strong peaks corresponding to the >C=O and >C=N groups are shifted from 1653 cm^{-1} and 1613 cm^{-1} (ligand) to 1590 cm^{-1} and 1548 cm^{-1} [Ni(II) complex], 1608 cm^{-1} and 1565 cm^{-1} [Co(II) complex] and 1647 cm^{-1} and 1600 cm^{-1} [Zn(II) complex] during complex formation and the shifts to lower values confirm that the oxygen and nitrogen atoms of these groups are the co-ordinating centres. The magnitude of the shift in each group follows the order Zn(II) < Co(II) < Ni(II), in agreement with the stability order of divalent metal complexes given by MELLOR and MALEY [14]. Moreover, the decrease in the shift is attributable to the reduced stability of the co-ordinate bond. The shift of the strong bands of the ligand from 1575 cm^{-1} and 1515 cm^{-1} to 1522 cm^{-1} and 1511 cm^{-1} (in the Ni(II) and Co(II) complexes) and to 1471 cm^{-1}, 1439 cm^{-1}, 1504 cm^{-1} (in all the three complexes) affords evidence for conjugation in the ligand during chelation. If the band at 820 cm^{-1} is considered to be due to *para* substitution, then its shift to 816 cm^{-1} 823 cm^{-1} and 816 cm^{-1} in the complexes indicates the possibility of change of the benzenoid structure of the ligand to a quinonoid structure in the course of chelation.

Table I

Principal infrared frequencies of anils and their complexes

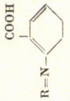	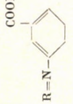		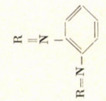	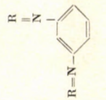	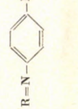	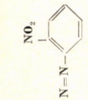	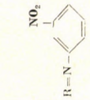	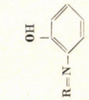	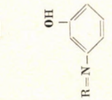		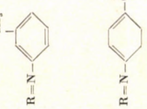			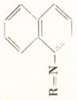	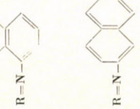	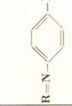					Assignment
3247 m	3390 m	3279 m	—	3333 s	3333 s	3333 s	3333 m	—	—	3333 s	3331 s	3333 m	3390 s	3289 s	3219 m	3448 s	3571 s	3509 s	C—H str. (alkyne)
—	—	—	—	—	—	—	—	3333 sh, m	3333 s	—	—	—	—	—	—	—	—	—	O—H str. (phenolic)
3030 sh, w	3030 w	—	3077 s	3030 sh, s	—	—	3077 sh, w	3030 s	—	3030 w	2985 w	3030 sh, w	—	—	2857 w	—	—	2667 m	C—H str. (aromatic)
2857 w, b	2899 w	2857 w	—	—	—	—	—	—	—	—	—	—	—	—	—	—	—	—	
2481 w	2500 w, b	2532 w	—	—	—	—	—	—	—	—	—	—	—	—	—	—	—	—	O—H str. (COOH)
—	—	2299 w	—	—	—	2326 w	2326 w	2326 w	2326 w	2326 w	2326 w	2353 w	2299 s	2326 m	2353 w	—	—	—	
—	—	—	—	—	—	—	—	—	—	1905 w	1905 w	1923 w	—	—	—	—	—	—	
1689 s	1724 s	1739 sh, m	1667 m	1695 sh, s	1667 s, b	1689 s	1675 s	1653 sh, m	1667 sh, s	1667 sh, s	1695 sh, m	1672 s	1681 s	1626 s	1653 s	1590 s	1608	1647 sh, s	C=O str.
1613 s	1613 s	1667 s	1587 sh, m	1603 s	1613 s	1618 s	1629 s	1613 s	1626 s	1603 s	1613 s	1613 sh, s	1626 sh, s	1587 s	1613 s	1548 s	1565 s	1600 s	C=N str.
—	—	1600 s	1563 s	—	—	1575 s	—	—	—	—	—	1600 s	—	—	1575 s	1522 s	1546 s	—	
1515 s	—	1515 s	1515 sh, m	—	1511 s	1515 s	1531 s	—	1493 m	1493 s	1508 s	1504 s	1527 s	1527 s	1515 s	1471 s	1439 s	1504 s	C=C str.
—	1460 m	1481 m	1504 s	1497 s	—	—	1481 sh, s	1481 s	—	—	—	—	1481 m	—	—	—	—	—	
—	—	—	—	—	—	—	—	—	—	1449 s	1449 s	—	—	—	—	—	—	—	C—CH_3 str.
1370 w	—	1418 m	—	—	—	—	1429 w	—	1418 m	—	—	1429 w	—	1449 s	1439 m	—	—	—	
—	1389 m	1379 m	1332 s	—	—	1351 s	1351 s	—	—	1389 m	1379 s	1370 m	1389 m	—	1370 m	1370 s	1370 s	1393 m	C—N str. (aromatic tertiary)
—	—	—	—	—	—	—	—	—	—	1342 s, b	1342 s	—	—	1342 s	—	—	—	1351 m	CH_3 symm. bending
1290 w	1307 sh, s	1282 s	—	—	—	1316 s	1307 sh, m	1299 m	1274 m, b	1307 m	1307 s	1307 m	1307 m	—	1282 s	1307 s	1300 s	1299 w	C—H in-plane bending
1227 s	1242 s	1227 sh, s	1250 s	1242 s	1250 s, b	—	—	—	—	1250 s	1235 s	1235 m	—	1258 m	1227 s	1221 s	1221 s	1235 m	
—	—	—	—	—	—	1235 s	1250 m	—	—	—	—	—	—	—	—	—	—	—	N—O str.
—	—	—	—	—	—	—	—	1247 s	1235 m	—	—	—	—	—	—	—	—	—	O—H bending + C—O str.
1183 w	1205 m	1212 m	1220 s	1205 m	—	—	1208 w	—	—	—	1205 m	—	—	—	—	—	—	—	
—	—	1176 s	—	—	—	—	1176 m	—	1163 m, b	1176 s	1176 s	1176 s	1176 m	1170 m, b	—	—	—	—	
1149 m	1149 s	1143 s	1144 s	—	—	1152 s	1143 sh, w	1143 w	—	1143 w	1143 w	—	—	1143 m, b	—	—	—	—	
—	1117 s	—	1106 s	1099 s	1093 m	1124 sh, m	1093 w	1117 s	1105 w	1099 w	1093 w	1093 w	1093 w	1087 m, b	—	—	—	—	
—	—	—	—	—	—	—	—	—	—	—	—	—	—	—	1170 v. s	1164 s	1164 s	1176 m	C—N str. (aliphatic)
															1103 w	1100 s	1100 s	1124 w	
1070 m	—	1087 m, *b*	1064 s	—	—	1074 s	—	1075 s	—	—	—	1053 sh, w	—	—	1081 w	1062 s	1062 s	1053 w	
1015 m	1044 s	—	1026 m	1044 m	1036 m	1042 s	—	1036 v. s	—	1036 m	—	1031 w	—	—	1034 w	1014 s	1014 s	1031 w	Benzene ring breathing
976 m	—	1000 m	—	—	—	985 m	1000 w	1000 s	1000 w	—	—	1000 w	1000 w	1000 m	—	—	—	985 w, b	
—	—	—	—	—	—	—	—	—	—	1000 m	1000 s	—	—	—	—	—	—	—	CH_3 rocking
—	—	—	966 s	—	—	—	—	980 s	976 w, b	966 w	—	943 w, b	—	—	948 m	951 m	943 s	948 sh, m	
939 w	—	—	—	—	—	922 w, b	893 w	939 s	—	—	—	—	—	—	—	—	—	—	
893 w	—	897 w	890 m	—	—	—	—	905 s	897 w	901 w	901 w, b	897 w, b	893 w, b	897 m	905 w	898 w	909 w	898 m	
—	—	—	—	—	—	866 w	870 w	—	—	—	—	—	—	—	—	—	—	—	ONO bending
870 w	870 w	858 sh, w	—	—	—	—	—	870 w	866 w	870 w	862 w, b	870 w, b	866 w, b	866 w	870 w	862 m	862 s	870 sh, m	
847 w	830 m	840 w	844 s	847 s	844 s, b	842 w	—	840 w	837 sh, w	—	842 sh, w	838 sh, w	—	—	851 m	853 s	850 s	844 m	
830 m	—	—	—	—	—	—	—	—	—	833 sh, w	—	—	—	—	—	—	—	—	
820 m	816 w	810 w	816 m, b	816 s, b	810 sh, s	820 s	813 s	814 v. s	810 s	813 s	810	813 s	810 s	810 s	820 s	816 s	823 s	816 m, b	C—H bending (two adjacent H atoms)
787 w	—	772 w	767 s	—	—	781 w	800 sh, w	784 sh, w	781 w	772 sh, w	772 sh, w	—	—	—	—	—	—	—	C—H bending (three adjacent H atoms)
755 s	752 s	743 w	758 s	749 s	746 s	742 s	746 sh, s	772 sh, w	746 m	746 s	746 s	743 s	746 s	746 s	752 w	746 m	755 s	746 s	C—H bending (four adjacent H atoms)
—	—	—	—	—	—	727 v. s	738 s	752 v. s	—	—	—	—	—	—	738 m	733 w	733 m	—	
725 w	—	730 w	716 m	—	—	714 w	710 w	—	717 w	714 m	714 m	712 w	714 m	714 m	719 w	704 m	708 m	709 w	C—H out-of-plane bending
709 w	—	709 w,b	—	—	—	—	—	—	—	—	—	685 w	—	—	676 w	692 w	694 w	—	

R = 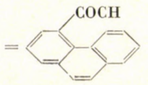

s, strong; sh, shoulder; v. s, very strong; m, medium; w, weak, b, broad; L, ligand

The intensity order of the bands due to the carbonyl and azomethine groups is the same as the order of stability of the complexes. Thus the most stable complex (co-ordinated bond) gives a highly intense band.

In view of the above facts, the change in ligand structure during chelation and the structures of the chelates may be shown as follows:

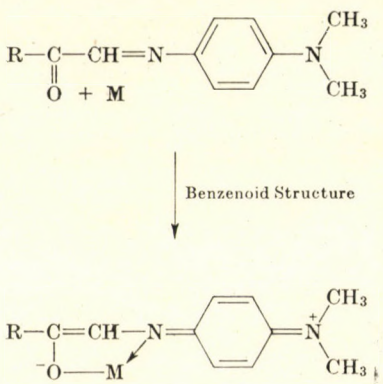

Benzenoid structure Quinonoid structure (M = Ni(II), Co(II) or Zn(II))

*

Suggestions from Prof. J. P. VAJPAI, D.S. College Aligarh are gratefully acknowledged. Thanks are also due to Dr. S. S. MISRA, Feroj Gandhi College, Rae Barely.

REFERENCES

[1] CROHNKE, F., GROSS, K. F.: Chem. Ber. **36,** 92 (1959)
[2] MALIK, W. U., GUPTA, B. R., TAPLOO, C. L.: J. Chem. Eng. Data **11,** 210 (1966)
[3] MALIK, W. U., SAXENA, R. C.: J. Indian Chem. Soc. **45,** 307 (1968)
[4] SINGH, P.: Ph. D. Thesis, Meerut University, Meerut (India) 1971
[5] DYER, J. R.: Applications of Absorption Spectroscopy of Organic Compounds. Prentice-Hall of India Pvt. Ltd., New Delhi, 1969 p. 37
[6] UPADHYAY, R. K., SAXENA, R. C.: J. Indian Chem. Soc. (Submitted for publication in 1972)
[7] SAXENA, R. C.: Ph. D. Thesis, Roorkee University, Roorkee (India), 1968
[8] UPADHYAY, R. K., SAXENA, R. C.: Indian J. Chem. **11,** 697 (1973)
[9] UPADHYAY, R. K., SAXENA, R. C.: Indian J. Chem. (Submitted for publication in 1973)
[10] UPADHYAY, R. K., PRASAD, R., MAHESHWARI, G. L.: J. inorg. nucl. Chem. (Submitted for publication in 1973)
[11] SAXENA, R. N., PANDAY, K. K.: J. Indian Chem. Soc. **49,** 782 (1972)
[12] NAKAMOTO, K.: Infrared Spectra of Inorganic and Co-ordination Compounds, John Wiley Sons Inc., N. Y. 1968
[13] UPADHYAY, R. K.: Ph. D. Thesis, Meerut University, Meerut (India) 1972
[14] MELLOR, D. P., MALEY, L. E.: Nature **159,** 379 (1947)

R. K. UPADHYAY
M. L. SINGHAL
A. K. SAXENA
57 Chhatta Street, Khurja 203131, India

R. PRASAD; J.A.S.I. College, Khurja, India.

Acta Chimica Academiae Scientiarum Hungaricae, Tomus 83 (3—4), pp. 303—308 (1974)

MEAN AMPLITUDES OF VIBRATION FOR CH_3NO_2, CF_3NO_2, CCl_3NO_2 AND CBr_3NO_2

B. VIZI, B. N. CYVIN and S. J. CYVIN

(University for Chemical Industries, Veszprém and Technical University of Norway, Trondheim)

Received February 14, 1974

Mean amplitudes of vibration for CH_3NO_2, CF_3NO_2, CCl_3NO_2 and CBr_3NO_2 were calculated on the basis of spectroscopic data from literature. The calculated values for CF_3NO_2 and CBr_3NO_2 were compared with the corresponding data from an electron diffraction investigation.

Symmetry co-ordinates and equilibrium parameters

The treated CX_3NO_2 molecular model has the symmetry of C_s. The symmetric structure of the molecular vibrations is given by

$$\Gamma_{\text{vib}} = 9A' + 6A''.$$

A set of symmetry coordinates is given in the legend of Fig. 1. Equilibrium parameters for CH_3NO_2, *viz.* C—N = 1.46 Å, N—O = 1.21 Å and ∠ O—N—O = 127°, are taken from BROCKWAY *et al.* [1]. These data are relatively old, but have been verified by the more recent microwave investigation of TANNENBAUM *et al.* [2]. In addition it was assumed C—H = 1.08 Å and tetrahedral angles in the methyl group.

The equilibrium parameters for CF_3NO_2 and CBr_3NO_2 were taken from the electron diffraction work of KARLE and KARLE [3] while those of CCl_3NO_2 were taken from BARSS [4] with the exception of the angles ONO, ClCN and CNO, which were put equal to 133°, 108.8° and 111.8°, respectively, as equal to the corresponding ones in the other halogenated compounds.

Observed frequencies and force constants

Observed frequencies for CH_3NO_2 are cited in the book of SVERDLOV *et al.* [5] and seem to fit exactly to the early infrared and Raman investigation of WELLS and WILSON [6] when the correlations $A' = A_1 + B_2$ and $A'' = B_1 + A_2$ are assumed, and the frequency 1413 cm^{-1} of A_1 has changed place with 1449 cm^{-1} of B_2. The observed frequencies for the other molecules are taken from a work of CASTELLI *et al.* [7]. In both of the cited works [6, 7] the C_{2v} sym-

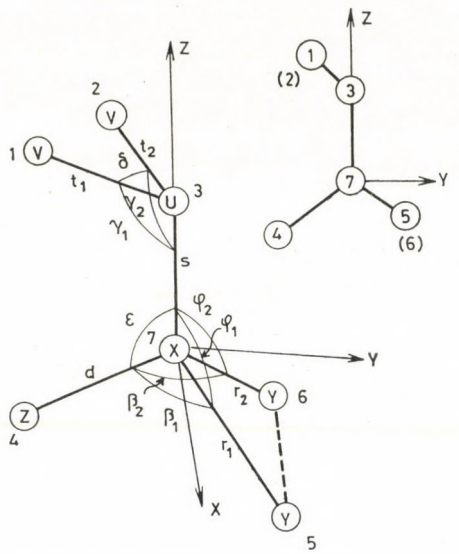

Fig. 1. The XY_2ZUV_2 molecular model (symmetry C_s) applied to CX_3NO_2 (X_1, X_2 and X_3 are atom numbers 4, 5 and 6, respectively). R, D, T and S are used to denote the equilibrium distances CX_2 or CX_3, CX_1, NO and CN, respectively. Valence co-ordinates are indicated. Torsional co-ordinates: τ_1 [1—3—7—4], τ_2 [2—3—7—4]. Symmetry co-ordinates are given by: (A′) $S_1 = 2^{-1/2}(r_1 + r_2)$, $S_2 = d$, $S_3 = s$, $S_4 = 2^{-1/2}(t_1 + t_2)$, $S_5 = (RS/2)^{1/2}(\varphi_1 + \varphi_2)$, $S_6 = (RD/2)^{1/2}(\beta_1 + \beta_2)$, $S_7 = (DS)^{1/2}\varepsilon$, $S_8 = (ST/2)^{1/2}(\gamma_1 + \gamma_2)$, $S_9 = T\delta$; A″ $S_1 = 2^{-1/2}(r_1 - r_2)$, $S_2 = 2^{-1/2}(t_1 - t_2)$, $S_3 = (RS/2)^{1/2}(\varphi_2 - \varphi_2)$, $S_4 = (RD/2)^{1/2}(\beta_1 - \beta_2)$, $S_5 = (ST/2)^{1/2}(\gamma_1 - \gamma_2)$, $S_6 = (DT/2)^{1/2}(\tau_1 + \tau_2)$

metry was assumed for the molecules in question. None of the torsional frequencies are available; therefore tentatively estimated values are used here. All the frequencies used in the present calculations are collected in Table I.

An initial force field was constructed with force constants mainly taken from the normal co-ordinae analysis of CASTELLI *et al.* [7] and with the C—H stretching constant equal to 4.9 mdyne/Å. The initial force constants were adapted to our symmetry co-ordinates. Through some steps of refinements they were made to fit exactly the observed frequencies. It seems to be of little interest to report further details of these calculations and the final force constants, especially because of the existence of the excellent normal co-ordinate analysis by CASTELLI *et al.* [7].

Mean amplitudes of vibration

The developed force fields were used to calculate the mean amplitudes of vibration according to conventional methods [8]. The results are given in Tables II—V. In Tables III and V the experimental values from the electron

Table I

Vibrational frequencies (in cm^{-1}) for CH_3NO_2, CF_3NO_2, CCl_3NO_2 and CBr_3NO_2

Species	No.	CH_3NO_2 [5]	CF_3NO_2 [7]	CCl_3NO_2 [7]	CBr_3NO_2 [7]
A'	1	3048	1310	1311	1311
	2	2965	1288	850	840
	3	1488	1151	717	669
	4	1449	860	677	618
	5	1384	750	442	397
	6	1153	527	425	304
	7	921	441	298	214
	8	647	430	289	191
	9	599	400	204	139
A''	1	3048	1620	1625	1606
	2	1582	1271	717	618
	3	1413	527	425	397
	4	1097	441	298	214
	5	476	400	204	139
	6	200[a]	154[a]	150[a]	100[a] or 150[a]

[a] Assumed

Table II

Mean amplitudes of vibration (u in Å) for CH_3NO_2

Distance	Equil. dist. (Å)	u		
		0 °K	25 °C	150 °C
1—3 N—O	1.210	0.040	0.041	0.041
3—7 N—C	1.460	0.048	0.049	0.049
4—7 C—H_1	1.080	0.077	0.077	0.077
5—7 C—H_2	1.080	0.078	0.078	0.078
1—2 O . . . O	2.166	0.050	0.051	0.052
1—7 O . . . C	2.218	0.058	0.062	0.063
1—4 O . . . H_1	2.620	0.133	0.155	0.158
1—5 O . . . H_2	2.419	0.142	0.162	0.164
1—6 O . . . H_3	3.110	0.100	0.103	0.103
3—4 N . . . H_1	2.085	0.100	0.100	0.101
3—5 N . . . H_2	2.085	0.105	0.106	0.106
4—5 H_1 . . . H_2	1.764	0.128	0.129	0.129
5—6 H_2 . . . H_3	1.764	0.133	0.134	0.134

Table III

Mean amplitudes of vibration (u in Å) for CF_3NO_2

Distance	Equil. dist. (Å)	u from spectroscopic data			u from electron diffraction data
		0 °K	25 °C	50 °C	50 °C [3]
1—3 N—O	1.210	0.040	0.041	0.041	0.050 ± 0.005
3—7 N—C	1.560	0.048	0.049	0.049	
4—7 C—F_1	1.325	0.044	0.044	0.045	0.050 ± 0.005
5—7 C—F_2	1.325	0.044	0.045	0.045	
1—2 O . . . O	2.211	0.048	0.049	0.049	0.067 ± 0.007
1—7 O . . . C	2.305	0.054	0.057	0.057	0.067 ± 0.007
1—4 O . . . F_1	2.885	0.067	0.083	0.085	0.084[a] ± 0.01
1—5 O . . . F_2	2.578	0.069	0.084	0.086	0.084[a] ± 0.01
1—6 O . . . F_3	3.383	0.057	0.063	0.064	0.084[a] ± 0.01
3—4 N . . . F_1	2.353	0.056	0.060	0.061	0.067 ± 0.007
3—5 N . . . F_2	2.353	0.055	0.060	0.061	
4—5 F_1 . . . F_2	2.170	0.055	0.060	0.061	0.057 ± 0.007
5—6 F_2 . . . F_3	2.171	0.057	0.063	0.064	

[a] Includes libration about the C—N bond

Table IV

Mean amplitudes of vibration (u in Å) for CCl_3NO_2

Distance	Equil. dist. (Å)	u		
		0 °K	25 °C	50 °C
1—3 N—O	1.210	0.041	0.042	0.042
3—7 N—C	1.590	0.051	0.052	0.052
4—7 C—Cl_1	1.750	0.055	0.059	0.059
5—7 C—Cl_2	1.750	0.054	0.057	0.058
1—2 O . . . O	2.219	0.052	0.055	0.055
1—7 O . . . C	2.328	0.060	0.065	0.066
1—4 O . . . Cl_1	3.194	0.069	0.093	0.096
1—5 O . . . Cl_2	2.806	0.077	0.111	0.115
1—6 O . . . Cl_3	3.777	0.058	0.069	0.071
3—4 N . . . Cl_1	2.717	0.057	0.065	0.067
3—5 N . . . Cl_2	2.717	0.057	0.071	0.073
4—5 Cl_1 . . . Cl_2	2.864	0.053	0.067	0.069
5—6 Cl_2 . . . Cl_3	2.881	0.055	0.073	0.075

Table V

Mean amplitudes of vibration (u in Å) for CBr_3NO_2

Distance	Equil. dist. (Å)	u from spectroscopic data[a]			u from electron diffraction data
		0 °K	25 °C	50 °C	50 °C [3]
1—3 N—O	1.220	0.043	0.043	0.044	0.050 ± 0.005
3—7 N—C	1.590	0.051	0.053	0.053	
4—7 C—Br_1	1.920	0.052	0.057	0.058	0.056 ± 0.005
5—7 C—Br_2	1.920	0.053	0.059	0.060	
1—2 O...O	2.246	0.055	0.058	0.058	0.070[c]
1—7 O...C	2.321	0.063	0.069	0.070	0.070[c]
1—4 O...Br_1	3.281	0.071	0.107	0.111[b]	0.069 ± 0.007
1—5 O...Br_2	2 889	0.072	0.111	0.115[b]	0.069 ± 0.007
1—6 O...Br_3	3.927	0.056	0.073	0.075[b]	0.069 ± 0.007
3—4 N...Br_1	2.852	0.056	0.068	0.070	0.062 ± 0.007
3—5 N...Br_2	2.852	0.053	0.071	0.073[b]	
4—5Br_1...Br_2	3.160	0.047	0.078	0.080[b]	0.089 ± 0.007
5—6Br_2...Br_3	3.151	0.049	0.081	0.084	

[a] With torsional frequency assumed 100 cm^{-1}.
[b] With 150 cm^{-1} for the torsional frequency the values at 50 °C are 0.105, 0.111, 0.072, 0.071 and 0.072, respectively, instead of the five marked values.
[c] Assumed by KARLE and KARLE [3].

diffraction work by KARLE and KARLE [3] are included for comparison. It seems to be satisfactory general agreement between the spectroscopic and electron diffraction values.

For CBr_3NO_2 calculations were performed with two different torsional frequencies, $\nu_6(A'') = 150$ and 100 cm^{-1}, in order to show the effect of such a change in the assumed frequencies. It was found that the mean amplitudes for the O...Br_1, N...Br_2 and Br_1...Br_2 are the only ones being significantly affected.

*

Financial support to BNC from The Norwegian Research Council for Science and the Humanities is gratefully acknowledged.

REFERENCES

[1] BROCKWAY, L. O., BEACH, J., PAULING, L.: J. Am. Chem. Soc. **57,** 2693 (1939)
[2] TANNENBAUM, E., MYERS, R. J., GWINN, W. D.: J. Chem. Phys. **25,** 42 (1956)
[3] KARLE, I. L., KARLE, J.: J. Chem. Phys. **36,** 1969 (1962)
[4] BARSS, W. M.: J. Chem. Phys. **27,** 1260 (1957)
[5] SVERDLOV, L. M., KOVNER, M. A., KRAINOV, E. P.: Kolebatelnye spektry mnogoatomnykh molekul (Vibrational spectra of polyatomic molecules), Izd. Nauka, Moscow 1970

[6] WELLS, A. J., WILSON, E. B., jr.: J. Chem. Phys. **9**, 314 (1941)
[7] CASTELLI, A., PALM, A., ALEXANDER, CH., jr.: J. Chem. Phys. **44**, 1577 (1966)
[8] CYVIN, S. J.: Molecular Vibrations and Mean Square Amplitudes. Universitetsforlaget, Oslo and Elsevier, Amsterdam 1968

Béla VIZI; H-8200 Veszprém, Schönherz Z. u. 12. Hungary,

B. N. CYVIN, S. J. CYVIN } N-7034 Trondheim-NTH, Norway.

Acta Chimica Academiae Scientiarum Hungaricae, Tomus 83 (3—4), pp. 309—313 (1974)

THE EXTREME VALUES OF CORIOLIS COUPLING CONSTANTS COMPATIBLE WITH THE MEASURED NORMAL FREQUENCIES

I. LUKOVITS and F. TÖRÖK

(Central Research Institute for Chemistry of the Hungarian Academy of Sciences and Department of General and Inorganic Chemistry, Eötvös Loránd University)

Received February 25, 1974

The authors have showed how the maximum and minimum values of the Coriolis coupling constants of a molecule can be estimated, when the elements of the **F** force constant matrix reproducing the measured normal frequencies are not fixed but are allowed to vary between well-defined limits. To achieve this task they used the parameter representation method and the projection gradient technique. A computer program has been written to perform these calculations for the HCHO molecule. They found that the experimentally determined ζ^x_{65} coupling constant was lying in the narrow range bounded by the maximum and minimum possible value of the estimated ζ^x_{65}.

Introduction

The force field of polyatomic molecules cannot be determined from the knowledge of the normal frequencies uniquely. Thus all quantities which are in principle computable from the **F** matrix (*e.g.* Coriolis coupling constants, mean square vibrational amplitudes, centrifugal distorsion constants) also cannot be obtained exactly. Our aim was to give an example, how to find the minimum and maximum values of the Coriolis coupling constants, when the elements of the **F** force constant matrix reproducing the measured normal frequencies are not fixed, but may vary within previously specified limits. This technique may be of use in finding and classifying the experimental Coriolis coupling constants.

The ζ^α matrix of the Coriolis coupling constants ($\alpha = x, y, z$) depends on the force field of the molecule [1]:

$$\zeta^\alpha = \mathbf{L}^{-1}\,\mathbf{C}^\alpha\,(\mathbf{L}^{-1})' \tag{1}$$

where $\mathbf{L}^{-1}$ denotes the inverse **L** matrix consisting of the eigenvectors of the **GF** matrix. The $\mathbf{C}^\alpha$ may be calculated from the $\mathbf{M}^\alpha$ matrices defined in [1]:

$$\mathbf{C}^\alpha = \mathbf{B}\mathbf{m}^{-1/2}\,\mathbf{M}^\alpha\mathbf{m}^{-1/2}\,\mathbf{B}'\,. \tag{2}$$

There $\mathbf{m}^{1/2}$ is a diagonal matrix whose elements are the square roots of the atomic masses. The **B** matrix connects the S and x vectors containing the symmetry and the Descartes co-ordinates, respectively:

$$S = \mathbf{B}x\,. \tag{3}$$

The force field of HCHO has been determined by several authors [2—4]. More recent calculations of MALLINSON and DUNCAN [5] yielded a refined force field, that was set up to reproduce the harmonic spectrum of formaldehyde and deuteroformaldehyde. An *ab initio* force field calculation for the H_2CO molecule was performed by PULAY [6].

Method and calculation

Our task was to find the maximum and minimum values of the ζ_{ij}^{α} matrix, on the condition that

$$l_{ij} \leqq \mathbf{F}_{ij} \leqq u_{ij} \tag{4}$$

where l_{ij} and u_{ij} are the lower and upper limits for the $\mathbf{F}_{ij}$ force constants, respectively. An iteration method based on the parameter representation of Coriolis coupling constants [8, 9] and the gradient projection method [10, 11] were applied. This method had been already applied by TÖRÖK and PULAY [7] for the estimation of maximal and minimal values of the $\mathbf{F}_{ij}$ force constants of ethane. The main feature of this procedure is to change the parameters in small steps in such a way that the ζ_{ij}^{α} under consideration should increase (or decrease) at the highest possible rate, keeping in mind that the restrictions of Eq. (4) imposed upon the elements $\mathbf{F}_{ij}$ must hold. In each step of the iteration process, a d gradient vector had to be calculated. The d_k component of this vector is the partial derivative of the ζ_{ij}^{α} constant:

$$d_k = \frac{\partial \zeta_{ij}^{\alpha}}{\partial \alpha_k} . \tag{5}$$

The next step is made in the direction of the vector $a = Nd$ .Here N denotes the normalization constant. The partial derivatives of the ζ_{ij}^{α} are given by TÖRÖK, PULAY and HUN-BOROSSAY [9, 17]. The elements of the gradient vector were used to set up the **K** matrix [8]. From the **K** matrix the new $\mathbf{L}^{-1}$ was computed using the relations given by TÖRÖK and PULAY [8]. The new **F** matrix was obtained by the formula:

$$\mathbf{F} = (\mathbf{L}')^{-1} \mathbf{\Lambda} \mathbf{L}^{-1} \tag{6}$$

where Λ denotes a diagonal matrix, whose elements λ_i are connected with the ith normal frequency according to: $\lambda_i = 4\nu_i^2\pi^2$ [12]. A new direction had to be chosen, when one or more of the prescribed restrictions (4) had been violated. In this case the new a' vector is obtained using equation (7):

$$a' = N\{\mathbf{I} - \mathbf{M}'(\mathbf{M}\mathbf{M}')^{-1}\mathbf{M}\}\, d \tag{7}$$

where **I** denotes a unit matrix of order $(n/2)$, here n denotes the number of the normal frequencies, **M** is a matrix which is made up from all the partial derivatives of those force constants that have violated the restrictions of Eq. (4) [7]. A further complication arises when one or more components of the vector a' are negative. ROSEN has proved that one row corresponding to the index of one of the negative components (that with the highest absolute value) can be omitted from matrix **M**. For this new **M*** matrix Eq. (7) also applies, a new direction a^* results. The iteration process may end in two ways:

a) it may lead to a local maximum or minimum

b) the number of rows of matrix **M*** equals $(n/2)$. Then the extreme value belongs to parameters being in a vertex of the region allowed.

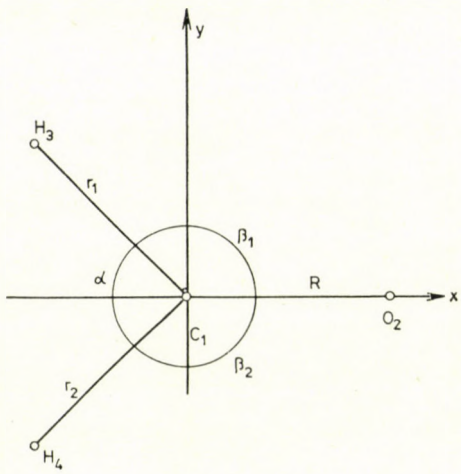

Fig. 1

On the Coriolis coupling constants of formaldehyde

In order to define the symmetry co-ordinates we have to set up the internal co-ordinates of the molecule. Figure 1 shows the placing of atoms and the definition of internal co-ordinates. The geometry has been taken from TAKAGI and OKA [3]. We used the following symmetry co-ordinates:

$$A_1 \text{ species:} \quad S_1 = R\,, \quad S_2 = 2^{-1/2}(r_1 + r_2)\,, \quad S_3 = 2^{-1/2}(\beta_1 + \beta_2 - 2\alpha)$$
$$B_1 \text{ species:} \quad S_4 = 2^{-1/2}(r_1 - r_2)\,, \quad S_5 = 2^{-1/2}(\beta_1 - \beta_2)\,.$$
$$B_2 \text{ species:} \quad S_6 = \delta.$$

Here δ denotes the out-of-plane vibration of the C—O bond. The values of the corresponding $\mathbf{F}_{ij}$ constants used were determined by MALLINSON and DUNCAN [5]. These force constants were fitted to approximate the "harmonized" spectrum of both H_2CO and D_2CO. Their force constants were adjusted by

JOHANSEN's method [13] in order to obtain the harmonic frequency values of HCHO exactly. Table I contains the elements of this **F** matrix. The harmonic spectrum of formaldehyde is for the A_1 species (in cm^{-1}): 2944.5, 1763.7, 1562.6; for the B_1 species: 3008.7, 1208.7; for the B_2 species: 1191.0.

Table I

The symmetry **F** *matrix of formaldehyde**

$\mathbf{F}_{11} = 12.97$	$\mathbf{F}_{33} = 0.58$
$\mathbf{F}_{12} = 0.74$	$\mathbf{F}_{44} = 4.82$
$\mathbf{F}_{13} = 0.44$	$\mathbf{F}_{45} = 0.16$
$\mathbf{F}_{22} = 4.97$	$\mathbf{F}_{55} = 0.76$
$\mathbf{F}_{23} = -0.08$	$\mathbf{F}_{66} = 0.41$

* The dimensions are for the stretching constants: mdyn/Å, for the stretch–bend–interaction: mdyn/rad, for the bending force constants: mdyn/rad²

The prescribed minimum and maximum values of the different $\mathbf{F}_{ij}$ force constants are given in Table II. According to JAHN's rule [1] the only

Table II

*Prescribed minimum and maximum values for the force constants of formaldehyde**

$12.60 \leq \mathbf{F}_{11} \leq 13.60$	$0.49 \leq \mathbf{F}_{33} \leq 0.63$
$0.60 \leq \mathbf{F}_{12} \leq 1.00$	$4.60 \leq \mathbf{F}_{44} \leq 5.00$
$0.35 \leq \mathbf{F}_{13} \leq 0.46$	$0.13 \leq \mathbf{F}_{45} \leq 0.20$
$4.69 \leq \mathbf{F}_{22} \leq 5.10$	$0.70 \leq \mathbf{F}_{55} \leq 0.90$
$-0.19 \leq \mathbf{F}_{23} \leq -0.07$	$0.35 \leq \mathbf{F}_{66} \leq 0.50$

* See footnote for Table I

non-vanishing ζ_{ij}^{α} Coriolis coupling constants are for $\alpha = x$: ζ_{64}^{x} and ζ_{65}^{x}; for $\alpha = y$: ζ_{61}^{y}, ζ_{62}^{y}, ζ_{63}^{y}; for $\alpha = z$: ζ_{41}^{z}, ζ_{51}^{z}, ζ_{42}^{z}, ζ_{52}^{z}, ζ_{43}^{z}, ζ_{53}^{z}. BLAU and NIELSEN [14] determined ζ_{65}^{x} experimentally, and found that $\zeta_{65}^{x} = 0.54$. But since the sum rule [1, 18] holds:

$$(\zeta_{64}^{x})^2 + (\zeta_{65}^{x})^2 = 1 \tag{8}$$

the ζ_{64}^{x} is also uniquely determined. Later OKA and MORINO [15] and NAKAGAWA and MORINO [16] analyzed the Coriolis interaction between ν_4 and ν_6.

Results

The calculation performed for the formaldehyde molecule yielded the initial Coriolis coupling constants and the possible maximum and minimum values of these constants. The results are summarized in Table III. It should be mentioned that the experimentally determined ζ_{ij}^{x} constants ($\zeta_{64}^{x} = 0.84$, $\zeta_{65}^{x} = 0.54$) lie within the theoretically estimated interval.

Table III

Evaluated minimum and maximum values for the non-vanishing ζ_{ij}^{α} Coriolis coupling constants of formaldehyde

ζ_{ij}^{α}	Initial value	Minimum value	Maximum value
ζ_{64}^{x}	0.843	0.838	0.847
ζ_{65}^{x}	0.537	0.532	0.546
ζ_{61}^{y}	−0.528	−0.534	−0.476
ζ_{62}^{y}	0.592	0.562	0.705
ζ_{63}^{y}	−0.609	−0.649	−0.514
ζ_{41}^{z}	−0.044	−0.055	0.023
ζ_{51}^{z}	−0.914	−0.918	−0.902
ζ_{42}^{z}	0.490	0.433	0.609
ζ_{52}^{z}	0.333	0.281	0.395
ζ_{43}^{z}	−0.871	−0.901	−0.789
ζ_{53}^{z}	0.233	0.173	0.296

REFERENCES

[1] Meal, J. H., Polo, S. R.: J. Chem. Phys. **24,** 1119 (1956)
[2] Hisatsune, I. C., Eggers, D. F.: J. Chem. Phys. **23,** 487 (1955)
[3] Takagi, K., Oka, T.: J. Phys. Soc. Japan **18,** 1174 (1963)
[4] Curtis, A.: J. Mol. Structure **14,** 279 (1964)
[5] Mallinson, P. D., Duncan, J. L.: Chem. Phys. Lett. to be published in 1974
[6] Pulay, P.: to be published
[7] Török, F., Pulay, P.: Acta Chim. Acad. Sci. Hung., **56,** 285 (1968)
[8] Török, F., Pulay, P.: J. Mol. Structure **3,** 1 (1969)
[[9] Török, F., Pulay, P.: J. Mol. Structure **3,** 283 (1969)
[10] Rosen, J. B.: J. Soc. Industrial and Applied Mathematics **8,** 181 (1960)
[11] Rosen, J. B.: J. Soc. Industrial and Applied Mathematics **9,** 514 (1961)
[12] Wilson, E. B., Decius, J. C., Cross, P. C.: Molecular Vibrations, McGraw-Hill, New York 1955
[13] Johansen, H.: Z. Phys. Chem. **227,** 305 (1964)
[14] Blau, H. H., Nielsen, H. H.: J. Mol. Spectroscopy **1,** 124 (1957)
[15] Oka, T., Morino, Y.: J. Mol. Spectroscopy **11,** 349 (1963)
[16] Nakagawa, T., Morino, Y.: J. Mol. Spectroscopy **38,** 84 (1971)
[17] Török, F., Pulay, P., Hun-Borossay, Gy.: Acta Chim. Acad. Sci. Hung. **61,** 39 (1969)
[18] Nemes, L.: Mol. Spectroscopy **28,** 59 (1968)

István Lukovits; H-1025 Budapest, Pusztaszeri út 59—67, Hungary
Ferenc Török; H-1088 Budapest, Múzeum krt. 6—8, Hungary.

Acta Chimica Academiae Scientiarum Hungaricae, Tomus 83 (3—4), pp. 315—319 (1974)

THE APPLICATION OF X-RAY-PHOTOELECTRON SPECTROSCOPY (ESCA) IN CO-ORDINATION CHEMISTRY, V*

STUDY OF THIOCYANATE AND ISOTHIOCYANATE COMPLEXES

K. BURGER, GY. LIPTAY and CS. VÁRHELYI

(Department of Inorganic and Analytical Chemistry, Eötvös Loránd University, Budapest, Department of Inorganic Chemistry, Technical University, Budapest and Department of Chemistry, Babes-Bólyai University, Cluj, Roumania

Received 1 March, 1974

The ESCA examination of some thiocyanate and isothiocyanate mixed complexes containing terminal thiocyanate ligands, and some polynuclear mixed complexes containing thiocyanate bridges, was used to demonstrate the effects of co-ordination of the sulphur atom or the nitrogen atom of the thiocyanate, or both at once, on the electronic structure of the thiocyanate.

In its metal complexes the thiocyanate ligand can co-ordinate to the central metal ion *via* a sulphur donor atom (thiocyanate complexes) or *via* a nitrogen donor atom (isothiocyanate complexes), and it can act too as a bridging ligand, co-ordinated *via* both of its donor atoms [1—5].

Infrared spectroscopic examinations have shown that the vibration spectrum of the thiocyanate ion varies, depending on which of its donor atoms is co-ordinated to the metal [5—8]. The C—S vibration frequency for the thiocyanate ion in potassium thiocyanate is 749 cm^{-1}; the corresponding frequency in thiocyanate complexes is about 720 cm^{-1}, and in isothiocyanate complexes is about 820 cm^{-1}. The C≡N vibration frequency for the thiocyanate ion in potassium thiocyanate is 2049 cm^{-1}; the corresponding value is 30—50 cm^{-1} higher in isothiocyanate complexes and 50—70 cm^{-1} higher in thiocyanate complexes, and attains the greatest value (about 2150 cm^{-1}) in thiocyanate bridges [3, 9—11].

By means of infrared spectroscopic examinations, therefore, it can be established how thiocyanate is bonded to the central atom of the complex. This is of great importance, for the manner of co-ordination of the thiocyanate ion showes quite clearly the PEARSON [4] 'soft' or 'hard' character of the central atom [12]. The thiocyanate ion is bound to soft central atoms *via* its sulphur donor atom, and to hard central atoms *via* its nitrogen donor atom. The hard or soft nature of the central atom depends on the overall electronic structure of the complex. Accordingly, in the case of mixed complexes, not only the central atom, but also both type of ligands, influences the nature of the bonding of the thiocyanate ion to the metal. It has been shown by TURCO and PE-

* The previous paper of this series: K. BURGER and Á. BUVÁRI: Inorg. Chim. Acta 11, 25 (1974).

CIL [8], for instance, that in the complex $Pd(NH_3)_2(SCN)_2$ the thiocyanate is bound to the palladium *via* the sulphur donor atom, whereas in the complex $Pd[P(C_2H_5)_3)_2(NCS]_2$ the nitrogen is the donor atom. Our earlier investigations [13] indicated that in the low spin number, mixed complex bis(dimethylglyoximato)dithiocyanatocobalt(II) the thiocyanate is bound to the cobalt *via* the sulphur donor atom, in contrast to the majority of cobalt(II) complexes examined, where the nitrogen is the donor atom. Prior to our present examinations there were not data on the manner of co-ordination of the thiocyanate in the analogous cobalt(III)-dimethylglyoxime mixed complexes.

As seen above, the infrared spectra of the complexes reflect well the changes in the electronic structure of the thiocyanate resulting from the various modes of co-ordination. The aim of the present work is to study how these changes appear in the electron-binding energies of the atoms of the thiocyanate in the ESCA spectra of the compounds.

Thus, the ESCA data for potassium thiocyanate were compared with the ESCA data for thiocyanate bonded in some nickel–pyridine and nickel–picoline mixed isothiocyanate complexes, in nickel–hexamine isothiocyanate, and in some cobalt(III)-dioxime mixed complexes. Infrared spectroscopy was used to determine how the thiocyanate is bound to the central cobalt(III) atom in these latter complexes.

Experimental

The ESCA examination of the complexes was performed as described earlier [14]. The pyridine and picoline complexes were kept at −50 °C during measurement, so that they should not undergo decomposition in the apparatus as a result of the vacuum.

The complex bands due to the presence of non-equivalent atoms were resolved by computer as reported previously [15].

A Zeiss UR 20 spectrophotometer was employed for the infrared examinations. The IR spectra of the complexes were taken in Nujol mull.

The complexes were prepared by procedures given in the literature [16–18].

The dipyridine and dipicoline derivatives were obtained from the tetrapyridine and tetrapicoline complexes in the vacuum chamber of the ESCA spectrometer, by cessation of the cooling and by appropriate heating of the sample.

The compositions of the pyridine and picoline complexes were checked thermogravimetrically, and the stoichiometry of the dimethylglyoxime mixed complexes was confirmed by determination of the cobalt contents.

Results and discussion

The C–S and C≡N vibration bands due to the thiocyanate ligand were identified in the infrared spectra of the mixed thiocyanate complexes of bis(dimethylglyoximato)cobaltate(III). On the basis of what was said in the introduction, the data in Table I show clearly that in these mixed complexes the thiocyanate is co-ordinated to the low-spin cobalt(III) central atom *via* its sulphur donor atom.

Table I

Infrared bands of thiocyanate mixed complexes of bis(dimethylglyoximato)cobalt(III), cm^{-1}

Complex	C≡N	C–S
$H[Co(HD)_2(SCN)_2]$	2108	718
$H[Co(HD)_2(SCN)Cl]$	2120	720
$[Co(HD)_2(SCN)H_2O]$	2115	720

It is already known from earlier studies of the pyridine and picoline complexes [10], that the thiocyanate is bound to the central atom in the tetrapyridine and tetrapicoline complexes *via* its nitrogen atom, whereas in the dipyridine and di-γ-picoline derivatives it acts as a bridge.

Each of the complexes examined contains only one type of sulphur atom, but in every complex there are two types of nitrogens and, with the exception of the nickel–hexamine complex, at least two types of carbon atom. The reliable separation of the bands due to the non-equivalent atoms, and the determination of the electron-binding energies of the thiocyanate atoms after such separation, could be performed only in those systems where the concentration of the disturbing atoms was not many times higher than that of the corresponding atoms of the thiocyanate and the difference of the electron-binding energies was not too small.

The charge arising on the insulating samples as a result of the ejection of the photoelectrons in the complexes of different types affected the electron-binding energy values in different ways. This may give the explanation for the fact that even after the ESCA examination of a large number of thiocyanate complexes JØRGENSEN and BERTHOU [19] did not detect the effect of the co-ordination of the sulphur or the nitrogen on the electron-binding energies. However, since this effect changes the electron-binding energy value of the various atoms within a single compound to the same extent, the electron-binding energies of the donor atoms referred to an appropriate reference atom within the molecule, can give data which are suitable for the drawing of reliable conclusions in co-ordination chemistry.

Table II contains the electron-binding energies of the S $2p_{1/2,3/2}$ and N 1*s* orbitals of the thiocyanate, referred to the C 1*s* orbital.

It can be seen that while the co-ordination of the nitrogen results in the increase of the energy difference C 1*s* — S $2p_{1/2,3/2}$ the co-ordination of the sulphur causes its decrease.

The electron-bonding energy difference N 1*s* — C 1*s* is smaller when the nitrogen in the thiocyanate ligand is co-ordinated, and larger when the sulphur.

Taking into account that the absolute value of the C 1*s* electron-binding energy is larger than that of the S $2p_{1/2,3/2}$, but smaller than that of the N 1*s*,

Table II

Electron-binding energies, of the donor atoms of the thiocyanate in various complexes, referred to the C 1s orbital of the thiocyanate, eV

Complex	C 1s—S $2p_{1/2,3/2}$	N 1s—C 1s
KNCS	122.35	112.75
$Ni(NH_3)_4(NCS)_2$	122.65	112.3
$H[Co(HD)_2(SCN)_2]$	121.4	114.2
$H[Co(HD)_2(SCN)Cl]$	120.7	—
$[Co(HD)_2(SCN)H_2O]$	121.3	—

and that the increase of the electron-binding energies shows the decrease of the electron density, the following conclusions can be drawn from the data in Table II.

1. The co-ordination of the nitrogen of the thiocyanate ion increases the electron density on both the sulphur and the nitrogen atoms and/or decreases that on the carbon atom.

2. The co-ordination of the sulphur, on the other hand, decreases the electron density on both the sulphur and nitrogen atoms, and/or increases that on the carbon atom.

In agreement with the results of infrared investigations, this apparently anomalous behaviour can be well explained *via* the following two structures of thiocyanate, showing the sulphur or the nitrogen atoms as donors:

$$\leftarrow\overline{\underline{S}}-C\equiv\overline{N} \qquad \overline{\underline{S}}=C=\overline{N}\rightarrow$$

The S $2p_{1/2,3/2}$ electron-binding energies referred to the aromatic carbon atoms in the pyridine and picoline complexes are given in Table III.

Table III

S $2p_{1/2,\,3/2}$ electron-binding energies, referred to the aromatic carbon atoms, in complexes containing terminal and brindging thiocyanate ligands

Complex	C 1s—S $2p_{1/2,3/2}$	State of thiocyanate
$Ni(py)_4(NCS)_2$	122.4	terminal
$Ni(py)_2(NCS)_2$	122.2	bridging
$Ni(\gamma\text{-pic})_4(NCS)_2$	122.2	terminal
$Ni(\gamma\text{-pic})_2(NCS)_2$	122.0	bridging

The data reveal that in the complexes $Ni(py)_4(NCS)_2$ and $Ni(\gamma\text{-pic})_4(NCS)_2$, which contain thiocyanate bound terminally through the nitrogen, the energy difference C 1*s* — S $2p_{1/2,3/2}$ is larger than in the corresponding *bis* complexes, which contain thiocyanate bridges. Since the tetrapyridine → dipyridine transformation and the development of the thiocyanate bridges in the analogous complexes cause no or only a very slight change in the electron density on the carbon atoms of the pyridine, the data in Table III clearly indicate that the formation of the thiocyanate bridge (the co-ordination of the sulphur) decreases the electron density on the sulphur atom. The data of Table III thus show that the energy differences for the thiocyanate complexes in Table II can be primarily attributed to the electron-density decrease on the sulphur, and only secondarily to the increase of the electron density on the carbon atom of the thiocyanate.

*

The authors express their thanks to Professor E. FLUCK, who made possible the recording of the ESCA spectra in the Department of Inorganic Chemistry, University of Stuttgart.

REFERENCES

[1] BASOLO, F., BADDELY, W. H., BURMEISTER, J. L.: Inorg. Chem. **3,** 1202 (1964)
[2] LINDQUIST, I., STRANDBERG, B.: Acta Crystall. **10,** 176 (1957)
[3] MITCHELL, P. C. H., WILLIAMS, R. J. P.: J. Chem. Soc. **1960,** 1912
[4] PEARSON, R. G.: J. Amer. Chem. Soc. **85,** 3533 (1963)
[5] TRAMER, A.: J. Chem. Phys. **1962,** 232
[6] CHAMBERLAIN, M. M., BAILAR, J. C., Jr.: J. Amer. Chem. Soc. **81,** 6412 (1959)
[7] LEWIS, J., NYHOLM, R. S., SMITH, P. W.: J. Amer. Chem. Soc. **1961,** 4590
[8] TUROC, A., PECIL, C.: Nature, London **191,** 66 (1961)
[9] BECK, W., LOTTES, K.: Z. anorg. allg. Chem. **335,** 258 (1965)
[10] LIPTAY, G., BURGER, K., PAPP-MOLNÁR, E., SZEBENI, SZ., RUFF, F.: J. Inorg. Nucl. Chem. **31,** 2359 (1969)
[11] BURGER, K., LIPTAY, G., KORECZ, L., KIRÁLY, I., PAPP-MOLNÁR, E.: Proc. 3rd Symp. Co-ord. Chem. Debrecen 1970, I, 465 (1970); II, 211 (1971)
[12] SCHMIDTKE, H. H., GARTHOHH, D.: Helv. Chim. Acta **50,** 1631 (1967)
[13] BURGER, K., RUFF, I., RUFF, F.: Proc. Symp. Co-ord. Chem. Tihany **1964,** 205. Akadémiai Kiadó, Budapest (1965)
[14] BURGER, K., FLUCK, E., BINDER, H., VÁRHELYI, CS.: J. Inorg. Nucl. Chem. (in press)
[15] BURGER, K., FLUCK, E., VÁRHELYI, CS., BINDER, H., SPEYER, F.: Z. anorg. allg. Chem. 408, 304 1974,
[16] ABLOV, A. V., SAMOT, N. M.: Zhur. Neorg. Khim. **3,** 1818 (1957)
[17] ABLOV, A. V., SYROTA, G. P.: Zhur. Neorg. Khim. **5,** 1221 (1960)
[18] SPACU, G., DICK, J.: Z. anal. Chem. **71,** 442 (1927)
[19] JORGENSEN, C. K., BERTHOU, H.: Photo-electron Spectra Induced by X-rays of above 600 Non-metallic Compounds containing 77 Elements. Danske Videnskab. Selskab. Mat-Fys. **38,** 15 (1972)

Kálmán BURGER
György LIPTAY } 1088 Budapest, Múzeum krt. 4/b, Hungary.

Csaba VÁRHELYI; Babes-Bólyai University, Cluj, Roumania.

Acta Chimica Academiae Scientiarum Hungaricae, Tomus 83 (3—4), pp. 321—329 (1974)

HARMONIC FORCE FIELDS AND CALCULATED MEAN AMPLITUDES FOR TUNGSTEN OXIDES: WO_2 AND WO_3 WITH COMMENTS ON THE WO_4^{--} ION

S. J. CYVIN and I. HARGITTAI

(University of Trondheim, Norway, and Hungarian Academy of Sciences, Budapest)

Received March 6, 1974

Harmonic force fields are developed for WO_2 and WO_3 and used to calculate the mean amplitudes of vibration for these molecules along with the shrinkage effect for WO_3. Previous calculations of mean amplitudes for WO_4^{--} are discussed. The influences on the mentioned quantities by varying certain frequencies of WO_2 and WO_3 are studied. The possibilities to estimate these frequencies by means of observed mean amplitudes or the shrinkage from gas electron diffraction are pointed out.

Much interest is attached to the structural and spectroscopical problems of tungsten oxides. The formation of vapours of tungsten oxides and their supposed water complexes is a part of important industrial processes at relatively high temperatures. A high-temperature gas electron diffraction investigation of $(WO_3)_3$ has been reported [1]. In the present work some spectroscopical computations for simple tungsten oxides are communicated. Mean amplitudes of vibration [2, 3] are discussed in particular as well as the BASTIANSEN—MORINO shrinkage effect [3, 4] for planar WO_3. The temperature dependence of these quantities is studied.

Hypothetical linear WO_2

A linear structure for the WO_2 molecule in gas phase is improbable. Nevertheless it has been assumed in different spectroscopical analyses. NAGARAJAN has reported the calculated mean amplitudes on the basis of the linear model [5] in addition to a previous analysis using a bent model [6]. We have reproduced the calculations for the hypothetical linear model and extended the range of temperatures. The vibrational frequencies of $\nu_1 = 770$ cm^{-1} and $\nu_3 = 835$ cm^{-1} were applied. Table I shows the calculated results. The values at 0, 298.15 and 500 K coincide with those reported by NAGARAJAN [5].

The corresponding calculations were performed with $\nu_1 = 992$ cm^{-1} and $\nu_3 = 928$ cm^{-1}. These frequencies were taken from JANAF Tables [7] and originate from infrared spectra in a neon matrix [8]. The resulting mean amplitudes are included in Table I.

Table I

Mean amplitudes of vibration (Å units) for WO_2 at given absolute temperatures (T in K)

Model	Linear (I)[a]		Linear (II)[b]		Bent (110°)[b]	
Distance	WO	OO	WO	OO	WO	OO
$T =$ 0	0.0378	0.0523	0.0346	0.0461	0.0346	0.0626
298.15	0.0386	0.0536	0.0350	0.0465	0.0349	0.0743
500	0.0417	0.0584	0.0369	0.0488	0.0369	0.0885
1000	0.0523	0.0737	0.0448	0.0589	0.0448	0.1195
1500	0.0623	0.0880	0.0529	0.0693	0.0528	0.1449
2000	0.0712	0.1007	0.0602	0.0788	0.0601	0.1668

[a] Frequencies as used by NAGARAJAN [5]
[b] Frequencies from JANAF Tables [7]

Bent WO_2

It is more realistic to assume a bent model for the WO_2 molecule. We have adopted an estimated valence angle of 110° in addition to the bond distance value of 1.81 Å [7]. The adopted ν_1 and ν_3 values [7, 8] are the same as those of the linear model (II) and are quoted above. In the present case the mean amplitudes also depend on the ν_2 frequency, which is unobserved. An estimated value of 300 cm^{-1} [7, 8] for gaseous WO_2 was used in the present calculations. The force field as obtained by means of the L-matrix approximation of MÜLLER [9, 10], which means that $L_{12} = 0$ was assumed. In the present case this approximation is justified in particular because the mass of the central atom is much greater than the mass of an end atom. The F and L matrix blocks of species A_1 are shown in Table II. The computed mean amplitudes of vibration are included in Table I. It is interesting to compare these results with those from the calculations using the linear model (II). The comparison shows the effect of nonlinearity in the molecular model. It is found that the bond mean amplitudes (WO) are affected to a negligible degree while the effect on the nonbond amplitudes (OO) is substantial; *cf.* Table I.

Table II

Force constants (in mdyne/Å) and L matrix elements (in $Amu^{-1/2}$) of species A_1 ($\nu_1 = 992$ cm^{-1}, $\nu_2 = 300$ cm^{-1}) for bent WO_2

F		L	
8.775	0.042	0.257	0.000
0.042	0.382	−0.028	0.373

The estimated value for the ν_2 frequency is very uncertain. We have therefore performed the calculation of mean amplitudes using a number of values for this frequency in the range between 200 and 350 cm^{-1}. The *L*-matrix approximation method was used throughout. As a consequence of this approximation the bond mean amplitude is not affected by changes in ν_2 *(cf.* Appendix). The nonbond mean amplitude on the other hand does depend on the ν_2 frequency. The calculated values at different temperatures are shown graphically in Fig. 1 as functions of ν_2.

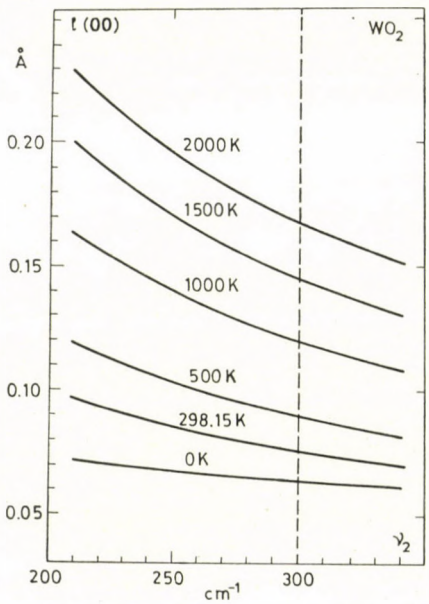

Fig. 1. Bent WO_2 (110°; $\nu_1 = 992$ cm^{-1}, $\nu_3 = 928$ cm^{-1}; $L_{12} = 0$): Mean amplitudes of vibration (*l*) for the nonbond distance (OO) at different temperatures as functions of the ν_2 frequency. 300 cm^{-1} is an estimated value [7, 8]

Planar trigonal WO_3

The planar trigonal structure with 1.81 Å for the bond distance has been adopted for the gaseous WO_3 molecule [7]. The vibrational frequencies were taken from JANAF Tables [7] and are different from those adopted by NAGARAJAN [5]. The present values contain the two estimated values $\nu_1 = 564$ cm^{-1} and $\nu_2 = 347$ cm^{-1} [8], one observed matrix-isolation frequency in infrared, *viz.* $\nu_3 = 1040$ cm^{-1} [8], and another estimated value, $\nu_4 = 320$ cm^{-1} [15]. The *L*-matrix approximation method (see above) was applied in order to determine the force constants of the *E'* species. These force constants along with the corresponding *L* matrix block are shown in Table III. Table IV

Table III

Force constants (in mdyne/Å) and L matrix elements (in $Amu^{-1/2}$) of species E′ ($\nu_3 = 1040\ cm^{-1}$, $\nu_4 = 320\ cm^{-1}$) for WO_3

F		L	
9.027	−0.058	0.266	0.000
−0.058	0.288	0.053	0.457

Table IV

Mean amplitudes of vibration (l in Å units) and Bastiansen–Morino shrinkage effect (δ in Å) for WO_3 at given temperatures (T in K)

T	l(WO)	l(OO)	δ
0	0.0372	0.0644	0.0014
298.15	0.0385	0.0736	0.0022
500	0.0421	0.0869	0.0033
1000	0.0531	0.1170	0.0063
1500	0.0634	0.1418	0.0093
2000	0.0724	0.1632	0.0124

shows the calculated mean amplitudes of vibration (l) and the BASTIANSEN—MORINO shrinkage effect (δ) at several temperatures.

Additional computations were made with varying frequencies because so many of them are very uncertain. Again the L-matrix approximation method was used throughout. Under these circumstances the l(WO) value depends only on ν_1 and ν_3, l(OO) depends on ν_1, ν_3 and ν_4, and δ depends mainly on ν_2, but also to a smaller extent on ν_3 and ν_4 (*cf.* Appendix). The value adopted for the equilibrium bond distance (1.81 Å) affects only the shrinkage, not the mean amplitudes. Fig. 2 shows the variation of l(OO) at different temperatures with the magnitudes of ν_4 under constant ν_1 and ν_3, which were kept at the values given above. Fig. 3 shows the variation of δ with ν_2 when ν_3 and ν_4 are kept constant at their original values.

Tetrahedral WO_4^{--}

Many spectroscopic investigations have been performed for the WO_4^{--} ion, which is known to have the tetrahedral structure. Calculated mean amplitudes have been reported [16—20]. Other spectroscopical studies on metal oxoanions including WO_4^{--} are due to MÜLLER *et al.* [21—24]; references

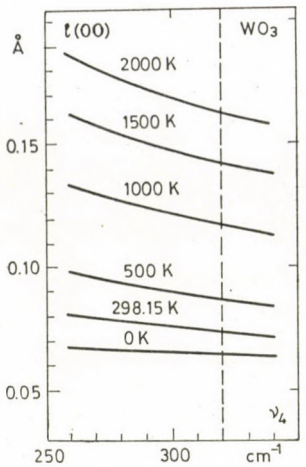

Fig. 2. Planar symmetrical WO_3 ($\nu_1 = 564\ cm^{-1}$, $\nu_3 = 1040\ cm^{-1}$; $L_{34} = 0$): Mean amplitudes of vibration (l) for the nonbond distance (OO) at different temperatures as functions of the ν_4 frequency. 320 cm^{-1} is an estimated value [7, 15]

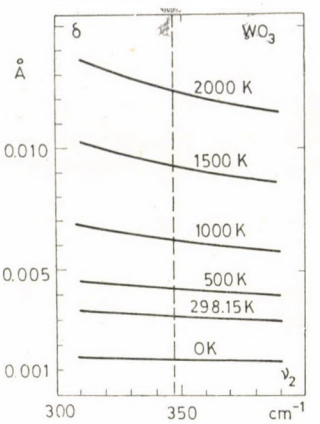

Fig. 3. WO_3 (1.81 Å; $\nu_3 = 1040\ cm^{-1}$, $\nu_4 = 320\ cm^{-1}$; $L_{34} = 0$): BASTIANSEN—MORINO shrinkage effect (δ) at different temperatures as functions of the ν_2 frequency. 347 cm^{-1} is an estimated value [7, 8]

Table V

Vibrational frequencies (cm^{-1}) for WO_4^{--}

Reference	[25]	[26]	[27]
ν_1	931	934	931
ν_2	(324)	325	373
ν_3	833	840	833
ν_4	324	452	320

cited therein may be consulted for additional works. Different vibrational frequencies are quoted in reference books [25—27]; *cf.* Table V.

Those from KRASNOV *et al.* [26] represent the oldest experimental data (1952). More recent references to experimental works are found in SIEBERT [25] and NAKAMOTO [27]. The assignment of frequencies from the latter reference [27] seems to be the preferable one. It contains the value $\nu_2 = 373\ cm^{-1}$ observed for crystalline substances. This assignment has also been adopted by MÜLLER *et al.* [17—19, 21—24]. The most reliable mean amplitudes based on the frequency assignment from NAKAMOTO [27] are supposed to be the ones of MÜLLER and CYVIN [18], *viz.* l(WO) = 0.037 Å at both 0 and 298 K, l(OO) = 0.062 Å and 0.071 Å at 0 and 298 K, respectively. MÜLLER *et al.* [19] obtained the same value for l(WO) according to an approximation method.

SANYAL *et al.* [20] have reported greatly simplified calculations with results comparable to those of Ref. [18]. Differing results from a previous publication [17] should be discarded, as also has been suggested previously [18]. In the present work we have not pursued the calculations of mean amplitudes and the shrinkage with varying frequencies. These quantities pertain to an ion and cannot be observed by the gas electron diffraction techniques.

For the sake of completeness we mention here that l(WO) in this case only depends on the frequencies ν_1 and ν_3 if we adher to the L-matrix approximation method. l(OO) depends on all the four frequencies, and the shrinkage effect on ν_2, ν_3 and ν_4.

Table VI

Force constants (in mdyne/Å) for WO stretchings in bent WO_2, WO_3 and WO_4^{--}

Compound	F_{11}	F_{22} or F_{33}	f_r	f_{rr}
WO_2 (C_{2v})	8.78	7.27	8.03	0.76
WO_3 (D_{3h})	3.00	9.03	7.02	−2.01
WO_4^{--} (T_d)[a]	8.17	5.84	6.42	0.58

[a] from Ref. [23]

Discussion

In Table VI we have collected some of the main force constants, *i.e.*, those of the WO stretchings, for the three tungsten oxides considered here. The principal and interaction valence force constants, *viz.* f_r and f_{rr}, are connected with the symmetry force constants through

$$F_{11} = f_r + f_{rr}\,, \qquad F_{22} = f_r - f_{rr}$$

for the bent WO_2 model (symmetry C_{2v}),

$$F_{11} = f_r + 2f_{rr}\,, \qquad F_{33} = f_r - f_{rr}$$

for the WO_3 (D_{3h}) model, and finally

$$F_{11} = f_r + 3f_{rr}\,, \qquad F_{33} = f_r - f_{rr}$$

for the tetrahedral WO_4^{--} (T_d) model. The f_r constants should be expected to have comparable magnitudes. It is reported, for instance, for the analogous row of sulphur oxides f_r = 10.02, 10.35 and 7.15 mdyne/Å [25] for SO_2, SO_3 and SO_4^{--}, respectively. On this background the f_r force constants developed

here for the tungsten oxides seem reasonable. However, the interaction constant f_{rr} for WO_3 (−2.01 mdyne/Å; *cf.* Table VI) seems to be too large in absolute magnitude. The main reason is probably a too low F_{11}, which is directly connected to one of the unobserved, estimated frequencies. The estimate of $\nu_1 = 564$ cm^{-1} [7, 8] is claimed to be based on the value of a WO stretching force constant. We believe that this frequency is too low, and in consequence that the l(WO) mean amplitudes for WO_3 shown in Table IV are too high. This applies also to l(OO), but probably to a smaller degree. In conclusion we feel that a possible recalculation of these quantities should await stronger experimental evidence, either from the spectroscopic or electron diffraction side.

Appendix

1. *Bent* WO_2

Following the notation of CYVIN [3] we have (*cf.* p. 195 of the cited reference)

$$l^2(\mathrm{WO}) = \frac{1}{2}\Sigma_1(A_1) + \frac{1}{2}\Sigma(B_1),$$

where

$$\Sigma(B_1) = L_{33}\delta_3 = G(B_1)\delta_3$$

depends only on ν_3. For $\Sigma_1(A_1)$ one has

$$\Sigma_1(A_1) = L_{11}^2\delta_1 + L_{12}^2\delta_2 .$$

In these equations δ_1, δ_2 and δ_3 are frequency parameters. By virtue of the L-matrix approximation ($L_{12} = 0$) one obtains

$$\Sigma_1(A_1) = L_{11}^2\delta_1 = G_1(A_1)\delta_1$$

and

$$l^2(\mathrm{WO}) = \frac{1}{2}G_1(A_1)\delta_1 + \frac{1}{2}G_1(B_1)\delta_3,$$

which proves that l(WO) does not depend on ν_2 under this approximation. For the nonbond mean-square amplitude on the other hand one has [3]

$$l^2(\mathrm{OO}) = 2\Sigma_1(A_1)\sin^2 A + 2^{1/2}\Sigma_{12}(A_1)\sin 2A + \Sigma_2(A_1)\cos^2 A,$$

which depends on both ν_1 and ν_2 (but not ν_3), since

$$\Sigma_{12}(A_1) = L_{11}L_{21}\delta_1 , \qquad \Sigma_2(A_1) = L_{21}^2\delta_1 + L_{22}^2\delta_2 .$$

2. *Planar symmetrical* WO_3

With reference to p. 196 of CYVIN [3] we have

$$l^2(\mathrm{WO}) = \frac{1}{3}\Sigma(A_1') + \frac{2}{3}\Sigma_1(E'),$$

which gives

$$l^2(\mathrm{WO}) = \frac{1}{3}L_{11}{}^2\delta_1 + \frac{2}{3}L_{33}{}^2\delta_3 = \frac{1}{3}G(A_1')\,\delta_1 + \frac{2}{3}G_1(E')\,\delta_3$$

under the approximation $L_{34} = 0$. Hence it is proved that l(WO) only depends on ν_1 and ν_3 under that assumption. For the nonbond mean amplitude one has [3]

$$l^2(\mathrm{OO}) = \Sigma(A_1') + \frac{1}{2}\Sigma_1(E') - 3^{-1/2}\Sigma_{12}(E') + \frac{1}{6}\Sigma_2(E'),$$

which depends on ν_1, ν_3 and ν_4. The expression for the shrinkage effect is found on p. 298 of Ref. [3], and is seen to contain $\Sigma(A_2'')$, $\Sigma_1(E')$, $\Sigma_{12}(E')$ and $\Sigma_2(E')$. Here

$$\begin{aligned}
\Sigma(A_2'') &= L_{22}{}^2\delta_2\,,\\
\Sigma_1(E') &= L_{33}{}^2\delta_3\,,\\
\Sigma_{12}(E') &= L_{33}L_{43}\,\delta_3\,,\\
\Sigma_2(E') &= L_{43}{}^2\delta_3 + L_{44}{}^2\delta_4\,.
\end{aligned}$$

3. *Tetrahedral* WO_4^{--}

From p. 196 of Ref. [3] one has

$$l^2(\mathrm{WO}) = \frac{1}{4}\Sigma(A_1) + \frac{3}{4}\Sigma_1(F_2),$$

which gives

$$l^2(\mathrm{WO}) = \frac{1}{4}L_{11}{}^2\delta_1 + \frac{3}{4}L_{33}{}^2\delta_3 = \frac{1}{4}G(A_1)\delta_1 + \frac{3}{4}G_1(F_2)\,\delta_3$$

when $L_{34} = 0$. Hence l(WO) depends only on ν_1 and ν_3. For the nonbond mean amplitude [3]:

$$l^2(\mathrm{OO}) = \frac{2}{3}\Sigma(A_1) + \frac{1}{9}\Sigma(E) + \frac{2}{3}\Sigma_1(F_2) - \frac{2}{3}\Sigma_{12}(F_2) + \frac{1}{6}\Sigma_2(F_2),$$

which depends on all the four frequencies. The expression for the shrinkage is found again on p. 298 and contains $\Sigma(E)$, $\Sigma_1(F_2)$, $\Sigma_{12}(F_2)$ and $\Sigma_2(F_2)$. Here

$$\Sigma(E) = L_{22}^2\delta_2 ,$$
$$\Sigma_1(F_2) = L_{33}^2\delta_3 ,$$
$$\Sigma_{12}(F_2) = L_{33}L_{43}\delta_3 ,$$
$$\Sigma_2(F_2) = L_{43}^2\delta_3 + L_{44}^2\delta_4 .$$

REFERENCES

[1] HARGITTAI, I., HARGITTAI, M., SPIRIDONOV, V. P., EROKHIN, E. V.: J. Mol. Structure **8,** 31 (1971)
[2] MORINO, Y., KUCHITSU, K., SHIMANOUCHI, T.: J. Chem. Phys. **20,** 726 (1952)
[3] CYVIN, S. J.: Molecular Vibrations and Mean Square Amplitudes. Universitetsforlaget, Oslo and Elsevier, Amsterdam 1968
[4] MORINO, Y., CYVIN, S. J., KUCHITSU, K., IIJIMA, T.: J. Chem. Phys. **36,** 1109 (1962)
[5] NAGARAJAN, G.: Indian J. Pure Appl. Phys. **4,** 158 (1966)
[6] NAGARAJAN, G.: Acta Phys. Austriaca **18,** 1 (1964)
[7] STULL, D. R., PROPHET, H. (Project Directors): JANAF Thermochemical Tables 2nd Edition, National Bureau of Standards, Washington, D.C. 1971
[8] WELTNER, W., MCLEAD, D.: J. Mol. Spectry. **17,** 276 (1965)
[9] MÜLLER, A.: Z. phys. Chem. **238,** 116 (1968)
[10] PEACOCK, C. J., MÜLLER, A.: J. Mol. Spectry. **26,** 454 (1968)
[11] STÖLEVIK, R., ANDERSEN, B., CYVIN, S. J., BRUNVOLL, J.: Acta Chem. Scand. **21,** 1581 (1967)
[12] CYVIN, S. J., BRUNVOLL, J., ANDERSEN, B., STÖLEVIK, R.: Selected Topics in Structure Chemistry (Ed.: ANDERSEN, P., BASTIANSEN, O., FURBERG, S.), p. 69, Universitetsforlaget, Oslo 1967
[13] CYVIN, S. J., BRUNVOLL, J., STÖLEVIK, R.: Acta Chem. Scand. **23,** 333 (1969)
[14] CYVIN, S. J., BRUNVOLL, J.: J. Mol. Structure **3,** 453 (1969)
[15] DE MARIA, G., BURNS, R. P., DROWART, J., INGHRAM, M. G.: J. Chem. Phys. **32,** 1373 (1960)
[16] NAGARAJAN, G.: Indian J. Pure Appl. Phys. **2,** 17 (1964)
[17] MÜLLER, A., NAGARAJAN, G.: Z. Naturforschg. **21b,** 508 (1966)
[18] MÜLLER, A., CYVIN, S. J.: J. Mol. Spectry. **36,** 315 (1968)
[19] MÜLLER, A., KREBS, B., PEACOCK, C. J.: Z. Naturforschg. **23a,** 1024 (1968)
[20] SANYAL, N. K., PANDEY, A. N., SINGH, H. S.: J. Quant. Spectrosc. Radiat. Transfer. **9,** 1035 (1969)
[21] KREBS, B., MÜLLER, A.: J. Mol. Spectry. **22,** 290 (1967)
[22] MÜLLER, A., KREBS, B.: J. Mol. Spectry. **24,** 180 (1967)
[23] KREBS, B., MÜLLER, A., FADINI, A.: J. Mol. Spectry. **24,** 198 (1967)
[24] MÜLLER, A., KREBS, B.: Mol. Phys. **12,** 517 (1967)
[25] SIEBERT, H.: Anwendungen der Schwingungsspektroskopie in der anorganischen Chemie. Springer-Verlag, Berlin 1966
[26] KRASNOV, K. S., TIMOSHININ, V. S., DANILOVA, T. G., KHANDOZHKO, S. V.: Molekularnye postoyannie neorganicheskikh soedinenii (Molecular Constants of Inorganic Compounds), Khimiya, Leningrad 1968
[27] NAKAMOTO, K.: Infrared Spectra of Inorganic and Co-ordination Compounds. 2nd Edition, Wiley-Interscience, New York 1970

Sven J. CYVIN; Division of Physical Chemistry, N-7034 Trondheim-NTH, Norway

István HARGITTAI; Central Research Institute for Chemistry, Hungarian Academy of Sciences, H-1088 Budapest, Puskin u. 11—13, Hungary.

Acta Chimica Academiae Scientiarum Hungaricae, Tomus 83 (3—4), pp. 331—342 (1974)

ON THE MOLECULAR GEOMETRY OF GASEOUS 1,3-DIOXANE AS STUDIED BY ELECTRON DIFFRACTION

GY. SCHULTZ and I. HARGITTAI

(Central Research Institute for Chemistry, Hungarian Academy of Sciences, H-1088 Budapest)

Received March 6, 1974

1,3-Dioxane molecules take a chair conformation according to the gas electron diffraction data in agreement with a microwave spectroscopy study (R. KEWLEY, [1]). The bond lengths and bond angles were also determined. In the course of the structure analysis data from the microwave spectroscopy study have been utilized.

Introduction

KEWLEY has recently studied the molecular conformation of 1,3-dioxane by microwave spectroscopy [1]. He has shown that considering the dipole moment components along the principal inertia axes, the chair form and one ("A") of the boat forms are to be examined while the other boat form and the

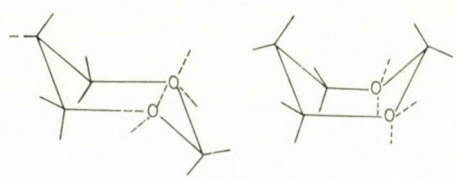

twist forms are ruled out. The cited work gave preference to the chair form convincingly, mainly on the basis of comparisons between the calculated and observed planar principal moments. It was also found on the basis of dipole moment data, that no flattening of the ring occurs as compared with cyclohexane, *e.g.*, although this could have been expected because of the presence of the oxygen lone electron pairs instead of C—H bonds. In the microwave spectroscopy study reasonable geometric parameters have been assumed and used but no attempt could be made to determine these parameters.

There has also been a recent vibrational spectroscopic study on 1,3-dioxane (not cited in Ref. [1]), in which PICKETT and STRAUSS [2] were able to assign all the observed low frequency bands to vibrational transitions arising from an expected chair conformation. They performed a normal-coordinate analysis and the rotational constants for the chair form geometry, they obtained, agree astonishingly well with the values observed by KEWLEY.

The two main purposes of our electron diffraction study were (i) to determine the geometric parameters *i.e.*, the bond distances and the bond angles of the 1,3-dioxane molecule, and (ii) to examine the mean amplitudes of vibration. It was also expected to gain further evidence concerning the molecular conformation, although it was clear from the very beginning of the electron diffraction study that strong correlation among the structural parameters including both geometric and vibrational quantities would prevent a detailed conformational analysis. It was for this reason, above all, that we decided to make partial use of the available experimental data from KEWLEY's microwave spectroscopy study in the course of the electron diffraction structure analysis. A similar approach has already been demonstrated to be extremely useful in other studies some of which have been performed in this laboratory [3, 4].

Experimental

The sample of 1,3-dioxane used in this study was kindly provided by Dr. M. BARTÓK (Szeged)*. The electron diffraction patterns were recorded with the Budapest apparatus, a modified EG-100A unit. The nozzle and sector systems used have been described elsewhere [5, 5]. The nozzle temperature was about 40°C. Nozzle-to-plate distance of 50 and 20 cm and a 60 kV nominal accelerating voltage were utilized. The data were treated as described elsewhere [7]. The ranges of intensity data used were $2.25 \leq s \leq 11.10$ Å^{-1} and $6.75 \leq s \leq 29.75$ Å^{-1} ($s = 4\pi\lambda^{-1}\sin\theta/2$, where λ is the electron wavelength and θ is the scattering angle). The data intervals were $\Delta s = 0.15$ Å^{-1} and

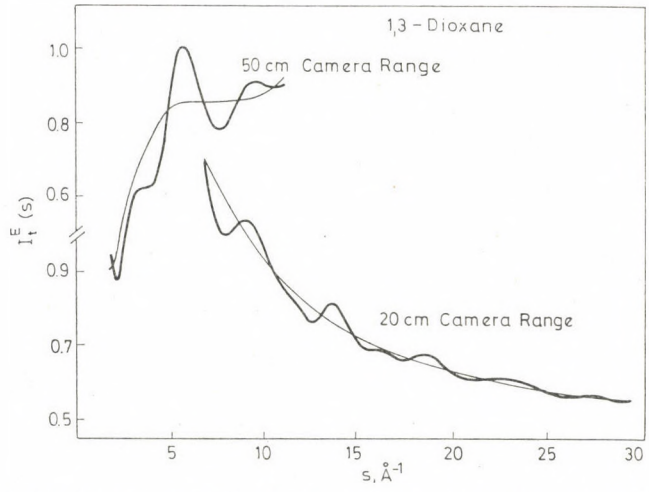

Fig. 1. The total experimental intensities and experimental backgrounds drawn in

* Department of Organic Chemistry, József A. University

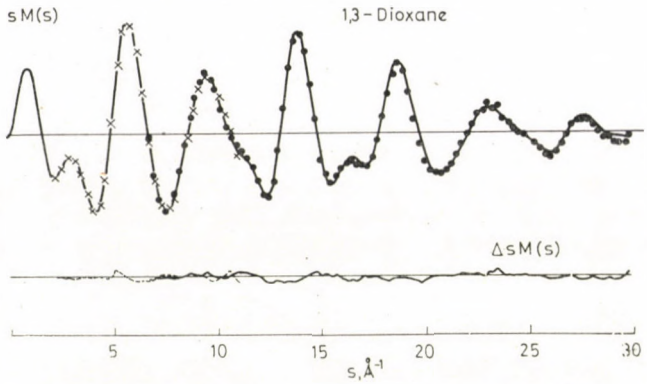

Fig. 2. Experimental (crosses and dots for 50 cm and 20 cm camera ranges, respectively) and theoretical (full line) molecular intensities. Δ represents $[sM^E(s) - sM(s)]$. The theoretical curve was computed for the model whose parameters are presented in column (*c*) of Table I

0.25 Å^{-1}, respectively, for the two camera ranges. The final versions of the experimental backgrounds are shown in Fig. 1. The scaled molecular intensities corresponding to the two camera ranges are shown in Fig. 2.

Structure analysis

The experimental radial distribution is presented in Fig. 3. As the (more important) individual interatomic distances and their relative weights are indicated also in this Figure assigned to the chair form, it can be well seen

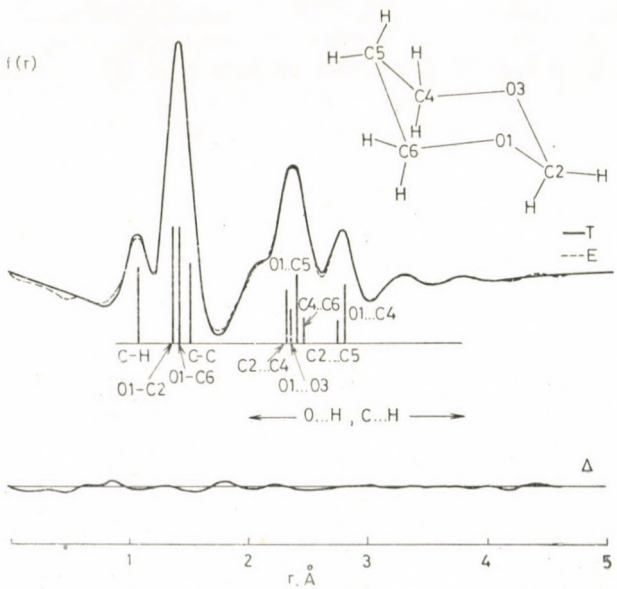

Fig. 3. Experimental (*E*) and theoretical (*T*) radial distributions and the difference curve (Δ). Curve *T* was computed for the model whose parameters are presented in column (*c*) of Table I. The more important individual interatomic distances and their relative weights are also indicated

that a unique determination of the 1,3-dioxane molecular geometry from electron diffraction data alone would be impossible. It was then decided, at least for the preliminary refinements of the structural parameters, to include experimental data from the microwave spectroscopy study into the least-squares procedure. SEIP's least-squares refinement program KCED21 [8] was modified so that the quantity to be minimized was

$$\sum_{s_{\min^1}}^{s_{\max^1}} W_s[M^E(s) - k_1 M^T(s)]^2 + \sum_{s_{\min^2}}^{s_{\max^2}} W_s[M^E(s) - k_2 M^T(s)]^2 + \\ + \sum_{j=a,b,c} W_j(I_j^E - I_j^T)^2 , \tag{1}$$

where $M(s)$ in the molecular intensity, k_2 and k_1 the respective scale factors for the two camera ranges, I_j the principal moment of inertia, and W_s and W_j the corresponding weights.

The molecular model of the chair form of 1,3-dioxane (see Fig. 3) as a whole was assumed to posses C_s symmetry. All C—H bond lengths and <H—C—H bond angles were taken equal. The bond configuration of the C5 atom and also that of the C2 atom has C_{2v} local symmetry. The following geometric parameters were chosen to be independent:

r(C—H)	<O—C—O
r(O1—C2)	<C—O—C
r(O1—C6)	<O—C—C
r(C—C)	<C—C—C
	<H—C—H
	<H—C—C

The mean amplitudes of vibration (l values) for the two types of C—O bounds were assumed to be equal. In most of the refinements the l values for non-bonding distances involving hydrogen atom and distances which occur only once, have not been varied. Because of strong correlation among the paraameters, the approach of block refinement of various groups of parameters [9] has been extensively used.

In the final stages of the structure analysis zero values were given to the weights W_j (Eq. (1), thus removing the constraints referring to the microwave spectroscopy measurements. No appreciable changes in the parameters, however, have been observed.

Two different trial structures have initially been used in the least-squares refinements. One of them was based on KEWLEY's [1] assumed parameters, while the other originated fron the values for bond angles and torsional angles given by PICKETT and STRAUSS [2]. For the latter case the parameters

Table I

Molecular parameters of 1,3-dioxane

	(a)	(b)	(c)	(d)	(e)	(f)	(g)
r(O1—C2), Å	1.410		1.393		0.018	1.393	0.025
r(O1—C6), Å	1.410		1.439		0.028	1.439	0.039
r(C—C), Å	1.533		1.528		0.009	1.528	0.013
r(C—H), Å	1.108		1.095		0.003	1.095	0.004
O—C—O	109°28′	109.95°	115.7°	114.4°	1.6°	115.0°	2.8°
C—O—C	111°43′	112.83°	110.3°	111.4°	0.7°	110.9°	1.5°
O—C—C	109°28′	108.43°	109.1°	109.3°	0.5°	109.2°	0.8°
C—C—C	109°28′	110.42°	107.6°	107.8°	0.7°	107.7°	1.1°
O—C—O—C		61.23°	58.9°				
C—O—C—C		57.59°	56.0°				
O—C—C—C		53.39°	57.4°				
l(O—C), Å			0.049		0.014	0.049	0.020
l(C—C), Å			0.053		0.012	0.053	0.017
l(C—H), Å			0.071		0.002	0.071	0.003
l(O1 . . . C4), Å			0.066		0.004	0.066	0.006
l(O1 . . . C5), Å			0.073		0.006	0.073	0.008
l(C . . . C), Å			0.062		0.008	0.062	0.011

(a) — Assumed geometric parameters in KEWLEY's work [1]
(b) — Bond angles and torsional angles given by PICKETT and STRAUSS [2]
(c) — Results of refinements using (a) as trial structure
(d) — Results of refinements using (b) as trial structure
(e) — Standard deviations obtained for (c)
(f) — Average parameters of (c) and (d)
(g) — Total errors obtained as described in the text

for the bond distances obtained in the previous refinements have been kept unvaried. The results of both refinements are presented in Table I. The mean values of these parameters are also given as representing the findings of this structure analysis. In estimating the total errors, the standard deviations were multiplied by $\sqrt{2}$ to take the correlation among the experimental intensities into account and then half of the differences between the results of the two refinement schemes were also added. This latter was felt to be necessary since the results of the least-squares refinements were somewhat sensitive to the choice of the trial structures. The standard deviations were so large that in all cases but for r(C—H) the experimental scale error, estimated to be about 0.2 per cent, was ignored in the calculations of the total error. As for the bond

Table II

Correlation coefficients (X1000)

	r1	r2	r3	r4	r5	r6	r7	r8	r9	r10	l1	l3	l4	l11	l12	l13	k1	k2
r1	1000																	
r2	−997	1000																
r3	958	−956	1000															
r4	−475	465	−387	1000														
r5	−584	571	−648	272	1000													
r6	322	−310	433	− 23	−786	1000												
r7	322	−336	190	−224	24	−328	1000											
r8	9	− 1	4	− 71	−550	456	−342	1000										
r9	−303	321	−163	295	−398	463	−463	427	1000									
r10	−283	290	−355	33	293	−115	−200	15	−423	1000								
l1	973	−979	953	−420	−556	324	301	− 5	−291	−314	1000							
l3	−959	959	−894	475	535	−261	−377	4	347	255	−889	1000						
l4	−434	429	−328	350	227	− 22	−310	− 44	224	65	−423	399	1000					
l11	325	−335	373	28	82	266	−142	−471	−219	25	382	−259	− 14	1000				
l12	−148	148	− 62	170	−331	385	143	238	279	− 48	−102	187	99	−169	1000			
l13	316	−303	425	− 35	−634	795	613	410	382	50	337	−219	18	359	86	1000		
k1	−213	184	− 18	422	117	141	−313	− 95	245	−173	− 32	343	359	317	278	232	1000	
k2	−198	209	− 92	− 78	−263	317	−311	323	542	−112	−146	291	74	−113	259	299	250	1000

$r1 = r(C2-O1)$, $r2 = r(O1-C6)$, $r3 = r(C4-C5)$, $r4 = r(C-H)$, $r5 = \sphericalangle OCO$, $r6 = \sphericalangle COC$, $r7 = \sphericalangle OCC$, $r8 = \sphericalangle CCC$, $r9 = HCH$, $r10 = HC4C5$, $l1 = l(C2-O1)$, $l3 = l(C4-C5)$, $l4 = l(C-H)$, $l11 = l(O1 \cdot C5)$, $l12 = l(O1 \cdot C4)$, $l13 = l(C2 \cdot C4)$, $k1$ and $k2$ scale factors for camera ranges 20 cm and 50 cm, respectively.

angles involving hydrogen atom, H—C—H 108.8 ± 2.5° and H—C—C 112.4 ± 1.1° were obtained in the refinements corresponding to column (c) of Table I. Closely related to the results of the least-squares refinements, presented in Table I, are the quantities of the correlation coefficients given in Table II.

Discussion

The geometric parameters of the 1,3-dioxane molecule obtained in this study are shown in column (*f*) with the total errors in column (*g*) of Table I. These parameters are represented in terms of r_a structure. It is well known that the r_a parameters, especially for bond angles, have no well-defined physical meaning, nevertheless, the large uncertainties do not warrant further pursuit for better defined parameters.

The electron diffraction data show excellent agreement with the chair conformation as demonstrated by Figs 2 and 3. Table III and IV provide a

Table III

Observed and calculated rotational constants for 1,3-dioxane

Rotational constant	Microwave spectroscopy [1]	PICKETT and STRAUSS (calculated) [2]	Electron diffraction	
			(c)	(d)
A	4999.94 ± 0.05	4977	5019	4969
B	4807.61 ± 0.05	4804	4795	4831
C	2757.12 ± 0.05	2750	2760	2752

(c) and (d) correspond to the parameters of the columns (c) and (d) of Table I

Table IV

Observed and calculated planar principal moments of 1,3-dioxane

	$\Sigma m_i a_i^2$	$\Sigma m_i b_i^2$	$\Sigma m_i c_i^2$
Microwave spectroscopy [1]	93.671	89.628	9.949
PICKETT and STRAUSS [2]	93.7	90.5	11.5
Electron diffraction	93.9	89.2	11.5

comparison between the rotational constants and the planar principal moments, respectively, obtained in the microwave spectroscopy study [1], calculated from the geometry of the vibrational spectroscopic work [2] and our electron diffraction structure analysis. The convenience of using the planar principal moments for this comparison was pointed out by KEWLEY [1]. When making

comparisons of this kind it should be remembered that a discrepancy between the microwave spectroscopy and electron diffraction data within, say, one per cent may well be expected to be due to the indeterminacy in the physical significance of the parameters originating from different techniques and not corrected for the effects of vibration and rotation. Accordingly, the agreement between the rotational constants from the present investigation and those of the microwave spectroscopy study can be considered also excellent. That the same can be stated for the calculated rotational constants of Ref. [2] indicate that several sets of geometric parameters may obviously reproduce the observed rotational constants. However, according to the least-squares refinement on the electron diffraction molecular intensities, the parameters like those presented in column (*f*) of Table I are to be preferred.

In addition to the structure refinements based on the chair conformation, refinements have also been attempted using a boat "A" model. These calculations, assuming the parameters for the bonds from the refinements on the chair form, yielded the following values for the bond angles:

O—C—O	111.5°
C—O—C	114.1°
O—C—C	108.7°
C—C—C	108.9°

The corresponding rotational constants

A	5115	(MHz)
B	4688	
C	2865	

and planar principal moments

$\Sigma m_i a_i^2$	(uÅ²)	92.7
$\Sigma m_i b_i^2$		83.7
$\Sigma m_i c_i^2$		15.1

Although the electron diffraction experimental distributions could be approximated quite well using a model with boat "A" conformation, the comparison of the above quantities with those observed in the microwave spectroscopy study rules out the boat form.

The choice between the ring conformations is the most important point for discussing the utilization of the microwave spectroscopy data in this electron diffraction structure analysis. The electron diffraction data alone could have not decided unambiguously between the different forms in this

particular case. The reason is that the molecule produces closely packed internuclear distances causing strong correlation among the parameters characterizing not only the bond angles but also the ring conformation. For deciding between the different conformational forms, however, simple comparisons like those given above and in Tables III or IV would have been sufficient. The inclusion of the microwave spectroscopy data into the least-squares procedure had further merits. First, it definitely facilitated a faster convergence of the refinement, and second, by selecting appropriate weights, the standard deviations could be reduced. Of these, the first merit proved to be very useful in the refinements. No advantage was taken of the second one in the final account, however, since it was preferred to present the findings for the geometric parameters in terms of r_a structure based solely on the electron diffraction intensities.

It is difficult to discuss the geometric parameters obtained in this study because of lack of reference data. That they are different from those given in Refs [1] and [2] does not mean that they are unusual, since in the cited works the geometric parameters were chosen, to a certain extent, arbitrarily. On the other hand, in discussing these parameters, the large uncertainties have to be taken into consideration.

The r(C—H) distance seems to be normal and well determined. The r(C—C) distance is not different from that in cyclohexane [10] within the uncertainty. The difference between the lengths of the two types of C—O bonds is not significant but the trend is real.

KEWLEY found no indication of flattening of the molecule by oxygen lone pair repulsions as compared with cyclohexane. This is very much in agreement with our findings. The torsional angles for 1,3-dioxane are presented in Table I. These could be compared to the torsion angles of cyclohexane and 1,3,5-trioxane. BASTIANSEN *et al.* [10] obtained $54.9 \pm 0.4°$ in terms of r_α structure for this angle in cyclohexane. The torsional angle around the O—C bond in 1,3,5-trioxane was calculated to be 58.6° from the r_a parameters given in CLARK and HEWITT's work [11]. No flattening seems then to occur in 1,3-dioxane and 1,3,5-trioxane as compared with cyclohexane. The data indicate the opposite trend although the effect may be not significant.

Appendix

The numerical values of the total experimental intensities, $I_t^E(s)$, and experimental backgrounds, $I_b^E(s)$

50 cm camera range

s	$I_t^E(s)$	$I_b^E(s)$	s	$I_t^E(s)$	$I_b^E(s)$
2.25	0.3838	0.4700	6.75	0.8442	0.8530
2.40	0.4215	0.5019	6.90	0.8173	0.8530
2.55	0.4682	0.5341	7.05	0.8011	0.8530
2.70	0.5079	0.5667	7.20	0.7861	0.8530
2.85	0.5505	0.5983	7.35	0.7787	0.8530
3.00	0.5778	0.6260	7.50	0.7737	0.8531
3.15	0.6006	0.6511	7.65	0.7757	0.8531
3.30	0.6139	0.6729	7.80	0.7811	0.8530
3.45	0.6181	0.6915	7.95	0.7903	0.8530
3.60	0.6208	0.7097	8.10	0.8024	0.8528
3.75	0.6199	0.7274	8.25	0.8162	0.8526
3.90	0.6209	0.7437	8.40	0.8315	0.8530
4.05	0.6283	0.7592	8.55	0.8486	0.8535
4.20	0.6438	0.7741	8.70	0.8641	0.8540
4.35	0.6680	0.7879	8.85	0.8751	0.8547
4.50	0.6987	0.8008	9.00	0.8860	0.8552
4.65	0.7405	0.8128	9.15	0.8947	0.8563
4.80	0.7899	0.8228	9.30	0.9009	0.8578
4.95	0.8474	0.8312	9.45	0.9031	0.8592
5.10	0.9068	0.8381	9.60	0.9033	0.8611
5.25	0.9445	0.8432	9.75	0.9021	0.8635
5.40	0.9763	0.8468	9.90	0.9008	0.8662
5.55	0.9927	0.8488	10.05	0.8984	0.8697
5.70	1.0000	0.8500	10.20	0.8969	0.8738
5.85	0.9953	0.8510	10.35	0.8926	0.8785
6.00	0.9790	0.8516	10.50	0.8930	0.8840
6.15	0.9571	0.8521	10.65	0.8919	0.8895
6.30	0.9307	0.8524	10.80	0.8921	0.9021
6.45	0.9021	0.8528	10.95	0.8933	0.9092
6.60	0.8693	0.8530	11.10	0.8955	0.9164

Appendix

20 cm camera range

s	$I_t^E(s)$	$I_b^E(s)$	s	$I_t^E(s)$	$I_b^E(s)$
6.75	1.1864	1.1955	14.25	0.7863	0.7450
7.00	1.1018	1.1707	14.50	0.7616	0.7379
7.25	1.0448	1.1480	14.75	0.7378	0.7312
7.50	1.0108	1.1263	15.00	0.7130	0.7252
7.75	0.9975	1.1020	15.25	0.7004	0.7194
8.00	0.9985	1.0796	15.50	0.6907	0.7133
8.25	1.0084	1.0570	15.75	0.6894	0.7079
8.50	1.0205	1.0349	16.00	0.6875	0.7028
8.75	1.0321	1.0155	16.25	0.6844	0.6976
9.00	1.0364	0.9967	16.50	0.6806	0.6921
9.25	1.0316	0.9790	16.75	0.6743	0.6873
9.50	1.0217	0.9618	17.00	0.6698	0.6822
9.75	0.9945	0.9441	17.25	0.6644	0.6773
10.00	0.9664	0.9275	17.50	0.6631	0.6722
10.25	0.9326	0.9129	17.75	0.6649	0.6673
10.50	0.9040	0.8990	18.00	0.6687	0.6626
10.75	0.8814	0.8855	18.25	0.6720	0.6580
11.00	0.8629	0.8730	18.50	0.6744	0.6538
11.25	0.8482	0.8617	18.75	0.6731	0.6499
11.50	0.8327	0.8500	19.00	0.6659	0.6460
11.75	0.8150	0.8389	19.25	0.6551	0.6419
12.00	0.7965	0.8278	19.50	0.6432	0.6382
12.25	0.7760	0.8167	19.75	0.6308	0.6345
12.50	0.7648	0.8061	20.00	0.6223	0.6305
12.75	0.7659	0.7960	20.25	0.6166	0.6272
13.00	0.7765	0.7863	20.50	0.6124	0.6241
13.25	0.7906	0.7770	20.75	0.6094	0.6211
13.50	0.8052	0.7688	21.00	0.6075	0.6181
13.75	0.8093	0.7604	21.25	0.6069	0.6154
14.00	0.8036	0.7528	21.50	0.6069	0.6128

20 cm camera range (continued)

s	$I_t^E(s)$	$I_b^E(s)$	s	$I_t^E(s)$	$I_b^E(s)$
21.75	0.6071	0.6100	26.00	0.5626	0.5675
22.00	0.6072	0.6074	26.25	0.5616	0.5656
22.25	0.6071	0.6046	26.50	0.5613	0.5640
22.50	0.6072	0.6020	26.75	0.5620	0.5624
22.75	0.6051	0.5994	27.00	0.5628	0.5608
23.00	0.6042	0.5968	27.25	0.5617	0.5594
23.25	0.6008	0.5942	27.50	0.5605	0.5580
23.50	0.5981	0.5914	27.75	0.5589	0.5566
23.75	0.5921	0.5886	28.00	0.5572	0.5554
24.00	0.5885	0.5860	28.25	0.5546	0.5542
24.25	0.5845	0.5834	28.50	0.5525	0.5532
24.50	0.5811	0.5808	28.75	0.5514	0.5522
24.75	0.5782	0.5784	29.00	0.5498	0.5513
25.00	0.5746	0.5760	29.25	0.5488	0.5505
25.25	0.5713	0.5735	29.50	0.5482	0.5497
25.50	0.5680	0.5715	29.75	0.5487	0.5490
25.75	0.5648	0.5695			

REFERENCES

[1] KEWLEY, R.: Can. J. Chem. **50,** 1690 (1972)
[2] PICKETT, H. M., STRAUSS, H. L.: J. Chem. Phys. **53,** 376 (1970)
[3] HARGITTAI, I., HARGITTAI, M.: J. Mol. Structure **15,** 399 (1973)
[4] HARGITTAI, M., HARGITTAI, I.: J. Mol. Structure **20,** 283 (1974)
[5] HARGITTAI, I., HERNÁDI, J., KOLONITS, M., SCHULTZ, GY.: Rev. Sci. Instrum. **42,** 546 (1971)
[6] HARGITTAI, I., HERNÁDI, J., KOLONITS, M.: Prib. Tekh. Eksp. 239 (1972)
[7] SCHULTZ, GY., HARGITTAI, I., HERMANN, L.: J. Mol. Structure **14,** 353 (1972)
[8] ANDERSEN, B., SEIP, H. M., STRAND, T. G., STØLEVIK, R.: Acta Chem. Scand. **23,** 3224 (1969)
[9] HARGITTAI, I., HEDBERG, K., in Molecular Structures and Vibrations, (ed.): S. J. Cyvin. Elsevier, Amsterdam, 1972
[10] BASTIANSEN, O., FERNHOLT, L., SEIP, H. M., KAMBARA, H., KUCHITSU, K.: J. Mol. Structure **18,** 163 (1973)
[11] CLARK, A. H., HEWITT, T. G.: J. Mol. Structure **9,** 33 (1971)

György SCHULTZ
István HARGITTAI
Central Research Institute for Chemistry, Hungarian Academy of Sciences, H-1088 Budapest, Puskin u. 11—13. Hungary.

Acta Chimica Academiae Scientiarum Hungaricae, Tomus 83 (3—4), pp. 343—346 (1974)

METAL-AMINO ACID INTERACTION, I

A STUDY OF THE COMPLEX COMPOUNDS OF TRIVALENT RARE EARTHS WITH L-ASPARTIC ACID

OMAR FAROOQ, ANEES UDDIN MALIK* and NASEER AHMAD

(Inorganic Research Laboratory, Chemistry Department, Aligarh Muslim University, Aligarh U.P. India)

Received March 25, 1974

A number of transition metal and inner transition metal complexes with α-amino acids have been studied mostly in solutions employing certain physicochemical techniques [1—10]. From the literature it appears that very limited attention has been paid to the isolation and elucidation of the structure of rare earth complexes with amino acids. The present communication deals with the interaction of L-aspartic acid with trivalent rare earth ions (Y, La, Ce—Lu except Pm). The complexes have been isolated and identified by IR, magnetic measurement, thermogravimetric analysis, molar conductance and elemental analysis.

Experimental

Freshly prepared rare earth carbonates were treated with L-aspartic acid in stoichiometric proportions in aqueous solution. The mixture was stirred, filtered and concentrated, mixed with dehydrated alcohol and allowed to evaporate slowly in vacuum at room temperature.

The complexes were analysed for C, H and N, by the Microanalytical Service, I.I.T. Kanpur (India) and rare earths were estimated as oxalates [11]. The IR spectra were taken on a Beckman Spectrophotometer model BK-56 in the range 2.5 to 16 in KBr pellets. Thermogravimetric analysis were performed on a Stanton thermobalance (London) between 25 and 900°C with a heating rate of 6°C per minute in air. Molar conductances were recorded by using a Philips conductivity bridge model PR 9500 in conjunction with a dip type cell (cell factor 1.48) and magnetic measurements were carried out at 27°C employing Faraday's method. Rare earth oxides were purchased from KOCH-Light (London). These compounds are highly hygroscopic and do not dissolve in common organic solvents, have high solubity in water. No melting is observed up to 360°C. Table I gives the characteristic data of these complexes.

Results and discussion

Elemental analyses and TGA studies exhibit the formula $M(Asp\text{-}H)_3 \cdot 3\ H_2O$ where M stands for Y, La, Ce, Pr, Nd, Sm, Eu, Gd, Tb, Dy, Ho, Er, Tm, Yb and Lu. The removal of water at 120—160°C (10—12% wt. loss) confirms that all molecules are co-ordinated to metal ions and are not just water of crystallization [12]. The partially dehydrated compounds are stable up to 230°C and then decomposition sets in. Most probably CO and CO_2 are pro-

* Department of Metallurgy and Material Science. University of Liverpool, Liverpool, England.

Table I

Complexes prepared in this study and some characteristic data

Complex	Colour	C		H		N		Metal		Magnetic moment (BM)	Molar cond. in mhos
		Calcd.	Found	Calcd.	Found	Calcd.	Found	Calcd.	Found		
$Y(Asp)_3 3H_2O$	White	26.70	26.62	4.45	4.27	7.78	7.75	16.48	16.42	Diamag	0.31
$La(Asp)_3 3H_2O$	White	24.44	24.38	4.07	4.10	7.13	6.89	23.58	23.54	Diamag	0.31
$Ce(Asp)_3 3H_2O$	Rosy pink	24.39	24.65	4.06	4.16	7.11	7.16	23.71	23.81	2.5	8.30
$Pr(Asp)_3 3H_2O$	Yellowish areen	24.35	24.25	4.06	4.18	7.12	7.07	23.83	23.90	3.5	0.30
$Nd(Asp)_3 3H_2O$	Pink	24.22	25.00	4.04	4.01	7.23	7.15	24.30	24.50	3.8	0.30
$Sm(Asp)_3 3H_2O$	White	23.96	23.87	3.99	3.95	6.99	6.92	23.36	23.42	2.0	0.30
$Eu(Asp)_3 3H_2O$	White	23.91	24.00	3.98	3.96	6.97	6.99	25.26	25.32	3.4	0.32
$Gd(Asp)_3 3H_2O$	White	23.70	23.94	3.95	4.05	6.91	7.29	25.89	26.02	7.8	0.31
$Tb(Asp)_3 3H_2O$	White	23.64	24.28	3.94	4.43	6.89	7.28	26.09	26.12	—	0.32
$Dy(Asp)_3 3H_2O$	Dirty white	23.51	24.61	3.92	4.02	6.86	6.84	26.59	26.55	9.8	0.32
$Ho(Asp)_3 3H_2O$	Dirty white	23.41	23.30	3.97	4.04	6.79	6.77	26.80	26.98	10.7	0.31
$Er(Asp)_3 3H_2O$	White	23.24	23.20	3.85	3.97	6.84	6.80	27.00	27.10	9.7	0.32
$Tm(Asp)_3 3H_2O$	White	23.08	23.20	3.84	3.75	6.78	6.75	27.20	27.90	6.8	0.32
$Yb(Asp)_3 3H_2O$	White	23.05	23.00	3.84	3.76	6.76	6.71	27.70	27.40	4.6	0.32
$Lu(Asp)_3 3H_2O$	White	23.03	23.10	3.84	3.88	6.72	6.70	28.13	28.20	Diamag	0.31

Asp = L-aspartic acid; H = $(C_4H_6O_4N)$

duced at 350—700°C leading to the formation of stable oxides. Ce(III) complex deviated from this behaviour and there is direct formation of CeO_2 from 340 °C onwards with a weight loss of about 70%.

The usual unequal double humped curve is obtained on plotting magnetic values in B. M. against atomic number [13]. The molar conductances of 2×10^{-4} *M* aqueous solution are of the order of 0.21 ± 0.01 mhos, but the corresponding trichlorides have about 2.8 times higher values then these complexes. These larger values of the rare earth halides might be due to the high ionic mobility of the halide ions as compared to those of large amino acid anions.

The bands which throw some light on the co-ordinating properties of amino acids are: NH_3^+ sym. asym [14], COO^- sym COO^- asym [15] CN stretchings and two unassigned medium intensity characteristic bands at 2060 and 1905 of L-aspartic acid [17]. The NH_3^+ asym stretchings of free aspartic acid appear as medium intensity bands at 1610 and 1510 cm^{-1}, respectively. The position of these bands remains unaltered on complexation, whereas a slight increase of 10—25 cm^{-1} in the sym vibrations is observed. The COO^- sym vibration (1420 cm^{-1}s) present in the free acid is lowered by 20—25 cm^{-1} and the COO^- asym (1640 cm^{-1} m) is reduced by 5—10 cm^{-1} only on complexation. The CN stretching band of medium intensity at 935 cm^{-1} in L-aspartic acid showed a lowering of 20—40 cm^{-1} on complex formation. Usually in amino acids, co-ordination takes place through the carboxylic group with consequent change in the position of NH_3^+ stretchings [18]. The presence of co-ordinated water is revealed by the presence of a medium intensity OH stretching band near 3400 cm^{-1} and OH rocking vibrations of strong intensity at 850 cm^{-1} [19, 20]. The exceptional bands of L-aspartic acid disappear on complexation.

Hence the formation of rare earth complexes is achieved through the displacement of the proton of the —COOH group by the rare earth ions. Moreover, aspartic acid (H_2L) is expected to loose a proton from —COOH ($pK_a \sim 4$) rather than from NH_3^+ ($pK_a \sim 9.8$) and the low affinity of lanthanide cations for NH_2 is unlikely to, in effect, reverse this order of acidities. It may be concluded that zwitter ion character of L-aspartic acid retained on complexation and that the possibility of co-ordination through nitrogen is ruled out.

*

It is a pleasure to thank Prof. W. RAHMAN for providing laboratory facilities. One of the authors (O. F.) is grateful to C.S.I.R., New Delhi for the award of a Senior Fellowship.

REFERENCES

[1] PEIFFER, P., WARNER, H.: Z. Physiol. Chem. **246,** 212 (1937)
[2] LIFSCHITZ, I.: Proc. Acad. Sci. Amsterdam **39,** 1192 (1937)
[3] CHABEREK, S., Jr., MARTELL, A. E.: J. Am. Chem. Soc. **74,** 6021 (1952)
[4] LI, N. C., DOODY, E.: J. Am. Chem. Soc. **74,** 4184 (1952)

[5] KROLL, H.: J. Am. Chem. Soc. **76,** 2034 (1954)
[6] VOLSHTEIN, L. M., MOTYAGIVA, G. G., ANAKHOVA, L. S.: Zh. Neorgan Khim. **1,** 2328 (1956)
[7] RYBCHIKOV, D. I., TERENT'EVA, E. A.: Izvest. Akad. Nauk SSSR. Otdel. Khim Nauk **44** (1944)
[8] BATYAEV, M., LARINOV, S. V., SHUL'MAN, V. M.: Zh. Neorgan Khim. **6,** 53 (1961)
[9] CEFOLA, M., TOMPA, A. S., CELIANO, A. V., GENTILE, P. S.: Inorg. Chem. **1,** 290 (1962)
[10] KRISS, E. E.: Ukr. Khim. Zh. **31,** 328 (1964)
[11] SPENCER, J. F.: The Metals of the Rare Earths. Longmans, London 1919 p. 105
[12] MATHUR, B. S., SRIVASTAVA, T. S.: J. Inorg. Nucl. Chem. **32,** 3277 (1970)
[13] SELBIN, J., AHMAD, N., BHACCA, N.: Inorg. Chem. **10,** No. 7, 1383 (1971)
[14] BELLAMY, L. J.: The Infrared Spectra of Complex Molecule. Methuen, London 1954 p. 238
[15] See reference [14], p. 240
[16] KOEGEL, R. J., GREENSTEIN, J. P., WINITZ, M., BIRNBAUM, S. M., MC CALLUM, R. A. J. Am. Chem.-Soc. **77,** 5708 (1955)
[17] RAO, C. N. R.: Chemical Application of Infrared Spectroscopy. Academic Press, New York 1963 p. 257
[18] LENOMANT, H.: J. Chim. Phys. **43,** 327 (1946)
[19] NAKAMOTO, K.: Infrared Spectra of Inorganic and Coordination Compounds. Wiley, New York. 1963 p. 156
[20] LUCCHESI, P J., GLASSON, W. A.: J. Am. Chem. Soc. **78,** 1347 (195 6)

OMAR FAROOQ
ANEES UDDIN MALIK
NASEER AHMAD
Inorganic Research Laboratory, Chemistry Department, Aligarh Muslim University, A.M.U. Aligarh (U.P.) India.

Acta Chimica Academiae Scientiarum Hungaricae, Tomus 83 (3—4), pp. 347—350 (1974)

DETERMINATION OF MANGANESE WITH N-BROMOSUCCINIMIDE

A. Aboul Kheir, M. Ayad,* and M. M. Amer

(Analytical Chemistry Department, Faculty of Pharmacy, Cairo University, Cairo)

Received April 1, 1974

A procedure is suggested for the semimicro determination of Mn(II) by its alkaline oxidation with N-bromosuccinimide (NBS). The reaction takes place at room temperature and in the presence of an excess of NBS, which is irreversibly reduced to succinimide. The excess NBS is back-titrated with standard arsenite solution and the end-point is detected potentiometrically.

The mechanism of the reaction has been studied, and the results are found to be equally precise and accurate as the complexometric and the formaldoxime colorimetric methods; the accuracy amounted to 99.63% ± 0.626 (P = 0.05).

The more common methods for the determination of manganese are the spectrophotometric [1—12], complexometric [13—15] and gravimetric [16, 17] methods.

N-bromosuccinimide has been applied in inorganic analyses [18—22]. Barakat *et al.* determined iodide [18], trivalent antimony [19] and cyanide and thiocyanate — either alone or in the presence of each other [20] — using N-bromosuccinimide. Berka and Zyka applied N-bromosuccinimide in the determination of As(III), Tl(I), tin(II), titanium(III) and sulphide [21]. The authors have also used N-bromosuccinimide for the semimicro determination of Cu(I) [22].

This communication describes a semimicro procedure for the determination of Mn(II), using NBS as an oxidizing agent.

Experimental

Apparatus

Beckman potentiometer (expanded scale); saturated calomel electrode; platinum electrode.

Reagents

1 — Standard manganous sulphate solution: 0.01*M*. 2 — Sodium hydroxide: T.S. 3 — Standard sodium arsenite solution: 0.0025*M*. 4 — Standard N-bromosuccinimide solution: 0.005*M*, aqueous solution. This solution must be freshly prepared and standardized against standard arsenite solution [19].

* The address: Research and Control Centre, Cairo.

Table I

Semimicro determination of manganous sulphate by the NBS and the complexometric [13] *procedures*

Mn(II) taken, mg	NBS procedure		Complexometric procedure	
	Mn(II) found, mg	Recovery, %	Mn(II) found, mg	Recovery, %
	1.070	97.3	1.070	97.3
1.100	1.070	97.3	1.100	100.0
	1.125	102.3	1.100	100.0
	1.375	100.0	1.348	98.0
1.375	1.375	100.0	1.348	98.0
	1.404	102.1	1.375	100.0
	1.674	101.6	1.593	96.5
1.650	1.650	100.0	1.622	98.3
	1.650	100.0	1.622	98.3
	2.795	101.6	2.698	98.1
2.750	2.750	100.0	2.717	99.0
	2.717	99.0	2.772	100.8
	5.428	99.0	5.500	100.0
5.500	5.428	99.0	5.395	98.0
	5.500	100.0	5.395	98.0
	8.132	98.6	8.099	98.2
8.250	8.132	98.6	8.132	98.6
	8.158	99.0	8.132	98.6
	10.850	98.6	10.791	98.1
11.000	10.904	99.1	10.823	98.4
	10.904	99.1	10.823	98.4
Mean recovery ($p = 0.05$)	99.63 ± 0.626%		98.6 ± 0.48%	
$t_{0.975}$	0.814 (2.021)*			
F	1.75 (2.18)*			

* Figures in parentheses are the theoretical values.

Procedure

In a beaker of 50 ml capacity, introduce an accurately measured volume of the manganous salt solution (containing 1.1 to 11.0 mg of Mn(II), render alkaline with sodium hydroxide solution (about 2 ml) and shake. Add the standard NBS solution in excess (10—30 ml), allow to stand for 3—5 minutes, whilst shaking, then titrate the excess NBS with standard arsenite solution detecting the endpoint potentiometrically.

Carry out a blank experiment simultaneously. 1 ml of 0.005*M* NBS solution is equivalent to 0.549 mg Mn(II) or 1.69 mg $MnSO_4 \cdot H_2O$.

Results

Table I includes the results obtained by applying the suggested NBS procedure and the complexometric method [13] on different volumes of the standard manganous sulphate solution, corresponding to 1.1—11 mg of Mn(II).

Discussion

Oxidation of Mn(II) in acidic solution is difficult; permanganate ion is formed only by the action of very strong oxidizing agents, such as PbO_2. In alkaline medium, Mn(II) is oxidized to Mn(III), as hydrated manganese(III) hydroxide [23]. $Mn_2O_3 \cdot nH_2O$ is the product of oxidation of precipitated $Mn(OH)_2$ which, on drying, gives $(Mn_2O_3H_2O)$ [24].

The reaction between NBS and Mn(II) in alkaline medium can be represented by the equation:

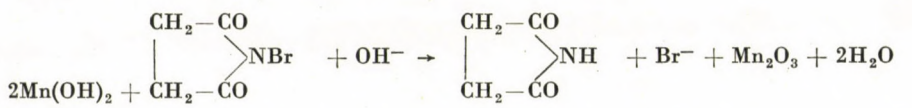

The presence of Br^- was confirmed by the silver nitrate and the chlorine water tests. Succinimide was isolated by filtering the reaction mixture, distilling the clear filtrate under reduced pressure and recrystallizing the solid residue from benzene; the colourless crystals were identified as succinimide of a m.p. 124—125°C.

Before the reaction was applied to the quantitative determination of Mn(II), the effect of the reaction medium was studied and it was concluded that no reaction takes place in acid medium while in alkaline medium the reaction is quantitative. Two moles of sodium hydroxide test solution were enough to render the solution sufficiently alkaline for the reaction between NBS and Mn(II) to be quantitative.

It is evident from the results in Table I that the accuracy of the proposed method amounts to $99.63 \pm 0.626\%$. Statistical analysis of the results in Table I reveals that both the variance ratios snd the *t*-tests are within the theoretical limits, indicating that the suggested NBS method is as equally precise and accurate as the complexometric method [13]; the same conclusion was also arrived at by comparison with the formaldoxime colorimetric method [8].

Applying the proposed method for the determination of Mn(II) in Ziemmermann's reagent almost the same accuracy has been obtained.

It is to be mentioned that manganous hydroxide is sensitive to the oxygen dissolved in water, however, the reaction between manganous hydroxide and NBS is considerably faster than that between manganous hydroxide and molecular oxygen. This fact has been shown by experiments; similar results were obtained when water was aerated and when it was boiled and cooled prior to the determination of its manganese content.

REFERENCES

[1] GOLSUYANAGI, T., GOTO, K., NAGAYAMA, M., AMURA, K.: Japan Analyst **18,** (4), 477—481 (1969)
[2] OTOMO, M.: Japan Analyst **14** (1), 45—52 (1965)
[3] HASHMI, M. H., QURESHI, T., CHUGHTAI, F. R., SACED, M.: Mikrochim. Acta **4,** 782—785 (1969)
[4] ISHU, H., EINAGA, .: Japan Analyst **15** (10), 1124—1129 (1966)
[5] AKAIWA, H., KAWAMOTO, H.: Anal. Chim. Acta **40** (3), 407—412 (1968)
[6] KAGRAMANOVA, N.;G., TALIPOR, SK. T., DZHIYAUBAEVA, R. KH.: Refart, Zhur Khim. 19GD (10) abst. No. 10 G 115 (1969); through Analyt. Abst. **18,** 181 (1970)
[7] MASCZEUKO, Z.: Anal. Chim. Acta **31** (3), 224—232 (1964)
[8] BRADFIELD, E. G.: Analyst **82,** 254 (1957)
[9] TRYBULA, Z., MURCZEWSHI, J.: J. Chem. Anal. Warsaw. **9** (2) 397—400 (1964); through Analyt. Abst. **12,** 3686 (1955)
[10] HARKAMP, H.: 2. Anal. Chem. **199** (3), 185—196 (1963)
[11] PIKE, L., YOE, J. H.: Anal. Chim. Acta **31** (4), 318—324 (1964)
[12] RADKO, V. A., YAKIMETO, E. M.: Ref. Zhur. Khim. 19GDE, (4) Abst. No. 4G14 (1); through Analyt. Abst. **12,** 105 (1965)
[13] VOGEL, I.: Text Book of Quantitative Inorganic Analysis, 3rd ed. 1961 p. 434
[14] BERNEJO MARTINEZ, M., MARGALET BARRAL, A.: Inf. Quim. Anal. **18** (2), 35—43 (1964); through Analyt. Abst. **12,** 2661 (1965)
[15] GAMAMURA, S. S.: Analyt. Chem. **40** (12), 1898—1901 (1968)
[16] PIRTEA, T. I.: Rivta. Chem. **15** (10), 635—636 (1964); through Analyt. Abst. **13,** 643 (1966)
[17] BUZÁGH-GERE, E., ERDEY, L.: Talanta **16** (10), 1434—1436 (1969)
[18] BARAKAT, M. Z.: Microchem. J. **13** (4), 517 (1968)
[19] BARAKAT, M. Z., SHEHAB, S. K.: Analyst **90,** 50 (1965)
[20] BARAKAT, M. Z., SHAKER, M., NANCY NAGUIB: Microchem. J. **11,** 485 (1966)
[21] BERKA, A., ZYKA, J.: Chem. Listy **51,** 1823 (1957)
[22] ABOUL KHEIR, A., AYAD, M., AMER, M. M.: Analyst (1974) (under publication)
[23] MOELLER, T.: Qualitative Analysis, An Introduction to Equilibrium and Solution Chemistry, 1st ed. McGraw-Hill Book Company 1958
[24] COLTON, A. F., WILKINSON, G.: Advanced Inorganic Chemistry, Intersci 1962

A. ABOUL KHEIR, M. M. AMER: Faculty of Pharmacy, Cairo University, Kasr El Aini, Cairo, Egypt.

M. AYAD; Research and Control Centre, Cairo, Egyipt.

Acta Chimica Academiae Scientiarum Hungaricae, Tomus 83 (3—4), pp. 351—358 (1974)

ACTIVITY AND ACTIVITY COEFFICIENT OF COUNTER IONS IN AQUEOUS POLYELECTROLYTE SOLUTIONS

E. A. HASSAN and M. M. B. EL-SABBAH

(Chemistry Department, Faculty of Science, Al-Azhar University, Nasr City, Cairo, E.A.R. Egypt)

Received April 10, 1974

The activity and activity coefficient were determined for silver ions in polyelectrolyte solutions of carboxyalkylated poly(vinylalcohol) with mono-, di- or trichloroacetic acid, and of two different weight exchange capacities.

The increase in the activity coefficient of counter ion (at equal concentrations of salt-free silver salt polyelectrolytes) in the above mentioned order of the polymer used, is significant in very dilute solutions ($6250 - 781.25 \times 10^{-7}N$). Although its value increases with the capacity of polymer, and sharply increases with decreasing the concentration of the silver salt polyelectrolyte, it does not reach unity at infinite dilutions.

For different mixtures of salt-free silver salt and acidform polyelectrolytes, the activity coefficient of silver ion increases with decreasing the relative quantity of silver salt polyelectrolyte and with decreasing the total concentration.

Introduction

Transport and thermodynamic properties of counterions in polyelectrolyte solutions are abnormally low as compared with the same properties in solutions of simple electrolytes. This phenomenon is related to counter ion binding [1—8]. The electrostatic interaction between the poly-ion and the counter ions may arise from localized effect of each charged site on the poly-ion *i.e.*, site binding, or from the overall charge density on the chains.

The counter ion activity coefficient of the sodium and silver (poly)-styrenesulphonates have been determined at different concentrations, and the results were analysed using simple electrostatic model which assumes the poly-ion to be parallel sheets of uniform charge density distributed in the volume of solution [7].

Experimental research on the activity of counterions in polyelectrolyte solutions, was carried out using the silver- or silver-sodium salt of the carboxymethylcellulose as a polyelectrolyte sample [6].

A number of workers have studied the activity of counterions in solutions of polyelectrolyte by immersing electrodes reversible to these ions in the solutions of poly(ethyleneimine hydrochloride) — and measuring the potential of such half-cell against a reference half-cell [6].

The aim of this work was to evaluate the activity and activity coefficient of counter silver ion in salt-free polyelectrolyte solutions of carboxyalkylated

poly(vinyl alcohol) with mono-, di- or trichloroacetic acid [9], at different concentrations. Moreover each silver salt polyelectrolyte was mixed with the respective acid-form polymer in different ratios at various total concentrations and the activity of silver ion was measured.

Experimental

Materials

Carboxyalkylated poly(vinylalcohol) with mono-, di- and trichloroacetic acid were prepared at 70°C (η_{sp}; 0.05 g/10 ml water at 25 °C = 0.27107, 0.2798 and 0.2955, and acid numbers = 34.064, 35.20 and 36.325 respectively); and at 30—40 °C (η_{sp} = 0.3010, 0.3040 and 0.3092, and acid numbers = 134.121, 150.20 and 166.72 [8]). The purified polymers were further diluted with deionized water, passed several times through a strong cation and then anion-exchange resin. The exchange capacities determined potentiometrically for the pure polyelectrolytes, in both deionized water and sodium chloride solutions (0.1, 0.5, 1.0 and 2*N*) are mentioned elsewhere [10].

Preparation of silver salt of polyelectrolyte

The polymer in the hydrogen form (1 g) was dissolved in deionized water (50 ml), then shaken with a large excess of fresh silver oxide [7], from time to time, in the darkness for a period of 2 days. The solution was then filtered of the remaining oxide, stored and handled in the absence of light.

The exchange capacity for each polyelectrolyte, relative to silver, was calculated, after boiling its silver salt with analar concentrated hydrochloric acid, to precipitate silver chloride, and the amount of silver was determined gravimetrically [11]. Their capacity, mequiv. g^{-1} relative to silver, were 0.6109, 0.6201 and 0.6522 for the first group of polymers prepared at 70 °C; and 2.4307, 2.5400 and 2.6770 for those prepared at 30—40 °C, which were more or less near to the respective values obtained from potentiometric titration curves (0.60720, 0.62744 and 0.64680 for the first group; and 2.4161, 2.6019 and 2.6550 for the second group [10]).

Measurement of the activity of silver ion

Potential measurements were made using a PYE potentiometer in conjunction with a scalamp galvanometer type MSZ-808 (Hungary). A constant voltage stabilized source ~2 volts, and also a 1.10191-volts standard cell (for standardization) were also used.

Measurements were carried out using the cell [6, 8]

$$+\text{Ag} \mid \text{Ag Cl, Sample soln.} \underset{\text{A}}{\parallel} \text{Sat. } KNO_3 \underset{\text{B}}{\parallel} \text{HgCl, Sat. KCl} \mid \text{Hg}^-$$

where A = saturated KNO_3 agar bridge, B = saturated KCl agar bridge, with the cell at 25 ± 0.1°. Neglecting the liquid junction potentials at the salt bridges A and B, the activity of silver ions a_{Ag^+} was calculated from the equation,

$$\log a_{Ag^+} = (\pi - \pi_0)/0.05909$$

in which π and π_0 are the respective electromotive forces for the studied polyelectrolyte solution and the standard solution (0.053*N* silver nitrate solution, where the silver ion activity is 0.0422 and the activity coefficient, γ_{Ag^+} is 0.789).

The concentrations (C_{Ag^+}) of salt-free silver-form solution were 7.8125, 15.625, 31.25, 62.5, 125, 250, 500, 1000, $2000 \times 10^{-5}N$.

Partially neutralized solutions were also prepared by mixing the desired proportions of the polyelectrolyte in the acid-form (C_{H^+}) with the respective solution in the silver-form (C_{Ag^+}) where $C_p = C_{Ag^+} + C_{H^+}$, and the activity of silver ion was calculated. The standard error in calculating the activity value was $\pm 0.3261 \times 10^{-8}$.

Results and discussion

Activity of counterion at different concentrations of polyelectrolyte in salt-free solution

Results given in Table I (Fig. 1 illustrates the polymers prepared at 70 °C as representative), show that, the activity coefficient of counterion increases with decreasing the polyelectrolyte concentration (from 0.2 to

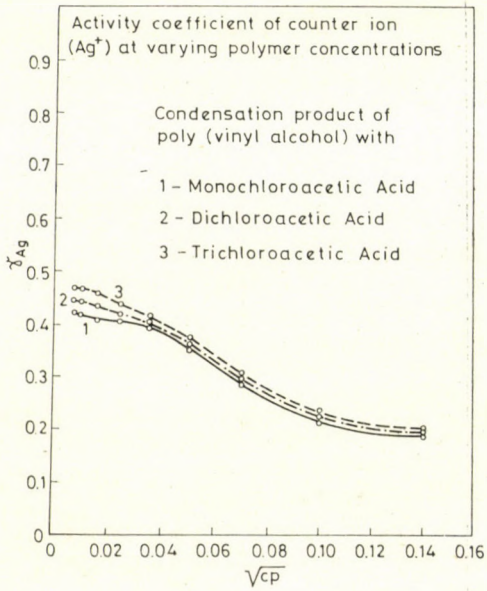

Fig. 1

0.000078125 *N*), in accordance with the previous findings for salt-free solutions of silver carboxymethylcellulose [6]. At equal concentrations the increase in the value of activity coefficient of counterion, in the following order of acid used for carboxyalkylating poly(vinylacohol): mono- < di- < trichloroacetic acid is significant in very dilute solutions (0.000625—0.000078125 *N*).

On extrapolating the activity coefficient curves to infinite dilution, it does not reach unity, differing therefore, from the behaviour of mean activity coefficients of simple electrolyte at low concentrations. It has been mentioned [6] that, the greater is the ionic charge of macroion, the greater is the decrease of activity coefficient, although it is rather difficult to treat separately the charge density distribution and the degree of polymerization.

Table I

Activity coefficient of Ag ion at varying polyelectrolyte concentrations

Concentration of silver C_{Ag^+}, $N\times10^{-7}$	$\sqrt{C_{Ag^+}}\times10^7$	Carboxylated poly(vinylalcohol) with					
		Monochloroacetic acid		Dichloroacetic acid		Trichloroacetic acid	
		$a_{Ag^+}\times10^8$	$\gamma_{Ag^+}\times10^6$	$a_{Ag^+}\times10^8$	$\gamma_{Ag^+}\times10^6$	$a_{Ag^+}\times10^8$	$\gamma_{Ag^+}\times10^6$
781.25	88,384	3261 (3962)	417,408 (507,136)	3491 (4218)	446,848 (539,904)	3622 (4446.1)	463,616 (569,088)
1562.5	102,710	6501 (7922)	416,064 (507,008)	6842.875 (8336)	43,944 (535,936)	7030 (8598.05)	459,920 (563,088)
3125.0	173,550	12,647 (15,804)	404,704 (505,728)	13,452 (16,255)	433,664 (533,504)	14,223 (17,415)	455,427.47 (557,280)
6,250	245,460	25,198 (31,013)	403,168 (496,208)	25,703 (32,531)	411,248 (520,496)	265,460 (34,515.99)	424,736 (552,256)
12,500	353,000	50,000 (61,000)	400,000 (488,000)	51,250 (62,400)	410,000 (499,200)	51,875 (65,000)	415,000 (520,000)
25,000	500,000	89,000 (98,700)	356,000 (394,800)	89,500 (94,000)	358,000 (380,000)	90,000 (100,000)	360,000 (400,000)
50,000	707,000	142,500 (153,000)	285,000 (306,000)	147,500 (155,000)	295,000 (310,000)	150,500 (157,000)	301,000 (314,000)
100,000	1 000,000	221,000 (232,000)	221,000 (232,000)	225,000 (243,000)	225,000 (243,000)	230,000 (237,000)	230,000 (237,000)
200,000	1 414,200	384,000 (395,000)	192,000 (197,560)	390,000 (397,000)	195 000 (198 500)	396,000 (399,000)	198,000 (199,500)

Data in brackets are for polymers prepared at 30—40°C

Activity coefficient of silver ion at different degrees of neutralization

The total concentrations (C_p) of mixture from salt-free silver salt, and the respective acid-form polyelectrolyte (in different ratios of (C_{Ag+}/C_{H+}) were 0.0025, 0.0075 and 0.20 *N*.

For every value of C_p *(cf.* Table II and Fig. 2), the activity coefficient of silver ion increases with the relative quantity of acid-form polyelectrolyte

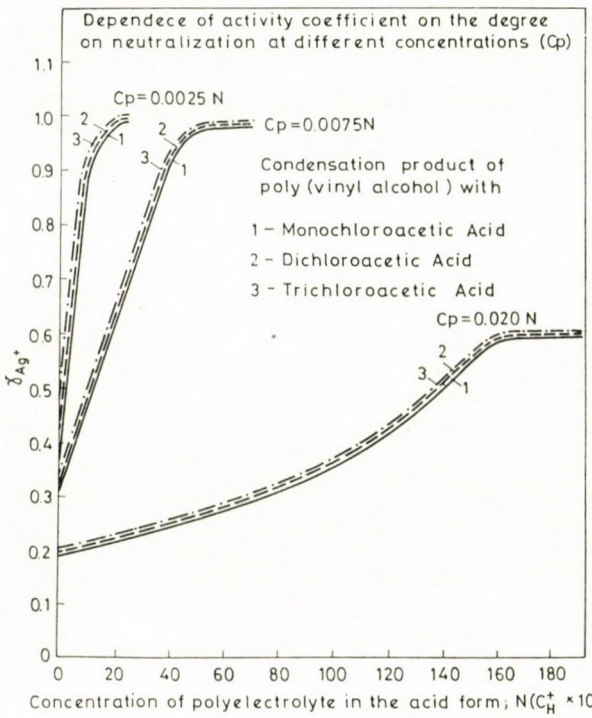

Fig. 2

(C_p). The slight change in the value of activity coefficient, with the type of carboxyalkylating acid (for the studied concentrations) is similar to that found in case of salt-free polyelectrolytes. As already reported [6], the activity of silver ion increases with increasing the degree of neutralization and falls after reaching a maximum.

The rate of increase in activity coefficient of silver ion with increasing the relative quantity of acid-form polyelectrolyte within relatively higher values (1—0.6) of the C_{Ag+}/C_p ratio is less at a C_p value of 0.02 *N*, as compared with the sharp increase in case of lower values of C_p (0.0075 and 0.0025 *N*). However, there is a slight increase in the obtained value of γ_{Ag+} at lower ratios (0.4—0.05) of C_{Ag+}/C_p.

Table II

Dependence of activity coefficient on the degree of neutralization

Total concentration $C_p = C_{Ag^+} + C_{H^+}$	Concentration of silver, C_{Ag^+} $N\times10^4$	Concentration of acidform polymer, C_{H^+} $N\times10^4$	C_{Ag}/C_p	Activity of silver ion, $a_{Ag^+}\times10^6$			Activity of coefficient, $\gamma_{Ag^+}\times10^2$		
				A	B	C	A	B	C
0.0025	1.25	23.75	0.05	125.27 (126.65)	125.713 (127.05)	125.805 (127.4)	100.216 (101.32)	100.57 (101.64)	100.645 (101.92)
	2.5	22.5	0.10	250.53 (253.025)	251.27 (253.8)	251.59 (254.575)	100.212 (101.12)	100.508 (101.52)	100.637 (101.86)
	5	20	0.20	501.0 (505.5)	502.0 (507.0)	503.0 (509.0)	100.20 (101.1)	100.40 (101.40)	100.60 (101.80)
	10	15	0.40	970.0 (980.0)	980.0 (985.0)	965.0 (990.0)	97.0 (98.0)	98.0 (98.5)	98.50 (99.0)
	15	10	0.60	1300 (1400)	1343 (1410)	1363 (1430)	86.7 (93.33)	89.53 (94.00)	90.89 (95.33)
	20	5	0.80	1200 (1260)	1220 (1270)	1260 (1290)	60.0 (63.0)	61.0 (63.5)	63.0 (64.5)
	25	0.0	1.0	890 (990)	895 (991)	900 (993)	35.6 (39.6)	35.8 (39.64)	36.0 (39.76)
0.0075	3.75	71.25	0.05	370.31 (376.574)	375.75 (377.325)	377.663 (377.70)	98.75 (100.42)	100.2 (100.62)	100.71 (100.72)
	7.50	67.5	0.1	740.62 (746.32)	741.75 (747.90)	750.75 (753.0)	98.75 (99.51)	98.9 (99.72)	100.1 (100.4)
	15	60.0	0.2	1480 (1492)	1482 (1494)	1485 (1496)	98.6 (99.47)	98.8 (99.6)	99.0 (99.73)
	30	45.0	0.4	2900 (2910)	2904 (2920)	2913 (2930)	96.66 (97.0)	96.8 (97.33)	97.1 (97.7)
	45	30.0	0.6	3500 (3610)	3555 (3620)	3564 (3640)	77.77 (80.22)	79.0 (80.44)	79.2 80.9)

	60	15.0	0.8	3250 (3360)	3264 (3380)	3288 (3400)	54.16 (56.0)	54.4 (56.33)	54.8 (56.7)
	75	0.0	1.0	2380 (2460)	2400 (2470)	2422 (2490)	31.73 (32.8)	32.0 (32.93)	32.3 (33.2)
0.20	10	190	0.05	609.4 (630.0)	612.1 (635.0)	622.3 (639.0)	60.94 (63.0)	61.21 (63.5)	62.23 (63.6)
	20	180	0.1	1208 (1238)	1218 (1258)	1238 (1270)	60.4 (61.9)	60.9 (62.9)	61.9 (63.5)
	40	160	0.2	2408 (2500)	2432 (2510)	2460 (2530)	60.2 (62.3)	60.8 (62.75)	61.5 (63.25)
	80	120	0.4	3400 (3510)	3440 (3530)	3488 (3550)	42.5 (43.87)	43.0 (44.125)	43.6 (44.375)
	120	80	0.6	3720 (3800)	3780 (3810)	3828 (3840)	31.0 (31.67)	31.5 (31.75)	31.9 (32.0)
	160	40	0.8	4000 (4110)	4080 (4121)	4128 (4160)	25.0 (25.688)	25.5 (25.76)	25.8 (26.0)
	200	0.0	1.0	3840 (3920)	3900 (3950)	3960 (3990)	19.2 (19.6)	19.5 (19.75)	19.8 (19.95)

Condensation product of poly(vinylalcohol) with monochloroacetic acid (A); dichloroacetic acid (B); trichloroacetic acid (C)

REFERENCES

[1] HERMANS, J. J., OVERBEEK, J.: Th. G., Rec. trav. chim. **67,** 761 (1948)
[2] KATCHALSKY, A., KOOZLE, O., KUHN, W.: J. Polymer Sci. **5,** 283 (1950)
[3] KIMBALL, G. E., CUTLER, M., SAMELSON, H.: J. Phys. Chem. **56,** 57 (1952)
[4] KATCHALSKY, A., LIFSON, S.: J. Polymer Sci. **11,** 409 (1953)
[5] OSAWA, F., IMAI, N., KAGAWA, I.: J. Polymer Sci. **13,** 93—111 (1954)
[6] KAGAWA, I., KATSUURA, K.: J. Polymer Sci. **17,** 365—374 (1955)
[7] FERNANDEZ-PRINI, R., BAUMGARTNER, R., LIBERMAN, S., LAGOS, A. E.: J. Phys. Chem. **73,** 1420—5 (1969)
[8] MILLER, M. L.: The structure of Polymers. Reinhold Book Corporation, New York 1966 pp. 597—600
[9] HASSAN, E. A., EL-SABBAH, M. M. B.: J. Chem. Cairo (in press).
[10] HASSAN, E. A., EL-SABBAH, M. M. B.: Indian J. of Chem. (in press).
[11] VOGEL, A. I.: A Text Book of Quantitative Inorganic Analysis. 3rd ed., Longmans, 1966

E. A. HASSAN
M. M. B. EL-SABBAH } Nasr City, Cairo, E.A.R. (Egypt).

Acta Chimica Academiae Scientiarum Hungaricae, Tomus 83 (3—4), pp. 359—365 (1974)

STUDIES ON 4-THIAZOLIDINONES,* II

REACTION OF SECONDARY AMINES WITH 5-ARYLIDENERHODANINES AND THEIR SALTS

A. R. A. RAOUF, M. T. OMAR, S. M. A. OMRAN and K. E. EL-BAYOUMY
(Faculty of Science, Ain Shams University, Cairo, Egypt)

Received October 8, 1973

5-Arylidenerhodanines **(1)** with secondary amines give a mixture of the amine salt **(2)** and 2-thiazolin-4-one **(3)** in varying proportions depending on the time of reaction. The route through which the amine salts **(2)** are converted to 2-thiazolin-4-ones **(3)** is discussed. The cleavage of 5-arylidene-3-phenylrhodanines with secondary amines has also been investigated.

Many organic bases react with rhodanines and attack the carbon atom in position 2 of the heterocyclic ring. In some cases the ring is sufficiently stable to withstand cleavage, while in others the ring is broken. Substitution at position 5 stabilizes the ring while at position 3 enhances the cleavage. Thus, whereas aniline condenses with rhodanine to give 2-phenylimino-4-thiazolidinone [1], 3-phenylrhodanine undergoes ring cleavage to give sym.-diphenylthiourea [2], and 5-benzylidenerhodanine gives phenylimino derivatives [2, 3]. Other primary amines behave similarly [4].

The present work discusses the route through which 5-arylidenerhodanines **1** are converted to the corresponding 2-thiazolin-4-ones **(3)** by reaction with secondary amines, and the cleavage of 5-arylidene-3-phenylrhodanines **4** with secondary amines. The 5-arylidenerhodanines used have been prepared using the sodium acetate–acetic acid method [5].

Refluxing each of **1a—f** with 1 or 2 mol of piperidine gives the corresponding 5-arylidene-2-piperidino-2-thiazolin-4-ones **(3a—f)** with evolution of hydrogen sulfide gas. Similar treatment with morpholine leads to the corresponding 2-morpholino derivatives **3g—l**. The structure of **3a—f** is substantiated by analytical data, the negative colour reaction previously reported by TURKEVICH and MAKUKHA [6] to characterize compounds containing a CSNH group, and by the infrared spectra *(cf.* Table I) which show a strong and a weak absorption between 1680—1690 cm^{-1} attributed to the stretching modes of the C=N and C=O groups, respectively. These are the same regions of absorptions as previously reported for 2-phenyl-2-thiazolin-4-one [7]. The structure of **3a** and **g** receives further support from m.p. and

* Part I: J. Prakt. Chem., **315**, 492 (1973).

Table I

Infrared (KBr disc) and UV spectra (in absolute methanol) of **3a—f**

Compound	Infrared spectra (cm^{-1})		Electronic spectra			
	ν C=O	ν C=N	λ_{max} (nm)	ϵ_{max}	λ_{max} (nm)	ϵ_{max}
3 a	1708	1690	239	9010	330	28 865
3 g	1710	1685	239	7700	331	28 860
3 b	1708	1685	243	8570	333	28 600
3 h	1710	1680	243	8980	334	29 670
3 c	1710	1690	~235—8	7380	337	28 660
			243	7970		
3 i	1710	1690	244	7995	337	30 750
3 d	1720	1690	~246—9	9070	307	11 915
			~296—9	11 240	353	30 125
3 j	1720	1695	251	8395	307	12 360
			~296—9	11 250	352	31 435
3 e	1710	1695	253	13 110	301	13 005
			272	12 635	358	30 135
3 k	1710	1695	253	11 315	302	11 220
			273	10 540	364	28 210
3 f	1710	1690	251	8385	300	11 910
			~280—9	10 615	361	33 135
3 l	1720	1690	251	10 205	301	21 680
			~280—8	12 145	364	29 480

~ inflection

maining 2-thiazolin-4-ones have been established from the analogy of their electronic spectra *(cf.* Table I) with those of **3a** and **g**.

However, treatment of the acetone or alcoholic solutions of **1a—f** with 1 mol or excess amine at room temperature gives mixtures of amine salts **2** and the corresponding 2-thiazolin-4-ones **3** in varying proportions depending on the time of reaction and the solubility of the salt in the reaction mixture. It is noteworthy that Lo et al. [10] has reported the isolation of the amine salts **2** only under similar conditions. The proportion of the amine salts **2** in the mixture obtained is increased in those cases when the salts are separated out quickly and the solution is worked up within a short time. For longer reaction times, the yield of thiazolinone **3** is increased at the expense of the amine salt **2**. The salts which are obtained in a pure crystalline form are **2a—e**. The remaining salts cannot be obtained in a pure state most probably because of their easy decomposition in the reaction mixture. Thus, treatment of **1a** and **b**

with piperidine gives a mixture of the amine salts **2a** and **b** and the 2-thiazolin-4-ones **3a** and **b**, respectively. Similar treatment of **1a**, **b** and **e** with morpholine gives a mixture of morpholine salts **2c**, **d** and **e** and 2-thiazolin-4-ones **3g**, **h** and **k**, respectively. The structure of **2a**—**e** is substantiated by analytical data, easy decomposition with acetic or hydrochloric acid [10], a positive colour reaction [6] and by the infrared spectra *(cf.* Table III), which show an intense broad absorption between 3050 and 3200 cm^{-1} characteristic of the stretching mode of the NH group. The structure of **2a** and **b** is further confirmed by the m.p. and mixture m.p. with authentic samples [10]. The structure of **3a**, **b**, **g**, **h** and **k** is based exclusively on a comparison (m.p. and IR) with the corresponding samples previously obtained.

The formation of rhodanine salts **2** can be explained by the acidity of the 3-H atom in rhodanines [11—13]; the problem of the conversion of amine salts **2** to the 2-thiazolin-4-ones **3** merits consideration. This reaction can be accomplished either by heating the solution of the salt for a short time or by allowing a cold solution to stand for a longer period. Thus, refluxing of the alcoholic solutions of the amine salts **2a** and **b** give the 2-piperidino-2-thiazolin-4-ones **3a** and **b**, respectively, as evidenced by m.p. and IR data. The mother liquors contain traces of 5-arylidenerhodanines **1a** and **b**, respectively, as confirmed by m.p. and a colour reaction [6]. Similarly, **2c**, **d** and **e** give 2-morpholino derivatives **3g**, **h** and **k** and traces of **1a**, **b** and **e**, respectively.

The formation of 5-arylidenerhodanines **1** as one of the decomposition products of amine salts **2** shows the reversibility of salt formation step. Further support is gained from the isolation of different thiazolinones on decomposing **2a** in the presence of morpholine. Thus, treatment of the alcoholic solution of **2a** with morpholine gives a mixture of the 2-piperidino- (**3a**) and 2-morpholino- (**3g**) -2-thiazolin-4-ones. The structures of **3a** and **g** are based on the identity with the appropriate compounds *(cf.* Experimental).

It has been reported that piperidylformanilide is obtained on refluxing 5-arylidene-3-phenyl-2,4-thiazolidinediones with excess piperidine [14]. Similar treatment of 5-arylidene-3-phenylrhodanines with secondary amines gives the corresponding thioformanilides. Thus, on refluxing the alcoholic solution of each of **4a**—**f** with piperidine or morpholine, piperidyl- (**5a**) and morpholyl- (**5b**) thioformanilides are obtained. The structures of **5a** and **b** are substantiated by analytical data and the IR spectra, which show ν_{NH} at 3265 cm^{-1} [15a] beside two strong bands at 700 and 740 cm^{-1} (5-adjacent hydrogen atoms)[15b].

Experimental

All melting points are uncorrected. The IR spectra were recorded on a Unicam SP 1200 spectrophotometer using the KBr Wafer technique. The UV absorption spectra were measured on a Model 4000 A Perkin-Elmer spectrophotometer in absolute methanol solutions.

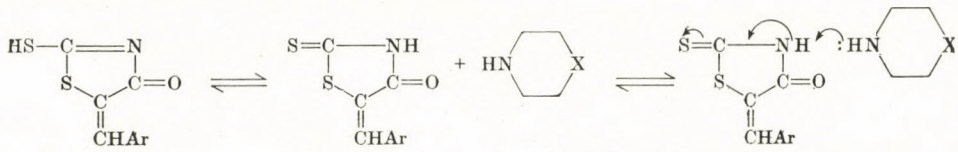

1 2

a; Ar = Phenyl
b; Ar = 4-Chlorophenyl
c; Ar = 4-Tolyl
d; Ar = 4-Methoxyphenyl
e; Ar = 3,4-Dimethoxyphenyl
f; Ar = 3,4-Methylenedihydroxyphenyl

a; Ar = Phenyl, X = CH_2
b; Ar = 4-Chlorophenyl, X = CH_2
c; Ar = Phenyl, X = O
d; Ar = 4-Chlorophenyl, X = O
e; Ar = 3,4-Dimethoxyphenyl, X = O

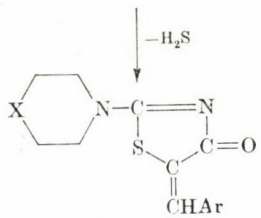

3

a; Ar = Phenyl, X = CH_2
b; Ar = 4-Chlorophenyl, X = CH_2
c; Ar = 4-Tolyl, X = CH_2
d; Ar = 4-Methoxyphenyl, X = CH_2
e; Ar = 3,4-Dimethoxyphenyl, X = CH_2
f; Ar = 3,4-Methylenedihydroxyphenyl, X = CH_2

g; Ar = Phenyl, X = O
h; Ar = 4-Chlorophenyl, X = O
i; Ar = 4-Tolyl, X = O
j; Ar = 4-Methoxyphenyl, X = O
k; Ar = 3,4-Dimethoxyphenyl, X = O
l; Ar = 3,4-Methylenedihydroxyphenyl, X = O

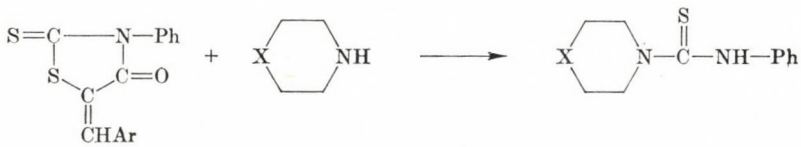

4 5

a; Ar = Phenyl
b; Ar = 4-Chlorophenyl
c; Ar = 4-Tolyl
d; Ar = 4-Methoxyphenyl
e; Ar = 3,4-Dimethoxyphenyl
f; Ar = 3,4-Methylenedihydroxyphenyl

a; X = CH_2
b; X = O

5-Arylidene-2-piperidino (or morpholino)-2-thiazolin-4-ones 3 a—l

A mixture of each of **1a—f** (5 mmol) and piperidine (or morpholine) (10 mmol) in ethanol, was refluxed until hydrogen sulfide gas ceases to evolve. The reaction mixture was concentrated, cooled, the separated solid filtered off, washed several times with light petroleum (b.p. 60—80°C) and dried. Recrystallization from the suitable solvents, gave the Title compounds. Results are shown in Table II.

Reaction of cyclic secondary amines with 1 a, b and e (without heating)

To a suspension of each of **1a—f** (5 mmol) in acetone or ethanol, piperidine (or morpholine) (10 mmol or excess) is added and the mixture is allowed to stand at room temperature for 30 min.

Table II

5-Arylidene-2-piperidino (or morpholino)-2-thiazolin-4-ones (**3a—f**)

1	Amine	3	m.p. (°C)	Yield %	Formula	Analysis: Calcd. Found			
						C	H	N	S
a	Pip.	*a*	202—4*	92	$C_{15}H_{16}N_2OS$	66.15 66.10	5.90 5.80	10.35 10.25	11.80 11.70
	Morph.	*g*	202—4**	90	$C_{14}H_{14}N_2O_2S$	61.30 61.50	5.10 5.20	10.25 10.25	11.70 11.40
b	Pip.	*b*	232—4*	92	$C_{15}H_{15}ClN_2OS$	58.75 58.60	4.90 5.10	9.15 9.10	10.45 10.50
	Morph.	*h*	218—9*	91	$C_{14}H_{13}ClN_2O_2S$	54.45 54.50	4.20 4.20	8.70 8.65	10.40 10.40
c	Pip.	*c*	183—4***	92	$C_{16}H_{18}N_2OS$	67.15 67.20	6.20 5.90	9.80 9.60	11.20 11.40
	Morph.	*i*	194—5**	93	$C_{15}H_{16}N_2O_2S$	62.50 62.30	5.55 5.50	9.70 9.65	11.10 11.10
d	Pip.	*d*	195—6*	91	$C_{16}H_{18}N_2O_2S$	63.50 63.30	5.90 5.90	9.60 9.50	10.50 10.60
	Morph.	i	200—2**	90	$C_{15}H_{16}N_2O_3S$	59.20 59.10	5.25 5.15	9.20 9.00	10.50 10.40
e	Pip.	*e*	204—5*	90	$C_{17}H_{20}N_2O_3S$	61.45 61.30	6.00 6.10	8.45 8.30	9.65 9.50
	Morph.	*k*	222—4**	95	$C_{16}H_{18}N_2O_4S$	57.50 57.20	5.40 5.30	8.40 8.30	9.60 9.80
f	Pip.	*f*	197—9*	90	$C_{16}H_{16}N_2O_3S$	60.75 60.50	5.05 5.10	8.85 8.80	10.15 10.20
	Morph.	*l*	268—9**	94	$C_{15}H_{14}N_2O_4S$	56.60 56.50	4.40 4.40	8.80 8.75	10.15 10.30

* From benzene–alcohol
** From ethanol
*** From benzene–light petroleum (b.p. 60—80°C)

The yellow-orange products which separated were filtered off and recrystallized from the suitable solvent to give the corresponding piperidine or morpholine salts. The salts which were obtained in a pure crystalline form are **2a—e**. Results are listed in Table III.

Evaporation of the mother liquors at room temperature gave a faint yellow solid, which was fractionally crystallized from benzene-alcohol to give the corresponding 2-thiazolin-4-ones. The relative amounts of the amine salts and the 2-thiazolin-4-ones at different times of the reaction shown in Table IV.

Decomposition of rhodanine salts 2 a—e

The ethanolic solution of each of the amine salts **2a—e** was refluxed until cessation of hydrogen sulfide gas (≈30 min). The solid precipitated after cooling was filtered off and recrystallized from a suitable solvent to give the corresponding 2-thiazolin-4-ones in a good yield (above 80%). Dilution of the mother liquors with water gave yellow solids, which were crystallized from a suitable solvent to give the corresponding 5-arylidenerhodanines (≈10% yield).

Table III

Rhodanine salts **2a—e**

1	Amine	Salt 2	m.p. (°C)	Formula	Analysis: Calcd. Found		IR Spectra (cm^{-1}) ν NH
					N	S	
a	Pip.	*a*	137—8* (decomp.)	$C_{15}H_{18}N_2OS_2$	9.10 8.90	20.90 21.10	3050—3200
	Morph.	*c*	148—9* (decomp.)	$C_{14}H_{16}N_2O_2S_2$	9.10 9.20	20.80 20.60	3050—3150
b	Pip.	*b*	159—60** (decomp.)	$C_{15}H_{17}ClN_2OS_2$	8.25 8.40	18.80 18.65	3050—3100
	Morph.	*d*	158—6** (decomp.)	$C_{14}H_{15}ClN_2O_2S_2$	8.15 8.00	18.70 18.60	3050—3100
e	Morph.	*e*	187—8*** (decomp.)	$C_{16}H_{20}N_2O_4S_2$	7.60 7.45	17.40 17.25	3050—3100

* From benzene
** From benzene–ethanol
*** From ethanol

Table IV

The relative amounts of **2** *and* **3** *at different intervals*

1	Amine	Total yield (%)	Product	Ratio of 2 to 3 after		
				30 min.	24 hrs	48 hrs
a	Pip.	80	3 *a* 2 *a*	10 90	60 40	95 Trace*
	Morph.	85	3 *g* 2 *c*	13 87	70 30	95 Trace*
b	Pip.	80	3 *b* 2 *b*	10 90	65 35	96 Trace*
	Morph.	82	3 *h* 2 *d*	10 90	75 25	97 Trace*
e	Morph.	90	3 *k* 2 *e*	20 80	80 20	95 Trace*

* Detected by a positive colour reaction [6]

Reaction of morpholine with 2 a

A mixture of **2a** (2.5 g) and morpholine (0.7 g) was refluxed in ethanol until no more hydrogen sulfide evolved. The reaction mixture was concentrated, treated with charcoal and allowed to stand overnight. The precipitated solid was filtered off and washed several times with light petroleum (b.p. 60—80°C). Fractional crystallization from alcohol gave **3g** (2.0g) as confirmed by m.p. and IR. The combined mother liquor was concentrated, dilute sodium hydroxide added and the whole mixture was warmed on a boiling water-bath. The insoluble fraction was filtered off (0.2 g) and crystallized from alcohol to give **3a** as evidenced by m.p. and IR.

Reaction of secondary amines with 4 a—f

A mixture of **4a—f** (5 mmol) and piperidine (or morpholine) (10 mmol) was refluxed in ethanol until all the solid dissolved (≈48 hr). The reaction mixture was concentrated, diluted with water and extracted with ether. Evaporation of the ethereal extract gave a semi-solid which was digested several times with light petroleum (b.p. 60—80°C). The combined petroleum ether extract was treated with charcoal, filtered and concentrated. The precipitated colourless needles were crystallized from light petroleum (b.p. 60—80°C) to give

Piperidylthioformanilide (77%), m.p. 88—90°C
$C_{12}H_{16}N_2S$ Calcd. C 65.4; H 7.27; S 14.5.
Found C 65.8; H 7.25; S 14.4%.

Morpholylthioformanilide (75%), m.p. 120—2°C
$C_{11}H_{14}N_2OS$ Calcd. C 59.5; H 6.3; S 14.5.
Found C 59.2; H 6.2; S 14.4%.

REFERENCES

[1] MAMELI, E., ZORZI, L.: Farmaco (Pavia) Ed. Sci. **9,** 691 (1954); Chem. Abst. **49,** 6229 (1955)
[2] GRANÄCHER, C.: Helv. Chim. Acta **3,** 152 (1920)
[3] DANIS, F. B., DAVIS, S. I.: Univ. Kansas Sci. Bull. **15,** 269 (1924); Chem. Abst. **20,** 600 (1926)
[4] BROWN, F. C.: Chem. Rev. **61,** 463 (1961)
[5] CAMPAIGNE, E., CLINE, R. E.: J. Org. Chem. **21,** 32 (1956)
[6] TURKEVICH, N. M., MAKUKHA, M. P.: Zh. Anal. Khim. **6,** 308 (1951); Chem. Abst. **46,** 1924 (1952)
[7] JENSEN, K. E., CROSSLAND, I.: Acta Chem. Scand. **17,** 144 (1963); Chem. Abst. **59,** 3912 *a*
[8] BESYADETS, KA. O. L.: Farm. Zh. (Kiev) **22,** 9 (1967); Chem. Abst. **67,** 82152 *w*
[9] TURKEVICH, N. M.: Besyadets Kaya USSR 196855; Chem. Abst. **68,** 21938 *f*
[10] LO, C.-P.: J. Amer. Chem. Soc. **80,** 3466 (1958)
[11] GIRARD, M. L., DREUX, C.: Compt. Rend. **260,** 2285 (1965); GIRARD, M. L., DREUX, C.: Bull. Soc. Chim. Fr. **3461** (1968)
[12] GINAK, A. I., SOCHILIN, E. G.: Zh. Org. Khim. **3,** 1711 (1967)
[13] COMRIE, A. M.: J. Chem. Soc. **3478** (1964)
[14] MUSTAFA, A., ASKAR, W., SOBHY, M. E. E.: J. Amer. Chem. Soc. **82,** 2597 (1960)
[15] BELLAMY, L. J.: The Infrared Spectra of Complex Molecules. Methuen and Co.-Ltd. 1960, (a) p. 65, (b) p. 13

A. R. A. RAOUF
M. T. OMAR
S. M. A. OMRAN
K. E. EL-BAYOUMY
Chemistry Department
Faculty of Science, Ain Shams University,
Abbassia, Cairo, Egypt.

Acta Chimica Academiae Scientiarum Hungaricae, Tomus 83 (1), pp. 367—372 (1975)

STUDIES ON 4-THIAZOLIDINONES, III

EVIDENCE FOR THE CLEAVAGE OF 2,4-THIAZOLIDINEDIONES WITH AMINES

A. R. A. RAOUF, M. T. OMAR and M. M. EL-ATTAL

(Department of Chemistry, Faculty of Science, Ain Shams University, Abbasia, Cairo, Egypt)

Received April 28, 1974

Cleavage of 5-(6-bromo-3,4-methylenedioxybenzylidene)-2,4-thiazolidinedione (**1b**) and its 3-phenyl derivative (**1a**) with piperidine under controlled conditions gives α-thiol-β-(6-bromo-3,4-methylenedioxyphenyl)-N-piperidylcarbonyl acrylamide (**2b**) and its N-phenyl substituted derivative (**2a**) respectively. However, the treatment of 5-arylidene-2,4-thiazolidinediones with excess benzylamine gives the corresponding arylacetic acids (**5**). The structures of these products have been confirmed by IR UV and NMR spectroscopy.

In a previous publication [1] it has been shown that 5-arylidene-3-phenyl-2,4-thiazolidinediones undergo ring cleavage with benzylamine and hydrazine at the 1,2- as well as the 4,5-bonds. The aim of the present work is to study the sequence of this cleavage.

Since it is not possible to isolate the products of 1,2-cleavage on treating 5-arylidene-3-phenyl-2,4-thiazolidinediones with benzylamine [1], our attempts here are aimed at cleaving these compounds with secondary amines such as piperidine.

Thus, short refluxing of an alcoholic solution of **1a** with 2 mol of piperidine gives α-thiol-β-(6-bromo-3,4-methylenedioxyphenyl)-N-piperidylcarbonyl-N-phenyl acrylamide (**2a**), as evidenced by analytical and spectral data. Thus, the infrared spectrum (*cf.* Table I) reveals $\nu_{C=O}$ at 1720 cm^{-1} (substituted non-cyclic imides [2]), and the electron spectrum (*cf.* Table I) is analogous to the spectra of 5-arylidene-2,4-thiazolidinediones (*cf.* Table IV). This indicates the presence of the same chromophore systems in all of these compounds. The structure of **2a** has been further confirmed, by chemical degradation. Thus refluxing of its alcoholic solution with excess piperidine gives piperidylformanilide as shown by m.p. and mixture m.p. with an authentic sample [3]. The same product is also obtained on refluxing **1a** for a long period with excess piperidine.

Similarly, cleavage of the 3-unsubstituted derivative **1b** with piperidine gives α-thiol-β-(6-bromo-3,4-methylenedioxyphenyl)-N-piperidylcarbonyl acrylamide **2b**. The structure of **2b** is evidenced by analytical as well as spectral data. Thus, its infrared spectrum (*cf.* Table I) shows ν_{NH} and $\nu_{C=O}$ (substituted non-cyclic imides [2]) and its electron spectrum (*cf.* Table I) is analo-

Table I

IR spectra KBr disc and UV spectra in absolute methanol of **2a**, **2b**, **5d** *and* **5e**

Compound	Infrared bands (cm^{-1})		Electronic bands	
	$\nu C=O$	νOH	λ_{max} (nm)	ε_{max}
2a	1720	—	370 251	23220 15100
2b	1710	3080*	366 250	16700 10565
5d	1750	3030—3700**	294 250	3075 2500
5e	1755	3030—3640**	287 250	2955 2710

* Characteristic of $\nu_N H$
** Broad absorption

Table II

NMR spectra (DMSO) of **2b** *and* **5d**

Compound	Olefinic proton	τ-values (p.p.m.)		Other absorption
		Aromatic protons	Methylenedioxy protons	
2b	2.5, 1H (S)	2.7, 1H (S) 2.87, 1H (S)	3.87, 2H (S)	6.1—8.6, 10H (M) (piperidyl protons)
5d	—	2.83, 1H (S) 3.08, 1H (S)	3.95, 2H (S)	5.93, 1H (D) 5.99, 1H (D) (α-methylene protons)

(S) = singlet; (D) = doublet; (M) = multiplet

Table III

5-*Arylidene*-2,4-*thiazolidinediones* **1a**, **1b** *and* **1c**

Compound	M.P. (°C)	Yield (%)	Formula	Analysis: Calcd. Found			
				C	H	N	S
1a	175—77 Canary yellow	74	$C_{17}H_{10}BrNO_4S$	50.5 50.2	2.47 2.60	3.64 3.90	7.9 7.9
1b	244—46 Pale yellow	76	$C_{11}H_6BrNO_4S$	40.2 40.6	1.8 2.0	4.26 4.10	9.7 9.9
1c	256—58 Pale yellow	87	$C_{12}H_{10}BrNO_3S$	41.9 42.2	2.9 3.0	4.06 3.8	9.0 9.1

Table IV

Infrared (KBr disc), UV (in glacial acetic acid) and NMR (DMSO) spectral data for **1a**, **1b** *and* **1c**

Compound	Infrared spectra (cm^{-1})		Electronic spectra		NMR spectra (τ-values)		
	$\nu C=O$	νNH	λ_{max}	ε_{max}	Olefinic protons	Aromatic protons	Other absorptions
1a	1740, 1695	—	369 255	17 870 11 655	2, 1H (S)	2.35—2.9 7H (M)	3.78, 2H (S) (Methylenedioxy protons)
1b	1760, 1715	3200	366 254	15 690 9500	2.17, 1H (S)	2.47, 1H (S) 2.98, 1H (S)	3.8, 2H (S) (Methylenedioxy protons)
1c	1760, 1710	3140	371 258	21 800 11 200	2.05, 1H (S)	2.57, 1H (S) 2.9, 1H (S)	6.28, 3H (S) 6.35, 3H (S) (Methoxy protons)

(S) = singlet; (M) = multiplet.

gous to those of **1a** and **2a**. The NMR spectrum which shows upon going from low to high fields, the signals characteristic of olefinic, aromatic, methylenedioxy and piperidyl protons with the integrated proton areas of 1 : 2 : 2 : 10, respectively, is consistent with the proposed structure. The assignment of the lowest field signal to the olefinic proton is based on comparison with the spectra of other 5-arylidene-4-thiazolidinones [4]. Furthermore, the observation of one olefinic singlet is consistent with a thiol rather than a thione form for acrylamides **2**. The analysis of its NMR spectrum is given in Table II.

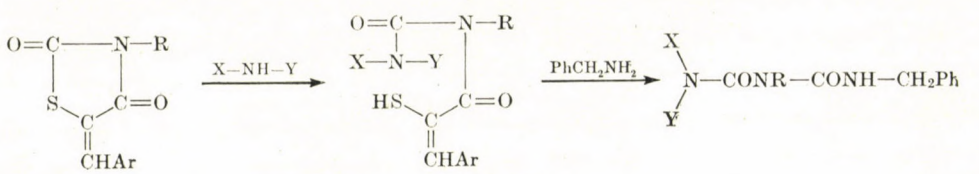

1 **2** **3**

X, Y = $-(CH_2)_5-$

\+ [$ArCH_2CHS$]

4

$ArCH_2COOH$

5

a; Ar = 6-bromo-3,4-methylenedioxyphenyl, R = Ph
b; Ar = 6-bromo-3,4-methylenedioxyphenyl, R = H
c; Ar = 6-bromo-3,4-dimethoxyphenyl, R = H
d; Ar = 6-bromo-3,4-methylenedioxyphenyl
e; Ar = 6-bromo-3,4-dimethoxyphenyl

The formation of **2a** and **2b** indicates that the cleavage occurs primarily at the 1,2-bond, which confirms the previously suggested route of cleavage [1].

However, refluxing the alcoholic solution of each of **1b** and **1c** with excess benzylamine gives 6-bromo-3,4-methylenedioxyphenyl- (**5d**) and 6-bromo-3,4-dimethoxyphenyl- (**5e**) acetic acids, respectively, with the evolution of hydrogen sulfide. In addition, an unidentified nitrogen-containing semi-solid is also obtained. The structure of both **5d** and **5e** is substantiated by analytical data, solubility in sodium carbonate solution and by infrared spectroscopy which shows $\nu_{C=O}$ and ν_{OH} characteristic of aliphatic acids [5] (*cf.* Table I). The structure of **5d** receives further support from NMR spectroscopy. Its NMR spectrum (*cf.* Table II) shows, upon going from low to high fields, the signals of aromatic, methylenedioxyl and α-methylene protons in the ratio of 2 : 2 : 2, respectively. The appearance of the α-methylene protons as two doublets points to their magnetic nonequivalence. The structure of **5e** is further proved by analogy of its electron spectrum with that of **5d** (*cf.* Table I). The nitrogen-containing semi-solids are supposed to be mixtures of different decomposition products.

It is noteworthy that arylacetic acids were prepared from 2,4-thiazolidenediones by the multistep GRÄNACHER synthesis [6]. Our procedure here provides a simple one-step method for obtaining arylacetic acids from the same starting materials.

Formation of **5d** and **5e** indicates that the cleavage of the primarily formed acrylamides **2** occurs at the 4,5-bond. This also supports our previously proposed route in which the 4,5-bond is cleaved.

Combination of these results and those reported earlier [1] permit the conclusion that the cleavage of 5-arylidene-2,4-thiazolidenediones, either substituted or unsubstituted at the 3-position, with amines involves a 1,2-bond rupture by attack at C — 2 to give **2**. In the presence of excess amine, after longer reaction times first cleavage is followed by attack at C — 4 with fission of the 4,5-bond and subsequent formation of **3** and **4**. Oxidation of **4** under the reaction conditions will lead to the formation of the arylacetic acids **5**. Further action of the amine on **3** gives nitrogen-containing decomposition products.

Experimental

Melting points are not corrected. Infrared spectra were recorded on a Carl Zeiss UR spectrophotometer. Ultraviolet spectra were taken on a Unicam SP 8005 spectrophotometer in glacial acetic acid solution. NMR spectra were obtained on a Perkin-Elmer R12 A instrument using DMSO as a solvent and TMS as internal reference.

Synthesis of bromoaldehydes

A solution of bromine (0.001 mol) and iodine (0.5 g) in 20 ml carbon tetrachloride–acetic acid mixture (1 : 1 *v/v*) was added dropwise over 30 min to a stirred solution of the appropriate aldehyde in 75 ml of the same mixture of solvents at room temperature. The reaction

mixture was stirred for 3 hrs, shaken for further 24 hrs, concentrated over a boiling water-bath and poured into cold water. The precipitated solids were filtered off and crystallized from a suitable solvent to give the title compounds.

Piperonal gave 6-bromo-3,4-methylenedioxybenzaldehyde (87%), m.p. 127—129°C, undepressed on admixture with an authentic sample [7].

Veratral gave 6-bromo-3,4-dimethoxybenzaldehyde (75%), m.p. 148—150°C, undepressed on admixture with an authentic sample [8].

Synthesis of 1a, 1b and 1c

These products were obtained by refluxing the appropriate 2,4-thiazolidinedione (0.002 mol), the bromaldehyde (0.002 mol) and fused sodium acetate (0.006 mol) in glacial acetic acid (20 ml) for 15 hrs. The reaction was carried out in the usual manner [9]. Results are given in Tables III and IV.

Action of 2 mol piperidine on 1a and 1b

To a suspension of **1a** (0.001 mol) in ethanol (15 ml), piperidine was added and the whole mixture refluxed for 3 hrs. The reaction mixture was concentrated, treated with charcoal and left standing overnight. The precipitated crude product was recrystallized from ethanol to give *α-thiol-β-(6-bromo-3,4-methylenedioxyphenyl)-N-piperidylcarbonyl-N-phenyl acrylamide* **2a** (72%) in yellow clusters, m.p. 187—189°C.

$C_{22}H_{21}BrN_2O_4S$	Calcd.	C 53.9;	H 4.2;	N 5.72;	S 6.4.
	Found	C 54.3;	H 4.0;	N 5.77;	S 6.9%.

Similar treatment of **1b** (0.001 mol) with piperidine (0.002 mol) gave a solid which was crystallized from methanol to give *α-thiol-β-(6-bromo-3,4-methylenedioxyphenyl-N-piperidyl--carbonyl acrylamide* **2b** (75%) in yellow crystals, m.p. 179—180°C.

$C_{16}H_{17}BrN_2O_4S$	Calcd.	C 46.68;	H 4.1;	Br 19.37.
	Found	C 46.50;	H 4.3;	Br 19.30%.

Action of excess piperidine on 1a

A solution of **1a** (0.001 mol) and excess piperidine was refluxed until hydrogen sulfide ceased to evolve. The reaction mixture was treated with charcoal, concentrated and the precipitated solid was recrystallized from dilute ethanol to give piperidylformanilide (60%), m.p. 158—159°C, undepressed on admixture with an authentic sample [3].

Degradation of 2a

To a solution of **2a** (0.001 mol) in ethanol (10 ml), excess piperidine was added and the mixture refluxed until hydrogen sulfide ceased to evolve. The reaction mixture was treated with charcoal, concentrated, diluted with water and the precipitated solid was recrystallized from dilute ethanol to give piperidylformanilide (50%), m.p. 158—159°C, undepressed on admixture with an authentic sample [3].

Action of benzylamine on 1b and 1c

To a suspension of **1b** (0.001 mol) in ethanol (15 ml), benzylamine (0.005 mol) was added and the mixture was refluxed for 3 hrs (or until hydrogen sulfide ceased to evolve). The reaction mixture was concentrated, treated with charcoal and allowed to stand overnight. The crude solid product was filtered off and recrystallized from n-butanol to give *6-bromo-3,4--methylenedioxyphenylacetic acid* **5d** (85%), m.p. 198—200°C.

$C_9H_7BrO_4$	Calcd.	C 41.3;	H 2.7.
	Found	C 41.6;	H 2.9%.

Similar treatment of **1c** (0.001 mol) with benzylamine (0.004 mol) gave a product which was crystallized from glacial acetic acid to give *6-bromo-3,4-dimethoxyphenylacetic acid* **5a** (85%), m.p. 193—195°C.

$C_{10}H_{11}BrO_4$	Calcd.	C 43.6; H 4.0.
	Found	C 43.3; H 4.3%.

Evaporation of the original mother liquors gave a semi-solid neutral fraction containing nitrogen; the separation and identification of these products is in progress.

REFERENCES

[1] RAOUF, A. R. A., OMAR, M. T., HABASHY, M. M.: J. Prakt. Chem. **315,** 492 (1973)
[2] UNO, J., MACHIDA, K.: Bull. Chem. Soc. Japan **34,** 545, 551 (1961); ABRAMOVICH: J. Chem. Soc. **1413** (1957)
[3] RUHEMANN, S.: J. Chem. Soc. **95,** 117 (1909)
[4] RAOUF, A. R. A., OMAR, M. T., EL-ATTAL, M. M.: Unpublished results
[5] BELLAMY, L. J.: The Infrared Spectra of Complex Molecules. John Wiley, New York 1961 p. 162
[6] GRANÄCHER, C.: Helv. Chim. Acta **5,** 610 (1922)
[7] OELKAR, A.: Ber. **24,** 2593 (1891)
[8] PSCHORR, R.: Annalen **391,** 32 (1912)
[9] CAMPAIGNE, E., CLINE, R. E.: J. Org. Chem. **21,** 32 (1956)

A. R. A. RAOUF
M. T. OMAR
M. M. EL-ATTAL
Department of Chemistry, Faculty of Science,
Ain Shams University, Abbasia, Cairo, Egypt.

Acta Chimica Academiae Scientiarum Hungaricae, Tomus 83 (3—4), pp. 373—379 (1974)

HEXITOL DERIVATIVES CONTAINING A 1,4-OXATHIANE RING, II*

J. KUSZMANN and P. SOHÁR

(Research Institute for Pharmaceutical Chemistry, Budapest)

Received March 15, 1974

The synthesis of 4-O-mesyl-3-O-tosyl- (**IIIc**), 3-O-mesyl-4-O-tosyl- (**IIId**) and 3,4-di-O-tosyl- (**IIIe**) derivatives of 2,5-anhydro-1,6-thioanhydro-D-glucitol is described. The tosyloxy groups of these compounds could be split by reduction with sodium amalgam, yielding the 3-hydroxy-4-O-methyl- (**IIIk**), 4-hydroxy-3-O-mesyl- (**IIIg**) and 3,4-dihydroxy (**IIIb**) derivatives.

Recently we described the synthesis [1] of 2,5-anhydro-3,4-di-O-methylsulfonyl-1,6-thioanhydro-D-glucitol (**IIIa**). Of the two mesyloxy groups present in **IIIa**, only the one at C-4 could be replaced by nucleophiles with retention of configuration, while the other at C-3 remained intact. As for our further experiments the corresponding 3,4-dihydroxy derivative **IIIb** was needed, a new synthesis had to be worked out.

Tosyl esters — which are very similar to mesyl esters in most of their reactions — can be easily split with sodium amalgam [2] whereby the hydroxyl group is recovered with retention of configuration. For this reason, the synthesis of the two mono-O-tosyl- (**IIIc** and **IIId**), as well as that of the di-O-tosyl derivative (**IIIe**) was decided.

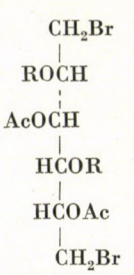

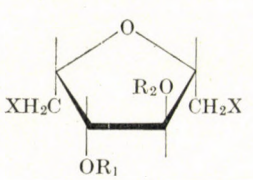

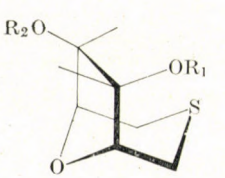

Ia R = H
Ib R = Ts

IIa X = Br, R_1 = H, R_2 = Ms
IIb X = Br, R_1 = Ts, R_2 = Ms
IIc 2X = BzS + Br, R_1 = Ts, R_2 = Ms
IId X = BzS, R_1 = Ts, R_2 = Ms
IIe X = Br, R_1 = H, R_2 = Ts
IIf X = Br, R_1 = Ms, R_2 = Ts
IIg 2X = BzS + Br, R_1 = Ms, R_2 = Ts
IIh X = BzS, R_1 = Ms, R_2 = Ts
IIi X = Br, R_1 = Ts, R_2 = Ts

IIIa R_1 = Ms, R_2 = Ms
IIIb R_1 = H, R_2 = H
IIIc R_1 = Ts, R_2 = Ms
IIId R_1 = Ms, R_2 = Ts
IIIe R_1 = Ts, R_2 = Ts
IIIf R_1 = H, R_2 = Ms
IIIg R_1 = Ms, R_2 = H
IIIh R_1 = Ts, R_2 = Bz
IIIi R_1 = Ts, R_2 = H
IIIj R_1 = Ac, R_2 = Ac
IIIk R_1 = H, R_2 = CH_3
IIIl R_1 = Ac, R_2 = CH_3

* Part I: Carbohyd. Res. **27**, 157 (1973).

Synthesis of the 3-O-tosyl derivative IIIc

Compound **IIIc** was synthesized according to the route described [1] for **IIIa**, starting from 2,5-anhydro-1,6-dideoxy-4-O-mesyl-D-glucitol (**IIa**), which on tosylation gave the corresponding 4-O-tosyl derivative (**IIb**). Treatment of **IIb** with one equivalent of potassium thiolbenzoate in acetone afforded a crude mixture, containing besides the desired mono-S-benzoyl derivatives (**IIc**) some unchanged starting material (**IIb**) and the corresponding di-S-benzoyl ester (**IId**). The latter could be obtained in pure state by treating the dibromide **IIb** with an excess of potassium thiolbenzoate.

As the mono-S-benzoyl derivatives **IIc** could not be purified by column chromatography, the crude mixture was treated with sodium methoxide, when a 1,6-thioanhydro link was formed and the 4-O-mesyl-3-O-tosyl derivative **IIIc** was obtained in a yield of nearly 50%.

The tosyl ester group in **IIIc** could be split reductively by sodium amalgam in aqueous methanol, but simultaneously the 4-O-mesyl group was substituted with retention of configuration by a methoxyl group, leading instead of the expected 3-hydroxy-4-O-mesyl compound **IIIf** to the corresponding 4-O-methyl derivative **IIIk**. Retention of the configuration at C-4 could not be proved by the NMR spectrum of compound **IIIk** itself, as the corresponding H-3 and H-4 protons gave an overlapping multiplet (see Table), therefore

Table

NMR data (δ, ppm) of 2,5-anhydro-1,6-thioanhydro-D-glucitol derivatives

Compd.	R_1	R_2	H-3 (2xd)	H-4 (d)	mesyl (CH_3)	tosyl (CH_3)	acetyl (CH_3)	methoxy (CH_3)
IIIa	Ms	Ms	5.33	5.67	3.32 3.34	—	—	—
IIIb	H	H	225—265*				—	—
IIIc	Ts	Ms	5.27	5.58	3.06	2.47	—	—
IIId	Ms	Ts	5.08	5.68	3.04	2.48	—	—
IIIe	Ts	Ts	4.99	5.50	—	—	—	—
IIIg	Ms	H	290—310*		3.22	2.42	—	—
IIh	Ts	Bz	5.28	5.70	—	2.23	—	—
II$_i$	Ts	H	4.85	5.05	—	2.50	—	—
IIIj	Ac	Ac	5.30	5.65	—	—	2.10 2.13	—
IIIk	H	CH_3	235—275*		—	—	—	3.45
IIIl	Ac	CH_3	5.15	4.40	—	—	2.10	3.36

* Overlapping multiplets (Hz)

IIIk was converted into the 4-O-acetyl derivative **III l**. In the NMR spectrum of the latter H-4 gave a doublet at 4.40 ppm, and H-3 appeared as a pair of doublets at 5.15 ppm, according to the different couplings of these protons with the adjacent H-3 and H-4 [1].

Synthesis of the 4-O-tosyl derivative IIId

For the synthesis of compound **IIId**, 2,5-anhydro-1,6-dibromo-1,6-dideoxy-4-O-tosyl-D-glucitol (**IIe**) was needed, which was prepared by converting 1,6-dibromo-1,6-dideoxy-3,5-di-O-acetyl-D-mannitol (**Ia**) into the corresponding 2,4-di-O-tosyl derivative (**Ib**) and treating the latter with hydrochloric acid in methanol. During this procedure deacetylation and elimination of *p*-tolylsulfonic acid took place resulting in the 2,5-anhydro derivative **IIe**. Mesylation of compound **IIe** afforded **IIf**, from which crystalline mono-S-benzoyl ester (**IIg**) was obtained on treatment with one equivalent of potassium thiolbenzoate in acetone. As by-product the corresponding di-S-benzoate **IIh** was isolated. When **IIg** was treated with sodium methoxide the 1,6-thioanhydro ring was formed, giving the expected 3-O-mesyl-4-O-tosyl derivative **IIId**. The tosyl ester group could be split reductively in this compound too, leading to the known [1] 4-hydroxy derivative **IIIg**.

Synthesis of the 3,4-di-O-tosyl derivative IIIe

For synthesizing the desired ditosyl ester **IIIe**, tosylation (to **IIi**) of 2,5-anhydro-1,6-dibromo-1,6-dideoxy-4-O-tosyl-D-glucitol (**IIe**) was attempted. Despite the fact that the bulky tosyl group could be introduced into the corresponding 4-O-mesyl compound **IIa**, the same reaction failed completely in the case of the 4-O-tosyl derivative **IIe**. Therefore another route had to be devised.

When the 4-O-mesyl-3-O-tosyl derivative **IIIc** was treated in hot dimethylformamide with sodium benzoate, the 4-O-mesyl group was selectively replaced by benzoate with retention of configuration. Debenzoylation of the obtained ester **IIIh** by a catalytic amount of sodium methoxide gave the 4-hydroxy-3-O-tosyl derivative **IIIi**, which on tosylation afforded the ditosyl ester **IIIe**. Both compounds (**IIIi** and **IIIe**) gave on treatment with sodium amalgam 2,5-anhydro-1,6-thioanhydro-D-glucitol (**IIIb**). Acetylation and mesylation of compound **IIIb** led to the di-O-acetyl **IIIj** and di-O-mesyl derivative **IIIa**, respectively, proving not only the presence, but also the configuration of the two hydroxyls, as the latter compound was identical with the known [1] 2,5-anhydro-3,4-di-O-mesyl-1,6-thioanhydro-D-glucitol (**IIIa**).

The IR and NMR data of the synthesized compounds were in full agreement with the proposed structures; the NMR data of the derivatives, corresponding to the general structure **III** are summarized in the Table.

Experimental

M.p.'s are uncorrected. TLC was effected on Kieselgel G with the solvent systems carbon tetrachloride ethyl acetate 1 : 1 (A), 2 : 1 (B), 5 : 1 (C), and 9 : 1 (D). A mixture of 0.1 *M* potassium permanganate ad 1 *M* sulfuric acid (1 : 1), with heating at 105°C, was used for detection. For column chromatography, silicic acid was used with carbon tetrachloride. The NMR spectra were recorded at 60 MHz, with a Varian A-60D spectrometer, for solutions in $CDCl_3$ with Me_4Si as internal standard. All evaporations were carried out in a rotary evaporator under diminished pressure, after drying the organic solutions over sodium sulfate. The light petroleum used had b.p. 60—80°C. Optical rotations were determined in chloroform (c = 1), unless otherwise stated.

3,5-Di-O-acetyl-1,6-dibromo-1,6-dideoxy-2,4-di-O-*p*-tolylsulfonyl-D-mannitol (Ib)

A solution of 3,5-di-O-acetyl-1,6-dibromo-1,6-dideoxy-D-mannitol (**Ia**) [3] (39.2 g) in dry pyridine (200 ml) was treated at 0°C with *p*-tolylsulfonyl chloride (42 g). The reaction mixture was kept for four days at room temperature and then poured into water. The oil which separated was extracted with chloroform to give, after the usual work-up, a syrup (51 g), which after crystallization from 10-fold methanol afforded pure **Ib** (42 g; 60%), m.p. 115—117°C; R_f 0.4 (solvent D); $[\alpha]_D^{20}$ +41.3°.

$C_{24}H_{28}Br_2O_{10}S_2$ (700.43). Calcd. C 41.15; H 4.03; Br 22.82; S 9.16.
Found C 41.32; H 4.19; Br 22.88; S 9.19%.

2,5-Anhydro-1,6-dibromo-1,6-dideoxy-4-O-methylsulfonyl-3-O-*p*-tolylsulfonyl-D-glucitol (IIb)

A solution of compound **IIa** [3] (156 g) and *p*-tolylsulfonyl chloride (242 g) in dry pyridine (500 ml) was kept at room temperature for five days. Water (17 ml) was then added to the reaction mixture and after further 2 hrs at room temperature it was poured into ice-water, containing conc. sulfuric acid (75 ml). The precipitate was filtered off, washed with water and dried to give, after recrystallization from methanol (1750 ml), pure **IIb** (149 g; 67.5%), m.p. 116—118 °C; R_f 0.40 (solvent C); $[\alpha]_D^{20}$ +46.2°.

$C_{14}H_{18}Br_2O_7S_2$ (522.25). Calcd. C 32.19; H 3.47; Br 30.60; S 12.28.
Found C 32.30; H 3.58; Br 30.78; S 12.34%.

2,5-Anhydro-1(6)-S-benzoyl-6(1)-bromo-6(1)-deoxy-4-O-methylsulfonyl-1(6)-thio-3-O-*p*-tolylsulfonyl-D-glucitol (IIc)

A solution of **IIb** (10.4 g) and potassium thiolbenzoate (3.8 g) in dry acetone (200 ml) was kept overnight at room temperature. The slurry was boiled for 15 min and evaporated. The residue was partitioned between chloroform and water, the organic solution was washed with water, dried and evaporated. Traces of solvent were removed from the remaining syrup at 100 °C and 0.01 torr. The syrupy product (11.4 g) contained, besides the desired mono-S-benzoyl derivatives **IIc**, some starting material (**IIb**) and the corresponding di-S-benzoyl ester **IId**, but no further purification could be achieved by chromatography because of the similar R_f values of these three components. $[\alpha]_D^{20}$ +38°; R_f 0.40 (solvent C).

$C_{21}H_{23}BrO_8S_3$ (579.51). Calcd. Br 13.79; S 16.60.
Found Br 13.90; S 16.43%.

2,5-Anhydro-1,6-di-S-benzoyl-4-O-methylsulfonyl-1,6-dithio-3-O-*p*-tolylsulfonyl-D-glucitol (IId)

A solution of **IIb** (1.04 g) and potassium thiolbenzoate (1.1 g) in dry acetone (10 ml) was treated as described for **IIh**. The crude ester obtained gave on recrystallization from methanol pure **IId** (0.96 g; 75.5%); m.p. 95—97°C; R_f 0.40 (solvent C); $[\alpha]_D^{20}$ +35.5°.

$C_{28}H_{28}O_9S_4$ (636.77). Calcd. C 52.81; H 4.43; S 20.14.
Found C 52.66; H 4.45; S 20.07%.

2,5-Anhydro-1,6-dibromo-1,6-dideoxy-4-*p*-tolylsulfonyl-D-glucitol(IIe)

Crude sirupy **Ib** (19.7 g) was boiled on a steam bath in a mixture of methanol (400 ml) and conc. hydrochloric acid (100 ml) for 7 hrs. The cooled solution was neutralized with solid sodium hydrogen carbonate, the salts were filtered off and the filtrate was concentrated to a syrup. This was dissolved in chloroform, washed with water, dried and evaporated. The residue was dissolved in methanol and treated with water till turbidity to obtain a crude material (5.4 g; 43%), which on recrystallization from methanol water afforded pure **IIe** (4.5 g; 36%); m.p. 118–120°C; R_f 0.45 (solvent D); $[\alpha]_D^{20}$ +43.1°.

$C_{13}H_{16}Br_2O_5S$ (444.28).	Calcd.	C 35.15;	H 3.63;	Br 35.99;	S 7.22.
	Found	C 35.19;	H 3.69;	Br 35.93;	S 7.53%.

2,5-Anhydro-1,6-dibromo-1,6-dideoxy-3-O-methylsulfonyl-4-O-*p*-tolylsulfonyl-D-glucitol (IIf)

A solution of **IIe** (8.9 g) in dry pyridine (50 ml) was treated with methylsulfonyl chloride (4 ml). The reaction mixture was kept at room temperature overnight to give, after usual work-up, 9.5 g crude diester, which on recrystallization from methanol (50 ml) afforded pure **IIf** (7.7 g; 74%); m.p. 79–81°C; R_f 0.55 (solvent C); $[\alpha]_D^{20}$ +42.8°.

$C_{14}H_{18}Br_2O_7S_2$ (522.25).	Calcd.	C 32.19;	H 3.47;	Br 30.60;	S 12.28.
	Found	C 32.46;	H 3.65;	Br 30.78;	S 12.32%.

2,5-Anhydro-1(6)-S-benzoyl-6(1)-deoxy-3-O-methylsulfonyl-1(6)-thio-4-O-*p*-tolylsulfonyl-D-glucitol (IIg)

A solution of compound **IIf** (8.8 g) and potassium thiolbenzoate (3.3 g) in acetone (170 ml) was boiled for 5 hrs. The slurry was evaporated, the residue treated with water, filtered and washed with water. Recrystallization of the crude material from chloroform-methanol afforded pure **IIg** (6.25 g; 64%); m.p. 194–196°C; R_f 0.50 (solvent C); $[\alpha]_D^{20}$ +42.2 (chloroform, c = 0.5).

$C_{21}H_{23}BrO_8S_3$ (579.51).	Calcd.	C 43.52;	H 4.00;	Br 13.79;	S 16.60.
	Found	C 43.75;	H 4.08;	Br 13.42;	S 16.75%.

2,5-Anhydro-1,6-di-S-benzoyl-3-O-methylsulfonyl-1,6-dithio-4-O-*p*-tolylsulfonyl-D-glucitol (IIh)

The mother liquor of compound **IIg** was evaporated and the crude mixture of the mono- and di-S-benzoyl derivatives was dissolved in dry acetone (20 ml) and boiled in the presence of potassium thiolbenzoate (2 g). The residue of the evaporated slurry was treated with chloroform–water. Evaporation of the washed and dried organic solution gave crude **IIh** (3.5 g) which was purified by recrystallization from chloroform–light petroleum to obtain the pure product (2.2 g; 20.6%); m.p. 126–127°C; R_f 0.50 (solvent C); $[\alpha]_D^{20}$ +55°.

$C_{28}H_{28}O_9S_4$ (636.77).	Calcd.	C 52.81;	H 4.43;	S 20.14;
	Found	C 52.64;	H 4.50;	S 19.91%.

2,5-Anhydro-1,6-thioanhydro-D-glucitol (IIIb)

A slurry of **IIIi** (9.5 g) or the ditosylate **IIIe** (14.1 g) and freshly prepared 4% sodium amalgam (95 g) in methanol containing 20% water (100 ml) was stirred for 3 hrs at room temperature. During the first period gentle cooling was necessary to maintain the temperature at 25°C. The decanted clear solution was neutralized with carbon dioxide, evaporated, the residue was treated with ethanol (200 ml) and the filtered solution was evaporated. The same procedure was repeated twice with acetone. The residue was treated with ether to give, after recrystallization from acetone, pure **IIIb** (4.3 g; 88.5%); m.p. 113–115 °C; R_f 0.40 (ethyl acetate); $[\alpha]_D^{20}$ +15° (chloroform, c = 0.5).

$C_6H_{10}O_3S$ (162.21).	Calcd.	C 44.43;	H 6.21;	S 19.77.
	Found	C 44.26;	H 6.35;	S 19.52%.

2,5-Anhydro-4-O-methylsulfonyl-1,6-thioanhydro-3-O-*p*-tolylsulfonyl-D-glucitol (IIIc)

Crude sirupy **IIc**, obtained from 10.4 g of **IIb** was dissolved in chloroform (50 ml) and 4 *N* methanolic sodium methoxide (6.8 ml) was added. The slurry was kept at room temperature for 24 hrs. After neutralization with carbon dioxide it was washed with water, dried and evaporated. The residue was treated with benzene–light petroleum, and the crude **IIIc** obtained was recrystallized from methanol (4.0 g; 48.8%); m.p. 147—149°C; R_f 0.35 (solvent C); $[\alpha]_D^{20}$ —15.9°.

$C_{14}H_{18}O_7S_3$ (394.48). Calcd. C 42.62; H 4.60; S 24.39.
Found C 42.61; H 4.58; S 24.42%.

2,5-Anhydro-3-O-methylsulfonyl-1,6-thioanhydro-4-O-*p*-tolylsulfonyl-D-glucitol (IIId)

A solution of **IIg** (6.25 g) in dry chloroform was treated with 4 *N* sodium methoxide (1.3 ml). After 1 hr at room temperature the solution was washed with water, dried and evaporated to yield crude **IIId** (2.45 g), which on recrystallization from methanol afforded the pure di-ester (2.1 g; 49.3%); m.p. 113—115 °C; R_f 0.50 (solvent B); $[\alpha]_D^{20}$ —13.15°.

$C_{14}H_{18}O_7S_3$ (394.48). Calcd. C 42.62; H 4.60; S 24.39.
Found C 42.63; H 4.62; S 24.24%.

2,5-Anhydro-1,6-thioanhydro-3,4-di-O-*p*-tolylsulfonyl-D-glucitol (IIIe)

A solution of **IIIi** (3.16 g) in dry pyridine (15 ml) was treated with *p*-tolylsulfonyl chloride (3 g). The reaction mixture was kept at room temperature overnight and then poured into water. The precipitated oil was extracted with chloroform to give, after the usual work-up, the ditosyl ester **IIIe** as a colorless and chromatographically pure syrup (4.5 g; 96%); R_f 0.75 (solvent B); $[\alpha]_D^{20}$ —13°.

$C_{20}H_{22}O_7S_3$ (470.57). Calcd. S 20.44. Found S 20.12%.

2,5-Anhydro-3-O-methylsulfonyl-1,6-thioanhydro-D-glucitol (IIIg)

Compound **IIId** (7.9 g) was treated with sodium amalgam as described for **IIIb**. The residue obtained after evaporating the acetone solution was dissolved in ethyl acetate, treated with ether until turbid, filtered with charcoal, and evaporated. Recrystallization of the residue from ethyl acetate–light petroleum afforded **IIIg** (1.85 g; 38.5%), m.p. 98—100°C, alone and in admixture with authentic material [1].

2,5-Anhydro-4-O-benzoyl-1,6-thioanhydro-3-O-*p*-tolylsulfonyl-D-glucitol (IIIh)

A solution of **IIIc** (19.7 g) and sodium benzoate (8.65 g) in dimethylformamide (200 ml) was boiled for 30 min. The residue obtained on evaporation was dissolved in chloroform and washed with water to give, after evaporation and treatment with methanol, pure **IIIh** (16.25 g; 77.5%), m.p. 184—195°C, R_f 0.65 (solvent C); $[\alpha]_D^{20}$ —126.3° .

$C_{20}H_{20}O_6S_2$ (420.49). Calcd. C 57.12; H 4.79; S 15.25.
Found C 57.08; H 4.82; S 15.23%.

2,5-Anhydro-1,6-thioanhydro-3-O-*p*-tolylsulfonyl-D-glucitol (IIIi)

A solution of **IIIh** (8.4 g) in dry chloroform (80 ml) and methanol (10 ml) was treated with 4 *N* sodium methoxide (0.1 ml). The reaction mixture was kept overnight at room temperature and then washed with water. The residue obtained after evaporation was treated with ether and filtered. Recrystallization from methanol gave pure **IIIi** (5.75 g; 91%); m.p. 159—160°C; R_f 0.6 (solvent A); $[\alpha]_D^{20}$ +13.9°.

$C_{13}H_{16}O_5S_2$ (316.39). Calcd. C 49.35; H 5.10; S 20.27.
Found C 49.56; H 5.24; S 20.25%.

3,4-Di-O-acetyl-2,5-anhydro-1,6-thioanhydro-D-glucitol (IIIj)

A solution of **IIIb** (4.85 g) in dry pyridine (40 ml) and acetic anhydride (30 ml) was kept at room temperature for 24 hrs and then poured into water. The filtered precipitate was washed with water (5.55 g) to give, after recrystallization from ether–light petroleum, the di-ester **IIIj** (5.0 g; 67.5%); m.p. 77–79°C, R_f 0.45 (solvent C), $[\alpha]_D^{20}$ −62°.

$C_{10}H_{14}O_5S$ (246.28).	Calcd.	C 48.77;	H 5.73;	S 13.02.
	Found	C 48.65;	H 5.82;	S 13.13%.

2,5-Anhydro-4-O-methyl-1,6-thioanhydro-D-glucitol (IIIk)

A slurry of **IIIc** (7.9 g) and freshly prepared 4% sodium amalgam (40 g) in methanol–water 4 : 1 (80 ml) was stirred overnight at room temperature and then worked up as described for compound **IIIb**. The semi-solid residue, obtained after the evaporation of acetone was dissolved in methanol and triturated with water. Unchanged starting material (0.17 g) was filtered off and the concentrated filtrate was chromatographed on a column (silicic acid, carbon tetrachloride) using solvent B for elution. Evaporation of the fractions with R_f 0.25 gave, after recrystallization from a mixture of ethyl acetate and ether, pure **IIIk** (2.2 g; 62%), m.p. 75—76°C; $[\alpha]_D^{20}$ +31°.

$C_7H_{12}O_3S$ (176.23).	Calcd.	C 47.70;	H 6.86;	S 18.19.
	Found	C 47.61;	H 6.93;	S 18.00%.

3-O-Acetyl-2,5-anhydro-4-O-methyl-1,6-thioanhydro-D-glucitol (III l)

A solution of compound **IIIk** (0.35 g) in dry pyridine (2 ml) was treated with acetic anhydride (1 ml). The reaction mixture was kept overnight at room temperature and then evaporated. The residue was treated with water and extracted with chloroform to give, after usual work-up, the crude ester (0.40 g), which on recrystallization from ether–light petroleum afforded pure **III** l (0.32 g; 76%), m.p. 80—82°C; R_f 0.75 (solvent A); $[\alpha]_D^{20}$ −27°.

$C_9H_{14}O_4S$ (218.27).	Calcd.	C 49.53;	H 6.47;	S 14.69.
	Found	C 49.54;	H 6.34;	S 14.65%.

REFERENCES

[1] KUSZMANN, J., SOHÁR, P.: Carbohyd. Res. **27,** 157 (1973)
[2] VARGHA, L., KUSZMANN, J.: Carbohyd. Res. **8,** 157 (1968)
[3] KUSZMANN, J., SOHÁR, P.: Carbohyd. Res. **16,** 261 (1971)

János KUSZMANN
Pál SOHÁR
1045 Budapest, Szabadságharcosok útja 47—49 Hungary.

Acta Chimica Academiae Scientiarum Hungaricae, Tomus 83 (3—4), pp. 381—389 (1974)

STUDY OF SOME HETEROCYCLES, XXXIV

BROMINATION AND NITRATION OF SOME 2-(*p*-X-PHENYL)-4-CHLOROMETHYLTHIAZOLES

I. SIMITI and M. FARKAS

(Institute of Medicine and Pharmacy, Cluj, Faculty of Pharmacy, Laboratory of Organic Chemistry)

Received March 15, 1974

The orientation in bromination and nitration reactions are studied in the 2-(*p*-X-phenyl)-4-chloromethyl- and 2-(*p*-X-phenyl)-4-chloromethyl-5-Y-thiazole systems by varying the substituents on the phenyl group and in position 5 of the thiazole ring.

In previous papers [1—3] we have reported on the bromination and nitration pattern of some 2-phenyl-4-R-thiazoles and of similar compounds substituted in *para* or *meta* position of the phenyl group.

To complete the studies on the behaviour of the 2-(*p*-X-phenyl)-4-R-thiazole system in various electrophilic substitution reactions [4], in the present paper we report the bromination and nitration of some of these compounds.*

Bromination was carried out in several solvents and with various amounts of bromine.

Upon brominating 2-(*p*-tolyl)-, 2-phenyl- and 2-(*p*-chlorophenyl)-4-chloromethylthiazole (**Ia, b, c**) in glacial acetic acid, acetic anhydride and conc. sulfuric acid and also 2-(*p*-bromophenyl)- and 2-(*p*-nitrophenyl)-4-chloromethylthiazoles (**Id, e**) in conc. sulfuric acid with a small excess of bromine, we have found that, regardless of the nature of the substituent on the phenyl rest and of the solvent used, only the corresponding 5-Br-derivatives (**IIa, b**(1), **c, d**(1), **e**(1)) were obtained.

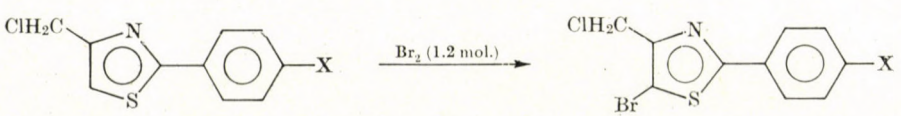

I a, b, c, d, e **IIa–e**

X = $-CH_3$, $-H$, $-Cl$, $-Br$, $-NO_2$

* The composition of the crude reaction products was studied by thin-layer chromatography on silica gel. The spots were visualized in UV light at 360 nm and their identification was made by comparing them with compounds of known structure, on the basis of RF values and the colour of fluorescence.

The presence of the bromine atom in position 5 of the thiazole ring is confirmed by the fact that the oxidative degradation of compounds **IIa, b, c, d, e** leads to the corresponding benzene mono- or dicarboxylic acids (terephthalic acid, benzoic acid, *p*-chlorobenzoic acid, *p*-bromobenzoic acid and *p*-nitrobenzoic acid, which were identified as such or as methyl esters). Like in former investigations [3, 5] also in this case compounds **II** do not show IR absorption at 3075—3100 cm^{-1}, a frequency characteristic for the C—H vibration in position 5 of the thiazole ring.

The experimental data, which indicate position 5 of thiazole to be the most reactive site in the system studied, is in agreement with quantum-chemical data on 2-phenylthiazole (the common framework of all the compounds studied) [6] and 2-(*p*-X-phenyl)-4-chloromethylthiazoles [7].

The rate of bromination depends on the nature of the substituent in the *para* position of the phenyl rest [8].

It was possible to prepare compound **IIa** also from 2-(*p*-tolyl)-4-hydroxi-4-chloromethyl-Δ^2-thiazoline hydrochloride [9] by boiling it with acetic anhydride and by adding bromine to the cold solution.

As the theoretical possibility of introducing the bromine atom into the phenyl ring exists, we have tried to carry out the bromination of compounds **Ia, b, c, d, e** with an excess of bromine (1 : 6 mol, in glacial acetic acid). Within the *para* position of the phenyl rest, a nitro group (**Ie**), a bromine (**Id**) or a chlorine (**Ic**) atom, only the corresponding 5-bromo derivatives (**IIe, d, c**) can be obtained. From 2-phenyl-4-chloromethylthiazole (**Ib**), besides the 5-bromo derivative (**IIb**) as the main product, also dibromo derivative (**IId**) with the bromine atoms in position 5 of the thiazole and in the *para* position of the phenyl rest is obtained. 2-(*p*-Tolyl)-4-chloromethylthiazole (**Ia**) furnishes the 5-bromo derivative (**IIa**) as the main product together with small amounts of the 5,5'(3')-dibromo and 5,2',5'-tribromo derivatives (**IIIa** and **IVa**):

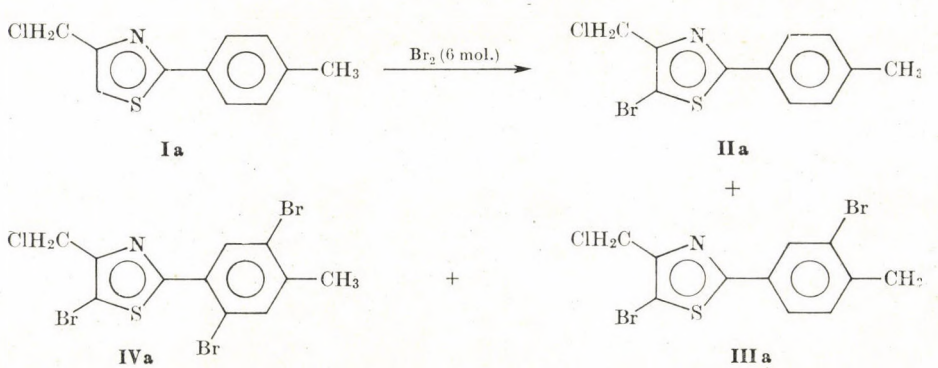

From these results we conclude that under the conditions applied the most reactive position for bromination is position 5 of the thiazole ring followed

by the *para* position of the phenyl rest if this position is free (**IIb**), or position 5'(3') of the phenyl rest if there is a methyl group (**Ia**) in *para* position.

In order to see whether a catalyst leads to a possible change in the selectivity of bromination, we have attempted the bromination of some 2-(*p*-X-phenyl)-4-chloromethylthiazoles with bromine, in conc. sulfuric acid, in the presence of a catalyst. Upon brominating compounds **Ia**, **b**, **d**, **e** with 1 mol of bromine in the presence of 0.5 mol Ag_2SO_4, the following compounds are obtained:

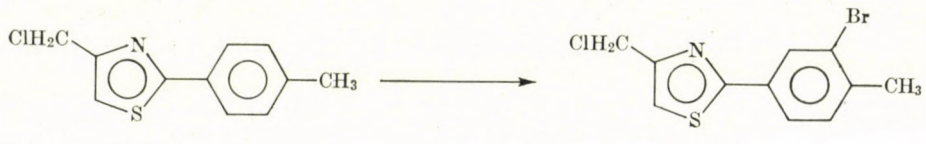

Ia **Va**

Ib **IIb**

IId **Id**

Upon brominating compound **Ia** with excess bromine (1 : 3.5 mol) in the presence of excess Ag_2SO_4 (1 : 2 mol) three compounds are obtained (**Va**, **IIIa** and **IVa**). The compounds obtained by bromination of 2-(*p*-tolyl)-4-chloro-

Id **IId**

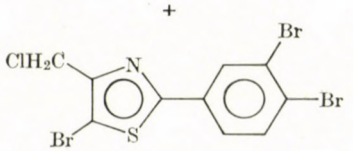

IIId

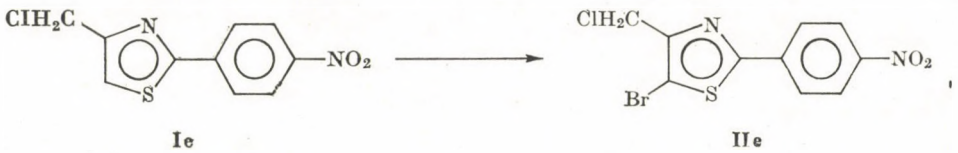

Ie IIe

methylthiazole (**Ia**) have prompted us to investigate also the bromination of compound **IIa** in similar conditions (using 2.5 mol of bromine and 2 mol of Ag_2SO_4). In these circumstances we have obtained compounds **IIIa** and **IVa**,

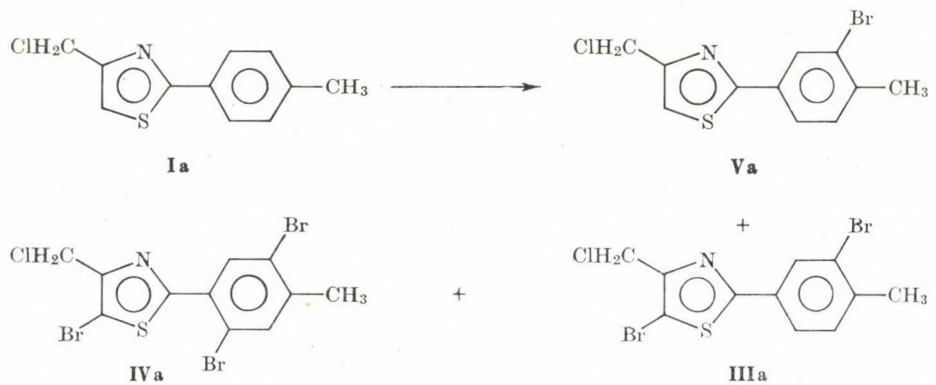

Ia Va

IVa IIIa

demonstrating that the presence of bromine in position 5 of the thiazole ring (**II a**) does not modify the orientation of the new substituents.

By brominating compound **Va** with bromine (1 : 1.2 mol) in acetic acid, we have obtained compound (**IIIa**) which is identical with that obtained before.

As the bromination of **Id** under the conditions mentioned also yields **IIId** together with **IId**, we have tried to brominate compound **IId** in the presence of a catalyst, obtaining compound **IIId**.

The structures of the new compounds (**IIIa**, **IVa**, **Va**, and **IIId**) were established in an identical way with those mentioned before.

In conclusion, the bromination of some 2-(*p*-X-phenyl)-4-chloromethyl-thiazoles (**Ia, b, d, e**) in conc. sulfuric acid in presence of Ag_2SO_4, at a mole ratio of 1 : 1 : 1/2, shows that, except for **Ie**, the catalyst increases the relative reactivity of certain positions of the aryl rest in comparison to the reactivity of position 5 of the thiazole. Thus, while bromination of **Ia, b, d** with bromine in conc. sulfuric acid leads only to the formation of the corresponding 5-bromo derivatives, in the same solvent and in the presence of Ag_2SO_4 compounds **Ib, d** are brominated not only in position 5 of the thiazole, but also in the aryl rest; in the case of compound **Ia**, however, total change of the orientation can be observed, the bromine atom entering only the aryl rest. The bromination of compounds **Ia** with NaOBr in acidic solutions, where the brominating agent is Br^+ or Br^+OH_2, occurs in position 5 of the thiazole, similarly to its bromi-

nation in conc. sulfuric acid in the absence of a catalyst. The change in bromine orientation for this compound under catalytic conditions, when the brominating agent is Br^+, is due, in our opinion, to the formation of a complex between compound **Ia** and Ag_2SO_4 prior to bromination. This problem will be discussed in one of our subsequent papers.

The nitration of **Ia, d** with a mixture of sulfuric and nitric acid affords compounds **VIa,**. The hydrochlorides of the corresponding 2-(*p*-X-phenyl)-4-hydroxy-4-chloromethyl-Δ^2-thiazolines (**I'a,**) are also converted into **VIa, d** in the presence of sulfuric and nitric acid:

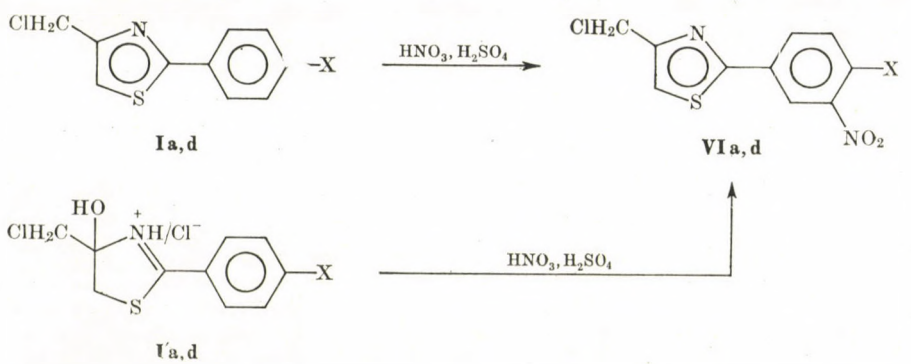

The nitration of **Ia** in acetic anhydride with conc. nitric acid leads to compound **VIIa**. It is interesting that in order to transform compound **Ia** into

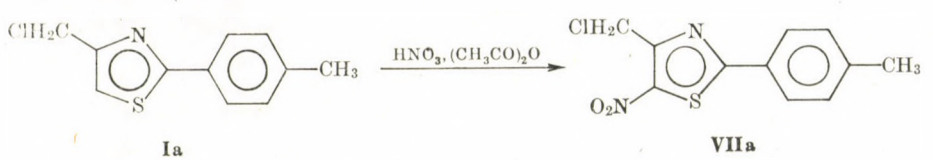

VIIa, it is absolutely necessary to leave the reaction mixture standing at room temperature before heating it up to 60°C. Otherwise compound **VIa** is obtained.

It should be emphasized that no nitration of compounds **Ia, b, d** can be effected in glacial acetic acid with nitric acid, regardless of the reaction temperature ($<$60 °C) and the quantity and concentration of the latter.

Nitration of compound **IIa, d** with a mixture of sulfuric and nitric acid affords products identical with those obtained by brominating **VIa, d**, *i.e.* **VIIIa, d**:

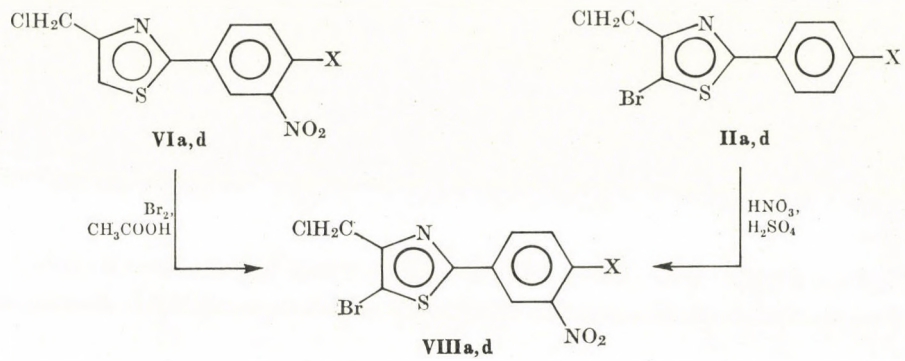

When compounds **VIIa**, **VIId** [1] are treated with a mixture of fuming nitric acid and conc. sulfuric acid, nitration occurs at position 3' (5') of the

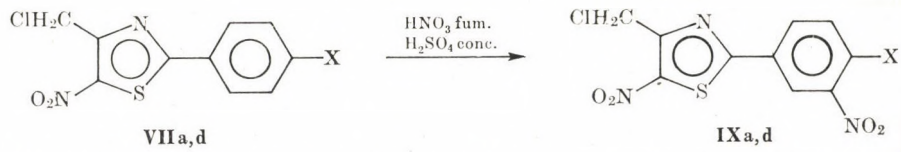

aryl rest: Under these conditions 2-phenyl-4-chloromethyl-5-nitrothiazole is nitrated also in position 3'(5') of the phenyl rest and not in the *para* position [1].

The position of the nitro group in the compounds obtained (**VIa**, **d**, **VIIa**, **IXa**, **d**) has been established by separation of the acids from their oxidative degradation and by IR spectroscopy.

From the results we can conclude that 2-aryl-4-chloromethylthiazoles are brominated easier than thiazole itself [10] and that, regardless of the solvents used, in the absence of a catalyst, the reaction occurs in position 5 of the thiazole ring. In the presence of Ag_2SO_4 as catalyst the reactivities of some aryl positions change relative to the reactivity of position 5 of the thiazole ring.

For the nitration reaction the orientation of the nitro group in the system studied depends on the nitrating agent. If the nitrating agent is acetyl nitrate protonated at the etheric oxygen [11], the nitro group predominantly enters position 5 of the thiazole ring. If the nitrating agent is the nitronium ion, nitration occurs on the aryl rest, in this case the position of the nitro group depends on the nature of the substituent in position 5 of the thiazole ring.

Experimental

Melting points have not been corrected. All recrystallizations have been carried out with added charcoal.

2-(p-X-phenyl)-4-chloromethyl-5-bromothiazole IIa, b, c)

a) To 0.001 mol of **Ia**, **b**, **c** dissolved in the minimum amount of glacial acetic acid is added 0.0012 mol of bromine with cooling the mixture, which is subsequently left at room temperature for 30 min. The mixture is then poured on ice, the precipitate filtered, washed with water and recrystallized.

Table I

Compound	Formula M.w.	m.p. (°C) (from ethanol)		N(%)		
				Calcd.	Found	
		a	b		a	b
IIa	$C_{11}H_9ClBrNS$ 302.63	138.5—139.5	137—138	4.63	4.73	4.75
IIb	$C_{10}H_7ClBrNS$ 288.60	88—89	—	4.85	5.08	—
IIc	$C_{10}H_6Cl_2BrNS$ (323.05)	127.5—128.5	—	4.34	4.41	—

b) 0.001 mol of **I'a** is heated for 5 min with 5 ml of acetic anhydride, then the solution is cooled and, keeping it cool, 0.0012 mol of bromine is added. Further processing as under (a).

2-[5'(3')-bromo-4'-methylphenyl]-4-chloromethylthiazole (Va)

To 0.002 mol of **Ia** dissolved in 15 ml of conc. H_2SO_4 is added 0.001 mol of Ag_2SO_4 and then 0.002 mol of bromine. The mixture is stirred for 4 hrs, then filtered through a G-filter and poured on ice. The precipitate is filtered, washed in abundance with water, dried and dissolved in absolute ethanol. From the filtered solution after adding water, compound **Va** is separated, which is then recrystallized from aqueous ethanol; m.p. 115°C.

$C_{11}H_9ClBrNS$ (302.63). Calcd. N 4.62; Found N 4.84%.

2-[5'(3')-bromo-4'-methylphenyl]-4-chloromethyl-5-bromothiazole (IIIa)

To 0.001 mol of **Va** dissolved in glacial acetic acid is added 0.0012 mol of bromine, the mixture is left standing at room temperature, for 30—40 min then poured on ice. The substance obtained is recrystallized from aqueous ethanol; m.p. 128—129°C.

$C_{11}H_8ClBr_2NS$ (381.54). Calcd. N 3.67; Found N 3.66%.

2-(2',5'-dibromo-4'-methylphenyl)-4-chloromethyl-5-bromothiazole (IVa)

To 0.003 mol of **IIa** dissolved in 15 ml of conc. H_2SO_4 is added 0.006 mol of Ag_2SO_4 and then 0.0075 mol of bromine. Further steps as for **Va**; m.p. 142—143°C (aqueous ethanol).

$C_{11}H_7ClBr_3NS$ (460.44). Calcd. N 3.04; Found N 3.35%.

2-(4',5'-dibromophenyl)-4-chloromethyl-5-bromo-thiazole (IIId)

To 0.004 mol of **IId** dissolved in 15 ml of conc. H_2SO_4 is added 0.008 mol of Ag_2SO_4 and then 0.006 mol of bromine. The further operations as for **Va**; m.p. 124—125°C (aqueous ethanol)

$C_{10}H_5ClBr_3NS$ (446.42). Calcd. N 3.13; Found N 3.35%.

2-(3'-nitro-4'-X-phenyl)-4-chloromethylthiazole (VIa, d)

a) To 0.001 mol of **Ia, d** dissolved in 0.6 ml conc. H_2SO_4 is added a mixture of 0.6 ml conc. H_2SO_4 and 0.4 ml HNO_3 ($d = 1.42$, g/cm^3) keeping the temperature below 60 °C. The reaction mixture is kept at 60 °C, for 30 min then poured on ice. The suspension formed is filtered, the precipitate washed with much water and recrystallized from ethanol.

Table II

Compound	Formula M.w.	m.p. (°C) (from ethanol)		N (%)		
				Calcd.	Found	
		a	b		a	b
VIa	$C_{11}H_9ClN_2O_2S$ 268.72	88—89	88—89	10.42	10.74	10.28
VId	$C_{10}H_6ClBrN_2O_2S$ 333.60	116—116.5	114	8.39	8.46	8.48

b) 0.001 mol of **I'a, d** is introduced in small portions into a mixture of 0.75 ml conc. H_2SO_4 and 0.5 ml HNO_3 (d = 1.42 g/cm³), keeping the temperature below 60°C. The procedure is continued as under (a).

2-(4'-methylphenyl)-4-chloromethyl-5-nitrothiazole (VIIa)

To 0.01 mol of **Ia**, dissolved in a minimum amount of acetic anhydride is added, under cooling, 10 ml HNO_3 (d = 1.42 g/cm³) keeping the temperature below 30°C. The reaction mixture is left standing at room temperature for 30 min then for 30 min at 60°C and subsequently poured on ice. The precipitate is filtered, washed with much water and recrystallized from ethanol; m.p. 124—125.5°C.

$C_{11}H_9ClN_2O_2S$ (268.72). Calcd. N 10.42; Found N 10.67%.

2-(3'-nitro-4'-X-phenyl)-4-chloromethyl-5-bromothiazole (VIIIa, d)

a) To 0.001 mol of **VIa, d** dissolved in a minimum amount of glacial acetic acid is added 0.076 ml of bromine. The solution is left at standing for 30 min at room temperature, then poured on ice. The precipitate is filtered, washed with water and the dry substance is recrystallized from ethanol.

b) To 0.001 mol of **IIa, d** dissolved in 1 ml of conc. H_2SO_4 is added a mixture of 0.9 ml conc. H_2SO_4 and 0.6 ml HNO_3 (d = 1.42 g/cm³), keeping the temperature below 60°C. The mixture is left for 30 min at 60°C and subsequently poured on ice. Further steps as under (a).

Table III

Compound	Formula M.w.	m.p. (°C) (from ethanol)		N (%)		
				Calcd.	Found	
		a	b		a	b
VIIIa	$C_{11}H_8ClBrN_2O_2S$ 347.63	122.5—123.5	122—123	8.06	8.15	8.27
VIIId	$C_{10}H_5ClBr_2N_2O_2S$ 412.51	147—148	148—149	6.79	6.99	7.03

2-(3'-nitro-4'-X-phenyl)-4-chloromethyl-5-nitrothiazole (IXa, d)

To 0.001 mol of **VIIa, d** dissolved in 1 ml of conc. H_2SO_4 is added a mixture of 1.65 ml conc. H_2SO_4 and 1.10 ml fuming HNO_3 keeping the temperature under 60 °C. The mixture is left standing at 60°C for 30 min, then poured on ice. The precipitate formed is filtered and washed with water. The dry substance is recrystallized from ethanol.

Table IV

Compound	Formula M.w.	m.p. (°C) (from ethanol)	N (%)	
			Calcd.	Found
IXa	$C_{11}H_8ClN_3O_4S$ 313.72	102.5—103.5	13.39	13.33
IXd	$C_{10}H_5ClBrN_3O_4S$ 378.60	123.5—124.0	11.09	10.89

REFERENCES

[1] SIMITI, I., FARKAS, M.: Chem. Ber. **98,** 3446 (1965)
[2] SIMITI, I., FARKAS, M.: Bull. soc. chim. Fr. **9,** 3862 (1968)
[3] SIMITI, I., FARKAS, M.: Acta Chim. (Budapest) **76,** 107 (1973)
[4] FARKAS, M.: Ph. D. Thesis, Univ. Babes-Bólyai, Cluj (1973),
[5] SIMITI, I., FARKAS, M.: Archiv der Pharmazie **367,** 81 (1974)
[6] BODOR, N., FARKAS, M., TRINASTIC, N.: Croat. chem. Acta **43,** 107 (1971)
[7] SCHWARTZ, I.: Studia Univ. Babes-Bólyai, ser. Chem. **1,** 51 (1971)
[8] SIMITI, I., FARKAS, M., SCHWARTZ, I.: Studia Univ. Babes-Bólyai, ser. Chem. **2,** 141 (1971)
[9] SIMITI, I., COMAN, M., SCHWARTZ, I.: Rev. Roum. **18,** 685 (1973)
[10] WIBAUT, J. P., JANSEN, H. E.: Rec. trav. chim. **53,** 77 (1934)
[11] BODOR, N., DEWAR, M. J. S.: Tetrahedron **25,** 5777 (1964)

M. FARKAS, I. SIMITI — Institute of Medicine and Pharmacy, Cluj, Faculty of Pharmacy, Laboratory of Organic Chemistry, Roumania.

Acta Chimica Academiae Scientiarum Hungaricae, Tomus 83 (3—4), pp. 391—403 (1974)

IR AND NMR STUDY OF α-AMINOOXYCARBOXYLIC ACIDS

P. SOHÁR, L. DANCSI* and L. KISFALUDY*

*(Research Institute for Pharmaceutical Chemistry, *Chemical Works of Gedeon Richter Ltd, Budapest)*

Received March 16, 1974

The IR and NMR spectra of ten simple representatives of α-aminooxycarboxylic acids and their hydrochlorides are discussed. Total assignment of the IR bands of racemic and optically active (L)- α-aminooxypropionic acid has been accomplished using the IR data of the hydrochlorids, and of alanine for comparison. The IR frequencies of the functional groups, among them the νC—O and νC—N bands being specific for this type of compounds, are characteristic of the spectra of the homologues, too.

The PMR parameters of R—CH(ONH_2)COOH type compounds are characteristic of the R substituent and not of the type of compound.

In the PMR spectrum of the isopropylidene derivative of α-aminooxypropionic acid and its ethyl ester there are two methyl signals owing to the diastereotopic relation of the methyl groups.

Although the first representative of α-aminooxycarboxylic acids — differing from natural amino acids by a single oxygen atom — had been known at the end of the last century [1], the physical and chemical properties of these compounds were not thoroughly investigated until the recognition that some of them inhibited the growth of *Mycobacterium tuberculosis* [2—4]. According to our studies, however, only certain derivatives possess significant activity [5—7]. Previously we reported about the synthesis of the parent substances [8] and their derivatives, as well as about some of their chemical and physical properties [9]. In the present paper, the IR and NMR characteristics of α-aminooxycarboxylic acids are discussed.

To our knowledge, no systematic IR and NMR studies of α-aminooxycarboxylic acids have been carried out so far. The IR spectrum of α-aminooxy-β-phenylpropionic acid and its hydrochloride is found in the literature [4] without any comment; furthermore, the νC=O and νC=N IR frequencies of some α-aminooxycarboxylic acid derivatives of the aldoxime and ketoxime ether type are described [10, 11]. Thus it seemed interesting to study the modifications of spectra caused by structural differences in comparison with simple amino acids and deviations of the chemical properties as reflected by differences in the spectra.

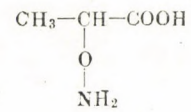

I

α-Aminooxypropionic acid (**I**) was chosen as a model for our investigations. First of all it had to be elucidated if the aminooxy analogues exist in a dipolar ion (zwitterion) structure as it is general for amino acids, or the non-ionic form predominates due to the lower basicity of the amine group. This non-ionic form might be stabilized by cyclic dimeric association of the carboxyl groups.

The IR spectrum (Spectrum 1) of **I** and all other α-aminooxycarboxylic acids investigated (*cf.* Table IV) have proved unambiguously that these substances exist exclusively in the zwitterion form (*cf.* Table I).

The IR spectrum of the enantiomers is, of course, completely identical, while that of the racemic forms is slightly different (Spectrum 2), a phenomenon also observed in several other compounds [11].

The divergence is the most significant in the shape of the νN^+H_3 band: the submaxima at about 3300 cm^{-1} which appear distinctly on the diffuse absorption between 3500 and 2200 cm^{-1} in the spectra of the optically active substances, are absent in the case of racemates. As the analogous band of primary amine salts appears in most cases with a maximum between 3000 and 3100 cm^{-1} [12], the lower-frequency part of the spectrum may be assigned to some secondary structure, which is possible only in zwitterionic compounds. (The shift of frequency is observable in the spectra of simple amino acids, too.) The absorption at lower frequency probably corresponds to polymeric 'molecular compounds' formed through the interaction of dipoles; furthermore, the equilibrium between these polymers and the analogous dimers is evidently shifted towards the former in the case of the racemate compared with the optically pure form. (The enantiomeric couples can easily establish a chain by alternation, by means of linking of the opposite poles.)

A similar tendency is observed when comparing the IR spectrum of substance **I** with that of L-alanine (Spectrum 3): the proportion of the polymeric compounds is higher than in **I**: the intensity distribution of the νN^+H_3 band is shifted in favour of the submaximum at about 3080 cm^{-1}. This can be explained by taking into consideration that the formation of a polymeric chain is favoured by the oxygen bridge rendering the ionic groups sterically more available. This is indicated by the structure of the νN^+H_3, $\delta_{as}^{+}N^+H_3$, $\nu_{as}CO_2^-$, $\nu_sCO_2^-$, etc. bands, belonging to the ionic groups, which are more diffuse in the spectrum of **I**, being the energy levels of the more flexible aggregates more diffuse. The assignments given in Table I are also confirmed by a comparison of the spectra.

Table I

IR data, cm^{-1} (KBr)[a]

Spectrum No.	Compound	νN^+H_3	δN^+H_3[b]	νCO_2^-[b]	δCH_3[b]	$\delta_{as}^- N^+H_3$	βCH γCH	$\nu C-O$ $\nu N-O$	$\nu C-C(O)$	$\delta_{as}^- CH_3$*	βCO_2^-[b]	$\nu C-C(H)$	γCO_2^- βCCC
1	I-L	3300—1900	1610[c]	1560[c]	1455		1335	1285		1090	840		490
		SM: 3030, 2600, 2140				1220			1135			900	
		(2940 : νCH_3)	1560[d]	1410	1370		775	990		1030	695		370
2	I-DL	3300—1900	1610[c]	1580[c]	1450 1440		1335	1290		1085	840		490
		SM: 2700, 2110				1210			1130			895	
		(2985 : νCH_3)	1580[d]	1410	1370		770	990		1025	695		360
3	L-Alanine [12]	3300—2000	1620[c]	1500[c]	1455		(1310)[e]	—[f]		1115	850		540
		SM: 3080, 2600				1235			1150			920	
		2120	1510	1415	1360		775	—		1015	650		410
4	I-L · HCl and	3300—2300	1575	—	1455		1325	1210[g]		1110	—		—
						1230[e]		1175	1090			880	
	I-DL · HCl	SM: —	1500		1370		770	1045		1000	—		—

[a] Concerning the vibration symbols, see Ref. [12, 13]

[b] Symmetric–antisymmetric vibration pairs

[c] The two bands are overlapped; an alternative assignment is also possible

[d] The $\delta_s N^+H_3$ band is completely overlapped by the diffuse $\nu_{as}^- CO_2$ band

[e] Overlapped

[f] The $\nu C-N$ band replacing the $\nu C-O$ and $\nu N-O$ bands and covering the βCH band appears at 1310 cm^{-1}, the $\beta C-N$ band appears at 650 cm^{-1}

[g] $\nu C-O$ type group vibration band of the carboxyl group. Frequencies of other bands characteristic of the carboxyl function are given in the text

* The two bands of the degenerated vibrations are split.
SM: Submaximum

The spectrum of the hydrochloride of **I** (Spectrum 4) affords further evidence for the original zwitterionic structure. Namely, the characteristic bands of the carboxylate ion are absent, but the spectrum contains absorptions characteristic of carboxylic acids, *e.g.* the most specific and very intense absorption of the carbonyl group at 1735 cm^{-1} (*cf.* Table II and Spectrum 4, resp.). The observation that the spectra of the racemic and optically active compounds are fully identical, supports our explanation of the divergences found between the zwitterionic parent substances. As the salts evidently and invariably form carboxylic acid dimers, further interaction between the molecules is possible only between the $-N^+H_3$ groups, and from this point of view the configuration is indifferent. (This configuration has importance only in the case when two optically active molecules are 'attached' at *two* points.)

By comparing the Spectra 1, 2, 3 and 4, the majority of the bands can be assigned with a relative great assurance.

The simplest way of deriving the normal vibrations of compound **I** is the separation of substituent and skeletal vibrations. The total number of the normal vibrations is $3N - 6 = 3 \cdot 14 - 6 = 36$.

The $-XY_3$ type groups show 5(8) bands, each having symmetric and antisymmetric stretching ($\nu_{as}XY_3$, ν_sXY_3) and deformation ($\delta_{as}^+CH_3$, δ_sCH_3) vibrations, further, a deformation vibration (the so-called rocking vibration) of identical phase ($\delta_{as}^-CH_3$) [12, 13]. The three antisymmetric vibrations are twofold degenerated; the two normal vibrations with coincident frequency belong to the corresponding bands. Thus, each methyl and ammonium group shows 5 bands (8 vibrations).

Each carboxylate ion has two, and each methine group one stretching vibration, in-plane vibrations and out-of-plane deformation vibrations (6 + 3 bands, 6 + 3 vibrations). Thus, in the spectrum 19 bands derived from 25 vibrations correspond to the substituents.

Among the 9 vibrations of the $\begin{matrix} C \\ C \end{matrix}\!\!>\!C-O-N$ skeleton ($N = 5$, $3N - 6 = 9$), 4 stretching vibrations (due to the 4 bonds), 3 in-plane and 2 out-of-plane vibrations are found. The latter five are the scissoring and rocking vibrations of the C—C—C chain (β_sCCC, $\beta_{as}CCC$), the bending vibration of the C—O—N chain (βCON), and the perpendicular vibration of the two atom triplets (γ_sCCC, γCON).

Finally, one in-plane and one out-of plane, originally non-genuine vibration (the βCCO in-plane and out-of-plane CCC-torsional: $\gamma_{as}CCC$ vibration) become genuine since the substituents counterbalance the moment of these vibrations, which therefore do not cause translation and rotation.

Table II contains the above-mentioned vibrations assorted according to their frequencies. Starting from this point, a likely assignment of the spectrum bands can be carried out.

Table II

Vibration types of α-aminooxypropionic acid and their presumed frequency regions

	4000–2000 cm^{-1}	2000–650 cm^{-1}		650–250 cm^{-1}		< 250 cm^{-1}
Vibrations of the substituents	$\nu_{as}CH_3$*	$\nu_{as}CO_2^-$	$\delta_{as}^+N^+H_3$*	$\beta_sCO_2^-$**	$\gamma_{as}CO_2^-$	—
	$\nu_{as}N^+H_3$*	$\nu_sCO_2^-$	$\delta_sN^+H_3$	$\beta_{as}CO_2^-$**	$\gamma_sCO_2^-$	
	ν_sCH_3	$\delta_{as}^+CH_3$*	$\delta_{as}^-N^+H_3$*	γCH**		
	$\nu_sN^+H_3$	$\delta_{as}^-CH_3$*	βCH			
	νCH	δ_sCH_3				
Vibrations of the skeleton	—	$\nu C(H_3)—C(H)$		β_sCCC		γ_sCCC
		$\nu C(O_2)—C(H)$		$\beta_{as}CCC$		${}_s^a\gamma CON$
		$\nu C—O$		βCON		γCCC
		$\nu O—N$		βCCO		

* Twofold degenerated vibration: two normal vibrations belong to one or two bands
** Frequencies of these vibrations are about 650 cm^{-1} and cannot be classified safely either into the region from 2000 to 650 cm^{-1} or into that from 650 to 250 cm^{-1}

From among the five high-frequency bands, those originating from the $—N^+H_3$ group are easy to identify and the $\nu_{as}CH_3$ band can be also recognized as a sharp maximum, being superimposed on the $\nu_{as}N^+H_3$ absorption (at 2940 cm^{-1} on Spectrum 1). Its symmetric pair and the νCH band are absent (completely overlapped by the $\nu_{as}N^+H_3$ band.) The $\nu_sN^+H_3$ band is found at about 2140 cm^{-1}.

From among the bands expectable in the middle (fingerprint) region of the spectrum, those originating from $\nu_{as}CO_2^-$, $\delta_{as}^+N^+H_3$ and $\delta_sN^+H_3$ show the highest frequencies. At about 1600 cm^{-1}, two maxima are distinguishable and as the absorption higher than 1600 cm^{-1} is absent from the spectrum of the hydrochloride, it is likely that $\nu_{as}CO_2^-$ absorbs at 1610 cm^{-1} and $\delta_{as}^+N^+H_3$, merged into the symmetric counterpart, absorbs at 1560 cm^{-1}. The $\delta_{as}^+CH_3$, δ_sCH_3 and $\nu_sCO_2^-$ bands are also easy to recognize at about 1460, 1370 and 1410 cm^{-1}, since they appear within a relatively narrow interval characteristic of the respective vibration forms [12] and are sharp. In contrast, the $\delta_{as}^-N^+H_3$ maximum can be assigned by the broad shape of the band at 1220 cm^{-1}. Presumably, the weak band at 1330 cm^{-1} corresponds to the βCH vibration.

Identification of the other bands of the fingerprint area is more difficult. It is expectable that these are the methyl rocking vibrations, the bands of the four skeletal stretching vibrations and, within these, the bands of νC—O and νO—N, respectively, characteristic of α-aminooxycarboxylic acids, furthermore one or both bands of the in-plane deformation vibration of the carboxylate group. It is possible that the band of the γCH vibration also appears here.

It seems likely that the intense pair of bands at about 1290 and 990 cm^{-1} belongs to the characteristic C—O—N system of α-aminooxycarboxylic acids. The former may arise from a νC—O and the latter from a νO—N type vibration. The assignment of the νC—O band is confirmed by the absence of this band from the spectrum (Spectrum 3) of alanine (it is replaced by the νC—N band being very intense and sharp at 1310 cm^{-1}) and by its broadening (the energy of vibration is influenced by the association structure, too; therefore, Spectrum 1 has a shoulder at about 1300 cm^{-1} and Spectrum 2 is sharper due to the more uniform association structure), finally by the high frequency; similarly to aromatic ethers, the CO bond order and thus, the νC—O frequency are increased by the electron-attracting effect of the N^+H_3 ion bound to the oxygen (*cf.* the mesomeric structure **Ia**). Of course, the frequency decreases in the case of the hydrochloride, as the flow of the electrons is pointing now in the opposite direction *i.e.* from the skeleton to the carbonyl oxygen. Therefore the νC—O band is found at 1175 cm^{-1}. A band of similar character belonging to the acid group [νC(=O)—O(H)] appears at 1210 cm^{-1}.

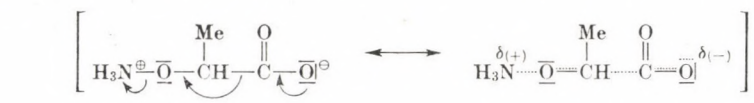

Ia **Ia**

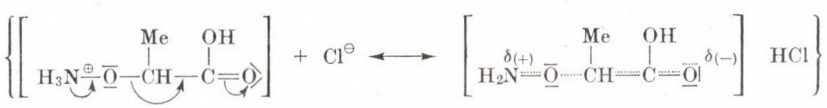

Ia · HCl **Ia′** · HCl

For similar reasons, the NO bond order and polarity are increased in the case of the hydrochloride (the mesomeric system is shifted towards structure **Ia** · HCl); as it is expected, the νN—O band becomes more intense and appears at higher wave-numbers. Of course, this band is absent from the spectrum of alanine. When all these factors are taken into consideration, it is likely that the band at 990 cm^{-1}, *i.e.* at 1045 cm^{-1} in the spectrum of the hydrochloride, belongs to the νN—O vibration.

The two bands between 1115 and 1000 cm^{-1} arise presumably from the methyl rocking vibration. This is indicated by the relatively stable frequency which is slightly increased due to the decreased electron density of the methine carbon in the case of alanine and hydrochloride.

Of the carbon–carbon skeletal stretching vibrations, the one adjacent to the carboxylate ion group has the higher frequency and is shifted strongly in the salt in consequence of coupling with the νC—O vibration; however, this frequency increases in the case of alanine, where the electro-attracting $—N^+H_3$

group is directly connected with the carbon atom. It is concluded from all these facts that in Spectra 1, 2, 3 and 4 the maxima at 1135, 1130, 1150 and 1090 cm^{-1}, respectively, should be assigned to this vibration.

It follows from the number of bands of the fingerprint region that two carboxylate, one skeletal deformation and even the γCH vibration absorb in the interval of frequencies higher than 650 cm^{-1}. The bands at 840 and 695 cm^{-1} can be assigned to the $\beta_s CO_2^-$ and $\beta_{as} CO_2^-$ vibrations respectively, according to their great intensity as well as because of their absence from the spectrum of the hydrochloride.

On the basis of these considerations, the two remaining bands (at 900 and 775 cm^{-1}, in Spectrum 1) should correspond to the vibrations νC—C(H_3) and γCH, according to their frequencies. The appearance of the γCH band may be due to the association structure: the molecule has a favoured plane in relation to which a βCH and γCH type vibration may really exist.

Between 650 and 250 cm^{-1} only the bands of two out-of-plane carboxylate ion and four in-plane deformation skeletal vibrations are expected (presumably, the three out-of-plane skeletal deformation vibrations have frequencies lower than 250 cm^{-1}). The bands of the carboxylate ion are intense and do not appear in the case of the acid; of the bands of the skeletal vibrations, only two (β_{as}CCC and β_sCCC) are found in the spectrum of alanine and the other two can be replaced by the δC—N band.

Based on the above considerations, the $\gamma_s CO_2^-$ and an in-plane bending skeleton frequency (an alternative assignment is also possible) appear at about 490 and 370 cm^{-1} in Spectrum 1, which is supported by the absence of these bands from Spectrum 4, and by their higher frequencies in Spectrum 3. (The $-CO_2^-$ and $-N^+H_3$ ion groups that are nearer in alanine, hinder the out-of-plane vibrations of each other and increase the energy of the vibration.) As an absorption at 650 cm^{-1} is found only in Spectrum 3, its interpretation as βCN band is undoubtful.

The assignments of the maxima of the salt not explained so far and appearing in the fingerprint region, are the following: νC=O: 1735, βOH: 1400, γOH: 825, βC—C(=O)—O: 795, 725, 715 cm^{-1} and γCO: 720 cm^{-1}.

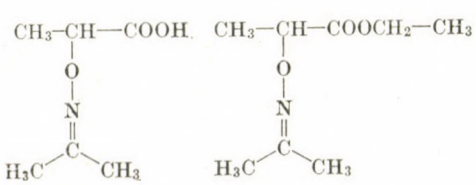

II III

It is interesting to note that the characteristic divergence described by UNDHEIM *et al.* [11], according to which the carboxylic carbonyl band of an

optically active compound will be split, did appear neither in the IR spectra of racemates and optically active modifications of the **I** hydrochloride, nor in the Schiff base **II** and ester **III**. Although the spectra are different for compound **II**, there is only one carbonyl band appearing at 1725 cm^{-1} (racemate) and at 1740 cm^{-1}. In the case of **I** · HCl and **III**, the spectra of the racemic and optically active modifications and the frequency of the carbonyl absorptions (at 1735 cm^{-1} in **I** · HCl and at 1755 cm^{-1} in **III**) are identical.

Although the data obtained by the detailed analysis of the IR spectrum of α-aminooxypropionic acid (**I**) are very useful in the interpretation of spectra of the homologues, the PMR spectrum of **I** (Spectrum 5) has few signals, giving very limited information for other α-aminooxy carboxylic acids. The reason is that the functional groups determining the IR spectrum are the same in all α-aminooxycarboxylic acids, whereas the PMR signals arise from CH groups building up the molecular skeleton and differing in every homologous compound,* furthermore there are no PMR signals characteristic of the functions CO_2^- and $O—N^+H_3$. (The ammonium proton signals are not characteristic, as their shape and positions depend on the experimental conditions, mainly due to exchange processes [14]).

However, the conclusions obtained from the IR spectra for the electron distribution of **I** and the corresponding hydrochloride, are supported by the PMR data. On the basis of the chemical shifts measured in DMSO-d_6 (Table III), a paramagnetic shift by 0.22 ppm of the methyl doublet and by 0.70 ppm of the methine quartet is observed in the case of the hydrochloride, under the influence of the electron-attracting carboxyl group replacing the carboxylate ion.

Optically active and racemic modifications of **I** give, of course, the same PMR spectrum in all achiral solvents. As mentioned above, these spectra are very simple: in addition to the doublet and quartet signals of the coupled methyl and methine groups, only the characterless absorptions of the acid protons appear, overlapped by the water content of the solvent (Spectrum 5). The spectral data are shown in Table III. When the values of the chemical shifts of alanine also listed in Table III are related to the corresponding data of **I**, the influence of the oxygen atom increasing the chemical shift of the methine proton is well observed, the difference being 0.76 ppm. The shift is hardly significant (—0.03 ppm) and of opposite direction in the case of the methyl signal. The reason for it is partly that the —**I** effect of the oxygen, which would shift the methyl signal paramagnetically is almost entirely isolated by the interpolated methine group, and partly that the decreased deshielding effect is compensated (and slightly even over-compensated according to the

* Table IV contains characteristic PMR data of the α-aminooxycarboxylic acids investigated in our experiments.

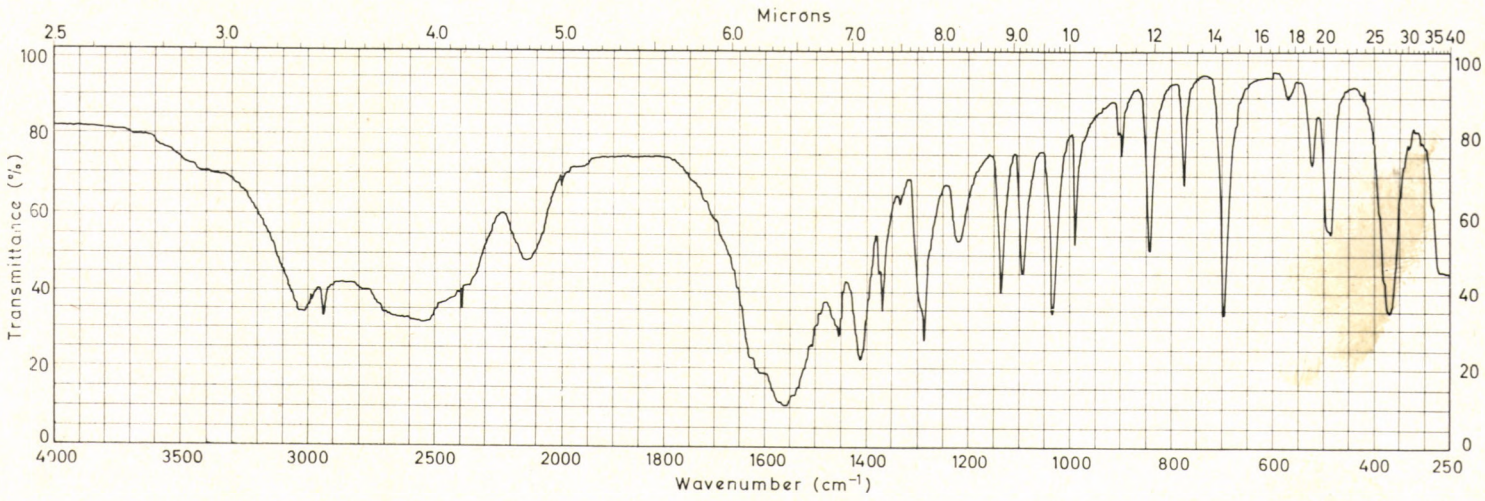

Spectrum 1. IR spectrum of **I** (L) in KBr

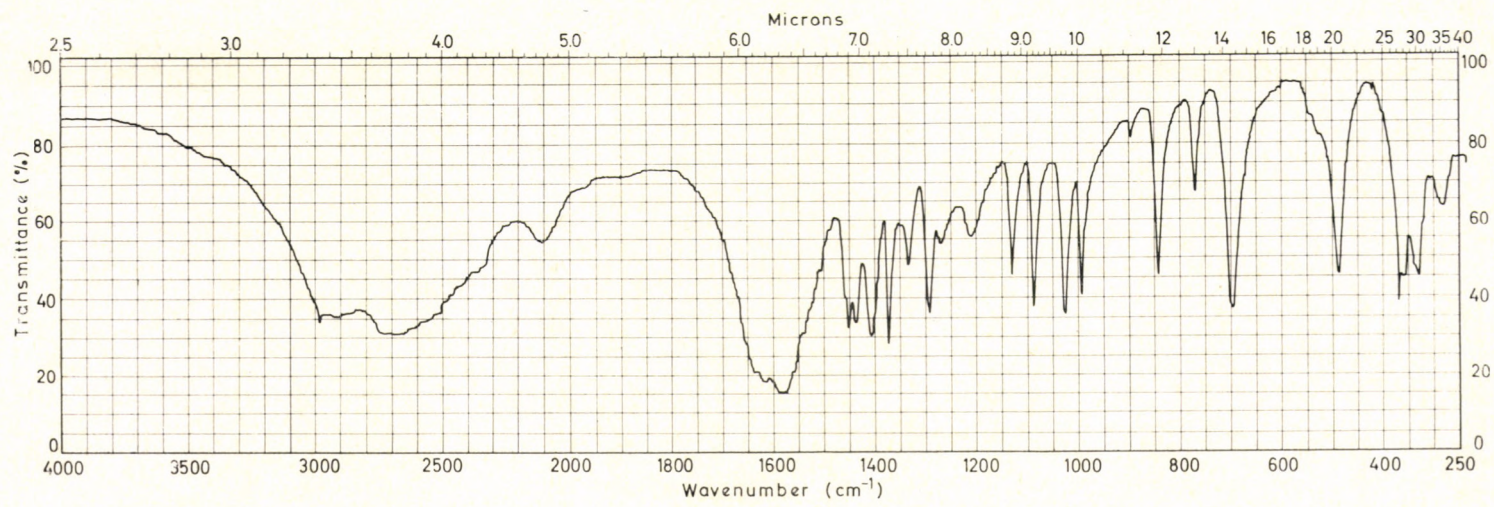

Spectrum 2. IR spectrum of **I** *(meso)* in KBr

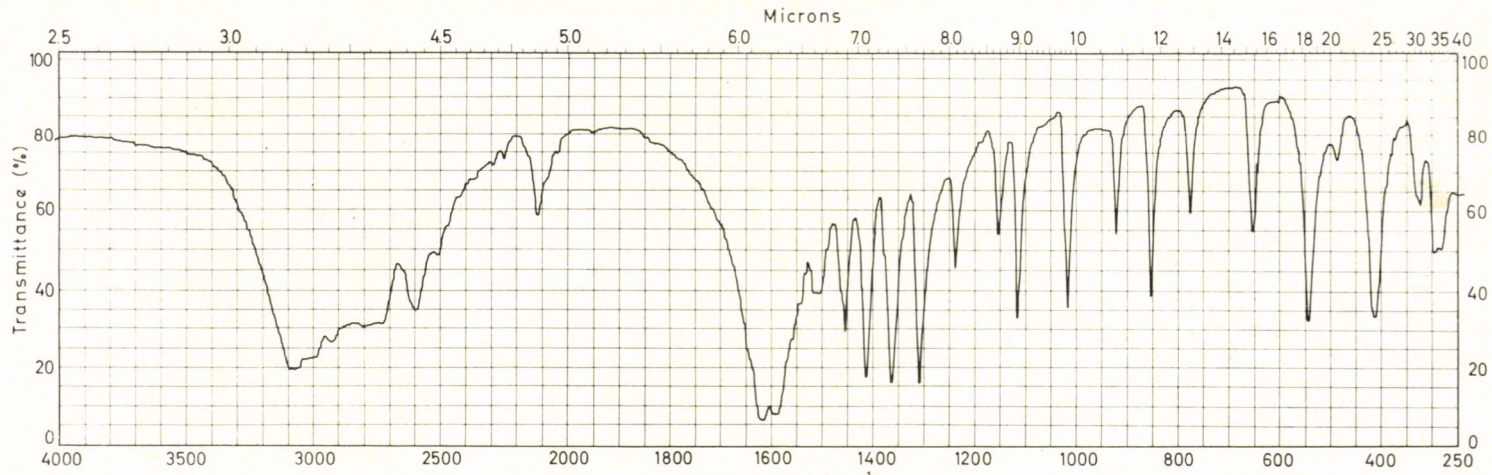

Spectrum 3. IR spectrum of L-alanine in KBr

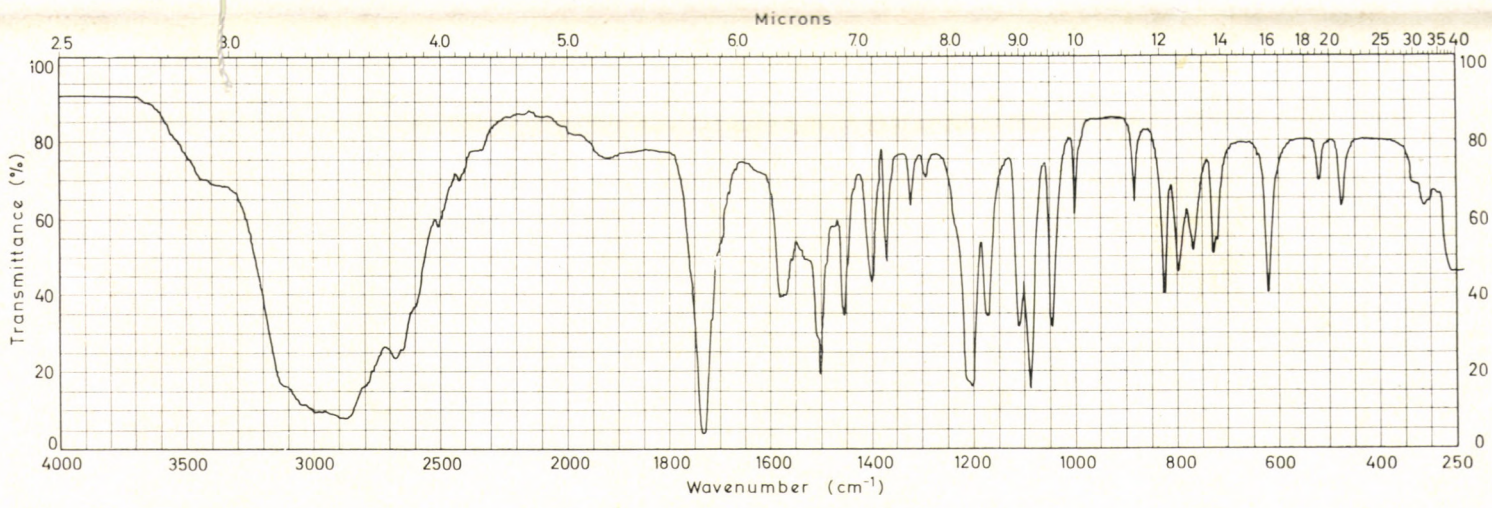

Spectrum 4. IR spectrum of the hydrochloride of **I** (L) in KBr

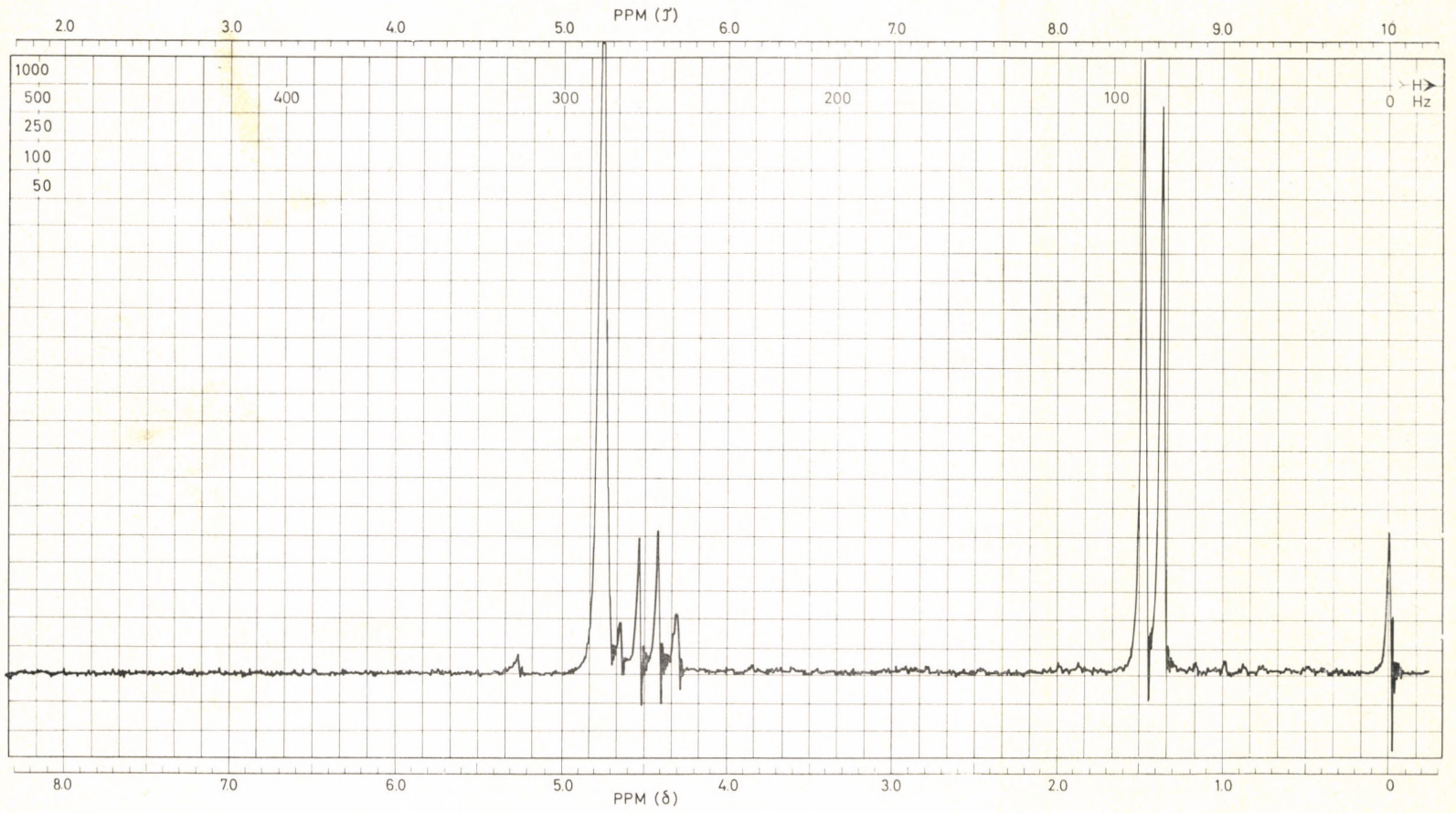

Spectrum 5. PMR spectrum of **I** in D_2O

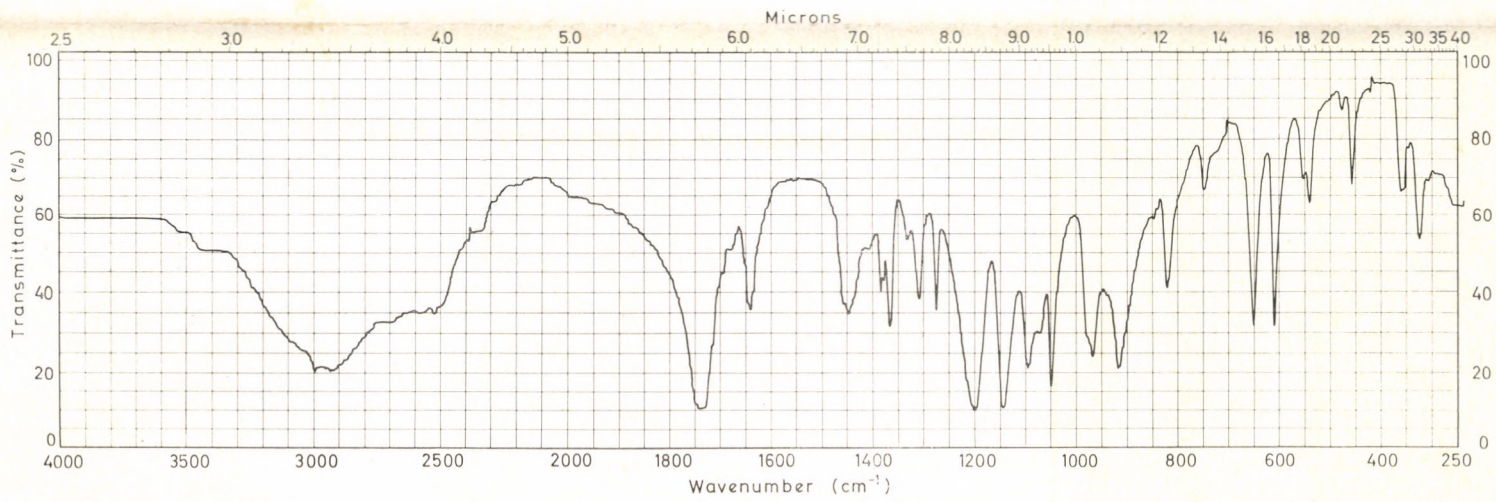

Spectrum 6. IR spectrum of **II** in KBr

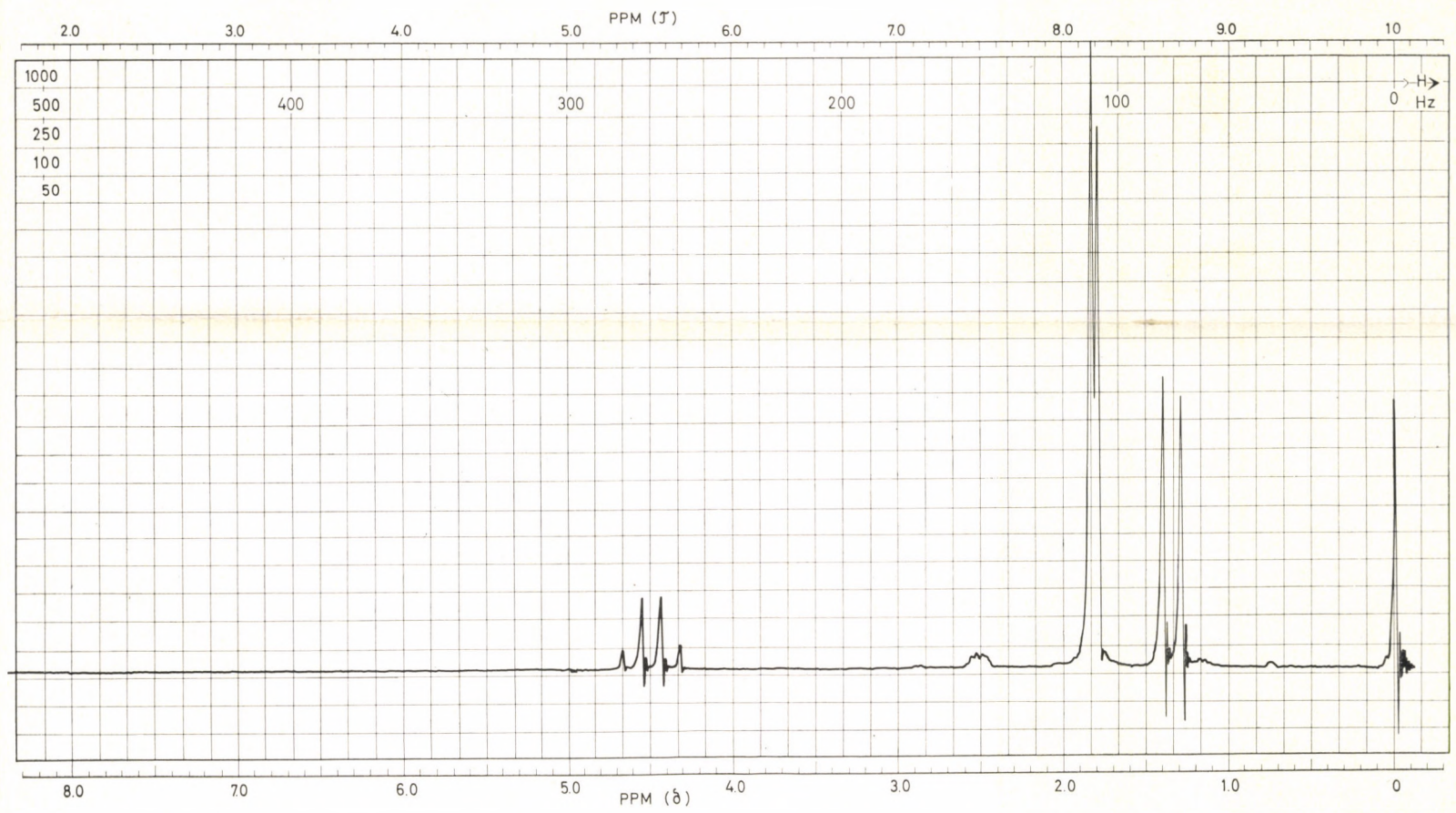

Spectrum 7. PMR spectrum of **II** in DMSO-d_6

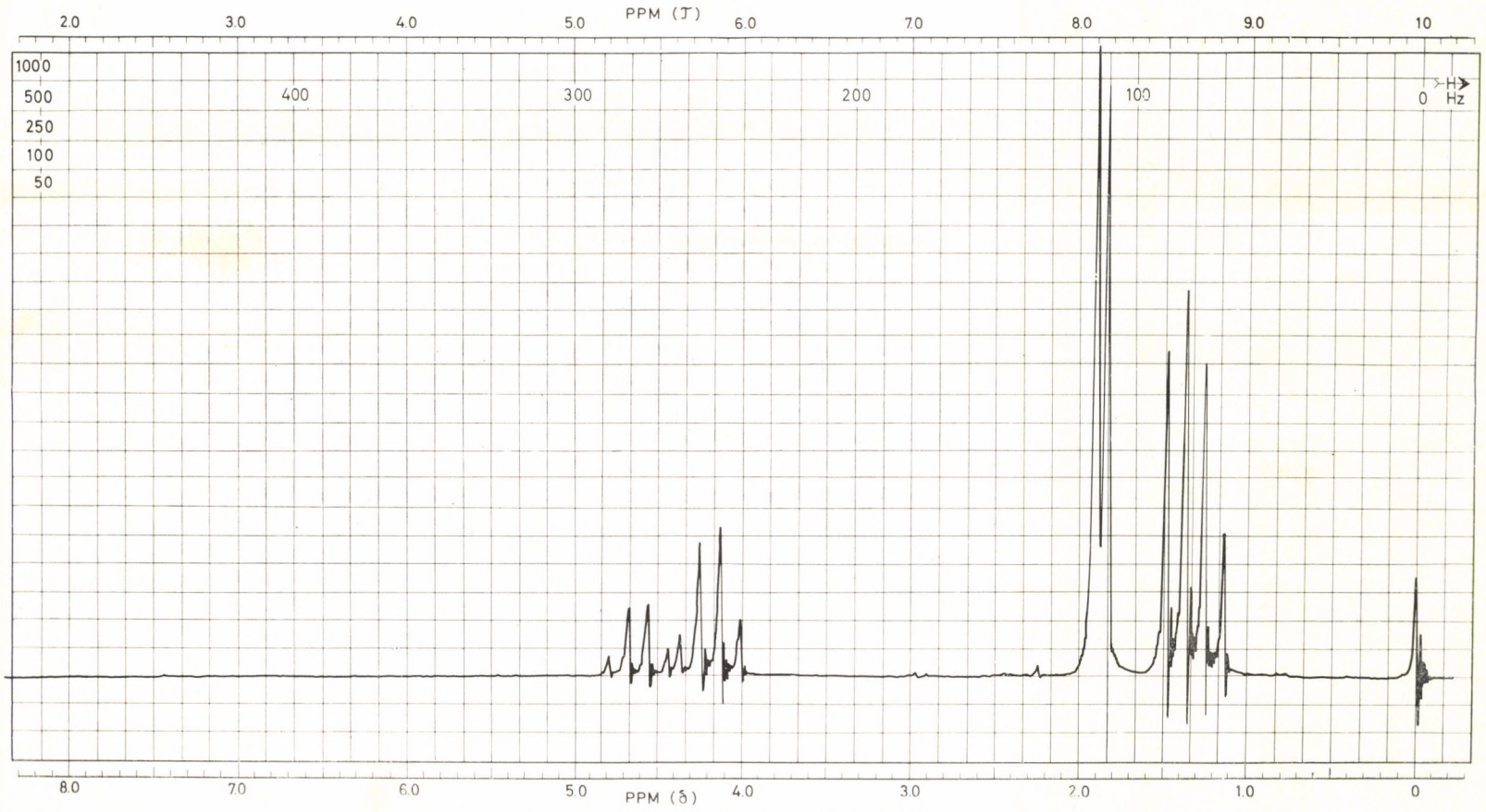

Spectrum 8. PMR spectrum of **III** in $CDCl_3$

Table III

PMR data of compounds **I**, **II**, **III** *and alanine (chemical shifts are given in ppm units, $\delta TMS = 0$ ppm)*

Spectrum No.	Compound	Solvent	δCH_3			δCH_2 Quartet* (ethyl) 2H	δCH Quartet* 1H
			Triplet* (ethyl) 3H	Doublet* 3H	Singlet (i-Pr) 2×3H		
5	I(D)=I(DL)	D_2O	—	1.42	—	—	4.48
		DMSO-d_6	—	1.20	—	—	4.07
—	I · HCl	DMSO-d_6	—	1.42	—	—	4.77
—	Alanine	D_2O	—	1.45	—	—	3.72
7	II	DMSO-d_6	—	1.35	1.80 1.83	—	4.50
8	III	$CDCl_3$	1.25	1.43	1.85 1.90	4.21	4.62

* $J = 7$ Hz

experimental data) by the anisotropic neighbouring group effect arising from the ammonium ion which becomes more pronounced in the vicinity of methyl protons because of the oxygen bridge (the $—N^+H_3$ ion can get nearer to the methyl protons).

When isolation of the α-aminooxypropionic acid (**I**) was first attempted by treatment with acetone, the IR spectrum of the product (Spectrum 6) indicated that it could not have the expected structure. Bands of ammonium and carboxylate ions characteristic of the zwitterionic structure did not appear, but absorptions of vibrations of free acids were identified in the spectrum: νOH (3500—2300 cm^{-1}), νC=O (1740 cm^{-1}), βOH (1450 cm^{-1}), νC—O (1205 cm^{-1}) and γOH (920 cm^{-1}). These bands and the band at 1640 cm^{-1} that can only arise from a double bond indicated that compound **I** was actually obtained in the form of an isopropylidene derivative **II**. This was proved by PMR investigation. This spectrum (Spectrum 7) had two singlets corresponding to the total number of six protons; in addition to these, the methyl doublet and methine quartet could only be detected. Thus, structure of **II** was accepted which was later supported by comparison with the physical data of an authentic sample.

In order to explain the appearance of two lines of the methyl signal of the isopropylidene group, the following possibilities were taken into consideration.

(*1*) Most probably, the two methyl groups are anisochronous because of the diastereotopy due to the presence of a centre of asymmetry. In this case,

Acta Chim. (Budapest) 83, 1974

Table IV

PMR data[a] of $R-CH\begin{matrix}COOH\\ONH_2\end{matrix}$ *type α-aminooxycarboxylic acids (in DMSO-d_6 solution), in ppm (δTMS = 0 ppm)*

Compound[b] R		δCH₃	δCCH₂	δXCH₂ (X = O, N, S, Ar)	δCCH	δOCH	δArH
—H	A	—	—	4.43, *s*	—	—	—
—H	B	—	—	4.08, *s*	—	—	—
$-CH_2-CH_3$	A	0.95, *t* (7 Hz)	1.80, *m*	—	—	4.70, *t* (5.5 Hz)	—
$-CH_2-CH_3$	B	0.90, *t* (6.5 Hz)	1.65, ~*qi*	—	—	3.95, *t* (6 Hz)	—
$-(CH_2)_2-CH_3$	A	0.90, *t* (7 Hz)	60—115 Hz *m* (4H)	—	—	4.75, *t* (5.5 Hz)	—
$-CH(CH_3)_2$	A	0.93, *d* (7 Hz) 1.03, *d* (7 Hz)	—	—	~2.3, *m*	4.55, *d* (5.5 Hz)	—
$-CH(CH_3)_2$	B	0.90, *d* (7 Hz) 0.95, *d* (7 Hz)	—	—	~2.0, *m*	3.95, *d* (6 Hz)	—
$-(CH_2)_3-CH_3$	A	0.90, *t* (7 Hz)	60—120 Hz *m* (6H)	—	—	4.70, *t* (5.5 Hz)	—
$-(CH_2)_3-CH_3$	B	0.90, *t* (7 Hz)	70—120 Hz *m* (6H)	—	—	4.00, *t* (6 Hz)	—
$-CH_2-CH(CH_3)_2$	A	0.97, *d* (7 Hz) (6H)	1.67, 2×*d* (5 and 7 Hz)	—	~2.1, *m*[c]	4.67, *t* (5.5 Hz)	—
$-CH_2-CH(CH_3)_2$	B	0.90, *d* (6 Hz)	~1.5, 2×*d* (5 and 6 Hz)	—	~1.5, *m*[c]	4.03, *t* (6 Hz)	—

$-(CH_2)_4-NH_2$	A	—	~2.8, *m* (6H)	~2.6, *t*	—	4.75, *t* (5.5 Hz)	—
$-(CH_2)_2SCH_3$	A	2.10, *s*	~2.10, *t*[d]	~2.6, *t*[e]	—	4.80, *t* (6 Hz)	—
$-(CH_2)_2SCH_3$	B	2.10, *s*	~1,95, *m*[f]	~2.6, *m*[f]	—	4.15, *t* (6 Hz)	—
$-CH_2Ph$	A	—	—	3.15, *m*[g]	—	5.05, $2\times d$[h] (5 and 7 Hz[i])	7.30, *s*
$-CH_2Ph$	B	—	—	3.18[g] 3.35[g] ($J_{AB}=15$ Hz)		5.03, $2\times d$[h] (5 and 7 Hz[i])	7.40, *s*

[a] The given spectral data of the optically active forms and racemates are identical in all cases investigated
[b] A: Hydrochloride, B: Base
[c] Overlapped by the δCH_2 signal
[d] Overlapped by the δSCH_3 signal
[e] Overlapped by absorption of the solvent
[f] A_2B_2 multiplet
[g] AB part of the ABX multiplet
[h] X part of the ABX multiplet
[i] Coupling constant J_{AX} and J_{BX}

the distance of the lines should be temperature-independent. However, the diastereotopic relation of methyl groups does not necessarily cause a splitting, as frequently an incidental isochrony occurs, first of all when the isopropylidene group is not directly attached to the asymmetric carbon atom, as in the case of **II**.

(*2*) In a zwitterionic structure, a splitting may be caused in the $N^+H{=}C\begin{smallmatrix}CH_3\\CH_3\end{smallmatrix}$ group by long-range coupling (the 2 Hz distance of the lines would be in good agreement with this phenomenon). However, it is unlikely that compound **II** with no zwitterionic form in the solid phase, might exist in this form in DMSO-d_6 solution.

(*3*) It is possible that a six-membered cycle is formed with hydrogen bond between the nitrogen atom and the hydroxyl group, leading to a different environment of the two methyl groups, owing to the sterically fixed structure.

(*4*) An anisochrony may also result from the geometrical (*syn–anti*) isomerism of the C=N double bond.

In order to clarify this problem, the PMR spectrum of the ethyl ester of **II** (**III**) was also investigated (Spectrum 8).

As in this spectrum (*cf.* Table III), the isopropylidene group gives invariably two lines, interpretations according to (*2*) and (*3*) should be rejected. For excluding the existence of inverse isomers according to (*4*), a temperature-dependent PMR examination was carried out. Since the distance of the two lines remained unchanged between 20 and 160°C, the separation of the line can be due only to the diastereotopic character of the methyl groups.

Experimental

Synthesis of the compounds mentioned in this paper has been reported elsewhere [8]. IR spectra were taken with a Perkin-Elmer 457 spectrometer in KBr pellets. NMR spectra were recorded at room temperature by a Varian A-60D device using tetramethylsilane as internal standard.

*

The authors are grateful to Dr. Mrs. Cs. MÉHESFALVI, Mr. A. FÜRJES, Mrs. B. CSÁKVÁRI and Miss V. WINDBRECHTINGER for the useful technical assistance.

REFERENCES

[1] WERNER, A.: Ber. **26,** 1567 (1893); *ibid.* **27,** 3350 (1894)
[2] FAVOUR, C. B.: J. Bact. **55,** 1 (1948)
[3] MCHALE, D., GREEN, J., MAMALIS, P.: J. Chem. Soc. **1960,** 225
[4] TESTA, E., NICOLAUS, B. J. R., MARIANI, L., PAGANI, G.: Helv. Chim. Acta **46,** 766 (1963)
[5] KISFALUDY, L., DANCSI, L., PATTHY, A., FEKETE, GY., SZABÓ, I.: Experientia **27,** 1055 (1971)
[6] KISFALUDY, L., DANCSI, L., PATTHY, A., FEKETE, GY., SZABÓ, I.: Hung. Pats. 160.181 (1971. IX. 29); 160.182 (1971. XII. 23); 162.469 (1972. XII. 29.)

[7] KISFALUDY, L., DANCSI, L., PATTHY, A., FEKETE, GY., SZABÓ, I.: Hung. Pat. Appls. RI-528; RI-529; RI-530
[8] KISFALUDY, L., DANCSI, L., PATTHY, A., KLUMPP, E.: Hung. Pat. Appls. RI-440; RI-525; RI-526
[9] KISFALUDY, L., LÖW, M., DANCSI, L., PATTHY, A., NYÉKI, O., SÁRKÖZI, M.: In "Peptides 1972" Proc. 12th Eur. Peptide Symp. 1972 (H. HANSON and H. D. JAKUBKE, eds.) North-Holland Publ. Comp., Amsterdam 1973. p. 409.
[10] RICHARDSON, A.: J. Med. Chem. **7**, 824 (1964)
[11] UNDHEIM, K., BAMBERG, P., SJÖBERG, B.: Acta Chem. Scand. **19**, 317 (1965)
[12] HOLLY, S., SOHÁR, P.: Infravörös Spektroszkópia. (In Hungarian) Műszaki Kiadó, Budapest 1968
[13] SOHÁR, P., HOLLY, S., VARSÁNYI, GY.: Kémiai Közlemények (In hungarian) **31**, 197 (1969)
[14] SOHÁR, P.: Mágneses Magrezonancia Spektroszkópia, (In Hungarian) I—II. Tankönyvkiadó, Budapest 1970

Pál SOHÁR; 1325. Újpest, 1 P.O.B. 82

Lajos KISFALUDI
Lajos DANCSI
} 1103 Budapest, Gyömrői út 19—21., Hungary.

Acta Chimica Academiae Scientiarum Hungaricae, Tomus 83 (3—4), pp. 405—407 (1974)

INVISIBLE EXCHANGE REACTION OF AROMATIC SCHIFF BASES*

(PRELIMINARY COMMUNICATION)

I. PINTÉR, G. TÓTH** and A. MESSMER

(Central Research Institute for Chemistry of the Hungarian Academy of Sciences, Budapest, and
***Research Institute for Pharmaceutical Chemistry, Budapest.*
Humboldt Postdoctoral Fellow at the Ruhr-University, Bochum, GFR, 1973—74)

Received September 18, 1974.

It has been proved that two identical molecules of a Schiff base can undergo an exchange reaction. Unlabeled and labeled benzylidene-*p*-anisidines investigated by NMR and MS techniques resulted in an equilibrium with a constant of $K = 1$. Some conclusions have been drawn on the mechanism of the azo coupling of aromatic Schiff bases.

In our previous paper [1] the exchange reaction of aromatic Schiff bases has been reported to (i) follow a second order rate law, (ii) lead to an equilibrium in all cases and (iii) to be proton catalyzed as shown by kinetic measurements.

According to the proposed mechanism, the initial step of exchange is the interaction of a neutral and a protonated Schiff base molecule, followed by the reversible reactions of the protonated dimeric intermediate thus formed.

The azo coupling of Schiff bases reported earlier [2, 3] takes place probably via an intermediate with the same dimeric structure. Since in these cases the reaction mixture contains only a single Schiff base, it seems necessary to demonstrate that two identical molecules of a Schiff base can similarly undergo an exchange reaction.

This chemically 'invisible' reaction was studied using doubly labeled benzylidene-*p*-anisidine as model compound. For this purpose benzylidene-*p*-anisidine-d (**I**) was prepared, in the NMR spectrum (1*a*) of which no azomethine proton could be detected as a consequence of labeling with deuterium. On the other hand, benzylidene-*p*-anisidine-^{15}N (**II**) gives spectrum 1*b* in which the NMR signal of the azomethine proton ($\delta = 8.30$ ppm) is split into a doublet as a result of interaction with the neighbouring ^{15}N atom ($J_{^{15}N=CH} = 3.9$ Hz). The coupling constant is in accordance with those of other ^{15}N-labeled Schiff bases [4]. The isotopic purity of both compounds was higher than 98% as shown by the mass spectra.

The rate of exchange can be determined from the variation of the intensity of the azomethine proton signal. The intensity of the starting doublet

* Presented in part at the IInd IUPAC Conference on Physical Organic Chemistry, Noordwijkerhout, The Netherlands, April 29—May 2, 1974.

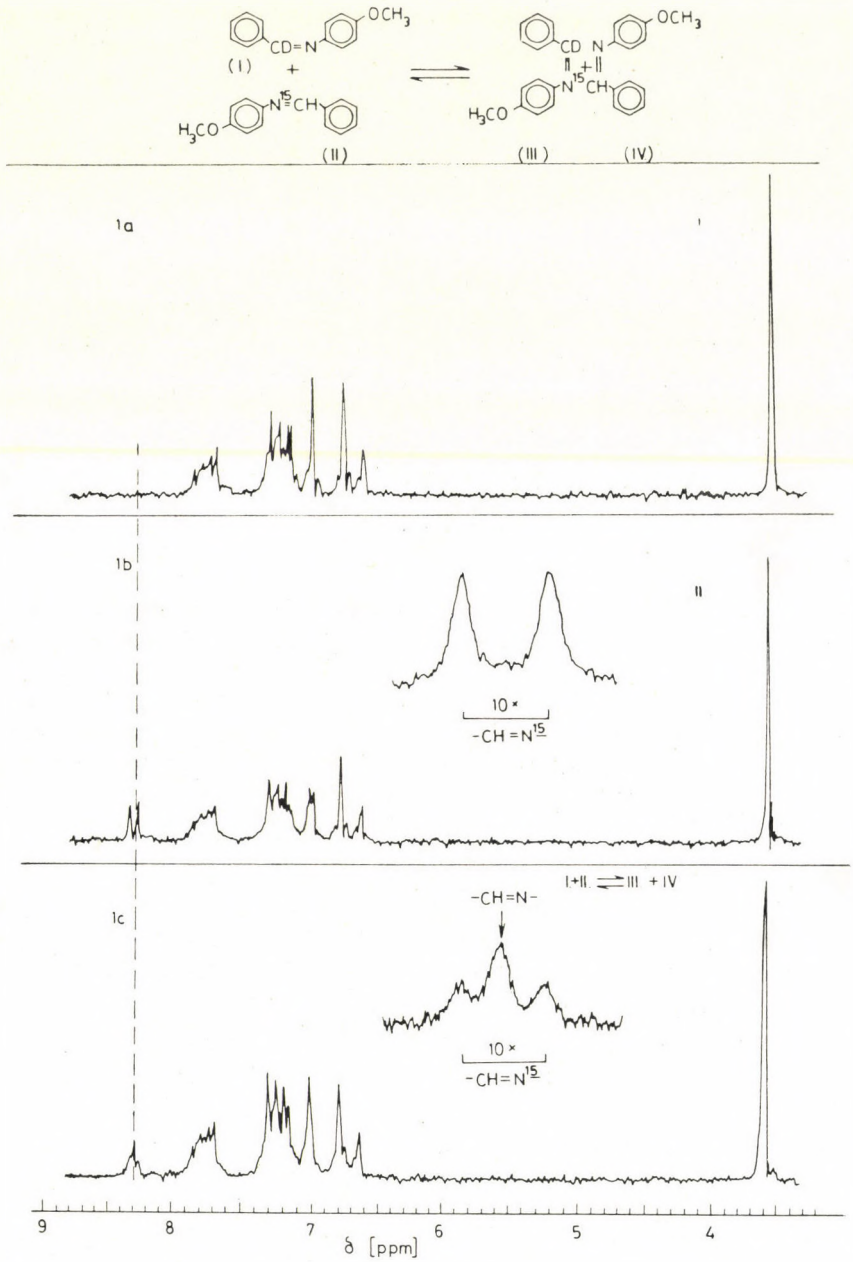
(I) +
(II)
(III)
(IV)
1a
1b
10 ×
-CH=N15
II
I+II ⇌ III + IV
1c
-CH=N-
10 ×
-CH=N15
9
8
7
6
5
4
δ [ppm]

Fig. 1

decreases during the reaction while the singlet of the unlabeled benzylidene-*p*-anisidine formed appears in the center of the doublet (Spectrum 1*c*). At equilibrium a virtual triplet is formed with the intensity ratio of 1 : 2 : 1, corresponding to an equilibrium constant of $K = 1$.

Kinetic measurements show that the reaction is of second order, the order of the rate constants being the same as for the exchange reaction of two different Schiff bases:

$k = 5.97 \times 10^{-4}$ l/mol sec (in tetrachloroethylene at 36°C)
$k = 3.50 \times 10^{-3}$ l/mol sec (in nitrobenzene at 36°C).

The reaction is proton catalyzed: in the presence of 0.01 mol trifluoroacetic acid the equilibrium is set up very rapidly and the NMR spectrum 1*c* can be immediately observed.

In the mass spectrum of the equilibrium mixture three molecular ions can be distinguished:

$M_1 = 213$, benzylidene-*p*-anisidine-^{15}N-d (**III**),
$M_2 = 212$, benzylidene-*p*-anisidine-^{15}N (**II**), and
benzylidene-*p*-anisidine-d (**I**),
$M_3 = 211$, benzylidene-*p*-anisidine (**IV**).

The intensity ratio of the three peaks is 1 : 2 : 1, in agreement with the NMR spectra.

The above results prove that two identical molecules of a Schiff base react in the same way as those of two different azomethines. This fact supports the suggestion that the azo coupling of aromatic Schiff bases may take place through a similar dimeric intermediate.

*

The authors are grateful to Dr. J. TAMÁS for the mass spectra, Dr. J. HEMELA for computing the kinetic data and Dr. J. WOLFORD for preparing the labeled starting materials.

REFERENCES

[1] TÓTH, G., PINTÉR, I., MESSMER, A.: Tetrahedron Letters, 735 (1974)
[2] MESSMER, A., SZIMÁN, O.: Angew. Chem., *78*, 237 (1967)
[3] MESSMER, A., PINTÉR, I., SZIMÁN, O.: IUPAC Symposium on Cycloaddition Reactions, München, 1970
[4] BINSCH, G., LAMBERT, J. B., ROBERTS, B. W., ROBERTS, J. D.: J. Amer. Chem. Soc., *86*, 5564 (1964)

István PINTÉR; 1025 Pusztaszeri u. 57—69
Gábor TÓTH; 1045 Szabadságharcosok u. 49
András MESSMER; 1025 Pusztaszeri u. 57—69, Hungary.

Acta Chimica Academiae Scientiarum Hungaricae, Tomus 83 (3—4), pp. 409—422 (1974)

STUDIES ON CHARATCHOK SYRIAN CRUDE OIL

CHEMICAL EVALUATION OF THE DISTILLATE FRACTIONS UP TO 300°C AND HYDROTREATING OF THE KEROSINE AND GAS OIL FRACTIONS

SAMIR A. KHATTAB,* MOHAMED F. KASSOUMEH,** FATHY S. ABO-LEMON** and MOHAMED I. ROUSHDY**

*(*Chemistry Department, Faculty of Science, University of Cairo*
***National Research Centre, Cairo, Egypt)*

Received July 30, 1973; in revised form January 20, 1974

The physicochemical characteristics of the Charatchok crude oil and its light and middle fractions obtained by technical distillation gasoline, kerosene and gas oil are reported.

Hydrotreating of the kerosine and gas oil fractions was carried out with the purpose of studying the possibility of their upgrading.

The crude oil was distilled under atmospheric pressure into five cuts. Further distillation under reduced pressure (40 torr) afforded two other fractions. The hydrocarbon type and the structural group analyses were carried out for the narrow cuts as well as for the fractions of technical distillation.

Introduction

The chemical evaluation of crude oils is of supreme importance from the point of view the refining and petrochemical industries. No systematic studies concerning the chemical nature and evaluation of Syrian crude oils have been reported. The first published data [1] were on Swidia Syrian crude oil. The Charatchok oil field is situated in the northeastern region of the Syrian Arab Republic, near the Swidia oil field.

The technique of hydrotreating has been widely adopted to improve the quality of the distillate fractions by reducing the sulfur, nitrogen and unsaturated hydrocarbon contents, as well as the carbon residue. A large number of catalysts have been developed for hydrogenating petroleum fractions [2, 3]. Nickel and platinum catalysts as well as cobalt molybdate [4] and tungsten sulfide [5] have been applied for this purpose. The reaction conditions, temperature, pressure and reaction time must be controlled in the hydrotreating of different feed stocks [6, 7].

The study of the residual fractions (above 300°C) of this crude will be reported in a future communication.

Experimental

The crude oil sample under investigation was kindly supplied by the Ministry of Petroleum of the Syrian Arab Republic.

1. Physicochemical characteristics of the crude oil

(A) *Physical characteristics*

The general characteristics of the crude oil and its products have been determined according to IP or ASTM standard methods unless otherwise stated.

(B) *Component analysis*

The scheme applied to the crude oil fractionation and component analysis is shown in Fig. 1.

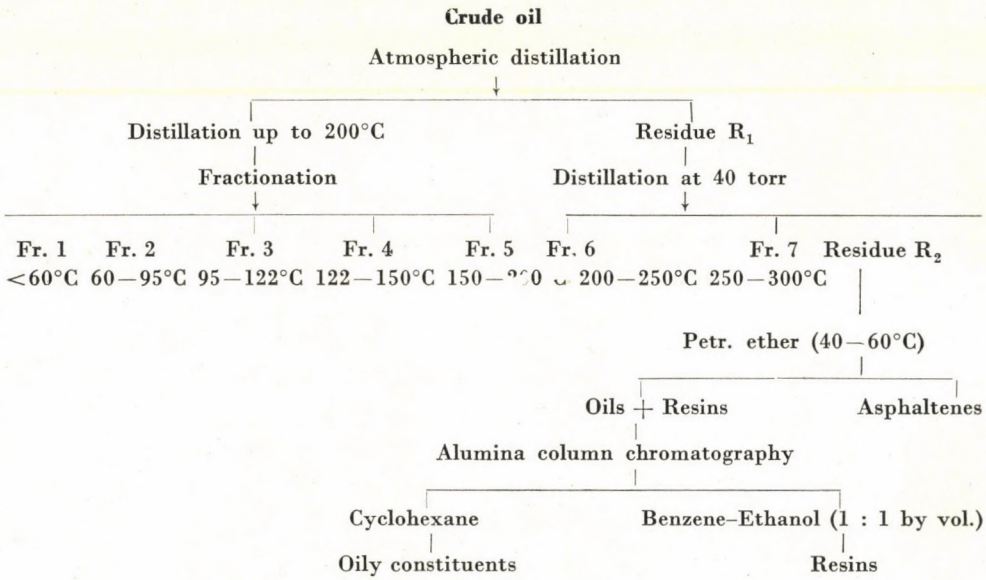

Fig. 1. Fractionation of Charatchok crude oil

(C) *Determination of vanadium and nickel in the crude oil, resins and asphaltenes*

Vanadium and nickel have been determined using the flame spectrophotometric method [8]. According to this method, the ash obtained from the crude oil was dissolved in sulfuric acid. Excess of the acid was evaporated and the sulfated ash was dissolved in distilled water. Measurements were carried out on a flame spectrophotometer (Unicam Model SP 900) at wave lengths of 352.5 and 550 nm for nickel and vanadium, respectively. The concentrations were estimated from the calibration curves of standard solutions against the galvanometer readings of the flame spectrophotometer.

2. Fractions obtained by technical distillation

The crude oil was distilled to obtain gasoline, kerosene, gas oil, a waxy distillate and residue (Table I).

Table I

Fractions obtained by technical distillation

Fraction	Cutting temp., °C (under 760 torr)	Pressure, torr (during distillation)
Gasoline	32—150	760
Kerosene	150—250	40
Gas oil	250—350	20
Waxy distillate	350—500	2
Residue	—	—

3. Hydrocarbon type analysis of the distillate fractions

The following methods have been adopted.

(*a*) Volumetric method by Fluorescent Indicator Adsorption (F.I.A), IP[156].

(*b*) Gravimetric methods:

1. Aniline point method for the determination of aromatics [9].
2. Determination of normal paraffins in fractions up to 200°C by gas chromatography [10]. An F & M Gas Chromatograph Model 500 was used with Katharometer as detector.
3. Urea adduct method [11] for the determination of normal paraffins in the fractions of boiling range 200—250° and 250—300°C.
4. Determination of naphthenes. Each fraction was dearomatized by sulfuric acid (98%) and the aniline point (t) of the saturates so obtained was determined. The content of naphthenes was calculated as follows:

$$\text{Naphthenes } (wt\ \%) = \frac{K}{d}(t_1 - t)$$

wher K is constant, d and t_1 are the density and aniline point respectively, of the pure naphthenes, obtained from tables cited in Ref. [9].

4. Investigation of bicyclic aromatics in fractions of boiling range 200—285 °C

Bicyclic aromatics were determined by cutting the fraction of boiling range 200—285 °C into four fractions and measuring the ultraviolet absorption at different wavelengths, using a Beckman Model DU spectrophotometer [12, 13].

Before carrying out the measurement the fractions were desulfurized with mercuric nitrate to avoid any interference of sulfur compounds with the spectral determination [13]. The investigation was then carried out as follows.

Fraction *a*, of boiling range 200—248°C was used for the determination of naphthalene, 1-methylnaphthalene and 2-methylnaphthalene by measuring the absorbance at the wavelengths 311, 314 and 319 nm.

Fraction *b*, 248—265°C, was applied for the determination of the C_{12}-naphthalenes by measuring the absorbance at the wavelengths 280 and 324 nm.

Fraction *c*, 265—275°C, served for the determination of C_{12}- and C_{13}-naphthalenes by measuring the absorbance at the wavelengths 280 and 324 nm.

Fraction *d*, 275—285°C, was used for the determination of C_{13}-naphthalenes by measuring the absorbance at 280 nm.

5. Structural group analysis

The structural group analysis of the middle distillate fractions of boiling range 200—300°C was carried out according to the n.d.M. method [14] using the Hasting correction.

6. Hydrotreating of Charatchok kerosine and gas oil distillate fractions

(A) *Catalyst WNiS/al*

This was provided by Badische Anilin und Soda Fabrik (Catalyst No. 8376): pellets (3 mm), composed of 25% tungsten sulfide and 3% nickel sulfide supported on activated alumina.

(B) *Hydrogenation technique*

A rocking batch autoclave (Andreas Hofer) of two liters capacity with electric heating device was used throughout this work. The weight of the feed as well as the weight of the catalyst were fixed. In each experiment, the feed (200 g) and a fresh sample of the catalyst (20 g) were introduced into the autoclave. It was purged once with nitrogen, then twice with low pressure hydrogen before filling with hydrogen to the required initial hydrogen pressure. By the "initial hydrogen pressure", it is meant the pressure inside the autoclave at room temperature before starting the hydrogenation experiment.

After checking for any leakage, heating was started to attain the desired working temperature which was automatically controlled. At required reaction temperature rocking was started and heating was continued during the desired reaction period, then heating and rocking were stopped. The autoclave was then left overnight to cool to room temperature.

In this work, the reported reaction period was considered to begin when the required working temperature was reached, lasting until heating was stopped.

The general characteristics of the hydrogenates were determined according to IP standard methods.

Results and discussion

1. General characteristics of Charatchok crude oil

The general characteristics of Charatchok crude oil as compared with Swidia crude oil are given in Table II. The data show that this crude oil has a higher sulfur content, carbon residues and asphaltanes than Swidia crude oil.

Table II

General characteristics of Charatchok and Swidia crude oils

Characteristics	Crude		Remarks
	Charatchok	Swidia [1]	
Sp. gr. 15/4 °C	0.9370	0.9010	IP 160
A.P.I. gravity	19.51	25.55	
Sulfur content, wt.-%	4.4	3.9	IP 63
Water content	Nil	Nil	IP 74
Engler viscosity at 37°C, sec/sec	15.09	8.40	
Pour-point, °C	−24.0	−10.0	IP 15
Carbon residue, Conradson wt.-%	14.9	11.55	IP 13
Ash content, wt.-%	0.0189	0.0178	IP 4
Wax content, wt.-%	2.10	3.38	Holds method
Asphaltanes, wt.-%	17.1	14.3	IP 6
Engler distillation I.B.P., °C	55.0	50.0	
Temp., °C %-Vol. Recovered, ml			
75	3.0	3.0	
100	8.0	7.0	
125	11.0	12.0	
150	16.0	18.0	
175	19.0	22.0	
200	23.0	26.0	
225	26.0	30.0	
250	30.0	34.0	
275	34.0	38.0	
300	41.0	50.0	
Residue	58.0	49.0	
Loss	1.0	1.0	
Total	100.0	100.0	

On the other hand, it is of a much better quality with regard to its pour-point; this is due to its lower max content. A higher percentage of distillate fractions up to 300°C is noticed in case of Swidia crude oil.

Generally, the Swidia crude oil can be considered as being of better quality.

(A) *Component analysis*

Component analysis was carried out using alumina column chromatography for the separation of the oily constituents from the resin components. The results obtained are given in Table III. It is seen that asphaltenes are present in a considerable amount (17.1%). The amounts of resinous components are higher than the asphaltenes, but lower than the oily constituents.

Table III

Component analysis of Charatchok crude oil

Component	wt.-% in crude oil
Distillate up to 300°C	29.20
Oil constituents	29.57
Resins	23.12
Asphaltenes	17.11
Gases and losses (by difference)	1.00

The amount of distillate up to 300°C is markedly lower than that obtained by the Engler distillation, due to the effect of fractionation.

(B) *Trace elements*

The vanadium and nickel contents in the crude oil and their fractional distribution in the crude oil components are shown in Table IV.

Table IV

Vanadium and nickel distribution in the crude oil, resins and asphaltenes [8]

	Crude oil	Resins	Asphaltenes
Ash content, wt.-%	0.0189	0.0	0.1167
Vanadium, ppm	46.0	0.0	268.0
Nickel, ppm	22.0	0.0	127.0
V/Ni ratio	2.11	—	2.11

It is of interest to notice the absence of both vanadium and nickel in the resinous components. Asphaltic components contain all the vanadium and nickel present in the crude.

(2) Characterization of the light and middle fractions obtained by technical distillation

The sample of Charatchok crude oil was fractionated into five cuts; gasoline, kerosene, gas oil, waxy distillate, and a residue. The boiling ranges of these fractions were selected taking into consideration the production of the highest possible yield of middle distillates (kerosene and gas oil), with the least possible content of sulfur compounds. The physical characteristics of gasoline, kerosene and gas oil are shown in Table V.

Table V

Physical characteristics of the light and middle fractions obtained by technical distillation

Characteristics	Fraction		
	Gasoline	Kerosene	Gas oil
Cutting temperature, °C	—150	—250	—350
Wt.-% on crude	12.8	10.2	13.0
Refractive index at 20°C	1.4096	1.4532	1.4886
Density at 20°C	0.7151	0.8079	0.8739
Mean molecular weight	103	187	251
Sulfur content, wt.-%	0.15	0.7	2.3
Aromatics content, vol.-%	2.4	26.2	40.2
Olefins content, vol.-%	0.3	0.7	1.2
Saturates content, vol.-%	97.3	73.1	58.6
Normal paraffins, wt.-%	10.6	7.3	7.4
Aniline pt., °C	61.4	57.6	61.2
Diesel index	—	—	42.28
Cetane number	—	—	46.0
Pour-point, °C	—	—	— 10.0
Freezing point, °C	—	— 47	—
Smoke point, mm.	—	20	—
ASTM distillation		Temp., °C	
Initial boiling point	55	150	246
%-Vol. recovered, ml			
10	76	171	262
20	88	185	274
30	95	192	280
40	104	199	286
50	113	204	293
60	122	212	304
70	132	223	314
80	145	235	326
90	158	251	344
Final boiling point	176	268	364

The aromatic, olefinic and sulfur contents increase from gasoline to kerosene to gas oil fractions, whereas the saturates content decreases in the same direction. The small amounts of olefins present may be due to some cracking during fractionation.

(A) *Gasoline*

The gasoline fraction contains a considerable amount of sulfur (0.15% by *wt.*). It is very poor in aromatics and normal paraffins. The major part of the fraction is thus composed of cycloparaffins and isoparaffins. It is expected therefore that this fraction constitutes a somewhat high grade motor gasoline, which could be further upgraded through a reforming process.

(B) *Kerosene*

The characteristics of the kerosene fraction are a high sulfur content and freezing point. The smoke point, being 20 mm, is in accord with specifications for illuminating purposes. However, in order to obtain a refined kerosene meeting jet fuel specifications, hydrotreating using catalysts with high hydrosulfurization and isomerization activities would be advantageous.

(C) *Gas oil*

The gas oil fraction is rich in aromatics and sulfur contents. On the other hand, the paraffinic content is low as reflected by its low pour-point. The aromatics content is 40.2% by vol. These aromatics can be of interest to the petrochemical industry. Solvent extraction and/or desulfurization of this fraction through hydrotreating would also be useful.

The structural group analysis (by the n.d.M. method) of the fractions (obtained by technical distillation) is given in Table VI.

Table VI

Structural group analysis of the kerosene and gas oil fractions (by n.d.M. method)

Characteristics	Fraction	
	Kerosene	Gas oil
% C_p	72.6	60.7
% C_A	11.8	19.4
% C_N	15.6	19.9
% C_R	27.4	39.3
R_A	0.27	0.60
R_N	0.30	0.60
R_T	0.57	1.20

The Hasting correction was used

It is noticed that the $\%C_A$ increases with the increase in boiling range. There is also an increase in the mean number of aromatic and naphthenic rings per molecule, going from kerosene to the gas oil fraction.

(3) Upgrading of Charatchok kerosene and gas oil distillate fractions through hydrotreating

The hydrotreating conditions, reaction temperature, initial hydrogen pressure, reaction period, and the tungsten nickel sulfide (on alumina) catalyst were selected on the basis of previous practical conditions [15]. The results of this investigation are cited in Table VII.

Table VII

Hydrotreating of Charatchok kerosene and gas oil distillate fractions

Conditions	Kerosene		Gas oil	
Reaction temp., °C	350		400	
Initial hydrogen pressure, atm	80		80	
Reaction period, hr.	4		4	
Catalyst	WNiS/alumina		WNiS/alumina	
Characteristics	Feed	Hydrogenate	Feed	Hydrogenate
Refractive index at 20°C	1.4532	1.4505	1.4886	1.4671
Density at 20°C	0.8079	0.8039	0.8739	0.8379
Mean molecular weight	187	191	251	212
Sulfur content, wt.-%	0.7	0.0	2.3	0.1
Sulfur removed, wt.-%, of total sulfur	—	100	—	95.6
Aromatics content, vol.-%	26.2	21.4	40.2	34.5
% aromatics reduced	—	18.3	—	14.2
Olefins content, vol.-%	0.7	0.2	1.2	0.3
Saturates content, vol.-%	73.1	78.4	58.6	65.2
Pour-point, °C	—	—	−10.0	−16.0
Freezing point, °C	−47	−37	—	—
Smoke point, mm	20	24	—	—
ASTM distillation		Temp., °C		
Initial boiling point	150	143	264	185
%-Vol. recovered, ml 10	171	176	262	235
20	185	184	274	242
30	192	198	280	254
40	199	208	286	263
50	204	218	293	273
60	212	223	304	281
70	227	236	314	290
80	235	250	326	303
90	251	269	344	319
Final boiling point	268	319	364	348

(A) *Kerosene*

From the kerosene fraction the sulfur compounds were completely removed. The saturation of aromatic hydrocarbons is evident. The content of aromatics is 21.4% in the hydrogenate, as compared with 26.2% in the feed.

This is evidenced also by the slight increase in molecular weight, and in the content of saturates. Refined kerosene with no sulfur and with a higher smoke point is obtained which will easily meet the domestic specifications.

It should be mentioned, however, that after hydrogenation of this fraction, some light fractions of the product have departed during degasification. Accordingly, the data of the hydrogenate should be considered as affected by this factor.

(B) *Gas oil*

The refractive index and density are decreased, which is due to a decrease in the aromatic content. The decrease in molecular weight is a result of the significant effect of hydrotreating. This is further shown by the initial and final boiling points of the product undergoing hydrogenation. Improvement in the pour-point is clearly noticed, being —16°C for the liquid hydrogenate, as compared with —10.0°C for the feed stock.

The sulfur removal nearly goes to completion, being 95.6%. Incomplete sulfur removal may be due to the presence of thiophenic sulfur compounds which are hardly desulfurized. The saturation of aromatic compounds is apparent as the percentage of aromatics reduced is 14.2%. However, the percentage of saturation of aromatics is greater in the kerosene fraction than in the gas oil fraction. This may be due to the complexity of the molecules in the higher fractions and to the larger amounts of the aromatic hydrocarbons present in the gas oil fraction. Incomplete saturation of the olefinic compounds is observed in both the kerosene and gas oil fractions.

(4) Detailed evaluation of the crude oil narrow cuts of boiling range up to 300°C

(A) *Physicochemical characteristics*

The physicochemical characteristics are shown in Fig. 2.

With increasing boiling range, there is an increase in the refractive index, density and a decrease in the aniline point. This indicates an increase in the aromatic content, which is justified by the hydrocarbon type analysis (Tables VIII and IX). An increase in the sulfur content is also observed.

The refractive index, the density and the aniline point of the saturated fractions increase with the increase in the boiling range.

(B) *Chemical composition*

The data of the gravimetric and volumetric hydrocarbon type analyses are given in Tables VIII and IX. A gradual increase in the contents of aromatic and naphthenic hydrocarbons with increasing boiling range is noticed. This

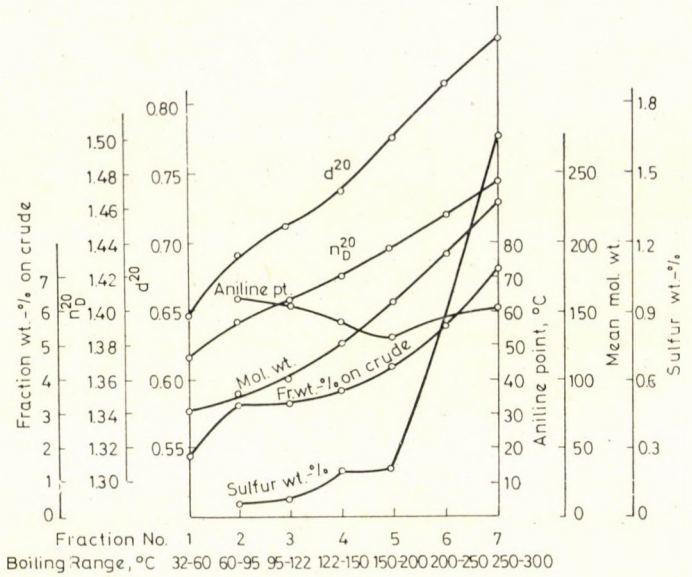

Fig. 2

Table VIII

Gravimetric hydrocarbon type analysis of distillate fractions up to 300°C

Hydrocarbon type wt.-%	Fraction No.					
	2	3	4	5	6	7
Aromatics, UOP method (1)	2.50	4.80	16.40	30.70	34.50	40.90
Aniline point method (2)	2.90	5.00	15.40	31.20	34.60	40.20
Average	2.70	4.90	15.90	31.00	34.60	40.60
Olefins; UOP method (1)	0.30	0.50	0.70	1.00	1.20	1.30
Naphthenes (2)	17.10	18.80	17.80	29.40	34.00	33.90
Normal paraffins (3 or 4)	11.20	9.50	11.70	21.30	6.10	7.30
Isoparaffins (by difference)	68.70	66.30	53.90	17.50	24.10	16.90
Isoparaffins/normal paraffins ratio	6.13	6.98	4.61	0.82	3.95	2.31

Methods used:
(1) UOP method [16]
(2) Manual Chimistului [9]
(3) Gas chromatography [10] (for fractions Nos 2—5)
(4) Urea adduct method [11] (for fractions Nos 6—7)

Table IX

Volumetric hydrocarbon type analysis of distillate fractions up to 300°C (F.I.A. method, IP[156])

Hydrocarbon, vol.-%	Fraction No.					
	2	3	4	5	6	7
Aromatics	0.9	1.4	7.0	22.1	29.6	31.3
Olefins	0.2	0.4	0.4	0.4	0.9	1.2
Saturates	98.9	98.2	92.6	77.5	69.5	67.5

increase is more pronounced in the case of aromatic hydrocarbons. At the same time, a marked decrease in the isoparaffins is observed. Aromatic hydrocarbons present in fractions Nos 2, 3 and 4 represent benzene, toluene and xylenes, respectively. It is apparent that these fractions are of a highly paraffinic nature. Fraction No. 4 can be considered a good source for the production of xylenes as it contains about 16% of these petrochemical raw materials. Fractions Nos 5, 6 and 7 are rich in aromatic hydrocarbons, therefore the paraffinic nature generally decreases with the increase in boiling range.

The ratio of iso- to normal paraffins decreases with the increase in boiling range, the decrease being noticeable in case of fraction No. 5. This is expected because of the decrease of isoparaffins with the increase in boiling range, this decrease being marked in fraction No. 5.

The integral chemical composition of the fractions of boiling range 60—200°C and 200—300°C is shown in Table X.

Table X

Integral chemical composition of light and middle distillates up to 300°C

Hydrocarbon, wt.-%	Fraction	
	Light distillate 60—200°C	Middle distillate 200—300°C
Aromatics	15.0	38.0
Olefins	0.7	1.3
Naphthenes	21.3	33.9
Normal paraffins	14.0	6.8
Isoparaffins	49.1	20.0

The light distillate of boiling range 60—200°C appears to be more aromatic than naphthenic in nature. The situation is reversed in the case of the middle fraction of boiling range 200—300°C.

(C) *Structural group analysis of the fractions of boiling range 200—250° and 250—300°C*

The analysis was carried out by applying the n.d.M. method and using the Hasting correction (Table XI). It is seen that the increase in $\%C_A$ in the fraction of boiling range 250—300°C has occurred mainly at the expense of the $\%C_p$. There is also an increase in the mean number of total rings per molecule from fraction No. 6 to fraction No. 7. This increase is due to an increase in the aromatic rings rather than naphthenic rings.

Table XI

Structural group analysis of fractions of boiling range 200—250 °C and 250—300°C by the n.d.M. method

Method characteristics	200—250°C	250—300°C
% C_p	68.48	63.79
% C_A	12.00	15.78
% C_N	19.52	20.43
% C_R	31.52	36.21
R_A	0.28	0.48
R_N	0.40	0.35
R_T	0.68	0.83

The Hasting correction was used

The results of carbon distribution coupled with those of the gravimetric type analysis (Table VIII) indicate that the increase in the aromatic hydrocarbons with increasing boiling range from 200—250°C to 250—300°C can be attributed to the presence of larger amounts of aromatics rather than to the increasing number of paraffinic side chains and/or the lengthening of the alkyl side chains attached to the aromatic ring structure. This observation is in agreement with the results obtained from the determination of naphthalene (Table XII), where the percentage of naphthalene hydrocarbons increases appreciably in the fractions above 248°C.

(D) *Distribution of alkylnaphthalenes in the fractions of boiling range 200—285 °C*

The production of naphthalene from petroleum through catalytic hydrodealkylation has gained recently great importance, since naphthalene is considered a valuable raw material in petrochemical industry.

Therefore, it was our objective in this work to evaluate the naphthalene hydrocarbon and its methyl derivatives up to the trimethyl isomers in the

Table XII

Quantitative determination of naphthalene [13] *in distillate fractions of boiling range 200—285°C*

Aromatics		Naphthalene	1-Methyl-naphthalene	2-Methyl-naphth.	Dimethyl-naphth.	Trimethyl-naphth.	Total diaromatics
Fractions boiling range, °C	wt.-%						
200—248	5.22	0.0	3.21	0.46	—	—	3.67
248—265	1.78	—	—	—	8.67	—	8.67
265—275	2.01	—	—	—	—	—	9.58
275—285	1.55	—	—	—	—	15	15

fractions of boiling range of 200—285°C. The results obtained (Table XII) indicate that the amounts of naphthalene hydrocarbons increase with the increase in boiling range. The fraction with boiling range 248—285°C of this crude, corresponding to that used for industrial production of naphthalene, is very suitable for this purpose.

*

Thanks are due to the National Research Centre, Giza, Cairo, for the facilities provided thoroghout this work and to the staff of the Petroleum Technology Laboratories for their help and co-operation.

REFERENCES

[1] Kelany, G. A., Riad, M. A., Mahmoud, B. H., Roushdy, M. I., Abdou, I. K.: 8th Arab Petroleum Congress, Paper No. 63 (C-3), Algiers, 1972
[2] Clough, H.: Ind. Eng. Chem. **49,** 673 (1957)
[3] Pier, M.: Proc. 4th World Petrol. Congr. Rome, Sec. III. 517 (1955)
[4] Langhout, W. C. *et al.*: J. Inst. Petroleum **41,** 263 (1955)
[5] Pier, M.: Z. Elektrochem. **53,** 291 (1949)
[6] Sachanen, A. N.: "Conversion of Petroleum", 2nd ed. Reinhold Publishing Corporation, New York 1948, p. 374
[7] Odasz, F. B., Sheffield, J. V.: Oil Gas J. **53** (No. 46), 203 (1955)
[8] Shalaby, A. A., Abdou, I. K., Faris, M. I.: Fifth Arab Petroleum Congress, Paper No. 53 (C-1), Cairo, 1965
[9] Mannual Chimistului, Volume II, Partea IV., Bucuresti 1948, p. 2117,
[10] Adlard, E. R., Whitham, B. T.: in "Gas Chromatography" (Eds Nathiol, Joseph and Narvin), 1962, p. 371
[11] (a) Hager, W.: Dissertation, Leipzig, 1954
(b) Schlief, H.: Chem. Techn. **6,** 456 (1954)
[12] Bálint, T.: Acta Chim. Acad. Sci. Hung. **15,** 139 (1958)
[13] Ayoub, S. M., Rushdy, M. I., Abdou, I. K.: Journal Chem. U.A.R. **10** (No. 2), 199 (1967)
[14] Van Nes, K., Van Westen, H. A.: "Aspects of the Constitution of Mineral Oils". Elsevier Publ. Co., New York 1951, p. 318
[15] Abo-Lemon, F. S.: Ph. D. Thesis, University of Cairo, 1970
[16] U.O.P. Laboratory Test Methods for Petroleum and its Products, Fourth Edition 2M, Oct. 1959, p. 305

Samir A. Khattab; Chemistry Department, Faculty of Science, University of Cairo

Mohamed F. Kassoumeh
Fathy S. Abo-Lemon
Mohamed I. Roushdy
National Research Centre, Cairo, Egypt.

RECENSIONES

K. DIMROTH: *Phosphorus–Carbon Double Bonds.* Topics in Current Chemistry, No. 38

Springer Verlag, Berlin—Heidelberg—New York 1973. pp. 147

In the excellent series "Topics in Current Chemistry", several interesting monographs have already been published. In this successful volume No. **38** three special types of compounds in organophosphorus chemistry are comprehensively treated, namely, the relatively less known phosphamethine-cyanines, and the trivalent (λ^3-) and pentavalent (λ^5-) phosphorins. Although research in this field was started hardly 10 years ago the theoretical and practical importance of these compounds is clearly indicated by the more than hundred publications dealing with them.

The first fundamental steps in the work for the synthesis and elucidation of the chemistry of the new organophosphorus compounds were made partly by the author of the present book, K. DIMROTH and his co-workers and partly by G. MÄRKL and his research team. It is not surprising thus that DIMROTH can handle the accumulated data so clearly and comprehensively.

In the structure of the book the well-known system is followed: synthesic methods, physical properties of the compounds, followed by the chemical characteristics in three successive chapters. The survey is supplemented by well-constructed tables comprising the data of the compounds prepared up to now. This system ensures a uniform approach and easy handling of the book.

The volume of the chapters is determined by the amount of information available rather than the importance of the individual compounds. Although the chapter dealing with phosphamethine-cyanines is the shortest, these compounds may still play a major role in the heterocyclic chemistry in the future, because their reactions are similar to, but the reactivities exceed those of methin and azamethin-cyanines.

The other two chapters in which the λ^3- and λ^5-phosphorin compounds are described are by no means less interesting. The two groups of compounds, which can be derived from one another and possess related properties from several points of view, represent a new type of heterocyclic systems, the phosphabenzenes, and can be considered as the phosphorus analogues of pyridine. The chemistry of λ^5-phosphorins, resonance-stabilized cyclic phosphinemethylenes, is particularly interesting. Although these phosphinemethylenes are quite unsuitable for the accomplishment of Wittig reactions, owing to the high degree of delocalization of the electrons, the reactivity of the phosphorus atom, together with the aromatic cyclic structure, provides possibilities for several other types of conversions which make the λ^5-phosphorins important not only from the theoretical but also from the synthetic point of view.

In accordance with the modern organic chemical concept applied in the book, these phosphorus compounds are not treated as isolated topics, but their properties are compared systematically with those of the analogous nitrogen compounds, including the correlation between experimental data and the results of quantum chemical calculations.

The introduction of fascinating experimental and unresolved theoretical problems arousing the interest of both practical and theoretical organic chemists is a very great merit of the book, which calls attention to the research of these compounds.

I. PINTÉR

K. CAMMAN: *Das Arbeiten mit ionenselektiven Elektroden*

Springer Verlag, Berlin—Heidelberg—New York 1973. 226 Seiten

Die ionenselektiven Elektroden zogen in den letzten 10 Jahren eine revolutionäre Entwicklung in der Potentiometrie nach sich. Mit Hilfe dieser Elektroden kann die Aktivität zahlreicher Ionen sowohl in wäßrigen, wie auch in nichtwäßrigen Lösungen unmittelbar ge-

messen werden. Es ist daher kein Zufall, daß in Verbindung mit ihrer Anwendung ein praktischer Bedarf für Bücher besteht, aus denen der Verwender jene wichtigsten Kenntnisse über die charakteristischen Eigenschaften der ionenselektiven Elektroden schöpfen kann, die deren Verwendbarkeit fördern bzw. einschränken. CAMMANs Buch ist diesem Ziel gewidmet. Im Buch wird Wert darauf gelegt, den Leser mit der Arbeitsweise der ionenselektiven Elektroden vertraut zu machen, um dadurch die Elektroden entsprechend anwenden zu können.

In einem Umfang von 226 Seiten ist das Buch auf 162 Literaturangaben aufgebaut. Im Rahmen der Grundlagen der Potentiometrie wird über 32 Seiten der wichtigste theoretische Hintergrund der ionenselektiven Elektroden behandelt.

Abschnitt 2 beschreibt über 20 Seiten das Messen des Elektrodenpotentials, wobei die Probleme der Bezugselektroden, das Diffusionspotential und die Herstellung der Bezugselektroden besprochen werden.

Der Verfasser beschäftigt sich über 56 Seiten mit den Einzelheiten der ionenselektiven Elektroden. Es werden die Eigenschaften der Glaselektroden, der Präzipitätelektroden sowie der flüssigen Ionenaustauscher-Elektroden diskutiert. Obzwar dieser Abschnitt eine sehr gute Orientation für Anfänger gibt, kann die Einteilung der Elektroden bei der Diskussion der wichtigsten Eigenheiten derselben theoretisch beanstandet werden. Diese Einteilung beruht nicht auf theoretischen Grundlagen. Dieser Abschnitt beschäftigt sich auch mit den Enzym-Elektroden und den Gasfühler-Elektroden. Schade daß diese sehr knapp im Buch behandelt werden, wo doch ihre Bedeutung, besonders die der Gasfühler-Elektroden in den letzten Jahren stark zunahm. Abschnitt 4 beschreibt über 17 Seiten die Messtechnik der ionenselektiven Elektroden. Der Abschnitt befaßt sich vor allem mit den Geräteproblemen der pX-Messung.

Abschnitt 5 beschreibt über 47 Seiten die bei der Anwendung von ionenselektiven Elektroden zu verwendenden Verfahren. Der Abschnitt umfaßt die Eichkurvenmethode, Titrierverfahren und verschiedene Konzentrations-Meßmethoden sowie deren Fehler. Dieser Abschnitt ist eine ausgezeichnete Hilfe für jeden sich mit praktischer Potentiometrie befassenden Fachmann bei der Wahl des richtigen Verfahrens in der Anwendung von ionenselektiven Elektroden.

Abschnitt 6 behandelt über 20 Seiten die Anwendung der ionenselektiven Elektroden auf verschiedenen wissenschaftlichen und technischen Gebieten. Es geht bereits aus der Kürze des Abschnittes hervor, daß hier keine konkreten Vorschriften zu erwarten sind, sondern es wird eher auf die durch die ionenselektiven Elektroden gebotenen Perspektiven hingewiesen. Dies wird durch einen Blick in die Zukunft über drei Seiten quasi zusammengefaßt und damit abgeschlossen, daß die weitere Verbreitung der Verwendung stark durch die Geschicklichkeit und Experimentierfreudigkeit des Verwenders dieser Elektroden entschieden wird.

Ein kurzer Anhang beschäftigt sich mit Problemen der Konzentration, Aktivität und dem Aktivitätskoeffizienten, sodann geben einige Tabellen über die Temperaturabhängigkeit einiger Bezugselektroden Aufschluß und schließlich wird zur Auswertung einiger im Buche angeführter Analyseverfahren eine tabellarische Hilfe geboten. Die letzte Tabelle gibt den Fluorid-Standard des NMS an.

Das Buch ist eine nützliche Einführung für jene, die sich im Themenkreis der ionenselektiven Elektroden zurechtfinden wollen.

E. PUNGOR

Topics in Current Chemistry 43. New Concepts III

Der Band umfaßt zwei Aufsätze:

1. P. CÁRSKY, R. ZAHRADNIK: *Approach to Electronic Spectra of Radicals*

Die Untersuchung von Radikalen ist in letzterer Zeit das Objekt vieler Strukturforschungsarbeiten. Die Untersuchung von Elektronenspektren ist ein wichtiges Mittel zur Erforschung der Radikalstruktur: das Elektronenspektrum ist eine unerläßliche Angabe zur Kontrolle der quantenchemischen Berechnungsmethoden für offenschalige Systeme. Zugleich sind die Ergebnisse der Berechnungen von großer Bedeutung in der Auslegung der Elektronenspektren und der allgemeinen Reaktivitätstheorie.

Der vorliegende zusammenfassende Aufsatz gibt auf 55 Seiten einen Überblick über die Elektronenspektren der Radikale. Die beiden Hauptabschnitte umfassen eine kurze Behandlung der Methoden und eine ausführliche Diskussion der Anwendungen. Die theoretische Einleitung befaßt sich mit der Problematik der Selbstkonsistenz und der Wahl der Konfigurations-Wechselwirkungsbasis. Anschließend wird das halbemprische SCF-CI-Verfahren von LONGUET-

HIGGINS und POPLE ausführlicher behandelt. Die Anwendungen sind nach der verwendeten Methode gruppiert. Ein beträchtlicher Teil befaßt sich mit den π-Elektronenberechnungen nach dem PPP-Verfahren, und innerhalb dessen mit der Deutung der Elektronenspektren einiger kleinen Moleküle und mehreren konjugierten Systeme. Die berechneten und experimentellen Ergebnisse sind in mehreren Abbildungen und Tabellen dargestellt; darunter befinden sich viele eigene Ergebnisse der Verfasser. Die mit dem Gesamt-Valenzelektronenverfahren erhaltenen Ergebnisse werden kurz erläutert. Abschließend folgt eine tabellarische Übersicht über einige *ab-initio*-Berechnungen.

Man kann mit der Meinung der Verfasser übereinstimmen, daß die π-Elektronen-Approximation noch lange das wichtigste Mittel zur Deutung der Elektronenspektren von großen konjugierten Radikalen bleiben wird. Die Zusammenfassung gibt einen guten Überblick über die Berechnung der π-Elektronenstruktur und der Elektronenspektren von Radikalen und leistet wertvolle Hilfe zur Forschung auf diesem Gebiet.

Á. KISS

2. H. HARTMANN, K. H. LEBERT, K. P. WANCZEK: *Ion Cyclotron Resonance Spectroscopy*

Die Ionen-Zyclotronresonanzspektroskopie ist eine eigenartige, äußerst genaue Methode der Massenspektroskopie. Bewegen sich Ionen mit einer konstanten Kreisfrequenz auf einer zentralen Bahn, so sind sie fähig, elektromagnetische Strahlung der gleichen Frequenz zu absorbieren. Die Kreisfrequenz des im Zyclotron sich bewegenden Ions ist seiner spezifischen Ladung proportional. Durch Radiofrequenz-Resonanz kann die Energie dies Ions gesteigert und das Ion von seiner Bahn abgelenkt werden. Je nach der Art des Detektierens unterscheidet man Ionen-Zyclotronresonanz (ICR), wo die Intensitätsänderung des Radiofrequenzfelds gemessen wird, d. h. die Absorption sowie das "Gesamtionenstrom-Verfahren" (TIC), wobei der Strom der von ihrer Bahn abgelenkten Ionen gemessen wird. Das Verfahren ist bei zahlreichen in der Gasphase verlaufenden Ionenreaktionen zur Untersuchung ihres Mechanismus verwendbar.

Der Aufsatz umfaßt 51 Seiten und besteht aus folgenden Abschnitten:

1. Grundprinzipien und Apparatur. Erwähnenswert is das Prinzip der Doppelresonanz, das in Ion—Molekül-Austauschreaktionen anwendbar ist. Mit seiner Hilfe wird dieAusbeute der Reaktion in Abhängigkeit von der Geschwindigkeit des reagierenden Ions gemessen.Die Geschwindigkeit des primären Ions wird dabei durch Radiofrequenzresonanz verändert und die Konzentration des sekundären Ions durch Anwendung der ihm entsprechenden Frequenz mit dem Gesamtionenstrom-Verfahren gemessen.

2. Linienformen und Geschwindigkeitskonstanten. In Resonanzabsorptionsmessungen ist die Linienbreite von der Lebensdauer des angeregten Ions abhängig. Geht das Ion schnell eine chemische Reaktion ein, wird die Absorptionslinie breiter. Die Linienbreite steht mit der Geschwindigkeitskonstante bzw. der Kollisionsfrequenz in eindeutigem Zusammenhang.

3. Anwendungen. Stoßquerschnitte und Kollisionsfrequenzen. Nukleophile Austauschreaktionen und Protonenaffinitäten. Photochemische Reaktionen. Reaktionen von Wasserstoff- und Deuteriummolekülen und Molekülionen. Reaktionen von Kohlenwasserstoffen. Untersuchung von Strukturen und Umlagerungen. Haloalkane und -alkene. Reaktionen von aliphatischen Alkoholen. Reaktionen von anorganischen Verbindungen (Hydride, Stickstoffoxide, Fluorverbindungen). Dieser Abschnitt enthält ausführliche Tabellen und Literaturhinweise.

Das neue Verfahren stellt ein einzigartiges Mittel zur Forschung der Kinetik von Gasreaktionen dar.

GY. VARSÁNYI

G. VARSÁNYI: *Assignments for the Vibrational Spectra of 700 Benzene Derivatives, Vols I, II*

Akadémiai Kiadó, Budapest 1973

After an introduction of about 20 pages, the author gives in the first volume the most important data of the vibrational spectra of about 700 benzene derivatives. The normal frequencies of the compounds, the assignment of the frequencies and the characterization of the intensities as well as the pertinent references are summarized in tables.

In the grouping of the compounds the author follows those principles the expedience of wich has been pointed out in his book "Vibrational spectra of benzene derivatives" (Akadé-

miai Kiadó). Light and heavy substituents are distinguished, depending on the fact whether the atomic weight of the first atom linked to the ring is lower or higher than 25. Molecules in which the number and position of the light or heavy substituents are identical belong to the same group. The usefulness of this grouping is emphasized by the fact that the author has succeeded in giving for both groups relatively narrow intervals in which the normal frequencies of the molecules are to be expected regardless of the nature of the light or heavy substituents.

The second volume contains the infrared spectra of most of the compounds discussed in the first volume. For 150 molecules, spectra recorded in the 250—4000 cm^{-1} region, and for 207 compounds spectra recorded in the 400—4000 cm^{-1} region are given. All the spectra were recorded in Hungary, the names of the contributors to this work are listed on page 4. Regrettably, the state in which the spectra were taken is not indicated. On the other hand, the subject index according to substituents at the end of Volume II is very useful.

The book is of great assistance to organic chemists and spectroscopists having assignment problems. The mass of data, compiled with great care and special knowledge, is easy to handle and will be very helpful for all those engaged in work on the physical chemistry of benzene derivatives.

F. TÖRÖK

Advances in Chemistry. Vol. 16. Ed. B. Csákvári

Akadémiai Kiadó, Budapest 1973. 240 pages, 25 figures, 5 tables

This volume of the series edited by Béla CSÁKVÁRI deals with chemical technology, and within this with three fields of chemical engineering science, which today are in the highlight of research. The surveys on these fields of science were written by Hungarian scientists most competent in the subject. In addition to an analysis of the present state of art, the volume predicts the direction of research in these fields.

The first part (70 pp.) "On some chemical operations involving component transfer", has been written by Antal LÁSZLÓ. It summarizes the development in rectification, absorption and extraction operations in the last decade. The survey is completed with 125 references and 15 major reviews primarily books.

The three operations selected comprise 70—80% of the operational units used in chemical industry. The author points out in connection with these classical operations that recent developments brought new results in the field of systems theory, computation techniques, optimization and process dynamics.

These advances are illustrated by numerous references to the work of distinguished representatives. First, a survey is given on equilibria, heat and component transfer and fluid mechanics; this is followed by the discussion of computation techniques introduced in design, a summary on the investigation of steady states, and finally, by the reviews of innovations introduced in the field of component separating apparatus. In the conclusions drawn, the author discusses the possible future development of results obtained so far.

The second part of the volume (100 pp.) has been written by Tibor BLICKLE under the title "Algebraic description of the systems of chemical engineering". It summarizes the results obtained in the Research Institute for Technical Chemistry of the Hungarian Academy of Sciences by the author and co-workers in the field of mathematical description of chemical technological systems. Based on a very thorough analysis of chemical production and applied natural sciences, the algebraic methods of systems theory have developed very rapidly. Results attained in Hungary are presented by the study.

In the introduction, systems and the fundamental information pertaining to the structure of systems are summarized. This is followed by the description of material system and their changes, and an analysis of the relationships between them. Finally, the study deals with chemical technological operator systems. The work reports on the first phase of a research project still in progress. The final aim is to explore the elements of technological processes, from which the technological systems can then be built up. The exactness of the discussion is ensured by the strict mathematical method using linear algebra.

The author complements the discussion by the concrete presentation of matrices and graphs, which makes the otherwise very abstract considerations easier to follow.

The third part is a survey (70 pp.) by József HOLDERITH: "On some problems of the stimulation of chemical reactors". The author presents the modern methods developed in this field and also reports some of his own work. A very valuable part of the survey is a critical analysis based on the 25 most important publications (mainly monographs) that have appeared on this subject in the world literature. The survey gives 140 references.

The Introduction deals with reactor models and the evaluation of the literature. Among the problems discussed, phenomenological reaction kinetics are of great importance. Within this, the stoichiometric degree of freedom, reaction rate and extent of reaction are those concepts around which the results presented are grouped. The final part of the study deals with the problems of heterogeneous catalytic reactors. The three-part model and various conditional equations are critically evaluated. The primary merit of the survey is the clear guideline given for this field of research, which is in a rapid phase of development and therefore not easy to review.

This volume of the series published by Akadémiai Kiadó deserves also special attention because in addition to informing Hungarian specialists engaged in this field, it is instrumental in pointing out the directions of theoretical research in Hungary.

P. SZOLCSÁNYI

Reaktionsmechanismen der Organischen Chemie
Ein Seminarbuch von HERMANN HÖVER

Verlag Chemie, Weinheim/Bergstr., John Wiley and Sons, Frankfurt am Main 1973. 565 Seiten.

HÖVER's Buch ist eine hervorragende Bearbeitung der wichtigsten Resultate und der neuesten Erkenntnisse der organischen Reaktionsmechanismen.

Das Buch ist aber nicht nur vom traditionellen Standpunkt aus eine gute Monographie, sondern zugleich "Ein Seminarbuch", mit anderen Worten, ein originelles Werk didaktischen Wertes. Das Buch besteht aus zwei Hauptteilen. Der erste Teil enthält die Problemstellungen (Seiten 1—75), der zweite Teil (Seiten 75—529) beschreibt in ca. 450 Seiten die "Lösungen" der Probleme. (Das Wort "Lösung" ist hier in übertragenem Sinne zu verstehen.) In diesem zweiten Teil sind natürlich zuerst die unmittelbaren Lösungen der aufgestellten Probleme angegeben, außerdem werden auch die, der gegebenen Reaktion analogen Prozesse sehr gründlich diskutiert, und auch die tieferen theoretischen organisch-chemischen Erläuterungen angegeben. Die folgenden Daten charakterisieren den ausgezeichneten Aufbau dieses Buches.

Der erste Teil stellt ca. 210 Probleme auf; diese beziehen sich auf Reaktionen, die aus verschiedenen Reaktionstypen der organischen Chemie, aufgrund Literaturangaben ausgewählt wurden: Die Reaktionen enthalten im allgemeinen die Struktur der Ausgangs- und Endverbindungen, die Reaktionsbedingungen, spektroskopische Daten und gegebenenfalls die Neben- und Folgereaktionen. Interessanterweise ist die Verteilung der 210 Probleme, den wichtigsten organisch-chemischen Reaktionstypen gemäß, die folgende:

Additionsreaktionen (A): 41, Cycloadditionen (C): 36, Valenzisomerisierungen (V): 13, Eliminierungen (E): 15, Fragmentierungen (F): 7, Aliphatische Substitutionen (S): 72, Aromatische Substitutionen (AS): 10, Radikal-Reaktionen (R): 6 und Photochemie (P): 11.

Die den Reaktionstypen entsprechende Verteilung der Aufgaben zeigt deutlich, daß die meisten Probleme noch immer in der Aliphatischen Substitution zu finden sind. Es darf freilich nicht vergessen werden, daß dieses Gebiet das bisher eingehendst untersuchte Mechanismen-Thema bildet.

Das Buch ist einerseits, als "Seminarbuch", ein Leitfader für Studenten und Seminarleiter. Es kann aber auch das Interesse der schon tätigen Forschungschemiker erregen, hauptsächlich deren, die den modernen Erläuterungen der Reaktionsmechanismen nachlesen wollen, da es die modernen Erörterungen in bündiger Form und klarem Aufbau darbietet.

Der zweite, Hauptteil des Buches befaßt sich nämlich mit den Grundzügen der Hückelschen MO-Theorie, der Anwendung der Woodward—Hoffmann-Regeln auf synchrone Reaktionen, den modernen Aspekten der Photochemie, der Bedeutung der nichtklassischen Carboniumionen, sowie mit noch vielen neuen Konzeptionen, bzw. neuen Erörterungen von älteren Konzeptionen. Die ca. 800 originalen Literaturangaben und das ca. 30seitige Register zeigen einerseits das inhaltliche Maß des Buches, andererseits vereinfachen sie dessen Gebrauch.

Ein kleiner, aber störender Mangel muß doch erwähnt werden. Dieser Mangel berührt hauptsächlich die sich für die organischen Reaktionsmechanismen fortlaufend interessierenden und die Fachliteratur lesenden Kollegen. Die neue deutsche Ausgabe enthält zwar den ursprünglichen Titel des Buches: "Problems in Organic Reaction. Mechanisms, by Hermann HÖVER, Wiley, New York 1970" — es wird aber nirgends, weder im Vorwort, noch in irgend einem anderen Teil — erwähnt, was übrigens allgemeiner Brauch ist, ob die neue deutsche Ausgabe eine umredigierte, erweiterte Form der früheren englischen Version ist, oder aber eine unveränderte Übersetzung. Der Rezensor muß also die Leser auf die erfreuliche Tatsache aufmerksam machen, daß hier von einer wesentlich erweiterten Ausgabe die Rede ist — zwar, wie

erwähnt, ist dies im Buch nicht angegeben. Diese Tatsache wird durch folgende Daten unten stützt: Der Umfang der neuen Ausgabe ist ca. um 100 Seiten gestiegen und enthält ca. 150 mehr Literaturangaben, von denen viele auf die 70er Jahre fallen. Von den modernen Inhaltsänderungen soll nur eine erwähnt werden: der englischen Ausgabe gemäß ist das Triphenylmethylradikal, durch Dimerisation, mit Hexaphenyläthan im Gleichgewicht, die deutsche Ausgabe berücksichtigt dagegen schon die neuere Erkennung, nach der das eine Radikal, im Dimeren, durch das zentrale Kohlenstoffatom an das Parakohlenstoffatom des anderen Radikals gebunden ist.

Zusammenfassend kann von der deutschen Ausgabe des HŐVER-Buches folgendes gesagt werden: Volle Anerkennung zur Ausgabe des Buches auf deutschem Sprachgebiet.

A. MESSMER

J. J. BIKERMAN: *Foams*

Springer Verlag, Berlin—Heidelberg—New York 1973. VIII + 337 pages.

Until the appearance of this work only two monographs dealing with foams proper, *i.e.* with gas/liquid systems, were known in the literature. One of these was written by the author himself and three co-authors in 1953 (Foams: Theory and Application), while the second, published in the same year, is the work "Schaum", written by E. MANEGOLD. This fact illustrates that the publication of a survey on this subject is of great interest. Indeed, during the last twenty years a large experimental material has accumulated particularly in connection with the most various practical applications of foams. However, in spite of this, only the first rudimentary experiments have been undertaken in connection with foams existing in the form of gas bubbles enclosed between thin liquid lamellae, and to interpret their properties as macroscopical physical systems, involving a definite structural combination of the two components with special regard to the properties of thin liquid films, differing in many respects from those of bulk phases. Several schools have developed in connection with thin films, of which the most notable are those of DERYAGUIN, MYSELS, OVERBEEK and SCHELUDKO in the Soviet Union, the United States, the Netherlands and Bulgaria, respectively. However, these schools centered their attention primarily on the thin films proper, so that even today there is no comprehensive theory relevant to the foam-like systems of these films.

BIKERMAN, a former pupil of FREUNDLICH and a well known author of many papers dealing with surface phenomena, did not aim at filling this gap. The present book is rather a revision of his earlier work mentioned, which takes into consideration the factual data accumulated since then, resulting partly in an extension and partly in a restriction. The latter is to be understood in the sense that, among others, the chapters on solid foams and flotation have been omitted because independent books have in the meantime been published on these subjects. The extension means primarily an updating of the references rather than an essential revision of the first variant. (The last reference stems from 1971, which may serve as a basis to comparison with the much-criticised publication times of manuscripts in this country.) Similarly to other works of BIKERMAN, Soviet literature is amply cited, which is often missing in many US publications.

The book is divided into 13 chapters (and within these, into 195 sub-chapters). The chapters are as follows: General introduction. Formation and structure. Measurement of foam-forming ability. Data on foam-forming ability. Three-phase films. Drainage. Mechanical properties. Optical properties. Electrical properties. Theories of foam stability. Foams in nature and industry. Separation with foams. Other applications.

The structure of the book is characterized by the frequent interlacing of the contents of various chapters, which leads to repetitions, and in fact, makes the work to a certain degree mosaic-like. This follows from the fundamental concept of the author; as his starting principle is the capillary theory in almost all chapters, considerations are traced back to LAPLACE, PLATEAU and MARANGONI. Remarkably, however, the not less classical work of BASFORTH and ADAMS on capillary surfaces is not mentioned.

Curiously, the "disjoining pressure", a concept already generally accepted today, is not mentioned in the book, at least not by this name, though the existence of the physical phenomenon proper is discussed to some extent in connection with the description of the basic experiment. However, the omission of a survey on modern thin film theory must be considered as a deficiency, even if the author may not agree with this theory, or, as mentioned already, it is not his aim to set forth a coherent foam theory on this basis. Neither is it easy to understand

why the book does not discuss intermolecular forces, the DLVO theory (which was developed in close connection with research on thin films), ion flotation, foams formed from polymer solutions (with the exception of a brief reference to foam fractionation), antifoam methods and foam columns.

Of course, demands with respect to deficiencies are always rather excessive and perhaps exaggerated, and might even obscure the actual merits of the work. It is not mere chance that this subject has not been worked up until 1953 or in the twenty years elapsed since then, or that MANEGOLD's work gives a leading role to a single aspect, the morphological one.

The great merits of BIKERMAN's work are the compilation of an extensive experimental material, the exceptionally concise and clear style, the demonstration of the subject on hand of simple numerical examples, and the richness in experimental and methodological detail. Therefore, notwithstanding a certain one-sidedness, the book is a valuable contribution to the literature on surface chemistry.

E. WOLFRAM

H.-H. PERKAMPUS: *Wechselwirkung von π-Elektronensystemen mit Metallhalogeniden*

Springer Verlag, Heidelberg, 1973. 215 Seiten.

Die Wechselwirkung von π-Elektronensystemen mit Metallhalogeniden (auch als Lewis- oder Ansolvosäuren zu bezeichnen) hängt von der Gegenwart von Protonen (aus protonhaltigen Lösungsmittels oder Verunreinigungen stammend) ab. Sind Protonen vorhanden, so resultieren sog. Proton—Additionskomplexe, fehlen Protonen, so entstehen π-Komplexe oder σ-Komplexe, letztere mit einer polaren Bindung zwischen Kohlenstoff und Metallatom. Diese drei Komplex-Typen werden in der vorliegenden Monographie behandelt. Besonders ausführlich werden die Ergebnisse der Untersuchungen an den reinen binären Systemen, π-Elektronensystem und Metallhalogenid dargelegt. Hier fehlte bisher eine umfassende Darstellung, die den Primärschritt der Wechselwirkung ohne Folgereaktionen zum Gegenstand hatte.

Nach einem kurzen historischen Überblick behandelt der erste Abschnitt die mit dem Gegenstand der Monographie zusammenhängenden Grundprinzipien. Der nächste Abschnitt befaßt sich mit den Eigenschaften der Donatoren und Akzeptoren mit besonderer Hinsicht auf die Struktur der Metallhalogenide. Der dritte Abschnitt behandelt die Untersuchung der Proton—Additions-Komplexe mit präparativen und spektroskopischen Methoden. Der vierte Abschnitt von größtem Umfang beschreibt die π-Komplexe auf Grund der Ergebnisse der an ihnen vorgenommenen Phasenstudien, spektroskopischen Untersuchungen (UV-, IR-, NMR NQR- und ESR-Messungen) und Dipolmoment-Messungen.

Der letzte Abschnitt beschäftigt sich mit den σ-Komplexen von Olefinen und Aromaten. Das Buch schließt mit einem Namenverzeichnis und Sachverzeichnis.

Die von einem in diesem Fachgebiet international bekannten Forscher geschriebene Monographie wurde schon seit langem entbehrt, und wird von jedem an diesem Gebiet interessierten Forscher mit Freuden begrüßt. Die Literaturverzeichnisse am Ende eines jeden Abschnittes fördern nur noch die Verwendbarkeit des Buches.

GY. DEÁK

Reaction Transition States

Proceedings of the 21st Annual Meeting of the Société de Chimie physique Paris, 20—24 September, 1970

Editor Dubois Jacques-Emile. Gordon and Breach Science Publ., New York—London—Paris 1972

The book is a collection containing the complete text of the lectures delivered at the 1970 Annual Meeting of the French Society of Chemical Physics on reaction transition states.

The timeliness of this subject is well demonstrated by the great progress of theories and methods in studying transition states over the last decade. Arising from the new and interesting quantitative results of the interpretation of kinetic and stereochemical processes in chemical

reactions, primarily the detection of short-lived active intermediates and the study of their role, this field has become the center of interest.

Thus it was the right moment to organize a symposium on this subject, where the outstanding international experts report their recent results, and call the attention to yet unsolved problems. The standard of the lectures was ensured by inviting appropriate contributors, who could inspire high-level discussions, giving a good insight into the problems to the audience and, through this volume, to the reader.

The broad spectrum of the papers embraces the discussion of general models on transition states, the theoretical and semi-empirical study of homogeneous and heterogeneous kinetics, mainly in the framework of organic chemical models and processes.

To deal even briefly with the 26 papers collected in the book is almost impossible in this review. Within the scope of the conference, the subjects of the lectures are extremely divergent, spanning from ab initio calculations on the transition state, through the interactions in the transition state and the stereochemistry of transition states, to the experimental kinetic investigation of isotope and medium effects. The only thing that can be done is to discuss some particularly interesting lectures, and thereby encourage the reader to study the voluem thoroughly.

Although the paper of M. KARPLUS (Harvard University) was read in the closing session of the symposium, its merits justify a priority in this review. The trajectory analysis of transition states applied in the paper permits to discuss in a general way the problems concerning the Eyring—Polányi theory of transition states. As well known, this subject has since then stimulated several theoretical and experimental investigations, and is still in the limelight.

K. J. LAIDLER (University of Ottawa) reports interesting results on the symmetry behaviour of transition states. According to his theoretical studies, based on the activated complex theory, there is a correlation similar to the Woodward—Hoffmann principle in such reactions, too, where no strict orbital symmetry control exists. Quantum chemical calculations on the structures and geometry of transition states have been reported in several papers. Interesting results were obtained, for instance, by L. SALEM (Faculté des Sciences, Orsay) on the geometrical isomerization of cyclopropane from SCF-MO *ab initio* calculations, and by W. Th. A. M. VAN DER LUGT and P. ROS (Koninklijke Shell Laboratorium, Amsterdam) on the intermediates of the electrophilic or nucleophilic substitution reactions at tetrahedral carbon atoms (CH_5 and CH_5^-) from LCAO-Hartree—Fock calculations.

The problem of pentacoordinate carbon atom was discussed from experimental aspects by G. A. OLÁH (Case Western Reserve University, Cleveland). The experimental results on the intermediate CH_5^+ of electrophilic substitution are in agreement with the quantum chemical calculations. Of the papers concerned primarily with experimental aspects, it is worth noting the report of J. E. DUBOIS and J. F. FORT (Laboratoire de Chimie Organique, Paris) on the interpretation of the stereochemical results of the aldolic "α,α'-diastereogenic" reaction, based on the measurement of kinetic and thermodynamic stereoselectivity.

In the investigation of transition states it is particularly important that the experimental methods applied enable to perform quick delicate kinetic measurements. From this aspect the results of F. TERRIER, Ch. DEARING and R. SCHAAL (ENSCP, Paris) should be noted. The authors, using the stopped flow method, have proved that two kinds of intermediates exist in the nucleophilic reactions of nitroanisols, one of which participates only in a fast pre-equilibrium. A differential method has been developed by W. J. ALBERY (Physical Chemistry Laboratory, Oxford) for the measurement of solvent isotope effect in solvolytic reactions. The accuracy of a few parts in a thousand allows to determine precisely the character of the transition state.

The standard of the reviewed papers is characteristic of the total content of the volume, making it a valuable collection.

It is perhaps only the edition that can be objected. Apparently, the editor insisted on the chronological order of the lectures, which causes difficulties for the reader in orientation. Completely theoretical papers often follow papers of experimental nature, and *vice versa*, without an underlying logical order. The book-form would have required a thematical arrangement instead of chronological, and this would probably have made the volume more consistent and easier to survey.

A second misfortune, occurring obviously with every publication of this kind, is that the book was published two years after the symposium. The results have since then been reported elsewhere, and further progress has been made in these subjects. The reader may be compensated at most by obtaining papers of comprehensive nature.

It must be stressed, however, as a great merit, that the discussions following the lectures are also reported, making the reader feel as an actual participant of the sessions.

On the basis of the high standard of the papers and discussions this volume can be recommended, irrespective of minor insufficiencies, to Hungarian chemists, particularly to those dealing with the research of reaction mechanisms.

I. PINTÉR

M. YUDKIN and R. OFFORD: *Comprehensible Biochemistry*

Longman Group Ltd., Harlow, 1973. 576 pages, 231 figures, 28 tables

The authors of the book are biochemistry professors of the University of Oxford, who published earlier a revised edition of the short work of HARRISON's "A Guidebook to Biochemistry". The present book is a considerably enlarged version of the former. On the flap of the bookjacket the volume is recommended as a textbook for university students studying biochemistry whether as the principal or a subsidiary subject. In accordance with modern didactic concepts, the aim of the authors was to give a sound fundation, *i.e.* a book not with comprehensive but comprehensible subject matter. Instead of learning the total body of knowledge of the rapidly developing science of modern biochemistry, the students must acquire an ability for independent thinking and the attitude of considering biological processes in all their interrelations.

In the reviewer's opinion the authors have attained their objectives. The mode of discussion suits fundamental biochemistry on cell-level, that is to say, subjects of higher level and those not generally characteristic of the living matter (*e.g.* hormones, nitrogen fixation) are omitted. Emphasis is laid on macromolecules occurring in the living substance and on the constantly changing, dynamic state of these molecules. Characteristic is further the thermodynamic consideration of the chemical changes and the technique of illustration by three-dimensional structures and the relevant functions. A large number of figures well support the text.

In addition to the introductory general chapters, the book consists of four main parts, dealing with macromolecules, intermediary metabolic processes, informational macromolecules and regulation.

In the introductory part, a separate chapter is concerned with the thermodynamics and the kinetics of biochemical processes, including non-equilibrium states. This foundation is successfully applied in the following parts of the book.

The main part, dealing with macromolecules, discusses the structure and the functions of proteins, particularly the enzymic function (with a thermodynamically emphasized interpretation of the mechanism of action). This is followed by a descripton of the structure of nucleic acids, polysaccharides and lipids. Here, the mode of discussion of the component elements, such as the steric structure of amino acids, is very fortunate, and the elementary interpretation of X-ray diagrams is also apposite.

In the second main chapter, the fundamental difference between the metabolic processes proceeding with the participation of NAD and NADP is well stressed. After an introduction and description of the cellular elements, the following topics are discussed: methods of investigation of metabolism, the respiratory chain and oxidative phosphorylation, the light reaction of photosynthesis, glycolysis, pyruvate oxidation and the citrate cycle (it would have been proper to mention also SZENT-GYÖRGYI in addition to KREBS), the oxidation of fatty acids, the pentose cycle, mechanical and chemo-osmotic utilization of ATP, synthesis of carbohydrates and lipids, the intracellular topology of carbohydrate and lipid metabolism, the metabolism of amino acids, and finally, the synthesis of the other important N-containing compounds. Here, the emphasizing of membrane effects is very successfully done.

The third main chapter deals with the synthesis of informational macromolecules (DNA, RNA, proteins); this is perhaps the most delectable part of the book. This subject, which is rather difficult on first reading, is expounded very wittily and logically. Following the chapter dealing with molecular genetics, the synthesis of DNA and RNA and protein synthesis are discussed. One chapter is dedicated to the evolutionary aspect of amino acid sequences.

The main chapter on regulation grasps similarly the essence. Here, regulations on the levels of enzyme action and enzyme synthesis are discussed.

The four main chapters are well complemented by the two parts of the Appendix. The first of them is a mathematical description of the fundamental phenomena of enzyme kinetics, while the second is concerned with the methods of separation of macromolecules, with witty explanations.

The list of literature contains, in addition to references to several biochemical series facilitating further orientation, 57 fundamental references pertaining to the material of the various chapters, from the period 1959 to 1973.

In accordance with its objective, the book had to omit dealing with a number of subjects. Evidently, depending on the individual sphere of interest, each reader might miss this or that theme. In the reviewer's opinion it could have been pointed out perhaps, in general, in connection with the intermediary metabolism that several small molecules, linked by covalent bonds to some carrier molecule, accompany the biochemical happenings (*e.g.* acetyl co-enzyme A, acyl-AMP, UDP-glucose, C_1-fragments, etc.). In connection with regulation, an example may have been given for zymogens, and in the discussion of the separation methods, affinity chromatography could have been mentioned.

A few minor faults occur, thus e.g. some symbols mentioned in the text are missing in the figures on pages 89 and 160. In the copy of the reviewer, the figures on pages 123 and 352/354 are interchanged, and the page number of the references in the text is erroneous on pages 228 and 271.

The book is very readable and unnecessary repetitions are avoided by the use of a number of cross-references.

The presentation of the book and the quality of the figures are nice, and good use can be made of the subject index.

The book can be used to good advantage by every biochemist.

P. TOLNAY

W. STRIEDER and R. ARIS: *Variational Methods Applied to Problems of Diffusion and Reaction*

Springer, Berlin—Heidelberg—New York, 1973. 118 pages, 12 figures

(Springer Tracts in Natural Philosophy, Vol. 24, Editor: B. D. Collman)

The use of variational methods is spreading also in technological sciences. A representant of this development process is the present work in which the two well known authors apply the classical method for the solution of problems in modern chemical engineering.

The first part of the book describes the mathematical apparatus. An important part of it is the presentation of those functionals, which are used to solve the envisaged tasks. This is followed by the discussion of some special diffusion problems. The basic principle of the method presented is the minimalization of the dissipation function. This tool is used by the authors for the solution of tasks in connection with models, which can be formulated only statistically in the phenomenological discussion of diffusion.

The basic question is answered, how computation formulas containing easily measurable parameters can be deduced for diffusion processes proceeding between particles statistically distributed in space.

The first topic is fluid flow in a set of random distribution solid particles both in the normal and Knudsen's region. In the relationships deduced the void fraction is used.

The second topic is the case of the range-dependent diffusion coefficient. Relationships, called nomenclaturally lower and upper limit cases, are obtained.

The third topic is mass transfer to randomly distributed solid particles. Limit case relationships, similar to the preceding, are deduced on the basis of the cell model.

The fourth topic is the inhibition by diffusion of reactions proceeding on porous solid catalysts. Using Thiele's modulus, relationships are derived for four types of limit cases.

The main merit of the book is to show the role of the dissipation function of the form $D \Delta c \Delta c$ in solving practical problems. Though not expressedly stated in the book, since the dissipation function is proportional to the entropy production function, the authors actually apply the thermodynamical concept of non-equilibrium processes to the deduction of macroscopic formulas describing diffusion processes and for a more exact outlining of their field of validity.

P. SZOLCSÁNYI

Garth L. LEE, Harris O. VAN ORDEN, Ronald O. RAGSDALE: *Laboratory Manual for General and Organic Chemistry*

W. B. Saunders Company, Philadelphia—London—Toronto 1973. 305 p.

The book is intended for undergraduates who work 2—3 hours weekly, or 2 hours twice a week in the laboratory. Although the book is a laboratory manual connected to the textbook "General and Organic Chemistry" by the same authors, it can also be used independently. The manual contains 32 exercises embracing most diverse fields of chemistry, including simple qualitative analysis, synthesis, polymer preparation, chemical equilibria, kinetics, stoichiometry, acid–base reactions and the determination of chemical formulae.

The exercises consist of four parts. In the first parts, the discussion, the required theoretical background is surveyed briefly. This is followed by the detailed description of the experiments to be performed. The third part is a pre-printed laboratory note-sheet, removable from the book, which facilitates the work of both the student and the teacher. The student is supposed to record his experimental data and observations, and to answer various questions concerning the experiments. The four part can also be removed, and presents further questions, problems and exercises in connection with the subject.

The experiments given in the book require relatively simple equipment. The excellent methods meet the purpose of the book: the undergraduates may grasp the laws of chemistry on the basis of own experiences, and study the fundaments of analytical and preparative chemistry by experiments.

In the reviewer's opinion, this book, on account of its size, has not been intended primarily for chemistry undergraduates. It attempts to familiarize the student with several fields of experimental chemistry in one year, through a few hours a week of laboratory practice, which is necessarily insufficient for a chemistry undergraduate. The required theoretical background is rather limited but the treatment is tractable, thus the book can be used to advantage in any field of education where chemistry is not a fundamental subject. Yet, this student-experiment book may provide assistance in the education of chemists. Moreover, it may supply ideas even for the chemistry teaching in secondary schools, because of the simplicity of the equipment required.

The book can be recommended to everyone who is engaged in chemical education, and intends to connect theoretical training to experimental work, particularly to student-experiments.

K. GYŐRBIRÓ

G. LIPTAY: *Atlas of Thermoanalytical Curves* (TG-, DTG-, DTA-curves measured simultaneously)

Akadémiai Kiadó, Budapest, and Heyden and Son Ltd., London—New York—Rheine, 1974
(160 pages, 75 derivatograms)

This volume of the series may command a wide range of interest since among the instrumental methods thermoanalysis plays a special role both from theoretical and practical points of view. The knowledge of the behaviour of a material towards heat treatment represents an important information as far as the structural properties are concerned and also in industrial technologies.

The simultaneous measurement of TG-, DTG- and DTA-curves results sometimes in very useful new experiences, as demonstrated also by the content of this volume. The arrangement of the volume follows the principle of the former ones. The two short Appendices at the beginning of the volume describe those technical data of the Derivatograph and Mettler Recording Thermoanalyser for the simultaneous testing of TG, DTA and DTG, according to which the individual samples were tested. These are followed by 75 thermoanalytical curves and the volume is terminated by a two-page index. Each curve was recorded by using the technique described in Vol. 1. A relatively small amount of the sample (20—120 mg) was tested at a slow rate of heating from 1 to 3°C · min^{-1} and a curve was recorded also by using (5 to 10 times) larger sample and a higher heating rate; the characteristics of the derivatogram are shown by two (red and black) curves.

The third volume is worthy continuation of the former volumes of the series, which contains the thermoanalytical curves of 23 Czechoslovakian, Hungarian, Polish and Roumanian

researchers from academic, university and industrial institutions. Among 75 carefully selected graphs, there are 24 organic compounds (aromatic molecules, sugars, amino acids and derivatives, etc.), 27 inorganic compounds (alkalies, earth-metal salts, lanthanides, heavy-metal compounds), 15 salts of organic acids with inorganic bases and 9 mine-industrial and mineral products. The success of the selection is characterized also by the fact that nearly every curves of the collection represents a material with particular and interesting thermal behaviour. The evaluation of the curves and the description of the thermal changes can also be used by the thermoanalytical chemist for the evaluation of analogous curves of other compounds.

The third volume of the Atlas is, therefore, a very useful manual for both specialists and for those getting acquainted with the field. An index containing the material of the former volumes of the series could eventually be included in one of the forthcoming volumes to facilitate orientation.

Á. DÁVID

C. D. JOHNSON: *The Hammett Equation*
Cambridge Chemistry Texts

Cambridge 1973. viii + 196 pages

"Since its conception over thirty years ago, the Hammett equation together with subsequent modifications, all of which owed their motivation to Hammett's original idea, has provided the main basis for quantitative structure reactivity relationships in organic chemistry" — writes the author in the introduction of his book. Indeed, very few semi-quantitative empirical relationships have found so far a wider application in organic chemistry than the Hammett equation

The book is intended for senior undergraduates and first year graduate students, who, although familiar with fundamental qualitative organic chemistry, often have little or no experience in the quantitative assessment of the reactivity of organic molecules. However, the book will be used to good advantage for the enlargement of their knowledge by those chemists graduated earlier, who in the course of their studies have not yet gone into the details of theoretical organic chemistry.

The author discusses the selected field of knowledge in five chapters. First, the Hammett relationship is explained, and this is followed by a detailed discussion of how the Hammett equation can be used for the elucidation of reaction mechanisms. The third chapter deals with the separation of the inductive resonance and steric effects, and with the application of the Hammett equation to aliphatic systems. The Taft equation and the Yukawa—Tsuno equation are discussed in this part.

The fourth chapter deals with the application of the Hammett equation to data other than side-chain reactivities of substituted benzenes. Consideration of the thermodynamic basis of the equation is delayed until the final chapter. This is the chapter in which the Hammond postulate is discussed.

To encourage full understanding, each chapter concludes with a series of problems, all drawn from research papers. A list of references helps the reader in the use of the book.

Gy. DEÁK

Topics in Current Chemistry 46: Photochemistry
J. MICHL, K.-D. GUNDERMANN, W. C. HERNDON, W. D. STOHRER, P. JACOBS, K. H. KAISER, G. WICH, G. QUINKERT

Springer-Verlag, Berlin—Heidelberg—New York, 1974. 236 pages

The publication of every volume of this series is received with great interest by chemists, information with excellent summaries, even if not in a spectacular form. This is true also for Volume 46, published recently.

The volume contains four surveys, dealing with organic photochemistry. The author of the first part is J. MICHL, professor of the University of Utah in Salt Lake City. His work summarizes the physical principles forming the basis of the qualitative evaluation of molecular orbitals, used in the photochemistry of organic compounds. In organic chemistry, physical models are generally developed on the basis of the Born—Oppenheimer approximation. However, if the bonds connecting the atoms of an organic molecule are not in the ground state

but are photochemically excited, this mode of approximation can only be used within very narrow limits, and the accuracy is usually unsatisfactory. Owing to this fact, in the last 10—12 years, when both the theory and the preparative methods of photochemistry have undergone very rapid development, several approximation methods have been developed, which partly correct the shortcomings of the Born—Oppenheimer method. The work of Professor Michl is actually a critical survey of these latter methods. The survey consists of three parts: the first summarizes the qualitative physical models of photochemical processes in a readily understandable way, omitting the complicated mathematical apparatus.

The second part is a concise, clearcut and well arranged summary of quantum mechanical calculations, while in the third part the author summarizes the use of qualitative molecular orbital calculations. 149 references are given comprising, almost without exception, the most important publications of the last 20 years.

In the second part, K.-D. GUNDERMANN, Professor of the University Clausthal-Zellerfeld, reviews recent results on the chemiluminescence of organic compounds. As a matter of fact this chapter is a complementation of a previous work of the author, entitled "Chemilumineszenz organischer Verbindungen", published similarly by Springer-Verlag. Though it is modestly mentioned in the introduction that instead of giving a complete survey of the field, only dealing with some problems, considered essential by the author, is intended, the paper with its 217 references actually covers, all important aspects.

In the third part of the book, W. C. HENDON, Professor of the Texas University, discusses the effect of substituents on photochemical cycloaddition reactions on hand of two photochemical models considered most important at present: the double bond–double bond and the double bond–carbonyl cycloaddition reactions. These two reaction types have become particularly interesting for preparative photochemists in the last 10 years. By means of examples, HENDON gives an account of the present knowledge on the mechanism of these reactions; the correctness of the conclusions are also proved on the basis of the current theories of molecular orbitals. 146 references are given.

The fourth part of the volume is the collective work of five authors on the staff of the University of Frankfurt. It summarizes the theory and experimental facts of the peculiar behaviour of four-membered cyclic ketones in the excited state.

The excitation possibilities of the cyclobutanone ring containing various substituents and the photochemical reactions taking place as a consequence of the various excitation states are discussed in detail also including a treatment of the steric conditions of the compounds formed. In this part of the volume 93 references are cited.

B. LOSONCZI

Karl HAUFE und S. Roy MORRISON: *Adsorption* (Eine Einführung in die Probleme der Adsorption)

Walter de Gruyter, Berlin—New York 1974. 174 Seiten

Das vom Verlager WALTER DE GRUYTER betreute Buch mit einem Umfang von 174 Seiten, mit 78 Abbildungen im Text und mit 257 Referenzen vermittelt über die Adsorption ein sehr gutes, umfassendes Bild.

Das Buch ist durch Autoren- und Sachregister ergänzt. In den 6 Abschnitten wird der Leser der Reihe nach mit den verschiedenen Problemen der Adsorption bekannt gemacht. Im ersten Abschnitt werden nach einer kurzen Übersicht der bei der Adsorption in Frage kommenden Wechselwirkungen die fundamentalen Zusammenhänge der Adsorptionsisothermen diskutiert. Die nächsten drei Abschnitte behandeln der Reihe nach die Ionenadsorption, die an Metallen und Halbleitern auf die Elektronen-Wechselwirkung zurückführbare Adsorption und die Rolle der Gitterdefekte. Der fünfte Abschnitt befaßt sich mit jenen Prozessen, in welchen die Adsorption eine Schlüsselrolle spielt, wobei Oberflächenreaktionen, Katalyse, Chromatographie, Flotation und Korrosion besprochen werden. Der letzte Abschnitt befaßt sich mit den Meßmethoden, von der Druck- bzw. Volumenmessung bis zur Spektroskopie, ESR und NMR, LEED und Auger-Spektroskopie. Es könnte vielleicht bemängelt werden, daß die Gemisch-Adsorption in den verschiedenen Prozessen nicht die ihr gebührende Betonung erhielt. Zufolge der Einstellung der Verfasser durchdringt die elektronentheoretische Betrachtungsweise das ganze Werk. Als Lehrbuch ist das Werk zur Aneignung der modernen Grundkenntnisse über Adsorption sehr geeignet.

D. KALLÓ

INDEX

ANALYTICAL CHEMISTRY – ANALITISCHE CHEMIE – АНАЛИТИЧЕСКАЯ ХИМИЯ

PHYSICAL CHEMISTRY AMD INORGANIC CHEMISTRY – PHYSIKALISCHE CHEMIE UND ANORGANISCHE CHEMIE – ФИЗИЧЕСКАЯ И НЕОРГАНИЧЕСКАЯ ХИМИЯ

Printed in Hungary

A kiadásért felel az Akadémiai Kiadó igazgatója Műszaki szerkesztő: Zacsik Annamária

A kézirat nyomdába érkezett: 1974. IX. 10- – Terjedelem: 18,90 (A/5) ív 78 ábra, 2 melléklet

75.872 Akadémiai Nyomda, Budapest – Felelős vezető: Bernát György

ACTA CHIMICA

ТОМ 83 — ВЫП. 3—4

РЕЗЮМЕ

Определение фосфора в силикатных породах с помощью активационного анализа

С. О. ХАЛИЛ

Метод нейтронной активации для определения фосфора в виде фосфата серебра и таллия Ag_2 Tl PO_4 из исходного осадка аммонийного фосформолибдата был применен к силикатным породам.

Фосфат аммония был добавлен к облученному порошку породы в качестве носителя, и фосфор был выделен в виде аммонийного фосформолибдата. Последний высаждали несколько раз в присутствии соответствующего задерживающего носителя для обеспечения его радиохимической чистоты, а затем, наконец, растворяли и высаждали в форме фосфата серебра и таллия (Ag_2TlPO_4) для взвешивания и счета.

Отделение небольших количеств палладия от платины и иридия с помощью гидрологического высаждения на слабокислых катионо-обменных смолах

Л. Л. КОЧЕВА и Б. ТАБАКОВА

Был разработан метод отделения небольших количеств палладия (0,15—1,5 мг) от платины и иридия. Метод основан на сорбции палладия на слабокислой катионо-обменной смоле Amberlite IRC-84 в натриевой форме, происходящей вследствие гидролитического высаждения при комнатной температуре. В этих условиях платина и иридий остаются полностью в растворе. Сорбируемый палладий элюируется 20 мл 2М соляной кислоты. Метод был использован для анализа бинарных смесей палладия и платины или палладия и иридия, находящихся в различных отношениях.

Исследование переохлажденной воды с помощью рассеивания света

ДЬ. БЕКЕ, ДЬ. ИНЗЕЛЬТ и Л. ЯНЧО

Рассеивание света водой было исследовано в интервале температур —8—+8°C Данные интенсивности света выше точки замерзания и в переохлажденном состоянии не различаются значительно. Приблизительно была определена область концентрации-агрегации ледяных зачаток, в которой, как можно было заключить на основе измерений, присутствием ледяных зачаток в переохлажденной воде можно пренебречь.

Электролитическая поляризация на индий-сурьмяных электродах

Т. М. САЛЕМ и А. А. ИЗМАИЛ

Для исследований был выбран антимонид индия в качестве межметаллического соединения с небольшим энергетическим барьером. Электрод одного кристалла был изучен в присутствии окислительно—восстановительной системы как под действием облучения, так и без него. Наблюдалось, что анодное растворение увеличивается под действием облучения по мере того, как дырки внедряются в валентную связь. Для всех окисляющих реагентов ток зависит от интенсивности света. Полагается, что избыток носителя может быть генерирован оптически, используя луч света, и что облучение может оказаться полезным при введении носителей на электрод полупроводников типа *n*.

Образование и устойчивость хелатов 1-аспарагина и 1-глутамина палладия (II), платины (IV), золота (III) и висмута (III)

Р. С. ТЕВАРИ и М. Н. СРИВАСТАВА

Металлические хелаты Pd(II), Pt(IV), Au(III) и Bi(III), образующиеся с 1-аспарагином, были изучены потенциометрически. Были рассчитаны их ступенчатые константы устойчивости.

Возможности использование окиси вольфрама при каталитическом гидрировании в жидкой фазе

ДЬ. ВЕРТЕШ и ДЬ. ХОРАНИ

Были рассмотрены возможности использования окисных вольфрамовых катализаторов, активированных добавками благородных металлов.

Было установлено, что окись вольфрама, содержащая небольшие количества платины и палладия, может быть с успехом использована при гидрировании различных органических соединений.

Спектрофотометрическое исследование пурпурина и хинализарина в буферных растворах, содержащих органические растворители

И. М. ИССА, Р. М. ИССА, К. А. ИДРИСС и А. М. ХАММАН

Спектры электронной абсорбции пурпурина и хинализарина были сняты как в чистых водных средах, так и в смесях воды с органическими растворителями, при различных pH. Были использованы следующие растворители: метанол, этанол, этиленгликоль, глицерин и ацетон. Обсуждается влияние полярности растворителя на положение полосы. Были определены величины pK для различных изученных равновесий, которые обсуждаются в связи с природой и количеством органического растворителя. Было найдено, что pK_1 и pK_2 для обоих соединений уменьшаются с увеличением пропорции этиленгликоля или глицерина, но увеличиваются с увеличением количества метанола, этанола или ацетона.

Комплексы α-диоксимина с переходными металлами. Комплексная кислота — цианогалогено-бис-диметилглиоксимато-кобальт (III) и гидратация ионов

З. ФИНТА и Ч. ВАРХЕЙИ

Три новые моноосновные комплексные кислоты — $H[Co(DH)_2(CN)X]$, где DH_2 = диметилглиоксим и X = Cl, Br и I — были получены с помощью реакций лигандного обмена из соответствующих дигалогенокислот — $H[Co(DH)_2X_2]$ и KCN. Было изолировано и охарактеризовано 18 солей этих смешанных кислот. Для определения силы этих кислот были проведены pH-метрические измерения. Были сняты и обсуждаются их ИК спектры. В водных растворах этих комплексных анионов галоидные ионы замещены водой. Была снята кинетика этих процессов гидратации в кислых средах и были определены их кинетические параметры. Обсуждается механизм гидратации.

Анализ функций Грина молекулярных колебаний изотопных молекул озона

К. Л. НАРАЯНА и Б. П. САБАЛЕ

С помощью анализа функций Грина и техники распределения, используя уравнения Деуэймса и сотр., были рассчитаны основные и симметричные средне-квадратичные амплитуды, силовые постоянные, кориолисовы постоянные и распределение потенциальной энергии для изотопных молекул озона.

ИК-спектроскопические исследования анилов и их комплексов, I

Р. К. УПАДАЙ, М. Л. СИНГАЛ, А. К. САКСЕНА и Р. ПРАСАД

ИК-спектры шестнадцати анилов (продукты конденсации 3-фенантрилглиоксалей с первичными ароматическими аминами) интерпретировались на основе различных типов колебаний и определялась их структура. Было изучено также влияние природы заместителя и его положения на валентное колебание азометиновой группы.

ИК исследования комплексов Ni(II), Co(II) и Zn(II) с п-диметиламиноанилом 3-фенантриглиоксаля указывают на то, что кислород карбонильной группы и азот азометиновой группы являются местами взаимодействия при образовании комплекса. Были определены стабильности связей металл-азот и металл-кислород.

Средние амплитуды колебаний соединений CH_3NO_2, CF_3NO_2, CCl_3NO_2 и CBr_3NO_2

Б. ВИЗИ, Б. Н. СИВИН и Ш. Й. СИВИН

На основе литературных спектроскопических данных были рассчитаны средние колебательные амплитуды CH_3NO_2, CF_3NO_2, CCl_3NO_2 и CBr_3NO_2. Данные для соединений CF_3NO_2 и CBr_3NO_2 сравнивались с результатами электронно-диффракционных измерений.

Определениеграничных значенийкорио лисовых постоянных, согласованных с зкспериментальными нормальными частотами

И. ЛУКОВИЧ и Ф. ТЕРЕК

Для оценки граничных значений кориолисовых постоянных данной молекулы $\zeta_j^{\alpha i}$ приводится способ, который может быть использован в случае, если элементы матрицы F не фиксированы, а изменяются в интервале заданных граничных значений. Для решения проблемы был использован метод параметрического изображения и градиентный способ проектирования. С этой целью была разработана программа для ЭВМ, которая применялась для расчета молекулы формальдегида.

Было установлено, что константа сопряжения ζ_{65}^*, измеряемая экспериментально, попадает в узкий интервал между рассчитанными максимальным и минимальным значениями ζ_{65}^*.

Применение рентген-фотоэлектронной спектроскопии (ESCA) в области координационной химии, V

Исследование комплексов тицианатов и изотицианатов

К. БУРГЕР, ДЬ. ЛИПТАИ и Ч. ВАРХЕЙИ

Было проведено ESCA исследование смешанных комплексов тиоцианатов и изотиоцианатов, содержащих конечные роданидные лиганды, а также многоядерных смешанных комплексов, содержащих роданидный мостик. Было установлено, что координация атома серы и атома азота роданида, а также одновременно их обоих оказывает влияние на электронное строение роданида.

Гармоническое силовое поле и расчетные средние амплитуды для окисей вольфрама: WO_2 и WO_3 с учетом иона WO_4^-

Ш. Й. СИВИН и И. ХАРГИТТАИ

Было разработано гармоническое силовое поле для WO_2 и WO_3, которое использовалось для расчета средних амплитуд колебаний этих молекул и эффекта сокращения в случае WO_3. Обсуждаются предыдущие расчеты средних амплитуд для WO_4^-. Было изучено влияние, оказываемое на эти величины изменением некоторых частот молекул

WO_2 и WO_3. Указываются возможности определения этих частот с помощью данных наблюдаемых средних амплитуд или эффекта сокращения, полученных методом газовой электронной дифракции.

Исследование молекулярной геометрии газового 1,3-диоксана методом электронной дифракции

ДЬ. ШУЛЬЦ и И. ХАРГИТТАИ

На основе данных электронной дифракции газа было заключено, что молекулы 1,3-диоксана принимают конформацию кресла, что находится в согласии с данными микроволновой спектроскопии [R. Kewley, Can, J. Chem. *50*, 1690 (1972))]. Были определены длины и углы связей. В ходе структурного анализа были использованы и данные микроволновой спектроскопии.

Взаимодействие между металлами и аминокислотами, I

Изучение комплексов трехвалентных редкоземельных элементов з L-аспарагиновой кислотой

О. ФАРУК, А. У. МАЛИК и Н. АХМАД

Внутренние комплексы переходных металлов с 0-аминокислотами были исследованы обычно в растворах, применяя некоторые физико-химические методы [1—10]. Как видно из современной литературы, очень ограниченное внимание уделялось изолированию и определению структуры комплексов редкоземельных элементов с аминокислотами. В настоящей работе занимаются взаимодействием L-аспарагиновой кислоты с трехвалентными ионами редкоземельных элементов (Y, La, Ce . . . Lu за исключением Pm). Комплексы были изолированы и идентифицированы на основе ИК спектроскопических исследований, магнитных измерений, термогравиметрического анализа, молярной проводимости и элементарного анализа.

Определение марганца с помощью N-бромосукцинимида

А. АБУЛЬ ХЕЙР, М. АЯД и М. М. АМЕР

Предлагается процедура для полумикро-определения Mn(II), основанная на его щелочном окислении с помощью N-бромосукцинимида (NBS). Реакция протекает при комнатной температуре и в присутствии избытка NBS, который необратимо восстанавливается до сукцинимида. Избыток NBS обратно титруют с помощью стандартного раствора арсенита, а конечная точка титрования детектируется потенциометрически.

Был изучен механизм реакции. Было найдено, что точность результатов не уступает точности, получаемой комплексометрическим титрованием и калориметрическим методом с помощью формальдоксима. Точность измерений соответствует 99,63 $\pm$ 0,6262% ($P = 0{,}05$).

Активность и коэффициент активности противоионов в водных полиэлектролитных растворах

Е. А. ХАССАН и М. М. Б. ЭЛЬ-САББАХ

Активность и коэффициент активности были определены для ионов серебра в полиэлектролитных растворах карбоксилалкилированного поли(винилового спирта) с моно-, ди- или трихлоруксусными кислотами при двух различных емкостях обмена.

Увеличение коэффициента активности противоиона (при равных концентрациях соли серебра полиэлектролита, свободного от других солей) в вышеупомянутом порядке используемого полимера является значительным в очень разбавленных растворах (6250—781,25 $\cdot$ 10^{-7}N). Хотя его величина увеличивается с емкостью полимера и сильно увели-

чивается с уменьшением концентрации соли серебра полиэлектролита, однако, не достигает единицы при бесконечном разбавлении.

Для различных смесей полиэлектролита в форме соли серебра, свободной от других солей, и в форме кислоты, коэффициент активности иона соли увеличивается с уменьшением относительных количеств серебряной соли полиэлектролита и с уменьшением общей концентрации.

Исследование 4-тиазолидинонов, II

Действие вторичных аминов на 5-арилиден роданины и их соли

А. Р. А. РАОУФ, М. Т. ОМАР, С. М. А. ОМРАН и К. Е. ЭЛЬ-БАЙОУМИ

Взаимодействие 5-арилиден роданинов (*1*) с вторичными аминами приводит к образованию смеси солей амина *2* и 2-тиазолин-4-онов (*3*) в различных отношениях в зависимости от времени контакта. Был обсужден ход реакции, приводящий к превращению солей амина *2* в 2-тиазолин-4-оны. Были также исследованы превращения 5-арилиден-3-фенил роданинов с вторичными аминами.

Исследование 4-тиазолидинонов, III

Ход разложения 2,4-тиазолидиндионов с аминами

А. Р. А. РАОУФ, М. Т. ОМАР и М. М. ЭЛЬ-АТТАЛЬ

Взаимодействие 5-(6-бром-3,4-метилендиоксибензилиден)-2,4-тиазолиндиона (*1в*) и его 3-фенил производного (*1а*) с пиперидином в определенных условиях дает 0-тиол-0-(6-бром-3,4-метилендиоксифнил)-N-пиперидилкарбонил акриламид (*2в*) и его N-фенил замещенное производное (*2в*), соответственно. Однако, обработка 5-арилиден-2,4-тиазолидиндиона избытком бензиламина приводит к соответствующим арилуксусным кислотам *5*. Структура этих продуктов была доказана на основе их ИК, УФ и ЯМР спектров.

Производные гекситола, содержащие 1,4-оксатиановое кольцо, II

Й. КУСМАН и П. ШОХАР

Был описан синтез 4-О-мезил-3-О-тозил-(IIIc), 3-О-мезил-4-О-тозил-(IIId) и 3,4-ди-О-тозил-производных (IIIe) 2,5-ангидро-1,6-тиоангидро-О-глуцитола. Тозилокси-группы этих соединений могут быть отщеплены за счет восстановления натриевой амальгамой. При этом образуются 3-гидрокси-4-О-метил-(III к), 4-гидрокси-3-О-мезил-(IIIg), и 3,4-дигидрокси-производные (IIIb).

Исследование некоторых гетероциклов, XXXIV

И. ШИМИТИ и М. ФАРКАШ

Была исследована ориентация в реакциях бромирования и нитрования 2-(п-X-фенил)-4-хлорметил- и 2-(п-X-фенил)-4-хлорметил-5-Y-тиазолей в зависимости от природы заместителей фенильного кольца или в положении 5 тиазоля.

Исследование 0-аминооксикарбоксильных кислот с помощью ИК и ЯМР спектроскопии

П. ШОХАР, Л. ДАНЧИ и Л. КИШФАЛУДИ

Хотя первые представители 0-аминооксикарбоксильных кислот — отличающихся от природных аминокислот одним атомом кислорода — были известны уже в конце прошлого столетия [1], однако, физические и химические свойства этих соединений не были тщательно изучены лишь до тех пор, пока не было установлено, что некоторые их них

ингибируют рост *Mycobacterium tuberculosis* charatchok, [2—4]. Согласно нашим исследованиям, однако, лишь некоторые представители обладают значительной активностью [5—7]. Авторами ранее уже были описаны синтез некоторых основных соединений [8] и их производных, а также их физические и химические свойства [9]. В настоящей статье обсуждаются ИК и ЯМР характеристики α-аминооксикарбоксильных кислот.

Были описаны физико-химические характеристики сырой нефти charatchok, а также ее легкой и средней фракций дестилляции (газолин, керосин и газовое масло).

Гидрообработка фракций керосина и газового масла была произведена с целью изучения возможности повышения их качества.

Сырую нефть подвергали дестилляции при атмосферном давлении с пятью отборами. Дальнейшая дестилляция при пониженном давлении (40 мм рт. ст.) приводит к двум другим фракциям. Был произведен анализ на углеводороды и на структурные группы как для узких отборов, так и для фракций технической дестилляции.

The Acta Chimica publish papers on chemistry, in English, German, French and Russian.

The Acta Chimica appear in volumes consisting of four parts of varying size, 4 volumes being published a year.

Manuscripts should be addressed to

Acta Chimica
Budapest 112/91 Műegyetem

Correspondence with the editors should be sent to the same address.

The rate of subscription is $ 32.00 a volume.

Orders may be placed with "*Kultúra*" Foreign Trade Company for Books and Newspapers (1389 Budapest 62, P.O.B. 149. Account No. 218 10990) or with representatives abroad.

Les Acta Chimica paraissent en français, allemand, anglais et russe et publient des mémoires du domaine des sciences chimiques.

Les Acta Chimica sont publiés sous forme de fascicules. Quatre fascicules seront réunis en un volume (4 volumes par an).

On est prié d'envoyer les manuscrits destinés à la rédaction à l'adresse suivante:

Acta Chimica
Budapest 112/91 Műegyetem

Toute correspondance doit être envoyée à cette même adresse.

Le prix de l'abonnement est de $ 32,00 par volume.

On peut s'abonner à l'Entreprise pour le Commerce Extérieur de Livres et Journaux «*Kultúra*» (1389 Budapest 62, P.O.B. 149 Compte-courant No. 218 10990) ou à l'étranger chez tous les représentants ou dépositaires.

«*Acta Chimica*» издают трактаты из области химической науки на русском, французском, английском и немецком языках.

«*Acta Chimica*» выходят отдельными выпусками разного объема. 4 выпуска составляют один том. 4 тома публикуются в год.

Предназначенные для публикации рукописи следует направлять по адресу:

Acta Chimica
Budapest 112/91 Műegyetem

По этому же адресу направлять всякую корреспонденцию для редакции.

Подписная цена — $ 32,00 за том.

Заказы принимает предприятие по внешней торговле книг и газет «*Kultúra*» (1389 Budapest 62, P.O.B. 149. Текущий счет № 218 10990) или его заграничные представительства и уполномоченные.

Reviews of the Hungarian Academy of Sciences are obtainable at the following addresses

ALBANIA

Drejtorija Qëndrone e Párhapjes
dhe Propagandimit të Librit
Kruga Konferenca e Pazes
Tirana

AUSTRALIA

A. Keesing
Box 4886, GPO
Sydney

AUSTRIA

GLOBUS
Höchstädtplatz 3
A-1200 Wien XX

BELGIUM

Office International de Librairie
30, Avenue Marnix
Bruxelles 5
Du Monde Entier
162, Rue du Midi
1000 Bruxelles

BULGARIA

HEMUS
11 pl Slaveikov
Sofia

CANADA

Pannonia Books
2, Spadina Road
Toronto 4, Ont.

CHINA

Waiwen Shudian
Peking
P. O. B. 88

CZECHOSLOVAKIA

Artia
Ve Směčkách 30
Praha 2
Poštovní Novinová Služba
Dovoz tisku
Vinohradská 46
Praha 2
Mad'arská Kultura
Václavské nám. 2
Praha 1
SLOVART A. G.
Gorkého
Bratislava

DENMARK

Ejnar Munksgaard
Nörregade 6
Copenhagen

FINLAND

Akateeminen Kirjakauppa
Keskuskatu 2
Helsinki

FRANCE

Office International de Documentation
et Librairie
48, rue Gay-Lussac
Paris 5

GERMAN DEMOCRATIC REPUBLIC

Deutscher Buch-Export und Import
Leninstraße 16
Leipzig 701
Zeitungsvertriebsamt
Fruchtstraße 3—4
1004 Berlin

GERMAN FEDERAL REPUBLIC

Kunst und Wissen
Erich Bieber
Postfach 46
7 Stuttgart S.

GREAT BRITAIN

Blackwell's Periodicals
Oxenford House
Magdalen Street
Oxford
Collet's Subscription Import
Department
Dennington Estate
Wellingsborough, Northants.
Robert Maxwell and Co. Ltd.
4—5 Fitzroy Square
London W. 1

HOLLAND

Swetz and Zeitlinger
Keizersgracht 471—487
Amsterdam C.
Martinus Nijhof
Lange Voorhout 9
The Hague

INDIA

Hind Book House
66 Babar Road
New Delhi 1

ITALY

Santo Vanasia
Via M. Macchi 71
Milano
Libreria Commissionaria Sansoni
Via La Marmora 45
Firenze
Techna
Via Cesi 16.
40135 Bologna

JAPAN

Kinokuniya Book-Store Co. Ltd.
826 Tsunohazu 1-chome
Shinjuku-ku
Tokyo
Maruzen and Co. Ltd.
P. O. Box 605
Tokyo-Central

KOREA

Chulpanmul
Phenjan

NORWAY

Tanum-Cammermeyer
Karl Johansgt 41—43
Oslo 1

POLAND

Ruch
ul. Wronia 23
Warszawa

ROUMANIA

Cartimex
Str. Aristide Briand 14—18
Bucureşti

SOVIET UNION

Mezhdunarodnaya Kniga
Moscow G—200

SWEDEN

Almquist and Wiksell
Gamla Brogatan 26
S—101 20 Stockholm

USA

F. W. Faxon Co. Inc.
15 Southwest Park
Westwood Mass. 02090
Stechert Hafner Inc.
31. East 10th Street
New York, N. Y. 10003

VIETNAM

Xunhasaba
19, Tran Quoc Toan
Hanoi

YUGOSLAVIA

Forum
Vojvode Mišića broj 1
Novi Sad
Jugoslavenska Knjiga
Terazije 27
Beograd

20. II. 1975 Index: 26.007